This is the manuscript of a book that was never completed and never published. I hope to update it and publish it sometime in the next few years. Large portions are adapted from my chapter "Gravitational Radiation" in the book ***300 Years of Gravitation***, eds. S.W. Hawking and W. Israel (Cambridge University Press, 1987), pp. 330-458..
- Kip Thorne, Caltech, September 2009.

GRAVITATIONAL RADIATION

A New Window onto the Universe

by Kip S. Thorne

draft of 16 September 1989

California Institute of Technology

1989

Contents

Preface xi

Part I. Overview 1

1. Introduction to gravitational waves 2

   A. Newtonian gravity and general relativity X
   B. The motivations for trying to detect gravitational waves X
   C. The physics of gravitational waves X
   D. Sources of gravitational waves X
   E. The information carried by gravitational waves X
   F. Gravitational waves as a tool for cosmology X

2. Introduction to wave detection 33

   A. Is detection outrageously impossible? X
   B. Frequency bands for detectors X
   C. Earth-based detectors: the high-frequency band X
   D. Solar-system-based detectors: the low-frequency band X
   E. Astronomical detectors: the very-low-frequency band X
   F. Burst waves: sources and detector sensitivities X
   G. Periodic waves: sources and detector sensitivities X
   H. Stochastic waves: sources and detector sensitivities X

3. A brief history of gravitational-wave research 68

A. Fundamental theory X
B. Wave detection and astrophysical theory X

Part II. Theory 89

4. Description of gravitational waves 90

A. The Riemann curvature tensor for a gravitational wave X
B. Proper reference frames, and the physics of Riemann curvature X
C. Metric theories of gravity, and gravitational-wave polarization X
D. Gravitational-wave field in general relativity X
E. Energy, momentum, and quantization of gravitational waves X
F. Transverse-traceless coordinates X

5. Propagation of gravitational waves 118

A. Geometric-optics propagation laws X
B. Linear perturbations of curved spacetime X
C. The shortwave formalism X
D. Geometric optics X
E. Interaction of waves with matter X
F. Interaction of waves with electromagnetic fields X
G. A catalog of wave-propagation effects X
H. Asymptotic analyses and exact solutions X

6. Generation of gravitational waves 160

A. Wave generation split off from wave propagation X
B. The quadrupole formalism for wave generation and radiation reaction X
C. Multipole expansions in the asymptotic rest frame X
D. Slow-motion sources: derivation of the quadrupole formalism X
E. General relativity as a nonlinear field theory in flat spacetime X
F. 3+1 formulation of general relativity X
G. Slow-motion formalisms X
H. Post-Minkowskii formalisms X
I. Post-Newtonian formalisms X
J. Perturbation formalisms X
K. Numerical relativity X

Part III. Sources 211

7. Burst sources 212

A. Characterization of bursts and of noise in a detector searching for them X
B. Supernovae (collapse to neutron star) X
C. Collapse of a star or star cluster to form a black hole X
D. Coalescence of neutron–star and black–hole binaries X
E. The fall of stars and small holes into supermassive holes X
F. Cherished beliefs X
G. Bursts with memory X

8. Periodic sources 254

A. Characterization of the waves from periodic sources and of the noise in a detector searching for them X
B. Rotating neutron stars: formal considerations X
C. Rotating neutron stars deformed by crystalline or magnetic stresses X
D. Rotating neutron stars deformed by the CFS instability X
E. Binary stars X

9. Stochastic sources 289 X

A. Characterization of stochastic waves and of noise in a detector searching for them X
B. Binary stars X
C. Population III stars X
D. Primordial gravitational waves X
E. Phase transitions in the early universe X
F. Cosmic strings X
G. Star clusters and plasmas X
H. Soliton and boson stars X

Part IV. Detection 297 X

10. Resonant bar detectors 298 X

A. How a resonant bar detector works X
B. Sensitivity of bar detectors to short bursts X
C. How to optimize the sensitivities of bar detectors X
D. Parameters of first– and second–generation bar detectors X

E. Sensitivities of bar detectors to periodic and stochastic waves X
F. Quantum limits and quantum nondemolition X
G. Looking toward the future X
H. Observations of supernova 1987A X

11. Beam detectors 314

A. How a beam detector works X
B. Noise in beam detectors X
C. Noise in the present prototypes X
D. Simple, recycling, and resonating receivers and their shot noise X
E. Quantum limit, quantum nondemolition, and squeezed vacuum X
F. Anticipated sensitivities of full-scale LIGO receivers X
G. Ideas for other types of beam detectors X
H. Networks of beam detectors
I. Signal processing of the output from beam detectors X

12. Other types of detectors 337

A. Earth-based detectors (frequencies above 10 Hz) X
B. Solar-system-based detectors (10 Hz to 10^{-5} Hz) X
C. Astronomical detectors (frequencies below 10^{-5} Hz) X
D. Hertz experiments X
D. Concluding remarks X

Notation and Conventions 349

References 350

Author Index X

Subject Index X

Preface

This book is an introduction to and thorough review of gravitational radiation, with emphasis on four topics: (i) The fundamental theory of gravitational waves (their generation, propagation, and detection). (ii) Cosmic sources of gravitational waves (black holes, neutron stars, supernovae, the big bang, inflation of the universe, cosmic strings, ...). (iii) Efforts to detect gravitational waves using resonant bars, laser interferometers, tracking of spacecraft, timing of pulsars, and other techniques. (iv) The prospects for such detection to revolutionize our understanding of the universe.

Part I of the book (Chaps. 1, 2, and 3) is an overview of the entire subject at roughly the Scientific American level. However, unlike the Scientific American, these chapters assume that the reader is familiar with elementary physics at the level of a good secondary-school course, and it uses mathematics at that level. These chapters are intended as an entré into gravitational radiation for the general, but elementary-physics-literate reader, as well as for people with more advanced training in physics or engineering.

The rest of the book requires, for full understanding, that the reader be trained in physics or engineering at the advanced undergraduate level. Two chapters (5 and 6), but only those two, require prior familiarity with Einstein's general theory of relativity at the level of track one of the textbook *Gravitation* by Misner, Thorne, and Wheeler (1973).

Part II of the book (Chaps. 4, 5, 6) is a pedagogical introduction to the theory of gravitational waves. It is not necessary to read or master these theory chapters in order to understand the remainder of the book; but mastering them will give the reader a deeper appreciation of many aspects of gravitational radiation. Were I to participate today in rewriting the textbook *Gravitation*, I would write the gravitational radiation section in the manner of these theory chapters. I expect these chapters to be useful as a supplement and update to general relativity textbooks, and as a text for courses on gravitational radiation.

Parts III (Chaps. 7, 8, 9) iandIV (Chaps. 10, 11, 12) are detailed descriptions of astrophysical sources of gravitational radiation, and of experimental efforts to detect gravitational waves. In these chapters I attempt to bring readers into full contact with the current state of the field and with the directions of near-future research.

This book attempts to be thorough in its coverage of topics and ideas. In this sense, it can serve as a useful handbook for researchers in the field as well as a thorough overview for newcomers. At one time I had hoped also to be thorough in my references to the primary literature — a glance at the length of the *References* section may leave the impression that I have been. Not so. Gravitational radiation has become such a large field of research that I was overwhelmed by the literature. As a result, in many places I have confined myself to citing for each idea or topic its earliest occurence in the literature, and several more recent, arbitrarily chosen but thorough discussions of it. For this I apologize to my many colleagues whose contributions are not cited explicitly.

A few words about the style of my prose: Much of the book is written in second person singular — "If we do this, then we discover that." The "we" refers to "you the reader and I the author", working together toward better understanding. From time to time there is a switch to first person singular — "I doubt that these things are correct." The "I" refers to the author, in this case offering his own personal viewpoint, with which other experts might disagree.

Parts III and IV of this book, and small pieces of Parts I and II, are adapted (with updating and extensive revision and expansion) from a chapter that I wrote in late 1986 for the book 300 *Years of Gravitation* (Thorne, 1987). The updating includes major developments in the field between January 1987 and August 1989.

For helpful comments on portions of the manuscript I thank a number of my colleagues: John Armstrong, Peter Bender, Jiří Bičak, David Blair, Roger Blandford, Herman Bondi, Alain Brillet, Carlton Caves, Frank Estabrook, Charles Evans, Sam Finn, Craig Hogan, Jim Hough, Ed Leaver, Brian Meers, Tsvi Piran, Roger Romani, David Shoemaker, Dan Stinebring, Kimio Tsubono, Alex Vilenkin, Bob Wagoner; and especially Ron Drever, Leonid Grishchuk, and Thibault Damour. Damour was particularly helpful in straightening me out about a number of historical issues.

This book includes some of my own research results that have not previously been published. My research and writing of the book have been supported in part by the National Science Foundation [grants AST-8514911 and AST-8817792 to the California Institute of Technology] and by funds associated with my William R. Kenan, Jr., Professorship at Caltech.

For their hospitality I would like to thank the Physics and Astronomy Departments and the Phenomenology Group at the University of Wisconsin in Madison, where much of this book was written.

Kip S. Thorne
Pasadena, California
30 September 1989

Part I
Overview

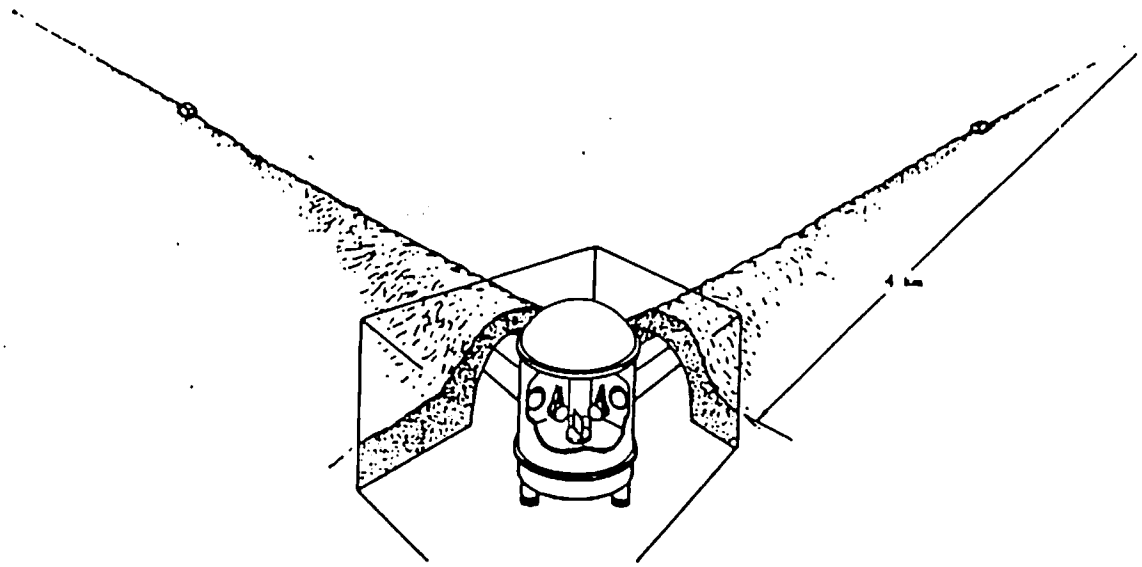

An artist's sketch of the Western site of the proposed American Laser Interferometer Gravitational-Wave Observatory (LIGO). The Eastern site, a similar facility, would be several thousand kilometers away. Searches for gravitational waves would be performed by cross correlating the data from "beam detectors" at the two sites. Extraction of all the information carried by the waves will require cross correlating also with similar detectors in Europe, Asia, and/or Australia. (KIP: SUPPLY FIGURE ATTRIBUTION.)

1 Introduction to Gravitational Waves

1.A Newtonian gravity and general relativity

For more than two centuries (1687 to 1915) Isaac Newton's theory of gravity reigned supreme as *the* definitive description of what gravity is, and how it governs an apple's fall, an ocean's tides, and the orbits of the moon and planets. Gravity, according to Newton, is a force by which any two particles of matter attract each other. This gravitational force points from one particle to the other; i.e., in the jargon of modern physicists it is "longitudinal". The force is directly proportional to the masses of the two particles and inversely proportional to the square of the distance between them. Put more precisely: the force *now* is inversely proportional to the square of the distance between the particles *now*; the force one second ago was inversely proportional to the square of the distance one second ago; and as the distance changes, the force changes.

This Newtonian description of gravity relied crucially on the concept of *universal time*. To determine the distance between the moving particles for insertion into Newton's gravitational law, one must know which moment of time at one particle is the same as a chosen moment at the other. Such a universal time was also built, inextricably, into Newton's other laws of mechanics.

Universal time and Newton's mechanical and gravitational laws achieved great triumphs in physics, astronomy, and engineering during the eighteenth and nineteenth centuries. However, at the beginning of the twentieth century Albert Einstein, Hendrik Lorentz, and Henri Poincaré discovered that electrical forces, magnetic forces, and their effects on charged particles are incompatible with absolute time. Absolute time cannot exist. This destruction of absolute time brought Newton's entire intellectual edifice tumbling down.

By 1905 Einstein had worked out a set of new physical laws, free of absolute time, to replace Newton's laws. These new laws came to be called special relativity theory, "special" because there was a key gap in the laws: they did not include gravity. Gravity remained a severe stumbling block until 1915, when Einstein finally developed a description of gravity that could be incorporated, consistently, into relativity theory. The result was Einstein's general theory of relativity.

During the seventy five years since 1915, a wide variety of high-precision experiments have tested Einstein's general relativistic laws of gravity, in competition with Newton's gravitational laws. In all these tests Einstein has prevailed. For details see, e.g. Will (1981, 1986b).

Einstein's description of gravity is radically different from Newton's. Newton described gravity as an instantaneous force between two particles of matter. Einstein describes it as a curvature of spacetime — "spacetime" being a unification of 3-dimensional space and time into an entity with four dimensions.

Despite this radical conceptual difference, Einstein's and Newton's laws of gravity give very nearly the same predictions when gravity is "weak" and the speeds of all particles of interest are small compared to the speed of light. This is the case throughout the solar system, which was the realm of eighteenth and nineteenth century science. Radically different predictions arise only when gravity becomes far stronger than in the solar system — near black holes and neutron stars, and in the early stages of the "big bang" that began our universe.

Because our everyday intuition relies so strongly on the language of Newtonian forces and accelerations, it is conceptually useful to recast Einstein's laws of gravity in Newtonian language. This is especially so when one is dealing with earth-based laboratories and solar-system physics, where gravity is almost Newtonian. Accordingly, in most sections of this book we shall use a Newtonian-language description of Einsteinian gravity.

When discussed in Newtonian language, Einsteinian gravity (spacetime curvature) breaks down into several pieces; see. e.g. Thorne (1988). The only piece familiar from everyday experience is the longitudinal, Newtonian-type. gravitational force. This force, which is analogous to the electrical force between two charged particles, is predicted by Einstein to differ from Newton's variant by about one part in a million in the solar system. That tiny difference has been measured, proving Einstein right, to a precision of about one per cent (see, e.g., Will, 1981, 1986b). A second, more esoteric, piece of Einsteinian gravity is the gravitational analog of the magnetic force. This "gravitomagnetic" force has never yet been detected directly by experiment, but there is strong indirect evidence for it, and it will be the target of a future NASA-flown earth-orbiting satellite called "Gravity Probe B" (KIP: GET REFERENCE). A third piece of Einsteinian gravity is the curvature of space (not spacetime; spacetime curvature is the whole thing, which we are breaking into pieces). This spatial curvature contributes, equally with the Newtonian-type gravitational force, to the sun's gravitational deflection of starlight. That deflection has been measured to a precision of 3 parts in 1000 by Robertson and Carter (1984), thereby verifying with better than one per cent precision Einstein's predictions for the existence and size of spatial curvature around the sun. A fourth piece of Einsteinian gravity is gravitational radiation.

Gravitational radiation is the gravitational analog of electromagnetic radiation, i.e. of light and radio waves. In Einstein's language, gravitational radiation consists of ripples in the curvature of spacetime that travel with the same speed as light. Translated into Newton's language, gravitational radiation is an oscillating, "transverse" force analogous to the oscillating transverse electrical force carried by an electromagnetic wave. By "transverse" is meant that the direction of the force is perpendicular to the direction of propagation of the wave, i.e. (in most situations) perpendicular to the direction to the source. Whereas the electrical force of an electromagnetic wave is proportional to the electrical charge of the particle on which the wave acts, the gravitational force of a gravitational wave is proportional to the particle's mass. Since all particles have mass, all particles experience the force of a gravitational wave. We shall explore the subtle but crucial consequences of this in Sec. 1.C below.

Although gravitational waves are an unequivocal prediction of Einstein's laws of gravity, they have never yet been detected by humans. The challenge of detecting them is a major theme of this

book.

The crucial experiments elucidating the nature of electromagnetic waves were carried out by Heinrich Hertz in the 1880's; see the papers collected in Hertz (1892). Hertz generated radio waves in his laboratory, and then detected them and measured their properties. [KIP: ADD MORE DETAILS?] To do the same for gravitational waves seems insuperably difficult. The gravitational waves that can be generated by human technology are so weak, according to general relativity's predictions, that there is no hope of detecting them (see Sec. XXXX, below). Accordingly, all present efforts to detect and study gravitational radiation rely on the astrophysical universe to produce the waves.

1.B The motivations for trying to detect gravitational waves

Before the 1930's human knowledge of the astrophysical universe was based almost entirely on observations of light using optical telescopes. Then in 1932, by chance, Karl Jansky at Bell Telephone Laboratories in New Jersey discovered radio waves coming from the sky. The detailed study of these cosmic radio waves in the 1940s, 50s, and 60s created a revolution in our understanding of the universe (Kellerman and Sheets 1983; Sullivan 1982, 1984). Previously the universe, as viewed by light, seemed serene and quiescent. It was dominated by stars and planets that wheel smoothly in their orbits, shining steadily and requiring millions or billions of years to change in any discernible way. By contrast, the universe as viewed by radio waves was violent: galaxies in collision, jets ejected from galactic nuclei, quasars with fluctuating luminosities brighter than our galaxy, and pulsars with gigantic radio beams rotating many times per second. These were the typical strong radio emitters.

The radio revolution was so spectacular because the information carried by radio waves was so different from that carried by light. The light, with its wavelength of a fraction of a micron, was emitted primarily by thermally excited atoms residing in the atmospheres of stars and planets. The radio waves, with their ten-million-fold greater wavelengths, were emitted primarily by high-energy electrons spiraling in the magnetic fields of intergalactic space or the fields of neutron stars.

Today, as we enter the 1990's, our knowledge of the astrophysical universe is based on a much wider variety of radiations than in Karl Jansky's day: radio, millimeter, infrared, light, ultraviolet, X-ray, and gamma-ray radiations. However, all of these radiations are

electromagnetic.

The differences between the light and radio waves of Jansky's day are pale compared to the differences between the electromagnetic waves of present-day astronomy, and gravitational waves. Let us dwell a bit on the electromagnetic-wave / gravitational-wave differences:

Cosmic gravitational waves should be emitted by large-scale, coherent motions of huge amounts of matter (e.g., the implosion of the core of a star), or by large-scale, coherent pulsations of spacetime curvature (e.g., the pulsations of newborn black holes). The coherence of the large-scale motions guarantees that the gravitational waves from the various atoms, or various pieces of curvature, will have the same time evolutions and thus will superpose coherently. The result is a net gravitational wave field that varies in time in a manner which describes the details of the source's coherent, large-scale motions. (We shall study an example in Fig. 1.4 below). By contrast, cosmic electromagnetic waves are usually superpositions of independent radiation from individual atoms, molecules, and charged particles. Because each emitter produces a wave with a different time evolution, the individual waves superpose incoherently. The resulting net wave fluctuates stochastically in time with no information in the wave's precise time evolution, but much information in the spectrum of its fluctuations (i.e. in the amount of power carried by the wave at various wavelengths). Thus, whereas astronomers today measure the electromagnetic spectra of cosmic sources, furture gravitational astronomers will measure the time variations of the gravitational-wave field.

Gravitational waves are emitted most strongly in regions of space where gravity is so intense that Newton's description fails and must be replaced by Einstein's, and where matter moves at near the speed of light. Examples are the big-bang origin of the universe, the collisions of black holes, and the pulsations of newborn neutron stars at the centers of supernova explosions. Since these strong-gravity regions are typically surrounded by thick layers of matter that prevent the passage of electromagnetic waves, the electromagnetic waves seen by astronomers come almost entirely from weak-gravity, low-velocity regions; for example, the surfaces of stars and supernovae, and magnetized clouds of gas in intergalactic space.

Gravitational waves pass through surrounding matter with impunity, in contrast to electromagnetic waves which are easily absorbed and scattered, and also in contrast to neutrinos which, although they easily penetrate normal matter, scatter thousands of times while leaving the

core of a supernova explosion.

These enormous differences between electromagnetic and gravitational waves make it likely that, if cosmic gravitational waves can be detected and studied, they will bring us entirely new kinds of information — information not now available to astronomers. Correspondingly, gravitational-wave astronomy has the potential to create a revolution in our understanding of the universe comparable to or greater than the radio-wave revolution.

It might be argued that our present, electromagnetically-based understanding of the universe is so complete, compared to the optically-based understanding of the 1930s, that a gravitational-wave revolution will be far less spectacular than was the radio revolution. This seems to me unlikely. I am painfully aware of our lack of understanding when I contemplate the sorry state of present estimates of the gravitational waves bathing the earth (see Part III of this book): For each type of gravitational-wave source that has been thought about, with the exception of binary stars and their coalescences, either (i) the strength of the source's waves for a given distance from earth is uncertain by several factors of ten; or (ii) the rate of occurrence of that type of source, and thus the distance to the nearest one, is uncertain by several factors of ten; or (iii) the very existence of the source is uncertain.

These uncertainties cause great frustration in the planning and design of gravitational-wave detectors. That is the down side. The up side is the fact that, when gravitational waves are ultimately detected and studied, we may be rewarded with major surprises. The waves may bring us extensive information about the universe that cannot be obtained in any other way.

Not only does gravitational radiation hold great promise as a tool for astronomy. It also is a potentially powerful tool for probing the fundamental nature of gravity:

Einstein's general relativity is not the only theory of gravity that is viable today, i.e. that agrees with all past experiments and meshes logically with the other laws of physics. Rather, it is the most simple and elegant theory in a group of viable theories called "relativistic theories of gravity". The theories in this class are relativistic in the sense that they all mesh nicely with Einstein's special relativity, which has been tested to far higher precision than general relativity. However, they

differ in their descriptions of the nature of gravity; and they also differ in their detailed predictions for the dynamics of the solar system, and for the properties of neutron stars, black holes, the early universe, and gravitational radiation. The class of *viable* relativistic theories of gravity has been narrowed enormously over the past two decades by high-precision measurements of the motions of the planets and the propagation of electromagnetic waves through the solar system; see Will (1981, 1986b) for details. However, some theories besides general relativity remain viable; and clever physicists have little difficulty inventing others that are viable, though ugly. Gravitational-wave observations would constitute a new tool for constraining such theoretical speculations — a tool so powerful that it might well quell all remaining doubts as to the correctness of general relativity.

The first discovery of gravitational waves would verify *directly* the prediction of general relativity, and other relativistic theories of gravity, that such waves exist. (There has already been an *indirect* verification; see Fig. 1.1.) Direct verification would confirm theorists' deeply held theoretical convictions that gravity, like light, must propagate at a finite speed: if the speed were infinite, the waves would not be waves and they could be used to define a Newtonian type of absolute time throughout the universe.

By comparing the arrival times of the first burst of light and the first gravitational waves from a distant supernova explosion, one could verify general relativity's prediction that electromagnetic and gravitational waves propagate with precisely the same speed, the "speed of light", 299,792.456 km/sec.

As an example, consider a supernova outburst in the Virgo cluster of galaxies, 30 million light years from earth, where there are several supernovae per year. Supernovae are rather well understood, both on theoretical grounds and as a result of detailed observations of light and of neutrinos that come from them; see, e.g. XXXXXX. Theory and observation agree that a supernova outburst is due to the explosion of a star's outer layers, and that this explosion is triggered by the implosion of the star's core. When the imploding core, initially the size of the earth, has shrunk to ~ 20 km size, the implosion is forced to a halt by the repulsive force of atomic nuclei being squeezed together. The core should then bounce and perhaps pulsate, and a burst of gravitational waves should be emitted. This gravitational-wave burst should last only a few milliseconds, but should carry off in that brief time detailed information about the core's implosion, bounce, and pulsations; see

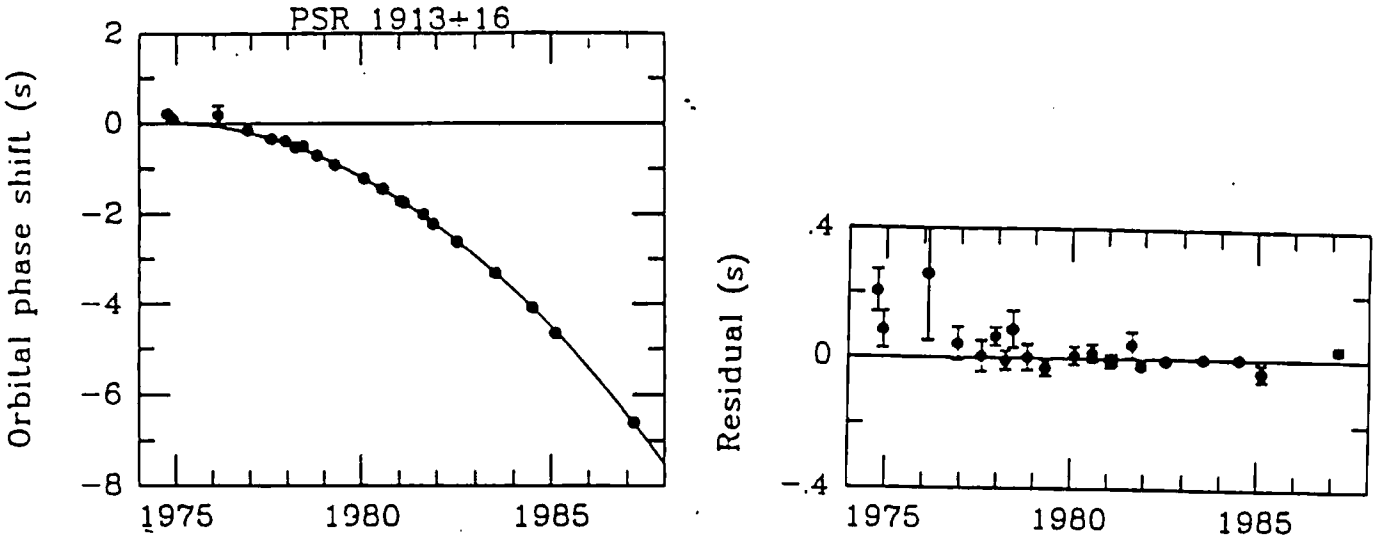

Fig. 1.1 Indirect evidence for the existence of gravitational radiation: General relativity predicts that two stars orbiting each other (i.e. a "binary star system") must emit gravitational waves, and that in reaction to their radiative loss of energy, the stars should very gradually spiral inward toward each other. This "radiation-reaction-induced" inspiral should produce a very gradual decrease in the stars' orbital period. When one of the two stars in the binary is a pulsar, its pulses of radio waves can be used as a clock for monitoring the orbital period: As the pulsar moves toward us in its orbit, the time interval between its pulses is shortened by the doppler shift; as it moves away, the time interval is lengthened. The duration of one cycle of shortening and lengthening is the orbital period. The "binary pulsar" PSR 1913+16 is a system of this type. It consists of two neutron stars orbiting each other, one of which is a pulsar. Precise measurement of the oscillating interval between pulses in PSR 1913+16 reveals that the orbital period, 7 hours 45 minutes and 7 seconds, is decreasing at a rate of 75.8 microseconds per year. This figure shows quantitatively the details of this period decrease. The upper graph depicts the measured "orbital phase shift", i.e. the time that the binary took to complete a given number of orbits since observations began in late 1974, minus the time that the binary would have taken had its period remained constant. The dots are the observational data; the curve is general relativity's prediction. The accuracy of the agreement between experiment and theory is indicated by their difference, the "residuals" shown in the bottom graph. These residuals demonstrate that the measured decrease of period agrees with theory to within the accuracy of the measurements, XX per cent at the 90 per cent confidence level. The data and analysis are due to Weisberg and Taylor (1984) and Taylor (1987). The details of the experiment and implications of the data are discussed by Weisberg, Taylor, and Fowler (1981) and Weisberg and Taylor (1981). This figure was kindly provided by Joseph Taylor. [KIP: CHECK WITH TAYLOR]

Fig. 1.4 below.

The core's implosion and bounce heat it to temperatures of hundreds of billions of degrees; and that heat produces a plethora of neutrinos which scatter thousands of times off the core's hot matter as they gradually (in several seconds time) work their way out of the core and escape. The bounce also produces a shock wave that propagates out through the core and into the star's envelope, ejecting the envelope with great force. An hour or so after the several millisecond gravitational-wave burst and the several second neutrino burst, the envelope's explosion has progressed far enough for the star's surface to start brightening enormously. After a few hours the surface, now ~ 100 million (10^8) kilometers in radius, is shining with light as brightly as ~ 10 million (10^7) suns. [KIP CHECK NUMBERS] Optical astronomers, alerted by gravitational astronomers that there has been a supernova at a certain location on the sky, might catch and study the stellar brightening within an hour or so of the initial gravitational-wave burst. Even without an alert, the supernova should become so brilliant after about a day that the optical astronomers' routine "supernova patrols" (KIP GIVE REFS), which cover the entire sky, should detect it. Without the alert, astronomers could deduce the difference in propagation speeds of the light and the gravitational waves to within a precision of (1 light day)/(30 million light years), i.e. 1 part in 10^{10}. With the alert the precision might be 1 part in 10^{11}. If both the neutrino burst and the gravitational-wave burst are seen, then astronomers could deduce the difference in the gravitational and neutrino propagations speeds (which should be equal according to conventional theory) to within (1 light second)/(30 million light years), i.e. 1 part in 10^{15}.

Such a comparison of propagation speeds has major theoretical implications: Theory says that all classical fields and forces are produced by collective, coherent motions of huge numbers of quantum mechanical particles called "bosons". (When only a few bosons are involved, the forces behave quantum mechanically. When many are involved, the forces are accurately described by classical physics.) The classical electromagnetic field is produced by huge collections of "photons", a specific type of boson; the classical gravitational field, by huge collections of "gravitons", another type of boson. Not surprisingly, the underlying bosons leave indelible imprints on their classical field. Nowhere do those imprints show up more clearly than in the field's waves. For example, if gravitons like photons have zero rest mass (and if they are affected by static gravity in the same way as are

photons; see below), then the propagation speeds of the gravitons' classical, gravitational waves must be precisely the same as the speed of light. If gravitons have nonzero rest mass, then the propagation speeds of their classical waves will be less than light and will depend on the waves' wavelength. Thus, from a high-precision comparison of the speeds of a supernova's light, neutrinos, and gravitational waves one can obtain a high-precision limit on the rest mass of the graviton.

Even if the graviton has zero rest mass, the propagation speed of its waves can differ from that of light. This is because gravitational waves and electromagnetic waves might respond to and be retarded by the static gravity of our Galaxy and other galaxies in different ways. Such, in fact, is the case in many relativistic theories of gravity, though not in general relativity. For examples and detailed discussions see Caves (1980b) and Sec. 10.1 of Will (1981).

Different relativistic theories of gravity predict different directions for the forces exerted on matter by a passing gravitational wave. In some theories the wave's forces must be longitudinal, i.e. along the direction of the wave's propagation. In other theories, including general relativity, the forces must be transverse; and in yet other theories they can be mixed, i.e. longitudinal and transverse. The possible force patterns are called the "polarizations" of the wave. General relativity's transverse waves can have two polarizations, i.e. two different patterns of transverse forces. We shall study these patterns in the next section (Fig. 1.3). For now the important fact is that they are called called "+" or "plus" and "×" or "cross"; and the evolution of each pattern's force with time is described by a "gravitational waveform": a function of time called $h_+(t)$ for the + polarization and $h_\times(t)$ for the × polarization.

Just as the rest mass of a boson places its imprint on the propagation speed of the boson's classical waves, so also the boson's spin places an indelible imprint on the polarization properties of the classical waves. An electromagnetic wave's polarization properties reveal that the underlying photon has spin one (i.e. its spin angular momentum is one in units of Planck's constant, $\hbar = 1.054\times10^{-27}$ g cm sec^{-2}). The polarization properties of a gravitational wave as predicted by general relativity reveal an underlying graviton spin of two. In other theories of gravity the graviton spin can be zero, one, or two; or there can be several types of gravitons each with its own spin; or the spin can even be ill-defined, thereby presenting serious obstacles to a quantum mechanical description of gravity. (For further details see Secs. 1.C

and 4.C below; also Eardley, Lee, and Lightman, 1973, and Eardley et. al., 1973). Thus, by measuring the polarization properties (force patterns) of gravitational waves, one can determine whether the spin of the graviton is two as demanded by general relativity, or is some other value or mixture of values.

If (as I strongly expect) general relativity turns out to be correct, then a central goal of gravitational-wave astronomy will be to monitor, for each source, the time evolutions $h_+(t)$ and $h_\times(t)$ of the waves' two polarizations. It is these time-evolving waveforms that carry detailed information about the source — e.g., in the case of waves from a supernova, information about the implosion, bounce, and pulsations of the supernova's core.

For most sources (e.g. supernovae and the big bang) we are far too ignorant today to predict the details of the waveforms. However, there is one type of source for which all tools of prediction are at hand: the spiraling together and coalescence of two black holes that are orbiting each other (a "black-hole binary"). Such a source is far simpler than a supernova or the big bang because it involves no matter. A black hole is made of pure spacetime curvature which holds itself together without the help of any matter. This means that calculations of the coalescence of a black-hole binary need not get embroiled in the messy and highly uncertain details of shock waves in matter, diffusion of photons through matter, emission of neutrinos by matter, etc. Being free of these complications, the black-hole coalescence and the gravitational waves it emits can be computed with confidence and precision by solving Einstein's gravitational equations (the "Einstein field equations"). To solve those equations analytically, in the case of coalescing black holes, is hopelessly difficult. However, they should be solvable numerically, using a supercomputer. Such computations, just now getting underway (Secs. 6.K and 7.D), are technically difficult, but well defined. They will take many person-years of programming effort, but are virtually guaranteed to reveal successfully general relativity's predictions.

From a detailed comparison of the resulting, predicted waveforms $h_+(t)$ and $h_\times(t)$ with gravity-wave detectors' observed waveforms there would follow major payoffs: Such a comparison could verify firmly that the sources are coalescing black holes. This would demonstrate unequivocally that black holes exist in our universe (the evidence thus far, while strong, is indirect and circumstantial; see, e.g., Blandford, 1987). Moreover, the comparison would serve as a probe of the nature of

gravity in a situation, the black-hole coalescense, where gravity is so extremely strong that Newton's laws should be flaunted violently. This probe would be by far the most stringent test ever of Einstein's general theory of relativity.

For the vast majority of sources, where we are too ignorant today to predict the waveforms $h_+(t)$ and $h_\times(t)$, the observed waveforms will bring us astrophysical information that we cannot get in any other way. For example, the waveforms from a supernova could show us the nonspherical, dynamical evolution of the imploding stellar core that triggers the supernova explosion: the flattening of the core due to centrifugal forces as it implodes, the breakup of the core into two pieces whirling about each other if that occurs, the bounce of the implosion when nuclear forces resist further compression, the spring-back of the core and recollapse and subsequent bounce, and the settling down into a rapidly rotating neutron-star state deep inside the now-ejecting stellar envelope. With so much surrounding matter to obscure the view, only the gravitational waveforms $h_+(t)$ and $h_\times(t)$ can bring us this information. The neutrinos cannot do so because they lose the information in their thousands of scatters, as they try to escape from the core. For further details see Secs. 1.E and 7.B below.

1.C The Physics of Gravitational Waves

We turn, now, to a more quantitative discussion of the nature of gravitational radiation. Throughout this discussion and throughout this book, except where otherwise stated, we shall assume that general relativity correctly describes classical gravity and gravitational radiation.

When an electromagnetic wave impinges on a particle, it exerts a force proportional to the particle's charge q, i.e. $F \propto q$. Similarly, when a gravitational wave impinges, its force is proportional to the particle's mass m, i.e. $F \propto m$. Since the particle's resulting acceleration a is equal to the force divided by the particle's mass, $a=F/m$, the acceleration a is proportional to q/m in the electromagnetic case and to $m/m = 1$ in the gravitational case.

Thus, in the gravitational case the acceleration is the same for all particles. This means that "free particles" (i.e. particles on which no forces except gravity act) all move in identically the same manner in response to a gravitational wave.

In order to discuss the particle motion quantitatively, it is helpful

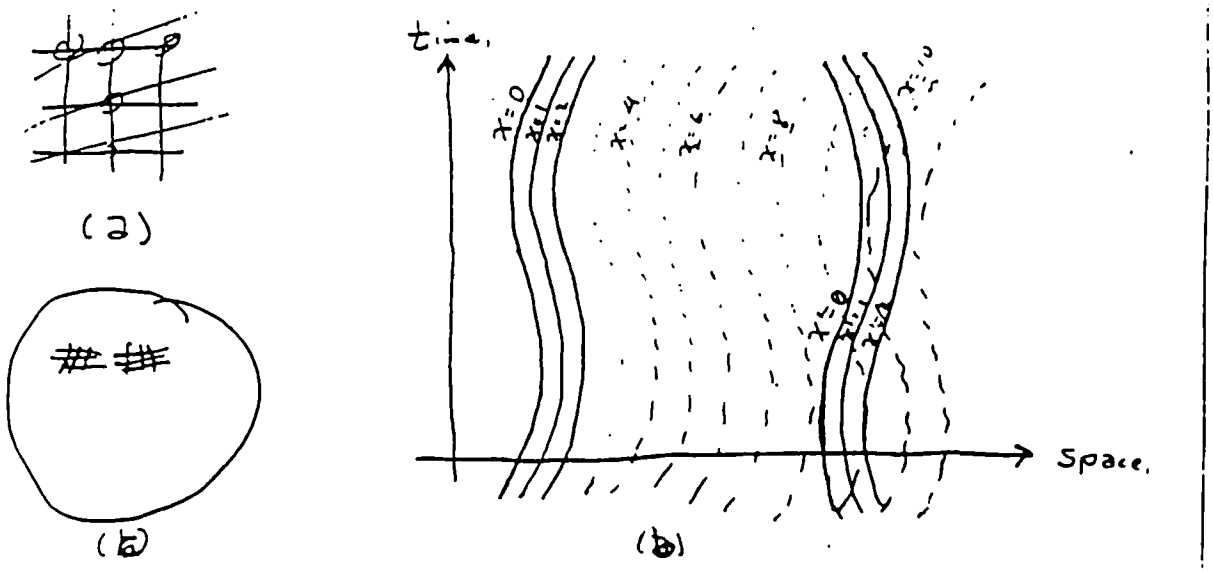

Fig. 1.2 (a) An inertial reference frame consisting of a rigid, rectangular latticework of measuring rods to which are attached ideal (perfect) clocks. (Reproduced from Fig. 9 of Taylor and Wheeler, 1966.) (b) The influence of a gravitational wave on two local inertial frames at two different locations in space. Plotted vertically is time; horizontally, one of the three directions of space. The three solid lines on the left represent the motion, through spacetime, of three lattice points in the first inertial frame; the three solid lines on the right, the motion of three lattice points in the second inertial frame. The two frames move relative to each other by an amount proportional to the distance between them [and also proportional to the gravitational waveform $h_+(t)$.] The dashed lines represent an extension of the first local inertial frame to form a larger, rigid, "proper reference frame" in which to analyze the wave's effects. (c) The influence of the curvature of the surface of the earth on two local, rectangular coordinate grids. Just as the earth's curvature prevents these grids from meshing to form a large, rectangular grid, so also Einstein attributes the gravitational-wave-induced nonmeshing of the two local inertial frames in (b) to a curvature of spacetime.

to introduce a *local inertial reference frame*. Such a frame (depicted in Fig. 1.2a and described at length in Sec. 4 of Taylor and Wheeler, 1966) is a small, conceptual, latticework of rigid rods. The smaller is the latticework, the more accurate will be the following discussion. The orientation of the latticework is held fixed by inertial-guidance gyroscopes. The gyroscopes prevent it from rotating. Throughout the latticework there reside ideal clocks, i.e. clocks which tick at uniform, identical rates and are synchronized with each other. (For a detailed discussion of ideal clocks see, e.g., Sec. 1.5 of Misner, Thorne, and Wheeler, 1973 — cited henceforth as MTW; for a discussion of clock

synchronization see, e.g., Sec. XXX of Taylor and Wheeler, 1966.) The reference frame moves freely through space, i.e. it moves in the same manner as free particles. In this sense it is inertial; if it did not move freely, i.e. if it were accelerated relative to free particles, then it would be noninertial.

If one seeks to detect a gravitational wave by monitoring the motions of free particles relative to such a local inertial frame, one will not see any effects of the wave whatsoever. The frame responds to the wave with exactly the same oscillatory motions as the particles, so relative to the frame the particles do not respond at all. Correspondingly, the gravitational wave is undetectable.

At least, this would be so if the wave's influence were identically the same everywhere in space. However, it is not. The wave pushes slightly differently here than there; and that difference gives rise to a motion of inertial reference frames (and particles) here relative to those there; see Fig. 1.2b. The farther apart are "here" and "there", the greater will be the relative motions. In fact, the relative motions are directly proportional to the distance between "here" and "there", so long as that distance is somewhat smaller than $\lambda\!\!\!^{-} \equiv (\text{wavelength of wave})/2\pi$. (For typical waves from cosmic sources, $\lambda\!\!\!^{-}$ is 5 km or longer; usually much longer. See Sec. 1.C below.)

This relative motion prevents us from meshing together the local inertial frames in one region of space with those in another, nearby region to form a global inertial frame. As Einstein was the first to realize, this nonmeshing of local inertial frames is analogous to the nonmeshing of surveyors' local rectangular coordinate grids on the surface of the earth (Fig. 1.2c) — i.e. it is analogous to the impossibility of making an accurate, flat map of the earth. Just as we say that the surveyor's local grids cannot mesh because of the curvature of the earth's surface, so Einstein's general relativity theory attributes the nonmeshing of local inertial frames to a *curvature of spacetime*. (For full details see, e.g., MTW — i.e. Misner, Thorne, and Wheeler, 1973.) Correspondingly, Einstein describes gravitational waves as *ripples in the curvature of spacetime that propagate with the speed of light*.

This description of gravitational waves is sophisticated and elegant. However, it is not easily incorporated into our ordinary, Newtonian-based intuition.

Fortunately, there is an alternative, Newtonian-language description of gravitational waves which requires no more mathematical

sophistication than that of elementary physics. This alternative description begins by selecting, somewhat arbitrarily, a specific local reference frame made from a rectangular, rigid-rod latticework. Along the latticework's rods are measured Cartesian coordinates x, y, z, and in the latticework are embedded ideal, synchronized clocks that measure time t. One might attach the latticework's spatial origin to an earth-bound laboratory and the axes to the laboratory's walls. In this case the frame is non-inertial and is called the laboratory's *proper reference frame* (Sec. 13.6 of MTW and Sec. 4.A of this book). Free particles, as studied in this proper reference frame, will exhibit Newtonian-type gravitational accelerations (which Einstein attributes to the frame's failure to move freely), and coriolis and centrifugal accelerations (which Einstein attributes to the frame's rotation, i.e. to one's failure to attach its latticework to inertial-guidance gyroscopes). This proper reference frame is precisely the kind of reference frame used in elementary physics and engineering. In the special situation where the laboratory moves freely (e.g. when it resides in an earth-orbiting satellite) and its walls are nonrotating, the proper reference frame is a local inertial frame.

Gravitational waves can be discussed using such a proper reference frame. To do so, one must extend its latticework (which previously was assumed to be arbitrarily small) out far enough to cover the entire region in which one measures the waves; and as one extends the axes, one must keep them rigid so they do not respond to the waves. Figure 1.2b depicts such a proper reference frame (dashed lines) with its latticework extended out to cover a large region of space. As an aid in discussing gravitational waves, we shall define the acceleration $\mathbf{a}$ of a particle in terms of this extended frame's t, x, y, z coordinates: $\mathbf{a} \equiv \ddot{x}\,\mathbf{e}_x + \ddot{y}\,\mathbf{e}_y + \ddot{z}\,\mathbf{e}_z$ where each dot denotes a time derivative and $\mathbf{e}_j$ denotes the unit vector along the j direction. It then turns out, according to general relativity, that a gravitational wave produces on any particle an acceleration that is proportional to the particle's distance from the origin of coordinates. (This gravitational-wave acceleration is in addition to the normal, Newtonian-type gravitational acceleration, which Einstein attributes to the laboratory's failure to fall freely.) More specifically, if the gravitational wave is propagating in the z direction with waveforms $h_+(t-z/c)$ and $h_\times(t-z/c)$ (where c is the speed of light), and the particle is moving at a speed much less than light, then the particle's acceleration is predicted by general relativity to be

$$\mathbf{a}=\tfrac{1}{2}\ddot{h}_{+}(x\,\mathbf{e}_x-y\,\mathbf{e}_y)+\tfrac{1}{2}\ddot{h}_{\times}(y\,\mathbf{e}_x+x\,\mathbf{e}_y) \qquad (1.1)$$

(cf. Sec. 4.C). Notice that this acceleration is transverse: **a** lies in the $x-y$ plane and thus is perpendicular to the propagation direction, $\mathbf{e}_z$.

Figures 1.3c,d depict this acceleration in terms of "lines of force". At each point in space and a specific moment of time the acceleration **a** is along the direction of the line of force there, and the magnitude of the acceleration is proportional to the density of force lines. The density of force lines, in turn (as is shown in the figure's insets), is proportional to the distance from the origin in the $x-y$ plane, i.e. to the distance from the z-axis. Note the differences between these gravitational-wave lines of force and the corresponding lines of force associated with an electromagnetic wave (Fig. 1.3a,b). In both cases the lines lie entirely in planes that are transverse to the propagation (z) direction. However, the electromagnetic lines point in the same, fixed direction throughout the transverse plane (not shown in detail in Fig. 1.3), while the gravitational lines have curved shapes that are called "quadrupolar".

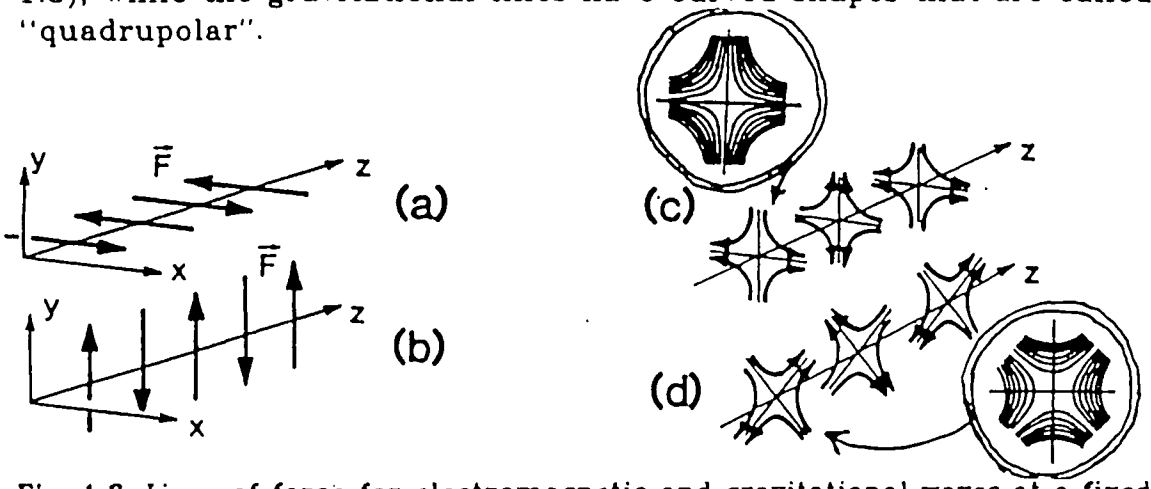

Fig. 1.3 Lines of force for electromagnetic and gravitational waves at a fixed moment of time, as measured in a proper reference frame. Left half: The electric forces produced on charged particles with speeds much less than light by an electromagnetic wave propagating in the z direction: (a) for a wave with x-polarization, and (b) for a wave with y-polarization. Right half: The forces produced on particles with mass and with speeds much less than light by a general relativistic gravitational wave propagating in the z direction: (c) for a wave with + polarization (i.e. with $h_{+}\neq 0$ and $h_{\times}=0$), and (d) for × polarization. The encircled insets in diagrams (c) and (d) show in greater detail the gravitational-wave lines of force in a specific, but arbitrary transverse plane.

This difference of field-line shape is the imprint, on the waves, of the spin S of the quantum mechanical particles which underlie the

waves (the waves' photons in the electromagnetic case; the waves' gravitons in the gravitational case). Rotate the lines of force of any kind of classical wave about the wave's propagation direction. The minimum angle of rotation that brings the force lines back to their original orientation is called the wave's "return angle" θ_{ret}. This return angle is related to the spin S of the underlying particles by

$$\theta_{ret} = \frac{360\,\text{degrees}}{S} \tag{1.2}$$

(except in the case of spin $S=0$ where the force lines are circularly symmetric so every rotation leaves them unchanged). For the electromagnetic waves of Figs. 1.3a,b, θ_{ret} is 360 degrees, so the photon must have spin S equal to one; for the gravitational waves of Figs. 1.3c,d, θ_{ret} is 180 degrees, so the graviton (according to general relativity) must have spin two. In other theories of gravity the force lines have other shapes and other return angles, and thus the graviton has other spins (Sec. 4.C; Eardley, Lee, and Lightman, 1973; Eardley et. al., 1973).

Correspondingly, for fundamental physics the key goal of gravitational polarization measurements will be to determine the waves' return angle and from it infer the graviton's spin.

Return to the quantitative formula (1.1) for the accelerations produced by a gravitational wave, as measured in a proper reference frame. If the proper reference frame is locally inertial (i.e. if its spatial origin moves freely and its axes are attached to inertial-guidance gyroscopes, so in it there are no Newtonian-type gravitational or coriolis forces), and if a test particle initially at rest at location (x,y,z) is free of electromagnetic or other nongravitational forces, then the particle's only acceleration will be that due to the wave. Thus, it will accelerate relative to the frame by the amount

$$\ddot{\mathbf{x}} = [\text{the } \mathbf{a} \text{ of Eq. (1.1)}] = \tfrac{1}{2}\ddot{h}_+(x\,\mathbf{e}_x - y\,\mathbf{e}_y) + \tfrac{1}{2}\ddot{h}_\times(y\,\mathbf{e}_x + x\,\mathbf{e}_y)\,. \tag{1.3}$$

Because the acceleration is so extremely weak, the particle's location will change in response to the waves by only a very slight amount, $\delta\mathbf{x} \equiv \delta x\,\mathbf{e}_x + \delta y\,\mathbf{e}_y + \delta z\,\mathbf{e}_z$. This means that to high accuracy the particle's coordinates (x,y,z) on the right hand side of Eq. (1.3) can be regarded as constants, the acceleration $\ddot{\mathbf{x}}$ on the left hand side can be regarded as due entirely to the displacement, $\ddot{\mathbf{x}} = \delta\ddot{\mathbf{x}}$, and Eq. (1.3) can be reexpressed as

$$\delta\ddot{x}\,\mathbf{e}_x + \delta\ddot{y}\,\mathbf{e}_y + \delta\ddot{z}\,\mathbf{e}_z = \tfrac{1}{2}\ddot{h}_+(x\,\mathbf{e}_x - y\,\mathbf{e}_y) + \tfrac{1}{2}\ddot{h}_\times(y\,\mathbf{e}_x + x\,\mathbf{e}_y)\,. \tag{1.3'}$$

From this equation one can infer that the gravitational wave produces the following particle displacements: If the wave has + polarization so $h_+ \neq 0$ but $h_\times = 0$, then

$$\delta x = \tfrac{1}{2} h_+ x \ , \quad \delta y = -\tfrac{1}{2} h_+ y \ , \quad \delta z = 0 \ . \tag{1.4a}$$

If the polarization is × so $h_+ = 0$ and $h_\times \neq 0$, then

$$\delta x = \tfrac{1}{2} h_\times y \ , \quad \delta y = \tfrac{1}{2} h_\times x \ , \quad \delta z = 0 \ . \tag{1.4b}$$

Notice that for both polarizations the displacement δz along the propagation direction vanishes, in accord with the transverse nature of the waves. Since the displacements (1.4) are proportional to the distance of the particle from the origin of the local inertial frame, with proportionality factor h_+ or $h_\times$, one can regard h_+ and $h_\times$ as dimensionless "strains of space". Correspondingly, the functions $h_+(t-z/c)$ and $h_\times(t-z/c)$ are sometimes called the *gravitational-wave strains*. They are also called *gravitational waveforms* and *gravitational-wave fields*.

The curvature of spacetime prevents one from holding rigid the axes of a proper reference frame if those axes are extended out to too great a length. Correspondingly, the force-field description of gravitational waves [Fig. 1.3 and Eqs. (1.1), (1.4)] becomes inaccurate if the particles are too far from the spatial origin of the frame. "Too far" turns out to mean at distances from the z-axis (transverse distances) of order or greater than the waves' reduced wavelength $\lambda\!\!\!^{-}$=(wavelength)/2π. All earth-based gravitational-wave detectors that are under development or in use (Sec. 2.C) have sizes small compared to the reduced wavelengths of the waves they seek, and thus can be analyzed using force diagrams and the acceleration equations (1.1). Not so for most solar-system-based or astronomical detectors (Secs. 2.D and 2.E); so they require a more sophisticated analysis (Sec. 4.F).

Although the force diagrams and acceleration equations break down over transverse distances $\gtrsim \lambda\!\!\!^{-}$, the gravitational-wave fields h_+ and $h_\times$ retain their identity over such distances — and, indeed, over arbitrarily large distances; see Chap. 4.

General relativity's demand that gravitational waves propagate from their source to the earth at precisely the same speed as light corresponds mathematically to the following statement: As the waves pass through any proper reference frame anywhere along their route, the functional forms of h_+ and $h_\times$ must be $h_+(t-z/c)$ and $h_\times(t-z/c)$ with c precisely the speed of light. (Here we presume for simplicity

that the frame's z-axis is oriented along the waves' propagation direction.)

1.D Sources of Gravitational Waves

As a theoretical physicist who has thought a lot about sources of gravitational radiation, I am often asked, by colleagues who build detectors, what kinds of waves they should look for. "What will be the strongest sources of gravitational waves in the universe?" they want to know; and "What will be the characteristics of these sources' waves: the amplitudes $\mathcal{A}$ of oscillation of the wave fields h_+ and $h_\times$ and the typical timescales τ on which they oscillate?" My answer is always the same: "Be prepared for surprises. Don't take too seriously what I or other theorists say. The strongest source is likely to be something we never thought of."

While this is good advice, it is not enough. Some guidance is needed. The effort to detect gravitational waves should not, and need not, be a completely blind search. General considerations tell us roughly (very roughly!) how strong the waves will be and on what timescales they will oscillate, and we know enough about the universe to identify a number of specific, promising sources. I shall focus in this section on the general considerations, and in Secs. 2.F–2.H on specific sources.

The amplitudes $\mathcal{A}$ of the strongest waves bathing the earth.

Some slightly sophisticated, general considerations that I shall sketch tell us roughly the amplitude $\mathcal{A}$ of the oscillations of h_+ and $h_\times$ to be expected from an astrophysical source. The source might be, for example, a pulsating star, or two stars orbiting each other, or two black holes colliding. It is the internal dynamical motion of the source that produces the gravitational waves – but it is not the entire motion; only that part which changes the source's shape. For example, when a spherical star pulsates spherically, with all points on its surface moving in and out radially in unison, no radiation is emitted. However, radiation *is* produced when the star pulsates nonspherically, with its poles moving in while its equator moves out, then its equator in and its poles out. (The reason will become clear below.) A quantitative measure of the strength of shape-changing motions is their kinetic energy; let us call it the "nonspherical kinetic energy" and denote it by $E_{\rm kin}^{\rm ns}$. This could be, for example, the energy of nonspherical pulsation, or the energy of orbital motion in a binary star system, or the energy of

collision of two black holes. It turns out that the shape-changing, dynamical motions cause the gravitational-wave fields h_+ and $h_\times$ to oscillate with amplitudes

$$\not{h} \sim \frac{G}{c^4}\frac{E^{\rm ns}_{\rm kin}}{r} \sim 10^{-20}\left[\frac{E^{\rm ns}_{\rm kin}}{M_\odot c^2}\right]\left[\frac{30\,\text{million light years}}{r}\right], \qquad (1.5)$$

where r is the distance to the source. Here the nonspherical kinetic energy is expressed in terms of the mass of the sun $M_\odot$, converted to energy units by multiplying with the square of the speed of light c^2. The distance to the source is expressed in units of 30 million light years (10 megaparsecs), which is roughly the distance to the Virgo Cluster of galaxies (the nearest large cluster to our own Milky Way Galaxy) and the distance to which one must go in order to encompass roughly 1000 galaxies. Equation (1.5) is a correct order-of-magnitude estimate not only for general relativity, but also for most other relativistic theories of gravity. [This generality of Eq. (1.5) can be inferred, e.g., from the analysis in Sec. 10.3 of Will, 1981.]

The strongest astrophysical sources are likely to have masses of order that of the sun, or a few factors of ten larger. (Sources more massive than this will be very rare.) The strongest sources will have the largest possible kinetic energies [cf. Eq. (1.5)] and thus are likely to have internal velocities v roughly equal to the speed of light or a few factors of ten smaller, and $E^{\rm ns}_{\rm kin} = \frac{1}{2}Mv^2$ roughly equal to $M_\odot c^2$. Strong ~~strong~~ sources are rare enough that they are likely to lie at roughly the distance of the Virgo cluster, give or take a few factors of ten. These estimates, when inserted into Eq. (1.5), imply that the strongest gravitational waves that bathe the earth are likely to have amplitudes $\not{h} \sim 10^{-20}$, give or take a few factors of ten. For comparison, the best 1989 gravitational-wave detectors (discussed below) are able to detect waves as strong as about 10^{-17}, an improvement from about 10^{-15} ten years ago; and the designers and builders of detectors think they know how to construct instruments that can detect $\not{h} \sim 10^{-22}$.

I shall now sketch the general considerations that lead to the estimate (1.5). These considerations, which involve *energy conservation, multipole moments, and dimensionality*, are somewhat more technical than the rest of Part I of this book, so I print them in smaller type. Readers not interested in wading through these technical details are encouraged to skip over the small-typed paragraphs.

Begin with energy conservation: Just as the energy flux (energy crossing a unit area per unit time) for an electromagnetic wave is proportional to the

square of the wave's force-producing electric field E, so also the energy flux for a gravitational wave is proportional to the square of the force-producing wave field h (i.e. h_+ or $h_\times$). As the wave propagates outward from its source to larger and larger distances r, it passes through spheres around the source of successively larger surface area $A = 4\pi r^2$. Energy conservation demands that the energy flux (proportional to E^2 or h^2) times the surface area (proportional to r^2) be independent of distance r traveled, and thus that E and h both die out as $1/r$.

Next, multipole moments: The multipole moments of a source are the quantities that produce the radiation; and they produce it by oscillating dynamically. Multipole moments describe, in a spatially-averaged sort of way, the shape and size of the source. The theory of gravitational multipole moments (Sec. 6.C) is similar to that of electromagnetic multipole moments (e.g. Jackson, XXXX), except for complications due to the "nonlinearity" of the gravitational field (Thorne, 1980b) which will not be important here. There are two families of gravitational multipole moments: *mass moments* (the analog of electric moments) and *current moments* (the analog of magnetic moments). These characterize, respectively, the source's distributions of mass and of mass current (the analog of electric current). There is a hierarchy of moments of each type, labeled by an integer l: the mass moments M_l and the current moments C_l (denoted I_L and J_L in Chap. 6). The moments of lowest order (smallest l, but $l > 0$) describe large-scale deformations of the source from sphericity; those of higher order (larger l) describe finer-scale deformations. The magnitudes of the moments of order l are

$$M_l \sim ML^l , \quad C_l \sim Mv L^l , \tag{1.6}$$

where M is the source's total mass, v is its average internal velocity, L is the average lengthscale of its deviations from spherical symmetry, and L^l is that lengthscale raised to the l power; cf. Eq. (6.31). These magnitudes are identical to those for the electric and magnetic moments of a charged source, except for the replacement of the source's total charge Q by its total mass M.

The mass moment of lowest order is the $l=0$ "mass monopole", M_0. It is precisely equal to the source's total mass M, and because that mass is conserved, M_0 cannot oscillate and thus cannot produce radiation. Instead it produces the steady, unchanging GM/r^2 gravitational acceleration that, for example, attracts planets to the source and keeps them in orbit around it. For a precisely spherical source this M_0 is the only nonzero moment; and thus all the other moments describe deviations from sphericity.

Just as classical electromagnetic sources have no magnetic monopole moment, so also gravitational sources (according to general relativity) have no

current monopole moment; C_0 vanishes. The next two multipole moments have $l=1$. They are the "mass dipole" M_1 and "current dipole" C_1. The current dipole is equal to the source's total angular momentum; and since angular momentum, like mass, is conserved, C_1 cannot oscillate and cannot produce radiation. Instead it produces a steady, unchanging gravitational analog of the Earth's dipole magnetic field (the *gravitomagnetic field*), which is thought to play a key role in the powering of quasars and the alignment of the jets that they emit; see, e.g., Chap. 4 of Thorne, Price, and Macdonald (1986). The mass dipole moment M_1 is also constrained: Its first time derivative is the source's total linear momentum, which is conserved and thus cannot oscillate or radiate.

Moving on upward in the hierarchy of moments, the next two are the $l=2$ "mass quadrupole" M_2 and "current quadrupole" C_2. These are not constrained by any laws of conservation, so they can and typically do oscillate and radiate — as also do the $l=3$ "octupole moments" M_3 and C_3 and all moments of still higher order. To summarize, all moments of order $l\geq 2$ can oscillate and thereby produce gravitational waves; but moments with $l<2$ cannot oscillate and thus cannot radiate. These conclusions, in fact, are a special case of a very general and fundamental aspect of the underlying quantum mechanical particles: Bosons of spin S can carry waves with multipoles $l\geq S$, but not waves with $l<S$. For gravitons S is 2 (according to general relativity plus quantum theory, which we shall assume correct unless otherwise stated), and thus gravitational waves must have $l\geq 2$. For photons S is 1 and thus electromagnetic waves must have $l\geq 1$.

Turn, finally, to dimensional considerations and their combination with energy conservation and multipole moments to obtain the estimate (1.5) of the gravitational-wave amplitude. It is the time variations, and hence time derivatives, of the multipole moments that produce the radiation. Since the wave fields h_+ and $h_\times$ are dimensionless, their amplitude of oscillation $\mathcal{H}$ must also be dimensionless, and so also must be the contributions to $\mathcal{H}$ of the moments of order l. Moreover, those contributions must be inversely proportional to the distance r of the source from earth (because of energy conservation); they must be proportional to some number of time derivatives of the moments; and besides that they can involve only the two fundamental constants that enter into the laws of gravity: Newton's gravitation constant $G=6.673\times10^{-8}$ cm^3 g^{-1} sec^{-2} and the speed of light $c = 2.998\times10^{10}$ cm/sec. Aside from a dimensionless factor of order unity this determines uniquely the form of the wave fields h_+ and $h_\times$, and via the magnitudes (1.6) of the moments, the amplitude $\mathcal{H}$ of the fields' oscillations

$$(h_+ \text{ and } h_\times) \sim \frac{G}{c^{l+2}}\frac{1}{r}\frac{d^l M_l}{dt^l} + \frac{G}{c^{l+3}}\frac{1}{r}\frac{d^l C_l}{dt^l}\ ; \qquad (1.7a)$$

$$\mathcal{H} \sim \frac{GM}{c^2 r}\left[\frac{v}{c}\right]^{l} + \frac{GM}{c^2 r}\left[\frac{v}{c}\right]^{l+1} . \qquad (1.7b)$$

Here we have estimated the time derivative of the size L of the deviations from sphericity as being equal to the source's average internal velocity: $dL/dt \sim v$.

Since the internal velocity v cannot exceed the speed of light, that moment in expression (1.7b) with the fewest factors of v/c will produce the waves of largest amplitude $\mathcal{H}$; i.e. it will be the strongest source of radiation, or among the strongest. This dominant moment is the mass quadrupole M_2 (since M_0, M_1, and C_1 cannot radiate, and C_2–radiation entails one more factor of v/c than M_2). The contributions to h_+ and $h_\times$ and to $\mathcal{H}$ of this dominant, mass quadrupole moment are, by Eq. (1.7),

$$(h_+ \text{ and } h_\times) \sim \frac{G}{c^4}\frac{1}{r}\frac{d^2 M_2}{dt^2} , \quad \mathcal{H} \sim \frac{G}{c^4}\frac{Mv^2}{r} . \qquad (1.8)$$

The quantity Mv^2 is approximately the kinetic energy $E_{\rm kin}^{\rm NS}$ associated with internal, nonspherical motions of the source; and correspondingly we can rewrite the amplitude $\mathcal{H}$ of h in the form (1.5) discussed above.

The nature of the strongest sources

Equation (1.5) shows that the strongest gravitational waves bathing the earth are likely to come from those sources with the largest nonspherical, internal kinetic energies, i.e. those with the largest masses and largest internal velocities. Since the internal velocities are generated by internal gravity, large internal velocities means large internal gravity, which means compact size. Thus it is that the strongest sources are likely to be cosmic events that produce large-scale, nonspherical internal motions of the most compact, massive objects in the universe: black holes and neutron stars. Examples are the violent births of black holes and neutron stars in stellar implosions, the spiraling together and coalescence of binary neutron stars and binary black holes in distant galaxies, and the rotation of neutron stars (pulsars), with deformed (lumpy) internal mass distributions, in our own galaxy. I shall discuss these and other examples in some detail in the next chapter (Secs. 2.F–2.H) in the context of efforts to detect their waves.

Frequencies of the strongest waves

In the design of gravitational-wave detectors, one needs estimates not only of the amplitude $\mathcal{H}$ of the strongest waves bathing the earth, but also estimates of the timescales τ on which the wave fields h_+ and $h_\times$ vary. It is conventional to quote instead of a wave's timescale (or period) τ, its frequency $f = 1/\tau$. That frequency will be the same as the frequency of the source's internal motions. For neutron stars the frequencies of vibration, orbital motion, and rotation are less than or of order a few kilohertz (a few thousand cycles per second, corresponding to periods τ greater than or of order a few tenths of a millisecond). For black holes of mass M the timescales τ of vibration or coalescence are about the time required for light, near the hole's horizon (its outer edge), to travel around the hole once. Since the hole's horizon has a circumference $\mathcal{C} \simeq 4\pi GM/c^2 = 18.5\,\mathrm{km} \times (M/M_\odot)$, these timescales are $\tau \sim 4\pi GM/c^3 = 6\times 10^{-5}\,\mathrm{sec} \times (M/M_\odot)$, which corresponds to a frequency $f = 1/\tau$ of

$$f \sim \frac{10\,\mathrm{kHz}}{M/2M_\odot} . \tag{1.9}$$

(Here $2M_\odot$ is an estimate of the smallest possible mass for a black hole that can form by stellar implosion). Thus, the strongest waves bathing the earth, whether they come from neutron stars or from black holes, are likely to lie at frequencies of 10 kHz and below.

As one moves downward from 10 kHz toward lower frequencies f, one is likely to see waves of greater amplitude $\mathcal{H}$. This shows up quite explicitly when one examines black holes as sources. For a black hole the wave frequencies [Eq. (1.9)] are inversely proportional to the hole's mass, $f \propto 1/M$, while the wave amplitudes [Eq. (1.5)] are directly proportional to its nonspherical kinetic energy $E^{\rm NS}_{\rm kin} \sim Mv^2$, which in turn is proportional to M. Since $f \propto 1/M$ and $\mathcal{H} \propto M$, as one goes to lower and lower frequencies f one should see waves from black holes of larger and larger mass M and correspondingly should see larger and larger wave amplitudes: $\mathcal{H} \propto 1/f$.

Actually, as one goes to lower frequencies one may run out of sources: For example, there are likely to be millions of black holes with mass $M \sim 3M_\odot$ in each galaxy, but typically only one or less with $M \gtrsim 10^7 M_\odot$; see, e.g., Blandford (1987). Correspondingly, in order to see waves of lower frequency one may be forced to look out to greater distances τ and as a result, the amplitudes of the waves at earth may increase less rapidly than the estimate $\mathcal{H} \propto 1/f$.

These kind of considerations, applied not just to black holes but to other sources as well, have led me to the very rough guess that the strongest waves at frequency f will have amplitudes

$$\not{h} \propto 1/f^n \quad \text{with } 0.2 \lesssim n \lesssim 1 \,. \tag{1.10}$$

More specifically, I expect the strongest waves at $f \sim 1000\,\text{Hz}$ to have $\not{h} \sim 10^{-21}$ (see Fig. 2.7), and correspondingly I expect the strongest at a factor million lower frequency, $f \sim 0.001\,\text{Hz}$, to have $\not{h}$ between $\sim 10^{-21} \times (10^6)^{0.2} \simeq 10^{-20}$ and $\sim 10^{-21} \times (10^6)^1 = 10^{-15}$.

In Secs. 2.F–2.H I shall discuss, briefly, a wide variety of possible sources and their estimated strengths. That discussion will show clearly the general trend, embodied in Eq. (1.10), for wave amplitudes to be stronger at lower frequencies. See, particularly, Figs. 2.7, 2.8, and 2.9.

1.E The Information Carried by Gravitational Waves

Gravitational waves carry substantial information about their sources. The total information carried to earth is embodied in the celestial coordinates ("right ascension" α and "declination" δ) of the source on the sky, plus the two gravitational waveforms $h_+(t)$ and $h_\times(t)$ evaluated at the location of a detector. A key goal of gravitational-wave astronomers will be to build a worldwide network of detectors that can extract from an incoming wave all four quantities, α, δ, $h_+(t)$, and $h_\times(t)$. For details of such a network and the extraction of α, δ, $h_+(t)$, $h_\times(t)$ from the waves it detects, see Sec. 11.H.

Having extracted a source's celestial coordinates, astronomers will use them to help identify which (if any) source of electromagnetic waves (radio, millimeter, infrared, light, ultraviolet, X-ray, gamma-ray) produced the gravitational waves. This identification of the source will permit a broad-fronted, many-radiations assault on the problem of understanding the source's nature, and will also be a key to studying the nature of gravity (e.g. by comparison of the arrival times of gravitational and electromagnetic waves from the same source).

Having extracted the waveforms $h_+(t)$ and $h_\times(t)$, astronomers will try to deduce from them details about their source. Suppose, for example, that the waves at earth were measured to have a vanishing $h_\times(t)$, and to have $h_+(t)$ of the form shown in Fig. 1.4. From the vanishing of $h_\times$ one can infer that the source is probably axisymmetric; i.e., like the earth, it is circularly symmetric about some axis, presumably a rotation axis. From the details of $h_+(t)$ (Fig. 1.4), one can infer

the following:

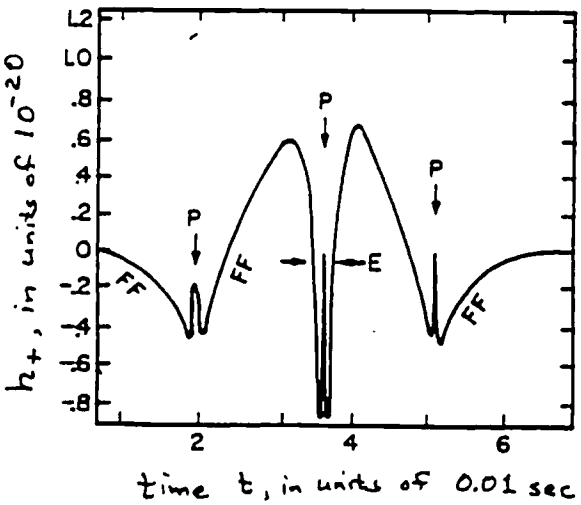

Fig. 1.4 The waveform $h_+(t)$ emitted by a specific scenario for the gravitational implosion of the core of a star, which triggers a supernova explosion. (Figure adapted from, and based on calculations by Saenz and Shapiro, 1978).

Because the shortest timescales present in the waveform are ~0.5 milliseconds, the source must either be a neutron star or a several-solar-mass black hole; no other known astrophysical object can have such short timescales of variation. Assuming, as usually will be the case, that the radiation is predominantly quadrupolar so $h_+ \sim (G/c^4)(1/r)d^2M_2/dt^2$ [Eq. (1.8)], one can infer from the waveform $h_+(t)$ the time evolution of the source's quadrupole moment M_2. In particular, one infers that during the time intervals marked *FF* in Fig. 1.4, when h_+ is varying as $h_+ \propto (t-\text{const})^{-2/3}$ or $(\text{const}-t)^{-2/3}$, the quadrupole moment varies as $M_2 \propto (t-\text{const})^{4/3}$ or $(\text{const}-t)^{4/3}$. This is precisely the quadrupole-moment evolution that Newtonian or Einsteinian theory predicts for the nonspherical, free-fall motion of a lump of mass. Moreover, the sharply reversed peaks marked *P* in Fig. 1.4 are just what one expects from a sharp acceleration in the direction opposite to the free fall. The natural and correct interpretation is that these waves are from the implosion of a stellar core; and that the implosion formed a neutron star which bounced, expanded, then reimploded three times. The fact that the three sharp peaks are all in the same direction in Fig. 1.4 (up, not down) indicates that the sharp

bounces were all along the same direction in the star: either along the star's polar axis, or on its equatorial plane. Surely the other direction should have bounced as well, or at least have stopped its implosion; so there should be at least one sharp peak in the down direction. Indeed there is; it is superposed on the central up peak (region labeled E). The natural interpretation is that the imploding star was centrifugally flattened by rotation; its pole imploded fast and bounced three times (up peaks P) while its equator imploded more slowly and bounced once (down peak E).

In fact, the wave form shown in Fig. 1.4 was not just made up for purposes of this discussion. Rather, it is the result of a numerical simulation by Saenz and Shapiro (1978) of the implosion of a stellar core; and the core's motions were precisely those deduced by the above argument.

Unfortunately those motions are not a firm prediction for realistic stellar implosion; they are but one of many scenarios that have resulted from computer simulations (Sec. 7.B and references therein). The true scenario will depend on issues (e.g. shock waves, emission and absorption of neutrinos, and nuclear reactions) that are not well understood and probably will not be well understood until gravitational radiation gives us direct, observational information. Correspondingly, theorists in the early years of gravitational-wave astronomy are likely to be relegated to the task of interpreting the observed waveforms, as above, rather than predicting them with confidence (an important exception being waves from the coalescence of two black holes; see the end of Sec. 1.B). From those interpretations we should learn much about the uncertain physics that governs gravitational-wave sources.

1.F Gravitational Waves as a Tool for Cosmology

All the gravitational-wave sources discussed above are discrete objects in the universe today. Theory insists that gravitational waves were also produced in the "big bang" that began the universe. Those primordial gravitational waves are a gravitational analog of the primordial microwave radiation which astronomers study with radio telescopes, and of primordial neutrinos which are thought also to have emerged from the big bang but have not yet been detected.

The early universe was filled with hot, dense matter as well as radiation. As the universe expanded, its density and temperature decreased and, correspondingly, the matter became more and more transparent to the passage of radiation.

For electromagnetic waves (photons), theory tells us that complete transparency was reached when the universe was several hundred thousand years old and its temperature had fallen to several thousand degrees. Earlier than this all photons were trapped by hot, ionized electrons; they were continually scattered and absorbed, destroyed and reemitted, and thereby kept in thermal equilibrium with the matter. At the few-hundred-thousand-year mark, the free electrons were captured by protons to form neutral hydrogen thereby liberating the photons to begin unimpeded travel through the universe. Astronomers today see those photons as the "primordial microwave radiation", and from that radiation they extract detailed information about conditions at the epoch of photon liberation, the few-hundred-thousand-year epoch. For further detail see, e.g., Barrow and Silk (1983), or at a more technical level, Zel'dovich and Novikov (1983).

For neutrinos, transparency was reached far earlier than for photons: theory predicts the universe to have become transparent to neutrinos when its expansion was only a few seconds old and its temperature was a few thousand million degrees (a few times 10^9K). Earlier than this time, when the temperature was higher, the neutrinos were trapped and were kept in thermal equilibrium by interaction with electron-positron pairs. At the few-second epoch the positrons were annihilated by electrons, thereby liberating the neutrinos to travel freely through the universe. Correspondingly, if and when astronomers detect primordial neutrinos, those neutrinos will give detailed information about their epoch of liberation, just a few seconds after the big bang (see, e.g., Barrow and Silk, 1983, or Zel'dovich and Novikov, 1983).

Gravitons are so penetrating, according to theory, that the universe has always been transparent to them (Sec. 7.2 of Zel'dovich and Novikov, 1983; Sec. 9.D below). Correspondingly, primordial gravitational waves (by contrast with photons and neutrinos) were probably never in thermal equilibrium with matter; and they have the potential to bring us direct information about the very earliest epochs of the universe – perhaps even about the *Planck* era, i.e. the era at the beginning of the big bang when space and time were coming into being and the initial conditions of the universe were being set. (This era, according to our best current understanding, comprised the first $\sim (G\hbar/c^5)^{1/2}$ $\sim 10^{-43}$ seconds of the universe's expansion.)

The details of the gravitational waves from the earliest epochs depend on physics that is very poorly understood: on the state of the gravitational-wave field as it emerged from the Planck era; on the

interaction of that field with the subsequent expansion of the universe during a possible "inflationary era" (an interaction that should have amplified the initial field; Sec. 9.D); on "phase transitions" in the early universe (Sec. 9.E); and on the formation of "cosmic strings" and their decay (Sec. 9.F). Some of these phenomena are so poorly understood that almost any strength of primordial gravitational radiation is allowed by present theory. However, currently fashionable scenarios predict fairly weak waves. If the primordial waves could be detected and studied, they would place stringent constraints on theories of the beginning of the universe. Interesting constraints on theory will also result if primordial waves are *not* found by the detectors planned for the turn of the century.

Gravitational waves also have the potential to become powerful tools for studying the large-scale structure of the universe today. Their role would be as precise indicators of the distances from earth to far-off galaxies.

Measurements of such distances are essential to cosmological understanding. Without distance measurements we cannot learn the actual size of the universe, the rate at which it is expanding, the rate that the expansion is slowing down, whether the expansion will continue forever, or whether it one day will halt and reverse into contraction and a "big-crunch" death.

Accurate distance measurements are possible in the solar system and for nearby stars, but when one looks into far-off parts of our Galaxy and beyond, the best distance measurements become less and less accurate. Their poorness is a source of enormous frustration for astronomers and cosmologists.

Remarkably, gravitational radiation shows promise of providing distance measurements more accurate than any so far (Schutz, 1986b). The key to such measurements is the inspiral of black-hole binaries (two black holes orbiting each other), and also of neutron-star binaries. During that inspiral (which precedes the final coalescence of the holes or stars) the holes or stars are gradually driven closer and closer together by reaction to emission of gravitational waves; and, as they near each other, their orbital period gradually shortens (cf. Fig. 1.1), i.e. their orbital frequency (equal to 1/period) gradually increases. The waveforms $h_+(t)$ and $h_\times(t)$ that the binary emits during this inspiral are precisely predicted by general relativity: They should have a sinusoidal form with a frequency f that is twice the orbital frequency and that increases with time, due to the inspiral, as

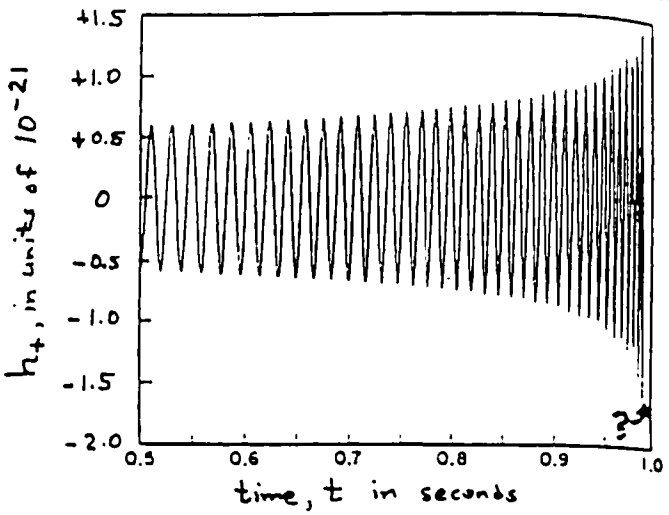

Fig. 1.5 The waveform $h_+(t)$ from a binary made of two $10M_\odot$ black holes 300 million light years from earth (10 times farther than the Virgo cluster of galaxies). This waveform is described mathematically by Eqs. (7.18). The binary's orbital plane is perpendicular to the line of sight to earth (its inclination angle ι is zero); and the waveform $h_\times(t)$ is identical to $h_+(t)$ except for being shifted in phase by 1/4 of a period. The two holes coalesce at time $t=1$ second. The waveforms during the final ~0.01 seconds of inspiral, and during the coalescence (region marked "?" on figure) are not yet known, but will be calculated using supercomputers in the next few years. It is those "?" waveforms that will provide the foundation for proving that black holes exist and for a stringent test of general relativity (Sec. 1.B). This figure is adapted from Smith (1987).

$f \propto (t_{\text{coalesce}}-t)^{-3/8}$. Their amplitudes should also increase with time, but at a different rate, $(t_{\text{coalesce}}-t)^{-1/4}$; see Fig. 1.5 and Eqs. (7.18). From those waveforms one can read off (i) the inclination of the orbit to the line of sight from earth (i.e. whether we are seeing the orbit edge on or face on or at some specific angle ι in between), (ii) the combination $(M_1M_2)^3/(M_1+M_2)$ of the masses M_1 and M_2 of the two holes or stars, and most importantly (iii) the distance r to the binary system. See Sec. 7.D for a detailed discussion of how this readout is done.

As we shall see in Chap. 2, gravitational-wave detectors now being planned have hope of detecting such binary systems, in their last few minutes of inspiral, throughout the universe (for black holes) or nearly so (for neutron stars). By contrast with distances obtained from electromagnetic observations, the gravitationally measured distances to these binaries would be free of ambiguity.

To make good cosmological use of these distances will require combining them with detailed information about the galaxies, or clusters of galaxies, in which the binaries live; most especially the galaxies'

speed of recession from earth (produced by the expansion of the universe), and their angular sizes on the sky. This galactic information can be obtained only from electromagnetic observations; it is not carried by the gravitational waves. The combination of electromagnetic and gravitational measurements will be possible only if astronomers can identify just which galaxy or cluster a gravitationally observed binary lives in. Fortunately, with a network of gravitational-wave detectors it should be possible to determine the location (α,δ) of the source to a precision of one degree on the sky, or better. This, together with a search for bursts of electromagnetic waves that accompany the binary's final coalescence, may often make possible the identification of the source's galaxy or cluster (Schutz, 1986b). For further details see Sec. 7.D.

2 Introduction to wave detection

2.A Is detection outrageously impossible?

The detection of gravitational waves with amplitudes $h \sim 10^{-20}$ is a rather daunting challenge. To see how daunting, note that it involves measuring fractional changes $\Delta L/L \sim h \sim 10^{-20}$ in the distance L between two objects. If the objects are in an earth laboratory of typical size $L \lesssim 10$ meters, as is the case for the "bar detectors" of Sec. 2.C below, then $\Delta L \lesssim 10^{-17}$ centimeters, one ten thousandth the diameter of the nucleus of an atom. If the objects are linked by the longest earth-based vacuum tube that seems reasonable, $L \sim 10$ kilometers, as is the case for the "interferometric detectors" discussed later in this section, then $\Delta L \sim 10^{-14}$ centimeters, one tenth the diameter of an atomic nucleus. If the objects are spacecraft in interplanetary space so $L \sim 10^9$ kilometers, as is the case for detectors discussed in Sec. 2.D below, then $\Delta L \sim 10^{-6}$ centimeters (0.01 micron; 0.02 of one wavelength of light).

As daunting as the measurement of such ΔL's may seem at first sight, it is not impossible. The best gravitational-wave detectors today are within a factor 1000 of this accuracy, and prospects are good for achieving $\Delta L/L \ll 10^{-20}$ by the end of the 1990s.

One can see that such measurements are not outrageously impossible by examining a specific example of a gravitational-wave detector: the *laser interferometer gravitational-wave detector* (also called an *interferometric detector*, or a *beam detector* to distinguish it from *bar detectors* discussed below). This type of detector was invented

independently by Michael Gertsenshtein and V. I. Pustovoit, Joseph Weber, and Rainer Weiss (see Sec. 3.B for discussion of the history) and is currently under development at laboratories in MIT, Caltech, Glasgow, Munich, Paris, Pisa, Tokyo, Moscow, Canberra, and Perth (see Sec. 2.C and Chap. 11 for current efforts, future plans, and references).

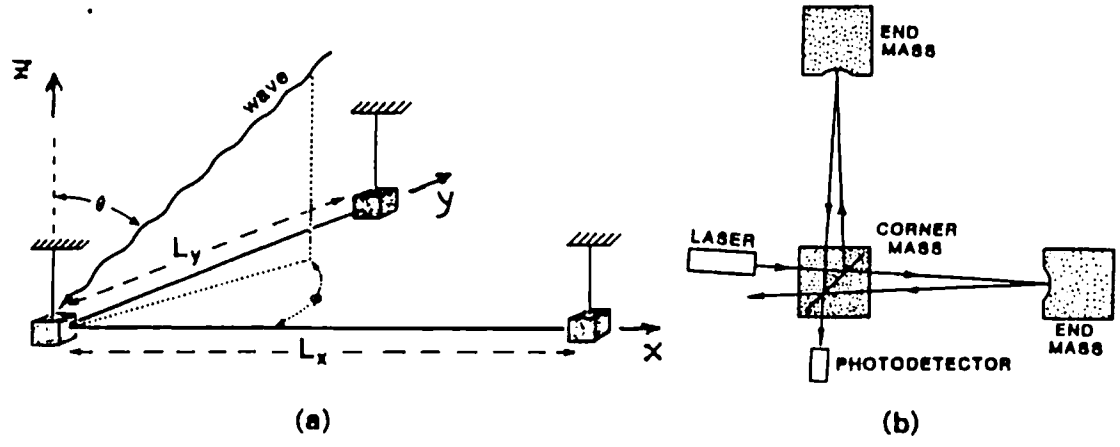

Fig. 2.1 Schematic diagram of a laser interferometer gravitational wave detector (also called an "interferometric" or "beam detector"). (a) Perspective drawing. (b) View from above.

The basic idea of this detector is as follows (see Fig. 2.1): Three masses, on which the gravitational waves will act, hang by wires from overhead supports at the corner and ends of an "L". The masses might, for example, be cubes of quartz or sapphire weighing 10 kilograms each, and the lengths of the L's arms (the distances between the masses) might be L = 1 kilometer. To discuss the effects of the waves, we introduce a proper reference frame with its spatial origin at the location of the corner mass, and with its x-axis along one arm of the L, its y-axis along the other, and its z-axis vertical. Denote by L_x and L_y the separations of the end masses from the corner masses, as measured using the rigid latticework of the proper reference frame. (Before the wave arrives, $L_x \cong L_y \cong L \equiv 1$ kilometer.)

Suppose, for simplicity, that a gravitational wave with + polarization propagates vertically through the laboratory (angle θ=0 in Fig. 2.1a), and that its waveform $h_+(t-z/c)$ oscillates a few times with a frequency $f \sim$500 Hertz. Because f is very high compared to the one

Hertz natural swinging frequency of the masses on their wires, the masses respond to the wave with 500-Hertz oscillatory motions that are unaffected by the natural swing. Those responses, as given by Eq. (1.3a), entail no motion of the corner mass (relative to our proper reference frame), a displacement $\Delta L_x = \frac{1}{2} h_+ L$ of the end mass on the x-axis, and a displacement $\Delta L_y = -\frac{1}{2} h_+ L$ of the end mass on the y-axis. Thus, when $h_+ > 0$ the gravitational wave lengthens the x-arm while shortening the y-arm; and then, on the next half cycle of oscillation ($h_+ < 0$), it shortens the x-arm while lengthening the y-arm. The wave-induced change in the fractional arm length difference (i.e. the wave-induced strain in the detector) is

$$\frac{\Delta L}{L} \equiv \frac{L_x - L_y}{L} = h_+(t) . \tag{2.1}$$

This wave-induced strain is monitored by techniques of laser interferometry.

"Isn't it outrageous," one is tempted to ask, "to think of monitoring with light the arm-length change $\Delta L \equiv L_x - L_y$ to a precision of $h_+ L \sim 10^{-20} \times 1$ kilometer $= 10^{-15}$ centimeters? After all, that is $\sim 10^{11}$ times smaller than the wavelength of the light!" The following considerations show that it is not at all outrageous:

As is depicted in Fig. 2.1b, light from the laser shines on a half-silvered mirror that rides on the corner mass. This mirror splits the laser beam in two, sending half the light down the x-axis toward one end mass and the other half down the y-axis toward the other end mass. These two beams bounce off mirrors attached to the two end masses, and return to the corner mass where they recombine with each other on the half-silvered mirror. A portion of the recombined light then goes back toward the laser, and the rest goes into a photodetector which measures its intensity.

In practice, the laser beams are made to bounce back and forth in the arms not just once as shown in Fig. 2.1b, but a large number B of round-trip times; see Fig. 2.2. With each round trip the two beams build up an increased phase difference. When the beams recombine in the beam splitter, their phase difference has reached

$$\Delta\Phi = \frac{2B(\Delta L_x - \Delta L_y)}{\lambda_0} = h_+ \frac{2BL}{\lambda_0} . \tag{2.2a}$$

This gravitational-wave-induced phase difference causes the recombining beams from the two arms to interfere with each other; and that

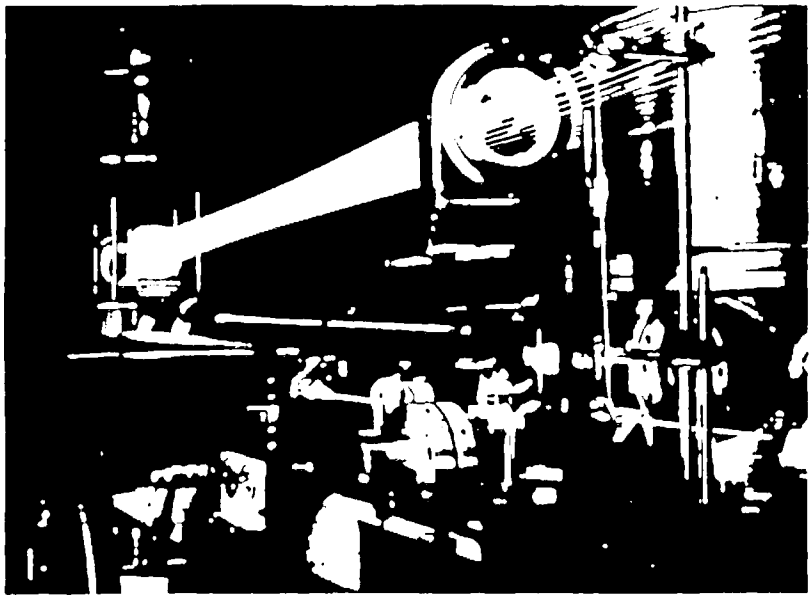

Fig. 2.2 Photograph of an early test rig for one arm of an interferometric detector in Garching, Germany (Billing et. al., XXXX). The laser beam bounces back and forth between the end mass and corner mass making, in this case, $B = XX$ round trips before recombining with the other arm's beam at a half-silvered mirror (not shown here). [Photograph courtesy XXXX]

interference produces a change

$$\frac{\Delta I}{I_o} \simeq \Delta\Phi = h_+ \frac{2BL}{\lambda\!\!\!^{-}} \qquad (2.2b)$$

in the intensity of the light going into the photodetector. Here $\lambda\!\!\!^{-}$ is the reduced wavelength (wavelength divided by 2π) of the light, approximately 0.1 microns (10^{-5} centimeters). Such a detector is called an "interferometric" detector because it is the interference of the light from the two beams that makes it possible to detect the gravitational-wave-induced phase difference.

The ultimate impediment to measuring the fluctuation $\Delta I/I_o \simeq \Delta\Phi$ in the light entering the photodetector is the discreteness of photons and the randomness of their arrival at the photodetector — phenomena embodied in the phrase *photon shot noise*. The photon shot noise limits the precision of monitoring to $\Delta I/I_o \sim 1/$(square root of number of photons available). The photodetector can collect the photons for a half period of the gravity wave, i.e. a time $1/2f \sim 1$ millisecond, during which time the x arm is shortened and the y arm lengthened. It must then start collecting all over again in the second half period, during which the x arm is lengthened and the y arm is shortened.

Correspondingly, the number of photons available during each measurement is N = (light energy available, $I_0/2f$)/(energy of one photon, $\hbar c/\lambda_0$). Putting these considerations together, we see that the gravitational wave can be detected if its amplitude exceeds

$$h_{\min} \simeq \frac{\lambda_0}{2BL}\frac{1}{\sqrt{N}} = \frac{\lambda_0}{2BL}\left[\frac{2\hbar cf}{I_0\lambda_0}\right]^{1/2}$$

$$\cong 6\times10^{-21}\frac{50}{B}\frac{1\text{km}}{L}\left[\frac{\lambda_0}{0.1\mu\text{m}}\right]^{1/2}\left[\frac{10\text{Watts}}{I_0}\right]^{1/2}\left[\frac{f}{1000\,\text{Hz}}\right]^{1/2}. \qquad (2.3)$$

These numbers show explicitly that the measurement is possible. The strategy is to increase the signal, by bouncing the light in the arms 50 times, to $\Delta I/I_0 \simeq \Delta\Phi \simeq 100\Delta L/\lambda_0 \sim 10^{-8}$, and then measure this tiny effect using $\sim 10^{16}$ photons.

"Okay, so the measurement is possible," one might say. "But does the measurement make any sense? After all, the random, thermally induced motions of the atoms in the faces of the mirrors are far far larger than the $\Delta L \sim 10^{-15}$ centimeter effect of the gravitational wave. Won't the effect of the wave be totally swamped by those motions?"

No, not at all. Because those atomic motions occur at very high frequencies, their influence on the laser light gets averaged away during the 1 millisecond collection of the 10^{16} photons. To see this quantitatively, one can regard a mirror's atomic motions as thermal sound waves propagating inside the 10 kilogram masses on which the mirror coatings are placed. Of all the thermal sound waves, the one of lowest frequency is the fundamental mode of "ringing" that the 10-kilogram mass would undergo if struck by a hammer. That fundamental mode, which has a frequency $f_0 \sim 10$ kilohertz, will be the most dangerous for the detector. All other thermal vibrations will be averaged away even more effectively than those of that mode. That mode's thermal vibrations will contain, on average, an energy of kT where k is Boltzmann's constant (1.38×10^{-16} g cm^2 sec^{-2} K^{-1}) and T is the mass's temperature (300 K). This vibration energy corresponds to an amplitude of vibration of the bar's ends given by

$$\Delta L = \frac{(kT/m)^{1/2}}{2\pi f_0} \sim 3\times10^{-14}\,\text{centimeters}. \qquad (2.4)$$

Note that this is only 1/3 the diameter of the nucleus of an atom! Although it is 30 times larger than the gravitational-wave signal, its effects will average away by much more than a factor 30 during the 1

millisecond time that the photodetector collects photons. Stated more precisely: the experimenters (who, we recall, are trying to study gravitational waves with frequencies of roughly 500 Hz) can and will filter their instrument's output to remove all frequencies above about 1 kilohertz; and the thermal vibrations (2.4) with their 10 kilohertz frequency will thereby be reduced in the data by much more than the needed factor of 30.

When one similarly goes through a very long list of other obstacles to the proposed measurement (an exercise first carried through for interferometric detectors by Weiss, 1972), one finds that they all have viable solutions. For a discussion of some of them see Sec. 11.B. Moreover, there are solutions to the obstacles not only in the case of interferometric detectors, but also for a variety of other detector designs described below.

2.B Frequency bands for detectors

There are likely to be astrophysically interesting gravitational waves at all frequencies from $f \sim 10\,\text{kHz}$ on down to $f \sim 1/(\text{the present age of the universe}) \sim 3\times10^{-18}$ Hz. Correspondingly, efforts are underway to detect waves throughout this vast domain.

Obviously, techniques that work well in one frequency region will not work so well in others. In this book, I shall distinguish three frequency bands in which three distinctly different types of detection techniques look optimal: the *high-frequency band* $10^4\,\text{Hz} \gtrsim f \gtrsim 10$ Hz, the domain of earth-based detectors; the *low-frequency band* $10\,\text{Hz} \gtrsim f \gtrsim 10^{-5}$ Hz, the domain of detectors flown in space within our solar system; and the *very-low-frequency band* $10^{-5}\,\text{Hz} \gtrsim f \gtrsim 3\times10^{-18}$ Hz, the domain of detectors that rely on distant astronomical bodies as part of the detection system.

The dividing lines between the bands are set by simple physical constraints on detector technology: At frequencies $f \gtrsim 10$ Hz it is possible to build good acoustical filters ("anti-seismic isolation systems") with which to isolate a detector from the vibrations of the laboratory floor. At these high frequencies one can also avoid the influence of fluctuating gravitational forces due to animals, people, automobiles, airplanes, etc., by building one's detectors at sites that are remote from civilization. By contrast, as one moves to frequencies below $f \sim 10$ Hz, antiseismic isolation will become extremely difficult, and fluctuating gravitational forces (not only due to animals, people, and their activities, but also due to fluctuations in the mass of atmosphere

above the detector) will become very serious. To circumvent this seismic and gravity noise, detectors below ~10 Hz will probably have to fly in space.

The optimal size L for a gravitational-wave detector depends on the reduced wavelength λ of the waves it seeks. If L is smaller than λ, then the displacement ΔL that a wave with amplitude h produces in the detector is $\Delta L \simeq hL$; thus, the larger the detector, the greater will be the displacement and the more sensitive will be the detector. However, when L is made larger than λ, the wave-induced displacement stops increasing; it remains of magnitude $\Delta L \sim \lambda L$ independently of how much larger L is made.† Thus, it is optimal wherever possible to make the detector's size comparable to a reduced wavelength, but nothing is gained by making it still larger.

At frequencies above $\sim 10^{-5}$ Hz (low-frequency band) the reduced wavelength is smaller than the distance from the Sun to Jupiter; and, correspondingly, solar-system-based detectors can be made roughly as large as a reduced wavelength. Below 10^{-5} Hz (very-low-frequency band) the reduced wavelength is so large that the optimal length L cannot be achieved within the solar system. Correspondingly, solar-system-based detectors start losing sensitivity as one pushes them down into this very-low-frequency band. In this band it is better to use detectors in which one of the masses is an astronomical body outside the solar system — e.g. a pulsar, with its precisely timed radio emissions.

In the next three sections I shall describe briefly the most promising detectors for each of the three frequency bands: high, low, and very low.

2.C Earth-based detectors: The high-frequency band

Two types of earth-based detectors are being developed for operation in the high-frequency band: *resonant-bar detectors* (also called, simply, *bar detectors*), and *laser-interferometer detectors* (also called *interferometric detectors* or *beam detectors*).

Bar detectors were invented by Joseph Weber (1960) and have since been developed into highly sophisticated instruments. Figure 2.3a is a

†Formally, mathematically, one can define a displacement ΔL that keeps increasing proportionally to L for $L \gtrsim \lambda$. However, such a definition is not relevant for gravitational-wave detection, since no real, physical apparatus can measure it. The displacement ΔL as measured by any detector ceases to increase when L exceeds λ.

photograph of the bar detector now operating at Stanford University (Michelson, Price, and Taber, 1987; Fairbank et. al., 1986; XXXX). As of summer 1989 this and a similar bar detector built by experimenters at the University of Rome but operating at CERN (Amaldi et. al., 1986; XXXX) are the most sensitive detectors in the world ($h \simeq 10^{-18}$).

The Stanford detector is built around a solid aluminum bar with length 3.1 meters, diameter 84.2 centimeters, and mass 4800 kilograms. The two ends of the bar play the roles of separated "particles" on which the waves act: Waves impinging on the bar should push the two ends in and out relative to the center. These gravitational pushes are like tapping the bar very lightly with two hammers, one on each end: they should make the bar ring like a bell. Stated more precisely, they should excite the fundamental mode of vibration of the bar, a mode in which the two ends move in and out while the center stays fixed.

In reality, because the bar is at a finite temperature (about 1.5 K), its fundamental mode will already be vibrating, thermally, with a far larger amplitude than the waves can induce. Consequently, the waves, instead of exciting it, will simply change slightly the amplitude and phase of its vibrations. The experimenters monitor the changes in amplitude and phase using a *transducer*: The bar's vibrating end pushes in and out on the rim of a drumhead-like, metal membrane, near which is mounted a superconducting coil of wire. (In Fig. 2.3a the membrane and coil are inside the "knob" at the center of the bar's end.) The membrane in turn vibrates in and out, and its vibrations modulate the inductance of the coil and thence modulate the current in the superconducting wire. The modulated current is monitored using a "superconducting quantum interference device" (SQUID).

The upshot of all this is that, when a gravitational wave alters the amplitude and phase of vibration of the bar's fundamental mode, those alterations change the output of the SQUID. The changed output is recorded on magnetic tape for future analysis by a computer.

This stanford detector (like all other detectors) responds to only one of the two polarizations of the gravitational wave. Which of the two it sees depends on its orientation in space. Suppose, for concreteness, that the orientation is chosen so the response is to the + polarization. Then, if it were possible to get a very tight electromechanical coupling between the transducer (superconducting coil) and the bar, the recorded output would contain enough detail to reconstruct that polarization's full waveform $h_+(t)$. Unfortunately, tight coupling to a

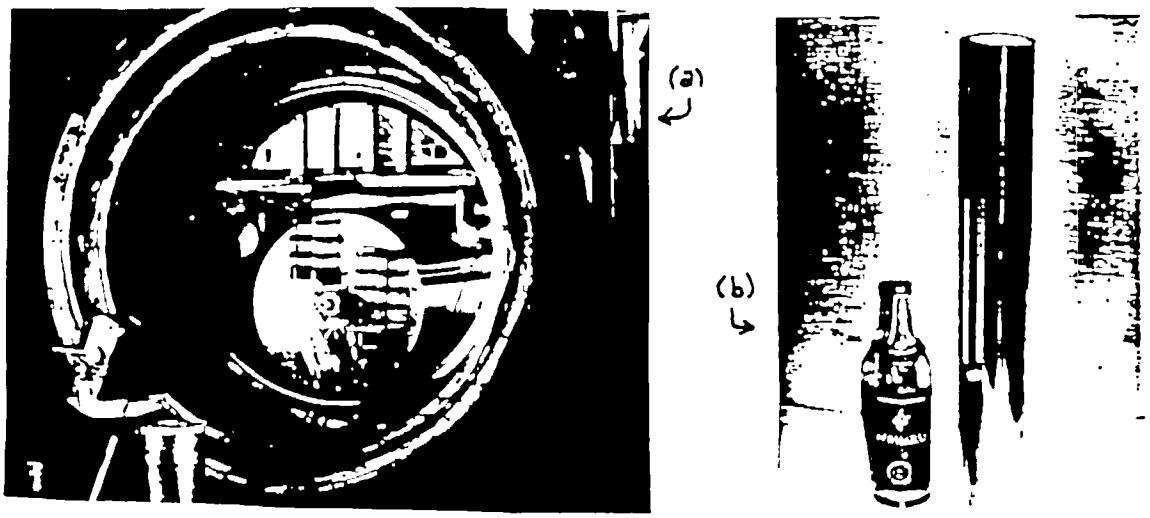

Fig. 2.3 Bar detectors for gravitational radiation. (a) The 4.8 tonne, aluminum bar detector at Stanford University, seen end-on inside its cryostat/vacuum chamber (Michelson, Price, and Taber, 1987; Fairbank et. al., 1986). The bar is the long cylinder with diameter about half that of the vacuum chamber. The "knob" at the center of the bar's end is the transducer that monitors the bar's vibrations; see text. The transducer's output is carried to the external world by electrical wires that are suspended on a set of mechanical filters (the two Chinese-bell-like assemblies in front of the bar's end) to prevent mechanical vibrations from traveling down them and exciting the bar. See text for further discussion. [Photograph courtesy XXXX] (b) A silicon-crystal bar, weighing about 10 kilograms, at Moscow University (Braginsky, 1983). This photograph, taken before the bar was instrumented with its transducer and suspended in its cryostat/vacuum chamber, shows the bar naked, alongside a Russian vodka bottle. This bar achieves high gravity-wave frequency (8000 Hz) by being small. As a byproduct, its smallness reduces its sensitivity (recall: $\Delta L \simeq hL$); but this is largely compensated by reduced internal frictional noise ("thermal noise"), which results from the bar's composition: it is made from a dielectric monocrystal (silicon) rather than a polycrystalline metal (aluminum alloy) like the huge Stanford bar. The long, thin, piece of the bar nearest the bottle is actually two "horns", one growing out of each end of the bar, with a several-micron-thick gap between them. This bar's transducer (not shown) is a microwave cavity which surrounds the horns in such a way that their gap provides the cavity's capacitance. As the bar vibrates, the gap oscillates, modulating the capacitance of the cavity and thereby modulating its response to microwaves that drive it. By monitoring that microwave response, the experimenters can monitor the bar's vibrations. [Photograph courtesy Vladimir B. Braginsky.]

bar detector is typically achieved only at a price of debilitating the overall sensitivity of the detector. The Stanford bar, having been designed for optimal sensitivity, incorporates somewhat weak coupling, which means that the transducer must average over ~ 100 periods of oscillation in order to read out the fundamental mode's amplitude and phase. As a result, each of the currently operating bar detectors is sensitive only to waves with frequencies within a narrow frequency

band, $\Delta f \lesssim 0.01 f_0$, centered on the bar's fundamental-mode frequency $f_0 \simeq 900$ Hz. There is hope in the future, however, of achieving bandwidths as large as $\Delta f \sim 0.2 f_0$, and then reconstructing the full waveform from the outputs of a "xylophone" of ~10 bars each tuned to a different frequency (Pizella, 1984; Richard, 1984, 1986 [KIP CHECK BOTH]; Michelson and Taber, 1984).

Most bar detectors, including Stanford's, are cooled to very low temperatures ($\lesssim 4$ K) so as to reduce the internal, thermal noise that can mask the effects of gravitational waves. They are also isolated so far as possible from the outside world by suspending them inside (cold) vacuum chambers and by supporting their suspension cables with acoustic filters ("antiseismic isolation"), see Fig. 2.3a.

Multitonne aluminum bar detectors with frequencies $f_0 \simeq 900$ Hz and bandwidths $\Delta f \sim 10$ Hz are presently operating or under construction at: Stanford University (Michelson, Price, and Taber, 1987; Fairbank et. al., 1986); Louisiana State University (Hamilton et. al., 1983, 1986); the University of Maryland (Carroll et. al., 1986); the University of Rome (in a collaboration with CERN; Amaldi et. al., 1986); and Zhongshan University in Guangzhou China (Hu En Ke, 1986). At Moscow State University, USSR, there are several ~10 kilogram bars with $f_0 \simeq 8000$ Hz, made of near-perfect monocrystals of sapphire and silicon (Fig. 2.3b; Braginsky, 1983). At the University of Western Australia (Perth) there is a 1.5 tonne niobium bar with $f_0 \simeq 700$ Hz (Veitch et. al., 1987). At Tokyo University in Japan there are specially shaped aluminum bars with $f_0 \simeq 60$ Hz designed for seeking periodic gravitational waves from the Crab pulsar (Owa et. al., 1986; Nagashima et. al., 1988). For further details and references see Sec. 10.C. [KIP: UPDATE THE REFERENCES]

Since 1986 the LSU, Rome, Stanford, and Perth detectors have been organized into a coordinated network called "Gravnet" (Blair, Frasca, and Pizzella, 1988a,b). They are brought into operation simultaneously and run for many months in a coordinated search for gravitational waves. Then they are shut down for a year or so of improvement before the next coordinated run. The negative results of the first such run (LSU, Rome, and Stanford; April–July 1986) are reported by Amaldi et. al. (1988). [KIP: UPDATE REFERENCES]

The sensitivity of a gravitational-wave detector can be described in a variety of ways (Secs. 2.F–2.H, 7.A, 8.A, and 9.A). One description is the *noise amplitude* h_n for detection of a gravitational wave which lasts for only one or two cycles of oscillation, i.e. a gravitational-wave

"burst". This h_n^{opt} is the amplitude $\not{h}$ that the waves' oscillations $h_+(t) = \not{h}\cos(2\pi f t)$ would need to have in order to be barely discernible above the noise (with "unity signal-to-noise ratio") — assuming, for concreteness, that the waves' direction of arrival and polarization are optimal for driving the detector. For a more precise definition see Eqs. (7.8) and (10.13) below. [KIP: FIX -- THOSE EQNS ARE NOT NOW FOR OPTIMAL ORIENTATION AND POLARIZATION]

As of summer 1989 the sensitivities of the Stanford and Rome bars are better than those of any other detector; they are $h_n^{opt} \simeq 10^{-18}$ for gravitational-wave bursts with frequencies f near the bars' fundamental-mode frequency $f_0 \simeq 900\,\text{Hz}$. This is a factor 30 improvement over the noise amplitudes of the mid 1970s. A further factor 10 improvement is likely within the next several years; and sensitivities in the neighborhood of $h_n^{opt} \sim 10^{-20}$ may well be achieved in the mid or late 1990s.

We shall discuss bar detectors in greater detail in Sec. 3.B and Chap. 10, and shall compare their sensitivities with the expected strengths of cosmic gravitational waves in Secs. 2.F–2.H.

Interferometric detectors were described conceptually in Sec. 2.A above and will be discussed in greater detail in Sec. 3.B and Chap. 11. Their sensitivities will be compared with expected wave strengths in Secs. 2.F–2.H.

Fig. 2.4 shows two photographs of the presently operating interferometric detector with 40-meter-long arms, at Caltech (Whitcomb et. al., 1983; Drever et. al., 1987). [KIP: UPDATE REFS] This detector is a small prototype for a future 4-kilometer, full-sized detector, being planned jointly by Caltech and MIT (Vogt et. al., 1987, 1989; see frontispiece to Part I, page 1). The swinging masses and the laser beams in Fig. 2.4 are hidden from view inside vacuum chambers, because at one atmosphere pressure air molecules would shake the masses far more than a gravitational wave does, and statistical fluctuations in the index of refraction of the air would produce fluctuating phase shifts in the laser beams far greater than the wave-induced phase shifts. In the center of the photograph, one sees the chamber in which resides the corner mass; extending out from that chamber are the vacuum pipes which house the two arms' laser beams. Barely visible at the far ends of those pipes are the chambers that house the end masses.

Interferometric detectors have been under development for 12 to

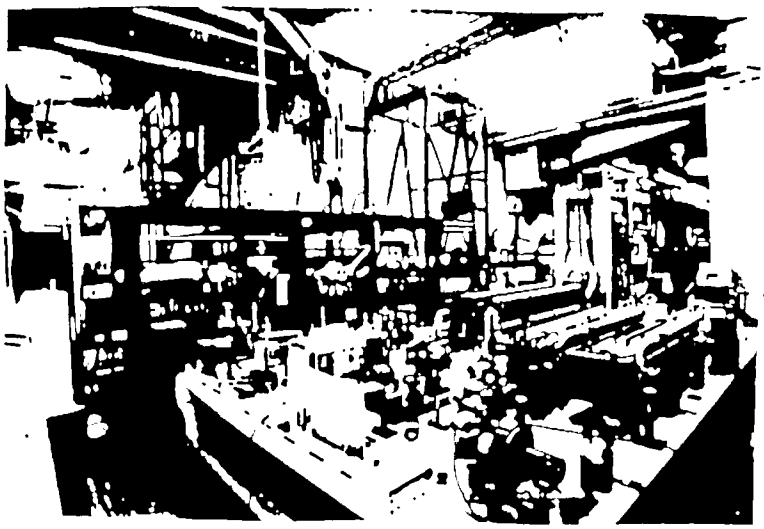

(a) (b)

Fig. 2.4 (a): The vacuum system that houses the prototype interferometric detector with 40-meter arms at Caltech. This photograph was taken when the detector was first being set up (ca. 1981). [Photograph courtesy R. W. P. Drever.] (b): The interferometric detector in 1987. The instrumentation in the foreground is prepares the laser beam for insertion into the detector. [Photograph courtesy XXXXX.]

18 years, depending on how one counts, by contrast with 25 to 30 years for bars. (See Sec. 3.B for a brief history.) Thanks to rapid improvements, the interferometric detectors' sensitivities have nearly caught up with the bars': At present (August 1989) the three most sensitive interferometric detectors – Munich (Shoemaker et. al., 1988), Glasgow (Ward et. al., 1988), and Caltech (Drever et. al., 1988) – all have noise amplitudes $h_n^{opt} \simeq 3\times10^{-18}$ for gravitational-wave bursts, which is a factor three worse than the Stanford and Rome bars. [KIP: UPDATE REFS]

Interferometric detectors easily achieve wide bandwidth, by contrast with bar detectors: The present Munich, Glasgow, and Caltech detectors all have good sensitivities over the frequency band from 500 Hz to 2.5 kHz – a band so wide that if waves were detected in it, the detectors would see nearly the full time evolution of the waveform.

These three interferometric detectors have arm lengths L = 40 meters at Caltech, 30 meters at Munich, and 10 meters at Glasgow. Detectors are also under construction, or technology or plans for them are being developed, by research groups at: MIT in Cambridge, Massachusetts (Livas et. al., 1986); a number of cooperating laboratories in

France and Italy (Brillet, 1985; Giazotto et. al., 1986); a number of cooperating laboratories in Japan (Kawashima, 1986; XXXX); the Shternberg Astronomical Institute in Moscow and the State Committee on Standards in Leningrad, USSR (Grishchuk, 1988a); and at the Australian National University and the University of West Australia in Canberra and Perth (XXXXX). These research efforts are all in preparation for future full-sized detectors with arm-lengths in the range 1 to 4 kilometers. (Vogt et. al., 1987, 1989; Hough et. al., 1986; Leuchs et. al., 1987; and Giazotto et. al., 1987). The present detectors are generally referred to as "prototypes" for the full-scale ones. [KIP: UPDATE REFS]

The prototype interferometric detectors have improved their sensitivities h_n^{opt} by about a factor 2 per year, on average, during the 1980's; and if the full-sized detectors are built by the mid 1990s as planned, there is good reason to expect this rate of improvement to continue through the turn of the century. If so, then 10^{-20} will be reached around 1996, and 10^{-22} around 2003. Somewhere between here and there gravitational waves will very likely be discovered.

Because the waves are likely to be somewhat stronger in amplitude at lower frequencies [see Eq. (1.9)], and because photon shot noise becomes less serious at lower frequencies [e.g. Eq. (2.3)], there has been and will continue to be a major effort to push interferometric detectors to lower and lower frequencies. In 1983 the best sensitivities were confined to frequencies $f \gtrsim 3000$ Hz. In 1989 they extend down to 500 Hz. By the late 1990s they are likely to extend well below 100 Hz. A reasonable ultimate goal is ~10 Hz.

All gravitational-wave detectors exhibit sudden glitches of internal noise a number of times per day. Some of these glitches can be explained and distinguished from gravitational waves, but many cannot. The only way to remove them from the data is by cross correlating the outputs of two (or preferably more) detectors that are far enough apart for their noise to be uncorrelated. For this reason, a single detector is of little value in searches for gravitational-wave bursts (the type of wave that I think will be the strongest). To carry out believable searches one needs at least two and preferably more detectors, on line at the same time, at widely separated sites. To optimize the searches, the detectors must have nearly identical sensitivities. (For two detectors with noise amplitudes h_{n1}^{opt} and h_{n2}^{opt} the net noise amplitude is $h_{n1}^{opt} h_{n2}^{opt} \left[(h_{n1}^{opt})^2 + (h_{n2}^{opt})^2 \right]^{-1/2}$. If, as is likely, the event rate varies as $(h_n^{opt})^{-3}$, then two identical detectors operating together are more sensitive than one by 180 per cent; but if the second detector has h_n^{opt} two times worse

than the first, it improves the sensitivity by only 40 per cent.)

For these reasons I am convinced that, to achieve a high probability of success in the search for gravitational radiation will require that a single, tightly knit group, with a single, reliable funding source, construct and operate two detection sites as a single "observatory". Detectors of near identical sensitivities must be brought on line at the two sites at the same time and must be run in tight coincidence with their data being cross correlated in real time, or near real time. Such a *Laser Interferometer Gravitational Wave Observatory* (*LIGO*) is currently being planned in the United States by a unified Caltech/MIT research group under the leadership of Rochus Vogt (Director), Ronald W. P. Drever, Fred Raab, and Rainer Weiss. A *detection system* in this LIGO will consist of two *receivers* (each an interferometric detector of the type shown in Fig. 2.1 and in the frontispiece to Part I, page 1), with one receiver at each site, together with the communications and data analysis systems that cross correlate the two receivers' outputs.

This LIGO, if built by the mid-1990s as planned, should be able to detect waves reliably in the late 1990s or early 2000s; but it will not by itself be able to measure the source directions (α,δ) or the two waveforms $h_+(t)$ and $h_\times(t)$ which are so crucial for astronomy. Moreover, it will not have the redundancy that is needed for detection when one receiver is inadvertently noisy or breaks down. For these reasons, it is of great importance to the future of gravitational-wave astronomy that several nations or consortia of nations build full-sized interferometric detectors. What is needed is a world-wide network of full-sized interferometric detectors, analogous to the present Gravnet network of bar detectors.

Such a network will determine source directions primarily by the time of flight of the waves between the network's sites. By time-of-flight measurements, a three-site network can determine the location of a source on the sky (or underfoot, since the waves penetrate the earth with impunity) to within an angular error

$$\Delta\Theta = \left[\frac{8}{\pi A\cos\mu}\right]^{1/2}\left[\frac{c}{2\pi f S/N}\right]$$

$$= 10\ \text{arcmin}\frac{1}{\sqrt{\cos\mu}}\frac{10}{S/N}\left[\frac{0.22R_\oplus{}^2}{A}\right]^{1/2}\frac{1\,\text{kHz}}{f}\ . \qquad (2.5)$$

(See Sec. XXXX for a derivation; and see Gürsel and Tinto, 1989, for a computer program and computer simulations that extract the source

direction from a network's gravitational-wave data with approximately this accuracy.) In Eq. (2.5) A is the area of the triangle formed by the three sites (the 3-*site triangle*), μ is the angle between the source direction and the normal to the 3-site triangle, f is the frequency of the waves, and S/N is the ratio of the signal S (i.e. the ΔL) that the waves make in each detector to the detector's noise N. (It is assumed for simplicity that S/N is the same for all three detectors.) For a network consisting of sites on the west coast and east coast of the United States and in western Europe, the area of the 3-site triangle would be about $0.22R_\oplus{}^2$, where $R_\oplus$ is the radius of the earth; and, correspondingly, the network is likely to reveal source directions (α,δ) to within a few tens of minutes of arc if $f \sim 1$ kHz, and a few degrees if $f \sim 100$ Hz. This is not wonderful precision, but it will be adequate for many purposes. For example, it is much smaller than the 6.6 degree by 6.6 degree size of each photograph in the Palomar Sky Survey, which will be a key tool in trying to identify sources.

Time-of-flight for a 3-site network actually leaves the source direction ambiguous: Both the true direction and its reflection in the plane of the 3-site triangle are compatible with the observed time delays. If the signal-to-noise ratio is adequate, this ambiguity can be resolved by the ratios of the amplitudes of the signals in the three detectors (Gürsel and Tinto, 1989). One of the two directions will be in accord with the measured amplitude ratios; the other will not.

Unfortunately, the errors in the measured source directions become large (tens of degrees) when the source is near the site triangle's plane. This is because the detector sensitivities are poorer for source directions near that plane and correspondingly S/N becomes smaller, and also because $\cos\mu$ becomes small; cf. Eq. (2.5). To get good accuracy over the entire sky and to deal with the (all too common!) situation of one detector being down or having unexpectedly large noise, it will be important for the network to include at least four detectors at four sites, and for the volume of the tetrahedron formed by the four sites to be as large as possible. Particularly attractive would be a network with two carefully placed sites in the United States, one or more in Europe, and one in Japan or Australia. A four-site network would also produce much more accurate wave-form measurements than one with only three sites.

For further details about networks of full-scale interferometric detectors see Sec. XXXX; and see, also, Schutz and Tinto (1987), Tinto (1987a,b), Livas et. al. (1987), Boulanger et. al. (1988a,b,c), and

Dhurandhar and Tinto (1988).

2.D Solar-system-based detectors: The low-frequency band

Three types of solar-system-based detectors have been used, or are being used, to search for gravitational waves in the low-frequency band (10 to 10^{-5} Hz): the normal modes of vibration of the earth (Sec. 12.B), the normal modes of the sun (Sec. 12.B), and the tracking of spacecraft. Of these, spacecraft tracking has been the most successful. [KIP: FIX SECTION REFS]

Spacecraft tracking uses an interplanetary spacecraft and the earth as the two masses perturbed by the wave. However, instead of monitoring their separation, one monitors their relative velocity. The reason is simple: velocity monitoring gives higher accuracy.

The monitoring is done by a radio tracking signal that is transmitted from an earth-based antenna to the spacecraft, received by the spacecraft and retransmitted to earth, and upon return to earth, compared with the outbound radio signal; see the frontispiece to Part IV, page XXX.

If the earth-spacecraft distance L is smaller than a reduced wavelength λ of the gravitational waves, then the wave-induced perturbations in distance and relative velocity are

$$\Delta L \simeq \mathcal{H} L \ , \quad \Delta v \simeq \frac{\Delta L}{\lambda/c} = c\mathcal{H}\frac{L}{\lambda} \quad \text{when } L \ll \lambda , \tag{2.6a}$$

where c is the speed of light. These perturbations increase, with increasing separation L. If $L \gtrsim \lambda$, then a proper reference frame cannot encompass both the spacecraft and the earth, expression (2.6a) breaks down, and the order-of-magnitude of the earth-spacecraft response,

$$\Delta L \sim \mathcal{H}\lambda , \quad \Delta v \sim c\mathcal{H} \quad \text{when } L \gtrsim \lambda , \tag{2.6b}$$

can be derived only using the concepts of spacetime curvature (see Secs. 4.F and 12.B; and see also the footnote on page XXXX). Note that this response for $L \gtrsim \lambda$ is independent of L in order of magnitude and is the same as the limit of (2.6a) as L approaches λ.

The relative velocity v of the spacecraft and earth is monitored by measuring the doppler shift $\Delta\nu$ of the returned radio signal's frequency relative to the outbound frequency ν:

$$\Delta\nu/\nu = \Delta v/c \sim h \quad \text{when } L \gtrsim \lambda . \tag{2.6c}$$

In recent years experimental teams at Caltech's Jet Propulsion

Laboratory have monitored the doppler shift of NASA's Voyager and Pioneer 10 and 11 spacecraft to a precision of $\Delta\nu/\nu \sim 3\times10^{-14}$, corresponding to a noise amplitude for gravitational-wave bursts $h_n^{opt} \sim 3\times10^{-14}$, in the band 10^{-2} to 10^{-4} Hz (see references and discussion in Sec. 12.B).

The earth-spacecraft separation ΔL is monitored by sending coded radio signals up, receiving them back, and measuring the round-trip travel time. The precision of this "ranging" technique is $\Delta L \sim$ (a few tens of meters) out of $L \sim 10^{12}$ meters, corresponding to $h_n^{opt} \sim 10^{-11}$, which is not nearly as good as the doppler-shift measurements.

Planned and projected improvements in spacecraft instrumentation and in NASA's tracking antennas should bring much better sensitivities: The Galileo spacecraft around XXXX should achieve $h_n^{opt} \sim 10^{-14}$ or a bit better, and subsequent missions may achieve 10^{-16}. [KIP: CHANGE TO 10^{-17}?] However, because of fluctuations in the interplanetary medium and the earth's troposphere, through which the radio waves must propagate, it is not likely that radio tracking will ever get much better than 10^{-16}. As we shall see in Secs. 2.F–2.H, these low-frequency-band sensitivities might bring success, but they might well not.

Interferometric detector in space. Soon after the turn of the century doppler tracking is likely to be replaced, in the low-frequency band, by interferometric detectors flown in space. Current design studies for such interferometric detectors (Bender et. al., 1989; Sec. 12.B below) entail three spacecraft at the corner and ends of an L, with arm lengths of roughly 1 million kilometers (Fig. 2.5). A one-watt laser in the corner spacecraft would send two light beams through 50-centimeter-diameter beam-collimating telescopes, one beam toward each end spacecraft. Each end spacecraft, instead of bouncing the beam back from a mirror, would receive the beam, lock a laser of its own onto the beam, and transmit phase-locked light from that laser back to the corner spacecraft. The two incoming beams would interfer at the corner in the same manner as for a ground-based spacecraft. This detector might achieve $h_n^{opt} \sim 10^{-22}$ at frequencies 10^{-2} to 10^{-3} Hz, and $h_n^{opt} \lesssim 10^{-20}$ throughout the band 1 Hz $\gtrsim f \gtrsim 10^{-5}$ Hz. As we shall see in Sec. 2.G, such a sensitivity would easily be adequate to detect and study waves from binary stars in the low-frequency band and might well detect other, more esoteric sources. [KIP: UPDATE DESCRIPTION?]

For further details on spacecraft tracking, interferometric detectors in space, and other solar-system-based detectors, see Sec. 12.B.

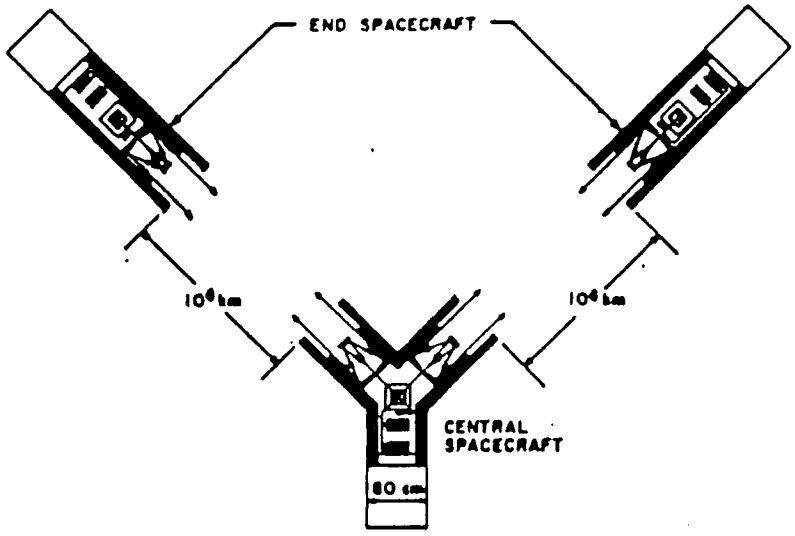

Fig. 2.5 An interferometric detector that might fly in space around the turn of the century. The corner and end masses are spacecraft with separations $L \sim$ one million kilometers (three times the earth–moon distance). These spacecraft would orbit the sun in the same orbit as the earth, and would monitor the difference in arm lengths using laser interferometry.

For comparisons with source strengths, see Secs. 2.F–2.H.

2.E Astronomical detectors: The very-low-frequency band

Very-low-frequency ($f \lesssim 10^{-5}$ Hz) gravitational radiation has been searched for by a number of different detection techniques which use astronomical bodies outside the solar system; see Sec. 12.D. Of these techniques two have produced especially impressive results: the timing of pulsars, and the isotropy of the primordial microwave radiation.

Pulsar timing. As a preliminary to discussing pulsar timing, I shall comment on the physical origin of the gravitational-wave-induced doppler shift. The doppler-shift signal $\Delta\nu/\nu \sim \Delta v/c \sim h$ [Eq. (2.6c)], for two bodies whose separation is large compared to a wavelength, can be thought of in two different ways: as due to a wave-induced relative velocity of the two bodies (see the above discussion of spacecraft tracking), or as due to a wave-induced "gravitational redshift" of clocks on one body relative to clocks on the other. These apparently contradictory viewpoints in fact are compatible and equivalent: When $L \gtrsim \lambda$, one cannot accurately discuss the waves using a proper reference frame; and the more sophisticated spacetime-curvature discussions

have "gauge freedom" (arbitrariness in the choice of coordinates) which permits one, by different choices of gauge, to develop different physical pictures. The physical pictures may differ, but the bottom line is the same: The propagating light or radio waves are shifted in frequency by $\delta\nu/\nu \sim \not{h}$. [KIP: FIX SCRIPT h THROUGHOUT]

A pulsar is a rotating neutron star from which shines a radio beam. As the star rotates, the beam rotates; and each time the beam swings past earth, we receive a pulse of radio waves. This pulsed beam is a precisely timed tracking signal, completely analogous to the signal sent by a spacecraft to earth — except that it is a one-way signal rather than round-trip.

When a gravitational wave sweeps over the earth, it will change the ticking rates ν of all clocks on earth relative to the rate of the distant pulsar's rotation, thereby producing a fluctuation $\Delta\nu/\nu \sim \not{h}$ in the pulsar's pulse rate ν, as timed by earth-based clocks. Similarly, when a wave sweeps over the pulsar it will change the pulsar's ticking rate (i.e. the rate of rotation of the neutron star) relative to all clocks on earth, again producing a fluctuation $\Delta\nu/\nu \sim h$ in the earth-measured pulse rate. Thus, by high-precision timing of the pulsar, one can search for gravitational waves at earth or at the pulsar.

The best instrument for such pulsar timing is at the Arecibo radio telescope in Puerto Rico (Fig. 2.6a). By monitoring with this telescope the most regular and fastest of all known pulsars, PSR 1937+21 (which resides in our galaxy at a distance of XXX thousand light years from earth), Davis et. al. (1985), Taylor (1987), and Rawley et. al. (1987) have placed the limit $\not{h} \lesssim 10^{-13}$ on the strengths of waves at a frequency $f \simeq 1/(\text{the four-year monitoring time}) \simeq 0.7\times10^{-8}$ Hz.

This limit might not look impressive compared to today's earth-based detectors' $h_n^{\rm opt} \sim 10^{-18}$, but because of the tendency for waves to be stronger at lower frequencies [Eq. (#1.10) and associated discussion], it is very impressive. For example, primordial gravitational waves which fill the universe and have amplitudes $\not{h}$ and frequencies between, say, $0.7f$ and $1.4f$, carry a total energy density [Eq. (9.5)]

$$\frac{dE_{\rm GW}}{d\,\text{Vol}} \simeq \frac{c^6}{G} f^2 \not{h}^2 . \tag{2.7a}$$

In units of the *critical energy density* required to close the universe (and make the universe ultimately recontract) this is [Eq. (9.7)]

$$\Omega_{\rm GW} \equiv \frac{dE_{\rm GW}/d\,\text{Vol}}{dE_{\rm crit}/d\,\text{Vol}} \simeq \left[\frac{\not{h}}{10^{-10}}\right]^2 \left[\frac{f}{10^{-8}\ \text{Hz}}\right]^2 . \tag{2.7b}$$

Fig. 2.6 The earth-based ends of two astronomical detectors for very-low-frequency gravitational radiation. (a) The radio telescope at Arecibo, Puerto Rico, which is used to time the pulses of radio waves from distant pulsars. (b) The XXXX telescope, which has been used to search for angular variations (anisotropy) in the intensity of the primordial microwave radiation.

(Here in evaluating $dE_{crit}/d\text{Vol}$, and throughout this book, I use the value $H_o = 100\,\text{km}\,\text{sec}^{-1}\,\text{Mpc}^{-1}$ for the Hubble expansion rate of the universe.) Because pulsar timing is sensitive to waves of 10^{11} times lower frequency than today's earth-based detectors, it needs only a 10^{11} times worse amplitude sensitivity in order to place the same limits on Ω_{GW}. In fact, its 10^{-13} amplitude sensitivity is only 10^5 times worse, so pulsar timing does far better than present earth-based detectors in limiting Ω_{GW}: From the pulsar data one infers that the energy density in gravitational waves in the band 0.5×10^{-8} to 1×10^{-8} Hz is less than 4×10^{-7} of that required to close the universe, $\Omega_{GW} \lesssim 4\times10^{-7}$ (Rawley et. al., 1987). For further details and discussion see Sec. 12.C and Fig. 2.9. (Of course, this impressive limit at gravity-wave frequencies $f \sim 10^{-8}$ Hz does guarantee anything about the strengths of the waves in the high-frequency band of earth-based detectors.) [KIP: UPDATE]

Isotropy of the primordial microwave radiation. The most distant of all sources of electromagnetic waves is the primordial gas, produced in the big-bang, which sends us its primordial microwave radiation. Although the primordial microwaves are not pulsed, they nevertheless can be used for gravitational-wave searches: Gravitational waves passing over the earth today or over the microwave-emitting gas at the

epoch of emission (universe age a few hundred thousand years) should produce fluctuating frequency shifts $\Delta\nu/\nu \sim$ ½ in the microwaves. In view of Eqs. (2.7), the most interesting such fluctuations will be at the lowest of frequencies. Although astronomers have not been searching long enough to see *temporal* microwave fluctuations at frequencies $f < 1/(25 \text{ years}) \sim 10^{-9}$ Hz, they can look for *spatial* fluctuations $\Delta\nu/\nu$ corresponding to frequencies far below this, and can do so with interestingly high precision. This is because the universe, at a few hundred thousand years' age, was so extremely homogeneous and so perfectly thermalized, that its primordial gas emitted thermal radiation which everywhere had the same temperature to within at least $\Delta T/T \sim$ a few times 10^{-4}.

A gravitational wave with wavelength of order the size of the universe today (frequency $f \sim 3\times10^{-18}$ Hz), sweeping over the earth, will produce a frequency shift $\Delta\nu/\nu \sim +$½ in one transverse direction and −½ in the other, and thence a microwave temperature difference $\Delta T/T = \Delta\nu/\nu \sim 2$½ between the two directions. Using the microwave antenna shown in Fig. 2.6b XXXXX have placed a limit $\Delta T/T \lesssim XXX$ on the large-scale (90-degree) anisotropy, which translates into $\Omega_{GW} \lesssim 10^{-5}$ in the extremely-low-frequency range (1.5 to 3)$\times10^{-18}$ Hz.

A much more impressive, but less reliable limit can be placed by considering the effects of gravitational waves that swept over the emitting, primordial gas, at the few-hundred-thousand-year epoch of its emission. Such waves, with wavelength that was the size of the observable universe then, should have produced fluctuations $\Delta T/T$ with angular scales on our sky today of a few degrees; i.e., because of them the microwave radiation should be mottled on scales of a few degrees. The best observational limits on such mottling, when combined with (somewhat uncertain) calculations of physical processes at the few-hundred-thousand-year epoch, produce a limit of $\Omega_{GW} \lesssim 10^{-13}$ at frequencies of (1 to 2)$\times10^{-13}$ Hz (Carr, 1980; Starobinsky, 1985). [KIP: GRISHCHUK SAYS 10^{-12} UNLESS ONE ASSUMES A SPECIFIC INFLATIONARY SCENARIO TO GET RATIO OF DENSITY PERTURBATIONS TO GW PERTURBATIONS; I MUST CHECK] This very impressive limit places severe constraints on theoretical speculations about the very early universe. See Sec. 12.C and references therein for further details.

2.F Burst waves: Sources and detector sensitivities

In the remainder of this chapter, I shall compare the sensitivities of present and planned detectors with estimates of the wave strengths from astrophysical sources. This comparison will give some indication of the difficulty of gravitational-wave detection, the prospects for future success, and the astrophysical information that gravitational astronomy may bring.

In my comparison I shall distinguish not only between the three different frequency bands (high, low, very low), each with its own types of detectors, but also between three different types of waveforms $h_+(t)$ [or $h_\times(t)$]: *bursts*, *periodic waves*, and *stochastic waves*. Bursts are waves whose waveforms oscillate for only a few cycles. Periodic waves are those whose waveforms oscillate on and on and on, in a coherent fashion (with, typically, a discrete number of frequencies present) for a time long compared to any gravitational-wave measurement. Stochastic waves are those whose waveforms have stochastically varying, i.e. random, time dependences. This section treats bursts, Sec. 2.G periodic waves, and Sec. 2.H stochastic waves.

To make a meaningful comparison of source strengths and detector sensitivities, one must express them on the same footing. I shall describe bursts by the *characteristic frequency* f_c at which the waveforms $h_+(t)$ and $h_\times(t)$ oscillate, and by a *characteristic amplitude* h_c, equal to the amplitude $\not h$ of the waveform oscillations multiplied by the square root of the number n_{cyc} of cycles of oscillation that the waveform undergoes with amplitude near $\not h$ and frequency near f_c:

$$h_c \equiv \not h \sqrt{n_{cyc}} . \tag{2.8}$$

The factor $\sqrt{n_{cyc}}$ is included because, when integrating up a signal that lasts for more than one cycle, a detector builds up an amplitude signal-to-noise ratio proportional to $\sqrt{n_{cyc}}$; thus, from the detector's point of view, a wave lasting n_{cyc} cycles with amplitude $\not h$ is as easy to detect as a wave lasting just one cycle with amplitude $h_c = \not h \sqrt{n_{cyc}}$.

The detector noise amplitude h_n^{opt} for bursts, introduced above, can be regarded as a function of the characteristic frequency f_c of the waves it seeks. When the detector receives waves with characteristic frequency f_c and characteristic amplitude h_c, and the waves come from that direction and with that polarization which will most optimally drive the detector, and the experimenter processes the detector's output using a technique called *optimal signal processing*, then the *amplitude signal-to-noise ratio* will be

$$\frac{S}{N} = \frac{h_c}{h_n^{\rm opt}} . \tag{2.9}$$

In comparing detector sensitivities with expected source strengths, it is more reasonable to assume random source directions and random polarizations rather than optimal ones. This reduces the signal-to-noise ratio by about a factor 2.2, so

$$\frac{S}{N} \simeq \frac{1}{2.2}\frac{h_c}{h_n^{\rm opt}} . \tag{2.9'}$$

How large must S/N be in order to know with confidence that an observed excitation in a detector is due to a wave burst and not to internal noise? If two detectors are being cross correlated to remove spurious noise spikes, the remaining internal noise will have a Gaussian probability distribution. If the bursts are extremely rare, say 3 per year, then for 90 per cent confidence that an apparent signal is not noise, the signal must exceed the level that the Gaussian noise randomly jumps to 3 times per year. From the Gaussian probability distribution one can infer that this critical S/N is

$$\frac{S}{N} \gtrsim \left[\ln[f_c \times (\tfrac{1}{3}\ \text{year})]\right]^{\frac{1}{2}} ; \tag{2.10}$$

i.e., $S/N \gtrsim 5$ for ground-based detectors operating in the band between 10 Hz and 10^4 Hz, and $S/N \gtrsim 3$ for solar-system detectors operating in the band between 10^{-2} Hz and 10^{-4} Hz. Combining this with Eq. (2.9'), we obtain the *minimum value* $h_{3/\rm yr}$ *that the waves' characteristic amplitude* h_c *must have in order to be detectable in a search that sees only three bursts per year*:

$$\begin{aligned} h_{3/\rm yr} &\simeq 11 h_n^{\rm opt} \text{ for earth-based detectors} \\ &\simeq 6 h_n^{\rm opt} \text{ for solar-system-based detectors.} \end{aligned} \tag{2.11}$$

When comparing detector sensitivities with source strengths we shall use this $h_{3/\rm yr}$ to characterize the detectors and regard it as a function of frequency f_c, and shall use h_c and f_c to characterize the sources. Much more careful definitions of $h_{3/\rm yr}$, h_c, $h_n^{\rm opt}$, and f_c are given in Eqs. (7.6)-(7.9), (10.12)-(10.14), and (11.14).

Figure 2.7 shows the best current estimates of the characteristic amplitudes h_c and frequencies f_c for burst waves from various astrophysical sources (thin curves), and the sensitivities $h_{3/\rm yr}(f_c)$ for present and planned detectors (thick curves and dots). Each source or

detector in this figure is discussed in detail in that section of the book which is shown beside its curve or dot. The figure covers the high-frequency band ($f_c \gtrsim 10\,\text{Hz}$; earth-based detectors) and the low-frequency band ($10\,\text{Hz} \gtrsim f_c \gtrsim 10^{-5}\,\text{Hz}$; solar-system-based detectors); but it omits the very-low-frequency band because no plausible sources of bursts have been identified there.

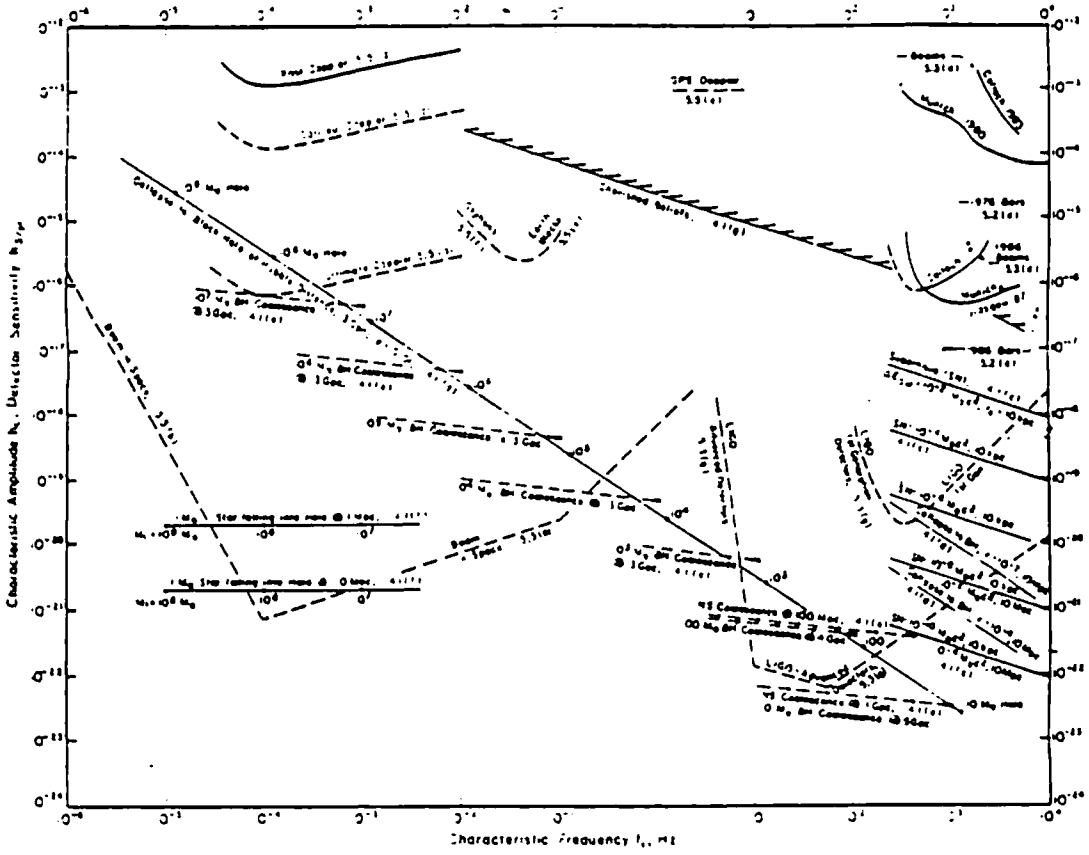

Fig. 2.7 Burst sources and detectors. Plotted vertically are the characteristic amplitudes h_c [Eqs. (2.7) or, more precisely, (7.6b)] of gravitational waves from several postulated *burst sources* (thin curves), and the sensitivities $h_{3/\text{yr}}$ of several existing and planned detectors (thick curves and circles). [$h_{3/\text{yr}}$ is the amplitude h_c of the weakest source that can be detected 3 times per year with 90% confidence by two identical detectors operating in coincidence; see Eqs. (2.11) or, more precisely, (7.9), (10.14), and (11.14).] Plotted horizontally is the characteristic frequency f_c of the waves [Eqs. (7.6a)]. The abbreviations BH, NS, and SN are used for black hole, neutron star, and supernova. The sources and detectors are discussed in detail in the indicated sections of this book.

Present and past earth-based detectors are shown in the upper right hand regions of Fig. 2.7 (dots for bar detectors because of their

narrow bandwidths; curves for the broad-band interferometric detectors). Note the improvements of bar detectors between 1976 and 1989, and the improvements of interferometric detectors between 1980/83 and 1989. Note also that the 1989 bar and interferometer sensitivities $h_{3/\mathrm{yr}}$ are a factor 11 worse than the 10^{-18} and 3×10^{-18} noise amplitudes h_n^{opt} quoted above, because of statistical, polarization, and directionality effects [cf. Eq. (2.11)].

In the $h_{3/\mathrm{yr}} = 10^{-18}$ to 10^{-20} region of the high-frequency band is a curve labeled "LIGO 1st Generation Detectors". This curve is an estimate of the performance to be achieved by the first full-sized interferometric detectors to operate in the proposed American Laser Interferometer Gravitational Wave Observatory (LIGO) — slated for completion in the mid 1990s. (Full-sized interferometric detectors in Europe, Australia and/or Japan should be comparable, but being closer to the American project, I am more familiar with its plans and projections.) Near the bottom of the low-frequency region is a "LIGO Advanced Detectors" curve. This is a sensitivity that might be achieved by detectors in the LIGO around the turn of the century, after some years of detector improvement and perfection. Section 11.F discusses some of the design parameters of such detectors. As one sees from the two LIGO curves, the experimenters expect to push their detectors gradually toward lower frequencies and better sensitivities as time passes.

The burst sources shown in the high-frequency region include supernovae, the collapse (implosion) of a stellar core to form a black hole, and the coalescences of neutron-star binaries ("NS") and black-hole binaries ("BH").

Supernovae should emit their gravitational waves in short bursts which accompany the implosion and bounce of the stellar core (neutron-star birth). Supernovae occur in our own galaxy (distances about 30 thousand light years, i.e. 10 kiloparsecs, labeled kpc on the figure) about once every 40 years (though because ~85 percent of the galaxy is obscured by interstellar dust, humans see them optically only once each ~250 years; cf. Tammann, 1981). At the distance of the Virgo cluster of galaxies (30 million light years, i.e. 10 Megaparsecs, labeled Mpc on the figure), supernovae occur several times per year. The characteristic amplitude of a supernova's waves is highly sensitive to the nonsphericity of its imploding core. If the core is precisely spherical, no waves at all are emitted. If it is highly nonspherical, as much as (a few)$\times10^{-2}M_\odot c^2$ (one hundredth of a solar rest mass) of energy might be emitted. The typical value might be far smaller than

$10^{-2}M_\odot c^2$; but of course the typical value is less relevant than the largest values that occur, say, once a year. The characteristic frequency of the waves is also highly uncertain; computer modeling of the stellar implosion is not yet good enough give predictions on which different modelers can agree. However, we can be fairly sure that f_c is between 200 Hz and 10^4 Hz. The curves shown in the figure are labeled by the amount of energy ΔE_{GW} that comes off in gravitational waves and the distance r_0 to the supernova. In addition, they are drawn for the entire uncertainty range of frequencies. For further details and references see Sec. 7.B.

Collapses of stars to form black holes are even more uncertain than supernovae: Not only are we ignorant of the nonsphericity of the imploding core, and thus ignorant of the amount of energy radiated, we don't even know how often such collapses occur. They might be a moderate fraction of the supernova rate, or they never occur. The curves in Fig. 2.7 are labeled with the fraction ε of the black-hole mass that gets radiated as gravitational-wave energy (i.e. the efficiency of the emission), and the distance r_0 to the source. The efficiency could be as high as 0.1 in an exceedingly nonspherical collapse, and as low as zero in a perfectly spherical one. The characteristic frequency should be $f_c \sim 10\,\text{kHz}\,(2M_\odot/M)$, where M is the newborn hole's mass [Eq. (1.8)]. For further details and references see Sec. 7.C.

Coalescence of neutron-star binaries. Of all sources that astrophysicists have identified in the high-frequency range, neutron-star coalescence is the least uncertain. From the statistics of observed neutron-star binaries in our own galaxy, Clark, van den Heuvel, and Sutantyo (1979) estimate that one must look out to a distance of 100^{+100}_{-40} Mpc (300 million light years) to see three coalescences per year. They argue that the quoted uncertainties correspond to 90 per cent confidence; but Schutz (XXXX) argues that this is overly optimistic, and 90 per cent confidence corresponds only to the range 10 Mpc to 1000 Mpc. The most easily detected waves from the coalescence event will be those produced in the last few minutes of inspiral, as the wave frequency sweeps upward from a few tens of Hertz to a few hundreds of Hertz (neutron-star analog of Fig. 1.5). The waves from this inspiral are understood with great confidence. The dashed arrow labeled "NS Coalescence @ 100 Mpc" shows the characteristic amplitude as a function of frequency during this sweep, assuming a distance to the binary of 100 Megaparsecs (300 million light years). For other distances r_0, the characteristic amplitude h_c scales as $1/r_0$. For further detail and

references see Sec. 7.D.

Coalescence of black-hole binaries. Of all sources that have been studied, the ones that I speculate will produce the strongest waves at earth are black–hole coalescences. However, because there is no firm proof that black holes even exist and because, if they do exist, the number of black–hole binaries in the universe is enormously uncertain, nobody can be fully confident about this source. The dashed arrows show the frequency sweep of the waves from the coalescence of two black holes with equal masses, assuming various distances and various masses. Fig. 1.5 shows the waveform $h_+(t)$ for the case of two $10 M_\odot$ holes at 100 Mpc (300 million light years). For further details and references see Sec. 7.D.

Cherished beliefs. If gravitational–wave bursts three times per year were to be stronger than the line in Fig. 2.7 labeled "Cherished beliefs", we would have to abandon some of our cherished beliefs about the laws of physics and the nature of the universe. If they are weaker, our cherished beliefs may be safe; see Sec. 7.F.

Comparison of high-frequency source strengths with detector sensitivities. By comparing the high–frequency burst sources of Fig. 2.7 with the present and projected detector sensitivities, we learn the following: (i) Present sensitivities are better than the cherished beliefs level, but just barely. Thus, detectors are now beginning to move into the realm where astrophysicists could comfortably adjust to wave discovery. (ii) The supernova 1987A in the Large Magellanic Cloud (distance 50 kiloparsecs, i.e. 150 million light years), under the most optimistic of estimates, should have been detectable with unity signal–to–noise ratio using the 1987 Stanford and Rome bar detectors. Unfortunately, both detectors were turned off for improvements (the Gravnet network was "down") at the time of the supernova. (iii) Full–sized interferometric detectors in the LIGO could have detected supernova 1987A even if its energy output was far below the most optimistic estimates. Unfortunately, the supernova came a decade too soon. (iv) If the advanced interferometric detectors in the LIGO achieve the projected sensitivities, they will have high confidence of detecting the inspiral of binary neutron stars (our least uncertain source). (v) Those advanced detectors will also be able to detect black–hole binaries throughout the universe if the holes' masses are between 10 and $1000 M_\odot$.

Turn, now, to the low-frequency band, $10\,\text{Hz} \gtrsim f_c \gtrsim 10^{-5}\,\text{Hz}$. The upper, long, thick curves depict present and projected sensitivities $h_{3/\text{yr}}$ for the Doppler tracking of spacecraft. The bottom long, thick curve is the projected sensitivity for an interferometric detector in interplanetary space with one-million-kilometer arms. Also shown are sensitivities for several other proposed detectors (skyhook, earth blocks, and GPS Doppler). For details on all these low-frequency detectors see Sec. 12.B.

The strongest burst sources in the low-frequency band involve supermassive black holes. [Recall that the characteristic frequency scales inversely with the mass of the hole; Eq. (1.8).] The rates of these supermassive-black-hole events are enormously uncertain. They may be so rare that none are seen in a human lifetime; or they may be frequent enough to produce exciting science with the planned detectors. See Secs. 7.C–7.E.

2.G Periodic waves: Sources and detector sensitivities

Turn, next, to periodic gravitational waves, as depicted in Fig. 2.9. The waves from each periodic source will be a superposition of one or more discrete frequencies f. For each f we shall call the amplitude of the sinusoidal oscillations of $h_+(t)$ and $h_\times(t)$, appropriately averaged over the two polarizations, the characteristic amplitude h_c; see Eq. (8.3) for precise details. By analogy with burst waves, we shall define a detector's sensitivity $h_{3/\text{yr}}$ to be the characteristic amplitude of a source with random direction that would be detectable with 90 per cent confidence after $\frac{1}{3}$ year (10^7seconds) of integration — assuming that the source's frequency f and phase are known in advance from electromagnetic studies. See Eqs. (8.5a), (10.23), and (11.15). If f and the phase are not known, $h_{3/\text{yr}}$ will be increased by a factor 5 for high-frequency detectors and 3 at low frequencies; cf. Eq. (8.5b).

During its 10^7sec integration the detector builds the signal-to-noise ratio up by a factor $(f \times 10^7\text{sec})^{1/2}$, relative to that for a one-cycle burst. For this reason, a given detector's $h_{3/\text{yr}}$ for periodic sources is smaller by the factor $\sim(f \times 10^7\text{sec})^{1/2}$ than its $h_{3/\text{yr}}$ for bursts. This explains the remarkably small values of $h_{3/\text{yr}}$ in the periodic-waves figure, Fig. 2.8.

Interferometric detectors can seek bursts and periodic waves simultaneously. They collect their data by sampling $\Delta L/L$ at short intervals of time, and those data are then searched, by computer, for whatever type of wave one wishes. By contrast, all present bar

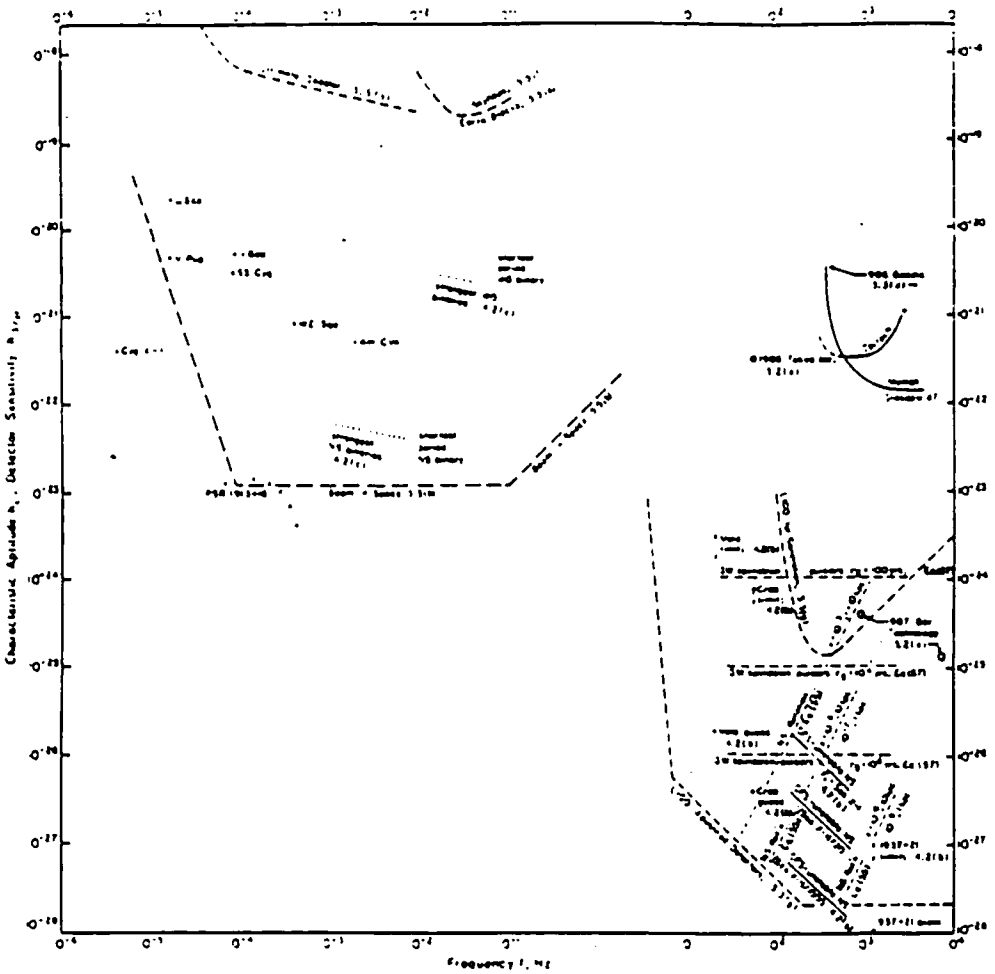

Fig. 2.8 The characteristic amplitudes h_c [Eq. (8.3)] and frequencies f of waves from several postulated *periodic sources* (thin curves), and the sensitivities $h_{3/\mathrm{yr}}$ of several existing and planned detectors (thick curves and circles). [$h_{3/\mathrm{yr}}$ is the amplitude h_c of the weakest source detectable with 90% confidence in a 1/3 year = 10^7 second integration, if the frequency and phase of the source are known in advance; see Eqs. (8.5a), (10.23), (11.15).] The sources shown in the high-frequency region, $f \gtrsim 10$ Hz, are all special cases of rotating, nonaxisymmetric neutron stars (Sec. 8.B). The steeply sloping dotted lines labeled "NS Rotation" refer to rigidly rotating neutron stars with moments of inertia $I_{zz} \simeq 10^{45}$ g cm^2, and with various ellipticities ε and distances r labeled on the lines [Eq. (8.11)]. The low-frequency sources, $f \lesssim 0.1$ Hz, are all binary star systems in our galaxy (Sec. 8.C): several specific, known binaries, which are indicated by name (μ Sco, V Pup,...); the strongest six spectral lines from the famous binary pulsar PSR1913+16; and the estimated strengths of our galaxy's strongest white-dwarf ("WD") and neutron-star ("NS") binaries. The sources and detectors are discussed in detail in the indicated sections of the book.

detectors must be physically adjusted to seek either bursts (Rome, Stanford, LSU, Maryland, Moscow, Perth) or periodic waves (Tokyo); Sec. 10.E. Accordingly, Fig. 2.8 shows the actual sensitivity $h_{3/\gamma r}$ to periodic waves for the 1988 Tokyo bar (solid circle), which operates at the rather low frequency 60 Hz of the Crab pulsar; and it shows the best that 1988 bar technology could do if detectors were built for periodic waves at the frequencies of Rome, Stanford, LSU, Maryland, Perth (900 Hz) and Moscow (8000 Hz). Also shown are the periodic sensitivities of the same interferometric detectors as were described above for bursts — except that the optical configurations of the advanced-LIGO detectors are altered to optimize them for periodic waves (Secs. 11.D and 11.F).

In the high-frequency band of earth-based detectors the only periodic sources identified by theorists are *rotating neutron stars* (Sec. 8.B). The strength of the waves from such a star depends crucially on its deviations from rotational symmetry, and those asymmetries are enormously uncertain. If the star emits radio waves and thus is a pulsar, by timing the pulses one can measure the slowdown of the star's spin. That slowdown places an upper limit on the gravitational-wave strength: If the waves are too strong, they will carry off too much angular momentum, producing too great a slowdown. Figure 2.8 shows the resulting limits on the characteristic amplitudes of waves from three pulsars: Crab, Vela, and PSR 1937+21. For each of these, a best guess of the wave strength is also shown (Zimmermann, 1978 for Crab and Vela; Alpar and Pines, 1985 for PSR 1937+21) — but the guesses are very-low-confidence ones.

The strongest neutron-star sources of gravitational waves almost certainly have not yet been detected electromagnetically. This is because so few pulsars have been detected (a few hundred out of perhaps 10^8 rotating neutron stars in our galaxy), and because the strongest gravitational-wave emitters are likely the fastest rotators, and the fastest rotators are the hardest to detect electromagnetically. To give a feeling for the possibilities, Fig. 2.8 shows two sets of dashed lines. The steeply sloped, dashed lines are labeled by distance r to the pulsar (recall that 10 kpc is the distance from the earth to the center of our galaxy), and by the ellipticity ε of the star's mass distribution about its spin axis; these lines are given by Eq. (8.11). Each horizontal dashed line refers to a hypothetical family of neutron stars whose rotations are being slowed down primarily by gravitational-wave emission, and not by electromagnetic emission. Each line is labeled by τ_B, the mean time between births of neutron stars in the family.

Remarkably, the characteristic amplitude of the strongest emitter depends only on τ_B and not (at least not sensitively) on anything else [Blandford, 1984; Eq. (8.13) below].

Also shown, as slanted solid lines, are the characteristic amplitudes for waves from neutron stars that are being spun up to high speeds by accretion from a companion star. It is presumed, here, that the accretion has triggered an instability, called the Chandrasekhar-Friedman-Schutz (CFS) instability (Sec. 8.B), in which density waves propagate around the star's envelope and radiate gravitational waves. The square of the resulting gravitational-wave strength h_c will be proportional to the accretion rate, as will be the flux of X-rays F_X produced by the accretion and received at earth (Wagoner, 1984). Correspondingly, h_c will be proportional to $\sqrt{F_X}$. The CFS lines in Fig. 2.8 are labeled by the X-ray flux, in units of the flux of SCO X-1 (the brightest of all the X-ray-emitting neutron stars); see Eq. (8.9).

By comparing the neutron-star wave strengths of Fig. 2.8 with the detector sensitivities, we can draw these conclusions: (i) It may well be possible to build bar detectors of sufficient sensitivity to detect the waves, though one probably would need to know in advance the frequency of a source and tune a bar to it. (ii) Full-sized LIGO interferometric detectors have a very good possibility of detecting and monitoring periodic waves. For further details and references on rotating neutron stars as sources of gravitational waves see Sec. 8.B.

Turn, next, to periodic waves in the low-frequency band (left portion of Fig. 2.8). The detectors shown here are the same as for burst waves in Fig. 2.7: doppler tracking of spacecraft, a future one-million-kilometer-arm interferometric detector in space, and (not to be discussed until Sec. 12.B) the skyhook and earth blocks. The sources are all *binary star systems* in our own galaxy.

Shown as discrete dots are the waves from specific, optically well-studied binaries. We can be highly confident of these predicted wave strengths. They are insensitive to unknown aspects of the binaries, and they depend on well-understood aspects of general relativity theory. All of the binaries shown have nearly circular orbits and thus emit waves with just one frequency f, except the binary pulsar PSR 1913+16. Its orbit is rather eccentric, so its waves include a fundamental frequency and a number of higher harmonics. Also shown as small dots are estimates of the strengths of waves from the strongest neutron-star binaries in our Galaxy and the strongest white-dwarf binaries. For further details and references on periodic waves from

binaries see Sec. 8.C.

It is evident from the figure that the only low-frequency detector with adequate sensitivity to reach the binaries' waves is the proposed interferometric detector in space. That interferometric detector would see the waves with ease. In fact, they may be so strong that the superposed waves from many binary stars might produce a stochastic background which hides other, more interesting stochastic waves; see Sec. 2.H.

As with burst sources, so also with periodic, no interestingly strong sources have been identified in the very-low-frequency domain, $f \lesssim 10^{-5}$Hz

2.H Stochastic waves: Sources and detector sensitivities

Turn, finally, to stochastic gravitational waves as depicted Fig. 2.9. The strengths of stochastic waves, like those of any other random process, are nicely described using spectral densities; see Sec. 9.A. However, in this elementary introduction we instead shall use a characteristic amplitude h_c which is a function of frequency f, and which is the root-mean-square amplitude that one would expect, on average, for just one cycle of oscillation at frequency f. Alternatively, we sometimes shall describe the wave strength by Ω_{GW}, the energy density of the waves between $0.7f$ and $1.4f$, divided by the critical energy density that would close the universe. Assuming, as is so for most stochastic sources, that the waves are isotropic in direction and that both polarizations are equally strong on average, these two descriptions of the wave strength are related by

$$h_c \simeq 10^{-10}\left[\frac{10^{-8}\text{Hz}}{f}\right][\Omega_{GW}(f)]^{\frac{1}{2}}; \qquad (2.12)$$

cf. Eqs. (2.7b) above and (9.7) below. The thin 45-degree lines in Fig. 2.9 show this wave strength for various values of Ω_{GW}.

One can best search for stochastic waves by multiplying together the outputs of two similar gravitational-wave detectors, and integrating for a long time. Because the detectors' noises are uncorrelated but the stochastic waves' forces on the detectors are the same (assuming they are closer together than a reduced wavelength, $\lambda = c/2\pi f$), the waves' effects gradually build up above the noise as the integration proceeds. The resulting sensitivity $h_{3/yr}$ (equal to the wave strength h_c that would be detectable with 90 per cent confidence after 1/3 year of

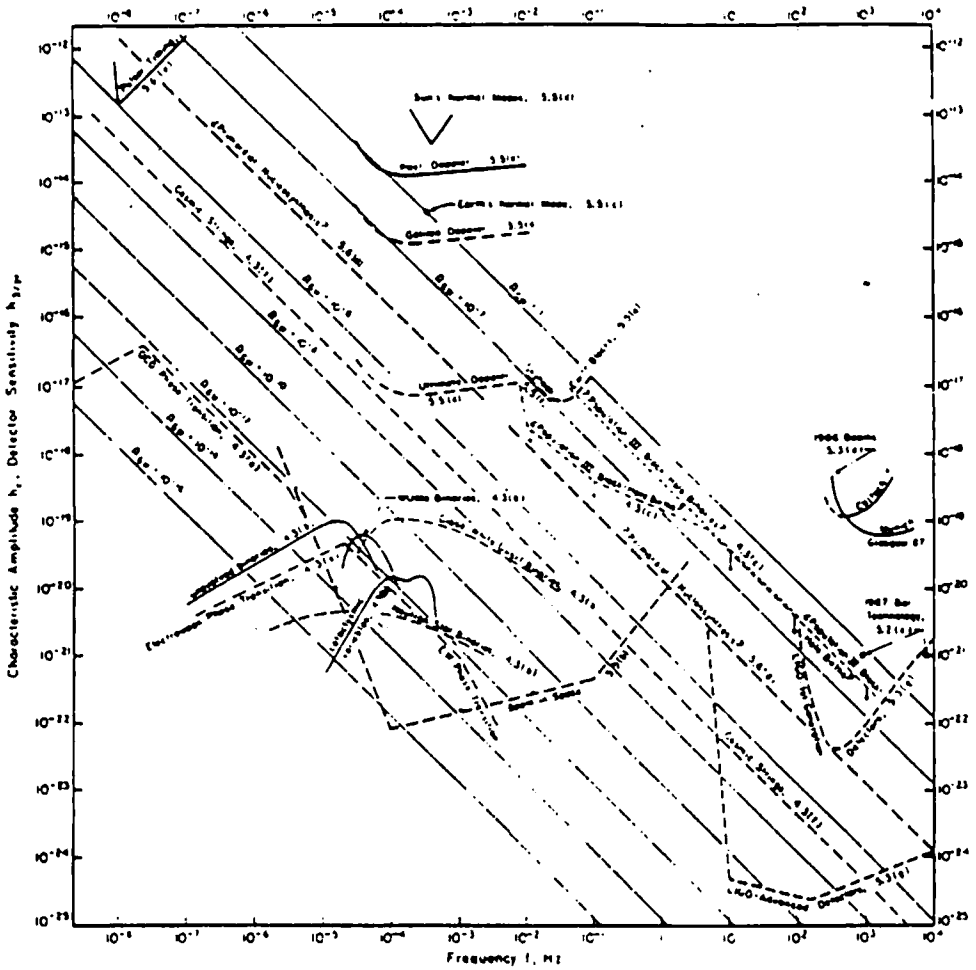

Fig. 2.9 The characteristic amplitudes h_c [Eq. (2.12) or, more precisely, Eq. (9.7)] as a function of frequency f for waves from several postulated *stochastic sources* (thin curves), and the sensitivities $h_{3/yr}$ of several existing and planned detectors (thick curves and circles). [$h_{3/yr}$ is the amplitude of the weakest source that can be detected with 90% confidence in a 1/3 year = 10^7 second integration; Eqs. (9.9), (10.25), (11.16)]. The very thin diagonal lines indicate values of h_c corresponding to constant $\Omega_{GW}(f)$ = (gravity wave energy in bandwidth $\Delta f = f$)/(energy to close the universe). (A Hubble constant of 100 km sec^{-1} Mpc^{-1} is assumed.) The sources shown as solid curves (background from various types of binary stars in our galaxy; Sec. 9.B) are rather firm predictions. The sources shown as dashed and dotted curves are much less firm; see Secs. 9.C–9.F for discussion and references on specific sources. Not shown are primordial waves from the big bang (Sec. 9.D), which could have Ω_{GW} as large as 1 or as small as 10^{-14} or less according to various plausible scenarios – but which are limited by observations as discussed in Secs. 2.E and 12.C. Each detector and source is discussed in detail in the section indicated beside its curve.

integration) is roughly the geometric mean between the burst-wave sensitivity and the periodic-wave sensitivity. This implies that it scales as $[f \times (\text{integration time})]^{-1/4}$. The sensitivity $h_{3/\text{yr}}$ also depends on the band of frequencies (bandwidth) Δf over which the two detectors' outputs are cross correlated; see Eqs. (9.9), (10.25), and (11.16).

Figure 2.9 shows this stochastic sensitivity for the same set of detectors as were discussed in the periodic-wave diagram, Fig. 2.8 - plus three other detectors in the low-frequency and very-low-frequency bands: timing of the "millisecond" pulsar PSR 1937+21 (upper left hand corner of figure; Secs. 2.E and 12.C), and the normal modes of vibration of the sun and the earth (upper middle of figure; Sec. 12.C). For each detector, the $h_{3/\text{yr}}$ shown is based on the largest cross-correlation bandwidth Δf, up to $\Delta f = f$, that is compatible with the detector's design.

Possible sources of stochastic gravitational waves include the following: (i) *The big bang*, whose waves, after amplification by coupling to background spacetime curvature in the very early universe (e.g. during "inflation" of the universe), could have $\Omega_{\text{GW}}(f)$ anywhere from utterly negligible to near unity (Sec. 9.D). (ii) Various vacuum phase transitions in the early universe (Sec. 9.E), of which two are shown: one due to quantum chromodynamic (QCD) forces and the other due to the electroweak force. (iii) Nonsuperconducting cosmic strings produced by phase transitions (Sec. 9.F). (iv) The superposed waves from huge numbers of binary star systems. For binary stars, the solid lines are fairly firm estimates for the waves from established families of binaries, and the dashed lines are estimates for poorly understood families of binaries. Except for the solid-line binaries, all of these stochastic sources in Fig. 2.9 are speculative.

We have already discussed in Part I waves from the big bang (Sec. 1.E) and binary stars (Sec. 2.G). Also of special note are cosmic strings. Such strings are microscopically thin defects in the structure of space, which can reach all the way across the observable universe or can form shorter, closed loops. A string's defect is easily described: The circumference C of any small circle that encloses the string, divided by 2π times the circle's radius r, is not unity as it should be, but instead is slightly less:

$$\frac{C}{2\pi r} = 1 - \frac{4G}{c^2}\mu . \qquad (2.13)$$

here μ is the string's mass per unit length. Most interesting are the

strings that *might* have been produced in the early universe by Grand Unified Theory (GUT) forces. If they exist, they should have $(G/c^2)\mu \sim 10^{-6}$ and defects $C/2\pi r \sim 10^{-5}$. If, moreover, these strings are not superconducting, they ultimately should destroy themselves by vibrating so violently that they break up into closed loops, which in turn vibrate so violently that they radiate themselves away as gravitational radiation. If such strings exist, the gravitational waves from their self-destructing loops should fill the universe with

$$\Omega_{GW} \sim 10^{-4}(Gc^{-2}\mu)^{\frac{1}{2}} \sim 10^{-7} \tag{2.14}$$

at frequencies $10^{-8}\,\text{Hz} \lesssim f \lesssim 10^{4}\,\text{Hz}$. For further details and references see Vilenkin (1987) [KIP: ADD REF] and Sec. 9.F.

The most interesting 1989 limits on stochastic waves come from the timing of pulsars (shown in Fig. 2.9) and from the isotropy of the primordial microwave radiation (not shown because the limits are at frequencies too low to fit onto Fig. 2.9.) Both limits severely constrain the waves produced by the big bang (Secs. 2.E and 12.C). In addition, the pulsar timing limits are almost good enough to confirm or refute the existence of GUT cosmic strings. Future detectors of all types have the prospect of placing interesting limits on stochastic waves. However, because our understanding of stochastic waves is so poor, it is impossible to predict firmly whether anything except binary-star waves will be seen at the projected levels of sensitivity.

For further discussion and references see Chap. 9 and Sec. 12.C.

Lest the reader be lulled, by Figs. 2.7–2.9 and the above discussion, into a false impression that gravitational-wave sources are moderately well understood, I shall reiterate my own view. If I were to make a bet as to what is the strongest source of gravitational waves in the universe, I would bet on none of the sources discussed in this book. More likely is some source that theorists have never yet thought of. I believe we are quite ignorant. Figures 2.7–2.9 give only a *rough* idea of where humans' detectors stand relative to the universe's waves.

3 A Brief History of Gravitational-Wave Research

In this chapter, to set into historical perspective our present understanding of gravitational radiation, I shall sketch the general themes and a few highlights of the history of gravitational-wave research, from Hendrick Lorentz's 1900 speculation that the gravitational force should not propagate faster than the speed of light, up to the 1989 planning for a trans-world network of full-sized interferometric detectors.

3.A Fundamental Theory

In the early 1900's Albert Einstein in Berne, Henri Poincaré in Paris, Hendrick Lorentz in Amsterdam, and others, were struggling to understand the laws that govern electromagnetism and the mechanics of particles moving at high velocities. It was a struggle that would lead to the formulation of special relativity. As part of that struggle, Lorentz (1900) conjectured that gravitation "can be attributed to actions which do not propagate with a velocity larger than that of light". With five years' more insight, Poincaré (1905) argued that all forces of nature, including gravity, should be "invariant under Lorentz transformations", and that correspondingly, there should exist gravitational waves which propagate with precisely the speed of light. He went on to argue (Poincaré, 1908) that as they orbit the sun, the planets of our solar system should emit gravitational radiation; and in

reaction to that emission, the planets should gradually spiral in toward the sun. However, he noted, this effect is much too weak to be detected. (For a more detailed discussion of Poincaré's contributions, see Damour, 1987a).

Poincaré's ideas, like those of the other great physicists in 1905–12, presumed that gravity could be regarded as a field residing in flat spacetime. Albert Einstein and Marcel Grossmann (1913) shattered that view by proposing instead that gravity is a manifestation of spacetime curvature, and that all other forces must be treated as fields which reside in the universe's gravitationally curved spacetime. It required two more years for Einstein (1915) to devise a fully self-consistent and satisfactory theory based on this idea, his general theory of relativity.

Fig. 3.1 [HERE I WANT A PHOTOGRAPH, IF POSSIBLE, OF POINCARE, LORENTZ, AND EINSTEIN TOGETHER; OR OF EINSTEIN AND GROSSMAN; OR OF EINSTEIN ALONE, FROM THE EPOCH 1900–1916]

With general relativity in hand, Einstein began immediately to explore its consequences: the gravitational redshift, the gravitational deflection of light by the sun, the perihelion shift of Mercury's orbit, and — in his seminal paper on the subject (Einstein, 1916) — gravitational radiation. Einstein limited his analysis of gravitational radiation to weak waves propagating in an otherwise flat spacetime, and to the emission of those waves by sources with negligible internal gravity. By doing so, he could expand his general relativistic "metric" $g_{\alpha\beta}$,

which describes distances in curved spacetime, around the metric $\eta_{\alpha\beta}$ of flat spacetime,

$$g_{\alpha\beta} = \eta_{\alpha\beta} + h_{\alpha\beta} , \tag{3.1}$$

and linearize the analysis in the difference $h_{\alpha\beta}$ between the two metrics. The result, in effect, was a treatment of gravity in terms of a field $h_{\alpha\beta}$ that resides in flat spacetime – a return, for approximation purposes, to the viewpoint of 1905–1912. Within this approximation Einstein, in just a few pages, laid the foundations for gravitational-wave theory. However, the details of his calculations contained a severe error which led him to conclude that gravitational waves will be emitted not only by dynamical deformations of a source, but also by the source's spherical motions. Two years later Einstein (1918) corrected his own error and worked out, in his approximation of a linearized $h_{\alpha\beta}$, most of the key features of gravitational waves: (i) the waves' two polarization states, which we now denote h_+ and $h_\times$; (ii) the production of gravitational waves by the dynamical deformations of their source, with no radiation being produced in the case of spherical motions; (iii) the fluxes of energy and momentum carried by the waves (but with a factor 2 error); and (iv) an expression (again with a factor 2 error) for the waves' total energy in terms of the square of the third time derivative of the source's quadrupole moment [Eq. (6.3) below].

During the next few years Weyl (1922), and Eddington (1922, 1924) elaborated on Einstein's initial work. Most notable were two contributions by Eddington: (i) Eddington computed "radiation reaction" (the reaction of the source to its own emission of gravitational waves) in a solid rod that rotates end-over-end. His calculation showed that the rod slows its rotation in reaction to emitting its waves, and its slowdown rate corresponds to a loss of kinetic energy at precisely the same rate that Einstein's formulas predicted energy was going into the waves. (ii) Eddington noted that for a source which, unlike the rotating rod, has internal gravity strong enough to influence its dynamics (e.g. a binary-star system), his linearized analyses, and those of Einstein and Weyl, were invalid.

Even for sources with negligible internal gravity, the Einstein-Weyl-Eddington analyses left one key issue murky: the details of the forces exerted on matter by a passing gravitational wave. Those gravitational-wave forces would not be clearly understood until the late 1950s (see below).

The study of sources with significant internal gravity was tackled in the 1930's by a number of researchers, among them Einstein, Infeld and Hoffman (1938), Levi-Civita (1937), and Fock (1939). Their analyses (building on earlier work of Droste, 1916; De Sitter, 1916; and Lorentz and Droste, 1917) entailed a simultaneous expansion in powers of the deviation $h_{\alpha\beta}$ of the metric from that of flat spacetime, and in powers of the velocities v of the system's bodies divided by the speed of light, v/c – treating $|h_{\alpha\beta}|$ as having the same magnitude as $(v/c)^2$. This expansion was called *post-Newtonian* because at lowest order the resulting formalism coincided with Newton's theory of gravity. The nonlinearites in these post-Newtonian analyses made them enormously more complex than the linearized analyses of Einstein, Weyl, and Eddington.

By the 1940s and 50s special attention was being focussed on the effects of radiation reaction on the evolution of post-Newtonian systems, and especially on the issue of whether two stars in a binary orbit spiral together, and at what rate, in reaction to their emission of gravitational waves. Tedious, complicated calculations by various researchers produced contradictory results: Hu (1947) found an outward spiral of the stars in a binary; Infeld and Scheidegger (1951), Scheidegger (1955), and Infeld and Plebanski (1960) argued for no radiation reaction at all; and Trautman (1958a,b) found an inward spiral, but at a different rate than one would infer from a less sophisticated analysis by Landau and Lifshitz (1941) (see below).

These results profoundly shook Western (and, because of Infeld, Polish) physicists' faith in their understanding of gravitational radiation. Some even questioned whether gravitational waves could be a real, physical phenomenon. Might they be a figment of our misunderstanding of the predictions of general relativity? Even Einstein (1936) fell pray to doubts, briefly. In autumn 1936 he wrote a letter to his friend Max Born saying "Together with a young collaborator, I arrived at the interesting result that gravitational waves do not exist, though they had been assumed a certainty to first approximation" [i.e. to first order in $h_{\alpha\beta}$]. Chandrasekhar (1986) discusses the origin of this remark and Einstein's rapid retraction of it.

In the USSR, isolated from the West by Stalin's "iron curtain", the climate of opinion was different. Lev Davidovich Landau's brilliance and charisma held sway over leading physics researchers. In 1941 Landau and his young colleague Yevgeny Michailovich Lifshitz published the first of a series of textbooks on theoretical physics which

ultimately would influence physicists throughout the world. This first book, *The Classical Theory of Fields* (Landau and Lifshitz, 1941), contained a terse and fairly simple analysis of the emission of gravitational waves by a body with significant self-gravity but slow internal velocities. The conclusion of the analysis seemed unequivocal: the formulas worked out by Einstein (1916, 1918) for the radiation field $h_{\alpha\beta}$ and the energy it carries, when expressed in terms of the source's quadrupole moment, are valid without change. The self-gravity of the source can profoundly affect the dynamical evolution of the quadrupole moment and thence the details of the waves; but the link of the quadrupole moment to the waves is preserved intact.

This conclusion, which was widely accepted by Soviet physicists and was verified in the USSR by Fock (1955) using a more sophisticated analysis, was viewed with caution in the West. The Landau-Lifshitz analysis was far too simplistic for Western taste; it lacked the rigor that was going into the controversial Western calculations. And Western physicists had difficulty seeing the true merits of Fock's analysis, after its translation into English (Fock 1959), because Fock preceded it, at the front of his book, by an ode to Marx and Lenin and he embellished it with clearly false claims that the coordinates which he used ("harmonic coordinates") have special physical significance. [KIP: CHECK IN FOCK'S BOOK] Western angst continued.

Only in the late 1950s and early 60s did Western physicists regain firm faith in gravitational radiation. The keys to the new faith were new viewpoints (see the reviews by Pirani, 1962a,b and in Trautman, Pirani, and Bondi, 1964): In Dublin and London, Felix Pirani (1957) — building on ideas of John Synge (XXXX), André Lichnerowicz (1955), A. Z. Petrov (1954), and others — focussed peoples' attention on the "Riemann curvature tensor" (a precise mathematical embodiment of spacetime curvature) as the key entity in terms of which to describe gravitational radiation. Pirani and others argued that discontinuities in this Riemann curvature tensor describe gravitational waves with arbitrarily short wavelengths, i.e. "gravitational shock waves" (cf. Sec. 5.F); and they showed that these shock waves propagate through curved spacetime with precisely the speed of light.† Most importantly, Pirani introduced an elegant way to describe with confidence the forces

†[KIP: IN SYNGE'S BOOK LOOK FOR A DISCUSSION, POINTED OUT TO ME BY DAMOUR, OF DISCONTINUITIES IN SOLUTIONS OF EFE PROPAGATING ALONG NULL GEODESICS AS HAVING BEEN IDENTIFIED BY VESSIOT (1918, PRELIMINARY ANALYSIS), DEDONDER (1921), DARMOIS (1927), AND STELLMACHER (1937).

exerted on matter by passing gravitational waves. His description, called the "equation of geodesic deviation"(Sec. 4.A below), not only filled in the one gap in the linearized analyses of Einstein, Weyl, and Eddington; it did more. It gave a description of gravitational forces that is valid in the domain of arbitrarily strong gravitational fields as well as for weak, linearized waves.

Building on this, Hermann Bondi (1957) in London devised a simple thought experiment to restore faith in the energy carried by the waves: Put two beads on a rigid stick and let gravitational waves push them back and forth relative to each other, and hence relative to the stick. Friction between the beads and the stick will heat the stick. Where did the energy for that heat come from? It had to come from the waves. Thus, the waves must carry energy. (Actually, Bondi used a "rigid friction disk", but I find it easier to think in terms of a stick.) Turning attention to nonlinear features of the waves, Bondi and his colleagues (Bondi, 1960; Bondi, van der Burg, and Metzner, 1962; Sachs, 1962, 1963; Newman and Penrose, 1962) developed a beautiful mathematical formalism for expanding the gravitational field of an isolated source in powers of 1/(distance from the source), including all nonlinear effects; and Penrose (1963a,b) added rigor and clarity to this expansion by introducing the concept of a "conformal treatment of infinity". This work, followed up in the 1970s and 1980s by many other researchers, has produced an elegant theory of the "asymptotic structure of spacetime" for sources that live alone in an otherwise empty universe (Sec. 4.F; Ashtekar, 1984; Blanchet and Damour, 1986)

Confidence in gravitational waves came also from Choquet-Bruhat's (1950, 1952 [KIP GET REFS FROM SYNGE]) rigorous mathematical proof that there exist exact solutions to Einstein's field equations which exhibit features characteristic of wave phenomena. Further confidence, in the 1950s and 1960s, came from a series of explicit exact solutions to the field equations, including (i) special solutions describing gravitational waves in all their nonlinear glory propagating through vacuum spacetime (e.g. Rosen, 1937; Einstein and Rosen, 1937; Bondi, Pirani, and Robinson, 1959; and other references in Sec. 5.F), and (ii) special solutions describing highly idealized sources that emit radiation into an otherwise empty universe (e.g. Robinson and Trautman, 1962; Bičak, 1968; and other references in Sec. 5.F).

Additional understanding and confidence came from Wheeler's (1955) and Power and Wheeler's (1957) insight that, when gravity is nonlinearly strong, one should identify as gravitational waves ripples of

spacetime curvature that have wavelengths short compared to the "background curvature" on which the ripples propagate. Such waves are similar to gravitational shocks, but with wavelength increased from zero to a finite but small size. To make their ideas quantitative, Wheeler and Power introduced a "two-lengthscale expansion" technique (also called "shortwave expansion") in which the spacetime metric $g_{\alpha\beta}$ was expanded in the dimensionless ratio (reduced wavelength of waves, λ)/(inhomogeneity lengthscale of background spacetime, $\mathcal{L}$). In the hands of two of Wheeler's students, Brill and Hartle (1964), and most especially in the hands of Isaacson (1968a,b; see also Choquet-Bruhat, 1964 and 1969), this shortwave expansion produced an elegant and appealing description of gravitational waves, a description appropriate to the real universe in which we live (Chap. 5 below).

In the 1940s and 50s, when the post-Newtonian, radiation-reaction calculations of Infeld and colleagues were giving unexpected and contradictory results, people began to question the Einstein (1916, 1918) and Landau-Lifshitz (1942) descriptions of the energy and momentum carried by a weak gravitational wave. [KIP: GIVE REFS.] Those descriptions relied on a mathematical object, called the "energy-momentum pseudotensor", whose physical interpretation was ambiguous: When one made infinitesimal changes in the coordinate system (gravitational analog of an electromagnetic "gauge transformation"), this pseudotensor changed its description of where a wave's energy was located: the energy could be moved, at will, from the crests of the wave, to its troughs, to in between. In other words, the distributions of energy and momentum in a gravitational wave were gauge-dependent. How awful! Moreover, the pseudotensors used by Einstein and by Landau and Lifshitz were different. In fact, Goldberg (1958) was able to show that there exist an infinite number of different energy-momentum pseudotensors, and that there is no obvious way to choose between them. This reinforced peoples' worries, in the 1950s, that gravitational waves were not being understood at all correctly.

Confidence began to return when Pirani (1957) exhibited a unique, gauge-invariant energy-momentum tensor (*not* pseudotensor) for waves of arbitrarily short wavelength, i.e. for gravitational shockwaves. And full understanding came when Isaacson (1968b) exhibited a unique, gauge-invariant energy-momentum tensor $T^{GW}_{\mu\nu}$ for waves of short but finite wavelength, $\lambda \ll \mathcal{L}$ – an energy-momentum tensor that "lives" in the background spacetime through which the waves

propagate (Sec. 5.C). Isaacson's $T^{GW}_{\mu\nu}$ did not attempt to localize the energy and momentum more finely than a wavelength; such localization has turned out to be impossible — one cannot say definitively whether the energy is in the wave's crest or its trough or in between. Instead, Isaacson's $T^{GW}_{\mu\nu}$ entailed an averaging (smearing) of the energy and momentum over a few wavelengths. Remarkably, this $T^{GW}_{\mu\nu}$ could be derived not only from "first principles"; one could also derive it by smearing over several wavelengths the Landau–Lifshitz energy–momentum pseudotensor, and other pseudotensors. The smearing removed the gauge–dependence from the waves' energy and momentum, making them fully respectable.

The confusion over radiation reaction has also abated, gradually, over the years since 1958. A first key step was Trautman's (1958a,b) realization that the post–Newtonian calculations of Hu, Infeld, and Scheiddeger were giving peculiar and conflicting results because of a failure to impose an outgoing–wave boundary condition far from the source. Although this failure might sound stupid to a sophisticated physicist, it was far from stupid. Post–Newtonian expansions are confined to the source's "near zone"; they lose their validity in the radiation zone (at radii $r \gtrsim \lambda$), so making sure that the expansions joined onto outgoing waves, and not onto standing or ingoing waves, was a very tricky task. Trautman formulated the outgoing–wave boundary condition properly, but made a small error in his calculations and got the wrong answer for the radiation reaction. Thus, in my opinion the credit for the first correct calculation goes to Peres (1960), rather than to Trautman. However Peres, too, can be criticized, as can be the many other analyses that were published between 1960 and the late 1970's; see, e.g., page 74 ff. of Damour (1983), and see below.

Greater rigor than that of Trautman and Peres became possible when Burke (1969) introduced into general relativity a new mathematical technique called "matched asymptotic expansions" (a technique that was just then gaining popularity in applied mathematics; see Cole, 1968). This technique gave a beautiful, simple, and reliable way of imposing Trautman's outgoing–wave boundary condition in a post–Newtonian expansion (Burke and Thorne, 1970). Its application produced not only a set of new, more satisfactory derivations of the radiation–reaction quadrupole formulas, but also the discovery of an elegant and simple, Newton–like "radiation–reaction potential" for describing the radiation–reaction forces in weakly gravitating systems (Burke 1969, 1971; Thorne 1969a; Burke and Thorne, 1970;

Chandrasekhar and Esposito, 1970; Sec. 6.B below). An additional improvement in rigor came from the realization that the correct boundary condition is not quite Trautman's outgoing-wave one, but rather a "no-incoming-wave" condition first introduced by Fock (1955) but largely ignored in the West until the mid 1970s. The difference between the two conditions becomes clear when one uses Penrose's (1963a,b) conformal description of infinity: Trautman's outgoing-wave condition is posed at "future null infinity", while Fock's no-incoming-wave condition is posed at "past null infinity".

In 1969, while thinking about the generation of gravitational waves in the language of matched asymptotic expansions, I came to the intuitive conclusion that weak internal gravity, $|h_{\alpha\beta}| \ll 1$, was totally irrelevant for the validity of the Einstein-Landau-Lifshitz quadrupole formulas; the sole key to those formulas was slow internal motion, $v/c \ll 1$. As a first test of this intuition, Ipser (1970) was able to prove that the quadrupole formulas are valid for the special case of a slowly rotating, non-axisymmetric neutron star. This motivated me, during the 1970s, to develop tools for studying general systems with arbitrarily strong gravity but slow internal motions (Thorne, 1980b). The most important tool was a multipole-moment formalism (based on earlier work of Bonnor, 1959, Pirani, 1964 and others). Using this formalism, I was able to give a proof that the quadrupole formulas are, indeed, valid for systems with arbitrarily strong gravity but slow internal velocities (Thorne, 1980b; Chap. 6 of this book; see also the discussion in Sec. 4 of Damour, 1987a).

In the mid and late 1970s, in response to assertions by me and others that gravitational radiation reaction was reasonably well understood, Ehlers et. al. (1976) produced a list of pitfalls that plagued all derivations of the quadrupole formulas; Walker and Will (1980) produced a list of mathematical errors in many of the derivations (including an error in the derivation that I wrote for MTW); and the Walker-Will list of errors was extended by Damour (1983) and by Blanchet and Damour (1984). The "quadrupole controversy" was thereby reignited; and it has continued to burn brightly until recently. It seems to me that the bottom-line answer was not in doubt: the standard formulas are valid. However, the controversy has been healthy in that it has produced a deeper understanding of radiation reaction and a series of powerful new tools that will be useful in future research. For examples of elegant, new derivations or explications of the quadrupole formulas, see the following references: Kerlick (1975); Anderson and

DeCanio (1975), Anderson (1980, 1987); Walker and Will (1979); Schutz (1980), Schutz and Futumase (1983), Futumase (1983, 1985, 1987), Futumase and Schutz (1985); Damour (1983); Isaacson, Welling, and Winicour (1985); Winicour (1987a,b); and Grishchuk and Kopeikin (1986). For detailed reviews of the quadrupole controversy see Ehlers (1979), Havas (1979), Ehlers and Walker (1984), Walker (1984), Will (1986a), Damour (1987a), and Schutz (1987b).

The issue of radiation reaction became a very practical one with the discovery of the binary pulsar PSR1913+16 by Hulse and Taylor (1975) and the measurement of its inspiral in reaction to emitting gravitational waves (Fig. 1.1). Because the duration of observations of the pulsar is short (12 years), the cumulative effects of radiation reaction on the orbit during those observations are 100 times smaller than the quadratic order, $O[(h_{\alpha\beta})^2]$, post-Newtonian effects. Consequently, the detailed effects of the radiation reaction could not be fully disentangled from non-radiation-reaction effects until the orbital equations were fully under control up through cubic, i.e. "post-post-Newtonian" order. Damour and Deruelle (1981, 1986) and Damour (1983a,b) have now brought the orbital equations fully under control; and there is a beautiful agreement between those equations — including the quadrupolar radiation reaction — and the observational data. For a detailed discussion see XXXX.

The foundations for gravitational radiation theory were fully laid by the early 1970s, but only the foundations. Extensive work by many researchers has been required to fill in the details of the theory, and that filling-in even now is not complete. We shall encounter many of the filled-in details in this book. For reviews of others see, e.g., XXXXXX.

[KIP: NOTE THAT HAVAS (1959), HAVAS AND GOLDBERG (1962), AND SMITH AND HAVAS (1965) ARE NO LONGER REFERRED TO. REINSERT THEM SOMEWHERE? DAMOUR SUGGESTS IN THE SAME PASSAGE AS ARE DISCUSSED SCHEIDEGGER AND HU. ALSO, CROSS REFERENCES TO PART 2 OF THE BOOK SHOULD BE INSERTED INTO THE ABOVE SECTION.]

3.B Wave Detection and Astrophysical Theory

The experimental search for gravitational waves was initiated by Joseph Weber (1960) at a time when almost nothing was known about astrophysical sources and nobody else had the vision to see that there were technological possibilities of ultimate success. Weber invented the resonant-bar detector, and developed it with vigor through the

1960s, including a transducer for measuring the bar's vibrations based on piezoelectric crystals. These crystals, glued around the side of his bar, were squeezed by the bar's vibrations, and when squeezed, produced voltages that could be amplified and measured; see Fig. 3.2. In parallel, and at a lower level of effort, Weber invented the idea of using the earth's vibrations as a detector for low-frequency waves and with colleagues developed the first instrument for this purpose (Forward et. al., 1961); and he invented but did not publish the basic idea of a laser-interferometer (interferometric) detector for gravitational waves.† Weber was a lonely figure: aside from coworkers in his own laboratory, only one other experimenter in the world took much interest in gravitational-wave detection — Vladimir Braginsky (1965) in Moscow, who, motivated by Weber's earliest publications, began exploratory experiments on wave-detection techniques.

Fig. 3.2 Joseph Weber with one of his original bar detectors for gravitational radiation, at the University of Maryland in 196XXX. Weber is inspecting the piezoelectric crystals, glued around the bar, which he used as transducers to monitor the bar's vibrations. [KIP: WRITE TO JOE FOR FIGURE; IT APPEARS, E.G., IN "GRAVITY, BLACK HOLES, AND THE UNIVERSE" BY IAN NICHOLSON WHO CITES IT AS COURTESY J. WEBER]

†Weber's 1964 concept of an interferometric detector had a single arm rather than two arms in the shape of an L. The separation between suspended masses at the ends of the arm would be monitored by making them the mirrors of a Fabry-Perot interferometer. Weber described this idea to Robert L. Forward by telephone on 13 September 1964, and Forward recorded it in his journal for that day (Forward, 1964).

After a decade of effort, Weber (1969) announced to the world tentative evidence that gravitational waves were exciting his resonant-bar gravity-wave detectors, one at the University of Maryland and the other at Argonne National Laboratory near Chicago. There followed a six-year period of excitement and feverish effort as many other research groups around the world constructed and operated similar, but not identical bar detectors. Braginsky et. al. (1972, 1974) in Moscow were the first — with negative results. Then came detectors and gravity-wave searches in America: at IBM by Levine and Garwin (1973, 1974) and Garwin and Levine (1973); at Bell Telephone Laboratories by Tyson (1973); and at the University of Rochester, jointly with Bell Laboratories, by Douglass et. al. (1975). Simultaneously detectors were developed and operated in Britain: at Glasgow University by Drever et. al. (1973, 1974) and Hough et. al. (1975); and at Reading University and the Rutherford Laboratory by Allen and Christodoulides (1975). In these British experiments the piezoelectric crystals were glued between two bars so as to give stronger coupling to the bars and much widened bandwidth, a technique invented at Bristol University by Peter Aplin (1972) and analyzed theoretically by Gibbons and Hawking (1971), Maeder (1974), and Buckingham and Faulkner (1973). There were also bars and experiments on the Western European continent: at Meudon France by Bonazzola et. al. (1974); at Frascati Italy by Bramanti, Maischberger and Parkinson (1973), and Maischberger (1974); and at Munich Germany by Billing et. al. (1975) and Billing and Winkler (1976).

While some of these groups occasionally saw statistically significant, coincident excitations between two independent detectors, as more data were collected the statistical significance went down. By 1975 there was general agreement that this massive experimental effort had produced no convincing evidence for gravitational waves. For detailed reviews of these first-generation bar experiments from several different viewpoints see de Sabbata and Weber (1977), Drever (1977), Tyson and Giffard (1978), Amaldi and Pizzella (1979), and Weber (1986).

The most extensive second-generation gravitational-wave search was that of the Munich-Frascati collaboration (Billing et. al., 1975; Kafka and Schnupp, 1978). In this search data were collected for 580 days using two nearly identical detectors with sensitivities $h_{3/\mathrm{yr}} = 3\times10^{-16}$. The strongest signal that these detectors saw in coincidence during that time had a characteristic amplitude within a few tens of per cent of their "3/yr" sensitivity, $h_c \simeq h_{3/\mathrm{yr}} = 3\times10^{-16}$. This is

about what one would expect from the Gaussian noise of the cross-correlated detectors. [KIP: CHECK AGAINST THE AMALDI PIZELLA REVIEW; ALSO, WHAT WAS THE ROCHESTER-BELL SENSITIVITY? ALSO, HAVE I TRANSLATED THEIR 5 GPU CORRECTLY?]

Motivated by these experimental efforts and by the discovery of the primordial microwave radiation (Penzias and Wilson, 1965, and Dicke et. al., 1965), relativity theorists in the late 60s and 70s invented techniques for seeking low-frequency and very-low-frequency gravitational waves: measurement of the anisotropy of the primordial microwave radiation (Sachs and Wolfe, 1967 and Dautcourt, 1969) and timing of pulsars (Sazhin, 1978 and Detweiler, 1979). Experimenters implementing those techniques have produced powerful limits on the strengths of the waves bathing the earth; see Secs. 2.D, 2.E, 2.H, 12.B, 12.C.

Also motivated by the bar detection efforts, astrophysicists worldwide struggled through the 1970s to milk, from electromagnetic observations of the universe and from fundamental theory, as much information as possible about the characteristics of the gravity waves that might be bathing the earth. By the mid-1970s a fuzzy but helpful picture had begun to emerge: While the detectors' sensitivities to kilohertz-frequency bursts arriving three times per year from random directions had improved during the early 70s from $h_{3/\mathrm{yr}} \simeq 1\times10^{-15}$ to $h_{3/\mathrm{yr}} \simeq 3\times10^{-16}$ (a factor 10 improvement in energy flux), it seemed highly unlikely that such bursts bathing the earth would exceed $h_{3/\mathrm{yr}} \sim 1\times10^{-16}$ (the "cherished beliefs" level of Fig. 2.7); a reasonable probability of success would require $h_{3/\mathrm{yr}} \sim 10^{-20}$ or better; and a high probability would require $h_{3/\mathrm{yr}}\sim10^{-21}$ to $h_{3/\mathrm{yr}}\sim10^{-22}$ (Epstein and Clark, 1979; Fig. 2.7 above). Although these estimates were discouraging, the theoretical efforts that produced them revealed the enormous potential payoff that could follow the successful detection of gravity waves.

Fortunately, the experiments of the early 1970s had pointed the way toward major possible improvements in bar detectors. Consequently, although many of the first-generation bar groups became discouraged and dropped out, some pushed onward into more sophisticated and sensitive, second-generation efforts: at Maryland, Weber (1977, 1983) and colleagues (Paik, 1980; Davis and Richard, 1980; Carroll et. al., 1986); in Moscow, Braginsky (1977, 1983) and colleagues; and at Rochester, Douglass et. al. (1982). These older groups were joined in the second-generation effort by several new research groups: at Stanford and Louisiana State University (LSU), Fairbank et. al. (1974,

1986) and Hamilton (1977, 1983); at the University of Rome, Amaldi and Pizzella (1975) and Amaldi et. al. (1986); at the University of West Australia in Perth, Blair (1980) and Veitch et. al. (1987); at Tokyo University, Hirakawa et. al. (1975, 1976, 1985); and at Regina, Canada, Strayer et. al. (1982). More recently, as China began recovering from the Cultural Revolution, bar detector efforts were mounted in Guangzhou and in Beijing (see Hu et. al., 1982; and Hu En Ke et. al., 1986); and in the meantime, the Regina group has left the field.

This second-generation effort has involved major technological changes, such as: (i) cooling the bars to liquid-helium temperatures to reduce their internal, frictional ("thermal") noise (initiated in 1970 at Maryland by Weber, see Weber, 1977, and in XXXXX at Stanford by Fairbank and Hamilton, see Fairbank et. al., 1974); (ii) changing to new bar materials that have much lower thermal noise (sapphire and silicon monocrystals initiated in Moscow by Braginsky, 1974; a aluminum alloy found in Tokyo by Suzuki, Tsubono, and Hirakawa, 1978; and superconducting niobium initiated in Perth by XXXX); and (iii) switching from piezoelectric transducers for monitoring the bar's vibrations to new, more sensitive transducers. These new transducers include: (a) a transducer in which the bar's vibrations modulate the capacitance of a cavity filled with microwave radiation, thereby moving microwave quanta in the cavity from one frequency to another (first developed in Moscow by Braginsky, 1974, see Fig. 2.3b; now used by the Moscow group and in other variants by the LSU and Perth groups); (b) a transducer in which the bar's vibrations deform a charged capacitor, thereby modulating the electrical energy in it and the voltage across it (also invented in Moscow by Braginsky et. al., 1972, and now used by the Rome group (Rapagnani, 1982) in a more sophisticated variant where the capacitor is a mechanical oscillator that is driven by the bar's vibrations); and (c) a transducer in which the bar's vibrations modulate the inductance of a superconducting coil of wire, thereby modulating the voltage across the inductance (first developed at Stanford by Paik, 1976, and now used at both Stanford and Maryland; Fig. 2.3a). At Stanford and Maryland techniques have been developed to mechanically amplify the bar's vibrations before they modulate the transducer (Paik, 1976; Richard, 1979, 1984, 1986); and all of the groups have developed or adopted new, lower-noise electronic amplifiers for the outputs of their transducers. Many other important techniques have been devised and implemented, but those mentioned are enough to give some feeling for the innovations. For further discussion see Sec. 10.D.

This second-generation bar effort reached partial fruition in January 1981 with the succesful operation of the Stanford cryogenically cooled bar (Boughn et. al., 1982). The bar's noise amplitude, $h_n^{opt} \simeq 4\times10^{-18}$ [KIP: CHECK - I NOW COMPUTE 1.5X10^-18 USING INTSIGMADF OF 1.5X10^-20 AND TN OF 20 MK] was a factor ten better than the best first-generation bars and would have corresponded to $h_{3/yr} \simeq 4\times10^{-17}$ had there been another cold bar with which to cross correlate. Unfortunately, there was none, and the room temperature bars still operating in Maryland and elsewhere, with their worse noise, were of little use as "mates" for Stanford. There was no way to know whether the occasional, unexpected excitations of the Stanford bar were due to gravitational-wave bursts or to non-Gaussian internal noise. The bar was beautiful to contemplate, but without a mate could do little real science.

For nearly five years the other research groups struggled with their cold bars (the intended mates for Stanford), trying to make them work, but to no avail. Each cycle of cooling down a bar to several degrees above absolute zero, running it and finding problems, warming up, fixing the problems, and beginning the next cooldown typically required a year or more. Each cycle brought new, unexpected difficulties. In the meantime, the Stanford experimenters improved to $h_n^{opt} \simeq 1\times10^{-18}$.

Finally in November 1985 the Rome bar (now moved to CERN near Geneva) began to work (Amaldi et. al., 1986) with slightly better performance than Stanford's best, and in 1986 the Louisiana bar worked, though with somewhat worse performance. At last, science could be done. The Gravnet network of bar detectors was established (Blair, Frasca, and Pizzella, 1988a,b); and gravitational-wave searches were carried out in earnest through the spring and summer of 1987 and then again in 1988 and 1989, with the expected result (Amaldi et. al., 1988): The excitations were internal noise; there was no sign of waves.

As this book is being completed (summer 1989), second-generation gravitational-wave observations continue; and in parallel the bar detector groups are planning, designing, and beginning to construct a third generation of bar detectors (Aguiar et. al., 1989; Aldcroft et. al., 1989; Amaldi et. al., 1989; Richard, Pang, and Hamilton, 1989). This new generation will entail cooling the bars to temperatures of 0.05 K or less; constructing new, improved transducers; and improvements in amplifiers. The sensitivity goal of these antennas, $h_n^{opt} \sim 10^{-20}$ may well be achieved by the mid 1990s.

For further detail on the second-generation bar detectors and their gravitational-wave searches and on the third-generation efforts, see Sec. 10.D.

On 23 February 1987, a supernova exploded in the Large Magellanic Cloud, one of the two nearest galaxies to our own. Unfortunately, at the time of the supernova all the world's second-generation bar detectors (and all the world's interferometric detectors as well) were turned off for improvements. The only gravitational-wave detectors in operation were two first-generation, room-temperature bars, one at the University of Rome and the other at the University of Maryland. Amazingly, these two detectors showed excitations, near the time of the supernova, that were correlated with each other and were strongly correlated with the times of neutrino "events" in neutrino detectors that monitored the supernova (Aglietta et. al., 1989; XXXXX [KIP ADD REFS ON KAMIOKA AND IMB]).

Conventional physics and astrophysics, in which I strongly believe, insist that these correlated events *cannot* have been gravitational waves and neutrinos from the supernova: (i) The conventional theory of the sensitivity of bar detectors (chap. 10), combined with the observed levels of excitation and the distance to the supernova, imply that, if the bar detectors' events were gravitational waves from the supernova and if the supernova emitted its waves isotropically, then the wave energy carried by each event was $2400\, M_\odot c^2$ (Aglietta et. al., 1989). Since the exploding star had a mass no larger than $\sim 20\, M_\odot$, this conclusion is a severe violation of the conservation of energy. (ii) The correlations with the Mont Blanc neutrino detector involve thirteen neutrino events spread over a time interval of 2 hours 37 minutes; and the end of this interval *preceeded*, by XXXXXXXX, the coincident bursts of neutrinos observed by the Kamiokande and IMB detectors. The Kamiokande and IMB neutrino bursts were in excellent accord with the standard theory of supernovae (XXXXXXREF). According to that theory, they were emitted during the first one second of the life of the newborn neutron star; and standard theory insists that there should have been a single gravitational wave burst, at the beginning of that one second interval. Standard theory has no place for thirteen neutrino bursts spread over some hours and occuring some hours before the neutron-star birth, nor for ultrastrong gravitational wave bursts accompanying those neutrino bursts.

Several years before the supernova, Weber (1984, 1986) published a new, unconventional theory of the sensitivities of bar detectors. This new theory predicted energy sensitivities that were larger by a factor $\sim 3\times10^6$ (detector noise levels $h_n^{\rm opt}$ and $h_{3/\rm yr}$ smaller by $\sqrt{3\times10^6}$) than conventional theory predicts. If Weber's new theory were correct, then each bar excitation would correspond to only $0.001\,M_\odot c^2$ rather than $2400\,M_\odot c^2$. However, I (and other experts on gravitational wave theory with whom I have discussed it) strongly disagree with the premise that underlie's Weber's new theory. We are convinced that the original, classic theory of bar detectors, as developed long ago by Weber himself (Weber, 1960), is the correct theory; see Sec. 10.XXXX. Correspondingly, we are deeply puzzled by the 1987 observations. Either there is some sort of earth-generated background, which excited both the neutrino detectors and the gravitational-wave detectors during the 2 hour 37 minute interval but has not excited them at other times (this would be rather surprising), or something is wrong with the data analysis (this seems unlikely), or some sort of completely new, unconventional physics is involved (this seems very unlikely).

The germ of the idea of a laser-interferometer gravitational-wave detector ("interferometric detector") can be found in Pirani (1956), but — so far as I am aware — the first explicit suggestion of such a detector and rough estimates of its sensitivity were made by Gertsenshtein and Pustovoit (1962). In 1964 Joseph Weber, unaware of the Gertsenshtein-Pustovoit work, reinvented the idea in primitive form, but left it lying in laboratory notebooks unpublished and unpursued. In 1969 Rainer Weiss at MIT, unaware of Gertsenshtein-Pustovoit or Weber, reinvented the idea in a much more detailed and sophisticated form and carried out a thorough design and feasibility study (Weiss, 1972) in which many of the techniques now being used were conceived. Unfortunately, Weiss was unable to obtain funding to mount a significant experimental effort.

Robert Forward at Hughes Research Laboratories in Malibu, California, having learned the concept of the interferometric detector from Weber (his former thesis advisor), was motivated indirectly by Weiss in 1969 to construct a prototype detector with funding from Hughes. By 1972 Forward and his colleagues at Hughes were operating the world's first prototype interferometric detector — an instrument that demonstrated the idea could really work, and that had remarkably good sensitivity considering the modest effort put into it:

$h_{3/yr} \simeq 1\times10^{-13}$ for 2500 Hz bursts (Moss, Miller, and Forward 1971; Forward and Moss 1972; Forward 1978). Regretably, Forward could not obtain funds to move from this first prototype to a more sophisticated instrument, and his project was shut down.

With the completion of the first-generation gravity-wave searches in the mid 1970s, each experimental group that decided to stay in the field looked carefully at a variety of possibilities for sensitivity improvement. While most groups decided to stick with bars, two switched to interferometric detectors: Munich, led by H. Billing, and Glasgow, led by Ronald Drever with Jim Hough second in command. The Munich group, motivated by the success and performance of the Hughes-Laboratory prototype, initiated their switch in 1974. The details of their design (Winkler, 1977) were strongly influenced by a proposal to develop interferometric detectors that Weiss submitted to NSF in the mid 1970s, and that NSF refused to fund. Most notably, they adopted Weiss's many-bounce "Michelson-interferometer" design (also called "delay line") — the design described above in Figs. 2.1 and 2.2. The Glasgow group initially built a small Michelson interferometer (Drever *et. al.* 1977), then because of problems with scattering of light inside the Michelson (discovered by the Munich group, Billing et. al., 1978, and confirmed by Glasgow) and a desire to use smaller mirrors, Glasgow switched to a new "Fabry-Perot" design invented by Drever (Drever *et. al.* 1980). See Sec. 9.B for details.

In 1979 Drever moved from Glasgow to Caltech (part time at first, full time later), leaving Hough as the Glasgow leader. At Caltech, Drever started up an interferometric-detector project; and NSF, finally recognizing that interferometric detectors were worth funding, agreed to support both Weiss at MIT to develop his original idea of a Michelson system and Drever at Caltech to develop his Fabry-Perot system. For eight years the Caltech and MIT groups operated in partial competition and partial cooperation with each other. Then, in 1987, they firmly united with each other under the leadership of Rochus Vogt, a cosmic-ray physicist and former Chief Scientist at JPL; and they selected the Fabry-Perot design for their first full-scale detector.

More recently, in 1983, Alain Brillet initiated an interferometric-detector effort in Orsay, France (Brillet and Tourrenc 1983; Brillet, 1985); in 1985 a group in Italy, led by Adalberto Giazotto, embarked on the development of antiseismic isolation for interferometric detectors (Giazotto et. al., 1986); and in 1986 the French and Italian groups joined forces in a united interferometric effort (Giazotto et. al., 1987).

The Japanese have also become convinced that interferometric detectors deserve vigorous development. The Japanese effort was initiated in 1986 by Nabuki Kawashima at the Institute for Space and Astronautical Sciences (ISAS) in Tokyo (Kawashima et. al., 1989); and more recently it has been expanded into a collaboration of a number of different Japanese research groups under the leadership of S. Hayakawa (Tsubono, 1989).

Soviet scientists developed an interest in interferometric detectors quite early; but their road toward a working detector has been a rocky one. The first Soviet interferometric effort was initiated in 1975 by a theorist, Erast Gliner, of the Ioffe Physico-Technical Institute in Leningrad (XXXXXXXXX), with participation by experimenters from Ioffe, from the Vavilov Optical Institute in Leningrad, from the Schmidt Institute of Earth Physics in Moscow, and from the Baksan Neutrino Laboratory. This initial effort was poorly funded — in large part, some of the participants think, because of the demands of the war in Afghanistan. Later, after Gliner emigrated to America, portions of this effort were taken over, with an enormous but temporary increase in funding, by a group at the State Committee on Standards in Moscow (Belousova et. al., 1983). The healthy funding lasted for several years then died, and the project went into decline. Most recently, in 1988, the project (including a 75-meter one-arm prototype interferometer at the Baksan Neutrino Observatory in XXXXcentral AsiaXXXXX) has been taken under the wing of the Shternberg Astronomical Institute in Moscow, with participation also by the State Optical Institute in Leningrad (Rudenko and Grishchuk, 1988).

The most recent entry into the field is Australia: In 1988 the Australian bar detector group decided to embark on a major interferometer effort (while *not* shutting down their bar effort); and they enlisted the collaboration of a number of other Australian research groups. Detailed plans for a full-scale Australian interferometer are now being developed under the joint leadership of Hans Beckel [KIP CHECK SPELLING] of the Australian National University in Canberra, and David Blair of the University of West Australia in Perth.

Thanks, in part, to the rapid cycle for each modification and test of an interferometric detector (as little as one day, since no bar-like, months-long cooldown and warmup is involved), interferometric detectors have improved far more rapidly than bars in the 1980s. The curves in the upper right-hand corner of Fig. 2.7 show the detectors' several-hundred-fold improvements in $h_{3/\mathrm{yr}}$. These improvements

have been achieved by extensive changes of design, made one after another as old problems were solved and new ones identified. See Chap. 11 for some details.

At this writing (summer 1989) the Munich group, the Glasgow group, and the Caltech/MIT group all are operating interferometric detectors with amplitude sensitivities ~2000 times better than that of Forward's first interferometer but ~3 times worse than the best bars. These detectors are small-scale (10 to 40 meter) prototypes for the full-scale (several kilometer) interferometric detectors that will be required for real success.

In 1981–3 the MIT group carried out a detailed design and feasibility study for full-scale detectors (Linsay et. al. 1983). The results were sufficiently promising to engage the vigorous interest of the U.S. National Science Foundation and to trigger a series of follow-on studies and proposals for full-scale systems in America (Drever et. al., 1985; Vogt et. al., 1987, 1989); in Europe (Maischberger et. al., 1985; Winkler et. al., 1986; Hough et. al., 1986; Leusch et. al., 1987; Giazotto et. al., 1987); in Australia (XXXXXXXXXX); and in Japan (XXXXXXXXX). The costs turn out to be far higher than for bar detection systems: 50 million dollars or more for the vacuum system and facilities at one site. However, once the facilities are built they can be used for many generations of interferometric detectors over tens of years, each detector costing several million dollars. Because of the large cost of the facilities, to move forward with full-scale interferometric detectors requires major commitments from funding agencies and the scientific community. If those commitments are made (none have been firmly made at the time of this writing, summer 1989), then a network of several full-scale interferometric detectors may be operating by the mid 1990s, with sensitivities in the region where gravity waves are expected.

During the late 1960s only Weber at Maryland and Braginsky in Moscow were working seriously on gravitational-wave detection. While the poor technological base of the Soviet Union made it difficult (but not impossible!) for Braginsky to compete with Western experimenters, his ingenuity made him a rich source of ideas that others could follow up. One such idea was the use of spacecraft doppler-tracking data for gravitational-wave searches (Braginsky and Gertsenshtein, 1967) – an idea that NASA has pursued with vigor and effectiveness since the mid 1970s (Sec. 12.B), but the Soviets with their poorer tracking accuracies have not attempted. Another was Braginsky's (1967, 1970) discovery

that the laws of quantum mechanics place worrisome limits on the sensitivities of gravitational-wave detectors (and other high-technology instruments), and his demonstration that, with clever changes of measurement strategy, one can circumvent those quantum limits (Braginsky and Vorontsov, 1974). "Quantum nondemolition" and "quantum measurement" techniques, invented by various people following up on Braginsky's seminal work, may play important roles in the gravitational-wave detectors of the 1990s and the 21st century (see Secs. 10.F and 11.E); and they are likely to be important in other branches of science and technology as well.

In parallel with the second-generation experimental efforts, theorists have redoubled their struggle to firm up their understanding of the waves bathing the earth, but with only modest success: The problem of knowing what kinds of sources actually occur and how frequently is hung up on a paucity of electromagnetic information. As a result, apparent recent improvements in our knowledge (e.g. theorists' discoveries of the possibilities of cosmic strings, phase transitions, and inflation in the early universe, Secs. 2.E, 2.H, 9.D–9.E) might be little more than changes of fashion. On the other hand, given a specific scenario for how a postulated source behaves, theorists have become far more adept than before — thanks not least to supercomputers — at computing the details of the gravitational waves it should emit (Chap. 6 below). As a consequence, when waves are ultimately detected, the prospects will be good for deciphering from them the details of their sources.

While the present, second-genration, gravity-wave searches might bring success, it is not likely they will. Thus, we must anticipate a continued vigorous effort at technology development during the coming years, with the prospects of success improving at each step along the way. In parallel, we must anticipate a continuing major effort by relativity theorists to refine their ability to decipher from measured waveforms the details of the source that produced them, and a continuing effort by astrophysicists and theoretical physicists to give better guidance as to what kinds of sources actually exist and in what numbers. The efforts will be considerable, but jointly they may bring an extremely valuable payoff.

GRAVITATIONAL RADIATION

A New Window onto the Universe

by Kip S. Thorne

draft of 16 September 1989

California Institute of Technology

1989

Part II
Theory

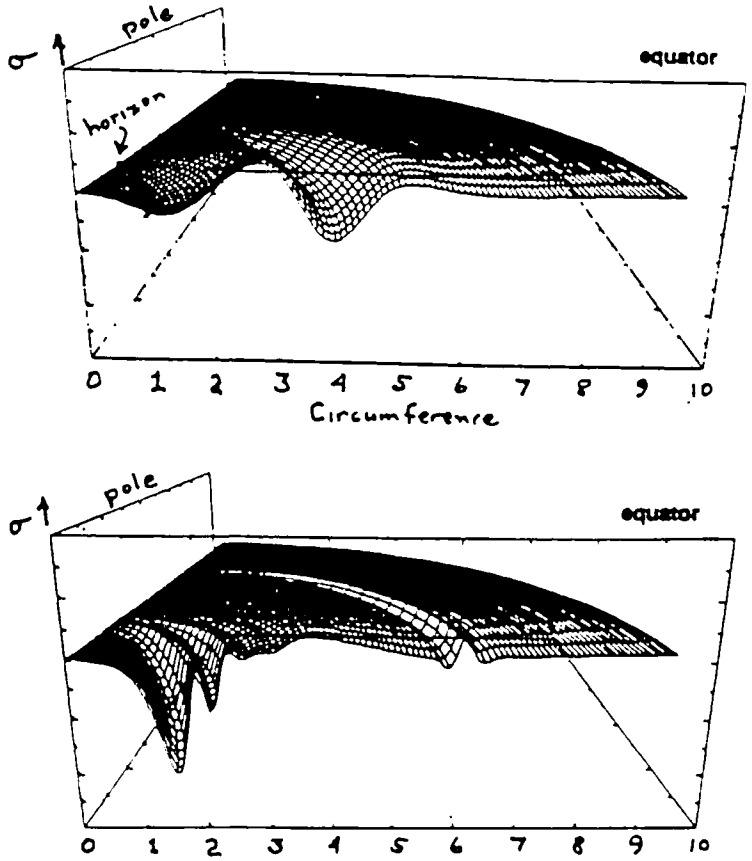

Gravitational waves being produced by axially symmetric pulsations of a non-rotating black hole, as calculated on a Cray-2 supercomputer by Bernstein, Hobill, and Smarr (1989). The two drawings show deformations of the hole's spacetime at two different times, one soon after the pulsations begin; the second a time $95GM/c^3$ later, where M is the hole's mass. In each diagram the height of the surface is a quantity, σ, called the "shear of the outgoing principal null vectors". This σ is a feature of the spacetime curvature that becomes, far from the hole, the rate of change of the gravitational-wave field, $\sigma = \partial h_+/\partial t$. This σ is shown as a function of position on a polar slice of space. The horizontal scale is circumference around the hole divided by the circumference of the hole's horizon. Initially (top diagram) the pulsations are concentrated in the region between 1.5 and 4 horizon circumferences. These pulsations give rise to two gravitational waves (bottom diagram): one propagating into the hole, the other propagating away from the hole. [This figure, based on the Bernstein, Hobill, and Smarr (1989) calculations, was produced by R. Idaszak and D. Cox using Wavefron Technologies software.]

4 Description of Gravitational Waves

We turn, now, in Part II of this book, to a detailed presentation of the theory of gravitational radiation. The fundamentals of the theory will be presented in pedagogical, textbook fashion; and the theory's principal consequences will be described.

Part II is divided into three chapters: Chap. 4 (this one) on the mathematical and physical description of gravitational waves, Chap. 5 on the propagation of gravitational waves, and Chap. 6 on the generation of gravitational waves.

Chapter 4 should be understandable to people familiar with physics or engineering at the advanced undergraduate level, including special relativity and vectors and tensors in special relativity's flat spacetime. Chapters 5 and 6 require, in addition, a prior familiarity with general relativity at the level, e.g., of track one of MTW.

The first section of this chapter (Sec. 4.A) introduces two concepts: a nearly Lorentz reference frame, and spacetime's Riemann curvature tensor. It then splits the curvature tensor into two parts, one associated with "background" gravity and the other associated with gravitational waves. Finally, it analyzes in a nearly Lorentz frame the mathematical properties of the waves' Riemann curvature $R^{GW}_{\alpha\beta\gamma\delta}$, including the propagation of that curvature with the speed of light. Section 4.B introduces a special type of nearly Lorentz frame — the proper reference frame of an observer — and it uses that frame to

discuss the physical forces produced by a gravitational wave's Riemann curvature. Section 4.C introduces the concept of metric theories of gravity (a wide class of theories which includes general relativity), and discusses the polarization properties of gravitational waves in any metric theory whose waves propagate with the speed of light. Most important is the connection between each polarization state and the spin of the gravitons that underlie that state's waves. Section 4.D (and the rest of this book) specializes to general relativistic gravitational waves and discusses those waves' "+" and "×" polarization states and their spin-two gravitons. Three different ways of describing the waves are introduced: the waves' Riemann curvature tensor $R^{GW}_{\alpha\beta\gamma\delta}$; a tensorial gravitational-wave field $h^{GW}_{\alpha\beta}$; and the wave fields h_+ and $h_\times$ associated with the two polarization states. It is shown that these three descriptions are completely equivalent: from any one the other two can be constructed. Section 4.E discusses the energy and momentum carried by a general relativistic gravitational wave, and shows that astrophysically realistic waves are highly classical: the fractional corrections to their properties due to quantum mechanics have magnitudes $\sim 10^{-37}$. Section 4.F introduces a special type of nearly Lorentz frame, called "transverse, traceless" or "TT" coordinates. It then discusses the fact that TT coordinates are powerful tools for analyzing gravitational-wave detectors which are large compared to the waves' reduced wavelength λ, but proper reference frames are preferable for detectors small compared to λ. Table 4.1, at the end of the chapter, summarizes the properties of the various coordinate systems and reference frames introduced in this chapter.

4.A The Riemann curvature tensor for a gravitational wave

In this book we shall use, as one fundamental entity for describing gravity, spacetime's *Riemann curvature tensor*, $R_{\alpha\beta\gamma\delta}$. This tensor is the full embodiment of the concept of spacetime curvature. It is sad, but true, that such full embodiment requires a tensor with four indices (by contrast with two indices for the electromagnetic field tensor $F_{\alpha\beta}$ and one for the electromagnetic vector potential A_α). I shall delay until the next section discussing the precise physical interpretation of the Riemann tensor $R_{\alpha\beta\gamma\delta}$.

A second fundamental entity in our description of gravity will be the metric $g_{\alpha\beta}$ of curved spacetime. This metric plays precisely the same role as that, $\eta_{\alpha\beta}$, of the flat spacetime of special relativity: Consider two neighboring events, with coordinate values x^α and $x^\alpha + dx^\alpha$.

These events are separated by the infinitesimal vector dx^α. From this separation vector and the metric we can compute the relativistic *squared interval* between the events: $ds^2 \equiv g_{\alpha\beta}dx^\alpha dx^\beta$. This squared interval is the vehicle by which one gives physical meaning to the metric: If the events' vectorial separation dx^α is spacelike (so $ds^2 > 0$), then one can stretch a perfect physical rod between the two events and measure with it the distance between them. That distance will be the square root of the squared interval, i.e. it will be $ds = \sqrt{g_{\alpha\beta}dx^\alpha dx^\beta}$. If the events' vectorial separation is timelike (so $ds^2 < 0$), then one can put a freely moving perfect clock into such a state of motion that it will pass through both events. The time interval $d\tau$ that the clock measures between the two events will be the square root of the negative of the squared interval, $d\tau = \sqrt{-ds^2} = \sqrt{-g_{\alpha\beta}dx^\alpha dx^\beta}$.

Full information about the curvature of spacetime resides in a (conceptual) table of distances between all neighboring pairs of events in the spacetime. Since such a table is equivalent to a knowledge of the spacetime metric $g_{\alpha\beta}$, full information about the curvature must reside in the metric. Correspondingly, one must be able to compute the Riemann curvature tensor from the metric. Indeed one can, by a complicated process that involves two differentiations [Eqs. (5.9) and (5.12) of Chap. 5]. In effect, the metric acts as a potential function for the Riemann curvature tensor; it is analogous to the vector potential for the electromagnetic field.

In our study of gravitational waves we shall make extensive use of coordinate systems that are as nearly like those of flat spacetime as possible, i.e. as nearly "Lorentz" (inertial) as possible. Spacetime curvature prevents us from constructing coordinates that are precisely Lorentz. However, the curvature in our universe is so weak, except near black holes and neutron stars, that over very large regions we can introduce coordinates $(t, x, y, z) \equiv (x^0, x^1, x^2, x^3)$ which are very nearly Lorentz, i.e. in which the spacetime metric takes the form

$$g_{\alpha\beta} = \eta_{\alpha\beta} + h_{\alpha\beta}\ , \quad \text{where } |h_{\alpha\beta}| \ll 1\ . \tag{4.1}$$

Here $\eta_{\alpha\beta}$ is the metric of flat spacetime [$\eta_{00} = -1$, $\eta_{0j} = 0$, $\eta_{ij} = \delta_{ij} \equiv (+1$ if $i = j$ and 0 otherwise)]. For example [cf. the paragraph following Eq. (4.41)], in a region whose size is 0.01 of the Hubble distance (size 100 million light years), we can introduce such coordinates with $|h_{\alpha\beta}| \lesssim (0.01)^2 = 10^{-4}$ – though to do so, we must cut a hole out of the coordinate system around each black hole or neutron star.

We shall use such a *nearly Lorentz coordinate system* (also called *nearly Lorentz reference frame*) throughout this chapter. When analyzing the properties of and propagation of the Riemann tensor, we shall approximate $g_{\alpha\beta}$ by $\eta_{\alpha\beta}$, thereby making fractional errors of order $|h_{\alpha\beta}|$. In other words, we shall treat the Riemann tensor as a field that lives in and propagates through flat spacetime. This is equivalent to adopting the linearized approximation to general relativity — the approximation on which Einstein, Weyl, and Eddington based their early studies of gravitational radiation. In Chaps. 5 and 6 we shall explore nonlinear effects, e.g. effects that are proportional to the square of $h_{\mu\nu}$, or the square of the Riemann tensor $R_{\alpha\beta\gamma\delta}$, or proportional to their product $h_{\mu\nu}R_{\alpha\beta\gamma\delta}$.

In most textbook treatments of linearized gravity, and in the original treatment by Einstein, Weyl, and Eddington, attention focusses on the metric perturbation $h_{\alpha\beta}$ rather than on the Riemann tensor. Such treatments are made complicated by the fact that, when one ripples the coordinate lines a bit (i.e., when one changes the nearly Lorentz coordinates by an amount $x^{\mu}_{\rm new} = x^{\mu}_{\rm old} + \xi^{\mu}$, where ξ^{μ} is small in the sense that $|\partial\xi^{\mu}/\partial x^{\nu}_{\rm old}| \sim |h_{\alpha\beta}| \ll 1$), then the metric perturbation $h_{\alpha\beta}$ changes substantially [see Eqs. (5.18)–(5.20) below]. By contrast, the Riemann tensor is unaffected, except for fractional changes of order $|h_{\alpha\beta}|$. One says that the Riemann tensor is "invariant under infinitesimal coordinate transformations", while the metric perturbation $h_{\alpha\beta}$ is not. By focusing on $R_{\alpha\beta\gamma\delta}$ rather than on $h_{\alpha\beta}$, we keep our analysis invariant under infinitesimal coordinate transformations.

Infinitesimal coordinate transformations in general relativity are closely analogous to gauge transformations in electromagnetic theory. The analogy is so close, in fact, that, when discussing gravity in this book, I shall use the phrase "gauge transformation" to mean "infinitesimal coordinate transformation", and "gauge invariant" to mean "invariant under infinitesimal coordinate transformations".

Our linearized analysis will rely on the mathematics of tensors in flat spacetime. We shall adopt, in that mathematics, the notation of Misner, Thorne, and Wheeler (1973) — denoted MTW throughout this book— including the use of Latin indices to denote spatial coordinates and spatial components of vectors and tensors (so S^i means S^1 or S^2 or S^3), and the use of Greek indices to denote spacetime coordinates and spacetime components of vectors and tensors (so x^{α} means $x^0 \equiv t$ or $x^1 \equiv x$ or $x^2 \equiv y$ or $x^3 \equiv z$). Because indices on vectors and tensors are lowered and raised with the flat metric $\eta_{\alpha\beta}$ and with its matrix inverse

$\eta^{\alpha\beta}$, those indices satisfy

$$S^0 = -S_0 , \quad S^j = +S_j . \tag{4.2a}$$

We shall denote the unit basis vectors along the coordinate axes by $\mathbf{e}_\alpha$ (with $\alpha = t, x, y, z$ or equivalently 0, 1, 2, 3). We shall denote partial derivatives by commas so that, for example, $S^\alpha{}_{,\mu} \equiv \partial S^\alpha / \partial x^\mu$ represents the gradient of the vector field S^α. Repeated indices, one up and the other down, are to be summed; for example,

$$S^\mu{}_{,\mu} \equiv \sum_{\mu=0}^{3} S^\mu{}_{,\mu} \tag{4.2b}$$

is the divergence of the vector field S^μ.

Finally, we shall use "geometrized units" in which Newton's gravitation constant G and the speed of light are set equal to unity, $G = c = 1$. This is equivalent to adopting the following conversion factors between units of length, time, mass, and energy:

$$1.0 = c = 2.997930\cdots\times 10^{10}\ \frac{\text{cm}}{\text{sec}} . \tag{4.3a}$$

$$1.0 = \frac{G}{c^2} = 0.7425\times 10^{-28}\ \frac{\text{cm}}{\text{g}} . \tag{4.3b}$$

$$1.0 = \frac{G}{c^4} = 0.826\times 10^{-49}\ \frac{\text{cm}}{\text{erg}} . \tag{4.3c}$$

If one wants to convert any of the geometrized-unit equations in this chapter (and the rest of the book) into cgs units, one need only insert enough factors of G and c to make the units come out correctly. For example, the equation $r_H = 2M$, which relates the radius r_H of the horizon of a black hole to the hole's mass M, is expressed in geometrized units. It presumes that r_H and M are both measured, e.g., in centimeters. To convert back to cgs units, one multiplies the M in this equation by $1.0 = G/c^2 = 0.7425\times 10^{-28}\,\text{cm/g}$, thereby obtaining $r_H = 2GM/c^2$ in which M can now be expressed in grams and r_H in centimeters.

General relativistic gravitational waves are ripples in the curvature of spacetime that propagate with the speed of light. Because gravity is nonlinear, it is not possible in a fully precise manner to separate the contributions to the curvature that are made by gravitational waves from the contributions made by the earth, the sun, or the galaxy. Since such a separation underlies the very concept of a gravitational wave, this means that gravitational waves are not precisely defined.

On the other hand, in realistic astrophysical situations the length-scale λ on which the waves vary (their reduced wavelength, $\lambda=\lambda/2\pi$) is almost always short compared to the lengthscales $\mathcal{L}$ on which all other important curvatures vary. This difference in lengthscale makes possible a high-accuracy, but approximate, split of the Riemann curvature tensor $R_{\alpha\beta\gamma\delta}$ into a "background curvature" $R^{B}_{\alpha\beta\gamma\delta}$ plus a contribution $R^{GW}_{\alpha\beta\gamma\delta}$ due to gravitational waves: The background $R^{B}_{\alpha\beta\gamma\delta}$ is the average of $R_{\alpha\beta\gamma\delta}$ over several wavelengths

$$R^{B}_{\alpha\beta\gamma\delta} \equiv \langle R_{\alpha\beta\gamma\delta} \rangle \tag{4.4a}$$

(the average $\langle \cdots \rangle$ being performed, for example, by multiplying the nearly Lorentz components of $R_{\alpha\beta\gamma\delta}$ by a Gaussian-shaped form factor and then integrating over the nearly Lorentz spacetime coordinates). The waves' curvature $R^{GW}_{\alpha\beta\gamma\delta}$ is the rapidly varying difference

$$R^{GW}_{\alpha\beta\gamma\delta} \equiv R_{\alpha\beta\gamma\delta} - R^{B}_{\alpha\beta\gamma\delta} \ . \tag{4.4b}$$

Heuristically, $R^{B}_{\alpha\beta\gamma\delta}$ is like the large-scale (10-centimeter) curvature of an orange, while $R^{GW}_{\alpha\beta\gamma\delta}$ is like the fine-scale granulation of the skin of the orange (lengthscale a few millimeters); see Fig. 4.1.

This method of defining a gravitational wave, introduced into general relativity by Wheeler (1955) and Power and Wheeler (1957), is a special case of what has since become a standard technique in mathematical physics. The technique is now called a "shortwave approximation" or "two-timing" or "two-lengthscale expansion" or "two-variable expansion" (see e.g. Chap. 3 of Cole, 1968); and it is intimately connected to the "WKB approximation", which is widely used in quantum mechanics. In Chap. 5 we shall present the general relativistic theory of gravitational-wave propagation in a form, based on this definition of waves, due to Brill and Hartle (1964), and especially to Isaacson (1968a,b). For the moment, the only feature of that theory which we shall need is the fact that $R^{GW}_{\alpha\beta\gamma\delta}$ propagates through the background spacetime with the speed of light. More specifically, in any nearly Lorentz reference frame and in the near vacuum of interstellar and intergalactic space it satisfies the standard vacuum wave equation

$$\Box R^{GW}_{\alpha\beta\gamma\delta} \equiv \eta^{\mu\nu} R_{\alpha\beta\gamma\delta,\mu\nu} = \left(-\frac{\partial^2}{\partial t^2} + \delta_{jk} \frac{\partial^2}{\partial x^j \partial x^k} \right) R^{GW}_{\alpha\beta\gamma\delta} = 0 \ . \tag{4.5}$$

For readers who know some general relativity, I sketch a quick derivation of this wave equation:

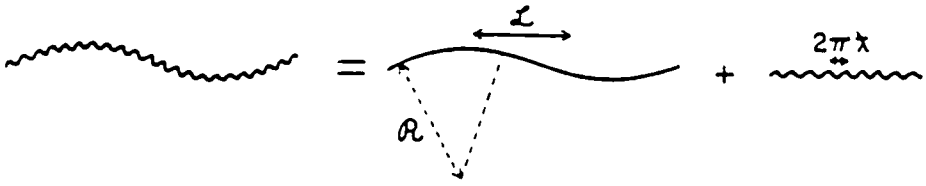

Fig. 4.1 Heuristic diagram describing the definition of a gravitational wave. The curvature of spacetime, like that of the line on the left, is characterized by changes on two lengthscales: a long lengthscale $\mathcal{L}$ (that of the background spacetime), and a short lengthscale λ (that of the wave). The background spacetime is defined by averaging over lengthscales bigger than λ but smaller than $\mathcal{L}$ (middle curve); and the gravitational waves are the piece of the spacetime curvature that thereby gets averaged away (right curve). The lengthscale $\mathcal{R}$ (radius of curvature of the background spacetime) is irrelevant to Chap. 4; it is introduced and used in Chap. 5. [This figure is reproduced from Thorne, 1983.]

Two foundations for the derivation are the "Bianchi identity" and symmetries satisfied by any Riemann tensor [see, e.g., MTW Eqs. (8.45) and (8.46), or Sec. 13.5 of MTW]. Because this identity and symmetries are linear, they must be satisfied not only by the full Riemann tensor, but also, individually, by its *slowly* varying (background) part and its rapidly varying (wave) part. In our nearly Lorentz frame, the Bianchi identity for the wave part of the Riemann tensor takes the form

$$R^{GW}_{\alpha\beta\gamma\delta,\mu} + R^{GW}_{\alpha\beta\delta\mu,\gamma} + R^{GW}_{\alpha\beta\mu\gamma,\delta} = 0 \; ; \tag{4.6}$$

and its symmetries include

$$R^{GW}_{\alpha\beta\gamma\delta} = -R^{GW}_{\beta\alpha\gamma\delta} \; , \quad R^{GW}_{\alpha\beta\gamma\delta} = -R^{GW}_{\alpha\beta\delta\gamma} \; , \quad R^{GW}_{\alpha\beta\gamma\delta} = +R^{GW}_{\gamma\delta\alpha\beta} \tag{4.7}$$

(antisymmetry on the first pair of indices, antisymmetry on the last pair, and symmetry under exchange of the first pair with the last pair). Another foundation is the Einstein field equation, which says that in the near vacuum of interstellar and intergalactic space the "Ricci curvature tensor" (contraction of the Riemann tensor on its first and third indices) vanishes. The rapidly varying part of this vacuum field equation is

$$R^{GW}_{\beta\delta} \equiv R^{GW\mu}{}_{\beta\mu\delta} \equiv -R^{GW\mu}{}_{\beta\delta\mu} = 0 . \tag{4.8}$$

(The second equality follows from antisymmetry on the last two indices.) By contracting the Bianchi identity (4.6) on its α and μ indices and using the definition and vanishing of the Ricci tensor [Eq. (4.8)], we learn that the Riemann tensor is divergence-free

$$R^{GW\mu}{}_{\beta\gamma\delta,\mu} = 0 . \tag{4.9}$$

The symmetries (4.7) imply that it is divergence-free not only on its first index, but on each of its four indices. By taking the divergence of the Bianchi identity (4.6) on its μ index and then commuting the μ and γ partial derivatives in the second term and the μ and δ partial derivatives in the third, and then invoking the vanishing of the divergence of the Riemann tensor, we find that $\Box R^{GW}_{\alpha\beta\gamma\delta} \equiv R^{GW}_{\alpha\beta\gamma\delta,\mu}{}^{,\mu} = 0$. Thus, in vacuum the Riemann tensor satisfies the wave equation, as claimed.

In Chap. 5 we shall derive and discuss the tiny deviations from the simple propagation law (4.5) that arise when waves propagate through matter or through electromagnetic fields, and some tiny nonlinear effects (e.g. coupling of the waves to background curvature and nonlinear wave-wave coupling) that were lost when we approximated our coordinates as precisely Lorentz.

4.B. Proper reference frames and the physics of Riemann curvature

Turn, now, to the physics of the Riemann tensor. As a tool in studying that physics we shall introduce a special type of nearly Lorentz reference frame: a *proper reference frame* (Sec. 13.6 of MTW). As was discussed in Sec. 1 B and Fig. 1.2a,b, a proper reference frame is the type of local coordinate system normally used by experimental physicists and engineers. More specifically, it is a reference frame constructed as follows: Select a specific observer, who moves through spacetime along a specific (possibly accelerated) world line. That observer's world line is taken as the spatial origin of the proper reference frame, and the proper reference frame is said to "belong to" that observer. Give the observer, to carry along this world line, a latticework of measuring rods; and insist that the latticework be as rectangular and Cartesian as is permitted by the spacetime curvature and by the observer's acceleration. At the latticework's spatial origin, place an ideal clock which measures the observer's proper time; and elsewhere in the latticework, place additional clocks which (to as great an extent as possible) are synchronized with the central clock. These clocks then measure the frame's coordinate time $t \equiv x^0$, and the

latticework measures its spatial coordinates $(x, y, z) \equiv (x^1, x^2, x^3)$.

In such a proper reference frame, the spacetime metric has the standard nearly Lorentz form (4.1), with this special additional feature: Because the latticework has been made as precisely Cartesian as possible and the clocks have been synchronized as perfectly as possible, the deviations from the flat-spacetime metric become arbitrarily small as one gets arbitrarily close to the spatial origin. For our purposes, the key, quantitative consequence of this is the following: When analyzing the interaction of gravitational waves with any detection system that is small compared to the waves' reduced wavelength λ, one can completely ignore the deviations of $g_{\alpha\beta}$ from the flat, special relativistic metric $\eta_{\alpha\beta}$. In Sec. 4.F below I shall justify these statements and shall make them more quantitative; for now I ask readers to accept them on faith.

(Note the strategy that I am adopting in this chapter: In discussing each feature of gravitational radiation, I use the most general coordinate system that permits the metric to be approximated as flat. For the propagation of the Riemann tensor, any nearly Lorentz reference frame will do; but for the forces produced by the Riemann tensor, I must restrict myself to a proper reference frame if I wish to retain the approximation that $g_{\alpha\beta} = \eta_{\alpha\beta}$. Section 4.F will explain why.)

Ask an observer to measure the "force of gravity" F^j that acts on a particle of mass m in the observer's proper reference frame. Assume, for simplicity, that the particle is momentarily at rest at a spatial location x^j, and attach the frame's latticework to inertial-guidance gyroscopes so there are no coriolis or centrifugal forces acting on the particle. To measure F_j, the observer might let the particle fall freely from rest, measure its acceleration d^2x^j/dt^2 in the proper reference frame, and multiply that acceleration by the particle's mass m, to get $F^j = md^2x^j/dt^2$. Alternatively, the observer might measure the force required to hold the particle at rest in the latticework of his proper reference frame and equate F^j to minus that force. Of course, this is not different in any way from what the observer would do were he a Newtonian physicist rather than a relativistic physicist. The difference lies in how he analyzes and thinks about the force of gravity F_j. As a relativist, he recognizes (see, e.g., Sec. 13.6 of MTW) that F_j is made up of a nearly steady force mg_j caused by the failure of the origin of the proper reference frame to fall freely, plus a force proportional to the particle's separation x^k from the spatial origin, which is caused by spacetime's Riemann curvature tensor $R_{\alpha\beta\gamma\delta}$

$$F^j = F_j = mg_j - mR_{j0k0}x^k \ . \qquad (4.10)$$

The Riemann-curvature-induced force is often called a *tidal force* because it is responsible for tides in the earth's oceans; see, e.g., the discussion in XXXXXXXX. The form $-mR_{j0k0}x^k$ of this tidal force can be inferred, e.g., from the "equation of geodesic deviation" (MTW Sec. 8.7 or 11.3). The two terms in Eq. (4.10) are just the first two in a power series in the separation x^k of the particle from the spatial origin. The higher-order terms (given, e.g., in Zhang, 1986 and Ni and Zimmermann, 1978) are negligible so long as $|\mathbf{x}| \equiv (\delta_{ij}x^i x^j)^{1/2}$ is small compared to the shortest lengthscale or timescale on which the curvature varies [i.e. small compared to $\lambda\!\!\!^{-}$ when the curvature is due to gravitational radiation; cf. Eq. (4.41b) below].

Had the observer been a Newtonian physicist, he would have regarded the gravitational force (4.10) as the particle's mass times the negative of the spatial gradient of a Newtonian gravitational potential Φ, i.e.

$$F_j = -m\frac{\partial\Phi}{\partial x_j} = -m\left[\frac{\partial\Phi}{\partial x^j}\right]_{\text{at } x^i=0} - m\left[\frac{\partial^2\Phi}{\partial x^j \partial x^k}\right]_{\text{at } x^i=0} x^k \ . \qquad (4.10\text{N})$$

Direct comparison of the relativistic expression (4.10) with the Newtonian expression (4.10N) reveals that in Newtonian situations

$$g_j = -\left[\frac{\partial\Phi}{\partial x^j}\right]_{\text{at } x^i=0} , \quad R_{j0k0} = \left[\frac{\partial^2\Phi}{\partial x^j \partial x^k}\right]_{\text{at } x^i=0} . \qquad (4.11)$$

However, when the spacetime curvature is due not to nearly-Newtonian gravity but instead to gravitational radiation, it is impossible to find any scalar field from which to compute R_{j0k0} as the double gradient.

Note that for a particle at rest in the proper reference frame it is the "space-time-space-time" part of the Riemann tensor, R_{j0k0}, which produces gravitational accelerations (tidal accelerations) relative to the spatial origin. The remaining parts of the Riemann tensor, e.g. R_{0jkl} and R_{ijkl}, produce accelerations proportional to the velocity v^l of the particle divided by the speed of light (unity), or to $v^k v^l$; see, e.g XXXXX. Those velocity-dependent accelerations will not be of interest to us because a gravity-wave detector's masses, on which gravitational waves act, are always at rest in the laboratory, or nearly so.

The split (4.4b) of the Riemann curvature tensor into background plus wave permits us also to split the gravitational force (4.10) into

that due to background gravity plus that due to the wave. The background force is the slowly varying component and of no interest here; the wave force is the rapidly varying, interesting one:

$$F_j^{GW} = -mR^{GW}_{j0k0}x^k \ . \tag{4.12}$$

We shall use this expression for the wave force over and over again in our discussion of the physical properties of gravitational waves and in analyses of gravitational-wave detectors.

The form of the force (4.12) shows that gravitational-wave detectors at rest in a proper reference frame are capable of measuring only the space-time-space-time part of $R^{GW}_{\alpha\beta\gamma\delta}$. Remarkably, from a measurement of that part, one can reconstruct the full Riemann tensor. This claim can be verified as follows:

Suppose, for simplicity, that the gravitational waves are propagating through the proper reference frame in the z-direction (x^3-direction). Then the wave equation (4.5) implies that the Riemann tensor is a function of $t-z$:

$$R^{GW}_{\alpha\beta\gamma\delta} = R^{GW}_{\alpha\beta\gamma\delta}(t-z) \ . \tag{4.13}$$

It is straightforward, by combining the functional form (4.13) of the waves' Riemann tensor with the Bianchi identity (4.6), to show that

$$R^{GW}_{\alpha\beta12} = 0 \ , \quad R^{GW}_{\alpha\beta13} = -R^{GW}_{\alpha\beta10} \ , \quad R^{GW}_{\alpha\beta23} = -R^{GW}_{\alpha\beta20} \ . \tag{4.14}$$

These relations, plus the symmetries (4.7), give all components of $R^{GW}_{\alpha\beta\gamma\delta}$ in terms of the components R^{GW}_{j0k0} that push on particles at rest. [Readers may find it interesting to carry out an alternative derivation of $R^{GW}_{\alpha\beta\gamma\delta}$ in terms of R^{GW}_{j0k0}, using Eqs. (4.24), (4.25), and (4.27) below.]

4.C Metric theories of gravity and gravitational-wave polarization

Many, but far from all, relativistic theories of gravity share with general relativity the features of: (i) using the metric of spacetime to define an invariant interval which is measured by physical rods and clocks; (ii) describing gravity as a consequence of the curvature of spacetime; and (iii) insisting that all the nongravitational laws of physics take on their standard, special relativistic forms in local inertial (local Lorentz) frames of the spacetime metric. Such theories are called *metric theories* (Thorne and Will, 1971; Will, 1981). In a wide variety of metric theories including general relativity, but not in all, gravitational waves propagate with the same speed as light. In this section we shall broaden our discussion to include not just general

relativity, but all metric theories with light-speed propagation. Our objective will be to elucidate the polarization properties of gravitational waves and the relationship of those properties to the spins of the waves' underlying quantum mechanical particles. Our discussion is based on the work of Eardley, Lee, and Lightman (1973) and Eardley *et. al.* (1973).

For any metric theory with light-speed wave propagation, all details of this chapter thus far [except the vacuum Einstein field equation (4.8) and the vanishing divergence of the Riemann tensor in vacuum, Eq. (4.9)] are valid without change. For such a theory, after one has chosen a small region of spacetime in which to study the gravitational waves, and after one has introduced a specific proper reference frame there, it is convenient to define in that frame a dimensionless *gravitational-wave field* h_{jk}^{GW} by

$$\frac{\partial^2 h_{jk}^{GW}}{\partial t^2} \equiv -2R_{j0k0}^{GW} . \tag{4.15}$$

The convenience of this gravitational-wave field lies in its relationship to displacements produced by the waves: Assume, for simplicity, that the origin of the proper reference frame is freely falling (so $g_j=0$), and its axes are attached to inertial-guidance gyroscopes. Then the frame is a *local inertial frame*. Assume, in addition, that the only spacetime curvature present is that due to the gravitational waves. Then the only force acting on a test particle of mass m, initially at rest in the frame's latticework, will be the gravitational-wave force (4.12). That force will produce tiny oscillatory changes δx^j in the position of the test particle relative to the rigid latticework:

$$m\frac{d^2\delta x^j}{dt^2} = F_j^{GW} = -mR_{j0k0}^{GW}x^k = \tfrac{1}{2}m\frac{\partial^2 h_{jk}^{GW}}{\partial t^2}x^k . \tag{4.16}$$

[This is actually the "equation of geodesic deviation", to which I have alluded, written in the language of our local inertial reference frame. It is also a generalization of Eq. (1.3')] Because any realistic wave is so weak that the oscillatory changes δx^j are minuscule compared to the distance of the particle from the origin, x^k can be regarded as essentially constant on the right-hand side, and Eq. (4.16) can then be integrated easily to give

$$\delta x^j = \tfrac{1}{2}h_{jk}^{GW}x^k . \tag{4.17}$$

This is a generalization of Eq. (1.4).

Thus, aside from a factor ½, h_{jk}^{GW} plays the role of the "dimensionless strain of space", or the "time-integrated shear of space": it is the ratio of the wave-induced displacement of a free particle δx^j to its original separation x^k from the origin. Because of the Riemann tensor's pair-exchange symmetry (4.7), this gravitational-wave field is symmetric in its two indices,

$$h_{jk}^{GW} = h_{kj}^{GW} . \tag{4.18}$$

Correspondingly, it has 6 independent components, which we shall take to be h_{xz}^{GW}, h_{zx}^{GW}, h_{xy}^{GW}, $\frac{1}{2}(h_{xx}^{GW}+h_{yy}^{GW})$, $\frac{1}{2}(h_{xx}^{GW}-h_{yy}^{GW})$, and h_{xy}^{GW}. Each of these components represents a different polarization state of the wave. In general relativity the Einstein field equation forces four of the polarization states to vanish leaving only the two states $\frac{1}{2}(h_{xx}^{GW}-h_{yy}^{GW}) \equiv h_+$ and $h_{xy}^{GW} \equiv h_\times$ (see Sec. 4.D below); but in other metric theories with light-speed propagation all six states can be present.

As an aid to understanding each of the six polarization states, consider a cloud of test particles surrounding the spatial origin of the local inertial reference frame. Initially no waves are present, and the cloud is static and precisely spherical. Then a gravitational wave passes through the cloud and deforms it. Assume that the cloud is small compared to the reduced wavelength $\lambda\!\!\!^{-}$ of the waves. This permits us to ignore higher-order terms in the gravitational force [see the brief discussion following Eq. (4.10) above] and to describe the wave-induced deformation of the cloud by the gravitational displacement equation (4.18). Consider, in turn, and with the help of Fig. 4.2, the deformations produced by each of the wave's six polarization states:

The component h_{zz}^{GW} produces the deformations

$$\delta x = \delta y = 0 , \quad \delta z = \tfrac{1}{2} h_{zz}^{GW} z . \tag{4.19a}$$

These equations say that, as $h_{zz}^{GW}(t-z)$ at the sphere's center ($z=0$) alternately oscillates positive and negative, the sphere expands and then contracts longitudinally (i.e., along the direction of wave propagation, z), and its transverse cross section remains unchanged. In this sense the wave is purely longitudinal. At any moment of time the deformed sphere is invariant under rotations about the propagation direction $\mathbf{e}_z$, i.e. it is circularly symmetric in the transverse plane. This means [cf. Eq. (1.2) and associated discussion] that the spin of the graviton that carries these waves must be $S=0$. Correspondingly, the polarization state embodied in h_{zz}^{GW} is called the waves' *longitudinal, spin-zero* or L0 state.

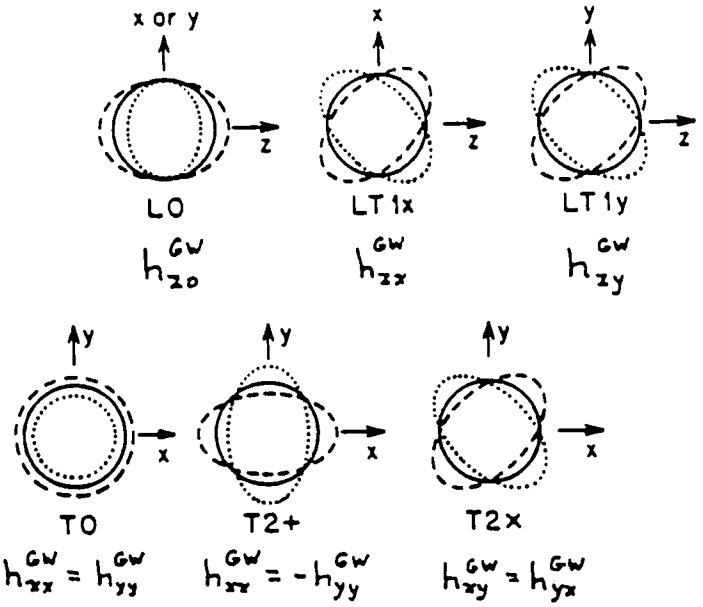

Fig. 4.2 The deformations of a sphere of test particles produced by gravitational waves with each of six polarizations. As the wave oscillates, the sphere (solid) first gets deformed in the manner shown dashed; then in the manner shown dotted. [This figure and the discussion of it in the text are adapted from Thorne, 1983.]

The component $h^{GW}_{zx} = h^{GW}_{xz}$ produces the deformations [Eq. (4.18)]

$$\delta x = \tfrac{1}{2} h^{GW}_{xz} z \ , \quad \delta y = 0 \ , \quad \delta z = \tfrac{1}{2} h^{GW}_{xz} x \ . \tag{4.19b}$$

These equations say that, as $h^{GW}_{zx}(t-z)$ oscillates at $z=0$, the sphere expands and then contracts at a 45 degree angle to the propagation direction $\mathbf{e}_z$, in the "longitudinal–transverse" $z-x$ plane, while remaining undeformed in the y–direction. At any moment the deformed sphere is invariant under a 360–degree rotation about the propagation direction, and 360 degrees is the smallest such angle of invariant rotation. Thus, as for an electromagnetic wave, so also for this gravitational wave, the "return angle" is 360 degrees [cf. Eq. (1.2) above and associated discussion]. Correspondingly, the quantum mechanical particle that carries this wave must have spin $S=1$, and the polarization state embodied in h^{GW}_{zx} is called the waves' *longitudinal-transverse spin-one*, or LT1 state.

The component $h^{GW}_{zy} = h^{GW}_{yz}$ produces the deformations

$$\delta x = 0 \ , \quad \delta y = \tfrac{1}{2} h^{GW}_{zy} z \ , \quad \delta z = \tfrac{1}{2} h^{GW}_{zy} y \ , \tag{4.19c}$$

and is thus also LT1. It is the LT1 polarization state orthogonal to h^{GW}_{zx}.

A wave with $h^{GW}_{xx} = h^{GW}_{yy}$ nonzero and all other h^{GW}_{jk} zero produces the deformations

$$\delta x = \tfrac{1}{2} h^{GW}_{xx} x \ , \quad \delta y = \tfrac{1}{2} h^{GW}_{xx} y \ , \quad \delta z = 0 \ . \tag{4.19d}$$

This wave alternately expands and compresses the sphere in the plane transverse to the wave's propagation while leaving it transversely circular and leaving it totally unchanged in the longitudinal direction. Thus, this wave is T0 (*transverse, spin-zero*).

A wave with $h^{GW}_{xx} = -h^{GW}_{yy}$ and all other h^{GW}_{jk} zero produces deformations

$$\delta x = h^{GW}_{xx} x \ , \quad \delta y = -h^{GW}_{xx} y \ , \quad \delta z = 0 \ . \tag{4.19e}$$

As $h^{GW}_{xx}(t-z)$ oscillates at $z = 0$, this wave expands the sphere in the x-direction and squeezes it in y, then expands it in y and squeezes it in x. Thus, the deformations are purely transverse, and at any moment the deformed sphere is invariant under a 180-degree rotation about the propagation direction; i.e. its return angle is 180 degrees corresponding to spin 2 for the underlying graviton [Eq. (1.2)]. This is the polarization state denoted + earlier in the book (Sec. 1 B); and its elliptical deformations [Eq. (4.19e) and Fig. 4.2] are the result of the "quadrupolar" force field of Fig. 1.3c. This + state is sometimes denoted T2 for *transverse, spin-2*.

Finally, $h^{GW}_{xy} = h^{GW}_{yx}$ produces the deformations

$$\delta x = h^{GW}_{xy} y \ , \quad \delta y = h^{GW}_{yx} x \ , \quad \delta z = 0 \ , \tag{4.19f}$$

which are also T2, but with the transverse deformation axes rotated 45-degrees to the frame's x- and y-axes. This is the polarization state denoted × above.

That each spin $S = 0$ wave (L0 and T0) has just one polarization state while the $S = 1$ (LT1) and $S = 2$ (T2) waves each have two orthogonal polarization states rather than $2S+1$ is familiar both from quantum mechanics and from canonical, classical field theory. It is a consequence of the fact that the waves propagate with the speed of light, i.e., their quanta have zero rest mass (KIP: REFER TO WIGNER IN RMP IN 40S??).

This familiar feature is deceptively reassuring. Actually, a nasty surprise awaits us if we try to check the fundamental tenet of canonical field theory that the spin of a wave must be Lorentz invariant. If we begin in one local inertial frame with a gravitational wave that is pure T0 or T2, we will find it to be pure T0 or T2 in any other inertial frame

moving at any arbitrary velocity relative to the first. However, if we begin with a pure LT1 wave in one frame, we will find a mixture of LT1, T0, and T2 in the other frame; and if we begin with pure L0 in one frame, we will find a mixture of L0, LT1, T0, and T2 in the other. Stated in more sophisticated language, if the L0 or LT1 states are present in the waves, then the Riemann tensor $R^{GW}_{\alpha\beta\gamma\delta}$ (for which h^{GW}_{jk} is a surrogate) generates an *indecomposible* representation of the "Little group" of the waves' propagation vector **k**, i.e. of that subgroup of the Lorentz group which leaves the components of the propagation vector unchanged. [These statements (due to Earley, Lee, and Lightman, 1973 and Eardley et. al., 1973) can be verified by: (i) in the first frame expressing R^{GW}_{j0k0} in terms of h^{GW}_{jk} via Eq. (4.15); then (ii) using Eqs. (4.14) and (4.7) to compute all the other components of $R^{GW}_{\alpha\beta\gamma\delta}$; then (iii) performing a Lorentz transformation on these components of $R_{\alpha\beta\gamma\delta}$ to get the components in the second frame; and finally (iv) reading off the h^{GW}_{jk} in the second frame from Eq. (4.15).]

These behaviors mean that any metric theory of gravity, with light-speed wave propagation, that possesses L0 or LT1 waves, violates the tenets of canonical field theory and cannot be quantized by canonical methods. For examples of such theories see Sec. 10.2 of Will (1981). By contrast, metric theories with purely transverse, light-speed gravitational waves obey the canonical tenets and are quantizeable by canonical means, at least in situations where the gravity is sufficiently weak that nonlinearities do not prevent convergence of Feynman-diagram expansions. Examples are general relativity, which as we shall see has pure T2 waves (spin-2 gravitons), and the Dicke-Brans-Jordan theory (Dicke, 1962; Brans and Dicke, 1961; Jordan, 1959), which has both T2 waves and T0 waves (a mixture of spin-2 gravitons and spin-0 gravitons). For further detail and references see Sec. 10.2 of Will (1981).

4.D Gravitational-wave field in general relativity

Throughout the rest of this book we shall specialize to general relativistic gravitational waves. As a first step in analyzing general relativity's waves, we introduce an arbitrary but specific nearly Lorentz reference frame.

That general relativity has only T2 waves follows from the vacuum Einstein field equation (4.8), evaluated in our chosen nearly Lorentz frame,

$$R^{GW}_{\alpha\beta} \equiv -R^{GW}_{0\alpha0\beta}+R^{GW}_{x\alpha x\beta}+R^{GW}_{y\alpha y\beta}+R^{GW}_{z\alpha z\beta} = 0 . \qquad (4.20)$$

The components $R^{GW}_{00}=0$ and $R^{GW}_{zz}=0$ of this field equation, together with properties (4.14) and (4.7) of the waves' Riemann tensor, guarantee that R^{GW}_{x0x0} and $R^{GW}_{x0x0}+R^{GW}_{y0y0}$ vanish, and thence that the L0 and T0 waveforms h^{GW}_{zz} and $h^{GW}_{xx}+h^{GW}_{yy}$ vanish. In the same way, the components $R^{GW}_{xz}=0$ and $R^{GW}_{yz}=0$ of the field equation guarantee the vanishing of the LT1 waveforms h^{GW}_{xz} and h^{GW}_{yz}. Only the T2 waveforms $h^{GW}_{xx}-h^{GW}_{yy}$ and h^{GW}_{xy} are left nonzero.

In general relativity the gravitational-wave field is often denoted h^{TT}_{jk} rather than h^{GW}_{jk},

$$h^{TT}_{jk} \equiv h^{GW}_{jk} \qquad (4.21)$$

because it is *transverse* (all components h^{GW}_{jz} along the propagation direction vanish) and *traceless* ($h^{TT}_{xx}+h^{TT}_{yy}+h^{TT}_{zz}=0$). However, in this book we shall use the superscript GW rather than TT.

The gravitational-wave fields $h_+(t-z)$ and $h_\times(t-z)$ used elsewhere in this book are related to h^{GW}_{jk} by

$$h_+ \equiv h^{GW}_{xx} = -h^{GW}_{yy} , \quad h_\times \equiv h^{GW}_{xy} = h^{GW}_{yx} . \qquad (4.22)$$

From these definitions it is straightforward to show that, if one rotates the x and y axes in the transverse plane through an angle $\Delta\psi$, the fields h_+ and $h_\times$ are changed to

$$h_+^{new} = h_+^{old}\cos2\Delta\psi + h_\times^{old}\sin2\Delta\psi ,$$
$$h_\times^{new} = -h_\times^{old}\sin2\Delta\psi + h_\times^{old}\cos2\Delta\psi . \qquad (4.23)$$

The factor 2 is yet another manifestation of the spin of the general relativistic graviton.

Let the $x-$ and $y-$axes be fixed. Then from h_+ and $h_\times$ one can reconstruct the TT gravitational-wave field h^{GW}_{jk}. The key to the reconstruction is the pair of *polarization tensors* $\mathbf{e}^+$ and $\mathbf{e}^\times$ defined by

$$e^+_{xx} \equiv -e^+_{yy} \equiv 1 , \quad e^\times_{xy} = e^\times_{yx} = 1 , \qquad (4.24)$$

with all other components vanishing. The obvious reconstruction formula is

$$h^{GW}_{jk} \equiv h_+ e^+_{jk} + h_\times e^\times_{jk} . \qquad (4.25)$$

From h^{GW}_{jk} one can construct a gravitational-wave field $h^{GW}_{\alpha\beta}$, which is a symmetric spacetime tensor residing in 4-dimensional spacetime. It is defined by giving its components in our chosen nearly Lorentz frame:

its space-space components are equal to those of h_{jk}^{GW}, and its space-time and time-time components are $h_{j0}^{GW} = h_{0j}^{GW} = 0$ and $h_{00}^{GW} = 0$. This 4-dimensional, gravitational-wave tensor can be expressed in terms of h_+ and $h_\times$ by a straightforward translation of Eqs. (4.25) and (4.24):

$$h_{\alpha\beta}^{GW} = h_+(a_\alpha a_\beta - b_\alpha b_\beta) + h_\times(a_\alpha b_\beta + b_\alpha a_\beta) . \qquad (4.26)$$

Here a_α and b_β are 4-vectors which, in our chosen frame, are purely spatial and are equal to $\mathbf{e}_x$ and $\mathbf{e}_y$, respectively; in other words, $a_\alpha = \delta_{\alpha x}$, $b_\alpha = \delta_{\alpha y}$. One can go on, if one wishes, to reconstruct the full Riemann curvature tensor for the waves from this $h_{\alpha\beta}^{GW}$. The reconstruction formula, derivable from Eqs. (4.15), (4.14), and (4.7), can be expressed most elegantly if we regard h_+ and $h_\times$, and thence $h_{\alpha\beta}^{GW}$, not as functions of $t-z$ but rather as functions of "the source's retarded time" τ_e.

This τ_e (subscript e for "emission") is defined as follows: Choose a specific event x^α in spacetime at which τ_e is to be evaluated. Consider the bit of gravitational wave which passes through this event. The proper time at which that bit of wave was emitted, as measured by the wave's source, is the quantity $\tau_e(x^\alpha)$. Since, in our chosen nearly Lorentz frame, the wave field is a function of $t-z$, the function $\tau_e(x^\alpha)$ will also be a function only of the combination $x^0 - x^3 = t-z$. That function, $\tau_e(t-z)$, will depend on the motion of the source relative to the chosen nearly Lorentz frame, and on the spacetime curvature between the source and the chosen frame. We shall study this τ_e in greater detail in Chap. 5.

The waves' Riemann tensor, as derived from Eqs. (4.15), (4.14), and (4.7), and as expressed in terms of τ_e, works out to be

$$R_{\alpha\beta\gamma\delta}^{GW} = \tfrac{1}{2}\left[\ddot{h}_{\alpha\gamma}^{GW} k_\beta k_\delta + \ddot{h}_{\beta\delta}^{GW} k_\alpha k_\gamma - \ddot{h}_{\alpha\delta}^{GW} k_\beta k_\gamma - \ddot{h}_{\beta\gamma}^{GW} k_\alpha k_\delta\right] . \qquad (4.27)$$

Here a dot is used to denote a derivative with respect to retarded time τ_e (*not* with respect to the coordinate time t of the chosen nearly Lorentz frame). Also, k_γ is the gradient of retarded time τ_e,

$$k_\gamma \equiv -\frac{\partial \tau_e}{\partial x^\gamma} , \qquad (4.28)$$

and is called the waves' *propagation vector*. Note that in the chosen nearly Lorentz frame, because τ_e is some function of $t-z$, the only nonzero components of this wave vector are $k_0 = -k_z = -\tau_{e,0}$; i.e. $\mathbf{k} = \tau_{e,0}(\mathbf{e}_0 + \mathbf{e}_z)$.

Thus far we have held fixed our chosen nearly Lorentz frame. What happens if we change it by boosting to a frame that moves with some high velocity relative to the original one? In other words, how do the wave fields h_+ and $h_\times$ depend on the velocity of the nearly Lorentz frame? The answer is buried in the general expressions (4.27), (4.26) for the Riemann tensor in terms of h_+ and $h_\times$: The Riemann tensor constructed from those expressions must be the same coordinate-indendent geometric object regardless of the frame one uses in the construction. To see the implications of this, one can argue as follows:

In both of the nearly Lorentz frames, "new" and "old", the polarization vectors a_α and b_α (denote them $a_\alpha^{\rm new}$, $a_\alpha^{\rm old}$, $b_\alpha^{\rm new}$, $b_\alpha^{\rm old}$) are orthogonal to the wave vector k_α. The set of all vectors orthogonal to k_α forms a 3-dimensional "hyperplane", spanned by 3 linearly independent such vectors. One set of spanning vectors is $\{a_\alpha^{\rm old}, b_\alpha^{\rm old}, \text{and } k_\alpha\}$ (note that k_α is orthogonal to itself, since it is null); and, thus, $a_\alpha^{\rm new}$ and $b_\alpha^{\rm new}$ can be expanded in terms of $\{a_\alpha^{\rm old}, b_\alpha^{\rm old}, k_\alpha\}$. By rotating the transverse spatial axes of the new frame so they coincide, so far as possible, with those of the old, we can bring those expansions into the form

$$a_\alpha^{\rm new} = a_\alpha^{\rm old} + Ck_\alpha\,, \quad b_\alpha^{\rm new} = b_\alpha^{\rm old} + Dk_\alpha\,, \tag{4.29}$$

where C and D are constants. (The coefficients in front of $a_\alpha^{\rm old}$ and $b_\alpha^{\rm old}$ are unity because both the old and the new a_α and b_α have unit squared length and k_α has vanishing squared length and is orthogonal to $a_\alpha^{\rm old}$ and $b_\alpha^{\rm old}$.) Now, insert Eq. (4.26) into (4.27) and add superscripts "new" to a_α, b_α, h_+, $h_\times$, so as to make clear that the resulting expression for $R^{\rm GW}_{\alpha\beta\gamma\delta}$ was constructed from quantities defined in the new frame. Then insert Eqs. (4.29) for $a_\alpha^{\rm new}$ and $b_\alpha^{\rm new}$ into the thus derived expression. The result, because of cancellations of all terms of the form $(C \text{ or } D)k_\alpha k_\beta k_\gamma k_\delta$, is identically the same as if one had calculated $R^{\rm GW}_{\alpha\beta\gamma\delta}$ in the old frame, except that $h_+^{\rm new}$ appears in place of $h_+^{\rm old}$ and $h_\times^{\rm new}$ appears in place of $h_\times^{\rm old}$.

From this one infers the remarkable result that

$$h_+^{\rm new}(\tau_e) = h_+^{\rm old}(\tau_e)\,, \quad h_\times^{\rm new}(\tau_e) = h_\times^{\rm old}(\tau_e)\,; \tag{4.30}$$

i.e., *the gravitational wave fields $h_+(\tau_e)$ and $h_\times(\tau_e)$ are the same in every nearly Lorentz frame, regardless of the frame's velocity*! Of course, no such equality holds for the new and old fields $h^{\rm GW\,new}_{\alpha\beta}$ and $h^{\rm GW\,old}_{\alpha\beta}$, since the old one is purely spatial in the old frame and the new one purely spatial in the new frame.

Sophisticated mathematical physicists describe the Lorentz-invariance (4.30) of h_+ and $h_\times$ by the statement that "the gravitational-wave field has boost-weight zero" (it is unaffected by boosts to new velocities), and they describe the behavior (4.23) under rotations by the statement that "the wave field has spin-weight two" [REF XXX KIP: GEROCH, HELD, AND PENROSE??]. Such physicists also sometimes use, instead of the wave fields h_+ and $h_\times$, and instead of $h_{jk}^{GW} \equiv h_{jk}^{TT}$, a quantity N called the *Bondi news function* (Bondi, van der Burg, and Metzner, 1962). Strictly speaking, this news function is defined only when the source of the waves resides alone in an otherwise flat and empty spacetime. Then, if r is the distance to the source and t is time in some chosen, asymptotically Lorentz coordinate system (i.e. in a coordinate system that becomes Lorentz as rapidly as possible as one moves away from the source toward infinity), the Bondi news function is a complex field given by

$$N = \frac{r}{2}\frac{\partial}{\partial t}(h_+ + i h_\times) , \tag{4.31}$$

where i denotes the square root of -1. The Bondi news function N will not be used in this book. In its place we shall use the wave fields h_+ and $h_\times$, which contain the same information as N.

4.E Energy, momentum, and quantization of gravitational waves

The shortwave description of gravitational waves, which will be developed in the next chapter, leads compellingly to a simple and elegant definition of the energy and momentum carried by the waves (Isaacson, 1968b). These energy and momentum are embodied in a stress-energy tensor $T_{\alpha\beta}^{GW}$ for the waves. This stress-energy tensor, like the background curvature $R^B_{\alpha\beta\gamma\delta}$, is smooth on the lengthscale λ. It is obtained, in fact, by averaging over several wavelengths the squared retarded-time derivative of the wave field, and then multiplying by two wave vectors:

$$T_{\alpha\beta}^{GW} = \frac{1}{16\pi}\langle (dh_+/d\tau_e)^2 + (dh_\times/d\tau_e)^2 \rangle k_\alpha k_\beta . \tag{4.32}$$

It is easy to show that, if the waves are propagating in the z direction, this stress-energy tensor takes the standard form for a bundle of zero-rest-mass particles (gravitons) moving at the speed of light in the z direction:

$$T_{00}^{GW} = -T_{0z}^{GW} = -T_{z0}^{GW} = T_{zz}^{GW} = \frac{1}{16\pi}\langle (\partial h_+/\partial t)^2 + (\partial h_\times/\partial t)^2 \rangle . \tag{4.33}$$

(Here, as for any stress–energy tensor, the 00 component is the energy density, the negative of the $0z$ component the energy flux, and the zz component the pressure along the propagation direction.)

By restoring the factors of G and c to Eq. (4.33) [i.e. by switching from geometrized units to cgs units; cf. Eq. (4.3) and associated discussion], and by setting $\langle(\partial h_+/\partial t)^2\rangle \simeq \frac{1}{2}(2\pi f \mathcal{H})^2$ and similarly for $h_\times$, we obtain the following approximate expression for the energy flux in the waves:

$$-T^{0z}_{GW} \simeq \frac{\pi}{4}\frac{c^3}{G} f^2 \mathcal{H}^2 = 320 \frac{\text{ergs}}{\text{cm}^2\,\text{sec}} \left|\frac{f}{1\ \text{kHz}}\right|^2 \left|\frac{\mathcal{H}}{10^{-21}}\right|^2 . \qquad (4.34)$$

Here $f = c/(2\pi\lambda\!\!\!^{-})$ is the waves' characteristic frequency and $\mathcal{H}$ is their amplitude. The numbers in this equation correspond to a strongly emitting supernova in the Virgo cluster of galaxies, where there are several supernovae per year. Contrast this huge gravity-wave energy flux with the peak electromagnetic flux at the height of the supernova, $\sim 10^{-9}$ erg cm^{-2} sec^{-1}; but note that the gravity waves should last for only a few milliseconds, while the strong electromagnetic output lasts for weeks.

Corresponding to the huge energy flux (4.34) in an astrophysically interesting gravitational wave is a huge "occupation number" for the quantum states of the gravitational-wave field, i.e. a huge value for the number of spin-2, zero-rest-mass gravitons in each quantum state. To compute that occupation number, we shall evaluate the volume in phase space occupied by the waves from a supernova and then divide by the volume occupied by each quantum state. At a time when the waves have reached a distance r from the source, they occupy a spherical shell of area $4\pi r^2$ and thickness of order $10\lambda\!\!\!^{-}$, where $\lambda\!\!\!^{-}$ is their reduced wavelength, so their volume in physical space is $V_x \sim 100 r^2 \lambda\!\!\!^{-}$. As seen by observers whom the waves are passing, they come from a solid angle $\Delta\Omega \sim (2\lambda\!\!\!^{-}/r)^2$ centered on the source, and they have a spread of angular frequencies ranging from $\omega \sim \frac{1}{2}c/\lambda\!\!\!^{-}$ to $\omega \sim 2c/\lambda\!\!\!^{-}$. Since each graviton carries an energy $\hbar\omega = \hbar c/\lambda\!\!\!^{-}$ and a momentum $\hbar\omega/c = \hbar/\lambda\!\!\!^{-}$, the volume that they occupy in momentum space is $V_p \sim (2\hbar/\lambda\!\!\!^{-})^3 \Delta\Omega$, i.e. $V_p \sim 10\hbar^3/(\lambda r^2)$. The gravitons' volume in phase space, then, is

$$V_x V_p \sim 1000\hbar^3 \sim 4(2\pi\hbar)^3 . \qquad (4.35)$$

Since each quantum state for a zero rest-mass particle occupies a volume $(2\pi\hbar)^3$ in phase space (see, e.g., XXXXX), this means that the

total number of quantum states occupied by the gravitons is of order unity! Correspondingly, the occupation number of each occupied state is of order the total number of gravitons emitted, which (since the total energy radiated in a strong supernova is of order $10^{-2}M_\odot c^2 \sim 10^{52}$ ergs, and each graviton carries an energy $\hbar c/\lambda\!\!\!^{-} \sim 10^{-23}$ erg), is

$$n_{\rm occ} \sim 10^{75} . \qquad (4.36)$$

This enormous occupation number means that the waves behave exceedingly classically; quantum-mechanical corrections to the classical theory have fractional magnitude $1/\sqrt{n_{\rm occ}} \sim 10^{-37}$ (see, e.g., XXXXXX).

Although the quantization of gravity is exceedingly difficult and not yet fully understood, the quantization of weak gravitational waves propagating through a smooth background spacetime — equivalent to weak waves in flat spacetime — has been well understood for decades; see, e.g., the most elementary aspects of Feynman (1963) or Dewitt (1967a,b). For some surprising insights into the coupling of gravitons to quantized fields see Ford (1982).

4.F Transverse-traceless coordinates

When a detector is small compared to the reduced wavelength $\lambda\!\!\!^{-}$ of the waves it seeks, one can analyze it with good accuracy in its proper reference frame using standard, flat spacetime techniques augmented by the gravitational-wave force (4.12) or (4.16). However, for a detector large compared to $\lambda\!\!\!^{-}$ that proper-reference-frame analysis fails [cf. the discussion following Eq. (4.10)]. The simplest way to analyze such a detector is using a so-called transverse-tracless (TT) coordinate system. To understand such a TT analysis, one must know a bit of general relativity; and I shall assume such knowledge in this, the last section of Chap. 4.

Although the detector may be large compared to $\lambda\!\!\!^{-}$, we shall assume it small enough to be covered by a single nearly Lorentz reference frame. (This is a good assumption for all detectors considered in this book, except gravitational-wave detection based on anisotropies of the primordial microwave radiation.) Moreover, we shall choose our nearly Lorentz frame to be at rest with respect to the detector's center of mass, or at least to have a velocity relative to the center of mass that is small compared to unity. I claim, and shall prove below, that the spacetime coordinates x^μ of this nearly Lorentz frame can be further adjusted so that in it the metric coefficients take the following special

form:

$$g_{\alpha\beta} = \eta_{\alpha\beta} + h^{B}_{\alpha\beta} + h^{GW}_{\alpha\beta} \ . \tag{4.37}$$

Here $\eta_{\alpha\beta}$ is the metric of flat spacetime; $h^{B}_{\alpha\beta}$ describes the (slowly varying) non-gravitational-wave component of gravity (e.g. the gravity of the earth, moon, sun, and planets); $h^{GW}_{\alpha\beta}$ is the gravitational-wave field (4.26); and both of the $h_{\alpha\beta}$'s are small compared to unity. When the coordinate system is so adjusted, it is called transverse-traceless (TT) because the gravitational waves' contribution, $h^{GW}_{\alpha\beta}$, to the metric $g_{\alpha\beta}$ is purely spatial, transverse, and traceless.

To verify that there exist TT coordinates in which the metric takes the form (4.37), all we need do is check that this form gives correctly the contribution (4.27) of the gravitational waves to the Riemann curvature tensor. This can be verified by inserting (4.37) into the standard expression for Riemann in terms of the metric [Eqs. (5.13) and (5.9) below], and by then linearizing in the small ($\ll 1$) $h^{B}_{\alpha\beta} + h^{GW}_{\alpha\beta}$. The result for the waves' contribution is (4.27).

If the spatial TT coordinate axes are oriented so that the wave propagates in the z-direction, then the only nonzero components of $h^{GW}_{\alpha\beta}$ are (4.22), and correspondingly the spacetime metric (4.37) takes the form

$$\begin{aligned} ds^2 = &- dt^2 + dz^2 + [1+h_+(t-z)]dx^2 + [1-h_+(t-z)]dy^2 \\ &+ 2h_\times(t-z)dxdy + h^{B}_{\alpha\beta}dx^\alpha dx^\beta \ . \end{aligned} \tag{4.38}$$

It is instructive to contrast the form (4.38) of the metric in TT coordinates with that in a proper reference frame. One can show (cf. Sec. 13.6 of MTW, or Ni and Zimmermann, 1978) that, with an appropriate slight adjustment of the spatial coordinates, the proper-reference-frame metric takes the following form:

$$\begin{aligned} ds^2 = &-(1-2g_jx^j+R_{j0k0}x^jx^k)dt^2 - 2(\varepsilon_{jkl}x^k\Omega^l+\tfrac{2}{3}R_{jkl0})dtdx^j \\ &+ (\delta_{ij}-\tfrac{1}{3}R_{ijm}x^lx^m)dx^idx^j \ , \end{aligned} \tag{4.39}$$

plus corrections of higher order. Here g_j is the "acceleration of gravity" in the proper reference frame, due to the failure of the frame to fall freely, and Ω^l is the frame's angular velocity of rotation with respect to the gyroscopes of an inertial guidance system. (For the proper reference frames used in this chapter Ω^l was set to zero.) Several aspects of this metric deserve discussion: (i) It is expressed as a power series expansion in spatial distance from the origin of

coordinates. Correspondingly, sufficiently near the spatial origin one can ignore the deviations of its $g_{\alpha\beta}$ from the flat metric $\eta_{\alpha\beta}$ and can carry out one's analyses using standard, flat-spacetime techniques augmented by the tidal force (4.10). This was the approach taken earlier in this chapter wherever proper reference frames were used (Secs. 4.B and 4.C). (ii) Since the waves' Riemann tensor has magnitude $\mathcal{H}/\lambda^2$, where $\mathcal{H}$ is the magnitude of h_+ and $h_\times$, the waves' contribution to the proper-reference-frame metric (4.39) has magnitude

$$\delta g^{GW}_{\alpha\beta} \sim \mathcal{H}\frac{|\mathbf{x}|^2}{\lambda^2}\,, \tag{4.40}$$

where $|\mathbf{x}|$ is spatial distance from the origin of coordinates. Note that $|\delta g^{GW}_{\alpha\beta}| \ll \mathcal{H}$ at distances $|\mathbf{x}| \ll \lambda$ from the origin. This means, for example, that when a detector is small compared to λ, the direct coupling of its internal electromagnetic fields to the gravitational waves (which produces effects of order $|\delta g^{GW}_{\alpha\beta}|$) can be ignored by comparison with the mechanical strains $\Delta L/L \sim \mathcal{H}$ produced by the waves' tidal force (4.10). However, when the detector has size $\gtrsim \lambda$, the $\delta g^{GW}_{\alpha\beta}$ of (4.40) will be $\gtrsim \mathcal{H}$, and one cannot ignore the coupling of the waves to electromagnetic fields. (iii) The higher-order corrections ignored in (4.39) include terms such as

$$\delta g^{GW}_{00} \sim \frac{\partial^2 R^{GW}_{ijkl}}{\partial t^2} x^i x^j x^k x^l \sim \mathcal{H}\frac{|\mathbf{x}|^4}{\lambda^4}\,. \tag{4.41a}$$

These corrections become comparable to (4.40) at distances $\sim \lambda$, as do corrections of arbitrarily high order in $|\mathbf{x}|$. (iv) Correspondingly, in a proper reference frame the geodesic equation for a slowly moving test particle takes the form

$$\frac{d^2x^j}{dt^2} = -\Gamma^j{}_{00} = \tfrac{1}{2}g_{00,j} = g_j + R^{GW}_{j0k0}x^k + 0\left(\mathcal{H}\frac{|\mathbf{x}|^3}{\lambda^4}\right); \tag{4.41b}$$

and since $R^{GW}_{j0k0}x^k \sim \mathcal{H}\,|\mathbf{x}|/\lambda^2$, the corrections to the standard wave force R^{GW}_{j0k0} become as large as that force at $|\mathbf{x}| \gtrsim \lambda$. (This same calculation, carried out in a general nearly Lorentz frame, shows that the frame must be a proper reference frame in order for the gravitational-wave acceleration to take on the simple form $R^{GW}_{j0k0}x^k$.)

In summary, the key feature of the proper reference frame which makes it so much better than TT coordinates for detectors with size $\ll \lambda$ is the fact that in it $|\delta g^{GW}_{\alpha\beta}| \ll \mathcal{H}$. This ceases to be true when the detector's size is $\gtrsim \lambda$; and, correspondingly, the proper reference frame

ceases being useful. By contrast, the TT coordinates are valid and useable over much larger regions. How large? The only constraint is that the metric perturbations h_+, $h_\times$, and $h^B_{\alpha\beta}$ of Eq. (4.38) be small compared to unity so we can linearize in them. As we shall see at the end of Sec. 5.D, gravitational radiation always has $|h_+| \ll 1$ and $|h_\times| \ll 1$. In the real universe the only localized objects that have strong gravity ($h^B_{\alpha\beta} \sim 1$) are neutron stars and black holes; and the cosmological contributions to the metric can be treated using local Lorentz coordinates [Eq. (4.39) with $g_j = 0$, $\Omega^l = 0$, and $R^B_{\alpha\beta\gamma\delta} \sim 1/(\text{Hubble distance})^2$, so $|h^B_{\alpha\beta}| \sim (\text{distance from earth})^2/(\text{Hubble distance})^2$]. As a result, we can cover the entire universe, out to 0.01 of the Hubble distance, with transverse-traceless coordinates in which: (i) we cut out holes around all black holes and neutron stars; (ii) the gravitational-wave contributions to the TT metric (2.28) have $|h_+| \ll 1$ and $|h_\times| \ll 1$; and (iii) the background-gravity contributions $h^B_{\alpha\beta}$ to the metric have magnitudes $\lesssim 10^{-4}$.

In the next chapter we shall develop a geometric optics description of gravitational waves that is valid over arbitrarily large distances.

TT coordinates are not the only nearly Lorentz ones in which the contributions of the waves to the metric have the "speed-of-light-propagation" form

$$g_{\alpha\beta} - \eta_{\alpha\beta} = h_{\alpha\beta}(t-z)\,, \tag{4.42}$$

with $|h_{\alpha\beta}| \ll 1$. There are many other such coordinate systems. In any such nearly Lorentz coordinate system the transverse components R^{GW}_{x0x0}, R^{GW}_{y0y0}, $R^{GW}_{x0y0} = R^{GW}_{y0x0}$ of the waves' Riemann curvature tensor take the form [derivable from the standard equations (5.13) and (5.9)]

$$R^{GW}_{a0b0} = -\tfrac{1}{2}\frac{\partial^2 h_{ab}}{\partial t^2} \text{ for } a = x, y \text{ and } b = x, y\,. \tag{4.43}$$

By comparing with Eq. (4.15) we see that in any such coordinate system the transverse part of the waves' metric perturbation must be equal to the gravitational-wave field:

$$h^{GW}_{jk} = (h_{jk})^{TT}\,. \tag{4.44}$$

Here TT means "throw away all components except those which are spatial and are transverse to the waves' propagation direction". Since h^{GW}_{jk} is trace-free as well as transverse, we are guaranteed that the transverse part of h_{jk} will be trace-free; i.e. $h_{xx} + h_{yy} = 1$. To emphasize this trace-free property it is conventional to write Eq. (4.44) in the

form

$$h_{jk}^{GW} = (h_{jk})^{TT} , \tag{4.45}$$

where the second T means "remove the trace, if the trace is not already zero". To repeat, Eq. (4.45) is true in any nearly Lorentz coordinate system where the waves' contribution to the metric has the "speed-of-light-propagation" form (4.42) — or, equally well (by rotation of spatial axes) the form

$$h_{\alpha\beta} = h_{\alpha\beta}(t - n_j x^j) . \tag{4.42'}$$

Here n_j is a unit vector ($n_j n_k \delta^{jk} = 0$) pointing in the direction of propagation.

We shall find it easier, in Chaps. 5 and 6, to compute the "trace-reversed metric perturbation" associated with the waves,

$$\bar{h}_{\alpha\beta} \equiv h_{\alpha\beta} - \tfrac{1}{2}\eta_{\alpha\beta}\eta^{\mu\nu}h_{\mu\nu} , \tag{4.46}$$

than to compute $h_{\alpha\beta}$ itself. Notice that, since $\bar{h}^{\alpha\beta}$ differs from $h_{\alpha\beta}$ only by a multiple of $\eta_{\alpha\beta}$, its spatial, TT part is identical to that of $h_{\alpha\beta}$ and thus to that of the gravitational-wave field:

$$h_{jk}^{GW} = (\bar{h}_{jk})^{TT} . \tag{4.47}$$

This is true in any coordinate system where $h_{\alpha\beta}$ has the speed-of-light-propagation form (4.42'). When the waves propagate in the z-direction, Eq. (4.47) simply says that

$$h_+ \equiv h_{xx}^{GW} = \bar{h}_{xx} - \tfrac{1}{2}(\bar{h}_{xx} + \bar{h}_{yy}) = \tfrac{1}{2}(\bar{h}_{xx} - \bar{h}_{yy}) , \quad h_\times \equiv h_{xy}^{GW} = \bar{h}_{xy} . \tag{4.48}$$

If the waves propagate along the direction of an (arbitrary) unit vector **n**, the TT projection can be performed with the aid of the tensor

$$P^{jk} \equiv \delta^{jk} - n^j n^k \tag{4.49}$$

that projects orthogonal to **n**:

$$h_{jk}^{GW} = (\bar{h}_{jk})^{TT} = P_j{}^l P_k{}^m \bar{h}_{lm} - \tfrac{1}{2}P_{jk}P^{lm}\bar{h}_{lm} . \tag{4.50}$$

Here the notation is that of Cartesian coordinates in flat Euclidean space, with $P_j{}^k = P^{jk} = P_{jk}$. We shall find this transverse-traceless projection procedure especially useful in analyses of gravitational-wave generation (Chap. 6).

Table 1 gathers together and summarizes the main properties of the various types of coordinate systems that I have introduced and used in this chapter.

Table 4.1
Nearly Lorentz coordinate systems

General, nearly Lorentz reference frame

1. *Form of metric*: $g_{\alpha\beta} = \eta_{\alpha\beta} + g_{\alpha\beta}$ with $|h_{\alpha\beta}| \ll 1$
2. *Size of coordinate system*: Can extend out from earth to a small fraction of the Hubble distance (e.g. 0.01 Hubble), with holes cut out around every black hole and neutron star.
3. *Uses of coordinate system*: All other coordinate systems in this table are special cases of this one. The mathematical properties of the Riemann tensor can be treated in this coordinate system, approximating $g_{\alpha\beta}$ by $\eta_{\alpha\beta}$ ("field theory in flat spacetime"); this includes, most importantly, the propagation of gravitational waves via $\Box R^{GW}_{\alpha\beta\gamma\delta} = 0$.

Proper reference frame

1. *Form of metric*: Eq. (4.39); in particular, the metric perturbation due to gravitational radiation has magnitude $\frac{1}{2}\mathcal{H}|\mathbf{x}|^2/\lambda\!\!\!^{-2}$, where $\mathcal{H}$ is the amplitude of the gravitational-wave fields h_+ and $h_\times$.
2. *Size of coordinate system*: Must be kept small compared to the inhomogeneity scale of the Riemann curvature. In studies of background gravitational effects this means small compared to $\mathcal{R}$; in studies of gravitational waves it means small compared to the waves' reduced wavelength $\lambda\!\!\!^{-}$.
3. *Uses of coordinate system*: Used to discuss local physical measurements by an arbitrarily moving observer, including measurements of gravitational effects. In it gravitational forces are described by $F_j = mg_j - mR_{j0k0}x^k$ in general, and gravitational-wave forces by $F_j^{GW} = -mR^{GW}_{j0k0}x^k = \frac{1}{2}m(\partial^2 h^{GW}_{jk}/\partial t^2)x^k$. It is ideally suited to analyses of gravitational-wave detectors with sizes small compared to $\lambda\!\!\!^{-}$.

Local Lorentz (local inertial) reference frame

1. *Form of metric*: Same as proper reference frame, Eq. (4.39), but with vanishing acceleration $-g_j$ and angular velocity Ω^l of the spatial latticework.

2. *Size of coordinate system*: Same as proper reference frame (see above).
3. *Uses of coordinate system*: Used to discuss local physical measurements by a freely falling observer. Gravitational forces in it are the same as in any proper reference frame (see above).

TT coordinate system

1. *Form of metric*: Eq. (4.38); in particular, the metric perturbation due to gravitational waves is equal to the gravitational-wave field $h^{GW}_{\alpha\beta}$.
2. *Size of coordinate system*: Huge; same as a general nearly Lorentz frame (see above).
3. *Uses of coordinate system*: Well suited to analyses of gravitational-wave detectors with size large compared to a reduced wavelength λ.

Nearly Lorentz coordinates in which the waves' metric perturbation propagates at the speed of light

1. *Form of metric*: Same as in a general, nearly Lorentz frame, but with the waves' metric perturbation propagating at the speed of light.
2. *Size of coordinate system*: Huge; same as a general nearly Lorentz frame (see above).
3. *Uses of coordinate system*: The gravitational-wave field $h^{GW}_{\alpha\beta}$ can be computed from the waves' metric perturbation $h_{\alpha\beta}$ by algebraically projecting out the spatial, transverse, traceless part [Eq. (4.50)].

5 Propagation of Gravitational Waves

In this chapter we shall study the propagation of gravitational waves from their source to the earth. We begin in Sec. 5.A by writing down the propagation laws in their simplest form, that appropriate to the *geometric-optics approximation*. Then in Secs. 5.B, 5.C, and 5.D we derive those geometric-optics propagation laws in a careful manner, identifying along the way the various assumptions that must be made. Each assumption entails discarding physical effects that might be important in special but unusual situations.

For simplicity, our geometric-optics laws are specialized to propagation through vacuum; however, as part of our derivation of them, we obtain in Secs. 5.B and 5.C a propagation equation that describes the interaction of the waves with matter and with electromagnetic fields. In Secs. 5.E and 5.F we seek insight into that interaction by calculations with this propagation equation. Our calculations show that, although the coupling of waves to matter and electromagnetism is fascinating in principle, it is almost never significant in practice: In realistic astrophysical situations the vacuum approximation to wave propagation is excellent.

In Sec. 5.G we study a wide variety of vacuum propagation phenomena (scattering and parametric amplification by background curvature, tails of waves, gravitational focusing and diffraction, nonlinear wave-wave coupling, ...); we describe how to analyze these effects; and we discuss their relevance to wave propagation in the real universe. We conclude the chapter in Sec. 5.H with a brief discussion of two special, non-geometric-optics analyses of wave propagation: a set

of exact solutions to the Einstein field equation, which describe propagating waves; and the theory of the asymptotic structure of the gravitational-wave field outside an isolated source in an asymptotically flat spacetime.

In order to understand this chapter and Chap. 6, the reader will need prior familiarity with general relativity at, e.g., the level of "track one" of MTW (Misner, Thorne, and Wheeler, 1973). Readers without such familiarity can move on to Chaps. 7–12, which should be understandable without mastery of Chaps. 5 and 6.

Our notation and mathematical conventions will be those of MTW. A key role will be played, in the mathematical formalism, by a split of the full, gravitational-wave-endowed spacetime into a background spacetime [obtained by averaging over several wavelengths of the waves, cf. Eqs. (4.4) above and (5.6) below], plus the waves. After the split has been made, the waves will be thought of as a field that propagates through the background spacetime. We shall use a vertical slash to denote covariant derivatives, i.e. gradients, in the background spacetime, so if S^α (also denoted abstractly as S) is a vector field that lives in the background spacetime, then $S^\alpha{}_{|\mu}$ (also denoted abstractly as ∇S) is its gradient. Similarly, we shall use a semicolon to denote covariant derivatives in the full, pre-split, wave-endowed spacetime, so if A^α lives in the full spacetime, then $A^\alpha{}_{;\mu}$ is its gradient.

5.A Geometric-optics propagation laws

Geometric optics is a very general formalism for studying the propagation of any kind of wave through any kind of medium. This formalism is valid whenever the wave's reduced wavelength λ is small compared to the radius of curvature of its wave fronts, and also small compared to all inhomogeneity scales of the medium through which it propagates.

For gravitational waves *in vacuum*, the geometric-optics propagation can be described as follows. (We shall derive this description in Secs. 5.B, 5.C, 5.D, and we shall show in Secs. 5.E and 5.F that it is also valid to high accuracy for gravitational waves propagating through astrophysically realistic matter.)

Consider, for concreteness, a source of gravitational waves somewhere far out in the universe. In the vicinity of the source but some wavelengths away from it (so as to avoid near-zone fields that will be discussed in Chap. 6), introduce a local Lorentz reference frame in

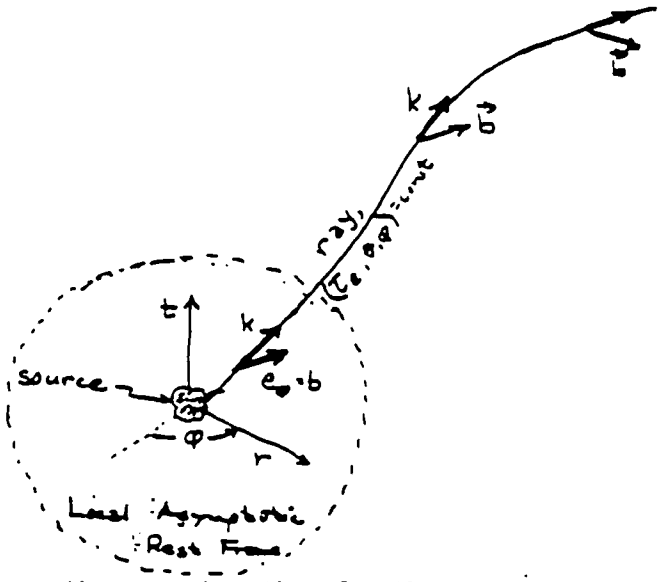

Fig. 5.1 Geometric-optics construction for the propagation of gravitational waves from a source's local asymptotic rest frame (region inside dotted circle) out through the external universe (region outside dotted circle).

which the source is at rest (the source's *local asymptotic rest frame*; Fig. 5.1). In that frame construct spherical polar coordinates (t,r,θ,ϕ) centered on the source and construct the associated orthonormal basis vectors $\mathbf{e}_0$, $\mathbf{e}_r$, $\mathbf{e}_\theta$, $\mathbf{e}_\phi$. The gravitational waves propagate radially through this asymptotic rest frame, with their retarded time τ_e and their wave vector $\mathbf{k} = -\nabla\tau_e$ (introduced in Sec. 4.D) given by

$$\tau_e = t - r\ , \quad \mathbf{k} = \mathbf{e}_0 + \mathbf{e}_r\ . \tag{5.1a}$$

The gravitational-wave field $h^{GW}_{\alpha\beta}$ associated with the asymptotic rest frame will have the form [Eq. (4.26)]

$$h^{GW}_{\alpha\beta} = h_+(a_\alpha a_\beta - b_\alpha b_\beta) + h_\times(a_\alpha b_\beta + b_\alpha a_\beta)\ . \tag{5.1b}$$

Here a_α and b_α are polarization vectors that are purely spatial in the source's asymptotic rest frame, have unit length, and are orthogonal to each other and to the waves' (radial) propagation direction. For example, we are free to choose them to be the unit vectors in the θ and ϕ directions

$$\mathbf{a} = \mathbf{e}_{\hat\theta}\ , \quad \mathbf{b} = \mathbf{e}_{\hat\phi}\ . \tag{5.1c}$$

Any other choice will be rotated relative to this choice by some angle ψ in the transverse plane, and correspondingly h_+ and $h_\times$ will be modified in the manner of expression (4.23). The propagation of the waves

(5.1b) through the source's asymptotic rest frame and then on out through the entire universe is described by the following geometric–optics construction:

(i) The waves propagate along a family of null geodesics of the background spacetime, which are called the waves' *rays*. These rays are the specific solutions to the geodesic equation

$$k_{\alpha|\beta}k^{\beta} = 0 \,, \tag{5.2a}$$

which begin in the asymptotic rest frame with $\mathbf{k} = \mathbf{e}_0 + \mathbf{e}_r$ and extend from there on out through the universe (Fig. 5.1). Each ray is labeled by the direction (θ,ϕ) in which it emerges from the source, and by the retarded time τ_e at which it emerges. By this labeling, τ_e, θ, and ϕ are carried out through the universe on the rays. The tangent vector $\mathbf{k}$ to the rays is given by

$$\mathbf{k} = -\nabla\tau_e \,, \tag{5.2b}$$

not just in the source's local asymptotic rest frame, but everywhere in the universe, as one can verify by checking that this $\mathbf{k}$ satisfies the geodesic equation (5.2a). [Specifically, $k_{\alpha|\beta}k^{\beta} = \tau_{e|\alpha\beta}\tau_e{}^{|\beta}$, which, by commutation of the covariant derivatives of a scalar field, is equal to $\tau_{e|\beta\alpha}\tau_e{}^{|\beta} = \frac{1}{2}(\tau_{e|\beta}\tau_e{}^{|\beta})_{|\alpha}$, which vanishes because $\tau_{e|\beta}$ is null.] (ii) Next, parallel transport the polarization vectors a_α and b_α along the waves' rays out through the universe,

$$a_{\alpha|\beta}k^{\beta} = 0 \,, \quad b_{\alpha|\beta}k^{\beta} = 0 \,. \tag{5.2c}$$

(iii) Define all along each ray a *radius function* r in the following way: Consider the 2–dimensional bundle of rays, surrounding the ray of interest, which all have the same τ_e as that ray but which have θ in the range $\Delta\theta$ and ϕ in the range $\Delta\phi$, so they subtend, as seen from the source, a solid angle $\Delta\Omega = \sin\theta\Delta\theta\Delta\phi$. As one moves out along the ray of interest, the cross–sectional area ΔA of this bundle (which is locally Lorentz–invariant; cf. Exercise 22.13 of MTW) changes, but by definition $\Delta\Omega$ remains fixed. The radius function is defined to be

$$r \equiv (\Delta A / \Delta\Omega)^{1/2} \,. \tag{5.2d}$$

Of course, in the source's local asymptotic rest frame this is just equal to the distance to the source. However, far out in the universe it might be quite different from that distance. For example, gravitational lenses (to be discussed in Sec. 5.G.c below) can make the area of the bundle and thence also r switch over from increasing along a ray to

decreasing. (iv) The (frame-invariant) gravitational-wave fields h_+ and $h_\times$ are carried outward along each ray unchanged, except for an overall alteration proportional to $1/r$ (which is required to conserve the waves' energy as they propagate):

$$h_+ = \frac{Q_+(\tau_e,\theta,\phi)}{r}\,, \quad h_\times = \frac{Q_\times(\tau_e,\theta,\phi)}{r}\,. \tag{5.2e}$$

The functions Q_+ and $Q_\times$ can be evaluated in the source's local asymptotic rest frame using the theory of gravitational-wave generation (Chap. 6), and then can be carried out along the rays unchanged. (v) The polarization tensors e_{jk}^{+} and $e_{jk}^{\times}$ associated with these fields, as measured in any proper reference frame anywhere in the universe, are

$$e_{jk}^{+} = (a_j a_k - b_j b_k)^{TT}\,, \quad e_{jk}^{\times} = (a_j b_k + b_j a_k)^{TT}\,, \tag{5.2f}$$

where the superscripts TT denote the transverse-traceless projection of Eq. (4.50). (vi) Correspondingly, the gravitational-wave field

$$h_{jk}^{GW} = h_+ e_{jk}^{+} + h_\times e_{jk}^{\times}\,, \tag{5.2g}$$

as measured in that proper reference frame, is given by

$$h_{jk}^{GW} = (h_{jk})^{TT} \tag{5.2h}$$

[Eq. (4.45)], where h_{jk} is the spatial part of the field

$$h_{\alpha\beta} \equiv h_+(a_\alpha a_\beta - b_\alpha b_\beta) + h_\times(a_\alpha b_\beta + b_\alpha a_\beta)\,. \tag{5.2i}$$

As a simple example, consider the propagation of gravitational waves through a closed Friedman model for our universe. The background metric [obtained by averaging over the waves' short-wavelength ripples in the manner of Eq. (4.4a)] has the standard Friedman form [MTW, Eqs. (27.46) and (27.23)]

$$ds^2 = a^2[-d\eta^2 + d\chi^2 + \sin^2\chi(d\theta^2 + \sin^2\theta d\phi^2)]\,, \tag{5.3}$$

where $a = a(\eta)$ is the universe's "expansion factor". (Never mind that this spacetime is filled with matter rather than being vacuum; as we shall see in Sec. 5.E the presence of matter has no significant influence on the propagation.) Place the source of gravitational waves at the origin of the spatial coordinates, $\chi = 0$. Then the waves' rays are the radial null geodesics $\chi = \eta - \eta_e$, where η_e is the coordinate time at which the ray is emitted. Retarded time on each ray is the proper time of emission, $\tau_e = \int_0^{\eta_e} a\,d\eta$; and the ray's radial function is $r = a\sin\chi$, which is the same radial function as appears in the expression for the optical

brightness of a source of electromagnetic radiation [Eq. (29.28) of MTW]. Expressed in terms of the "deceleration parameter" q_0 and "Hubble expansion rate" H_0 of the universe, and the redshift z of the source as viewed optically from earth, this radial function is [Eq. (29.33) of MTW]

$$r = \frac{H_0^{-1}}{q_0^2(1+z)}[-q_0+1+q_0 z+(q_0-1)(2q_0+1)^{1/2}] . \tag{5.4}$$

Note that, if the waves are emitted in an epoch when the universe's expansion factor is a_e and are received at earth when it is a_0, then in terms of proper time t as measured in the earth's local proper reference frame, the source's retarded time is $\tau_e = (a_e/a_0)t$ + const. $= t/(1+z)$ + const., where $z = a_0/a_e$ is the source's "cosmological redshift". Correspondingly, the time dependence of the waveform as measured at earth is unchanged by the waves' propagation, except for a frequency-independent redshift $f_{\text{received}}/f_{\text{emitted}} = 1/(1+z)$ which is identically the same as for electromagnetic waves.

In fact, this similarity to electromagnetic waves is completely general: If one develops the geometric-optics formalism for electromagnetic wave propagation, one finds that the electromagnetic vector potential has the form

$$A_\alpha = A_1 a_\alpha + A_2 b_\alpha , \tag{5.5a}$$

where a_α and b_α are precisely the same polarization vectors as we used for gravitational waves; and that

$$A_1 = \frac{Q_1(\tau_e,\theta,\phi)}{r} , \quad A_2 = \frac{Q_2(\tau_e,\theta,\phi)}{r} , \tag{5.5b}$$

where τ_e, θ, ϕ, r are precisely the same functions as we used above in the gravitational-wave formulas. (See, e.g., the treatment of monochromatic, electromagnetic geometric optics in Sec. 22.5 of MTW, translated into the notation of this book and with many frequencies superposed to give waveforms with arbitrary time dependences.) By comparing Eqs. (5.2e) and (5.5b) we infer that, in the geometric optics limit, the gravitational-wave fields h_+ and $h_\times$ experience precisely the same amplitude changes and redshift changes as do the components A_1 and A_2 of the electromagnetic vector potential.

5.B Linear perturbations of curved spacetime

As a foundation for deriving the above geometric-optics description of vacuum wave propagation (and also for discussing the effects discarded by geometric optics, the energy and momentum carried by gravitational waves, the generation of gravitational waves, and propagation through nonvacuum regions of spacetime), we shall develop in this section some mathematical formalism. This formalism will describe linearized perturbations of an arbitrary, nonvacuum spacetime geometry.

Whereas our description of gravitational waves thus far has focussed on the Riemann curvature tensor, our analysis here will focus on the metric $g_{\alpha\beta}$ of spacetime. We shall write that metric as the sum of a *background* metric $g^{\rm B}_{\alpha\beta}$ and a perturbation $h_{\alpha\beta}$:

$$g_{\alpha\beta} = g^{\rm B}_{\alpha\beta} + h_{\alpha\beta} \,. \tag{5.6a}$$

The precise way of making the split into background plus perturbation will depend on the situation. The background might be a smooth part, defined by averaging $g_{\alpha\beta}$ over several wavelengths of gravitational radiation, and the perturbation then will be the remaining, rippled part; or the background might be a spherically symmetric part, and the perturbation the deviations from spherical symmetry; or the background might be the equilibrium spacetime for a rotating black hole, and the perturbation the deviations from that equilibrium. In order to be able to handle, with one formalism, all these situations and more, we shall here regard the split (5.6a) as a purely formal one: The *background* metric $g^{\rm B}_{\alpha\beta}$ is one solution to the Einstein field equation with one stress-energy tensor $T^{\rm B}{}^{\alpha\beta}$ as its source; the *full* metric $g_{\alpha\beta}$ is another solution, with another stress-energy tensor $T^{\alpha\beta}$; and the two solutions are nearly but not quite the same. Nearly identical coordinate systems are set up in the spacetimes of these two solutions, the coordinates are given the same names x^μ, and events in the background spacetime and the full spacetime are regarded as "the same" if they have the same coordinate values. The perturbation $h_{\alpha\beta}$ at location x^μ is then the difference between the two functions $g_{\alpha\beta}(x^\mu)$ and $g^{\rm B}_{\alpha\beta}(x^\mu)$.

We shall regard the metric perturbation $h_{\alpha\beta}$ as a symmetric tensor field that lives in the background spacetime, and correspondingly, we shall raise and lower indices on $h_{\alpha\beta}$ using the background metric $g^{\rm B}_{\alpha\beta}$. Because $g^{\alpha\beta}$ is the inverse of $g_{\alpha\beta}$ ($g_{\alpha\beta}g^{\beta\gamma} = \delta_\alpha{}^\gamma$), $g^{\alpha\beta}$ takes the form

$$g^{\alpha\beta} = g_{\rm B}^{\alpha\beta} - h^{\alpha\beta}\,, \quad \text{where } h^{\alpha\beta} = g_{\rm B}^{\alpha\mu} g_{\rm B}^{\beta\nu} h_{\mu\nu}\,. \tag{5.6b}$$

Note the opposite signs in expressions (5.6a,b) for $g_{\alpha\beta}$ and $g^{\alpha\beta}$, and note that there is no significance to whether the B (for background) is placed up or down.

The difference between the stress–energy tensor of the full spacetime and that of the background spacetime, at the same coordinate locations x^μ, we shall write in the form

$$T^{\alpha\beta} = T_{\rm B}^{\alpha\beta} + \mathcal{T}^{\alpha\beta} - h^{\mu(\alpha} T_{\rm B}^{\beta)}{}_{\mu}\,. \tag{5.7a}$$

Here and henceforth the parentheses on indices denote symmetrization:

$$h^{\mu(\alpha} T_{\rm B}^{\beta)}{}_{\mu} \equiv \tfrac{1}{2}(h^{\mu\alpha} T_{\rm B}^{\beta}{}_{\mu} + h^{\mu\beta} T_{\rm B}^{\alpha}{}_{\mu})\,.$$

Equation (5.7a) serves as a definition of the stress–energy perturbation field $\mathcal{T}^{\alpha\beta}$. We choose this specific definition because it simplifies subsequent equations [e.g. Eqs. (5.33) and (5.34)]. We shall regard this $\mathcal{T}^{\alpha\beta}$, like $h_{\alpha\beta}$, as a linear field that resides in the background spacetime, with indices to be raised and lowered using $g_{\alpha\beta}^{\rm B}$. By lowering indices on $T^{\alpha\beta}$ with $g_{\alpha\beta} = g_{\alpha\beta}^{\rm B} + h_{\alpha\beta}$ and linearizing in $\mathcal{T}^{\alpha\beta}$ and $h_{\alpha\beta}$, we obtain

$$T_{\alpha\beta} = T_{\alpha\beta}^{\rm B} + \mathcal{T}^{\alpha\beta} + h^{\mu}{}_{(\alpha} T_{\beta)\mu}^{\rm B}\,. \tag{5.7b}$$

Note the opposite signs on the last terms in expressions (5.7a) and (5.7b), completely analogous to the opposite signs in (5.6a) and (5.6b).

The evolution of $\mathcal{T}^{\alpha\beta}$ will be governed by first-order perturbations of the law of energy–momentum conservation; and the evolution of $h_{\alpha\beta}$, by first-order perturbations of the Einstein field equation. In discussing these evolution laws, we shall use a semicolon to denote a covariant derivative in the full spacetime, a vertical bar for a covariant derivative in the background spacetime, and a comma for an ordinary partial derivative with respect to our chosen coordinates. Correspondingly, the laws of energy–momentum conservation in the full and background spacetimes are

$$T^{\alpha\beta}{}_{;\beta} \equiv T^{\alpha\beta}{}_{,\beta} + \Gamma^{\alpha}{}_{\mu\beta} T^{\mu\beta} + \Gamma^{\beta}{}_{\mu\beta} T^{\alpha\mu} = 0\,; \tag{5.8a}$$

$$T_{\rm B}^{\alpha\beta}{}_{|\beta} \equiv T_{\rm B}^{\alpha\beta}{}_{,\beta} + \Gamma^{{\rm B}\alpha}{}_{\mu\beta} T_{\rm B}^{\mu\beta} + \Gamma^{{\rm B}\beta}{}_{\mu\beta} T_{\rm B}^{\alpha\mu} = 0\,; \tag{5.8b}$$

Here $\Gamma^{\alpha}{}_{\beta\gamma}$ is the connection coefficient for the full spacetime, and $\Gamma^{{\rm B}\alpha}{}_{\beta\gamma}$ is that for the background spacetime:

$$\Gamma^{\alpha}{}_{\beta\gamma} = \tfrac{1}{2} g^{\alpha\mu}(g_{\mu\beta,\gamma} + g_{\mu\gamma,\beta} - g_{\beta\gamma,\mu})\,, \quad \Gamma^{{\rm B}\alpha}{}_{\beta\gamma} = \tfrac{1}{2} g_{\rm B}^{\alpha\mu}(g_{\mu\beta,\gamma}^{\rm B} + g_{\mu\gamma,\beta}^{\rm B} - g_{\beta\gamma,\mu}^{\rm B}) \tag{5.9}$$

[see, e.g., Eqs. (8.24b,c) of MTW]. Their difference can be evaluated to linear order with the help of Eqs. (5.6). The result, expressed in terms of the background's covariant derivative of $h_{\alpha\beta}$, is

$$S^{\alpha}{}_{\beta\gamma} \equiv \Gamma^{\alpha}{}_{\beta\gamma} - \Gamma^{B\alpha}{}_{\beta\gamma} = \tfrac{1}{2} g^{B\alpha\mu}(h_{\mu\beta|\gamma} + h_{\mu\gamma|\beta} - h_{\beta\gamma|\alpha}) . \qquad (5.10)$$

(For a sophisticated method of deriving this and the equations that follow, see Exercise 35.11 of MTW. However, sophistication is not needed; one can derive these equations by elementary algebra and index shuffling, plus a lot of sweat.)

It is a straightforward calculation to take the difference between the full and the background laws of energy–momentum conservation [Eqs. (5.8a,b)] and express it in terms of the perturbations of the stress–energy tensor and of the connection coefficients. The result, after also using Eq. (5.10), is the following *evolution equation for the stress-energy perturbation*:

$$\mathcal{T}^{\alpha\mu}{}_{|\mu} = \tfrac{1}{2}(h_{\mu\nu}{}^{|\alpha} - h^{\alpha}{}_{\mu|\nu})T_B^{\mu\nu} + \tfrac{1}{2}(h_{\mu\nu}{}^{|\nu} - h^{\nu}{}_{\nu|\mu})T_B^{\mu\alpha} . \qquad (5.11)$$

This shows how gradients of the metric perturbations $h_{\alpha\beta|\gamma}$ couple to the background stress–energy to generate stress–energy perturbations $\mathcal{T}_{\alpha\beta}$.

One application of this equation is to gravitational-wave detection: there $h_{\alpha\beta}$ is the metric perturbation associated with the gravitational radiation, $T_B^{\alpha\beta}$ is the stress–energy tensor of an unperturbed detector, and $\mathcal{T}^{\alpha\beta}$ is the influence of the waves on the detector. When the detector involves a set of masses on which the waves act, and the coordinate system is a proper reference frame of $g_{\alpha\beta}$ and also of $g^{B}_{\alpha\beta}$, in which the masses are nearly at rest, then the dominant spatial term (driving force) on the right-hand side of (5.11) is

$$\tfrac{1}{2} h_{00}{}^{|j} T_B^{00} = -(R^{GW}_{j0k0} x^k) T_B^{00}$$

[cf. Eq. (4.39)]. This is the "per-unit-volume" version of the gravitational-wave force (4.12) of Chap. 4.

The Riemann curvature tensors of our two spacetimes can be expressed in terms of the connection coefficients and their derivatives by the standard formula [MTW, Eq. (8.44)]

$$R^{\alpha}{}_{\beta\gamma\delta} = \Gamma^{\alpha}{}_{\beta\delta,\gamma} - \Gamma^{\alpha}{}_{\beta\gamma,\delta} + \Gamma^{\alpha}{}_{\mu\gamma}\Gamma^{\mu}{}_{\beta\delta} - \Gamma^{\alpha}{}_{\mu\delta}\Gamma^{\mu}{}_{\beta\gamma} , \qquad (5.12)$$

and the same formula for the background but with a superscript B on all quantitities. By taking the difference between these two formulas and discarding terms nonlinear in the metric perturbation, we obtain

$$\delta R^{\alpha}{}_{\beta\gamma\delta} \equiv R^{\alpha}{}_{\beta\gamma\delta} - R^{\mathrm{B}\alpha}{}_{\beta\gamma\delta} = S^{\alpha}{}_{\beta\delta|\gamma} - S^{\alpha}{}_{\beta\gamma|\delta}$$
$$= \tfrac{1}{2} g^{\mathrm{B}\mu}(h_{\mu\beta|\delta\gamma} + h_{\mu\delta|\beta\gamma} - h_{\beta\delta|\mu\gamma} - h_{\mu\beta|\gamma\delta} - h_{\mu\gamma|\beta\delta} + h_{\beta\gamma|\mu\delta}) . \qquad (5.13)$$

Since the Ricci curvature tensors are obtained by contracting on the first and third indices of the Riemann tensors, Eq. (5.13) yields immediately for the perturbation of the Ricci tensor

$$\delta R_{\beta\delta} \equiv R_{\beta\delta} - R^{\mathrm{B}}_{\beta\delta} = \tfrac{1}{2}(h_{\mu\beta|\delta}{}^{\mu} + h_{\mu\delta|\beta}{}^{\mu} - h_{\beta\delta|\mu}{}^{\mu} - h_{|\beta\delta}) , \qquad (5.14)$$

where the h with no subscripts denotes the contraction of $h_{\mu\nu}$ (using, of course, the background metric: $h \equiv h_{\mu\nu} g^{\mathrm{B}\mu\nu}$).

It is the Einstein tensor, $G_{\mu\nu} \equiv R_{\mu\nu} - \frac{1}{2} R g_{\mu\nu}$ (where $R \equiv R_{\alpha\beta} g^{\alpha\beta}$) that appears on the left-hand side of the Einstein field equation. The perturbation in the Einstein tensor is readily computed from Eq. (5.14) and the perturbation (5.6) in the metric. The result is most nicely expressed not in terms of the metric perturbation $h_{\alpha\beta}$, but rather in terms of the trace-reversed metric perturbation

$$\bar{h}_{\alpha\beta} \equiv h_{\alpha\beta} - \tfrac{1}{2} h g^{\mathrm{B}}_{\alpha\beta} . \qquad (5.15)$$

The result is brought into the nicest form by commuting a pair of background covariant derivatives [at the price of introducing a term proportional to the background Riemann tensor; cf. Eqs. (16.6) of MTW]. The resulting, "nicest form" is

$$G_{\alpha\beta} - G^{\mathrm{B}}_{\alpha\beta} \equiv G^{(1)}_{\alpha\beta}(h) = -\tfrac{1}{2}(\bar{h}_{\alpha\beta|\mu}{}^{\mu} + g^{\mathrm{B}}_{\alpha\beta}\bar{h}^{\mu\nu}{}_{|\mu\nu} - 2\bar{h}_{\mu(\alpha|}{}^{\mu}{}_{\beta)} + 2R^{\mathrm{B}}_{\mu\alpha\nu\beta}\bar{h}^{\mu\nu}$$
$$- 2R^{\mathrm{B}}_{\mu(\alpha}\bar{h}_{\beta)}{}^{\mu} - R^{\mathrm{B}}_{\mu\nu}\bar{h}^{\mu\nu} g^{\mathrm{B}}_{\alpha\beta} + R^{\mathrm{B}}\bar{h}_{\alpha\beta}) . \qquad (5.16)$$

Here $R^{\mathrm{B}} \equiv R^{\mathrm{B}\mu}{}_{\mu}$ is the background scalar curvature, and the parentheses on indices denote symmetrization. This is the nicest form of $G^{(1)}_{\alpha\beta}$ because it simplifies so much when one specializes the *gauge*:

By "gauge" we mean "the choice of which points in the full spacetime correspond to which points in the background spacetime". To change the gauge, we can hold fixed the coordinates in the background spacetime, but change those in the full spacetime by the following very small amount (i.e. the following "infinitesimal coordinate transformation"):

$$x^{\alpha}_{\mathrm{old}} = x^{\alpha}_{\mathrm{new}} - \xi^{\alpha}(x^{\mu}_{\mathrm{new}}) . \qquad (5.17)$$

This gauge change produces the following change in the metric coefficients of the full spacetime:

$$g^{\mathrm{new}}_{\alpha\beta}(x^{\mu}_{\mathrm{new}}) = g^{\mathrm{old}}_{\rho\sigma}(x^{\mu}_{\mathrm{old}}) \frac{\partial x^{\sigma}_{\mathrm{old}}}{\partial x^{\alpha}_{\mathrm{new}}} \frac{\partial x^{\sigma}_{\mathrm{old}}}{\partial x^{\beta}_{\mathrm{new}}} . \qquad (5.18)$$

By combining this with Eq. (5.17) and with Eq. (5.6) for both the old and the new gauges, we obtain the relationship between the new and the old metric perturbations

$$h^{\rm new}_{\alpha\beta} = h^{\rm old}_{\alpha\beta} - \xi_{\alpha|\beta} - \xi_{\beta|\alpha} \,. \tag{5.19}$$

Thus, the *generator of the gauge change* ξ_α, viewed as a field living in the background spacetime, produces the change (5.19) in the metric perturbation. This is completely analogous to gauge changes in electromagnetism: The $h_{\alpha\beta}$ here is the analog of the electromagnetic vector potential A_α; the generator of the gauge change ξ_α is the analog of the electromagnetic gauge-change generator ψ; and Eq. (5.19) is the analog of $A^{\rm new}_\alpha = A^{\rm old}_\alpha - \psi_{,\alpha}$. Moreover, just as the electromagnetic evolution equation for A_α takes on an especially simple form when one specializes to the "Lorentz gauge" ($A^\alpha{}_{|\alpha} = 0$), so also the Einstein-tensor perturbation and thence the Einstein equation take on especially simple forms when one specializes to the *gravitational Lorentz gauge*

$$\bar{h}^{\alpha\beta}{}_{|\beta} = 0 \,. \tag{5.20}$$

If one is not initially in this Lorentz gauge, one can go there by the gauge change whose generator satisfies the wave-equation-with-source

$$\xi_{\alpha|\beta}{}^{\beta} = -R^{\rm B}_{\alpha\beta}\xi^\beta + h^{\rm old}_{\alpha\beta}{}^{|\beta} \,. \tag{5.21}$$

In Lorentz gauge the perturbation (5.16) of the Einstein tensor simplifies to

$$G^{(1)}_{\alpha\beta}(h) = -\tfrac{1}{2}(\bar{h}_{\alpha\beta|\mu}{}^{\mu} + 2R^{\rm B}_{\mu\alpha\nu\beta}\bar{h}^{\mu\nu} - 2R^{\rm B}_{\mu(\alpha}\bar{h}_{\beta)}{}^{\mu} - R^{\rm B}_{\mu\nu}\bar{h}^{\mu\nu}g^{\rm B}_{\alpha\beta} + R_{\rm B}\bar{h}_{\alpha\beta}) \,, \tag{5.22}$$

which involves only the wave operator plus the coupling of $\bar{h}_{\alpha\beta}$ to background curvature.

The perturbed Einstein equation [with Newton's gravitation constant G set to unity as we shall do throughout Chaps. 5 and 6, cf. Eqs. (4.3)] equates this $G^{(1)}_{\alpha\beta}$ to 8π times the stress-energy perturbation [Eq. (5.7b)]

$$G^{(1)}_{\alpha\beta}(h) = 8\pi(T_{\alpha\beta} - T^{\rm B}_{\alpha\beta}) = 8\pi(\mathcal{T}_{\alpha\beta} + h^\mu{}_{(\alpha}T^{\rm B}_{\beta)\mu}) \,. \tag{5.23}$$

By combining Eqs. (5.22), (5.23), and the background Einstein equation $G^{\rm B}_{\alpha\beta} = 8\pi T^{\rm B}_{\alpha\beta}$, we obtain our final Lorentz-gauge form for the first-order, perturbed Einstein equation:

$$\bar{h}_{\alpha\beta|\mu}{}^{\mu} + 2R^{\rm B}_{\mu\alpha\nu\beta}\bar{h}^{\mu\nu} = -16\pi(\mathcal{T}_{\alpha\beta} - \tfrac{1}{2}\bar{h}_{\mu\nu}T^{\mu\nu}_{\rm B}g^{\rm B}_{\alpha\beta} - \tfrac{1}{2}\bar{h}T^{\rm B}_{\alpha\beta} + \tfrac{1}{4}\bar{h}T_{\rm B}g^{\rm B}_{\alpha\beta}) \,. \tag{5.24}$$

The equation of motion (5.11) for $\mathcal{T}_{\alpha\beta}$, which goes hand-in-hand with this wave equation, takes the following form when expressed in terms of $\bar{h}_{\alpha\beta}$ rather than $h_{\alpha\beta}$, and when specialized to Lorentz gauge:

$$\mathcal{T}^{\alpha\mu}{}_{|\mu} = \tfrac{1}{2}(\bar{h}_{\mu\nu}{}^{|\alpha} - \bar{h}^{\alpha}{}_{\mu|\nu})T_{\mathrm{B}}{}^{\mu\nu} + \tfrac{1}{2}\bar{h}_{|\mu}T_{\mathrm{B}}{}^{\mu\alpha} - \tfrac{1}{4}\bar{h}^{|\alpha}T_{\mathrm{B}} . \qquad (5.25)$$

In Eqs. (5.24) and (5.25), $\bar{h}$ and T_{B} without indices denote the traces of $\bar{h}_{\alpha\beta}$ and $T_{\mathrm{B}}{}^{\alpha\beta}$: $\bar{h} \equiv \bar{h}_{\alpha\beta}g_{\mathrm{B}}{}^{\alpha\beta}$ and $T_{\mathrm{B}} \equiv T_{\mathrm{B}}{}^{\alpha\beta}g^{\mathrm{B}}{}_{\alpha\beta}$.

Equations (5.24) *and* (5.25) *describe the joint, coupled evolution of the gravitational perturbations* $\bar{h}_{\alpha\beta}$ *and the stress-energy perturbations* $\mathcal{T}_{\alpha\beta}$. In the remainder of this chapter we shall use these coupled equations to study the propagation of gravitational waves in the presence of matter and electromagnetic fields. In Chap. 6 we shall use them to study the generation of gravitational waves by astrophysical sources.

5.C The shortwave formalism

Turn, now, from general formalism to a specific situation: the propagation of gravitational radiation with reduced wavelength $\sim\lambda$ through a background spacetime with inhomogeneity scale $\mathcal{L}$. Assume, as in Chap. 4, that $\lambda \ll \mathcal{L}$ so the waves are well defined. Then the propagation is beautifully described using a *shortwave formalism* due to Isaacson (1968a,b). In this section we shall develop that formalism.

In our analysis we shall need, in addition to λ and $\mathcal{L}$, a third lengthscale: the radius of curvature $\mathcal{R}$ of the background spacetime. We define it to be the inverse square root of the largest components of the background Riemann tensor, evaluated in a proper reference frame

$$\mathcal{R} \equiv (\text{minimum value of } |R^{\mathrm{B}}{}_{\alpha\beta\gamma\delta}|^{-1/2}): \qquad (5.26)$$

This lengthscale is depicted heuristically in Fig. 4.1 on page XX. We shall always define the inhomogeneity lengthscale $\mathcal{L}$ to be no larger than the curvature lengthscale,

$$\mathcal{L} \lesssim \mathcal{R} , \qquad (5.27)$$

because of a philosophical viewpoint that curvature itself is a form of inhomogeneity. (This also simplifies some of the conceptual issues that follow.)

We introduce into the full spacetime a coordinate system which, for the moment, we constrain in only one way: we demand that in it the metric coefficients $g_{\alpha\beta}$, like the physical curvature, vary on lengthscales $\sim\lambda$, $\sim\mathcal{L}$, and possibly $\gg\mathcal{L}$, but not on any lengthscales between λ and $\mathcal{L}$. Following Isaacson (1968a), we shall call such a coordinate

system *steady*. We then define the background spacetime by the demand that there exist in it coordinates in which the background metric coefficients are the average over several wavelengths of the steady coordinates' $g_{\alpha\beta}$:

$$g^{B}_{\alpha\beta}(x^{\mu}) \equiv \langle g_{\alpha\beta}(x^{\mu}) \rangle . \tag{5.28}$$

The difference between $g_{\alpha\beta}$ and $g^{B}_{\alpha\beta}$ describes, of course, the gravitational radiation. In analyzing this radiation we shall be interested not only in linear effects, but also in nonlinear ones — for example, the energy and momentum carried by the waves. In preparation for discussing nonlinear effects, we shall write the difference between $g_{\alpha\beta}$ and $g^{B}_{\alpha\beta}$ not as a single field $h_{\alpha\beta}$, but rather as a power series:

$$\underset{1,\ \lambda/\mathcal{L}}{g_{\alpha\beta}} = \underset{1,\ \lambda/\mathcal{L}}{g^{B}_{\alpha\beta}} + \underset{\lambda/\mathcal{L},\ \lambda}{h_{\alpha\beta}} + \underset{\lambda^2/\mathcal{L}^2,\ \lambda}{j_{\alpha\beta}} + \cdots . \tag{5.29}$$

Below each term we show the characteristic magnitude (1, $\lambda/\mathcal{L}$, $\lambda^2/\mathcal{L}^2$) of the term, and also the lengthscale (λ or $\mathcal{L}$) on which it varies. Note that $j_{\alpha\beta}$ is a nonlinear correction to the propagating waves. This nonlinear correction is not yet precisely defined. We are free to shove pieces of it in and out of $h_{\alpha\beta}$ in such a way as to make the computational formalism as simple as possible.

Similarly, we split up the covariant components of the stress-energy tensor in the following way:

$$T_{\alpha\beta} = T^{B}_{\alpha\beta} + \mathcal{T}_{\alpha\beta} + h^{\mu}{}_{(\alpha} T^{B}_{\beta)\mu} + j^{\mu}{}_{(\alpha} T^{B}_{\beta)\mu} + \cdots \tag{5.30a}$$

[cf. Eq. (5.7b)]. Here, by definition, $T^{B}_{\alpha\beta}$ is the average of $T_{\alpha\beta}$ over several wavelengths

$$T^{B}_{\alpha\beta} \equiv \langle T_{\alpha\beta} \rangle ; \tag{5.30b}$$

and $\mathcal{T}_{\alpha\beta} + h_{\mu(\alpha} T^{B}_{\beta)\mu} + j^{\mu}{}_{(\alpha} T^{B}_{\beta)\mu} + \cdots$ is the fluctuating part, which averages to zero. Our chosen form (5.30a) of $T_{\alpha\beta}$ amounts to a definition of the stress-energy perturbation field $\mathcal{T}_{\alpha\beta}$. This specific definition is carefully chosen to make the fluctuating parts of the field equations [Eqs. (5.33) and (5.34) below] especially simple. We shall meet evidence of that simplicity in specific calculations with the formalism in Sec. 5.E.

In formulating the mathematics of our shortwave formalism, as in the linear perturbation theory of Sec. 5.C, we shall treat $h_{\alpha\beta}$, $j_{\alpha\beta}$, $\mathcal{T}_{\alpha\beta}$, and all other quantities except $T_{\alpha\beta}$ and $g_{\alpha\beta}$, as fields that reside in the background spacetime. Correspondingly, we shall raise and lower their

indices using the background metric $g^{B}_{\alpha\beta}$.

By a calculation analogous to that of the last section, but one which includes nonlinear terms as well as linear, one can derive a power-series expansion for the Einstein curvature tensor $G_{\alpha\beta}$ of the full spacetime:

$$G_{\alpha\beta} = \underset{\lesssim \mathcal{H}^{-2},\, \mathcal{L}}{G^{B}_{\alpha\beta}} + \underset{\mathcal{H}\lambda^{-2},\, \lambda}{G^{(1)}_{\alpha\beta}(h)} + \underset{\mathcal{H}^{2}\lambda^{-2},\, \lambda}{G^{(2)}_{\alpha\beta}(h)} + \underset{\mathcal{H}^{2}\lambda^{-2},\, \lambda}{G^{(1)}_{\alpha\beta}(j)} + \cdots . \tag{5.31}$$

Here, as in Eq. (5.29), we write below each term its magnitude and the lengthscale on which it varies. The notation has the following meanings: $G^{B}_{\alpha\beta}$ is the Einstein curvature tensor of the background spacetime, computed from the metric $g^{B}_{\alpha\beta}$; $G^{(1)}_{\alpha\beta}(h)$, the piece that is linear in the radiation field $h_{\alpha\beta}$, is given by expression (5.16); $G^{(1)}_{\alpha\beta}(j)$ is this same expression, but with $h_{\alpha\beta}$ replaced by $j_{\alpha\beta}$; and $G^{(2)}_{\alpha\beta}(h)$ is the piece that is quadratic in $h_{\alpha\beta}$ [derivable from MTW Eqs. (35.58)].

Following Isaacson (1968a,b), we split the Einstein field equation $G_{\alpha\beta} = 8\pi T_{\alpha\beta}$, through order $\mathcal{H}^{2}$, into three parts: a part which varies on scales $\mathcal{L}$ (obtained by averaging over a few wavelengths)

$$G^{B}_{\alpha\beta} = -\langle G^{(2)}_{\alpha\beta}(h)\rangle + 8\pi T^{B}_{\alpha\beta} \; ; \tag{5.32a}$$

a part whose individual terms have magnitude $\mathcal{H}\lambda^{-2}$ or smaller, vary on scales λ, and average to zero on larger scales

$$G^{(1)}_{\alpha\beta}(h) = 8\pi(T_{\alpha\beta} + h^{\mu}{}_{(\alpha}T^{B}_{\beta)\mu}) \; ; \tag{5.32b}$$

and a part whose terms have magnitude $\mathcal{H}^{2}\lambda^{-2}$ or smaller, vary on scales λ, and average to zero on larger scales

$$G^{(1)}_{\alpha\beta}(j) = -\,G^{(2)}_{\alpha\beta}(h) + \langle G^{(2)}_{\alpha\beta}(h)\rangle + 8\pi j^{\mu}{}_{(\alpha}T^{B}_{\beta)\mu} \; . \tag{5.32c}$$

This choice of how to split up the field equations determines the details of the split of the waves into $h_{\alpha\beta}+j_{\alpha\beta}$. Changing the split-up [pulling a piece of Eq. (5.32c) into Eq. (5.32b)] would shove a piece of $j_{\alpha\beta}$ into $h_{\alpha\beta}$. Our specific choice of the split is guided by a desire to make the first-order equation (5.32b) identical to the linearized equation (5.23), so that when a weak wave enters a region of rapidly varying curvature $\mathcal{L} \lesssim \lambda$ (e.g. when it impinges on a black hole), our first-order equation continues to be valid.

The first-order equation (5.32b) is a wave equation for the propagation of the first-order gravitational wave $h_{\alpha\beta}$. By specializing to Lorentz gauge, expressing the background Ricci tensor in terms of the

background Einstein tensor, using Eq. (5.36) below for the background Einstein tensor, and discarding terms of the form $\bar{h}_{\alpha\beta}T^{GW}_{\gamma\delta}$ because they are cubic in the wave amplitude $\mathcal{H}$ (one order smaller than the accuracy of our analysis), we bring Eq. (5.32b) into the standard linearized form (5.24):

$$\Box\bar{h}_{\alpha\beta} \equiv \bar{h}_{\alpha\beta|\mu}{}^{\mu} = -2R^{B}_{\mu\alpha\nu\beta}\bar{h}^{\mu\nu} - 16\pi(\mathcal{T}_{\alpha\beta} - \tfrac{1}{2}\bar{h}_{\mu\nu}T_{B}{}^{\mu\nu}g^{B}_{\alpha\beta} - \tfrac{1}{2}\bar{h}T^{B}_{\alpha\beta} + \tfrac{1}{4}\bar{h}T_{B}g^{B}_{\alpha\beta}) . \tag{5.33}$$

Much of the rest of this chapter will be devoted to a discussion of this wave equation and the physical effects associated with it.

In Lorentz gauge and in vacuum, Eq. (5.32c) takes on the form

$$\Box\bar{j}_{\alpha\beta} = -2R^{B}_{\mu\alpha\nu\beta}\bar{j}^{\mu\nu} + 8\pi(\bar{j}_{\mu\nu}T_{B}{}^{\mu\nu}g^{B}_{\alpha\beta} + \bar{j}T^{B}_{\alpha\beta} - \tfrac{1}{2}\bar{j}T_{B}g^{B}_{\alpha\beta}) + 2G^{(2)}_{\alpha\beta}(h) - 2\langle G^{(2)}_{\alpha\beta}(h)\rangle . \tag{5.34}$$

Here $\bar{j}_{\alpha\beta} \equiv j_{\alpha\beta} - \frac{1}{2}j_{\mu}{}^{\mu}g^{B}_{\alpha\beta}$, and $\bar{j} \equiv \bar{j}_{\mu}{}^{\mu}$. The terms on the right-hand side involving $G^{(2)}(h)$, which are quadratic in $h_{\alpha\beta}$, act as a source for the nonlinear corrections $j_{\alpha\beta}$ to $h_{\alpha\beta}$. Thus, this equation describes nonlinear wave-wave coupling ("3-wave coupling" in the standard jargon of nonlinear physics) analogous to that which occurs in plasma physics or for electromagnetic waves in a nonlinear medium. We shall discuss the effects of this wave-wave coupling in Sec. 5.G.e below.

Equation (5.32a) describes the waves' nonlinear generation of background curvature. This equation, in fact, is the foundation for Isaacson's (1968b) description of the energy and momentum carried by the waves: Isaacson defines the *gravitational-wave stress-energy tensor* by

$$T^{GW}_{\alpha\beta} \equiv -\frac{1}{8\pi}\langle G^{(2)}_{\alpha\beta}(h)\rangle , \tag{5.35}$$

and then notes that in terms of this tensor Eq. (5.32a) takes on the same form as the standard Einstein field equation

$$G^{B}_{\alpha\beta} = 8\pi(T^{B}_{\alpha\beta} + T^{GW}_{\alpha\beta}) . \tag{5.36}$$

Equation (5.36) shows that the gravitational-wave stress-energy tensor, like any nongravitational stress-energy tensor, generates spacetime curvature. Isaacson points out, moreover, that because $G^{B}_{\alpha\beta}$, like any Einstein tensor, automatically has vanishing divergence, the sum $T^{B}_{\alpha\beta} + T^{GW}_{\alpha\beta}$ is guaranteed also to have vanishing divergence:

$$(T^{\mathrm{B}\alpha\beta} + T^{\mathrm{GW}\alpha\beta})_{|\beta} = 0 \,. \tag{5.37}$$

In other words, when averaged over a few wavelengths, the sum of the gravitational-wave energy-momentum and the nongravitational energy-momentum is conserved. For example, when a gravitational-wave detector is driven into motion by a passing wave, the detector's energy (embodied in $T^{\mathrm{B}\alpha\beta}$) goes up, and the wave's energy (embodied in $T^{\mathrm{GW}\alpha\beta}$) goes down.

A straightforward but tedious calculation (Isaacson, 1968b; Eq. (35.70) of MTW and associated discussion) gives the following explicit expression for $T^{\mathrm{GW}}_{\alpha\beta}$ in an arbitrary gauge:

$$T^{\mathrm{GW}}_{\alpha\beta} = \frac{1}{32\pi}\langle \bar{h}_{\mu\nu|\alpha}\bar{h}^{\mu\nu}{}_{|\beta} - \tfrac{1}{2}\bar{h}_{|\alpha}\bar{h}_{|\beta} - \bar{h}^{\mu\nu}{}_{|\nu}\bar{h}_{\mu\alpha|\beta} - \bar{h}^{\mu\nu}{}_{|\nu}\bar{h}_{\mu\beta|\alpha}\rangle \,. \tag{5.38}$$

Here $\bar{h}_{\alpha\beta}$ is the trace-reversed, first-order metric perturbation [Eq. (5.15)]. Note that in Lorentz gauge the last two terms vanish; and in a nearly Lorentz frame and TT gauge, because $\bar{h}_{00} = \bar{h}_{0j} = 0$ and $\bar{h}_{jk} = h^{\mathrm{GW}}_{jk}$ which is trace free, Eq. (5.38) reduces to

$$T^{\mathrm{GW}}_{\alpha\beta} = \frac{1}{32\pi}\langle h^{\mathrm{GW}}_{jk,\alpha} h^{\mathrm{GW}}_{jk,\beta}\rangle \,. \tag{5.39}$$

Here there is an implied summation on j and k, which are Cartesian, spatial indices. When, moreover, the waves propagate in the z-direction of a nearly Lorentz frame so $h^{\mathrm{GW}}_{xx} = -h^{\mathrm{GW}}_{yy} = h_+(t-z)$, $h^{\mathrm{GW}}_{xy} = h^{\mathrm{GW}}_{yx} = h_\times(t-z)$, this becomes the expression (4.33) that was discussed in Chap. 4.

Note that the magnitude of the gravitational-wave stress-energy tensor is $T^{\mathrm{GW}}_{\alpha\beta} \sim (\lambda\!\!\!^{-}/\lambda)^2$; cf. Eq. (4.34). Since this stress-energy is a source of background curvature through the averaged Einstein equation $G^{\mathrm{B}}_{\alpha\beta} = 8\pi(T^{\mathrm{B}}_{\alpha\beta} + T^{\mathrm{GW}}_{\alpha\beta})$ [Eq. (5.36)], it must be that $G^{\mathrm{B}}_{\alpha\beta} \gtrsim (\lambda\!\!\!^{-}/\lambda)^2$. However, because $G^{\mathrm{B}}_{\alpha\beta}$ is constructed as a sum of components of the background Riemann tensor, the largest of which have magnitudes $1/\mathcal{R}^2$, it must be that $G^{\mathrm{B}}_{\alpha\beta} \lesssim 1/\mathcal{R}^2$. From these relations and $\mathcal{R} \gtrsim \mathcal{L}$ we infer that

$$\lambda\!\!\!^{-} \lesssim \lambda/\mathcal{R} \lesssim \lambda/\mathcal{L} \,. \tag{5.40}$$

Since the very concept of a gravitational wave has meaning only when $\lambda \ll \mathcal{L}$, Eq. (5.40) tells us that *gravitational radiation always has a small dimensionless amplitude*,

$$\lambda\!\!\!^{-} \ll 1 \,. \tag{5.41}$$

Equation (5.37) is only one portion of the law of conservation of energy–momentum: the portion obtained by averaging $T^{\alpha\beta}{}_{;\beta} = 0$ over a few wavelengths. The other portion, that which fluctuates on scales of order λ and averages to zero, has the linearized form (5.25):

$$\mathcal{T}^{\alpha\mu}{}_{|\mu} = \tfrac{1}{2}(\bar{h}_{\mu\nu}{}^{|\alpha} - \bar{h}^{\alpha}{}_{\mu|\nu})T_{\rm B}^{\mu\nu} + \tfrac{1}{2}\bar{h}_{|\mu}T_{\rm B}^{\mu\alpha} - \tfrac{1}{4}\bar{h}^{|\alpha}T_{\rm B} . \qquad (5.42)$$

The right side is the force exerted by the waves on the matter or fields through which they propagate, and the left side is the response of the matter or fields to this gravitational force.

5.D Geometric optics

Turn, next, to the task of solving the wave equation (5.33) for the propagation of $\bar{h}^{\alpha\beta}$ from its source to the earth. As we shall see in Secs. 5.E and 5.F, in the real astrophysical universe (except near the Planck time) the effects of matter and electromagnetic fields on the propagating waves are minuscule. This permits us to simplify our analysis by setting to zero, in the propagation equation (5.33), the nongravitational stress-energies $\mathcal{T}_{\alpha\beta}$ and $T^{\rm B}_{\alpha\beta}$ — a procedure we shall call the *vacuum approximation* for wave propagation.

The wave equation (5.33) has already been simplified by specializing to Lorentz gauge; and we shall now simplify it further by an additional specialization of the gauge: It is not difficult to verify that the gauge will remain Lorentz ($\bar{h}^{\alpha\beta}{}_{|\beta} = 0$ will continue to be satisfied) if the generator ξ_α of the gauge change (5.19) satisfies the wave equation $\Box\xi_\alpha = 0$. Note, further, that the trace of the propagation equation (5.33) guarantees (in vacuum) that $\bar{h} = \bar{h}^{\alpha}{}_{\alpha}$ satisfies the wave equation $\Box\bar{h} = 0$. Accordingly, if we choose ξ_α to be a solution of the wave equation $\Box\xi_\alpha = 0$ such that $\xi^{\alpha}{}_{|\alpha} = \frac{1}{2}h^{\rm old} = -\frac{1}{2}\bar{h}^{\rm old}$, then the gauge change (5.19) will remove the trace of $h_{\alpha\beta}$. We make this gauge change, thereby guaranteeing that

$$h = \bar{h} = 0 , \quad \bar{h}_{\alpha\beta} = h_{\alpha\beta} . \qquad (5.43)$$

This permits us to omit bars from $h_{\alpha\beta}$ in what follows.

We expect the field $h_{\alpha\beta}$ to be a rapidly varying function of the source's retarded time $\tau_{\rm ret}$, and a slowly varying function of all other spacetime coordinates. More specifically, it should vary in $\tau_{\rm ret}$ on a lengthscale λ (the reduced wavelength of the waves); and all its other variations should have lengthscales no longer than

$$\mathcal{L} \equiv \text{minimum of } \mathcal{R} \text{ and radius of curvature of wave fronts.} \qquad (5.44)$$

Accordingly, we shall seek a solution of the propagation equation which is accurate only to leading order in the small dimensionless parameter $\lambda\!\!\!^{-}/\mathcal{D}$ — in other words, we shall solve for the propagation using the *vacuum, geometric-optics approximation.*

As a formal mathematical tool in the solution, we introduce a parameter ε which tells us at a glance the relative orders of magnitude of various terms: If a specific term is of order $(\lambda\!\!\!^{-}/\mathcal{D})^n$ relative to other terms with which it is compared, then we shall prepend to it a factor ε^n. However, we shall take the numerical value of ε to be one, thereby allowing ourselves to drop it when it ceases to be useful. In this spirit, we write the field $h_{\alpha\beta}$ in the form ("geometric optics expansion")

$$h_{\alpha\beta} = h^{[0]}_{\alpha\beta}(\tau_e/\varepsilon, x^\mu) + \varepsilon h^{[1]}_{\alpha\beta}(\tau_e/\varepsilon, x^\mu) + \varepsilon^2 h^{[2]}_{\alpha\beta}(\tau_e/\varepsilon, x^\mu) + \cdots . \quad (5.45)$$

The term $h^{[0]}_{\alpha\beta}$ is the geometric optics approximation to $h_{\alpha\beta}$, and $h^{[1]}_{\alpha\beta}$, $h^{[2]}_{\alpha\beta}$, ... are "post-geometric-optics corrections". It will be straightforward to read off our formalism the equations governing the corrections, but we will focus attention in the end only on the leading term, $h^{[0]}_{\alpha\beta}$. Each $h^{[n]}_{\alpha\beta}$ varies in τ_e on the scale $\lambda\!\!\!^{-}$ and in its argument x^μ on the scale $\mathcal{D}$; i.e. it can be thought of as varying on scales of order unity in both $\tau_e/\lambda\!\!\!^{-}$ and $x^\mu/\mathcal{D}$ — which means that by comparison with x^μ, the τ_e in the functional form requires a factor ε^{-1}. That is why we write the functional form as $h^{[n]}_{\alpha\beta}(\tau_e/\varepsilon, x^\mu)$. Because of this functional form, we write the covariant derivative (gradient) of $h^{[n]}_{\alpha\beta}$ as

$$h^{[n]}_{\alpha\beta|\mu} = -\varepsilon^{-1}\dot{h}^{[n]}_{\alpha\beta}k_\mu + h^{[n]}_{\alpha\beta|\mu'} . \quad (5.46)$$

Here the dot denotes a derivative with respect to τ_e

$$\dot{h}_{\alpha\beta} \equiv \left[\frac{\partial h_{\alpha\beta}}{\partial \tau_e}\right]_{x^\mu} ; \quad (5.47a)$$

k_μ is the negative of the gradient of τ_e

$$k_\mu \equiv -\tau_{e|\mu} ; \quad (5.47b)$$

and the prime on the last μ index indicates that the covariant derivative is to be taken holding τ_e constant.

This notation makes straightforward the geometric-optics expansion of the propagation equation (5.33), the Lorentz gauge condition (5.20), and our auxiliary gauge condition (5.43). The result of those expansions is:

$$\varepsilon^{-2}\ddot{h}^{[0]}_{\alpha\beta}k_\mu k^\mu + \varepsilon^{-1}(-2\dot{h}^{[0]}_{\alpha\beta|\mu'}k^\mu - \dot{h}^{[0]}_{\alpha\beta}k^\mu{}_{|\mu} + \ddot{h}^{[1]}_{\alpha\beta}k_\mu k^\mu) + \varepsilon^0(2R^{\mathrm{B}}{}_{\mu\alpha\nu\beta}h^{[0]\mu\nu}$$

$$+ h^{[0]}_{\alpha\beta|\mu'}{}^{|\mu'} - 2h^{[1]}_{\alpha\beta|\mu'}k^{\mu} - h^{[1]}_{\alpha\beta}k^{\mu}{}_{|\mu} + h^{\alpha\beta[2]}k_{\mu}k^{\mu}) + O(\varepsilon) = 0 ; \quad (5.48a)$$

$$-\varepsilon^{-1}h^{[0]}_{\alpha\beta}k^{\beta} + \varepsilon^{0}(h^{[0]}_{\alpha\beta}{}^{|\beta'} - h^{[1]}_{\alpha\beta}k^{\beta}) + O(\varepsilon) = 0 ; \quad (5.48b)$$

$$h^{[0]}_{\alpha}{}^{\alpha} + \varepsilon h^{[1]}_{\alpha}{}^{\alpha} + \varepsilon^{2}h^{[2]}_{\alpha}{}^{\alpha} + O(\varepsilon^{3}) = 0 . \quad (5.48c)$$

By equating to zero the leading two orders in (5.48a) and the leading order in (5.43b,c), we obtain the geometric-optics equations that govern $h^{[0]}_{\alpha\beta}$:

$$k_{\mu}k^{\mu} = 0 , \quad h^{[0]}_{\alpha\beta|\mu'}k^{\mu} = -\tfrac{1}{2}k^{\mu}{}_{|\mu}h^{[0]}_{\alpha\beta} , \quad h^{[0]}_{\alpha\beta}k^{\beta} = 0 , \quad h^{[0]}_{\alpha}{}^{\alpha} = 0 . \quad (5.49)$$

The higher-order terms in (5.48) govern the post-geometric-optics corrections to the propagation.

The first of Eqs. (5.49) tells us that the wave vector $\mathbf{k} = -\nabla\tau_{e}$ is null, as it surely should be since we chose τ_{e} to be retarded time. By taking the gradient of $k_{\mu}k^{\mu} = 0$, then noting that $k_{\mu|\nu} = -\tau_{e|\mu\nu} = -\tau_{e|\nu\mu} = k_{\nu|\mu}$, we deduce that $k_{\nu|\mu}{}^{|\mu} = 0$. Thus, the wave vector is the tangent vector to a null geodesic. That null geodesic is a *ray* of the propagating waves.

The second of Eqs. (5.49) tells us how the field $h^{[0]}_{\alpha\beta}$ propagates along its rays. Note that, because τ_{e} is constant along any ray, we do not need the prime on the gradient in this propagation equation: with or without the prime, the left-hand side of the propagation equation is sensitive only to the changes in $h_{\alpha\beta}$ that hold τ_{e} constant.

The third of Eqs. (5.49) tells us that the field $h^{[0]}_{\alpha\beta}$ is orthogonal to its wave vector; and the fourth tells us it is trace-free.

Henceforth we shall ignore all post-geometric-optics corrections, and shall use $h^{[0]}_{\alpha\beta}$ as a high-accuracy approximation to $h_{\alpha\beta}$. Accordingly, we shall rewrite the equations (5.49) governing it as

$$k_{\mu}k^{\mu} = 0 , \quad k_{\nu|\mu}k^{\mu} = 0 , \quad (5.50a)$$

$$h_{\alpha\beta}k^{\beta} = 0 , \quad h_{\alpha}{}^{\alpha} = 0 , \quad (5.50b)$$

$$h_{\alpha\beta|\mu}k^{\mu} = -\tfrac{1}{2}k^{\mu}{}_{|\mu}h_{\alpha\beta} . \quad (5.50c)$$

Notice that the curvature-coupling term $R^{B}{}_{\mu\alpha\nu\beta}h^{\mu\nu}$, which appeared in the original propagation equation (5.33), is gone in the geometric-optics limit. It shows up only as a post-geometric-optics correction [the $O(\varepsilon^{0})$ part of Eq. (5.48a), where the coupling of $h^{[0]}_{\alpha\beta}$ to the curvature helps generate the tiny correction $h^{[1]}_{\alpha\beta}$]. Because that curvature coupling is gone, in the geometric-optics limit $h_{\alpha\beta}$ satisfies the wave

equation $\Box h_{\alpha\beta} = 0$; and because the waves' Riemann tensor is a linear sum of gradients of $h_{\alpha\beta}$ [Eq. (5.13)], it also satisfies the wave equation:

$$\Box R^{GW}_{\alpha\beta\gamma\delta} = 0 \,. \tag{5.51}$$

This is the propagation equation (4.5) which was derived in a very different manner in Sec. 4.A and was used as the foundation for the description of gravitational radiation in Chap. 4. Note, further, that in the geometric-optics approximation the waves' Riemann tensor (5.13) takes the form

$$R^{GW}_{\alpha\beta\gamma\delta} = \tfrac{1}{2}(\ddot{h}_{\alpha\delta}k_\beta k_\gamma + \ddot{h}_{\beta\gamma}k_\alpha k_\delta - \ddot{h}_{\alpha\gamma}k_\beta k_\delta - \ddot{h}_{\beta\delta}k_\alpha k_\gamma) \,. \tag{5.52}$$

This is identical in form to expression (4.27), except that here the field used is the geometric-optics approximation to the trace-free, Lorentz-gauge metric perturbation $h_{\alpha\beta}$, while in Chap. 4 the field used was the "gravitational-wave field" $h^{GW}_{\alpha\beta}$. Recall that in Chap. 4 there was a separate gravitational-wave field $h^{GW}_{\alpha\beta}$ associated with each nearly Lorentz reference frame, but that all those fields, when inserted into (5.52), produced the same frame-invariant Riemann tensor. In fact, in any specific small region of spacetime, one can adjust $h_{\alpha\beta}$ to be the same as the $h^{GW}_{\alpha\beta}$ of any desired nearly Lorentz frame there by a gauge change with a generator that has the geometric-optics form

$$\xi_\alpha = \xi_\alpha(\tau_e/\varepsilon, x^\mu) \,, \quad \text{where } \xi_\alpha k^\alpha = 0 \text{ and } \xi_{\alpha|\mu}k^\mu = 0 \,. \tag{5.53}$$

This gauge change, in fact, has precisely the same effect as the transverse-traceless projection process introduced in Eq. (4.50). Correspondingly, in the chosen nearly Lorentz frame the gravitational-wave field is

$$h^{GW}_{jk} = (h_{jk})^{TT} \,, \tag{5.54}$$

where the superscript TT means "perform the TT projection process of Eq. (4.50)".

We are ready, now, to make contact with the vacuum, geometric-optics propagation laws presented in Sec. 5.A: The field (5.2i) constructed there is the solution $h_{\alpha\beta}$ of the equations of propagation (5.50). To verify this is straightforward, except for one detail: it is necessary to know that the cross sectional area ΔA of a bundle of rays obeys the differential equation

$$\Delta A_{\,|\mu}k^\mu = k^\mu{}_{|\mu}\Delta A \,. \tag{5.55}$$

This is proved, for example, in Exercise 22.13 of MTW.

Finally, we note that for this geometric-optics solution (5.2i) to the propagation equations, Isaacson's gravitational-wave stress-energy tensor (5.38) reduces to

$$T^{GW}_{\alpha\beta} = \frac{1}{16\pi}\langle(\dot{h}_+)^2+(\dot{h}_\times)^2\rangle k_\alpha k_\beta = \frac{1}{16\pi r^2}\langle(\dot{Q}_+)^2+(\dot{Q}_\times)^2\rangle k_\alpha k_\beta , \quad (5.56)$$

in accord with an assertion made in Chap. 4 [Eq. (4.32)].

5.E Interaction of waves with matter

In developing the geometric optics formalism for gravitational-wave propagation, we ignored the coupling of the waves to the matter and nongravitational fields through which they propagate; i.e., we introduced the "vacuum approximation". In this section we shall study the coupling to matter, and in the next section, the coupling to electromagnetic fields. These studies will show that the vacuum approximation is highly accurate in the real astrophysical universe: the coupling to matter and electromagnetic fields can change only slightly the properties of the propagating waves. The sole exception is for waves emerging from the Planck era of the big bang. Near the Planck era, individual elementary particles and gravitons were so energetic that they could interact significantly (Sec. 7.2 of Zel'dovich and Novikov, 1983).

When gravitational waves pass through matter, they can be absorbed and scattered, and can develop dispersion (frequency-dependent propagation speeds). In this section we shall study absorption and dispersion, and shall describe and give references for scattering.

In our studies of absorption and dispersion, initially we shall confine attention to matter which, before the waves arrive, is static and has isotropic stresses and self-gravity that is negligible on length-scales somewhat larger than the waves' reduced wavelength. More specifically, we shall assume that in the region of spacetime we are studying there exists a local Lorentz frame of $g^B_{\alpha\beta}$ with size $\mathcal{D} \gg \lambda$ in which

$$T^{00}_B = \rho_B , \quad T^{0j}_B = 0 , \quad T^{jk}_B = p_B \delta^{jj} , \quad (5.57)$$

with ρ_B (the density) and p_B (the pressure) independent of time $t = x^0$ but possibly dependent on x^j; and we shall insist that throughout this frame the gravitational interactions of the matter are negligible. By "negligible interactions" I mean that (i) $g^B_{\alpha\beta}$ can be approximated by

$\eta_{\alpha\beta}$, and (ii) when the matter is perturbed on scales $\lesssim \lambda\!\!\!^{-}$, the gravitational influence of one element of matter on any other can be ignored. This rules out, for example, using our analysis to study the coupling of gravitational waves to quadrupolar normal modes of the earth; but it permits a study of coupling to short-wavelength sound waves inside the earth, to the quadrupolar modes of resonant-bar gravitational-wave detectors, and to primordial plasma in the early universe. Note that our local Lorentz frame must always be small compared with the background radius of curvature, $\lambda\!\!\!^{-} \ll \mathcal{R}$, since one can never approximate $g^{B}_{\alpha\beta}$ by $\eta_{\alpha\beta}$ on scales of order $\mathcal{R}$.

Specific examples that we shall study are a homogeneous perfect fluid (subsection *a* below), a homogeneous viscous fluid (subsection *b*), an inhomogeneous elastic medium, e.g. the earth (subsection *c*), a medium made of a large number of quadrupolar oscillators (subsection *d*), and a plasma (subsection *e*).

We presume that gravitational waves propagate into our local Lorentz frame from very far away, and thus are plane fronted on the scale of our frame. To simplify our calculations, we shall describe the waves in a gauge that is TT as the waves enter our frame. Since, as we shall see, interaction with the matter has only a tiny effect on the waves, on the right-hand side of the wave equation (5.33) we can treat the waves as having the undisturbed TT form

$$\bar{h}_{00} = \bar{h}_{0j} = 0, \quad \bar{h}_{jk} = h^{TT}_{jk}(t - n_j x^j) . \tag{5.58a}$$

Here n_j is a unit vector in the propagation direction, and h^{TT}_{jk} is the transverse-traceless gravitational-wave field

$$h^{TT}_{jk} n^k = 0 , \quad h^{TT}_{jk} \delta^{jk} = 0 . \tag{5.58b}$$

This form of $\bar{h}_{\alpha\beta}$ has $\bar{h} = 0$, and when contracted into the background stress-energy tensor (5.57) it gives $\bar{h}_{\alpha\beta} T^{\alpha\beta}_{B} = 0$, thereby bringing the wave equation (5.33) into the form

$$\Box \bar{h}_{\alpha\beta} + 2R^{B}_{\mu\alpha\nu\beta} \bar{h}^{\mu\nu} = -16\pi \mathcal{T}_{\alpha\beta} . \tag{5.59}$$

[Our original definition (5.7) of $\mathcal{T}_{\alpha\beta}$ was carefully crafted so that it alone would remain on the right-hand side of (5.59). If we had used the more naive definition $\mathcal{T}_{\alpha\beta} = T_{\alpha\beta} - T^{B}_{\alpha\beta}$, then the right-hand side of (5.59) would have contained an additional term $16\pi p_B \bar{h}^{\alpha\beta}$, thereby complicating our calculations but, of course, not changing their final physical conclusions.]

Notice that in (5.59) only the TT part of $\mathcal{T}_{\alpha\beta}$ can contribute to the physically measurable waves. All other parts (e.g. $\mathcal{T}_{00}$ and $\mathcal{T}_{jk}n^k$) produce changes in $\bar{h}_{\alpha\beta}$ that are pure gauge, i.e. that contribute nothing to the waves' Riemann tensor and thus can be removed by a gauge transformation.

In the equation of motion (5.42) for the matter, as on the right-hand side of the wave equation, we can use the undisturbed wave field (5.58). When Eqs. (5.58) and (5.57) are inserted into Eq. (5.42), all terms on the right-hand side are found to vanish, leaving only

$$\mathcal{T}^{\alpha\mu}{}_{|\mu} = 0 \,. \tag{5.60}$$

At first sight one might think that this equation of motion implies the waves have no influence at all on the matter. On the contrary, as we shall see, there is a coupling of waves and matter embodied in $\mathcal{T}^{\alpha\beta}$ and hence in (5.60). Equation (5.60) governs the dynamical response of the matter to that coupling, and (5.59) governs the response of the waves.

Although Eqs. (5.59) and (5.60) are valid only in a local Lorentz frame of size $\mathcal{D} \ll \mathcal{R}$, they can be used to study wave propagation on scales $\gtrsim \mathcal{R}$: All one need do is string a series of local Lorentz frames together along the route of the waves, and as the waves enter each frame transform them to that frame's TT gauge.

To make these remarks more concrete and to get physical insight into wave-matter coupling, we shall now study several specific situations.

a) Homogeneous perfect fluid

The coupling of gravitational waves to a homogeneous, perfect fluid has been studied by a number of researchers over the years. The analysis which I like most is that of Gayer and Kennel (1979). The following calculation is patterned on it.

For a homogeneous perfect fluid, the stress-energy tensor in the full spacetime has the general form

$$T^{\alpha\beta} = (\rho + p)u^\alpha u^\beta + p g^{\alpha\beta} \tag{5.61}$$

(see, e.g., Sec. 22.3 of MTW). Here u^α is the fluid 4-velocity, and ρ and p are the density and pressure as measured in the fluid's local rest frame. Our background stress-energy tensor (5.57) has this form with $u_{\hat{0}} = 1$ and $u_{\hat{j}} = 0$. Suppose that the fluid is perturbed slightly, so that a particle originally at location x^j gets moved to coordinate location

$x^j+\xi^j$. This displacement produces a fractional increase in fluid volume $\delta V/V = \xi^j{}_{|j}$; and correspondingly (by energy conservation), the density changes by $\delta\rho = -(\rho_B+p_B)\xi^j{}_{|j}$, and the pressure changes by $\delta p = -K\xi^j{}_{|j}$, where K is the fluid's bulk modulus. The time-dependent displacement ξ^j also produces a first-order change $\delta u^0 = 0$, $\delta u^j = \dot{\xi}^j$ in the 4-velocity, where the dot denotes $\partial/\partial t$. These perturbations, together with $\delta g^{\alpha\beta} = -h^{\alpha\beta}$, all contribite to the stress-energy perturbation

$$T^{\alpha\beta} - T^{\alpha\beta}_B = (\delta\rho+\delta p)u_B^\alpha u_B^\beta + 2(\rho_B+p_B)u^{(\alpha}\delta u^{\beta)} + \delta p g_B^{\alpha\beta} - ph^{\alpha\beta} . \quad (5.62)$$

Our definition (5.7a) of $\mathcal{T}^{\alpha\beta}$ has been carefully crafted so that the wave-dependent term $-ph^{\alpha\beta}$ will drop out of it. More specifically, by combining Eqs. (5.62) and (5.7a) and inserting the above values of $\delta\rho$, δp, and δu^α, we obtain

$$\mathcal{T}^{00} = -(\rho_B+p_B+K)\xi^i{}_{|i} , \quad \mathcal{T}^{0j} = (\rho_B+p_B)\dot{\xi}^j , \quad \mathcal{T}^{jk} = -K\xi^i{}_{|i}\delta^{jk} . \quad (5.63)$$

Notice that nowhere at all in this $\mathcal{T}^{\alpha\beta}$ is there any gravitational-wave field $\bar{h}^{\alpha\beta}$, and recall that there is no explicit appearance of the wave field in the fluid's equation of motion (5.60). Correspondingly, as Gayer and Kennel (1979) conclude (see also p. 420 of Grishchuk and Polnarev, 1980 and references therein; XXXXXXX), *a gravitational wave cannot couple to a homogeneous, perfect fluid.* This is true in two senses: (i) When a wave hits the fluid, it leaves $\xi^i = 0$ and $\mathcal{T}^{\alpha\beta} = 0$; and correspondingly, the wave propagates through the fluid in accord with the standard, vacuum propagation equation $\Box\bar{h}_{\alpha\beta} + 2R_{\mu\alpha\nu\beta}\bar{h}^{\mu\nu} = 0$. (ii) When sound waves, governed by $\mathcal{T}^{\alpha\mu}{}_{|\mu} = 0$, propagate through the fluid, they carry a nonzero $\mathcal{T}_{\alpha\beta}$ [Eq. (5.63)] whose spatial part (at first order in the fluid displacement) is a pure trace. Correspondingly, they generate via (5.59), a $\bar{h}^{\alpha\beta}$ wave whose spatial part is pure trace, and hence is pure gauge: it can be removed by a subsequent gauge transformation. In other words, pressure waves in a homogeneous perfect fluid cannot radiate gravitational radiation, at first order in the fluid displacement. [KIP: HOW ABOUT HIGHER ORDERS? I THINK IT IS REPUTED TO VANISH THERE ALSO.]

b) *Homogeneous, viscous fluid*

If our homogeneous fluid has shear viscosity as well as pressure and density, then its full stress-energy tensor (5.61) is augmented by $-2\eta\sigma^{\alpha\beta}$, where η is the coefficient of shear viscosity and $\sigma_{\alpha\beta}$ is the fluid's rate of shear (the symmetric, trace-removed part of the

gradient of the 4-velocity, projected orthogonal to the 4-velocity); see, e.g., Exercise 22.6 of MTW. For the unperturbed fluid, with 4-velocity $u_{\underline{0}}^{\underline{0}} = 1$ and $u_{\underline{0}}^{\underline{j}} = 0$, the shear vanishes and the stress-energy tensor $T_{\underline{\alpha}}^{\underline{\alpha\beta}}$ has the form (5.57) considered above. However, when the fluid undergoes the displacement ξ^j and a gravitational wave of the form (5.58) is passing, the fluid experiences a rate of shear

$$\sigma_{00} = \sigma_{0j} = 0 , \quad \sigma_{jk} = \xi_{(j|k)} - \tfrac{1}{3}\xi^{i}{}_{|i}\delta_{jk} + \tfrac{1}{2}\dot{h}_{jk}^{\rm GW} . \tag{5.64}$$

(The term $\frac{1}{2}\dot{h}_{jk}^{\rm GW}$ arises from a connection coefficient $\Gamma^0{}_{jk}$ in the computation of the gradient of the 4-velocity.) Correspondingly, the stress-energy perturbation $\mathcal{T}_{\alpha\beta}$ has the standard form for a slightly perturbed viscous fluid in flat spacetime, augmented by the coupling term

$$\delta\mathcal{T}_{jk} = -\eta\dot{h}_{jk}^{\rm GW} . \tag{5.65}$$

This term has a nonzero TT part. Thus, it produces a genuine coupling of the fluid to the gravitational waves.

The influence of this term on the waves can be studied by inserting it onto the right-hand side of the wave equation (5.59), taking the TT part of that wave equation so as to get rid of all extraneous, pure-gauge parts, and dropping the tiny curvature-coupling term (which we shall study in Sec. 5.G below). The result is

$$\Box h_{jk}^{\rm GW} = 16\pi\eta\dot{h}_{jk}^{\rm GW} . \tag{5.66}$$

A straightforward solution shows that the time-derivative term on the right-hand side produces a damping of the waves: The amplitude of the waves dies out as $\exp(-l/2l_{\rm atten})$, and the energy dies out as $\exp(-l/l_{\rm atten})$, where l is the distance travelled and $l_{\rm atten}$ is the energy attenuation length

$$l_{\rm atten} = \frac{1}{32\pi\eta} . \tag{5.67}$$

By restoring the factors of G and c, i.e. converting to cgs units via Eqs. (4.3), we bring this attenuation length into the form

$$l_{\rm atten} = \frac{c^6/G}{32\pi\eta} = (4.2\times10^{18}\ \text{lt yr})\left[\frac{1\ \text{poise}}{\eta}\right] . \tag{5.67'}$$

When we recall that 1 poise is 1 dyne cm sec^{-2}, and that the viscosity of water is about 0.01 poise, we recognize that the gravitational waves' viscosity-induced attenuation length is exceedingly long.

Where does the gravitational waves' energy go? Into the fluid, of course. The wave-induced rate of shear, $\sigma_{jk} = \frac{1}{2}\dot{h}^{GW}_{jk}$, working against the viscosity, produces heat, thereby increasing the background energy density of the fluid at a rate $\partial\rho_B/\partial t = 2\eta\sigma_{jk}\sigma^{jk}$ (MTW, Exercise 22.7). This rate of heating is precisely equal to the rate of loss of gravitational-wave energy,

$$\frac{\partial\rho_B}{\partial t} = -T^{0j}_{GW|j} = \frac{T^{0j}_{GW}n_j}{l_{atten}}, \tag{5.68}$$

as one can readily verify using expression (4.33) for the gravitational-wave energy flux and expression (5.67) for the waves' attenuation length. Notice, moreover, that this energy-balance relation (5.68) is just the general law of energy-momentum conservation (5.37), specialized to the present situation.

In order to estimate the magnitude of the attenuation length (5.67), we must consider the microscopic, particulate nature of the fluid. If the fluid is made of particles that move with mean speed v and that scatter off each other after traveling, on average, a mean free path $s \ll \lambda =$ (inhomogeneity scale of the perturbed fluid), then kinetic theory dictates that $\eta \sim \rho_B v s$; see, e.g., XXXX. If $s \gtrsim \lambda$, the diffusion approximation which underlies the theory of viscous fluids breaks down, but one can show that the above formula for viscous heating remains valid in order of magnitude if we set $\eta \sim \rho_B v s(\lambda/s)^2$. These expressions for the viscosity η, together with the fact that the fluid produces a background radius of curvature $\mathcal{R} \sim 1/(\text{Riemann tensor due to fluid})^{1/2} \sim 1/(\text{Einstein tensor due to fluid})^{1/2} \sim 1/(\text{energy density } \rho_B \text{ due to fluid})^{1/2}$, implies that

$$\frac{l_{atten}}{\mathcal{R}} \sim \frac{\mathcal{R}}{\lambda}\frac{1}{v}\max\left[\frac{\lambda}{s}, \frac{s}{\lambda}\right]. \tag{5.69}$$

The magnitudes of the terms on the right-hand side are $\mathcal{R}/\lambda \gg 1$ by virtue of the definition of a gravitational wave, $1/v \gtrsim 1$ since the fluid's particles cannot travel faster than light, and $\max(\lambda/s, s/\lambda) \gtrsim 1$. Consequently, the attenuation length is always much larger than the background radius of curvature of spacetime $\mathcal{R}$ produced by the fluid. Since the size of the fluid cannot exceed by much the radius of curvature $\mathcal{R}$ (when it reaches a size a bit larger than $\mathcal{R}$, it curls space up into closure around itself), this means that *no viscous fluid can produce significant attenuation of gravitational radiation.*

For more detailed treatments of the interaction between a viscous fluid and gravitational waves see, e.g., Esposito (1971a,b), Papadopoulos and Esposito (1985), Szekeres (1971), Sec. 4.2 of Grishchuk and Polnarev (1980) [KIP: CHECK THESE REFERENCES].

c) *Inhomogeneous, elastic medium*

For an inhomogeneous, elastic medium (e.g. a resonant-bar gravitational-wave detector), the background stress-energy tensor $T^{\alpha\beta}_{\rm B}$ has the standard form (5.57), and the stress-energy perturbation $\mathcal{T}^{\alpha\beta}$ is that of a perfect fluid (5.61), augmented by a shear restoring force

$$\delta\mathcal{T}^{\alpha\beta} = -2\mu\Sigma^{\alpha\beta} , \tag{5.70a}$$

where μ is the shear modulus and $\Sigma^{\alpha\beta}$ is the shear (the time integral of the rate of shear $\sigma^{\alpha\beta}$. By time integrating expression (5.64) we obtain

$$\Sigma_{00} = \Sigma_{0j} = 0 , \quad \Sigma_{jk} = \Sigma^{\xi}_{jk} + \tfrac{1}{2}h^{\rm GW}_{jk} , \tag{5.70b}$$

where Σ^{ξ}_{jk} is the part of the shear produced by the displacement ξ^i

$$\Sigma^{\xi}_{jk} = \xi_{(j|k)} - \tfrac{1}{3}\xi^{i}{}_{|i}\delta_{jk} . \tag{5.70c}$$

By augmenting (5.70) onto the $\mathcal{T}_{\alpha\beta}$ of Eq. (5.63) and then inserting that $\mathcal{T}^{\alpha\beta}$ into the equation of motion (5.60) and specializing to the nearly Newtonian regime $p_{\rm B} \ll \rho_{\rm B}$, $K \ll \rho_{\rm B}$, we obtain

$$\rho_{\rm B}\ddot{\xi}_j - (K\xi^{i}{}_{|i})_{|j} - 2(\mu\Sigma^{\xi}_{jk})^{|k} = \mu^{|k}h^{\rm GW}_{jk} . \tag{5.71}$$

This is the standard equation of motion for a slightly perturbed, inhomogeneous, nonrelativistic elastic medium, augmented by the gravitational-wave driving term $\mu^{|k}h^{\rm GW}_{jk}$. This equation was first derived by Dyson (1969) and was subsequently generalized and studied in more elegant ways by Carter and Quintana (1977) and Carter (1983). Notice that *the waves drive the medium only through inhomogeneities of its shear modulus*.

For an elastic body that is small compared to λ (e.g. a resonant-bar gravitational-wave detector), one can study the waves' influence using the TT-gauge equation of motion (5.71), or one can study it in the body's proper reference frame, where the full metric $g_{\alpha\beta} = g^{\rm B}_{\alpha\beta} + h_{\alpha\beta}$ has the form (4.39). In the proper reference frame, the body's equation of motion will be the same as (5.71) but with the driving term $\mu^{|k}h^{\rm GW}_{jk}$ replaced by the standard gravitational-wave driving term $-\tfrac{1}{2}\rho_{\rm B}\ddot{h}^{\rm GW}_{jk}x^k$ [Eqs. (4.12) and (4.15)]. The two driving terms look completely

different, and they give different displacement functions ξ^j. The reason is that the spatial coordinates of the TT gauge wiggle dynamically relative to those of the proper reference frame, thereby producing

$$\xi_j^{\rm TT} = \xi_j^{\rm PRF} - \tfrac{1}{2} h_{jk}^{\rm GW} x^k \ . \tag{5.72}$$

If one wants to be able to rely on ordinary physical intuition, one should use spatial coordinates that are as rigid as possible: proper reference-frame coordinates. However, if one wants only to solve the equations of motion of the medium without refering to elementary physical intuition, one is free to use either approach, proper-reference-frame or TT. If the medium is large compared to a reduced wavelength (e.g. for studies of the interaction of kilohertz waves with the earth's crust), one is stuck: only the TT analysis [Eq. (5.71)] is valid. The proper-reference-frame analysis fails. See the discussion in Sec. 4.F.

Turn attention from the influence of the waves on the medium to the influence of a homogeneous, elastic medium on the waves. The shear stress $\mathcal{T}_{jk} = -\mu h_{jk}^{\rm GW}$, acting back on the waves, produces dispersion; in addition, if there is viscosity, it will give rise to a shear stress $\mathcal{T}_{jk} = -\eta \dot{h}_{jk}^{\rm GW}$ [Eq. (5.65)] that damps the waves. We can see this quantitatively with the help of the waves' propagation equation (5.59). By (i) inserting into that propagation equation the above elastic and viscous contributions to $\mathcal{T}_{jk}$ along with the fluid contributions (5.63), (ii) taking the transverse-traceless part of the resulting equation [in accord with the paragraph following Eq. (5.59)], and (iii) ignoring the tiny curvature-coupling term, we obtain

$$\Box h_{jk}^{\rm GW} = 16\pi(\mu h_{jk}^{\rm GW} + \eta \dot{h}_{jk}^{\rm GW}) \ . \tag{5.73}$$

For waves with the sinusoidal form $h_{jk}^{\rm GW} \propto e^{i(kz-\omega t)}$, Eq. (5.73) gives the dispersion relation

$$\omega^2 = k^2 + 16\pi(\mu - i\omega\eta) \ . \tag{5.74}$$

Since, as we shall see, $16\pi|\mu - i\omega\eta|$ is always extremely small compared to $\omega^2 \cong k^2 = 1/\lambda\!\!\!^{-2}$, this dispersion relation corresponds to (i) an attenuation of the waves with an energy attenuation length the same as for a viscous fluid [Eq. (5.67)]

$$l_{\rm atten} = \frac{1}{32\pi\eta} \ , \tag{5.75}$$

and (ii) propagation with phase velocity $v_{\rm ph} = \omega/k$ and group velocity $v_{\rm gp} = \partial\omega/\partial k$ given by

$$v_{ph} = 1+8\pi\mu\lambda\!\!\!^{-2}\,, \quad v_{gp} = 1-8\pi\mu\lambda\!\!\!^{-2}\,. \tag{5.76}$$

Ordinary solid bodies have $\eta \sim 10^3 \,\mathrm{g\,cm^{-1}\,sec^{-1}}$ and $\mu \sim 10^{10}$ dyne $\mathrm{cm^{-2}}$ which, by virtue of $c = 3\times10^{10}\,\mathrm{cm\,sec^{-2}} = 1$ and $G/c^2 = 0.7\times10^{-28}$ $\mathrm{cm/g} = 1$, is the same as $\eta \sim 10^{-36}\,\mathrm{cm^{-1}}$ and $\mu \sim 10^{-39}\,\mathrm{cm^{-2}}$. Correspondingly, *when propagating through an ordinary solid such as the earth, the gravitational waves' attenuation length is* $l_{atten} \sim 10^{34}$ cm $\sim 10^6$ *Hubble distances; and their phase and group velocities differ from the speed of light by fractional amounts* $\sim 10^{-24}(\lambda\!\!\!^{-}/100\,\mathrm{km})^2$. *Thus, kilohertz-frequency gravitational waves would have to propagate through earth-type matter a distance* $l_{disp} \sim 10^{24}\lambda\!\!\!^{-} \sim 10^{31}\,\mathrm{cm} \sim 10^3$ *Hubble distances in order for dispersion to cause their phase to slip by just one radian.*

More generally, because the velocity of propagation of shear waves in any elastic medium is $\simeq \sqrt{\mu/\rho_B}$ and cannot exceed light speed, it should always be true that $\mu \lesssim \rho_B \sim 1/\lambda\!\!\!^{-2}$. This means that gravitational waves in *any* elastic medium will have their phase shifted by one radian due to dispersion only after traveling a distance

$$l_{disp} \sim \frac{1}{\mu\lambda\!\!\!^{-}} \gtrsim \lambda\!\!\!^{-}\frac{\lambda\!\!\!^{-}}{\lambda}\,. \tag{5.77}$$

Since the medium cannot be much larger than $\lambda\!\!\!^{-}$, and since gravitational radiation by definition must have $\lambda/\lambda\!\!\!^{-} \ll 1$, *dispersion in an elastic medium can never produce a slippage of phase by even one radian.* Similarly, as was shown in Eq. (5.69), *attenuation can never be significant in an elastic medium.*

d) Medium made of quadrupolar oscillators

Turn, next, to the attenuation of gravitational radiation by that type of medium which, so far as I am aware, is the most effective of all realistic media for absorbing gravitational radiation: a medium made of a large number of "quadrupolar oscillators" with internal damping. By "quadrupolar oscillator", I mean a solid body with size $L \lesssim \lambda$ and with a normal mode of oscillation that has a quadrupolar shape. Examples include resonant-bar gravitational-wave detectors, planets like the earth, stars like the sun, neutron stars, and black holes.

We can estimate the attenuation length in such a medium as $l_{atten} = 1/n\sigma$, where σ (not to be confused with the rate of shear of a fluid) is the cross section for an individual oscillator to absorb gravitational-wave energy and n is the number density of oscillators.

To evaluate the cross section σ we compute the response of an oscillator to a passing, monochromatic gravitational wave. That response, in the oscillator's proper reference frame (*not* in TT gauge), is governed by the equation

$$\frac{d^2\delta L}{dt^2} + \frac{1}{\tau_*}\frac{d\delta L}{dt} + \omega_0{}^2\delta L \simeq L\frac{d^2h_+}{dt^2}\ ; \tag{5.78}$$

cf. Exercise 37.10 of MTW. Here δL is the generalized coordinate of the oscillator's quadrupolar normal mode, so normalized as to be equal to the physical displacement of a representative piece of the oscillator's surface, and h_+ is the gravitational-wave field evaluated at the oscillator's location. (Since the oscillator is smaller than a reduced wavelength of the waves, $L \lesssim \lambda$, spatial variations of h_+ are unimportant inside the oscillator.) The left-hand side of (5.78) is the standard harmonic-oscillator equation for the normal mode's generalized coordinate, and the right-hand side is an order-of magnitude estimate of the gravitational-wave driving force, based on Eqs. (4.12), (4.16) and (4.25). The parameter ω_0 is the eigenfrequency of the normal mode, τ_* is its damping time, L is the oscillator's linear size, and below we shall denote by M the oscillator's mass and by $Q \equiv \omega_0\tau_*/\pi$ the normal mode's "quality factor".

The approximate equation of motion (5.78) and the order-of-magnitude analysis that follows are valid for bodies with strong self-gravity (e.g. neutron stars and black holes) as well as weak (the earth or a resonant-bar gravitational-wave detector).

By setting $h_+ = \mathcal{H}e^{-i\omega t}$ (where $\omega = 1/\lambda$ is the wave's angular frequency and $\mathcal{H}$ is its amplitude), solving (5.78) for δL, then computing the energy of oscillation $E_{osc} \sim \frac{1}{2}M\omega_0{}^2\times(\text{amplitude of } \delta L)^2$, and then multiplying by $1/\tau_*$, we obtain the rate that energy is fed into internal damping of the oscillator — a rate which, in this steady-state situation, must equal the power absorbed by the oscillator from the gravitational wave, P_{abs}. By equating this P_{abs} to the product of the cross section σ and the waves' energy flux $(1/16\pi)\omega^2\mathcal{H}^2$ [Eq. (4.34)], we obtain the following expression for the oscillator's cross section

$$\sigma(\omega) \sim \frac{ML^2\omega^2/\tau_*}{\omega^2-\omega_0{}^2+(2/\tau_*)^2}\ . \tag{5.79}$$

We shall return to the frequency dependence of this expression in Chap. 10, when discussing gravitational-wave detectors. For now, in order to put an upper limit on the effects of absorption, we shall suppose that

the waves are precisely on resonance, $\omega = \omega_0$. Then σ achieves its maximum value of

$$\sigma_{\max} \sim \frac{M}{L}\frac{L}{\lambda}QL^2 , \tag{5.80}$$

and the attenuation length achieves its minimum possible value, $l_{\text{atten}} = 1/n\sigma_{\max}$. Expressed in terms of the radius of curvature of the background spacetime produced by the attenuating oscillators, $\mathcal{R} \sim 1/\rho^{1/2} = (1/nM)^{1/2}$, this works out to be

$$\frac{l_{\text{atten}}}{\mathcal{R}} \sim \frac{\mathcal{R}}{\lambda}\left[\frac{\lambda}{L}\right]^2\frac{1}{Q} . \tag{5.81}$$

The first term, $\mathcal{R}/\lambda$, is $\gg 1$ by the definition of a gravitational wave. The second term, $(\lambda/L)^2$, is equal to the speed of light divided by the velocity of sound inside the oscillating body, squared, and thus is always $\gtrsim 1$. [For a black hole $(\lambda/L)^2 \sim 1$, for a neutron star $(\lambda/L)^2 \sim 10$, for a white dwarf $(\lambda/L)^2 \sim 10^4$, for normal stars like the sun $(\lambda/L)^2 \sim 10^6$, for the earth or a resonant-bar gravitational-wave detector $(\lambda/L)^2 \sim 10^{10}$.] By contrast, the third term, $1/Q$, is generally $\ll 1$. However, for realistic astrophysical situations $1/Q$ is never sufficiently small to make up for the large product of the first two terms. Moreover, when the resonant angular frequencies of the many oscillators are spread out randomly over a band $\Delta\omega_0 \sim \omega_0$, only a fraction $\sim 1/Q$ of the oscillators will be near enough resonance to have $\sigma \sim \sigma_{\max}$; and correspondingly the factor $1/Q$ in (5.81) will be replaced by unity. Thus, *although, in principle, gravitational waves could be attenuated significantly by a medium of quadrupolar oscillators, in realistic situations the attenuation length greatly exceeds the radius of curvature $\mathcal{R}$ produced by the oscillators; and thus, as in the case of a viscous medium, attenuation cannot be astrophysically important.*

A simple extension of this argument shows that dispersion also cannot be significant: the total phase shift, due to dispersion, in traveling the distance $\mathcal{R}$ through a realistic astrophysical medium is generally $\ll 1$; see Sec. 2.4.3 of Thorne (1983). It is instructive and fun, however, to imagine and study theoretically an unrealistic form of matter ("respondium") with such strong dispersion that it actually reflects gravitational waves (Press 1979).

The specific problem of the absorption and scattering of gravitational waves by black holes has been studied in extensive detail. Those studies reveal a great richness of scattering phenomena (superradiant

scattering, "glories", rotation of the waves' polarization, ...); see De Logi and Kovacs (1977), Matzner and Ryan (1978), Matzner et. al. (1985), Futterman, Handler, and Matzner (1988), and references therein. For studies of absorption and scattering by neutron stars and other stars see Linet (1984). For a study of how the energy levels of atoms are shifted by the tidal gravity of passing gravitational waves [fractional shifts no larger than $\mathcal{H}\times(\text{size of atom})^2/\lambda^2$, which is almost certainly too small in the real universe to be measurable], see Leen, Parker, and Pimentel (1983).

e) Plasmas

The most astrophysically ubiquitous of all media is a magnetized plasma. Careful studies of the propagation of gravitational waves through plasmas are only now in process (Ehlers, Prasanna, and Breuer, 1986; Bondi and Pirani, 1988), and there are no definitive results at this writing, with one exeption: Gayer and Kennel (1979), and Grishchuk and Polnarev (1980, p. 420 -- KIP: CHECK) have shown that in an unmagnetized plasma, as in the media studied above, dispersion is so extremely small that there is no hope for particles with mass to "ride along with the crests" of a gravitational wave and produce Landau damping. *Landau damping of gravitational radiation in a plasma is totally negligible.* This result, and intuition built up from the above calculations for other media, make me rather confident that a magnetized plasma cannot have any significant influence on gravitational waves that propagate through it. Nevertheless, there are likely to be a number of fascinating but tiny effects of the waves on the plasma and the plasma on the waves.

5.F Interaction of waves with electromagnetic fields

Turn attention from propagation of gravitational waves through matter, to propagation through electromagnetic fields.

Because gravitational and electromagnetic waves should propagate with the same speed, they can interact in a coherent way (Gertsenshtein, 1962). The interaction is so weak, however, that a substantial transformation of one into the other requires propagation over a distance of order the radius of curvature $\mathcal{R}$ of the background spacetime which their own energy density produces. Thus, such coherent interaction is not likely ever to be important in the real universe -- except possibly in gravity-wave detectors; see Sec. 12.A below. For a review of the extensive literature on this subject see Grishchuk and

Polnarev (1980). For a brief pedagogical discussion see Sec. 17.9 of Zel'dovich and Novikov (1983).

The situation in which one might have expected the strongest resonant interaction is for electromagnetic and gravitational waves propagating parallel to each other through an otherwise empty spacetime. Remarkably, in this situation there is no interaction whatsoever (Braginsky and Grishchuk, 1977 KIP: LEONYA CLAIMS THIS PAPER DOES NOT EXIST AND SAYS TO CITE BRAGINSKY ET AL 1973; Grishchuk, 1977b -- KIP: LEONYA SAYS THIS REFERENCE IS NOT NECESSARY). It is easy to see why, for the special issue of whether the stress-energy tensor of a propagating electromagnetic wave generates a gravitational wave propagating along with it. That stress-energy tensor, in a local Lorentz frame of the background metric, has the form

$$T^{00} = T^{0z} = T^{z0} = T^{zz} = \frac{E_o^{\,2}}{4\pi}\cos^2\omega(t-z)\,, \tag{5.82}$$

where E_o is the amplitude of oscillation of the electric field and the wave is presumed to be plane polarized and to propagate in the z-direction. The oscillatory part of $T^{\mu\nu}$, which one might expect to generate gravitational waves, is

$$\mathcal{T}^{00} = \mathcal{T}^{0z} = \mathcal{T}^{z0} = \mathcal{T}^{zz} = \frac{E_o^{\,2}}{8\pi}\cos 2\omega(t-z)\,. \tag{5.83}$$

When fed into the wave equation (5.33) (with the coupling of $\bar{h}_{\alpha\beta}$ to the background fields $R^{\rm B}_{\alpha\beta\gamma\delta}$ and $T^{\rm B}_{\alpha\beta} \equiv \langle T_{\alpha\beta}\rangle$ ignored because it can be important only over the extremely long lengthscale $\mathcal{R}$), this $\mathcal{T}^{\alpha\beta}$ produces a trace-reversed metric perturbation $\bar{h}_{\alpha\beta}$ that propagates along with the electromagnetic waves at the speed of light, growing linearly with the distance traveled. However, this $\bar{h}_{\alpha\beta}$, like the $\mathcal{T}_{\alpha\beta}$ that generates it, is purely longitudinal; i.e. it has 00, $0z$, $z0$, and zz components but no components in transverse directions. This implies that this wavelike $\bar{h}_{\alpha\beta}$ is "pure gauge": it can be transformed to zero by a change of gauge, as one can see most easily by noting that its transverse-traceless projection (4.50) vanishes and therefore that it is associated with a vanishing gravitational-wave field $h^{\rm GW}_{jk}$.

To achieve a resonant interaction between parallely propagating electromagnetic and gravitational waves, one can send them through a time-independent ("DC") electric or magnetic field (Gertsenshtein, 1962). As a simple example, let a pure electromagnetic wave, with electric field $\mathbf{E} = E_o\cos\omega(t-z)\mathbf{e}_x$, propagate from vacuum at $z < 0$ into

a region of homogeneous, DC field $\mathbf{E} = E_{DC}\mathbf{e}_x$ at $z > 0$; and assume that $E_{DC} \gg E_o$. Then the beating of the wave's electric field against the DC field produces an oscillating stress-energy tensor which has (among others) the transverse components

$$\mathcal{T}_{xx} = -\mathcal{T}_{yy} = \frac{E_{DC}E_o}{4\pi}\cos\omega(t-z) \quad \text{for } z > 0\,. \tag{5.84}$$

Fed into the wave equation (5.33) (with background-coupling effects neglected as above), these $\mathcal{T}_{\alpha\beta}$ generate a trace-reversed metric perturbation

$$\bar{h}_{xx} = -\bar{h}_{yy} = \frac{2E_{DC}E_o}{\omega} z\sin\omega(t-z) \quad \text{for } z > 0. \tag{5.85}$$

The TT projection of this $\bar{h}_{\alpha\beta}$ [Eq. (4.50)] gives a gravitational-wave field

$$h_+ = \frac{2E_{DC}E_o}{\omega} z\sin\omega(t-z)\,, \quad h_\times = 0 \quad \text{for } z > 0. \tag{5.86}$$

The amplitude of this wave grows linearly with the distance z travelled, and correspondingly its energy density grows quadratically. It is easy to verify that the ratio of the energy in the growing gravitational wave to that in the original electromagnetic wave is of order $(z/\mathcal{R})^2$, where $\mathcal{R}$ is the background radius of curvature produced by the DC field. By virtue of total energy conservation, there is a back-action on the electromagnetic wave which saps energy from it as the gravitational wave grows. A detailed analysis (XXXXX) shows that, once all the wave energy has been fed into the gravitational wave, the beating of that gravitational wave against the DC field begins to regenerate the electromagnetic wave. The wave energy thereafter sloshes back and forth between electromagnetic and gravitational waves, with a sloshing lengthscale of order $\mathcal{R}$. [KIP: SEE GRISHCHUK'S REFS. PRIVATELY HE SAYS ZEL'DOVICH JETP 65, 1311 (1973), SOV PHYS JETP 38, 652 (1974); ALSO GERLACH PRL 32, 1023 (1974)]

Because the background field cannot have a longitudinal extent much larger than $\mathcal{R}$ (see above), the sloshing cannot continue for more than a few cycles. And, for realistic laboratory or astrophysical parameters, there cannot be any sloshing at all; there is only a fractionally tiny interconversion of one wave type into the other.

A specific, well-studied example of the above process is the interconversion of gravitational and electromagnetic waves as they propagate near an electrically charged black hole (XXXXXX). Another cute

application is a proof that in principle (though never in practice) this interconversion, plus interaction of the electromagnetic waves with thermal matter, can be used to thermalize initially nonthermal gravitational radiation (Garfinkle and Wald, 1985). A third application is to gravitational-wave detectors in which a strong, DC field (e.g. the electric field in a parallel-plate capacitor) is driven by incoming gravitational waves to produce a tiny amount of electromagnetic radiation (Braginsky et. al., 1973; Sec. 12.A, below).

Interactions between gravitational and electromagnetic waves can be catalyzed not only by a background, DC electromagnetic field, but also in other ways: (i) Parallely propagating electromagnetic and gravitational waves can be coupled by a dielectric medium, but the coupling is proportional to $n-1$ where n is the dielectric's index of refraction, and the coupling is so weak that it probably is of no practical interest (Grigor'ev, 1982). (ii) When electromagnetic and gravitational waves propagate through vacuum in nonparallel directions, they interact weakly. For example, if the wavelength of the gravitational wave is much longer than that of the electromagnetic wave, then the gravitational wave can produce electromagnetic polarization (Polnarev, 1985), it can rotate the plane of electromagnetic polarization (Cruise, 1983), and it can produce fluctuations in the frequency, intensity, and direction of the electromagnetic wave (Zipoy, 1966; Bergman, 1971; Bertotti and Catenacci, 1975; Adams, Hellings, and Zimmerman, 1984). Such interactions have only minuscule influence on either the gravitational or the electromagnetic wave; but, thanks to high-precision technology, the tiny electromagnetic effects can be used in a variety of promising ways for gravitational-wave detection (Sec. 12.C).

5.G A catalog of vacuum wave-propagation effects

Having seen that the interaction of gravitational waves with matter and electromagnetic fields is almost never significant, we now return to the vacuum approximation. There are a number of peculiarities of vacuum wave propagation. Some show up in the equations of geometric optics, while others are removed by the approximations that underlie the geometric-optics formalism. In this section we shall discuss the most interesting and important of the vacuum propagation phenomena, and we shall examine their relationship to geometric optics and their relevance to the real universe.

a) Scattering by background curvature, and tails of waves

Gravitational waves can sometimes encounter regions of spacetime where the background radius of curvature becomes comparable to or shorter than the reduced wavelength, $\mathcal{R} \lesssim \lambda$. When this happens, not only do the shortwave and geometric optics formalisms break down, but the very concept of a gravitational wave becomes meaningless. Nevertheless, one can continue to analyze the evolution of the metric perturbations $h_{\alpha\beta}$ using the formalism of Sec. 5.B.

Of particular interest when $\mathcal{R} \lesssim \lambda$ is the scattering of the perturbations by the background curvature. Such scattering shows up in the vacuum wave equation $\Box\bar{h}^{\alpha\beta}+2R^{B}_{\mu\alpha\nu\beta}\bar{h}^{\mu\nu} = 0$ [Eq. (5.24)] as a result not only of the curvature–coupling term, but also of the influence of the background on the wave operator $\Box$. This scattering is very important in some sources of waves, as the waves are trying to form. For example, it is responsible for the normal–mode vibrations of black holes (Press, 1971; Goebel, 1972; Sec. 6.J), and it leads to the formation of "tails" of the waves in a source's near zone (Price, 1972a,b; Thorne, 1972; Cunningham, Price, and Moncrief, 1979) and to radiative tails in the wave zone (Leaver, 1986; Blanchet, 1987b; XXXX) — which, though they are very important in principle (Newman and Penrose, 1965; Blanchet and Damour, 1988a), are not likely ever to be observationally important. Remarkably, in a homogeneous cosmological model filled with perfect fluid with vanishing pressure or with pressure equal to 1/3 the energy density, there is no backscatter off the spacetime curvature whatsoever (Janis, 1985; Gayer and Kennel, 1979).

b) Parametric amplification by background curvature

In regions of a dynamical spacetime (e.g. the expanding universe) in which the characteristic wavelength λ of gravitational waves is larger than or comparable to the background radius of curvature $\mathcal{R}$, $\lambda \gtrsim \mathcal{R}$, the waves can be parametrically amplified by interaction with the dynamical background (Grishchuk, 1974, 1975a,b, 1977a; Grishchuk and Polnarev, 1980; Allen, 1988; Sec. 9.D). Viewed quantum mechanically, the interaction causes stimulated emission of new gravitons (XXXX). Viewed classically, the interaction can be analyzed using the standard, perturbed, vacuum Einstein equation $\Box\bar{h}^{\alpha\beta} + 2R^{B}_{\mu\alpha\nu\beta} = 0$; and the parametric amplification comes about because of the time dependence not only in $R_{\mu\alpha\nu\beta}$ but also in the background connection coefficients that appear in the wave operator. Such parametric amplification may well have enabled the expansion of the universe to

take gravitational vacuum fluctuations that emerged from the Planck era of the big-bang, and enlarge them into a strong, stochastic background of gravitational waves today; see Sec. 9.D below.

c) Gravitational focusing

Lumps of background curvature associated with black holes, stars, star clusters, and galaxies will focus gravitational waves in precisely the same manner as they focus electromagnetic waves; i.e., they act as "gravitational lenses" for the waves. Just as this focusing is observationally important for the light and radio waves from a few very distant quasars, so it might also be important for distant discrete sources of gravitational waves. Focusing by the sun, in the case of waves with sufficiently short wavelength, can be significant, but not at earth; the focal point lies farther out in the solar system, near the orbit of Jupiter (Cyranski and Lubkin, 1974). Gravitational focusing shows up clearly in the waves' geometric-optics propagation: A bundle of rays, along which the waves are propagating, is focussed gravitationally. This causes the bundle's cross sectional area $\Delta\mathcal{A}$ and radial variable r [Eq. (5.2d)] to decrease, and the h_+ and $h_\times$ of Eq. (5.2e) to increase.

d) Diffraction

Near the focal point of a gravitational lens, the radii of curvature of the wave fronts are no longer huge compared to the waves' reduced wavelength. As a result, the waves cease to propagate along null rays and begin to diffract, thereby lessening the strength of the focusing. The analysis of this is no different for gravitational waves than for electromagnetic or scalar waves, since polarization plays no important role. The analysis can be carried out using the flat-spacetime wave equation $\Box h_{\alpha\beta} = 0$ in a nearly Lorentz frame of the focal region. One switches from geometric optics to this wave equation as the waves near the focal point. Then, once the waves are well past the focal point, one can return to geometric optics. One thereby finds that diffraction almost completely wipes out the effects of gravitational focusing, unless the waves' reduced wavelength λ is small compared to the lens's gravitational radius $2GM/c^2 = 3\,\mathrm{km}(M/M_\odot)$. (Here M is the lens's mass.) This criterion applies whether the lens is a black hole, or a star like the sun, or a galaxy. For an order of magnitude discussion see, e.g. Sec. 2.6.1 of Thorne (1983); for full details see Bontz and Haugan (1981).

e) Nonlinear wave-wave coupling (frequency doubling, etc.)

Because general relativistic gravity is nonlinear, there is a nonlinear self–coupling of gravitational waves ("wave–wave coupling"). In principle this leads to such nonlinear conversion processes as frequency doubling. One can compute the effects of nonlinearities using an explicit version of Eq. (5.32c). Such a calculation shows that in practice wave–wave coupling effects are not important in regions where the waves *are* waves (where $\lambda \ll \mathcal{L}$). This is because, in such regions, the dimensionless amplitude $\mathcal{H}$ of the waves is small compared to unity [Eq. (5.41) above]. For details see Sec. 2 of Thorne (1985). However, in idealized situations where λ becomes temporarily $\sim \mathcal{L}$ and $\mathcal{H}$ becomes temporarily of order unity, significant frequency doubling can occur. An example is the focusing of beams of gravitational radiation into a region so small (of order λ) and with such great beam intensity ($\mathcal{H} \sim 1$) that the focused radiation almost but not quite forms a black hole. Upon diffracting and reexploding, the radiation shows signficant frequency doubling (Abrahams, 1987).

Even when the waves' amplitude $\mathcal{H}$ becomes of order unity (and, as a result, the distinction between background curvature and wave curvature begins to break down), there is no evidence in any calculations to date for a steepening of the waves to form gravitational shocks (discontinuities in the waves' Riemann tensor). This remains true even when one adds additional nonlinearities to the Einstein field equation by augmenting the Einstein–Hilbert Lagrangian by terms quadratic in the curvature tensor (Tomimatsu, 1987).

f) Generation of background curvature by the waves

The generation of background curvature by the stress–energy of the waves [Isaacson, 1968b; MTW Sec. 35.15; Eq. (5.38) above] is important in cosmological models in any epoch when the waves are sufficiently strong that their energy density is comparable to that of matter, or larger; see, e.g. Hu (1978) and Chap. 17 of Zel'dovich and Novikov (1983). It is also important in a gravitational "geon" – i.e. a bundle of gravitational waves that is held together by its own gravitational pull on itself (Wheeler, 1962; pp. 409–438 of Wheeler, 1964; Brill and Hartle, 1964). But geons surely do not exist in the real universe. There is no reason to expect them to form, and if they did form they would quickly disrupt due to a large–scale, global instability (XXXXXX). Nevertheless, geons are important theoretical entities: they are useful for exploring issues in fundamental physics.

g) Nonlinear effects in collisions of gravitational waves

The head-on collisions of precisely planar gravitational waves (with infinite transverse extent) have been studied using exact, rather than approximate solutions of the vacuum Einstein field equation; see Sec. 5.H below. These solutions, and exact theorems about them, reveal a number of interesting nonlinear features: (i) The background curvature produced by each wave acts as a lens to focus the other wave. Because the waves have infinite transverse extent, diffraction does not occur, and each focussed wave converges onto its focal plane to produce a spacetime singularity (Kahn and Penrose, 1971; Szekeres, 1972; Nutku and Halil, 1977; Tipler, 1980; Matzner and Tipler, 1984). (ii) The singularity has an "inhomogeneous Kasner structure" with infinite tidal squeezing along two spatial axes and infinite stretching along the third (Yurtsever, 1987a, 1988). (iii) For special forms of the pre-collision waves, some or all of the singularity gets replaced by a "Cauchy horizon". However, those special forms are nongeneric: arbitrarily weak changes in them cause the collision to produce an all-embracing singularity rather than a Cauchy horizon (Chandrasekhar and Xanthopoulos, 1986, 1987; Yurtsever, 1987a, 1988).

Exact theorems show that, in the more realistic case of colliding waves that are almost planar but die out slowly at large transverse distances, if the transverse size is sufficiently large compared to the initial wave amplitude, then the focusing still drives the amplitude up far enough, before diffraction can act, to make nonlinear effects take over and produce singularities (Yurtsever, 1987b, 1988). If the "cosmic censorship conjecture" is correct, those singularities must be hidden inside one or two black-hole horizons; but it has not yet been possible to determine whether this is so. Unfortunately, the wave size required to produce a singularity is so huge that wave-wave collisions almost certainly do not form singularites in the real universe, except possibly near the big bang (Yurtsever, 1987b, 1988).

Collisions of gravitational waves produce not only focusing, but also a rotation of the polarization axes of one wave by the gravitational action of the other — a phenomenon discovered in collisions of cylindrical waves by Piran and Safier (1985).

5.H Asymptotic analyses and exact solutions

We conclude this chapter with a brief description of studies of gravitational-wave propagation in special circumstances.

a) Asymptotic analyses

Much has been learned about the geometric properties of gravitational radiation by studying the idealized problem of the propagation of waves outward from a source that resides alone in an otherwise empty and asymptotically flat spacetime: In analyses that were central to building up confidence in our understanding of gravitational waves, Bondi (1960), Bondi, van der Burg, and Metzner (1962), and Sachs (1962, 1963) expanded the spacetime curvature along the outgoing light cone in inverse powers of the distance to the source. Their expansions, carefully formulated and combined with conformal transformations that bring "infinity" in to finite locations (Penrose 1963a,b) revealed an elegant asymptotic structure for waves in asymptotically flat spacetime. The study of this asymptotic structure has been pursued with vigor in recent years; for reviews and references see Newman and Todd (1980), Ashtekar (1981, 1984), Walker (1983), Schmidt (1979, 1986), Hobill (1984), Penrose and Rindler (1986), Friedrich (1986), Blanchet and Damour (1986), Blanchet (1987a), and Winicour (1988).

b) Exact solutions to the vacuum Einstein field equation

Much insight into gravitational radiation has come from exact solutions to the vacuum Einstein field equation.

One broad class of exact solutions, called "boost-rotation symmetric spacetimes", describes an idealized class of gravitational-wave sources that radiate into a (nearly) asymptotically flat spacetime. The sources are axially symmetric and invariant under a Lorentz-like "boost". They include such idealized configurations as two black holes with a spring between them, which forces them to accelerate uniformly away from each other (the "C-metric", discovered by Levi-Civita, 1918 and explored and interpreted physically by Kinnersley and Walker, 1970; Bonnor, 1983; and others). The spacetime into which these special sources radiate is asymptotically flat (like Minkowskii spacetime), except for a weak, cosmic-string-type structure (circumference, divided by $2\pi\times$radius, equal to a constant slightly less than one) along the direction of acceleration (the symmetry axis). For the general theory and reviews of boost-rotation-symmetric spacetimes see Bičak

(1968); Bičak, Hoenselaers and Schmidt (1983); Bičak and Schmidt (1984); and Bičak (1985, 1988).

Although there are no other known exact solutions describing waves that propagate out into asymptotically flat spacetime, there is a general formalism for a much broader and more realistic class of solutions — a formalism sufficiently powerful to permit proof of interesting theorems and to give promise of ultimately producing exact solutions. This formalism, due to Robinson and Trautman (1962), describes wave-carrying spacetimes whose rays are "geodesic and hypersurface orthogonal" (properties shared by the rays of geometric optics) and in addition are free of shear. [KIP: CHECK - HOW CAN THEY BE SHEAR-FREE?] Among the important, rigorous theorems that have been proved for such spacetimes is one which says that the waves must die out at late times, leaving behind the Schwarzschild spacetime of a nonrotating black hole (Forster and Newman, 1967; Lucacs et. al., 1984). For reviews and references on the Robinson-Trautman formalism see, e.g., Kramer et. al. (1980) and Schmidt (1987). For a first step in generalizing the Robinson-Trautman theory to spacetimes whose rays have "twist", see Chinea (1988).

Nonlinear interactions of gravitational waves with themselves and each other have been studied extensively using exact solutions which are plane symmetric or cylindrically symmetric — and, thus, which extend outward infinitely far in one or two transverse directions. Powerful, soliton-theoretic techniques for generating such exact solutions have been devised by Belinsky and Zakharov (XXXX); and other solution-generating techniques have been developed by Chandrasekhar (1986 and refs. therein) and by Ernst, Garcia, and Hauser (1988). For applications of these techniques see, e.g., Cespedes and Verdaguer (1987); Garriga and Verdaguer (1987); and Ferrari, Ibanez, and Bruni (1987). The physical properties of cylindrical gravitational waves have been explored, e.g., by Einstein and Rosen (1936) and Weber and Wheeler (1957), who pioneered the subject; and by Thorne (1965a,b), Schmidt (1981), Piran, Safier, and Katz (1986), Chandrasekhar and Ferrari (1987), and others. For detailed studies of planar gravitational waves see Rosen (1937), Bondi, Pirani, and Robinson (1959), and Ehlers and Kundt, 1962 (the pioneering papers), and, more recently, the papers cited in Sec. 5.G.g in connection with gravitational-wave collisions.

Insight into cosmological gravitational waves originating in the early universe comes from a family of exact solutions generated by the

Belinsky–Zakharov (XXXX) technique. These solutions describe universes which, at early times, contain "frozen–in" inhomogeneities. As the cosmological horizon expands and becomes larger than the inhomogeneities' reduced wavelength λ, the inhomogeneities unfreeze and are smoothly transformed into gravitational radiation propagating dynamically through an otherwise homogeneous universe. For specific solutions of this type see Carr and Verdaguer (1983), Belinsky and Francaviglia (1984), and Adams, Hellings, and Zimmerman (1985).

A final type of exact solution which is useful for insight is the extreme limit of geometric optics, where the wavelength becomes so short that the radiation is compacted into a *gravitational shock wave*. For the exact theory of gravitational shocks see, e.g., Pirani (1957), Papapetrou (1977), and references therein.

6 Generation of gravitational waves

In chapter 5 we learned how gravitational waves propagate from the asymptotic rest frame of their source to the earth. In this chapter we shall discuss how waves are generated and move from their source's interior into its asymptotic rest frame. We begin in Sec. 6.A by formulating the match of the wave-generation problem (this chapter) to the wave-propagation problem (preceding chapter). Then in Sec. 6.B we present, without derivation, the "quadrupole formalism" for computing wave generation. This formalism is easy to use, and is accurate when the source's internal motions are slow compared to the speed of light; but it breaks down for sources with large internal velocities, and these probably include the strongest sources in the universe. As a foundation for deriving the quadrupole formalism and deriving other techniques of computing wave generation, we develop in Sec. 6.C a multipole expansion of the gravitational field in the source's local asymptotic rest frame; then in Sec. 6.D we use that expansion to derive the quadrupole formalism. In Secs. 6.E and 6.F we develop two other tools that underlie a variety of techniques for computing wave generation: a formulation of general relativity as a nonlinear field theory in flat spacetime, and the 3+1 formulation of general relativity. We conclude the chapter, in Secs. 6.G—6.K by cataloging a wide variety of formalisms for computing wave generation, each of which is based on one or more of the tools we have developed: *slow-motion formalisms*, applicable to sources with sizes small compared to a reduced wavelength (Sec. 6.G); *post-Minkowski formalisms*, applicable to sources with weak internal gravity (Sec. 6.H); *post-Newtonian formalisms*, applicable to

sources with both slow motion and weak internal gravity (Sec. 6.I); *perturbation formalisms*, applicable to sources that are weakly perturbed away from a nonradiating state (Sec. 6.J); and *numerical relativity*, applicable to any kind of source (Sec. 6.K). The application of these wave-generation methods to specific astrophysical sources will be discussed in Chaps. 7–9.

6.A Wave generation split off from wave propagation

Mathematically, the problems of computing wave generation and computing the propagation of the waves from their source to the earth are both difficult — though for very different reasons, so that to handle the difficulties requires two very different sets of mathematical tools and approximations. This dictates a split of the propagation problem from the generation problem. Such a split is accomplished (Thorne, 1977 and 1980b) by dividing the space around the source into three regions: a *wave-generation region* at distances from the source $r \lesssim r_I$ = ("inner radius"); a *local wave zone* at distances $r_I \lesssim r \lesssim r_0$ = ("outer radius"); and a *distant wave zone* at distances $r \gtrsim r_0$. See Fig. 6.1. The theory of wave generation is developed with one set of mathematical tools in the wave-generation region and the local wave zone, i.e. at distances $r \lesssim r_0$. The theory of propagation to earth is developed with the other set of tools in the local wave zone and the distant wave zone, i.e. at distances $r \gtrsim r_I$. The two theories are matched together in their domain of overlap, the local wave zone $r_I \lesssim r \lesssim r_0$.

The inner radius r_I is far enough out to be in the wave zone, $r_I \gg \lambda$, far enough to be in a region where the source's gravity is weak, $r_I \gg 2M \equiv$ (Schwarzschild radius of source) = 2×(mass of source), and far enough to be outside the source, $r_I \gg L \equiv$ (size of source). The outer radius r_0 is far enough beyond the inner radius to leave many wavelengths in the local wave zone, $r_0 - r_I \gg \lambda$, but not so far that the gravitational redshift can produce a significant net phase shift during propagation through the local wave zone, $\delta\phi = (M/\lambda)\ln(r_0/r_I) \ll 1$, and not so far that the background curvature of the external universe can significantly affect the propagation, $r_0 - r_I \ll \mathcal{R}_B \equiv |R^B_{\alpha\beta\gamma\delta}|^{-1/2}$ ≡ (radius of curvature of background spacetime). These choices of r_I and r_0 permit one to ignore, in the local wave zone $r_I \lesssim r \lesssim r_0$, the background curvature both of the source and of the external universe; i.e. they permit one to regard the waves in the local wave zone as propagating through flat spacetime. This greatly simplifies calculations.

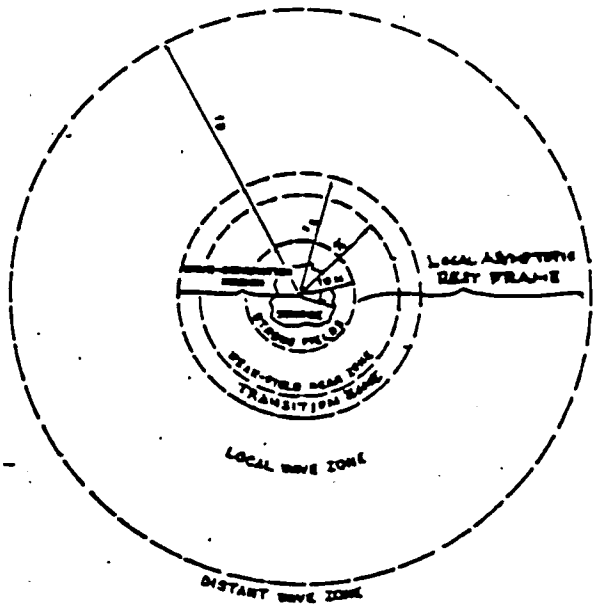

Fig. 6.1 Regions of space around a source of gravitational radiation, drawn for the special case of a source whose size is not much larger than its gravitational radius. [KIP: USE THE VERSION FROM ERICE BUT ADD ON THE SOURCE'S LOCAL ASYMPTOTIC REST FRAME AND THE TRANSITION ZONE]

The entire region over which one can regard the waves as propagating through flat spacetime is called the source's *local asymptotic rest frame* or, simply *asymptotic rest frame*. That asymptotic rest frame includes the local wave zone plus, if the waves' reduced wavelength is huge compared to its gravitational radius $2M$, a *weak-field near zone* that extends over the range $2M \ll r \ll \lambda\!\!\!^{-}$ and a transition zone $r \sim \lambda\!\!\!^{-}$. Not included is the *strong-field region* where $r \lesssim M$.

For a given, astrophysically interesting source, the wave-generation task consists of computing with reasonable accuracy the dynamical behavior of the source's gravitational field in the wave-generation region $r \lesssim r_1$, and further computing how that dynamical curvature develops into outward propagating waves in the local wave zone, $r_1 \lesssim r \lesssim r_0$. Once this is done, the theorist can switch tasks and mathematical formalisms from wave generation to wave propagation. The wave-propagation task takes as input the propagating waves in the local wave zone and carries those waves outward (typically using the geometric-optics formalism of Chap. 5) through the universe from the source to earth.

As an addendum to the wave-generation task, one sometimes computes the back-reaction effects of the wave emission on the

source, i.e. the "radiation reaction".

6.B The quadrupole formalism for wave generation and radiation reaction

Of all the techniques for computing wave generation, one, the "quadrupole formalism", is especially important because it is highly accurate for many sources and is accurate in order of magnitude for most. The quadrupole formalism was derived originally by Einstein (1916, 1918) for sources with negligible self-gravity and slow internal motions. Later, in a series of steps by Landau and Lifshitz (1941), Fock (1959), Ipser (1971), and Thorne (1980b, Secs. VII and XII) — see Sec. 3.A for historical detail —, it became clear that the quadrupole wave-generation formalism requires for high accuracy no constraints whatsoever on the strength of the source's internal gravity. All that is required is slow motion — more specifically, that the source's size L be small compared to the reduced wavelength λ of the waves it emits. In other words, the quadrupole formalism is to gravity-wave generation what the "poor-antenna approximation" (dipole formalism) is to radio-wave generation. Moreover, as in the radio-wave problem, the quadrupole formalism typically is accurate to within factors of order 2 even for sources with sizes of order a reduced wavelength λ [see discussion following Eq. (6.32) below]. Since very very few astrophysical systems are larger than a reduced wavelength of the waves they emit, this justifies the use of the quadrupole formalism for order-of-magnitude astrophysical estimates in almost all situations.

The quadrupole formalism writes the gravitational-wave field in the source's local-wave zone (where the background curvature can be ignored) in the following simple form:

$$h_{jk}^{GW} = \frac{2}{r}\frac{\partial^2}{\partial t^2}[I_{jk}(t-r)]^{TT} . \qquad (6.1)$$

Here r is the distance to the source's center and t is proper time as measured by an observer at rest with respect to the source (i.e. in the source's local asymptotic rest frame), $t-r$ is retarded time, the superscript TT means "algebraically project out and keep only the part that is transverse to the (radial) direction of propagation and is traceless" [Eq. (4.50)], and $I_{jk}(t-r)$ is the source's mass quadrupole moment evaluated at the retarded time $t-r$.

The meaning of "mass quadrupole moment" is well known when the source has weak internal gravity and small internal stresses, so

Newtonian gravity is a good approximation to general relativity inside and near the source. Then I_{jk} is the symmetric, trace-free (STF) part of the second moment of the source's mass density ρ, as computed in a Cartesian coordinate system centered on the source:

$$I_{jk}(t) = [\int \rho(t) x^j x^k d^3x]^{\rm STF} \equiv \int \rho(t)[x^j x^k - \tfrac{1}{3} r^2 \delta_{jk}] d^3x \ . \qquad (6.2a)$$

Equivalently, I_{jk} is the coefficient of the $1/r^3$ part of the source's Newtonian gravitational potential:

$$\Phi = -\frac{M}{r} - \frac{3}{2}\frac{I_{jk}(t)x^j x^k}{r^5} - \frac{5}{2}\frac{I_{ijk}x^i x^j x^k}{r^7} + \cdots$$

$$= -\frac{M}{r} - \frac{3}{2}\frac{I_{jk}(t)n^j n^k}{r^3} - \frac{5}{2}\frac{I_{ijk}n^i n^j n^k}{r^4} + \cdots , \qquad (6.2b)$$

where $n^i \equiv x^i/r$ is the unit radial vector. Moreover, the second time derivative of this quadrupole moment, which appears in the radiation field (6.1), can be rewritten in terms of the source's mass flux ρv^j as

$$\frac{\partial^2 I_{jk}}{\partial t^2} = \frac{\partial}{\partial t}[\int 2\rho v^j x^k d^3x]^{\rm STF} \qquad (6.2c)$$

[a formula readily derivable from (6.2a), mass conservation $\partial\rho/\partial t + (\rho v^i)_{,i} = 0$, and integration by parts]. The second time derivative of I_{jk} can also be written as an integral over the source's stress tensor T_{jk} and its "gravitational stress":

$$\frac{\partial^2 I_{jk}}{\partial t^2} = \int [T_{jk} + \frac{1}{4\pi}(\Phi_{,j}\Phi_{,k} - \tfrac{1}{2}\delta^{ab}\Phi_{,a}\Phi_{,b}\delta_{jk})] d^3x \qquad (6.2d)$$

[a formula derivable from (6.2c), the law of momentum conservation $\partial(\rho v^j)/\partial t + T^{jk}{}_{,k} + \rho\Phi_{,j} = 0$, the Newtonian field equation $\delta^{ab}\Phi_{,ab} = 4\pi\rho$, and integration by parts]. In numerical calculations of $h_{jk}^{\rm GW}$, Eqs. (6.2c) and (6.2d) are generally superior to the second time derivative of (6.2a) because they involve fewer numerically-inaccurate time derivatives. Equations (6.2c) has the numerical advantage over (6.2d) that its integrands is confined to the source's interior, while (6.2d) has the numerical advantage over (6.2c) that it entails no time derivatives at all. For detailed discussions of these and other numerical issues in applying the quadrupole formalism, see Finn (1988), and Finn and Evans (1989),

If the source has strong internal gravity, one can no longer express its mass quadrupole moment as the simple integral (6.2a). However, so long as the source has slow internal motions (size $L \ll \lambda$), there will be a

region of space far enough from the source to be in vacuum ($r > L$) and far enough for gravity to be weak ($r \gg 2M$), yet near enough for retardation and wave behavior to be unimportant ($r \ll \lambda$). In this vacuum part of the weak-field near zone, gravity can be described with high accuracy as Newtonian; and the Newtonian potential is $\Phi \cong -\frac{1}{2}(g_{00}+1)$, where g_{00} is the time-time part of the metric in a coordinate system that is as Minkowski as possible throughout the weak-field, vacuum near zone. The mass quadrupole moment can then be read off this Newtonian potential using the standard formula (6.2b). We shall discuss this readoff more carefully in the first paragraph of Sec. 6.D and in Sec. 6.G.

From the quadrupole formula (6.1) for the wave field in the local wave zone and Isaacson's formula (5.38) for the stress-energy tensor of the waves, one can compute the fluxes of energy and angular momentum carried by the waves. By integrating those fluxes over a sphere surrounding the source in the local wave zone, one obtains for the rates of emission of energy (Einstein 1916, 1918) and angular momentum (Peters 1964)

$$\frac{dE^{GW}}{dt} = \frac{1}{5}\sum_{j,k}\left\langle \left| \frac{d^3 I_{jk}}{dt^3} \right|^2 \right\rangle , \tag{6.3}$$

$$\frac{dJ_i^{GW}}{dt} = \frac{2}{5}\sum_{j,k,l}\varepsilon_{ijk}\left\langle \frac{\partial^2 I_{jl}}{\partial t^2}\frac{\partial^3 I_{lk}}{\partial t^3}\right\rangle . \tag{6.4}$$

The linear momentum carried off by the waves vanishes when one computes it by the quadrupole formalism; but when one includes higher-order corrections to the gravitational-wave field of a slow-motion source [Eq. (6.25) below], one finds for the rate of emission of linear momentum (first derived by Papapetrou 1962, 1971; for a more modern derivation in the notation of this chapter see section IV.C of Thorne, 1980b)

$$\frac{dP_i^{GW}}{dt} = \frac{2}{63}\sum_{j,k}\left\langle \frac{\partial^3 I_{jk}}{\partial t^3}\frac{\partial^4 I_{jki}}{\partial t^4}\right\rangle + \frac{16}{45}\sum_{j,k,a}\varepsilon_{ijk}\left\langle \frac{\partial^3 I_{ja}}{\partial t^3}\frac{\partial^3 S_{ka}}{\partial t^3}\right\rangle . \tag{6.5}$$

Here I_{ijk} is the source's "mass octupole moment" and S_{ij} is its "current quadrupole moment" (gravitational analog of magnetic quadrupole moment). For sources with weak internal gravity and weak stresses (nearly Newtonian sources), these moments are computable from the simple volume integrals

$$I_{ijk} = \left(\int \rho x^i x^j x^k d^3x\right)^{STF} , \tag{6.6a}$$

$$\mathcal{I}_{ij} = \left(\int \rho \varepsilon_{ipq} x^p v^q x^j d^3x\right)^{\rm STF} , \tag{6.6b}$$

where, as in Eq. (6.2a), STF means "make it symmetric and trace-free", i.e. "symmetrize on all free indices and remove the traces on all pairs of free indices". Independently of the strengths of the internal gravity and stresses, the moments can be read off the Newtonian potential $\Phi \cong -\frac{1}{2}(g_{00}+1)$ [Eq. (6.2b)] and off the "gravitomagnetic potential" $\beta_i \equiv g_{0i}$ in the source's weak-field near zone:

$$\beta_i = -2\varepsilon_{ipq}\frac{J^p x^q}{r^3} - 4\varepsilon_{ipq}\frac{\mathcal{I}_{pa}x^q x^a}{r^5} - \cdots . \tag{6.7}$$

In Eq. (6.7), J^p, the moment in the leading, dipolar term, is the source's angular momentum. For further details, discussions, and derivations see Thorne (1983) or Thorne (1980b) and Sec. 6.G below. For a discussion of the gravitomagnetic potential see, e.g., Chap. 3 of Thorne, Price, and Macdonald (1986).

The laws of conservation of energy, angular momentum, and linear momentum imply that radiation reaction should deplete the source's energy, angular momentum, and linear momentum at just the right rates to compensate for the losses (6.3), (6.4), and (6.5); and a detailed analysis of the radiation reaction forces reveals that this is so. See the extensive list of references in Sec. 3.A. Particularly convenient in analyzing the radiation reaction in a source with weak internal gravity is a Newtonian-type radiation-reaction potential (Burke 1969, Thorne 1969b, Chandrasekhar and Esposito 1970, section 36.8 of MTW). This potential is expressed in terms of the fifth time derivative $^{(5)}\mathcal{I}_{jk} \equiv d^5\mathcal{I}_{jk}/dt^5$ of the source's quadrupole moment as

$$\Phi^{\rm react} = \tfrac{1}{5}{}^{(5)}\mathcal{I}_{jk}x^j x^k . \tag{6.8}$$

If one adds this onto the source's standard Newtonian potential

$$\Phi(t,x^i) = \int \frac{\rho(t,x'^i)}{[\delta_{jk}(x^j-x'^j)(x^k-x'^k)]^{1/2}}dx'dy'dz' \tag{6.9}$$

in the source's interior and analyzes the source's dynamical evolution using the gravitational acceleration $\boldsymbol{g} = -\nabla(\Phi+\Phi^{\rm react})$ produced by that combined potential, one will obtain the correct long-term evolution of the source, including the dominant radiation-reaction effects.

For example, whereas the standard potential Φ conserves energy, the radiation-reaction potential $\Phi^{\rm react}$ removes it at just the same *time-averaged* rate (6.3) that it is carried off by gravitational waves. To

see this, one can compute the rate of change of the source's energy as the volume integral of the radiation–reaction force per unit volume dotted into the source's internal velocity $\mathbf{v}$:

$$\frac{dE^{\text{source}}}{dt} = \int(-\rho\nabla\Phi^{\text{react}})\cdot\mathbf{v}dxdydz = -\frac{2}{5}{}^{(5)}I_{ij}\int\rho v^i x^j dxdydz$$

$$= -\frac{1}{5}{}^{(5)}I_{jk}\int\rho v^i(x^j x^k)_{,i}dxdydz = +\frac{1}{5}{}^{(5)}I_{jk}\int(\rho v^i)_{,i}x^j x^k dxdydz$$

$$= -\frac{1}{5}{}^{(5)}I_{jk}\int\frac{\partial\rho}{\partial t}x^j x^k dxdydz = -\frac{1}{5}{}^{(5)}I_{jk}\frac{d}{dt}\int\rho x^j x^k dxdydz \qquad (6.10)$$

$$= -\frac{1}{5}{}^{(5)}I_{jk}{}^{(1)}I_{jk} = -\frac{1}{5}{}^{(3)}I_{jk}{}^{(3)}I_{jk} - \frac{1}{5}\frac{d}{dt}({}^{(4)}I_{jk}{}^{(1)}I_{jk} - {}^{(3)}I_{jk}{}^{(2)}I_{jk}) .$$

Here the second equality follows from the definition (6.8) of Φ^{react}, the fifth follows from the law of mass conservation $\partial\rho/\partial t + (\rho v^i)_{,i} = 0$, the seventh follows from the definition (6.2a) of I_{jk} and from the fact that ${}^{(5)}I_{jk}$ is trace–free, and all other equalities are straightforward. When one time averages this relation over a number of periods of oscillation of the source, one finds

$$\left\langle\frac{dE^{\text{source}}}{dt}\right\rangle = -\frac{1}{5}\langle{}^{(3)}I_{jk}{}^{(3)}I_{jk}\rangle = -\frac{dE^{\text{GW}}}{dt} ; \qquad (6.11)$$

cf. Eq. (6.3). The necessity to time average in order to get energy conservation goes hand–in–hand with the fact that the waves' energy is well defined only when averaged over a number of wavelengths.

The gravitational acceleration due to radiation reaction can be written in many different, but mathematically equivalent, ways. The above way, $\mathbf{g}^{\text{react}} = -\nabla\Phi^{\text{react}}$ with Φ^{react} given by Eq. (6.8), is the simplest and conceptually the nicest. Other ways differ from it in their (extremely small) short–term effects, but they all have the same long–term, time–integrated effects as the "standard" way, $\mathbf{g}^{\text{react}} = -\nabla\Phi^{\text{react}}$. For numerical computations some of the alternative ways are superior to the standard way, because they entail computing fewer numerically touchy time derivatives. For the alternative ways and detailed comparisons of them, see: Miller (1974); Schäfer (1983, 1985, 1989); Secs. 4.15–4.17 of Damour (1987a); and Blanchet, Damour, and Schäfer (1989).

Different physicists feel comfortable with different levels of rigor. Such differences have shown up strongly and publicly in a controversy over derivations of the quadrupole wave–generation formula (6.1) and especially the formula for the energy sapped from a source by

radiation reaction [negative of Eq. (6.3)]. For a brief history of this "quadrupole controversy" and of how it is finally being resolved and the above formalism is coming to be fully accepted, see Sec. 3.A. For a quantitative study of the accuracy of the quadrupole formalism as applied to the pulsations of compact stars, where L is not terribly small compared to λ, see Balbinsky et. al. (1985).

The quadrupole formalism has been used in computations of the gravitational waves from a wide variety of astrophysical sources. Two examples are the waves emitted by binary star systems (Peters and Mathews, 1963; Wahlquist, 1987; Sec. 8.C of this book), and the waves emitted by Newtonian models of supernovae (e.g. Müller, 1982; Saenz and Shapiro, 1978, 1981; Fig. 1.4 and Sec. 7.B of this book). The radiation-reaction potential (6.8) has also been used in a wide variety of astrophysical studies. Examples are the evolution of a binary system made of two disks (rotationally flattened stars, star clusters, or galaxies) (Eriguchi, Futamase, and Hachisu, 1989); XXXXXX.

6.C Multipole expansions in the asymptotic rest frame

As a foundation for deriving the quadrupole formalism and other formalisms for wave generation, we shall now develop the theory of multipole moments of gravitational-wave sources.

Our goal is to expand a source's external gravitational field in multipole moments. To make the expansion (relatively) easy, we shall restrict it to the source's asymptotic rest frame, a region with sufficiently weak gravity and sufficiently small size that the gravitational field can be treated as a linear perturbation of flat spacetime. Recall (Fig. 6.1 and associated discussion) that this asymptotic rest frame includes all of the local wave zone. In addition, for a *slow-motion source*, i.e. a source whose waves have reduced wavelength huge compared to the source ($\lambda \gg L$ and $\lambda \gg 2M$), it also includes the transition zone and a vacuum, weak-field near zone. We shall carry out our multipole expansion in such a way as to be uniformly valid throughout the asymptotic rest frame, including (when they all exist) the vacuum, weak-field near zone, the transition zone, and the local wave zone.

The foundation for our expansion is the theory of linear perturbations of curved spacetime (Sec. 5.B), specialized to a vacuum, flat-spacetime background. In the background spacetime we adopt Lorentz coordinates $(t, x, y, z) = (x^0, x^1, x^2, x^3)$ with the spatial origin centered on the source. In this coordinate system the background metric coefficients are $g^{\rm B}_{\alpha\beta} = \eta_{\alpha\beta}$ (where, as usual, $\eta_{00} = -1$, $\eta_{xx} = \eta_{yy} = \eta_{zz} = +1$,

and all others vanish), and the background connection coefficients vanish, so background covariant derivatives reduce to partial derivatives, $h_{\alpha\beta|\gamma} = h_{\alpha\beta,\gamma}$. We shall adopt Lorentz gauge from the outset, so the trace-reversed metric perturbation

$$\bar{h}_{\alpha\beta} \equiv h_{\alpha\beta} - \tfrac{1}{2} h^{\mu}{}_{\mu} \eta_{\alpha\beta} , \quad \text{where } h_{\alpha\beta} \equiv g_{\alpha\beta} - \eta_{\alpha\beta} , \tag{6.12}$$

satisfies the gauge and field equations [Eqs. (5.20) and (5.24)]

$$\bar{h}^{\alpha\mu}{}_{,\mu} = 0 , \tag{6.13a}$$

$$\Box \bar{h}_{\alpha\beta} \equiv \eta^{\mu\nu} \bar{h}_{\alpha\beta,\mu\nu} = 0 . \tag{6.13b}$$

Our task will be to construct, as a multipole expansion, the general solution to Eqs. (6.13) with purely outgoing waves (no incoming waves). Our method of solution will be that of Thorne (1980b, Sec. VIII), which was based on earlier work of Sachs and Bergmann (1958), Bonnor (1959), [KIP: CHECK] Sachs (1961), Pirani (1964), and Campbell and Morgan (1971).

Multipole moments are the coefficients that appear in spherical-harmonic expansions. Most modern, elementary introductions to spherical harmonics are based on spherical harmonic functions denoted $Y^{lm}(\theta,\phi)$ (with θ,ϕ spherical polar coordinates centered on the source). If a function $f(\theta,\phi)$ is expanded in these functions,

$$f(\theta,\phi) = \sum_{l=0}^{\infty} \sum_{m=-l}^{+l} F^{lm} Y^{lm}(\theta,\phi) , \tag{6.14a}$$

the coefficients F^{lm} are called the multipole moments of f.

There is an alternative approach to spherical harmonics, which predates the functions $Y^{lm}(\theta,\phi)$ (see, e.g., Kelvin and Tate, 1879; Hobson, 1931), and which turns out to be superior to $Y^{lm}(\theta,\phi)$ for many purposes, including that of this section. This alternative is to replace the angles θ,ϕ by the Cartesian components of the unit radial vector n (i.e. by $n_x = \sin\theta\cos\phi$, $n_y = \sin\theta\sin\phi$, $n_z = \cos\theta$), and to expand f in powers of those components:

$$f = \sum_{l=0}^{\infty} \mathcal{F}_{a_1 a_2 \cdots a_l} n^{a_1} n^{a_2} \cdots n^{a_l} . \tag{6.14b}$$

Here and below repeated Latin indices such as a_1 and a_2 are to be summed even when they are both down or both up (a practice that should not produce confusion since the background spatial metric is Cartesian, $\eta_{jk} = \delta_{jk}$). The expansion coefficients $\mathcal{F}_{a_1 a_2 \cdots a_l}$ are rank-l tensors which are symmetric under interchange of any two pairs of

indices and have vanishing trace on every pair of indices, and therefore are called *symmetric and trace-free*, or STF. These coefficients are the STF version of the multipole moments of the function f.

The STF approach to spherical harmonics is based on the fact that the set of all symmetric trace-free tensors of rank l (STF-l tensors) generates an irreducible representation of the rotation group, of weight l (Gel'fand, Minlos, and Shapiro, 1963; Courant and Hilbert, 1953). One aspect of this is the fact that, just as the index m can take on $2l+1$ independent values in the spherical harmonics $Y^{lm}(\theta,\phi)$, so also the space of STF-l tensors has dimension $2l+1$ (i.e. any STF-l tensor can be expanded in terms of $2l+1$ such tensors). The mapping between spherical harmonics $Y^{lm}(\theta,\phi)$ and STF-l tensors is exhibited in detail in Sec. II of Thorne (1980b). As a simple example of that mapping, consider the axially symmetric quadrupolar function

$$f(\theta,\phi) = F^{20}Y^{20} = (3/16\pi)^{1/2}(3\cos^2\theta - 1) . \tag{6.15a}$$

This same function, expressed in terms of Cartesian components of the unit radial vector is

$$f = F^{20}(3/16\pi)^{1/2}(3n_z n_z - 1) = F^{20}(3/16\pi)^{1/2}(2n_z n_z - n_x n_x - n_y n_y)$$
$$= \mathcal{F}_{jk} n_j n_k , \tag{6.15b}$$

from which we read off the STF multipole moments

$$\mathcal{F}_{zz} = -2\mathcal{F}_{xx} = -2\mathcal{F}_{yy} = (3/4\pi)^{1/2}F^{20} . \tag{6.15c}$$

For ease of notation we shall denote the tensor product of l unit radial vectors by

$$N_{a_1 a_2 \cdots a_l} \equiv n_{a_1} n_{a_2} \cdots n_{a_l} ; \tag{6.16a}$$

we shall denote long strings of indices by capital letters whose corresponding lower-case letter is the number of indices in the string:

$$N_L \equiv N_{a_1 a_2 \cdots a_l} , \quad \mathcal{F}_J \equiv \mathcal{F}_{b_1 b_2 \cdots b_j} ; \tag{6.16b}$$

and, accordingly, we shall write (6.14b) in the compact form

$$f = \sum_{l=0}^{\infty} \mathcal{F}_L N_L . \tag{6.17}$$

(The compact notation $\mathcal{F}_L$, due to Blanchet and Damour, 1986, replaces the $\mathcal{F}_{A_l}$ used in Thorne, 1980b.) All tensors such as $\mathcal{F}_L$ that are denoted by capital script letters will be STF. WARNING: The L in $\mathcal{F}_L$, which stands for $a_1 \cdots a_l$, must not be confused with L = (size of source). The

former L appears only in subscripts and the latter is never in subscripts.

One demonstration of the power of the STF formalism is the following elegant multipolar expansion for the general outgoing-wave solution to the scalar wave equation $\Box\psi = 0$:

$$\psi = \sum_{l=0}^{\infty} \left[\frac{I_{a_1 \cdots a_l}(t-r)}{r} \right]_{,a_1 \cdots a_l} = \sum_{l=0}^{\infty} \left[\frac{I_L(t-r)}{r} \right]_{,L} . \tag{6.18}$$

The first expression is in standard notation; the second, in compacted notation. In this expression $r \equiv (x^2+y^2+z^2)^{1/2}$ is distance from the source, and the multipole moments $I_L(t-r)$ are STF-l tensors which are functions of retarded time $t-r = \tau_e$. One can easily verify that this expression is a solution of the wave equation by checking that any function of the form $f(t-r)/r$ satisfies the wave equation, and by noting that the wave operator $\Box$ commutes with Cartesian-coordinate spatial derivatives. Contrast the simplicity of expression (6.18) with the greater complexity of the corresponding expansion in terms of the Fourier inverse of $h_l^{(1)}(\omega r)e^{-i\omega t}Y^{lm}(\theta,\phi)$ (where $h_l^{(1)}$ are the spherical hankel functions). The contrast is even more extreme when we deal, as we must, with spherical-harmonic expansions of vector fields and tensor fields.

Return now to the task of writing down the general outgoing-wave solution to the linearized, vacuum Einstein field equation (6.13b). We shall write down separately the solutions for $\bar{h}_{00}$, which can be thought of as a spatial scalar field; for $\bar{h}_{0j} = \bar{h}_{j0}$, a spatial vector field; and for $\bar{h}_{jk}$, a symmetric spatial tensor field. Since $\bar{h}_{00}$ has only one component, it requires just one set of multipole moments. Since $\bar{h}_{0j}$ has four independent components, it requires four sets of moments. Since $\bar{h}_{jk}$ has six independent components, it requires six sets of moments. By trial and error, motivated by the solution (6.18) to the scalar wave equation, one can arrive at the following general solution to $\Box\bar{h}_{\alpha\beta} = 0$:

$$\bar{h}_{00} = \sum_{l=0}^{\infty} \left[\frac{A_L(t-r)}{r} \right]_{,L} \tag{6.19a}$$

$$\bar{h}_{0j} = \sum_{l=0}^{\infty} \left[\left[\frac{B_{jL}(t-r)}{r} \right]_{,L} + \left[\frac{\varepsilon_{jpq} C^{qL}(t-r)}{r} \right]_{,pL} + \left[B_L \frac{(t-r)}{r} \right]_{,jL} \right] , \tag{6.19b}$$

$$\bar{h}_{jk} = \sum_{l=0}^{\infty} \left[\left[\frac{\delta_{jk} I_L(t-r)}{r} \right]_{,L} + \left[I_{jkL} \frac{(t-r)}{r} \right]_{,L} + \left[\frac{\varepsilon_{pqj} C_{kqL}(t-r)}{r} \right]_{,pL} \right.$$

$$+\left[\frac{\mathcal{H}_{jL}(t-r)}{r}\right]_{,kL}+\left[\frac{\varepsilon_{jpq}\mathcal{J}_{qL}(t-r)}{r}\right]_{,kpL}+\left[\frac{\mathcal{K}_L(t-r)}{r}\right]_{,jkL}\Bigg]^{S}. \quad (6.19c)$$

Here the superscript S in Eq. (6.19c) means "symmetrize on the free indices jk"; i.e., $(A_{jk})^S \equiv \frac{1}{2}(A_{jk}+A_{kj})$.

This general outgoing-wave solution to the Einstein field equations $\Box\bar{h}^{\alpha\beta}=0$ does not yet satisfy the Lorentz gauge condition $\bar{h}^{\alpha\mu}{}_{,\mu}=0$. By imposing that gauge condition we obtain, straightforwardly, the following four connections between the ten families of multipole moments,

$$\mathcal{B}_L=\dot{\mathcal{A}}_L-\ddot{\mathcal{B}}_L\,,\qquad \mathcal{F}_L=\ddot{\mathcal{A}}_L-\dddot{\mathcal{B}}_L-\tfrac{1}{2}\ddot{\mathcal{H}}_L\,,$$
$$\mathcal{E}_L=\ddot{\mathcal{B}}_L-\tfrac{1}{2}\ddot{\mathcal{H}}_L-\dddot{\mathcal{K}}_L\,,\qquad \mathcal{G}_L=2\dot{\mathcal{C}}_L-\ddot{\mathcal{J}}_L\,, \quad (6.20a)$$

plus the following special relations which result from the absence of the monopole moments $\mathcal{B}, \mathcal{C}, \mathcal{F}, \mathcal{G}, \mathcal{H}, \mathcal{J}$ and the dipole moments $\mathcal{F}_j$ and $\mathcal{G}_j$ from the solution (6.19):

$$\dot{\mathcal{A}}-\ddot{\mathcal{B}}=0\,,\quad \mathcal{E}-\ddot{\mathcal{B}}+\dddot{\mathcal{K}}=0\,,\quad \dot{\mathcal{C}}_j-\tfrac{1}{2}\ddot{\mathcal{J}}_j=0\,,\quad \ddot{\mathcal{A}}_j-\dddot{\mathcal{B}}_j-\tfrac{1}{2}\dddot{\mathcal{H}}_j=0\,. \quad (6.20b)$$

Here, and throughout, a dot means a derivative with respect to time t. The six remaining families of moments can be reduced to two by a gauge transformation [Eq. (5.19)] with generator

$$\xi_0=\sum_{l=0}^{\infty}\left[\left[\frac{\mathcal{B}_L(t-r)}{r}\right]_{L}+\frac{1}{2}\left[\frac{\dot{\mathcal{K}}_L(t-r)}{r}\right]_{L}\right], \quad (6.21a)$$

$$\xi_j=-\sum_{l=0}^{\infty}\left[\frac{1}{2}\left[\frac{\mathcal{H}_{jL}(t-r)}{r}\right]_{L}+\frac{1}{2}\left[\frac{\varepsilon_{jpq}\mathcal{J}_{qL}(t-r)}{r}\right]_{,pL}+\frac{1}{2}\left[\frac{\mathcal{K}_L(t-r)}{r}\right]_{,jL}\right]. \quad (6.21b)$$

This gauge change brings to zero the moments $\mathcal{B}_L$, $\mathcal{H}_L$, $\mathcal{J}_L$, and $\mathcal{K}_L$; and together with (6.20) it leaves $\mathcal{A}_L$ and $\mathcal{C}_L$ as a complete set of moments. For reasons to be explained below, we shall renormalize and rename our two remaining families:

$$\mathcal{A}_L\equiv(-1)^l\frac{4}{l!}\mathcal{I}_L\,,\quad \mathcal{C}_L\equiv(-1)^l\frac{4l}{(l+1)!}\mathcal{S}_L\,. \quad (6.22)$$

The Lorentz gauge conditions (6.20b), with $\mathcal{P}$, $\mathcal{P}_j$, $\mathcal{H}_j$, and $\mathcal{J}_j$ brought to zero and with the renaming (6.22), imply that

$$\mathcal{I} = 0\ ,\quad \mathcal{S}_j = 0,\quad \dot{\mathcal{I}}_j = 0\ . \tag{6.23}$$

These constraints have simple physical meanings: As we shall see below (and as one can infer from the discussions in Chaps. 19 and 20 of MTW), $\mathcal{I}$ is the source's total mass, $\mathcal{S}_j$ is its total angular momentum, $\mathcal{I}_j$ is its mass dipole moment, and $\dot{\mathcal{I}}_j$ is its total linear momentum. Correspondingly, Eqs. (6.23) are the laws of conservation of mass, angular momentum, and linear momentum. (This formalism is insensitive to the loss of mass, angular momentum, and linear momentum to the waves because those losses are quadratic in the metric perturbation $h_{\alpha\beta}$, and this formalism is linearized.) Since we have asked that our coordinate system be at rest relative to the source, it must be that the conserved linear momentum, $\dot{\mathcal{I}}_j$ vanishes. By insisting further that our origin of spatial coordinates coincide with the source's center of mass — i.e. that the coordinates be *mass centered*, we guarantee, further, that $\mathcal{I}_j = 0$. If we then denote the constant values of the mass $\mathcal{I}$ by M and of the angular momentum $\mathcal{S}_j$ by J_j, and combine Eqs. (6.19), (6.20), (6.22), and $\mathcal{P}_L=\mathcal{H}_L=\mathcal{J}_L=\mathcal{K}_L=0$, we can write $\bar{h}_{\alpha\beta}$ in the following, final form:

$$\bar{h}_{00} = \frac{4M}{r} + \sum_{l=2}^{\infty}(-1)^l\frac{4}{l!}\left[\frac{\mathcal{I}_L(t-r)}{r}\right]_{\mathcal{L}}\ , \tag{6.24a}$$

$$\bar{h}_{0j} = -2\frac{\varepsilon_{jpq}J^p n_q}{r^2} + \sum_{l=1}^{\infty}(-1)^{l+1}\frac{4l}{(l+1)!}\left[\frac{\varepsilon_{jpq}\mathcal{S}_{pL}(t-r)}{r}\right]_{,qL} + \sum_{l=0}^{\infty}(-1)^l\frac{4}{l!}\left[\frac{\dot{\mathcal{I}}_{jL}(t-r)}{r}\right]_{\mathcal{L}}\ , \tag{6.24b}$$

$$\bar{h}_{jk} = \sum_{l=2}^{\infty}\left[(-1)^l\frac{4}{l!}\left[\frac{\ddot{\mathcal{I}}_{jkL}(t-r)}{r}\right]_{\mathcal{L}} + (-1)^{l+1}\frac{8l}{(l+1)!}\left[\frac{\varepsilon_{pqj}\dot{\mathcal{S}}_{kpL}(t-r)}{r}\right]_{,qL}\right]^{S}\ . \tag{6.24c}$$

Notice, in keeping with the discussion in Sec. 1.C, that the gravitational field, in the source's asymptotic rest frame, is determined by two families of multipole moments, the *mass moments* $\mathcal{I}_L$ and the *current moments* $\mathcal{S}_L$, and that the laws of conservation of mass, angular momentum, and linear momentum imply that the only moments which can oscillate, and thus radiate, are those with multipole order

$l \geq 2$; i.e. $l \geq$ (the spin of the general relativistic graviton).

Turn attention to the radiation produced by the moments with $l \geq 2$. In the local wave zone that radiation is described by the transverse-traceless part of the $1/r$ piece of the field $\bar{h}_{jk}$ [cf. Eq. (4.50)]:

$$h_{jk}^{GW} = (\bar{h}_{jk})^{TT} = \sum_{l=0}^{\infty} \left[\frac{4}{l!} \frac{{}^{(l)}I_{jkL}(t-r)N_L}{r} + \frac{8l}{(l+1)!} \frac{\varepsilon_{pqj}{}^{(l)}S_{kpL}(t-r)n_q N_L}{4} \right]^{S,TT} . \tag{6.25}$$

Here the superscript S means that one must symmetrize on the two free indices j and k, while the superscript TT means that one must take the transverse-traceless part in the manner of Eq. (4.50). Equation (6.25) is the general multipolar expansion of a gravitational-wave field. It contains two pieces: that described by the mass moments I_L with $l \geq 2$ (analog of electric multipole radiation), and that described by the current moments S_L with $l \geq 2$ (analog of magnetic multipole radiation). Any radiation field in the local wave zone can be expanded in moments in this way.

By inserting the expansion (6.25) into expression (5.39) for the waves' stress-energy tensor and performing surface integrals of the energy and momentum fluxes over a sphere r = const in the local wave zone, one can derive expressions for the energy and linear momentum carried by the waves (Sec. IV of Thorne, 1980b):

$$\frac{dE^{GW}}{dt} = \int T^{GW0k} n^k r^2 d\Omega = \frac{1}{32\pi} \int \langle h_{jk,t}^{GW} h_{jk,t}^{GW} \rangle r^2 d\Omega$$

$$= \sum_{l=2}^{\infty} \left[\frac{(l+1)(l+2)}{(l-1)l} \frac{1}{l!(2l+1)!!} \langle {}^{(l+1)}I_L \, {}^{(l+1)}I_L \rangle \right. \tag{6.26a}$$

$$\left. + \frac{4l(l+2)}{(l-1)} \frac{1}{(l+1)!(2l+1)!!} \langle {}^{(l+1)}S_L \, {}^{(l+2)}S_L \rangle \right] ,$$

$$\frac{dP_j^{GW}}{dt} = \int T^{GWjk} n^k r^2 d\Omega = \frac{1}{32\pi} \int \langle h_{jk,t}^{GW} h_{jk,t}^{GW} \rangle n^j r^2 d\Omega$$

$$= \sum_{l=2}^{\infty} \left[\frac{2(l+2)(l+3)}{l(l+1)!(23+3)!!} \langle {}^{(l+2)}I_{jL} \, {}^{(l+1)}I_L \rangle + \frac{8(l+3)}{(l+1)!(2l+3)!!} \right. \tag{6.26b}$$

$$\left. \times \langle {}^{(l+2)}S_{jL} \, {}^{(l+1)}S_L \rangle + \frac{8(l+2)}{(l-1)(l+1)!(2l+1)!!} \langle \varepsilon_{jpq} {}^{(l+1)}I_{pL-1} \, {}^{(l+1)}S_{qL-1} \rangle \right] .$$

Here $(2l+1)!!$ means $(2l+1)(2l-1)(2l-3)\cdots 1$. A similar, but more delicate calculation produces general expressions for the angular momentum carried by the waves. The calculation is more delicate because the averaging process that underlies expression (5.39) for the gravitational waves' stress-energy tensor treats as zero "tiny corrections" which die out as $1/r^3$, and it is precisely the $1/r^3$ part of the stress-energy tensor that carries off the angular momentum. Two independent calculations that treat with care the $1/r^3$ part have been carried out (DeWitt, 1971; Sec. IV D of Thorne, 1980b); and they produced the same final formula for the angular momentum in the waves [first line of Eq. (6.26c)]. That formula, when combined with the multipole expansion (6.25) for the radiation field, yields

$$\frac{dJ_j^{\rm GW}}{dt} = \frac{1}{16\pi}\int \varepsilon_{jpq}x^p\langle (h^{\rm GW}_{qa}h^{\rm GW}_{ab,t})_{,b} - \tfrac{1}{2}h^{\rm GW}_{ab,q}h^{\rm GW}_{ab,t}\rangle r^2 d\Omega$$

$$= \sum_{l=2}^{\infty}\left[\frac{(l+1)(l+2)}{(l-1)l!(2l+1)!!}\langle \varepsilon_{jpq}{}^{(l)}I_{pL-1(l+1)}I_{qL-1}\rangle \right. \qquad (6.26c)$$

$$\left. + \frac{4l^2(l+2)}{(l-1)(l+1)!(2l+1)!!}\langle \varepsilon_{jpq}{}^{(l)}S_{pL-1}{}^{(l+1)}S_{qL-1}\rangle\right],$$

The quadrupole formalism's expressions for the loss of energy, linear momentum, and angular momentum [Eqs. (6.3)–(6.5)] are the lowest-order terms in the infinite sums (6.26).

6.D Slow-motion sources: derivation of the quadrupole formalism

In this section we shall specialize our multipole expansions to slow-motion sources (i.e. sources whose size and gravitational radius are small compared to a reduced wavelength of the waves they emit), and shall use the expansions to derive the quadrupole formalism. In the weak-field near zone of a slow-motion source, the expression (6.24) for the trace-reversed metric perturbation $\bar{h}_{\alpha\beta}$ reduces to

$$\bar{h}_{00} = \frac{4M}{r} + \sum_{l=2}^{\infty}\frac{4(2l-1)!!}{l!}\frac{I_L N_L}{r^{l+1}}, \qquad (6.27a)$$

$$\bar{h}_{0j} = -2\frac{\varepsilon_{jpq}J_p n_q}{r^2} + \sum_{l=2}^{\infty} -\frac{4l(2l-1)!!}{(l+1)!}\frac{\varepsilon_{jpq}S_{pL-1}n_q N_{L-1}}{r^{l+1}}, \qquad (6.27b)$$

$$\bar{h}_{jk} = 0, \qquad (6.27c)$$

plus fractional corrections to each moment's contributions that are of

order r/λ. The corresponding metric perturbations $h_{\alpha\beta} = \bar{h}_{\alpha\beta} - \frac{1}{2}\bar{h}\eta_{\alpha\beta}$ are

$$h_{00} = \tfrac{1}{2}\bar{h}_{00}\ , \quad h_{0j} = \bar{h}_{0j}\ , \quad h_{jk} = \tfrac{1}{2}\delta_{jk}\bar{h}_{00}\ . \tag{6.28}$$

Thus, in our linearized approximation, the source's mass moments I_L can be read off the time–time part of the weak-field, near-zone metric perturbation $h_{00} = \frac{1}{2}\bar{h}_{00}$, and its current moments can be read off the time–space part. We shall return to this readoff in Sec. 6.G.

If the source has weak gravity throughout its interior and is small compared to a reduced wavelength, then one can compute the near-zone field $\bar{h}_{\alpha\beta}$ by dropping the (negligible) time derivatives from the field equation, $\Box\bar{h}_{\alpha\beta} \cong \delta_{jk}\bar{h}_{\alpha\beta,jk} = -16\pi T_{\alpha\beta}$ [Eq. (5.24)], and by then inverting this field equation to obtain

$$\bar{h}_{\alpha\beta}(t,x^i) = 4\int \frac{T_{\alpha\beta}(t,x'^i)}{[\delta_{jk}(x^j - x'^j)(x^k - x'^k)]^{1/2}} dx'dy'dz' \ . \tag{6.29}$$

This is the relativistic analog of the Newtonian Eq. (6.9). By then expanding the denominator in powers of x'^j/r one can obtain the external gravitational field written as an STF multipolar expansion. After a gauge change to bring $\bar{h}_{0j}$ into the canonical form (6.27b) [KIP: CHECK], and a specialization to sources with small internal stresses $|T^{jk}| \ll T^{00}$, and a change to Newtonian-type notation with $T^{00} = \rho =$ (mass density), $T^{0j} = \rho v^j =$ (mass flux) (with v^j the internal velocity field of the source), one obtains the multipolar expressions (6.27) for $\bar{h}_{\alpha\beta}$ along with the following formulas for the moments as integrals over the source:

$$M = \int \rho dxdydz\ , \quad I_{a_1a_2\cdots a_l} = \left[\int \rho x^{a_1}x^{a_2}\cdots x^{a_l}dxdydz\right]^{\rm STF}\ , \tag{6.30a}$$

$$J_j = \int \varepsilon_{jpq}x^p\rho v^q dxdydz\ , \quad S_{a_1a_2\cdots a_l} = \left[\int \varepsilon_{a_1pq}x^p\rho v^q x^{a_2}\cdots x^{a_l}dxdydz\right]^{\rm STF}\ . \tag{6.30b}$$

Here the superscript STF means to symmetrize on all pairs of indices and remove the trace on all pairs. Thus, M is the source's mass, J_j is its angular momentum, I_L is the STF part of the lth moment of its mass distribution, and S_L is the STF part of the $l-1$th moment of its angular momentum distribution.

Note: Our normalizations (6.22) for the moments I_L and S_L were chosen so that there would be no numerical coefficients in front of Eqs.

(6.30); i.e. so that $\mathcal{I}_L$ could be interpreted as precisely the STF part of the l'th moment of the mass distribution, and $\mathcal{S}_L$ as precisely the STF part of the l'th moment of the angular momentum distribution. Note further that the source's mass and current moments are of order

$$\mathcal{I}_L \sim ML^l\ , \quad \mathcal{S}_L \sim Mvl^l \sim M(L/\lambda)L^l\ , \tag{6.31}$$

where M is the source's mass, L *not in a subscript* is its linear size, and v is its characteristic internal velocity. This will be true in rough order of magnitude not just for sources with weak internal gravity, but for those with strong. Correspondingly, the contributions of the l'th moments to the gravitational-wave field (6.25) have magnitudes

$$(h_{jk}^{\rm GW})_{\mathcal{I}_L} \lesssim \frac{M}{r}\left[\frac{L}{\lambda}\right]^l\ , \quad (h_{jk}^{\rm GW})_{\mathcal{S}_L} \lesssim \frac{M}{r}\left[\frac{L}{\lambda}\right]^{l+1}\ . \tag{6.32}$$

This justifies the order-of-magnitude discussion in Sec. 1.C. It also shows that, for slow-motion systems, unless the mass quadrupole is artificially suppressed (e.g. by special symmetries in the source), it will be the dominant producer of gravitational waves. This justifies ignoring higher-order multipoles in the quadrupole-moment formalism. Finally, Eq. (6.32) shows that when $L \sim \lambda$ the higher-order moments give contributions to the waves that are of the same order of magnitude as the mass quadrupole contribution. This justifies our claim, above, that the quadrupole formalism typically will give correct order-of-magnitude results even when L is as small as the waves' reduced wavelength.

We turn, next, to a derivation of expression (6.8) for the radiation-reaction potential. This potential is valid only for nearly Newtonian sources, i.e. for sources with mass M, size L, internal speeds v, timescales of variation λ, internal Newtonian potential Φ, mass density $\rho = T^{00}$, mass flux $T^{0j} = \rho v^j$, and internal stress T^{jk} satisfying

$$v \sim \frac{\lambda}{L}\ , \quad |\Phi| \sim \frac{M}{L} \sim v^2\ , \quad \frac{|T^{j0}|}{T^{00}} \sim v\ , \quad \frac{|T^{jk}|}{T^{00}} \sim v^2\ . \tag{6.33a}$$

In the interior of such a source, so long as

$$|\bar{h}_{0j}| \lesssim |\bar{h}_{00}|\ , \quad |\bar{h}_{jk}| \lesssim |\bar{h}_{00}|\ , \tag{6.33b}$$

one can identify $\bar{h}_{00}$ with -4 times the Newtonian potential Φ, and the source's general relativistic equation of motion $T^{j\beta}{}_{;\beta} = 0$ will reduce to the Newtonian law of momentum conservation

$$(\rho v^j)_{,t} + T^{jk}{}_{,k} = -\rho\Phi_{,j}\ . \tag{6.33c}$$

The source's internal gravitational field $\bar{h}_{\alpha\beta}$ must match smoothly onto the external field (6.24). Note that the external field contains only outgoing waves; no incoming waves. By definition, *radiation reaction is that set of effects, in the source's evolution, which would change sign if the source's distant field were to consist of incoming waves rather than outgoing waves.* Correspondingly, radiation reaction is embodied in that part of the trace-reversed metric perturbation $\bar{h}_{\alpha\beta}$ which would change sign if the time dependence $t-r$ in Eq. (6.24) were changed to $t+r$. To compute that radiation-reaction field near but outside the source, we can replace $t-r$ by $t-\varepsilon r$ (with $\varepsilon = \pm 1$) in Eq. (6.24), expand in powers of r and pluck out the pieces sensitive to the sign of ε. The expansion of (6.24) produces, outside but near the source

$$\bar{h}_{00} = \frac{6I_{jk}x^j x^k}{r^5} - \frac{{}^{(2)}I_{jk}x^j x^k}{r^3} + \frac{{}^{(4)}I_{jk}x^j x^k}{4r} - \frac{2}{15}\varepsilon\,{}^{(5)}I_{jk}x^j x^k + 0_8\,, \quad (6.34a)$$

$$\bar{h}_{0j} = -2\frac{{}^{(1)}I_{jk}x^k}{r^3} + \frac{{}^{(3)}I_{jk}x^k}{r} - \frac{2}{3}\varepsilon\,{}^{(4)}I_{jk}x^k + 0_7\,, \quad (6.34b)$$

$$\bar{h}_{jk} = 2\frac{{}^{(2)}I_{jk}}{r} - 2\varepsilon\,{}^{(3)}I_{jk} + 0_6\,. \quad (6.34c)$$

Here 0_n means terms of order v^n. The leading piece that is *not* sensitive to the sign of ε is $\bar{h}^{00} = (6/r^5)I_{jk}x^j x^k$. Together with the leading piece $\bar{h}_{00} = 4M/r$ of the monopole field and the leading pieces of the higher mass multipoles, it adds up to expression (6.27a), which is -4 times the full external Newtonian potential, and which matches smoothly onto the source's internal Newtonian field

$$\bar{h}_{00}^{\text{Newton}} = -4\Phi\,. \quad (6.35)$$

The higher-order terms in (6.34) that are not sensitive to the sign of ε join onto post-Newtonian corrections to the internal field. Those, plus nonlinear post-Newtonian corrections which are lost in this linear analysis, are important in many astrophysical sources; but we shall ignore them here because they have nothing to do with radiation reaction. The dominant radiation reaction terms in the field (6.34) outside but near the source are

$$\bar{h}_{00}^{\text{react}} = -\frac{2}{15}{}^{(5)}I_{jk}x^j x^k\,, \quad \bar{h}_{0j}^{\text{react}} = -\frac{2}{3}{}^{(4)}I_{jk}x^k\,, \quad \bar{h}_{jk}^{\text{react}} = -2\,{}^{(3)}I_{jk}\,. \quad (6.36)$$

These are simplified by the gauge change whose generator is

$$\xi_0 = \frac{1}{6}{}^{(4)}I_{jk}x^j x^k\,, \quad \xi_j = -{}^{(3)}I_{jk}x^k\,. \quad (6.37)$$

In the new gauge they become

$$\bar{h}_{00}^{\text{react}} = -2\Phi^{\text{react}} = \frac{2}{5}\mathcal{I}_{jk}^{(5)} x^j x^k \,, \tag{6.38a}$$

$$|\bar{h}_{0j}^{\text{react}}| \ll |\bar{h}_{00}^{\text{react}}| \,, \quad |\bar{h}_{jk}^{\text{react}}| \lesssim |\bar{h}_{00}^{\text{react}}| \,. \tag{6.38b}$$

Thus, in this gauge the radiation reaction field $\bar{h}_{\alpha\beta}$ outside but near the source has Newtonian form. Moreover, it satisfies the vacuum near-zone Einstein field equation $\delta^{jk}\bar{h}^{\text{react}}_{\alpha\beta,jk} = 0$, which is the same as the vacuum Newtonian field equation $\delta^{jk}\Phi^{\text{react}}_{,jk} = 0$; and, therefore, it extends on into the source's interior without change. In the interior this field gives rise to the radiation reaction force $-\rho\Phi^{\text{react}}_{,j}$ [Eq. (6.33c)], in accord with the discussion in Sec. 6.A.

One can think about the above derivation in the following way: The source produces the Newtonian gravitational field Φ, inside itself and in its near zone, by way of the Newtonian field equation $\delta^{jk}\Phi_{,jk} = 4\pi\rho$. This Newtonian field becomes relativistic because of retardation effects (finite speed of propagation) as it emerges from the near zone into the transition zone and then the local wave zone. As a relativistic field, it must join onto outgoing gravitational waves. This join is possible only if the near-zone and inside-source Newtonian field is accompanied by the radiation-reaction field Φ^{react}. With outgoing-wave boundary conditions the full internal field (in Newtonian approximation) is $\Phi+\Phi^{\text{react}}$. If the boundary conditions were changed to ingoing-wave the internal field would be changed to $\Phi-\Phi^{\text{react}}$.

This description, and the above derivation, take on a more elegant, sophisticated, and rigorous form if one reformulates them using the mathematics of *matched asymptotic expansions*. For details, see Burke (1970, 1971), Burke and Thorne (1970).

Historical remark: The radiation-reaction potential (6.8) was originally derived by Burke (1969) using an argument similar to the above. Having learned the idea from Burke, I included a derivation along the above lines, but in a different gauge (the "Regge-Wheeler gauge") in a paper on vibrations of stars (Thorne, 1969b). (Most people browsing my paper fail to notice that the derivation is carried out for *any* slow-motion, weak-gravity, small-stress system, not just for pulsating stars; see the first paragraph of Sec. III.a of the paper.) Shortly thereafter, Chandrasekhar and Esposito (1970) gave a correct derivation in a Lorentz-like gauge. [KIP: CHECK] Two years later, when writing Sec. 36.11 of MTW, I included a derivation in Lorentz gauge — but, to my everlasting chagrin, the variant of Lorentz gauge that I chose was

one where nonlinear terms must be taken into account in the derivation, and I stupidly ignored those terms. My error was caught and explained by Walker and Will (1980). The variant of Lorentz gauge used in the above derivation, like Regge–Wheeler gauge, has the nice property that no nonlinear terms need enter the derivation.

In this section we have focused attention on near–zone features of the gravitational field of a slow–motion source. Equations (6.24) contain, also, full information about the transition zone $r \sim \lambda$, where near–zone field is gradually transformed into wave–zone field. For a thorough discussion of the transition–zone gravitational field and how it compares and contrasts with scalar and electromagnetic transition–zone fields, and what a gravitational–wave detector would measure in the transition zone, see Finn (1985).

6.E General relativity as a nonlinear field theory in flat spacetime

Although one can analyze gravitational waves in the local wave zone of any source with good accuracy using a linearized approximation to general relativity, when analyzing the interiors of strongly gravitating sources, one must deal with nonlinearities. In this book we shall study three techniques for handling the nonlinearities. The first (this section) reformulates general relativity as a nonlinear field theory in flat spacetime and then uses flat–spacetime methods to solve, iteratively and analytically, the fully nonlinear Einstein equation. The second technique (Secs. 6.F and 6.K) splits the fully nonlinear Einstein equation into initial–value equations plus dynamical, evolution equations and then solves those equations numerically on a computer. The third technique (Sec. 6.J) linearizes around a fully nonlinear equilibrium configuration in order to treat, by a mixture of analytic and numerical methods, waves from weakly perturbed, fully nonlinear sources. All three techniques have proved valuable in computations of wave generation by sources with strong self–gravity.

The foundations for the nonlinear–field–theory–in–flat–spacetime formulation of general relativity were laid by deDonder (1921) and Lanczos (1923); and the theory has been developed to varying degrees of sophistication and completeness by a large number of researchers, including: Rosen (1940, 1963), Papapetrou (1948), Kraichnan (1955), Gupta (1957), Thirring (1961), Feynman (1963), Halpern (1963), Burlankov (1963), Ogievetsky and Polubarinov (1965), Weinberg (1965a), Deser (1970), Grishchuk, Petrov, and Popova (1984), Zel'dovich and Grishchuk (1986). In its most complete form (e.g., Grishchuk,

Grishchuk and Petrov (1987)

it is not

Petrov, and Popova, 1984 [KIP: MORE REFS?]), the theory includes all features that one might wish for any classical field theory: It has a Lagrangian and associated action; by varying the action one obtains field equations that are completely equivalent to Einstein's field equation, and one also obtains an energy–momentum tensor for the gravitational field and conservation laws that correspond to the symmetries of the flat background spacetime; it is invariant under general coordinate transformations; it also is invariant under a certain, broad, class of gauge transformations; and it also possesses a Hamiltonian formulation. In this book we shall not treat all these features of the theory; rather, we shall focus only on those features that are especially important for gravitational-wave computations.

In this section I shall present the nonlinear-field-theory-in-flat-spacetime formulation of general relativity without derivation. The derivation, were I to give one, could consist of two steps: First, a derivation (given, e.g., in Sec. 100 of Landau and Lifshitz, 1962) of an explicit expression for the Einstein field equation $G_{\mu\nu} = 8\pi T_{\mu\nu}$ in terms of the "metric density" $(-g)^{1/2} g^{\alpha\beta}$ (where g is the determinant of the covariant components of the metric, $g \equiv \det\|g_{\mu\nu}\|$); then second, a straightforward translation of that formalism into a form which is generally covariant with respect to the metric $g^{B}_{\alpha\beta}$ of a flat, background spacetime. In my presentation of the formalism, I shall indicate where, in Landau and Lifshitz (1962) (cited below as LL), and where in MTW, one finds the original, "untranslated" version of key equations.

The field-theory formalism can be understood conceptually as follows: We begin with two different spacetimes, one the *full spacetime* of general relativity which we wish to study; the other a flat, empty, *background spacetime*. We denote by $g_{\alpha\beta}$ and $g^{B}_{\alpha\beta}$ the metrics of these two spacetimes. We introduce an (initially arbitrary) one-to-one map of events $\mathcal{P}$ in the full spacetime into events $\mathcal{P}_B$ in the background spacetime. By means of this map we conceptually merge the two spacetimes to obtain a single spacetime manifold on which reside the two metrics $g^{B}_{\alpha\beta}$ and $g_{\alpha\beta}$. This is the same conceptual procedure as we used in Sec. 5.B when studying linear perturbations of a curved spacetime. However, here the background is flat while in Sec. 5.B it was curved; and here we shall compute the difference between the full and background metrics with complete, nonlinear precision while in Sec. 5.B we studied that difference only in a linear approximation.

The field theory formalism, by itself, is unaware of the curved-spacetime metric $g_{\alpha\beta}$. Only after fully analyzing an astrophysical

system with that formalism does one compute $g_{\alpha\beta}$, and also the curved-spacetime stress-energy tensor $T_{\alpha\beta}$. Correspondingly, all quantities that appear in the formalism (e.g. the fields $\bar{h}^{\alpha\beta}$, $t_{\alpha\beta}$, and $H^{\mu\alpha\nu\beta}$ defined below) are flat-spacetime tensors, with indices raised and lowered using the flat-spacetime metric $g^{\rm B}_{\alpha\beta}$.

As a tool in our analysis we introduce a scalar field ψ defined by

$$\psi \equiv \left(\frac{\det\|g^{\rm B}_{\alpha\beta}\|}{\det\|g^{\alpha\beta}\|}\right)^{1/2} = \left(\frac{\det\|g_{\alpha\beta}\|}{\det\|g^{\rm B}_{\alpha\beta}\|}\right)^{1/2} . \tag{6.39}$$

It is straightforward to show that, although neither the numerator nor the denominator of each of these expressions is a scalar field (because it is different in different coordinate systems), the ratio ψ of numerator to denominator is a scalar field. In a global Lorentz coordinate system of the flat background metric, ψ reduces to $\sqrt{-g} \equiv (-\det\|g_{\alpha\beta}\|)^{1/2}$.

As a second tool in our analysis we introduce a symmetric tensor field $\bar{h}^{\alpha\beta}$:

$$\bar{h}^{\alpha\beta} \equiv g^{\rm B}_{\alpha\beta} - \psi g^{\alpha\beta} . \tag{6.40}$$

We shall call this field the *gravitational field* of our formalism and shall regard it as the "unknown" in the Einstein equation. In keeping with our field theory's ignorance of the curved-spacetime metric, this gravitational field will be treated as residing in the flat spacetime. It is a tensor field in that flat spacetime; and, accordingly, its indices are lowered and raised with the flat background metric $g^{\rm B}_{\alpha\beta}$. Our goal will be to develop flat-spacetime field-theory techniques for solving the Einstein field equation for $\bar{h}^{\alpha\beta}$, and then from that solution to construct the full spacetime metric.

Suppose that we have solved for the gravitational field $\bar{h}^{\alpha\beta}$ via field-theory techniques. How, from it, do we construct the full spacetime metric? The first step is to construct the scalar field ψ using the relation [which follows from Eqs. (6.39) and (6.40)]

$$\psi = \left(\frac{\det\|g^{\rm B}_{\alpha\beta} - \bar{h}^{\alpha\beta}\|}{\det\|g^{\rm B}_{\alpha\beta}\|}\right)^{1/2} = 1 - \bar{h} + \tfrac{1}{2}[(\bar{h})^2 - \bar{h}^{\alpha\beta}\bar{h}_{\alpha\beta}] + O_3 . \tag{6.41a}$$

Here $\bar{h} \equiv \bar{h}^{\alpha\beta} g^{\rm B}_{\alpha\beta}$ is the trace of $\bar{h}^{\alpha\beta}$, and O_3 means terms cubic in $\bar{h}^{\alpha\beta}$. The next step is to construct the contravariant components of the full metric using

$$g^{\alpha\beta} = \frac{g^{\rm B}_{\alpha\beta} - \bar{h}^{\alpha\beta}}{\psi}$$

$$= g^{\alpha\beta} - (\bar{h}^{\alpha\beta} - \tfrac{1}{2}\bar{h} g^{\alpha\beta}) - \tfrac{1}{2}\bar{h}\bar{h}^{\alpha\beta} + \tfrac{1}{8} g^{\alpha\beta}[(\bar{h})^2 + 2\bar{h}^{\mu\nu}\bar{h}_{\mu\nu}] + O_3 , \qquad (6.41b)$$

which follows from Eqs. (6.40) and (6.41a). The final step is to construct the covariant components of the full metric, which are the matrix inverse of the contravariant components:

$$\| g_{\alpha\beta} \| = \| g^{\alpha\beta} \|^{-1} ; \qquad (6.41c)$$

i.e.

$$g_{\alpha\beta} = g^{B}_{\alpha\beta} + \bar{h}_{\alpha\beta} - \tfrac{1}{2}\bar{h} g^{B}_{\alpha\beta} + \bar{h}_{\alpha\mu}\bar{h}^{\mu}{}_{\beta} - \tfrac{1}{2}\bar{h}\bar{h}_{\alpha\beta} + \tfrac{1}{8}[(\bar{h})^2 - 2\bar{h}^{\mu\nu}\bar{h}_{\mu\nu}] g^{B}_{\alpha\beta} + O_3 . \qquad (6.41c')$$

From the exact expressions in Eqs. (6.41) one can construct power series expansions in $\bar{h}^{\alpha\beta}$ to as high an order as one wishes. The linear and quadratic terms in those expansions are shown in Eqs (6.41).

Notice that at linear order the covariant metric perturbation $g_{\alpha\beta} - g^{B}_{\alpha\beta}$ is the trace reversal of $\bar{h}_{\alpha\beta}$. Equivalently, $\bar{h}_{\alpha\beta}$ at linear order is the trace-reversed metric perturbation. This shows that *the gravitational field $\bar{h}_{\alpha\beta}$ of the present formalism is a generalization, to full, nonlinear general relativity, of the linearized, trace-reversed metric perturbation.*

The Einstein field equation is most easily formulated in terms of $\bar{h}^{\alpha\beta}$ with the aid of the fourth-rank tensor field

$$H^{\mu\alpha\nu\beta} \equiv (g^{\mu\nu} - \bar{h}^{\mu\nu})(g^{\alpha\beta} - \bar{h}^{\alpha\beta}) - (g^{\alpha\nu} - \bar{h}^{\alpha\nu})(g^{\mu\beta} - \bar{h}^{\mu\beta}) \qquad (6.42a)$$

and the second-rank tensor field

$$t^{\alpha\beta} \equiv \frac{1}{16\pi\psi^2}\Big[\bar{h}^{\alpha\beta}{}_{|\lambda}\bar{h}^{\lambda\mu}{}_{|\mu} - \bar{h}^{\alpha\lambda}{}_{|\lambda}\bar{h}^{\beta\mu}{}_{|\mu} + \tfrac{1}{2} g^{\alpha\beta} g_{\lambda\mu}\bar{h}^{\lambda\nu}{}_{|\rho}\bar{h}^{\rho\mu}{}_{|\nu}$$

$$- (g^{\alpha\lambda} g_{\mu\nu}\bar{h}^{\beta\nu}{}_{|\rho}\bar{h}^{\mu\rho}{}_{|\lambda} + g^{\beta\lambda} g_{\mu\nu}\bar{h}^{\alpha\nu}{}_{|\rho}\bar{h}^{\mu\rho}{}_{|\lambda} + g_{\lambda\mu} g^{\nu\rho}\bar{h}^{\alpha\lambda}{}_{|\nu}\bar{h}^{\beta\mu}{}_{|\rho}$$

$$+ \tfrac{1}{8}(2g^{\alpha\lambda} g^{\beta\mu} - g^{\alpha\beta} g^{\lambda\rho})(2g_{\nu\rho} g_{\sigma\tau} - g_{\rho\sigma} g_{\nu\tau})\bar{h}^{\nu\tau}{}_{|\lambda}\bar{h}^{\rho\sigma}{}_{|\mu}\Big] . \qquad (6.42b)$$

Here, as earlier, the vertical slashes mean covariant derivatives with respect to the (flat) background metric. In a global Lorentz coordinate system of the background metric these vertical slashes reduce to partial derivatives (commas), and Eq. (6.42b) reduces to Eq. (100.7) of LL (Landau and Lifshitz, 1962) and to Eq. (20.22) of MTW. Similarly, Eq. (6.42a) reduces to an integral of Eq. (100.2) of LL and to Eq. (20.20) of MTW. The quantity $H^{\mu\alpha\nu\beta}$ is sometimes called a *superpotential* because of the role that it plays in the Einstein field equation, below. The

quantity $t^{\alpha\beta}$ is sometimes called the *Landau-Lifshitz energy-momentum complex* and sometimes (for historical reasons) the *Landau-Lifshitz pseudotensor*. In actuality, both $H^{\mu\alpha\nu\beta}$ and $t^{\alpha\beta}$, like $\bar{h}^{\alpha\beta}$, are true tensors in the background spacetime; but also like $\bar{h}^{\alpha\beta}$ depend on our choice of map between the background spacetime and the full spacetime; i.e. they are "gauge-dependent".

Thus far, the formalism seems horrendously arbitrary. However, it has been carefully crafted to produce powerful forms of the Einstein field equation $G_{\alpha\beta} = 8\pi T_{\alpha\beta}$ and the equation of motion $T^{\alpha\beta}{}_{;\beta} = 0$. The form of the field equation is the following [Eq. (100.4) of LL and Eq. (20.21) of MTW]:

$$H^{\alpha\mu\beta\nu}{}_{|\mu\nu} = 16\pi\psi^2(T^{\alpha\beta}+t^{\alpha\beta}) . \tag{6.43}$$

Notice that, whereas the left-hand side of (6.43) involves double derivatives of the gravitational field, the right-hand side involves (through ψ^2 and $t^{\alpha\beta}$) only products of single derivatives. By virtue of the antisymmetry of $H^{\alpha\mu\beta\nu}$ on its first pair of indices and also on its second pair, and the vanishing curvature of the background (which implies that background covariant derivatives commute), the divergence of the left-hand side of (6.43) is identically zero. Correspondingly, the right-hand side must have vanishing divergence:

$$[\psi^2(T^{\alpha\beta}+t^{\alpha\beta})]_{|\beta} = 0 \tag{6.44}$$

[Eq. (100.8) of LL and Eq. (20.23a,b) of MTW]. This is the equation of motion $T^{\alpha\beta}{}_{;\beta} = 0$, rewritten in the notation of field theory in flat spacetime.

The Einstein field equation (6.43) takes on an especially simple form when one specializes the gauge. Here, as in Sec. 5.B and elsewhere in this book, by *gauge* we mean the choice of which events $\mathcal{P}_B$ in the background spacetime correspond to which events $\mathcal{P}$ in the full spacetime. (For the mathematical structure of the "gauge transformations" which change the mapping of points $\mathcal{P}_B$ into points $\mathcal{P}$, see, e.g., Grishchuk, Petrov, and Popova, 1984.) [KIP: CHECK; MAYBE CITE GRISHCHUK AND ZEL'DOVICH, 1986?] Because the spacetimes have four dimensions, by special adjustments of the gauge we can impose four constraints on the gravitational field $\bar{h}^{\alpha\beta}$. As in our linearized analysis, so also here, we shall adjust the gauge so that

$$\bar{h}^{\alpha\beta}{}_{|\beta} = 0 . \tag{6.45}$$

In the linearized analysis this gauge was called Lorentz, by analogy with

the corresponding gauge of electromagnetic theory. In this fully nonlinear analysis *this gauge is variously called Lorentz, deDonder, Lanczos, and harmonic*. The names deDonder and Lanczos are in recognition of the fact that deDonder (1921) and Lanczos (1923) were the first to introduce this gauge in the nonlinear context. The name harmonic recognizes the fact that this gauge brings the Einstein field equations (6.43) into a form whose only second derivatives are those of a wave operator:

$$(g^{\mu\nu}-\bar{h}^{\mu\nu})\bar{h}^{\alpha\beta}{}_{|\mu\nu} = -16\pi\psi^2(T^{\alpha\beta}+t^{\alpha\beta}) + \bar{h}^{\alpha\mu}{}_{|\nu}\bar{h}^{\beta\nu}{}_{|\mu} . \qquad (6.46)$$

This form of the Einstein equations is nicely suited both to approximate solutions of the Einstein equations and to proofs of fundamental theorems about relativistic gravity.

A straightforward example of an approximate solution based on Eq. (6.46) is the following *post-linear (or post-post-Minkowski) formalism for computing wave generation*: Consider a source of gravitational waves whose internal gravity is sufficiently strong that linearized theory is a poor approximation, but weak enough to be well approximated by the first few terms of a power-series expansion in the strength ε of the gravitational field (i.e. in the magnitude ε that the largest components of $\bar{h}^{\alpha\beta}$ have in Lorentz coordinates of the background spacetime). For this system we can construct a succession of ever more accurate approximations to the gravitational field and the stress-energy tensor as follows: The first, linear approximation, denoted $\bar{h}_1^{\alpha\beta}$ and $T_1^{\alpha\beta}$, satisfies the linearized versions of the field equation (6.46), the harmonic gauge condition (6.45), and the equation of motion (6.44):

$$g^{\mu\nu}\bar{h}_1^{\alpha\beta}{}_{|\mu\nu} = -16\pi T_1^{\alpha\beta} , \quad \bar{h}_1^{\alpha\beta}{}_{|\beta} = 0 , \quad T_1^{\alpha\beta}{}_{|\beta} = 0 . \qquad (6.47a)$$

Having solved these equations for $\bar{h}_1^{\alpha\beta}$ and $T_1^{\alpha\beta}$, one is ready to compute an improved gravitational field and stress-energy tensor $\bar{h}_2^{\alpha\beta}$ and $T_2^{\alpha\beta}$ with accuracies of one order higher in ε. These *post-linear approximations* (also called *post-post-Minkowski approximations*) are governed by the following quadratic-order-accurate versions of Eqs. (6.44)-(6.46):

$$(g^{\mu\nu}-\bar{h}_1^{\mu\nu})\bar{h}_2^{\alpha\beta}{}_{|\mu\nu} = -16\pi(T_2^{\alpha\beta}+t_2^{\alpha\beta}) + \bar{h}_1^{\alpha\mu}{}_{|\nu}\bar{h}_1^{\beta\nu}{}_{|\mu} ,$$

$$\bar{h}_2^{\alpha\beta}{}_{|\beta} = 0 , \quad T_2^{\alpha\beta} = (\bar{h}_1 T_1^{\alpha\beta} - t_2^{\alpha\beta})_{|\beta} . \qquad (6.47b)$$

Here $t_2^{\alpha\beta}$ is the quadratic-order approximation to expression (6.42b), constructed from $\bar{h}_1^{\alpha\beta}$:

$$t_2^{\alpha\beta} \equiv \frac{1}{16\pi}\Big[\bar{h}_1^{\alpha\beta}{}_{|\lambda}\bar{h}_1^{\lambda\mu}{}_{|\mu} - \bar{h}_1^{\alpha\lambda}{}_{|\lambda}\bar{h}_1^{\beta\mu}{}_{|\mu} + \tfrac{1}{2}g_B^{\alpha\beta}g^B_{\lambda\mu}\bar{h}_1^{\lambda\nu}{}_{|\rho}\bar{h}_1^{\rho\mu}{}_{|\nu}$$

$$- (g_B^{\alpha\lambda}g^B_{\mu\nu}\bar{h}_1^{\beta\nu}{}_{|\rho}\bar{h}_1^{\mu\rho}{}_{|\lambda} + g_B^{\beta\lambda}g^B_{\mu\nu}\bar{h}_1^{\alpha\nu}{}_{|\rho}\bar{h}_1^{\mu\rho}{}_{|\lambda} + g^B_{\lambda\mu}g_B^{\nu\rho}\bar{h}_1^{\alpha\lambda}{}_{|\nu}\bar{h}_1^{\beta\mu}{}_{|\rho}$$

$$+ \tfrac{1}{8}(2g_B^{\alpha\lambda}g_B^{\beta\mu} - g_B^{\alpha\beta}g_B^{\lambda\rho})(2g^B_{\nu\rho}g^B_{\sigma\tau} - g^B_{\rho\sigma}g^B_{\nu\tau})\bar{h}_1^{\nu\tau}{}_{|\lambda}\bar{h}_1^{\rho\sigma}{}_{|\mu}\Big]. \qquad (6.47c)$$

These equations, being linear in $\bar{h}_2^{\alpha\beta}$ and $T_2^{\alpha\beta}$, can be solved analytically. One can go on, in a similar manner, to construct linear equations for the post-post-linear fields $\bar{h}_3^{\alpha\beta}$ and $T_3^{\alpha\beta}$ in terms of nonlinear combinations of lower-order fields. If, instead, one truncates at second order and uses $h_{jk}^{\rm GW} = (\bar{h}_{2jk})^{\rm TT}$ in the local wave zone as one's estimate of the gravitational waves emitted by the source, one obtains the so-called "post-linear" (or "post-post-Minkowski") formalism for gravitational-wave generation (Thorne and Kovacs, 1975; Crowley and Thorne, 1977). For a concrete calculation with this formalism (evaluation of the gravitational-wave field emitted when two stars fly past each other at high velocity, i.e. "gravitational bremsstrahlung radiation") see Kovacs and Thorne, 1977, 1978).

One aspect of the post-linear formalism deserves special mention: The left-hand side of the field equation (6.47b) for $\bar{h}_2^{\alpha\beta}$ is written with a wave operator $\Box_1$ appropriate to a curved spacetime: $\Box_1\bar{h}_2^{\alpha\beta} \equiv (g_B^{\mu\nu} - \bar{h}_1^{\mu\nu})\bar{h}_2^{\alpha\beta}{}_{|\mu\nu}$. We could equally well have written the term $-\bar{h}_1^{\mu\nu}\bar{h}_2^{\alpha\beta}{}_{|\mu\nu}$ as $-\bar{h}_1^{\mu\nu}\bar{h}_1^{\alpha\beta}{}_{|\mu\nu}$ and moved it onto the right-hand side as part of the source, thereby converting over to the flat-spacetime wave operator on the left, $\Box_B\bar{h}_2^{\alpha\beta} \equiv g_B^{\mu\nu}\bar{h}_2^{\alpha\beta}{}_{|\mu\nu}$. This altered form of the field equation, with $\Box_B$, would be much easier to solve than the original form with $\Box_1$. However, the altered form is more dangerous: It causes the field $\bar{h}_2^{\alpha\beta}$ to propagate on characteristics of flat spacetime, whereas the form (6.47b) with $\Box_1$ causes propagation on characteristics of the first-order curved spacetime. Because the flat characteristics are farther from the truth than the first-order curved ones, they are in greater danger of causing bits of field from different parts of the source to slip by a quarter wavelength or more relative to each other. Such slippage can produce serious errors in the computed waves. In fact, such slippage is sometimes the most serious source of error in gravitational-wave calculations. For this reason, wave-generation formalisms often use curved-spacetime wave operators such as $\Box_1$ rather than flat-spacetime wave operators $\Box_B$. The price paid is the necessity to use a curved-spacetime Green's function to solve the wave equation. Such a Green's function, accurate to first order in

perturbations away from flat spacetime, has been derived by DeWitt and DeWitt (1964) and in an alternative form by Thorne and Kovacs (1975). Crowley and Thorne (1977) exhibit the relationship between these two forms and discuss their relative merits. This Green's function is used, for example, in the post-linear wave-generation formalism of Thorne and Kovacs (1975), Crowley and Thorne (1977), and Kovacs and Thorne (1977, 1978). For the Green's function of the wave operator in a strongly curved spacetime see DeWitt and Brehme (1960). We shall return to the post-linear wave-generation formalism in Sec. 6.H.

Not only is the field-theory-in-flat-spacetime formalism powerful for deriving approximate solutions of the Einstein equation, it is also powerful for proving general theorems. As an example, we shall use it to prove that when a source emits gravitational waves, its total energy, momentum, and angular momentum decrease at the same rate as the waves carry these quantities away; i.e. we shall prove the conservation of the total (source plus waves) energy, momentum, and angular momentum. The same proof, applied to a gravitational-wave detector, shows that when a detector absorbs energy from a wave, the wave's energy goes down by just the amount absorbed.

For the emission problem, the source's total energy (including rest mass, internal kinetic energy, gravitational binding energy, and all other forms of energy), by definition, is the mass monopole moment M of its external field [Eq. (6.24a)]. The source's total momentum P_i, by definition, is the time derivative of the external field's mass dipole moment (which we have set to zero in Eqs. (6.24) by going to the source's center-of-mass frame). The total angular momentum J_i, by definition, is the current dipole moment of the external field (6.24b). The motivation for these definitions is discussed at length in Chap. 19 of MTW. The total energy M and momentum P_i make up a 4-vector P^α which resides in the source's asymptotic rest frame. The integral

$$P^\alpha = \frac{1}{16\pi}\oint H^{\alpha\mu 0j}{}_{|\mu} d^2S_j . \tag{6.48}$$

over a closed 2-surface in the asymptotic rest frame (e.g. a sphere of constant r and t) plucks that 4-momentum out of the external field (which appears in $H^{\alpha\mu 0j}$) and discards everything else; see Chap. 20 of MTW. The time derivative of this surface integral is the rate of change of the source's 4-momentum:

$$\frac{dP^\alpha}{dt} = \frac{1}{16\pi}\oint H^{\alpha\mu 0j}{}_{|\mu 0} d^2S_j = \frac{1}{16\pi}\oint (H^{\alpha\mu\nu j}{}_{|\mu\nu} - H^{\alpha\mu ij}{}_{|\mu i}) d^2S_j . \tag{6.49}$$

In terms of the 3-vector field $V_k \equiv \frac{1}{2}\varepsilon_{jk\ell}H^{a\mu\ell j}{}_{|\mu}$, the integral of the last term can be rewritten as

$$\oint \nabla\times\mathbf{V}\cdot d^2\mathbf{S}\,,$$

which vanishes by Stokes' theorem in the flat, 3-dimensional background space. The remaining first term in (6.49) can be rewritten using the vacuum Einstein equations (6.43) as

$$\frac{dP^a}{dt} = -\oint \psi^2 t^{aj} d^2S_j\,. \tag{6.50}$$

If we now average over several periods of oscillation of the source, we convert this into

$$\langle\frac{dP^a}{dt}\rangle = -\oint\langle\psi^2 t^{aj}\rangle d^2S_j\,.$$

Since the field is weak in the local wave zone, $|\bar{h}^{\alpha\beta}| \ll 1$, we can evaluate $\psi^2 t^{aj}$ using its leading, quadratic-order piece $t_{\mathcal{L}}^{\alpha\beta}$:

$$\langle\frac{dP^a}{dt}\rangle = -\oint\langle t_{\mathcal{L}}^{aj}\rangle d^2S_j\,. \tag{6.51}$$

A straightforward but tedious calculation shows that the average of $t_{\mathcal{L}}^{\alpha\beta}$ over several cycles of oscillation is equal to the gravitational-wave stress-energy tensor (5.37):

$$\langle t_{\mathcal{L}}^{\alpha\beta}\rangle = T^{\mathrm{GW}}_{\alpha\beta}\,, \tag{6.52}$$

and correspondingly that the source's 4-momentum decreases at the same rate, Eq. (6.26a,b), as the waves carry off 4-momentum:

$$\langle\frac{dP^a}{dt}\rangle = -\oint T^{\mathrm{GW}}_{aj} d^2S^j = -\frac{dP^{\mathrm{GW}}_a}{dt}\,. \tag{6.53}$$

An analogous calculation for angular momentum begins with the surface integral [MTW Chap. 20]

$$J_j = \frac{1}{16\pi}\oint \varepsilon_{jpq}(x^p H^{q a 0 i}{}_{|a} + H^{pi0q})d^2S_i \tag{6.54}$$

for the source's angular momentum; here x^p is the vector in the background flat space reaching from the source's center of mass to the point of integration. By taking the time derivative of this expression, applying Stokes' theorem and the Einstein field equation (6.43), using the leading, quadratic approximation to $t^{\alpha\beta}$, and averaging over a few

cycles of oscillation of the source, one obtains for the rate of change of the source's angular momentum

$$\langle \frac{dJ_j}{dt} \rangle = -\oint \varepsilon_{jpq} x^p \langle t^{qi} \rangle d^2 S_i \ . \qquad (6.55)$$

By performing the average of expression (6.47c) with care to keep those terms of order $1/r^3$ that will contribute to the surface integral (6.55), and by expressing the answer in terms of the local-wave-zone gravitational-wave field $h_{jk}^{GW} = (\bar{h}_{1\,jk})^{TT}$, one obtains the DeWitt (1971) formula

$$\langle \frac{dJ_j}{dt} \rangle = -\frac{1}{16\pi} \int \varepsilon_{jpq} x^p \langle (h_{qa}^{GW} h_{ab,t}^{GW})_{,b} - \tfrac{1}{2} h_{ab,q}^{GW} h_{ab,t}^{GW} \rangle r^2 d\Omega = -\frac{dJ_j^{GW}}{dt} \ ; \quad (6.56)$$

cf. Eq. (6.26c). Thus, the source loses angular momentum at the same rate as the waves carry it off.

The above two analyses (post-linear wave generation, and conservation laws for radiating sources) are just two among many important applications of the nonlinear-field-theory-in-flat-spacetime formulation of general relativity. In Sec. 6.G we shall meet several additional methods of computing wave generation that are based on this formalism. Some other applications of it are these: (i) It underlies analyses of the full nonlinear structure of gravitational waves propagating outward from an isolated source in asymptotically flat spacetime (Blanchet and Damour, 1986, 1988a,b; Blanchet, 1987a; Damour, 1986, 1987a). (ii) It underlies derivations of high-accuracy equations of motion for binary systems in general relativity (e.g. Damour, 1983 and 1987b), including the equations of motion now used to analyze the orbit of the binary pulsar. (iii) It underlies derivations of equations of motion and precession for black holes (e.g. Thorne and Hartle, 1985). (iv) It underlies a proof that the classical Euler equations for the precession of a rigid, nongravitating body are valid without change if the body has arbitrarily strong self-gravity and rotates slowly and rigidly (Thorne and Gürsel, 1983). (v) It underlies the post-Newtonian approximation to general relativity (Einstein, Infeld, and Hoffman, 1938; Fock, 1959; Chandrasekhar, 1965; Chandrasekhar and Nutku, 1969; Chandrasekhar and Esposito, 1970). (vi) It underlies the ephemeris which the Caltech Jet Propulsion Laboratory uses in high-accuracy tracking of spacecraft and the planets (XXXX). (vii) It underlies theoretical frameworks for interpreting tests of general relativity (Nordtvedt, 1968; Will, 1981). (viii) It underlies derivations of general

relativity that begin with canonical field theory for spin-two gravitons and iterate until the theory becomes fully self-consistent (e.g. Feynman, 1963b; Weinberg, 1965a; Deser, 1970). (ix) It underlies perturbation-theory (Feynman-diagram) approaches to the quantization of gravity (e.g. Feynman, 1963 and DeWitt, 1967a,b).

Occasionally this nonlinear field theory is reinvented and is asserted to be a new theory of gravity, different from general relativity (e.g. Logunov and Vlasov, 1984; Vlasov, Logunov, and Mestvirishvili, 1984; Logunov, Loskutov, and Mestvirishvili, 1988; Pei-Yuan, XXXX). However, because this nonlinear field theory is mathematically equivalent to general relativity, the only way it can give different predictions for experiment is if one changes the physical interpretation of the mathematics. The obvious change is to assert that some forms of physical apparatus measure proper times or proper distances of the background metric $g^{B}_{\alpha\beta}$ rather than those of the full metric $g_{\alpha\beta}$. Such an assertion, however, leads to severe contradictions with experiment. If, instead, one retains the standard rule that all physical apparatus measures proper distances of the full metric $g_{\alpha\beta}$, one is dealing unequivocally with the general theory of relativity. For further discussion, see Zel'dovich and Grishchuk (1986, 1988). For an elegant reformulation of general relativity as a nonlinear field theory on an arbitrary, possibly curved background $g^{B}_{\alpha\beta}$, see Grishchuk, Petrov, and Popova (1984).

Some researchers have argued that the Landau-Lifshitz complex $t^{\alpha\beta}$ should be regarded as a full-fledged stress-energy tensor for the gravitational field, on an equal footing with the stress-energy tensors of other fundamental fields. Such a proposal has little merit: $t^{\alpha\beta}$ does not exist until one introduces the flat background spacetime, and it depends crucially on the chosen map between the flat background and the full spacetime, i.e. on the chosen gauge. The background has no physical reality, since (according to general relativity) physical apparatus measures the full spacetime metric, not the background; and, correspondingly, $t^{\alpha\beta}$ cannot have physical reality. Moreoever, the gauge is arbitrary, and correspondingly the value of $t^{\alpha\beta}$ at any event in the full spacetime is arbitrary. Even if one insists that the gauge be fixed as harmonic, there remains additional gauge arbitrariness [e.g., that involved in the linearized gauge transformations (6.21)], and correspondingly $t^{\alpha\beta}$ retains much arbitrariness.

Nevertheless, $t^{\alpha\beta}$ is a powerful mathematical tool: it is central to the proofs of a number of important theorems (see the references cited

above). More generally, despite the background spacetime's lack of physical reality and despite the failure of $t^{\alpha\beta}$ to be a full-fledged stress-energy tensor for the gravitational field, the field-theory formulation of general relativity is a powerful tool for gravitation research.

6.F 3+1 Formulation of general relativity

As nice as nonlinear field theory in flat spacetime is for analytical calculations, it is not well suited to numerical solutions of the Einstein field equations. The reason is that it contains no provision for carefully adjusting the coordinate system, at each point in a numerical calculation, so as to avoid pitfalls that make the calculation prematurely grind to a halt. Examples of such pitfalls are the creation of a coordinate singularity; and integrating one's way, in some regions of spacetime, into a physical singularity (e.g. at the center of a black hole), thereby forcing the calculation to stop before other regions of spacetime (e.g. the waves in the local wave zone) have been explored.

The formulation of general relativity which gives one the fullest and clearest, step-by-step control over the coordinate system is Arnowitt, Deser, and Misner's (1962) 3+1 *formulation*, as adapted to numerical relativity by Smarr and York (1978). This section is a brief introduction to the 3+1 formulation. For more detailed presentations see, e.g., Chap. 21 of MTW, and York (1979, 1983).

The geometric foundation for the 3+1 formulation is shown in Fig. 6.2. One slices spacetime with a foliation of three-dimensional, spacelike hypersurfaces, one and introduces a time coordinate t which is constant on each hypersurface. Special observers (called *fiducial observers* or FIDOs) move along the world lines orthogonal to the chosen hypersurfaces. The 4-velocity of a FIDO is denoted N, and his proper time is denoted τ. The ratio $d\tau/dt$ of the FIDO proper time lapse $d\tau$ to the coordinate time lapse dt, in going from one hypersurface to the next, is denoted α and is called the *lapse function*. Correspondingly, the vector that reaches orthogonally from one hypersurface to the next is $N\Delta\tau = \alpha N\Delta t$ (Fig. 6.2). On an initial hypersurface, $t = t_o$, the FIDOs set up a spatial coordinate system x^i; and then, instead of carrying the coordinate grid with themselves along their own world lines, they force the grid to shift by an amount $\beta^i\Delta t$ in going from the hypersurface t to the hypersurface $t+\Delta t$; see Fig. 6.2. The quantity β^i, called the *shift*, is a 3-vector which lives in the hypersurface of constant t. These definitions guarantee that the spacetime metric, in the coordinate system

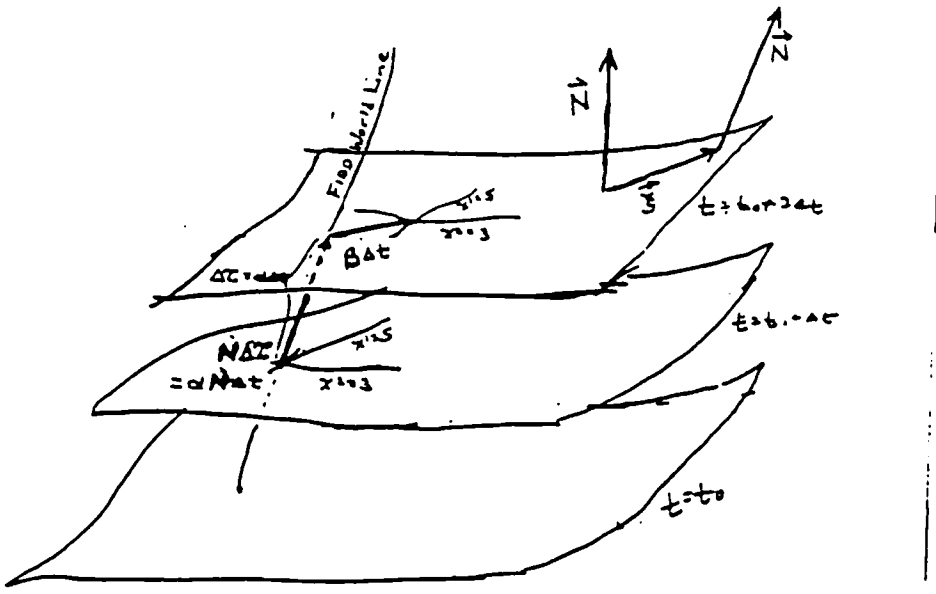

Fig. 6.2 The slicing and coordinates that underlie the 3+1 formulation of general relativity.

(t, x^i), takes the form

$$ds^2 = -\alpha^2 dt^2 + \gamma_{ij}(dx^i + \beta^i dt)(dx^j + \beta^j dt)\,, \qquad (6.57)$$

where γ_{ij} is the 3-*metric* of the 3-dimensional hypersurfaces t = const.

The 3+1 formalism gets its name from its split of spacetime into three-dimensional space (the hypersurfaces of constant time t) plus one-dimensional time t. This split is followed rigorously: Instead of expressing the equations of physics in covariant, 4-dimensional spacetime language, the formalism expresses all laws and equations in covariant, 3-dimensional, spatial language – i.e., in terms of scalars, spatial 3-vectors, and spatial 3-tensors that reside in the hypersurfaces t = const. Some people find it helpful to mentally collapse all these hypersurfaces into a single 3-dimensional space and think of that space as a generalization of the *absolute space* of Newtonian physics, and to regard t as the generalization of Newtonian *universal time*. If one takes such an approach, however, one should always keep in mind that the geometry of absolute space, as embodied in its 3-metric γ_{ij}, is curved, not flat, and evolves in time; and also that, by making different choices of spacetime slicing (corresponding to different choices of the lapse function α, see below), one changes the details of absolute space. Thus, the space is far less absolute than in Newtonian physics!

Because the hypersurfaces of constant time t are orthogonal, in a spacetime sense, to the world lines of the FIDOs, the FIDOs regard them as hypersurfaces of physical simultaneity. More specifically, if a FIDO uses Einstein's synchronization-by-means-of-light-rays technique to determine which events near his world line are simultaneous, he will discover that the nearby simultaneous events all lie in the same hypersurface $t = \text{const}$. (This is true despite the fact that different FIDOs at different locations on the same hypersurface see different lapses of proper time $\Delta\tau = \alpha\Delta t$ between the same adjacent hypersurfaces.) Thus, the 3-vectors and 3-tensors of the 3+1 formalism represent quantities which a FIDO would recognize, physically, as purely spatial objects.

Just as the 3+1 formalism splits the 4-dimensional spacetime metric $g_{\alpha\beta}$ into a 3-metric γ_{jk} plus the 3-vector shift β^i plus the scalar lapse α, so the formalism also splits the 4-dimensional stress-energy tensor $T^{\alpha\beta}$ into 3-dimensional quantities: The FIDO-measured energy density ρ, momentum density J^i, and spatial stress S^{ij}:

$$\rho = T_{\mu\nu}N^\mu N^\nu = \alpha^2 T^{tt} , \quad J_i = T_{i\mu}N^\mu = \alpha T_i{}^t , \quad S_{ij} = T_{ij} . \qquad (6.58)$$

Here the expressions in terms of components of the stress-energy tensor are written in the coordinate system (t, x^i). (In deriving these expressions it is helpful to note that the basis vectors $\partial/\partial x^i$ lie in the hypersurfaces of constant t, and the FIDO 4-velocity N has components $N_t = -\alpha$, $N_i = 0$ and $N^t = \alpha^{-1}$, $N^i = -\alpha^{-1}\beta^i$.)

In formulating the 3+1 version of the Einstein field equation it will be helpful to use the *extrinsic curvature* K_{ij} of the hypersurfaces $t = \text{const}$. This extrinsic curvature measures the way in which each hypersurface is embedded in spacetime; i.e. it measures the manner in which the hypersurface's normals N at adjacent points deviate from being parallel. Expressed in 4-dimensional language, K_{ij} is the spatial part of the 4-dimensional gradient (defined, of course, with respect to parallel transport in 4-dimensional spacetime) of N:

$$K_{ij} = -N_{i;j} = -\alpha {}^{(4)}\Gamma^t{}_{ij} . \qquad (6.59)$$

Here the quantity in the second expression is the 4-dimensional connection coefficient for our coordinate system, and because that connection coefficient is symmetric in its indices ij, the 3-tensor K_{ij} is symmetric. Note that, if ξ^j is a vector lying in the hypersurface $t = \text{const}$, then $N_{i;j}\xi^i\xi^j = -K_{ij}\xi^i\xi^j$ is the difference (distance between tips of normals N at the two ends of ξ) – (distance between tails of those

same normals); see Fig. 6.2.

In the 3+1 formalism one uses the lapse function α to control the slicing of spacetime: By choosing α a little larger here and a little smaller there, one pushes one's hypersurfaces forward in spacetime a little more here and a little less there. If one is clever, one thereby can assure, for example, that the forward march of the hypersurfaces is slowed inside a black hole, preventing them from hitting the singularity there, while it is speeded up in the local wave zone so as to explore there the full details of the emitted waves. Similarly, one can use the shift function β^i to control the spatial coordinates. For example, by careful adjustment of β^i one can prevent the spatial coordinate grid from collapsing to zero thickness in one direction while stretching in other directions.

With the lapse and shift reserved for the control of the slicing and the spatial coordinates, one characterizes gravity by the 3-metric γ_{ij} and extrinsic curvature K_{ij}; and one describes the stress-energy which generates gravity by the FIDO-measured energy density ρ, momentum density J_i, and stress S_{ij}. The stress is determined from ρ and J_i by *equations of state* for the matter or fields that are generating the gravity:

$$S_{ij} = f_{ij}(\rho, J_a) . \tag{6.60}$$

The evolution of the remaining quantities, γ_{ij}, K_{ij}, ρ, and J_i is governed by 3+1 versions of the Einstein field equation $G_{\alpha\beta} = 8\pi T_{\alpha\beta}$ and of the equation of motion $T^{\alpha\beta}{}_{;\beta} = 0$.

The 3+1 Einstein field equation breaks up into two sets of equations: *initial-value equations* (also called *constraint equations*) which constrain the choices, on some initial hypersurface (at some initial time $t = t_0$), of γ_{ij}, K_{ij}, ρ, and J_i; and *dynamical equations* which evolve the gravitational field forward from the initial hypersurface.

The first of the initial value equations, $G_{\mu\nu}N^\mu N^\nu = 8\pi T_{\mu\nu}N^\mu N^\nu = 8\pi\rho$, written in 3+1 notation, says

$$^{(3)}R + (K^i{}_i)^2 - K_{ij}K^{ij} = 16\pi\rho , \tag{6.61a}$$

where $^{(3)}R$ is the 3-dimensional scalar curvature of the hypersurface, i.e. the scalar curvature computed from the 3-metric γ_{ij}. This is sometimes called the *Hamiltonian constraint* because of its role in the "canonical (Hamiltonian) formulation" of general relativity; see, e.g., XXXXX. The remaining initial-value equation, $G_{i\mu}N^\mu = 8\pi T_{i\mu}N^\mu = 8\pi J_i$, says in 3+1 notation

$$K_i{}^j{}_{|j} - K_j{}^j{}_{|i} = 8\pi J_i \ , \qquad (6.61b)$$

where the vertical bar denotes a 3-dimensional covariant derivative in the 3-dimensional hypersurface (i.e. with 3-dimensional connection coefficients computed from the spatial metric γ_{ij}).

In practice, the first step in a numerical solution of the 3+1 Einstein equations is to solve these constraint equations (6.61) to get "initial data" γ_{ij}, K_{ij}, ρ, J_i at time $t = t_o$. One tries to adjust those initial data so they describe as closely as possible the physical system one wishes to study (for example, a star which is beginning to implode to form a black hole, or two black holes that are orbiting each other and soon will begin to coalesce). Getting some sort of solution to the constraint equations is not all that hard, but getting a solution corresponding to a physically realistic, interesting situation is difficult. In fact, this is the most difficult part of numerical relativity.

Once the constraint equations have been solved at time t_o, one is ready to integrate forward in time. Part of that integration is governed by the 3+1 form of the dynamical Einstein field equations $G_{ij} = 8\pi T_{ij}$:

$$\frac{\partial K_{ij}}{\partial t} = \alpha[{}^{(3)}R_{ij} - 2K_{ia}K_j{}^a - K_{ij}K_a{}^a - 8\pi(S_{ij} - \tfrac{1}{2}\gamma_{ij}S_a{}^a) - 4\pi\rho\gamma_{ij}]$$

$$-\alpha_{|ij} + K_{ij|a}\beta^a + K_{ia}\beta^a{}_{|j} + K_{ja}\beta^a{}_{|i} \ . \qquad (6.62)$$

These equations are used to evolve the extrinsic curvature K_{ij} forward. The 3-metric γ_{ij} is evolved using the following expression for its time derivative in terms of the extrinsic curvature:

$$\frac{\partial \gamma_{ij}}{\partial t} = -2\alpha K_{ij} + \beta_{i|j} + \beta_{j|i} \ . \qquad (6.63)$$

[This expression is the definition (6.59) of K_{ij}, with ${}^{(4)}\Gamma^t{}_{ij}$ evaluated from the 4-metric (6.57).] Finally, the FIDO-measured energy density ρ and momentum density J_i are evolved using the following 3+1 version of the equation of motion $T^{\alpha\beta}{}_{;\beta} = 0$:

$$\frac{\partial \rho}{\partial t} = \alpha(\rho K_a{}^a + S^{ab}K_{ab}) - \alpha J^a{}_{|a} - 2\alpha_{|a}J^a + \beta^a\rho_{|a} \ , \qquad (6.64a)$$

$$\frac{\partial J^i}{\partial t} = \alpha(J^i K_a{}^a + 2J_a K^{ai}) - \alpha S^{ia}{}_{|a} - S^{ia}\alpha_{|a} - \rho^{|i} + J^i{}_{|a}\beta^a - \beta^i{}_{|a}J^a \ . \qquad (6.64b)$$

At each step in the evolution one adjusts α and β^i so as to keep the slicing and coordinates well behaved.

By evolving gravity and the stress-energy in this way [using Eqs. (6.62)–(6.64)], one automatically guarantees that the initial-value equations (6.61) will be satisfied at all times. This is because of the redundancy between the 4-dimensional Einstein field equation and equation of motion, i.e. because the field equation $G_{\alpha\beta} = 8\pi T_{\alpha\beta}$ implies the equation of motion $T^{\alpha\beta}{}_{;\beta} = 0$ [cf. the passage from Eq. (6.43) to (6.44) above]; and, correspondingly, the 3+1 equations of motion and dynamical field equations together imply the time derivative of the 3+1 initial-value equations.

This redundancy permits an alternative approach to evolution: After constructing initial data as a solution to the 3+1 constraint equations (6.61), one can evolve forward with the equations of motion (6.64), the definition (6.62) of K_{ij}, just two of the six dynamical Einstein equations (6.63), and the four constraint equations (6.61). In other words, at each time step one can replace four of the six dynamical Einstein equations (6.63) by the four constraint equations (6.61). The fact that one thereby reduces to two the number of dynamical Einstein equations used is intimately connected with the fact that the gravitational field has two dynamical degrees of freedom, i.e. two independent polarizations for its gravitational waves. For a discussion of the relative advantages and pitfalls of these two approaches (6 dynamical equations vs. 2 dynamical and 4 initial-value) and mixtures thereof, see Detweiler (1987).

This 3+1 formulation of general relativity has played major roles in a variety of aspects of gravitation research. We shall describe, in Sec. 6.K, its role in numerical-relativity computations of gravitational-wave generation. Other roles have been the following: (i) It is used in numerical-relativity studies of the evolution of inhomogeneities (voids and galaxy formation) in the expanding universe (XXXX). (ii) It is used in numerical studies of accretion of gas onto black holes and the formation of jets by accreting matter (XXXX). (iii) It is used in the "membrane paradigm" formulation of black-hole physics (Thorne, Price, and Macdonald, 1986). (iv) It has been used to prove rigorous theorems about the dynamical structure of general relativity (e.g. existence and uniqueness of solutions to the Einstein field equation) (XXXX). (iv) It is used in the canonical (Hamiltonian) approach to classical gravity (XXXXX), in the canonical quantization of gravity (XXXXXX) and in the Wheeler-DeWitt and Hawking-Hartle approaches to quantum gravity (XXXXX).

6.G Slow-motion formalisms

The remainder of this chapter is a catalog of formalisms (i.e. methods) of computing wave generation. To be tractable with a minimum of numerical computation, such a formalism must break the extreme nonlinearity of the Einstein field equation by imposing a power-series expansion in some small quantity and keeping only the lowest, linear order or the lowest few orders. Wave-generation formalisms can be classified according to their choice of the small expansion parameter. *Slow-motion formalisms* (this section) expand in L/λ = (size of source)/(reduced wavelength of waves). *Post-Minkowski formalisms* (Sec. 6.H) expand in the strength of the gravitational field inside the source, i.e. in the magnitude ε of the deviations of the metric from that of flat spacetime. *Post-Newtonian formalisms* (Sec. 6.I) expand simultaneously in L/λ and ε. *Perturbation formalisms* (Sec. 6.J) expand in the deviations of the metric from its form for some nonradiative, astrophysical system. Of all astrophysical sources, the very strongest emitters will entail gravitationally induced large-amplitude, high-velocity, nonspherical internal motions — e.g. the inspiral and coalescence of a binary black hole or binary neutron star. For such sources, there is no small parameter in which to expand. The only way to compute in detail waves emitted by such sources is by the techniques of *numerical relativity* (Sec. 6.K), i.e., the numerical solution of the Einstein field equation on a supercomputer.

Turn, now, to slow-motion formalisms. Equation (6.32) shows that for a slow-motion source (one with size L small compared to reduced wavelength λ), the amplitude of the waves from the mass l-pole is typically $(M/r)(L/\lambda)^l$ and that from the current l-pole is typically $(M/r)(L/\lambda)^{l+1}$. Correspondingly, the strongest radiation will be from the mass quadrupole unless its oscillations are suppressed, in which case some higher-order multipole will dominate. To compute the waves, then, all one need do is calculate the time evolution of the dominant multipole moments, and then insert those multipoles into Eqs. (6.1), (6.3)–(6.5), and/or (6.25), (6.26). All slow-motion wave-generation formalisms are based on this.

In practical calculations one must use wisdom in deciding which moments will dominate, and thus which to compute. Such wisdom comes from past experience: From gravitational bremsstrahlung calculations (Kovacs and Thorne, 1978, and Turner and Will, 1978) one gets quantitative insight into how, as the source's internal motions are gradually speeded up, the higher moments gradually become more and

more important. The torsional oscillation of a neutron star (Schumaker and Thorne, 1983) provides an example in which the mass quadrupole moment vanishes because of parity considerations, leaving the current quadrupole to dominate the radiation. The Chandrasekhar (1970)–Friedman–Schutz (1978) (CFS) instability in neutron stars provides another example in which the mass quadrupole is suppressed, in this case because the CFS instability probably does not occur at all for the star's quadrupole modes (e.g. Managan, 1985); instead, it preferentially excites the mass octupole ($l=3$) or perhaps even the hexadecapole ($l=4$) or the $l=5$ multipole; see Secs. 2.G and 8.B for discussion.

For a slow-motion source with weak internal gravity and small internal stresses (e.g. a binary star system or the oscillations of the sun), the gravity and dynamical evolution are accurately governed by Newtonian theory; and the lowest multipoles are accurately computable by integrating over the source's Newtonian mass, momentum, and stress distributions [Eqs. (6.2), (6.6) and (6.30)]. The result is the standard version of the quadrupole formalism (Sec. 6.B), and its obvious generalization to higher-order moments [Eqs. (6.30), (6.25), (6.26)].

For a slow-motion source with strong internal gravity (e.g. a rotating neutron star or a torsionally oscillating neutron star), if one can compute by some method the gravitational field in the weak-field near zone, one then can read the quadrupole and other low-order moments off that field. In the linear approximation for the source's asymptotic rest frame (including its weak-field near zone), and in a very specially chosen version of Lorentz gauge, the near-zone field takes the form (6.27), and one reads the mass moments off that form's $\bar{h}_{00}$ and the current moments off its $\bar{h}_{0j}$. Unfortunately, one typically will compute the near-zone field in a gauge very different from (6.27), and the transformation to this gauge may be extremely difficult. Fortunately, one need not make that full transformation:

Using the formalism of nonlinear field theory in flat spacetime (Sec. 6.E), Thorne (1980b, Sec. XI) has derived the following procedure for reading off the l'th mass moment I_L and the lth current moment J_L: Compute that portion of the near-zone metric $g_{\alpha\beta}$ which is of zero order in L/λ (i.e. which treats gravity as though it propagates instantaneously across the source), and transform that *instantaneous-gravity metric* to a coordinate system which is *asymptotically Cartesian and mass centered to order* $l-1$, i.e. ACMC$-(l-1)$. By this is meant a system in which the $O[(L/\lambda)^0]$ metric coefficients, when expanded in powers of $r \equiv (\delta_{ij}x^i x^j)^{1/2}$ and in multipoles of $n^j \equiv x^j/r$, take the

following form:

$$g_{00} = -1 + \frac{2M}{r} + \frac{S_0}{r^2} + \sum_{j=2}^{l-1} \frac{1}{r^{j+1}}(S_0 + S_1 + \cdots + S_j) + 0\left(\frac{1}{r^{l+1}}\right),$$

$$g_{0j} = \sum_{j=1}^{l-1} \frac{1}{r^{j+1}}(S_0 + S_1 + \cdots + S_j) + 0\left(\frac{1}{r^{l+1}}\right),$$

$$g_{jk} = \delta_{jk} + \sum_{j=1}^{l-1} \frac{1}{r^{j+1}}(S_0 + S_1 \cdots + S_j) + 0\left(\frac{1}{r^{l+1}}\right). \qquad (6.65)$$

Here S_k means any spherical harmonic of order k. In words, the ACMC-$(l-l)$ coordinate system involves, for $j \le l-1$, only multipoles of order $\le j$ in the $1/r^{j+1}$ part of the metric, and it has vanishing mass dipole moment. In any such coordinate system, one can read the mass moment I_L off the $1/r^{l+1}$ part of g_{00}, and the current moment J_L off the $1/r^{l+1}$ part of g_{0j}:

$$(r^{-(l+1)},\ l\text{-pole part of } g_{00}) = \frac{2(2l-1)!!}{l!}\frac{I_L N_L}{r^{l+1}}, \qquad (6.66a)$$

$$\left[\begin{matrix} r^{-(l+1)},\ l\text{-pole,} \\ \text{parity } (-1)^{l+1} \text{ part of } g_{0j} \end{matrix}\right] = -\frac{4l(2l-1)!!}{(l+1)!}\varepsilon_{jpq}\frac{J_{qL-1}N_{L-1}}{r^{l+1}}. \qquad (6.66b)$$

(Note: in the STF notation, multipoles with no ε_{jpq} have parity $(-1)^l$, while those with one ε_{jpq} have parity $(-1)^{l+1}$; see Sec. II of Thorne, 1980b.) As a specific example, to read off the quadrupole moments one need only be sure that the $1/r$ part of the metric involves only monopoles, the $1/r^2$ part of g_{00} involves only monopoles, and the $1/r^2$ parts of g_{0j} and g_{jk} involve only monopoles and dipoles. In practical situations it is not difficult to construct a coordinate system with this property.

With this readout prescription in hand, and the multipolar radiation formulas in hand, the key remaining task of a slow-motion wave-generation calculation is to compute the near-zone, instantaneous-gravity metric $g_{\alpha\beta}$ to the leading few orders in $1/r$. This has been done by several different techniques: (i) for rigidly rotating and precessing bodies, using Sec. 6.E's formalism of nonlinear field theory in flat spacetime (Thorne and Gürsel 1983); (ii) for pulsating stars, using the perturbation theory formalism discussed in Sec. 6.J below (e.g. Schumaker and Thorne, 1983); (iii) for models of stellar collapse to form a neutron star, by techniques of numerical relativity, Sec. 6.K (Abrahams and Evans, 1988), and by the post-Newtonian

wave-generation formalism of Sec. 6.I (Turner and Wagoner, 1979).

One final remark: Because of the nonlinearities of general relativity, the moments which one reads off the weak-field, near-zone, instantaneous-gravity metric (6.65), (6.66) differ very slightly from the true moments of the radiation field. Those tiny differences (i.e. the errors made by the above formalism) have been estimated by Thorne (1980b, Sec. IX.H) to have magnitude

$$\frac{(\text{moment in wave zone})}{(\text{moment in near zone})} - 1 \sim \frac{M}{\lambda}\ln\left[\frac{\lambda}{L}\right]; \qquad (6.67)$$

and the differences have been studied with elegance and in detail by Blanchet (1987a), Damour (1987a), and Blanchet and Damour (1988a).

6.H Post-Minkowski formalisms

Post-Minkowski wave-generation formalisms are sometimes called *post-linear* because they entail expanding in the strength of the gravitational field beyond linear order; and they are sometimes called *fast-motion* to contrast them with slow-motion formalisms. They generally are based on the nonlinear-field-theory-in-flat-spacetime formalism of Sec. 6.E.

There is a systematic way to take a post-Minkowski wave-generation formalism that is accurate to a given order in the strength ε of the source's internal gravity, and iterate it to obtain a formalism of one-order-higher accuracy (Thorne and Kovacs 1975, Thorne 1977). The step involved in going from Eq. (6.47a) for $\bar{h}_1^{\alpha\beta}$ to (6.47b) for $\bar{h}_2^{\alpha\beta}$ is the prototype for this iteration.

The wave-generation formalism that is accurate to first post-Minkowski order (first order in the strength ε of internal gravity) is *linearized theory*, i.e. the linear approximation to general relativity. It is the formalism embodied in Eqs. (6.47a) for $\bar{h}_1^{\alpha\beta}$. By solving the field equation (6.47a) with the usual flat-spacetime Green's function and inserting the resulting field into the local-wave-zone expression $h_{jk}^{GW} = (\bar{h}_{1jk})^{TT}$, one obtains the following linearized-theory formula for the gravitational-wave field

$$h_{jk}^{GW}(t, x^i) = \left[\int \frac{4T_{jk}(t' = t - |\mathbf{x}-\mathbf{x}'|, \mathbf{x}')}{|\mathbf{x}-\mathbf{x}'|} dx'dy'dz'\right]^{TT}, \qquad (6.68)$$

where $|\mathbf{x}-\mathbf{x}'|$ is the flat-space distance from the source point $\mathbf{x}'$ to the field point $\mathbf{x}$. Here the stress-energy tensor $T^{\alpha\beta}$ is to be computed

ignoring all gravitational effects, i.e. using the gravity-free equation of motion $T^{\alpha\beta}{}_{|\beta} = 0$ [Eq. (6.47a)]. An alternative, and equivalent formula for the wave field, derived independently by Halpern and Desbrandes (1969) and by Press (1977), is

$$XXXXXXXXX \tag{6.69}$$

Note that this formula reduces to the quadrupole wave-generation formula when the source is small compared to its reduced wavelength (slow-motion limit).

Examples of gravity-wave generation that have been analyzed by linearized theory are: (i) the coherent (but painfully slow) transformation of electromagnetic waves into gravitational waves, which occurs when the waves are propagating through a steady magnetic or electric field (Gertsenshtein, 1962; Sec. 4.1 of Grishchuk and Polnarev, 1980; Sec. 5.F of this book); and (ii) the waves emitted by the explosion of a nonspherical nuclear bomb (Wheeler, 1962; Wood et. al., 1971).

Linearized theory is completely ignorant of the source's internal gravity; it can correctly predict the emitted waves only if the source's motions are governed by nongravitational forces — typically electric or magnetic. For systems with significant but weak internal gravity (e.g. stellar pulsations, binary systems, and high-speed stellar encounters), one must use a wave-generation formalism accurate to the next, "post-post-Minkowski" or "post-linear" order. Such a *post-linear theory*, based on Eqs. (6.47) plus $h_{jk}^{GW} = (\bar{h}_{2jk})^{TT}$ in the wave zone, has been constructed by Thorne and Kovacs (1975) and Crowley and Thorne (1977); see the discussion accompanying and following Eqs. (6.47) above. For the application of the post-linear theory to high-speed stellar encounters (gravitational bremsstrahlung radiation) see Kovacs and Thorne (1977, 1978). [Waves from ultra-high-speed ($v \cong 1$), head-on black-hole collisions have been computed using a rather different technique, one closely related to the theory of collisions of plane gravitational waves (Sec. 5.G.g), by Curtis (1978), D'Eath (1978), and Payne (1983)]. For a recent review of research using post-linear theory see Westpfahl (1985). [KIP: CHECK]

Thus far, nobody has developed in detail a post-post-linear wave-generation formalism — i.e. a formalism accurate to post-post-post-Minkowski order. There has been no great need for such a formalism, and the post-linear formalism is sufficiently hard to work with in practice (cf. Kovacs and Thorne 1977) that it is not clear whether post-post-linear would be significantly easier than full-

blown numerical relativity.

On the other hand, the external gravitational field of a completely general, radiating system that lives alone in an asymptotically flat spacetime has been studied *to all orders* in a post–Minkowski expansion by Blanchet and Damour (1986) and Blanchet (1987a). These studies have led to a number of powerful theorems about the properties of the radiation field; cf. the last paragraph of Sec. 6.G above.

6.I Post–Newtonian formalisms

Post–Newtonian approximations to general relativity make the assumption — in accord with the virial theorem for gravitationally bound systems — that inside the source the deviation of the metric from Minkowski (i.e. the dimensionless strength ε of the source's gravity) has a magnitude

$$\varepsilon \sim (L/\lambda)^2 ; \tag{6.70}$$

and accordingly they expand the Einstein field equations simultaneously in ε (post–Minkowski expansion) and L/λ (slow–motion expansion). See, e.g., Burke (1979) for a review of the method. The slow–motion expansion, by virtue of Eq. (6.32), is accompanied by a multipolar expansion; and as a result, post–Newtonian formalisms become specific methods of computing the dominant, lowest–order multipoles for insertion into the standard radiation–field multipole formulas (6.25), (6.26).

The lowest–accuracy post–Newtonian formalism is called the *Newtonian wave-generation formalism* because it computes the evolution of the source using Newton's laws of gravity and mechanics, then evaluates the source's time–evolving quadrupole moment using one of the standard Newtonian volume integrals (6.2a,c,d), and then inserts that quadrupole moment into the standard quadrupole wave–generation formulas (6.1), (6.3)–(6.5). It is this Newtonian version of the quadrupole formalism that has been especially controversial (see Secs. 3.A and 6.B), but is now almost universally agreed to be highly reliable.

There have been a large number of important wave–generation calculations with this formalism. Some examples are: (i) the waves emitted by binary systems with Newtonian, elliptical orbits (Peters and Mathews 1963); (ii) the waves emitted by a variety of models of stars that collapse to form neutron stars (Saenz and Shapiro 1978, 1981); and (iii) the waves emitted in the head–on collision of two compact

stars (Gilden and Shapiro 1984).

The Newtonian wave-generation formalism starts losing accuracy when the source's internal gravity becomes too strong ($\varepsilon \sim 0.05$) and its internal velocities too high ($v \sim 0.2$) (Turner and Will 1978) — e.g. in the late stages of the spiraling together of a neutron-star binary system. In such a situation it is useful to include the next higher-order corrections (one order higher in the strength of gravity ε, two higher in the speed L/λ). The resulting *post-Newtonian wave-generation formalism* (Epstein and Wagoner 1975; Wagoner, 1977; Tsvetkov, 1984; Blanchet and Damour, 1989); Blanchet, Damour, and Schäfer, 1989) is a specialization, to the post-Newtonian regime, of the field-theory-in-flat-spacetime formalism of Sec. 6.E. In the post-Newtonian formalism, the radiation is produced by the mass quadrupole moment I_{ij}, the mass octupole moment I_{ijk}, and the current quadrupole moment S_{ij}. The formalism provides formulas for computing these moments, accurate to post-Newtonian order; and it then inserts the moments into the standard multipole expansions (6.25) and (6.26) of the radiation field.

Examples of calculations that have been performed with the post-Newtonian formalism are: the radiation from a system of bodies whose sizes are all small compared to their separations, including as a special case binary systems (Wagoner and Will 1976; Gal'tsov, Matiukhin, and Petukhov, 1980; Krolak, 1988; Blanchet and Schäfer, 1989); gravitational bremsstrahlung at moderate velocities (Turner and Will 1978); the radiation emitted by a slowly rotating star as it collapses to a neutron star (Turner and Wagoner 1979); and radiation from a rapidly rotating neutron star deformed by the pressure of an off-axis magnetic field (Tsvetkov and Tsirulev, 1987).

The foundations for a post-post-Newtonian wave-generation formalism have also been worked out using the field-theory-in-flat-spacetime formalism of Sec. 6.E: Chandrasekhar and Esposito (1970) have developed the post-post-Newtonian equations governing the internal dynamics of the source, and Thorne (1980b, Sec. V.E) has given post-post-Newtonian formulas for the moments that generate the radiation: the mass moments of orders 2, 3, and 4 and the current moments of orders 2 and 3. Much further work is needed, however, to bring the formalism into a computationally robust form — work analogous to that carried out, in the post-Newtonian case, by Blanchet, Damour, and Schäfer (1989). Such work would be well worthwhile: I expect that the resulting formalism — by contrast with the post-

post-linear formalism — would be far more tractable than full-blown numerical relativity. It may one day prove useful, for example, in computing the gravitational waves from the late stages of coalescence of neutron-star binaries and black-hole binaries; see Sec. 7.D. [KIP: UPDATE IN LIGHT OF CLIFF WILL'S STUDENT; OR UPDATE THE POST-NEWTONIAN DISCUSSION OF THIS ISSUE, ABOVE]

6.J Perturbation formalisms

Perturbation formalisms for computing wave generation are applicable to any source which is weakly perturbed from a nonradiating configuration. Examples are pulsating neutron stars and black holes, the infall of a small hole or star into a large hole, and small deviations of the early universe from perfect homogeneity and isotropy (primordial gravitational waves).

Perturbation formalisms treat the nonradiating configuration as a "background spacetime" and the perturbed configuration and its waves as a corresponding "full spacetime". The perturbations and waves are then analyzed using the theory of linear perturbations of curved spacetime (Sec. 5.B above).

The central tasks in any perturbation formalism are (i) to devise a clear and concise description of the unperturbed background spacetime, including a coordinate system well suited to it, (ii) to find a gauge (i.e. a mapping of the full spacetime onto the background) which makes the perturbation equations especially tractable, and (iii) to solve those perturbation equations in sufficient detail for deducing the radiation field.

Such a formalism has been developed for the waves from nonradial pulsations of nonrotating relativistic stars by Thorne and Campolattaro (1967), Price and Thorne (1969), Thorne (1969a), Ipser and Thorne (1973), Detweiler and Ipser (1973), Detweiler (1975), Schumaker and Thorne (1983), Detweiler and Lindblom (1985), and Finn (1986). For a review of the early work see Thorne (1978). This stellar pulsation formalism uses "Schwarzschild coordinates" for the unperturbed star and a gauge due to Regge and Wheeler (1957) for the perturbations. Among its recent applications are computations by Lindblom and Detweiler (1983) of the normal modes of neutron stars with a variety of equations of state, and a study by Balbinsky et. al. (1985) of the accuracy of the quadrupole formalism when applied to pulsations of moderately relativistic stars.

For the waves from pulsations of rotating stars there is a formalism due to Chandrasekhar and Friedman (1973), Will (1974), and especially Friedman and Schutz (1975a,b). [KIP: ADD MORE REFS FROM SCHUTZ (1987)] For a recent review of the formalism and its applications see Schutz (1987). The most important recent applications are studies of the waves emitted by the "Chandrasekhar–Friedman–Schutz instability" in rapidly rotating neutron stars; see Sec. 8.B.

For waves from pulsations of nonrotating (Schwarzschild) black holes there is a perturbation formalism due to Regge and Wheeler (1957), Edelstein and Vishveshwara (1970), Zerilli (1970), Moncrief (1974), Bardeen and Press (1973), Chandrasekhar (1975), and Chandrasekhar and Detweiler (1975). For reviews see Chandrasekhar (1983) and Thorne (1978). Recent applications include a definitive numerical evaluation of the eigenfrequencies and damping times of a Schwarzschild hole's quasinormal modes (Leaver, 1985a,b), and of the Green's function for arbitrary perturbations of a Schwarzschild hole (Leaver, 1986), extensive studies of gravitational waves from objects orbiting or falling into a black hole (Sec. 7.E of this book; review in Nakamura, Oohara, and Kojima, 1987), and a general analysis of the excitation of black–hole normal modes by any process (Sun and Price, 1988).

For waves from pulsations of rotating (Kerr) black holes the formalism is due to Teukolsky (1972, 1973), Teukolsky and Press (1974), Starobinsky (1973), Wald (1973), Chrzanowski (1975), Cohen and Kegeles (1975), Kegeles and Cohen (1979), Chandrasekhar and Detweiler (1976b), Detweiler (1977), Chandrasekhar (1983), and Sasaki and Nakamura (1982). For detailed reviews see Chandrasekhar (1983), and Nakamura, Oohara, and Kojima (1987). Recent applications include an analytic proof that the normal modes of a Kerr black hole are stable (Whiting, 1989), the evaluation of the eigenfrequencies and damping times of a Kerr hole's quasinormal modes (Detweiler 1980, Leaver 1985a,b), and evaluations of the gravitational waves emitted when a compact body orbits a Kerr hole (Detweiler, 1978), scatters gravitationally off a Kerr hole (Kojima and Nakamura, 1984b), or plunges into a Kerr hole (Detweiler and Szedenits, 1979; Kojima and Nakamura, 1984a). For reviews see Sec. 7.E of this book, and Nakamura, Oohara, and Kojima (1987).

A generalization of the formalisms for nonrotating stars and black holes to gravitational perturbations of *any* spherically symmetric spacetime has been developed by Gerlach (1980). For waves from

gravitationally collapsing stars with slight deviations from sphericity see the formalism and calculations by Cunningham, Price, and Moncrief (1978, 1979), and by Seidel and Moore (1987, 1989).

Primordial gravitational waves (waves created in or near the big-bang) cannot be analyzed by splitting space into a wave-generation region plus wave zones (Sec. 6.A), because the transition from wave generation to wave propagation is a temporal one rather than spatial: the transition occurs when the size of the cosmological horizon expands to become much larger than a wavelength, thereby unfreezing a set of frozen-in perturbations. Correspondingly, the wave-generation region is the earliest phases of the universe, and the propagation region is later phases.

The perturbation formalism for the generation of primordial waves takes as the unperturbed, background spacetime a nonradiative, Friedman-Robertson-Walker cosmological model. The linear perturbation equations were originally derived by Lifshitz (1946), and the advantages and disadvantages of various gauges were elucidated by Bardeen (XXXX). Parker (XXXX) showed how to quantize the perturbations, a step which is crucial to matching them onto the Planck-Wheeler era. References to explicit model calculations are given in Sec. 9.D.

6.K Numerical relativity

Numerical solution of the fully nonlinear Einstein equation is the only way today to study wave generation in the strongest and most interesting of all gravity-wave sources: those with high internal velocities, strong internal gravity, and large deviations from a nonradiating spacetime. During the past decade several dozen researchers have worked vigorously to develop the field of numerical relativity. Almost all these efforts have focussed on numerical implementations of the 3+1 formalism (Sec. 6.F); but some work has been done with an alternative approach, called *Regge Calculus* (Regge, 1961; recent work reviewed by Piran, 1987) — which we shall not study here.

Most 3+1 numerical work thus far has focussed on spherically symmetric, plane-symmetric, cylindrically symmetric, and axially symmetric systems. In the spherical, planar, and cylindrical cases the spatial grid can be made one dimensional, and in the axial case it can be made two dimensional, thus simplifying the calculations. For spherical calculations (where there is no radiation), see Shapiro and Teukolsky (1985, 1988a,b) and references therein. For planar

calculations (where the spacetime cannot be asymptotically flat), see Centrella (1980a,b) and XXXX. For cylindrical calculations (where again it cannot be asymptotically flat), see Piran (1979, 1985) and references therein.

The most astrophysically interesting calculations thus far are axially symmetric (two nontrivial space dimensions and one time). For research on viable ways, in the axisymmetric case, to slice spacetime (i.e. to fix the lapse function α), and to choose the spatial coordinates (i.e. to fix the shift function β^i), and to compute the emitted gravitational waves, see Smarr and York (1978), Piran (1983), Bardeen and Piran (1983), Sasaki (1984), Stewart and Friedrich (1983), Isaacson, Welling, and Winicour (1983), Gomez *et al.* (1986), Anderson and Hobill (1986), and Abrahams and Evans (1988).

Numerical relativists call the choice of spatial coordinates their *gauge*. Accordingly, in this section and only here we shall use the word "gauge" in this way. Two axisymmetric gauges that have been used extensively are the *quasi-isotropic gauge* (also called *isothermal gauge*) (Smarr, 1979; Wilson, 1979; Evans, 1986), in which the 3-metric γ_{ij} takes the form

$$ds^2 = A^2(dr^2+r^2d\theta^2)+B^2(\sin\theta d\phi+\xi d\theta)^2 ; \qquad (6.71)$$

and the *quasi-radial gauge* (Bardeen and Piran 1983), in which

$$ds^2 = A^2dr^2+B^{-2}d\theta^2+B^2r^2(\sin\theta d\phi+\xi d\theta)^2 . \qquad (6.72)$$

In both these metrics A, B, and ξ are functions of t, r, and θ. The spatial coordinates are kept in these forms by careful choice of the shift function at each time step of the integration. The components $\beta^r(t,r,\theta)$, $\beta^\theta(t,r,\theta)$, and $\beta^\phi(t,r,\theta)$ of the shift that achieves this are determined at each time step by numerical solution of differential equations in r and θ (see, e.g. Bardeen and Piran, 1983, where β^j is denoted $-N^j$).

One popular and powerful choice of slicing in the axisymmetric case is to insist that the trace of the hypersurfaces' extrinsic curvature vanish, $\mathrm{Tr(K)} \equiv K^i{}_i = 0$ (Estabrook et. al., 1973). This is called *maximal slicing* because slight deformations of a hypersurface away from this choice produce no first-order change in the hypersurface's 3-volume, and produce a decrease in 3-volume at second order; i.e. the 3-surfaces have maximal 3-volume. Maximal slicing is achieved by forcing $\alpha(t,r,\theta)$ to satisfy an elliptic differential equation in r and θ at each time step in the evolution (see, e.g., Bardeen and Piran, 1983, where α

is denoted N). The reason for the popularity of maximal slicing is that, as one approaches most physical singularities, the infinitely diverging Riemann curvature of spacetime forces all hypersurfaces to have infinitely diverging Tr(K), which means that maximal hypersurfaces cannot run into such singularities (Eardley and Smarr, 1979) [KIP: ADD TO REFS]. Correspondingly, as a numerical calculation proceeds, in regions of spacetime where its maximal hypersurfaces are nearing a singularity, α is automatically driven to zero (the so-called "collapse of the lapse"), forcing the evolution into an exponentially slow crawl; while in regions where there is no impending singularity, α automatically remains large and the evolution moves forward rapidly.

Polar slicing, in which $\mathrm{Tr(K)} = K^r{}_r$, is a reasonable alternative to maximal slicing (Bardeen and Piran, 1983). When combined with radial gauge [Eq. (6.72)], not only does it avoid black-hole singularities; it even avoids reaching inside the apparent horizon of a black hole. The lapse α automatically collapses to zero at the apparent horizon but remains large outside, thereby permitting exploration of the exterior of the hole but not the interior. Polar slicing, when combined with radial gauge, produces parabolic equations for the lapse and shift functions, which are easier to solve at each step of numerical integration than the elliptic equations of maximal slicing and quasi-isotropic coordinates.

A third popular choice of slicing and gauge in axisymmetric spacetimes (Maeda *et. al.*, 1980, Sasaki, 1984) begins by writing the four-dimensional metric in the form

$$g_{\alpha\beta} = h_{\alpha\beta} + \lambda^{-2}\xi_\alpha\xi_\beta \,, \tag{6.73}$$

where ξ_α is the "Killing vector" that generates rotations about the symmetry axis (equal to $\partial/\partial\phi$ in the quasi-isotropic or radial gauge). The quantity $h_{\alpha\beta}$ is regarded as a 3-dimensional metric for a 3-dimensional spacetime in which lives the scalar field λ. This 3-dimensional spacetime is then sliced into 2-dimensional hypersurfaces, in a 2+1 analog of the 3+1 formalism of Sec. 6.F. The resulting so-called (2+1)+1 *formalism* has been used in extensive numerical calculations by Nakamura, Sasaki, Maeda, Miyama, and their coworkers; see the reviews by Nakamura (1983), Sasaki (1984), and Nakamura, Oohara, and Kojima (1987).

A fourth choice of slicing, one which is not yet as highly developed and tested numerically as the other three, uses outgoing light cones as the 3-dimensional hypersurfaces of constant time ("retarded time").

This is called *null slicing*. Because the slices are null instead of spacelike, the formalism takes a somewhat different form from that of Sec. 6.F, and the numerical techniques and pitfalls are somewhat different. A potential advantage of this approach is the fact that on a slice of constant retarded time in the wave zone, the wave field is a constant (divided by radius) rather than an oscillating function. For details of the formalism and/or numerical calculations see, e.g., Corkill and Stewart (1983); Stewart and Friedrich (1983); Isaacson, Welling, and Winicour (1983); Gomez and Winicour (1989); Piran, Safier, and Stark (1985); and Anderson and Hobill (1986).

Until recently, the gravitational radiation produced in axisymmetric calculations was computed by numerically evolving the spacetime metric in the innermost regions of the wave zone, as well as in the strong-gravity region. The waves were then computed numerically in the inner regions of the wave zone as the TT part of the numerically-evolved $g_{\alpha\beta}$. This method was so fraught with numerical error (due to gauge and near-zone effects partially obscuring the waves) that only one calculation was able to give reliable wave forms: that of Stark and Piran (1986) and Piran and Stark (1986), which used polar slicing and radial gauge. A potentially better method, recently developed by Abrahams and Evans (1988) (and in a different, null-slicing variant by Anderson and Hobill, 1987), relies on the fact that the quadrupole and higher-order moments show up much more strongly, in the numerically computed metric, in the near zone and transition zone than in the wave zone. Abrahams and Evans (and Anderson and Hobill) propose comparing the near-zone/transition-zone numerical metric with a gauge-transformed version of Eqs. (6.24), and from that comparison (via numerical surface integrals) extracting the dominant multipole moments. Those moments can then be inserted into the standard radiation formulae (6.25), (6.26). Numerical tests (Abrahams, 1989) show that this method will enable calculations with quasi-isotropic gauge and maximal slicing to produce reliable wave forms. It is likely to do so also with the other choices of slicing and gauge.

For details of some computer codes that have been constructed for evolving axisymmetric systems and computing their waves see Smarr (1977a, 1979) and Evans (1986), who use maximal slicing and quasi-isotropic gauge; Stark and Piran (1986) and Piran and Stark (1986), who use polar slicing and quasi-radial gauge; and Nakamura (1983) and Nakamura, Oohara, and Kojima (1987), who use the (2+1)+1 slicing and gauge. Among the problems that have been studied successfully

with these codes are the gravitational radiation produced by a head-on collision of two Schwarzschild black holes (Smarr 1977a), the waves from the collapse of a rotating star to form a Kerr black hole (Stark and Piran 1986), and waves from the vibrations of a neutron star (Evans 1986).

The experts in numerical relativity are now beginning to move on from axisymmetric systems to generic systems with three nontrivial spatial dimensions and one time (e.g. Nakamura 1987, 1990). This full 3+1 numerical effort will require using the world's largest supercomputers, and will require new techniques for slicing spacetime into space plus time, for choosing the spatial coordinates (gauge), and for differencing the 3+1 Einstein equations. The effort may absorb almost as many person-years as the development of gravitational-wave detectors, but it will be well worthwhile. The payoffs will include the ability to compute in detail the waveforms from the strongest gravity-wave sources in the universe, such as the spiraling together and coalescence of two black holes — waveforms that will be crucial to the interpretation of gravity-wave observations and to their use for strong-field, highly dynamical tests of general relativity.

One should not be misled into believing that numerical relativity will be the totally dominant tool for realistic gravitational-wave calculations in the coming years. On the contrary, we can expect a healthy interaction between numerical and analytical techniques; for discussions see Schutz (1986c) and Damour (1986). [KIP: WHICH - 1986a OR 1986b?]

Moreover, in the mature era of gravitational-wave astronomy, when waves have been discovered and are being milked for their astrophysical information, we can expect rich interactions among all the tools of research: numerical and analytical relativity, astrophysical modeling of sources, gravitational detector design, gravitational data analysis, and electromagnetic astronomy.

GRAVITATIONAL RADIATION

A New Window onto the Universe

by Kip S. Thorne

draft of 16 September 1989

California Institute of Technology

1989

Part III
Sources

Optical photograph of the central regions of the Virgo cluster of galaxies, the nearest large cluster to earth. Most bursts of gravitational waves strong enough for detection at earth and frequent enough to be seen several times per year are expected to come from the Virgo cluster or beyond. [Photograph courtesty XXXX.]

7 Burst sources

Part III of this book describes in detail the present (1989) knowledge and speculations about various sources of gravitational waves. Attention is restricted to those sources that are most promising for detection by present or planned detectors, with Chap.7 focusing on burst sources, Chap. 8 on periodic sources, and Chap. 9 on stochastic sources.

As was noted in Sec. 1.2, for each source, with the exception of binary stars and their coalescences, either (i) the strength of the source's waves for a given distance from earth is uncertain by several orders of magnitude; or (ii) the rate of occurrence of that type of source, and thus the distance to the nearest one, is uncertain by several orders of magnitude; or (iii) the very existence of the source is uncertain. Despite these uncertainties, it is important in the wave-detection effort to estimate as best one can, for each source, the strengths of the waves bathing the earth. Such estimates were displayed graphically and compared with detector sensitivities in Secs. 2.F–2.H (Figs. 2.7–2.9). Part III provides the details behind those estimates.

This chapter on burst sources begins, in Sec. 7.A, by defining with care the characteristic amplitude h_c and frequency f_c by which we characterize a burst source, and the corresponding noise amplitude h_n and sensitivity $h_{3/yr}$ of a detector searching for bursts. Then

subsequent sections treat specific burst sources: supernovae (Sec. 7.B); the collapse of a star or star cluster to form a black hole (Sec. 7.C); the coalescence of neutron-star and black-hole binaries (Sec. 7.D); and the fall of stars and small black holes into supermassive holes (Sec. 7.E). Section 7.F estimates how strong the strongest bursts bathing the earth could be without violating our cherished beliefs about the laws of physics and the nature of the universe. Finally, Sec. 7.G describes peculiar types of bursts that leaves behind themselves, in the geometry of spacetime near earth, "memories" of their passage.

7.A Characterization of bursts and of noise in a detector searching for them

Burst sources are best characterized by their full waveforms $h_+(t)$ and $h_\times(t)$. However, when comparing with detector sensitivities, it is helpful to have a more compact characterization. Past discussions have used a loosely defined "characteristic amplitude" h_c and "characteristic frequency" f_c. However, the factors of order 3 that are glossed over by the loose definitions are beginning to be important in the planning of laser-interferometer gravitational-wave observatories (LIGOs), especially in the case of the inspiral and coalescence of binary neutron stars (Sec. 7.D below). I therefore shall be quite careful in my definitions of h_c and f_c and in my corresponding discussions of detector sensitivities.

As an aid to defining h_c and f_c with care, Fig. 7.1 shows a diagram of the emission, propagation, and absorption of the wave. We introduce, in the source's local asymptotic rest frame, preferred local Cartesian axes $(\bar{x},\bar{y},\bar{z})$ with respect to which the source's internal structure or its emitted waves are especially simple, and we denote by (ι,β) the direction toward Earth (spherical polar angles) relative to those axes. Similarly, we introduce in the detector's proper reference frame local Cartesian axes (x,y,z) with respect to which the detector's geometry is especially simple; and we denote by (θ,ϕ) the direction toward the source (spherical polar angles) relative to those detector axes. The waves themselves, as they pass through the detector, are most simply described in a third set of Cartesian axes (x',y',z') with origin at the detector's center of mass, z' axis along the waves' propagation direction, and x' and y' axes so oriented in the polarization plane as to make the waveforms $h_+ = h^{GW'}_{x'x'} = -h^{GW'}_{y'y'}$ and $h_\times = h^{GW'}_{x'y'} = h^{GW'}_{y'x'}$ especially simple. We shall denote by ψ the angle between the x' polarization axis and the $\phi = 0$ plane.

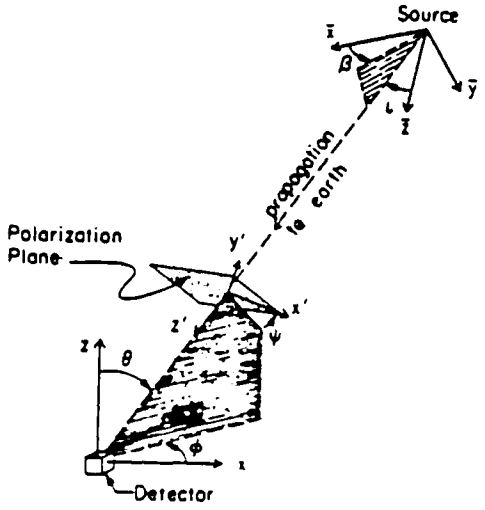

Fig. 7.1 The angles $\iota,\beta,\psi,\theta,\phi$ which characterize the emission, propagation, and detection of a gravitational wave.

From a model for the source one can compute the waveforms $h_+(t-z';\iota,\beta)$ and $h_\times(t-z';\iota,\beta)$ arriving at the detector. If the detector is small compared to a reduced wavelength (as is the case for all earth-based detectors), then it will feel a simple linear combination of h_+ and $h_\times$; i.e. it will detect the waveform

$$h(t) = F_+(\theta,\phi,\psi)h_+(t;\iota,\beta) + F_\times(\theta,\phi,\psi)h_\times(t;\iota,\beta) . \qquad (7.1)$$

Here F_+ and $F_\times$ are detector beam-pattern functions (to be discussed in Chaps. 10 and 11 below), which depend on the direction of the source (θ,ϕ) and the orientation ψ of the polarization axes relative to the detector's orientation (Fig. 7.1), and which have values in the range $0 \le |F_A| \le 1$. There will be some special choice of θ, ϕ, ψ for which $F_+ = 1$ and $F_\times = 0$. We shall call this the "optimum source direction and polarization" for the waves' + mode.

The most precise way to characterize the noise in a detector is by a frequency-dependent spectral density $S_h(f)$ (with dimensions Hz^{-1}) defined as follows: If a precisely sinusoidal gravitational wave with known phase α, known frequency $f>0$, and unknown rms amplitude h_o

$$h(t) = [\text{expression (7.1)}] = \sqrt{2}h_o\cos(2\pi ft+\alpha) , \quad \alpha = \text{const} , \qquad (7.2a)$$

impinges on the detector, and if the experimenters seek to detect the wave by Fourier analyzing the detector output with a bandwidth Δf

(integration time $\hat{\tau} = 1/\Delta f$), then the amplitude signal-to-noise ratio will be

$$\frac{S}{N} = \frac{h_o}{\sqrt{S_h(f)\Delta f}} . \tag{7.2b}$$

In much of the gravitational-wave literature this spectral density, $S_h(f)$, is denoted $[h(f)]^2$ or $[\tilde{h}(f)]$; i.e. $h(f) \equiv \sqrt{S_h(f)}$ or $\tilde{h}(f) \equiv \sqrt{S_h(f)}$ (with dimensions $\mathrm{Hz}^{-1/2}$).

To understand the next few paragraphs and occasional sections of the remainder of this book, the reader will need to be familiar with the concept of spectral density and how spectral densities are influenced by linear signal processing. These issues are part of a subject called the "theory of random processes", which is treated in some statistical physics textbooks, and also in textbooks on the theory of noise or the theory of signal processing; see, e.g., XXXXXXXXXX.

In this chapter we are interested not in the sinusoidal gravitational waves of Eqs. (7.2), but rather in bursts — i.e. in waves with complicated time dependences $h(t)$ and with durations short compared to the experimenters' observation time. As an aid in defining the characteristic amplitude h_c and frequency f_c of such a burst, we shall assume that the burst's waveform $h(t)$ is known, and that our only question is whether the wave is really present or not in a detector's noisy output, with some postulated starting time t_o. (Later we shall discuss the statistical consequences of an unknown starting time.) There is a well-known optimal strategy for searching for such a wave in the presence of noise with known spectral density: (i) One constructs a *Wiener optimal filter* $K(t)$, that function of time whose Fourier transform $\tilde{K}(f)$ is the same as the transform $\tilde{h}(f)$ of the signal $h(t)$ weighted by $1/S_h(f)$ (so that noisy frequencies are suppressed):

$$\tilde{K}(f) \equiv \frac{\tilde{h}(f)}{S_h(f)} , \quad \tilde{h}(f) \equiv \int_{-\infty}^{+\infty} h(t) e^{i2\pi f t} dt , \tag{7.3a}$$

$$K(t) = \int_{-\infty}^{+\infty} \tilde{K}(f) e^{-i2\pi f t} df . \tag{7.3b}$$

(ii) One then takes the output of the detector, which includes noise and possibly signal. From the output one computes the gravitational waveform $h_{\mathrm{output}}(t)$ that would have been required to produce the observed output if there were no noise present, and one then computes a quantity

$$W = \int_{-\infty}^{+\infty} K(t-t_o) h_{\text{output}}(t)\,dt \ . \tag{7.3c}$$

(iii) This quantity will have a root-mean-square contribution N from noise; and if the signal was actually present with starting time t_o, it will have a signal contribution S (i.e. $W = N+S$), with squared signal-to-noise ratio

$$\frac{S^2}{N^2} = \int_0^{\infty} \frac{2|\tilde{h}(f)|^2}{S_h(f)} df \ . \tag{7.4}$$

See Wiener (1949), Secs. 25–27 of Wainstein and Zubakov (1962), Kafka (1977), and Michelson and Taber (1984) for proofs and discussion. The integral in Eq. (7.4) is from 0 to ∞ rather than $-\infty$ to $+\infty$ and there is a factor 2 present because $S_h(f)$ is a "one-sided spectral density" (defined only for $f \geq 0$; negative frequencies are folded into positive). The squared signal-to-noise ratio (7.4) will be the basis for our definitions of h_c and f_c.

Expression (7.4) is the squared signal-to-noise ratio for a specific ("fiducial") source at some specific distance r_o from earth. Suppose that space is uniformly filled with sources, all identical to this fiducial source but with random directions (θ,ϕ), orientations (ι,β), and polarization angles ψ. Suppose, further, that inside the source's distance r_o there is, on average, one burst each D_o days. Then what, on average, will be the squared signal-to-noise ratio $(S^2/N^2)_{\text{strongest}}$ of the strongest burst that occurs each D_o days? One might expect the answer to be the fiducial S^2/N^2 of (7.4), averaged over all the angles $\theta,\phi,\psi,\iota,\beta$. Not so. There is a statistical preference for directions and polarizations that give larger values of S^2/N^2, because they can be seen out to greater distances where the event rate is greater. This effect gives, assuming the event rate goes up as r^3 and h_{jk}^{TT} goes down as $1/r$, $(S^2/N^2)_{\text{strongest}} = \langle S^3/N^3\rangle^{2/3}$ where $\langle \cdots \rangle$ denotes an average over randomly distributed angles. Now, the 2/3 power is a pain to deal with in subsequent calculations, so we shall switch to a straightforward angular average $\langle S^2/N^2\rangle$ and to compensate we shall insert a multiplicative factor 3/2, which is (approximately) the ratio of $\langle S^3/N^3\rangle^{2/3}$ to $\langle S^2/N^2\rangle$ if both source and detector have quadrupole beam patterns ("slow-motion, poor-antenna regime"). This, together with $\langle F_+^2\rangle = \langle F_\times^2\rangle$ and $\langle F_+ F_\times\rangle = 0$ (true for any quadrupole-beam-pattern gravity-wave detector), permits us to write $(S^2/N^2)_{\text{strongest}}$ in the following approximate form, where we omit the subscript "strongest" for ease of notation and where $\langle|\tilde{h}_+|^2+|\tilde{h}_\times|^2\rangle$ is averaged over source angles (ι,β):

$$\frac{S^2}{N^2} \cong 3\langle F_+^2(\theta,\phi,\psi)\rangle \int_0^\infty \frac{\langle |\tilde{h}_+|^2 + |\tilde{h}_\times|^2\rangle}{S_h(f)} df \ . \tag{7.5}$$

We shall now specialize, for the remainder of this section, to gravity-wave searches with broad-band detectors, i.e. detectors for which the noise $S_h(f)$ is small over a band of frequencies $f_{\min} \lesssim f \lesssim f_{\max}$, with $f_{\max} \gtrsim 2f_{\min}$. Narrow-band detectors will be treated separately in Sec. 10.B. For broad-band detectors Eq. (7.5) motivates us to define the characteristic frequency and amplitude of our fiducial source, at distance r_0, by

$$f_c \equiv \left[\int_0^\infty \frac{\langle |\tilde{h}_+|^2 + |\tilde{h}_\times|^2\rangle}{S_h(f)} df\right]^{-1} \left[\int_0^\infty \frac{\langle |\tilde{h}_+|^2 + |\tilde{h}_\times|^2\rangle}{S_h(f)} f df\right] , \tag{7.6a}$$

$$h_c \equiv \left[3\int_0^\infty \frac{S_h(f_c)}{S_h(f)} \langle |\tilde{h}_+|^2 + |\tilde{h}_\times|^2\rangle f df\right]^{1/2} , \tag{7.6b}$$

where the average is over randomly-distributed source orientation angles ι,β. Similarly, we shall define a characteristic detector noise amplitude at frequency f by†

$$h_n(f) \equiv \sqrt{f S_h(f)} \ . \tag{7.7}$$

Note that this noise amplitude describes the detector's rms noise fluctuations in a bandwidth $\Delta f = f$ at frequency f, when the detector is looking at a source with optimal direction and polarization. In terms of these quantities, Eq. (7.5) reads

$$\frac{S}{N} = \frac{h_c}{h_n(f_c)} \langle F_+^2(\theta,\phi,\psi)\rangle^{1/2} \ . \tag{7.8}$$

This is the S/N of the strongest burst that arrives at earth, on average, at the same rate as bursts occur inside the fiducial source's distance r_0.

In Sec. 2.F and Fig. 2.7 we characterized detector burst sensitivities not by $h_n(f)$, but rather by a quantity $h_{3/\mathrm{yr}}$ that answers the following question: *What is the characteristic strength $h_c = h_{3/\mathrm{yr}}$ of a source with*

†In a previous presentation of this material, Thorne (1987), I used a slightly different definition of the detector's noise amplitude. I used $h_n(f) = \sqrt{f S_h(f)}/\langle F_+^2(\theta,\phi,\psi)\rangle^{1/2}$, and, correspondingly, I omitted the factor $\langle F_+^2(\theta,\phi,\psi)\rangle^{1/2}$ from Eq. (7.8); see Eqs. (32) and (33) of Thorne (1987). In this book I have changed the definition of h_n to that of Eq. (7.7) because it has become common for experimenters working on interferometric gravitational-wave detectors to quote their sensitivities in terms of this quantity.

sufficiently large S/N [Eq. (7.8)] that, if it is seen 3 times per year (once each 10^7 seconds) by two identical detectors operating in coincidence, we can be 90% confident the detectors are not just seeing their own noise? The use of two detectors permits the elimination of non-Gaussian noise; see Sec. XXXX. Then the Gaussian distribution of the amplitude noise, together with the use of two detectors and the fact that in $\hat{\tau} = 10^7$ sec the experimenters must try roughly $2\pi f_c \hat{\tau} \simeq f_c/10^{-8}$ Hz starting times t_0 for their Wiener optimal filter, implies that we require $S/N \simeq [\ln(f_c/10^{-8}\text{Hz})]^{1/2} \simeq (3 \text{ to } 5)$. The range 3 to 5 corresponds to the range of frequencies of interest for most burst searches, 10^{-4} Hz to 10^{+4} Hz. Correspondingly, the detector's burst sensitivity is

$$h_{3/\text{yr}} \simeq \left[\ln\left(\frac{f_c}{10^{-8}\text{ Hz}}\right)\right]^{1/2} \frac{[f_c S_h(f_c)]^{1/2}}{\langle F_+^2(\theta,\phi,\psi)\rangle^{1/2}} \simeq (7 \text{ to } 11) h_n(f_c) . \quad (7.9)$$

Here we have used the value $\langle F_+^2(\theta,\phi,\psi)\rangle^{1/2} = 1/\sqrt{5} = 0.447$, which is precisely correct for interferometric detectors [Eq. (11.13)] and approximately correct for the quadrupolar beam pattern of any detector whose size is small compared to the waves' reduced wavelength. The range 7 to 11 in Eq. (7.9) corresponds to the range of frequencies 10^{-4} Hz $\lesssim f_c \lesssim 10^{+4}$ Hz. Note that because the events being sought are so far out on the tail of the Gaussian probability distribution, changing by a factor 10 or 100 the number of trial starting times t_0, or asking for 99% or 99.9% confidence rather than 90%, would have a negligible effect on this $h_{3/\text{yr}}$.

It is often useful to rewrite the f_c and h_c of Eqs. (7.6) in terms of the total gravitational-wave energy per unit frequency dE_{GW}/df emitted by the source. From Eq. (4.33) for the waves' energy flux together with Parseval's theorem we infer that the energy per unit area per unit frequency is

$$\frac{dE_{\text{GW}}}{dA\,df} = \frac{\pi}{2} f^2 (|\tilde{h}_+(f)|^2 + |\tilde{h}_\times(f)|^2) , \quad (7.10)$$

where the extra factor 2 comes from folding negative frequencies into positive (so $f > 0$). When this quantity is integrated over a sphere of radius r_0 surrounding the source, where r_0 is the distance from the source to the earth, it gives

$$\frac{dE_{\text{GW}}}{df} = 2\pi^2 r_0^2 f^2 \langle |\tilde{h}_+(f)|^2 + |\tilde{h}_\times(f)|^2 \rangle ; \quad (7.11)$$

and consequently Eqs. (7.6) become

$$f_c = \left[\int_{-\infty}^{\infty} \frac{dE_{GW}/df}{f S_h(f)} d\ln f\right]^{-1} \left[\int_{-\infty}^{\infty} \frac{dE_{GW}/df}{S_h(f)} d\ln f\right], \tag{7.12a}$$

$$h_c = \left[\int_{-\infty}^{\infty} \frac{S_h(f_c)}{S_h(f)} \frac{3}{2\pi^2 r_0^2} \frac{dE_{GW}}{df} d\ln f\right]^{1/2}. \tag{7.12b}$$

For most burst sources (e.g. supernovae) the waveform is so uncertain that a careful calculation of h_c is unjustified. In such cases it is useful to reexpress h_c [Eq. (7.12b)], approximately, in terms of the total energy radiated, ΔE_{GW}:

$$h_c \simeq \left[\frac{3}{2\pi^2} \frac{\Delta E_{GW}/f_c}{r_0^2}\right]^{1/2} = 2.7\times10^{-20} \left[\frac{\Delta E_{GW}}{M_\odot c^2}\right]^{1/2} \left[\frac{1\text{ kHz}}{f_c}\right]^{1/2} \left[\frac{10\text{ Mpc}}{r_0}\right], \tag{7.13}$$

where $M_\odot$ is the mass of the sun and 10 Mpc is the distance to the center of the Virgo cluster of galaxies (assuming a Hubble constant of 100 km/sec Mpc^{-1}).

When the waveform is well understood but the detector and its spectral density of noise $S_h(f)$ are unspecified, as sometimes will be the case in this chapter, we shall use one of two "standard" spectral densities in our evaluations of the waves' characteristic amplitude h_c. The first of our standard spectral densities is an idealized version of the one appropriate for an interferometric detector in space, Eq. (12.XXXX):

$$S_h(f) = 1 \text{ for } f_{\min} < f < 10 f_{\min} \tag{7.14a}$$

$$= \infty \text{ for } f < f_{\min} \text{ and } f > 10 f_{\min}. \tag{7.14b}$$

Here the noise is large (idealized as infinite) in the region below the cutoff frequency $f_{\min}$ because the detector's test masses there are being shaken severely by nongravitational forces; and it is large (idealized as infinite) above $10 f_{\min}$ because the detector's arm length is larger than a reduced wavelength of the waves it seeks. In the band $f_{\min} < f < 10 f_{\min}$, photon shot noise is the dominant noise source, and it produces a flat $S_h(f)$. The precise value of this flat S_h is irrelevant in Eqs. (7.6) and (7.12) for the source's characteristic frequency f_c and characteristic amplitude h_c; and, accordingly, we have simplified our standard S_h by setting it to unity. We shall call this standard S_h [Eq. (7.14)] the *band-pass spectral density*.

Our second, standard S_h we shall call the *recycling spectral density*

because it is a reasonable idealization for an earth-based interferometric detector with nonresonant recycling of light [Eq. (11.20c), Fig. 11.5, and associated discussion]. As for the band-pass spectral density (7.14), we choose the normalization of our recycling spectral density so as to make it take on an especially simple form:

$$S_h(f) = f_k[1+(f/f_k)^2] \quad \text{for } f > f_{\min} \tag{7.15a}$$

$$= \infty \quad \text{for } f < f_{\min} . \tag{7.15b}$$

Here $f_{\min}$ is a cutoff frequency below which seismic forces severely shake the detector's test masses; and f_k is a "knee frequency" which the experimenters can adjust by changing the reflectivities of certain mirrors in their detector. Notice that the larger is the chosen f_k, the greater will be the bandwidth of the band $f_{\min} < f \lesssim f_k$ in which the noise takes on its minimum value; but also, the larger will be that minimum value. In using the spectral density (7.15) to compute a source's f_c and h_c, we shall adjust the knee frequency f_k in such a way as to maximize $h_c(f_c)$. This, of course, is just what an experimenter would do when searching for waves with a specific, known waveform.

These two standard spectral densities, (7.14) and (7.15), when inserted into Eqs. (7.6) or (7.12), will produce characteristic frequencies and amplitudes that depend on the noise's cutoff frequency $f_{\min}$. The qualitative features of their dependence on $f_{\min}$ are governed by the low-frequency and high-frequency behaviors of the source's waveforms. At high frequencies the waveforms always die out rapidly with increasing frequency; but at low frequencies there can be a variety of behaviors, depending on the early-time and/or late-time behavior of the source (Smarr, 1977b; Bontz and Price, 1979; Wagoner, 1979; KIP: CHECK THESE REFS). Specific examples are shown in Fig. 7.2. The examples include: (a) the gravitational collapse of a rotating stellar core, with the deformation of the core at early times being produced solely by centrifugal forces (Evans, 1989); (b) the free-fall collapse of nonrotating matter (cf. Fig. 1.4); (c): the "memory" of a "burst with memory" (Sec. 7.G), i.e. a net change in h_+ or $h_\times$ between the beginning of the burst and its end; (d): the radiation-reaction-induced inspiral of a binary star system (Sec. 7.D); and (e): the "memory" of a "burst with memory of velocity" (Sec. 7.G), i.e., a long segment, at the beginning or end of the burst, in which h_+ or $h_\times$ varies linearly with time.

It is easy to see from Eqs. (7.6) or (7.12) that, if the waveform goes to zero both at the beginning of the burst and the end [e.g. the waveforms from rotating collapse and free-fall collapse (Fig. 7.2a,b),

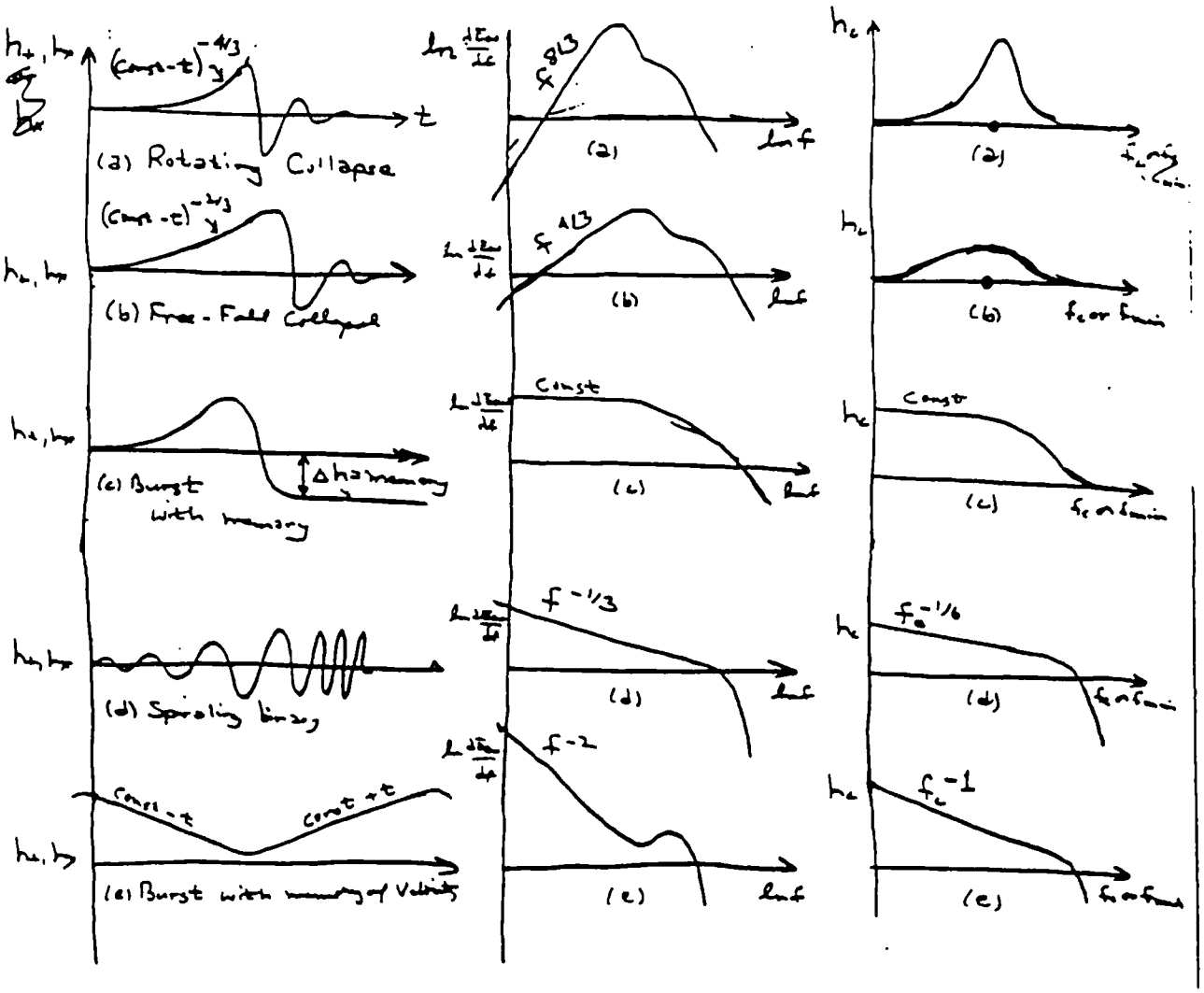

Fig. 7.2 Schematic diagrams showing: (i) five qualitatively different waveforms (left column of diagrams); (ii) their corresponding energy spectra [Eq. (7.11)] (center column of diagrams); and (iii) their characteristic amplitudes h_c [Eq. (7.12b)] as a function of the cutoff frequency $f_{\rm min}$ in the detector's noise spectrum (7.14) or (7.15), or equally well as a function of the waves' characteristic frequency f_c [Eq. (7.12a)] (right column of diagrams).

and the generic, axisymmetric supernova waveform (Fig. 7.4 below)], then dE_{GW}/df will go to zero at low frequencies (as it does at high), and there will be a specific value of the noise's cutoff frequency f_{min} that maximizes the characteristic amplitude h_c. See the large dots in the right-hand segments of Figs. 7.2a,b. In such cases it is reasonable to characterize the waveform by just two numbers: its maximum value of h_c and the corresponding f_c. If, instead, the waveform goes to different constant values at its beginning and end, i.e. if the burst has a memory as in Fig. 7.2c, then dE_{GW}/df will approach a constant at low frequencies; and for f_{min} in the low-frequency region, h_c will be independent of f_{min}. In this case there might be no value of the cutoff f_{min} that produces a maximum h_c. Then it is reasonable to characterize the waveform by the function $h_c(f_c)$, with f_c varying continuously because f_{min} varies continuously; see right segment of Fig. 7.2c. In cases where dE_{GW}/df grows with decreasing frequency (e.g. the inspiraling binary in Fig. 7.2d, and the burst with memory of velocity in Fig. 7.2e), the characteristic amplitude h_c will grow with decreasing f_{min}; and, again, it will be appropriate to characterize the burst by a function $h_c(f_c)$.

We turn now to a discussion of specific burst sources, and their characteristic frequencies f_c and amplitudes h_c.

7.B Supernovae (collapse to neutron star)

Supernovae of "type II" are believed, with a high level of confidence, to be created by the gravitational collapse, to a neutron-star state, of the cores of massive, highly evolved stars. Supernovae of "type I", by constrast, are thought to result from nuclear explosions of white dwarfs that are accreting mass from close companions — explosions in which the stellar core probably does not collapse to a neutron-star state. In addition to these two types of optically observed supernovae, theoretical models suggest that there may be many stellar collapses to a neutron star that produce little optical display ("optically silent supernovae"), and that some accreting white dwarfs in close binaries might implode to form neutron stars. For details and references see, e.g., Woosley and Weaver (1986); Evans, Iben, and Smarr (1987); and Iben (1988); Grindley and Bailyn (1989) [KIP CHECK].

The rate of occurrence of supernovae of types I and II is fairly well determined observationally; see, e.g. Tammann (1981). In our Galaxy, there is roughly one type I each 40 years and one type II each 40 years (though, because interstellar dust obscures nearly 90 percent of the

Chanmugam and Brecher (1985)

galaxy to view by optical telescopes, supernovae are discovered optically in our galaxy only once every several hundred years). Out to the distance of the center of the Virgo Cluster of Galaxies (10 Mpc), there are several type I and several type II supernovae per year. Near and beyond Virgo, the rate increases roughly as (distance)^3; but between earth and Virgo it increases much more slowly than that. Thus, to have an interesting event rate one must have adequate sensitivity to reach the center of Virgo, about 10 Mpc.

Optically silent supernovae could be as much as 10 times more frequent than the optically observed supernovae: Statistics on normal stars massive enough to form neutron stars when they die permit a neutron-star birth rate that could be as high as one each 4 years in our galaxy, if mass loss in the late stages of stellar evolution is smaller than normally thought. [KIP: CHECK. GIVE REFS] However, negative results in searches for bursts of neutrinos from optically silent supernovae suggest that there have been no such supernovae in our galaxy in the past ten years (Bahcall and Piran, XXXX), and it is conceivable that optically silent supernovae never occur.

The strengths of the gravitational waves from a supernova depend crucially on the degree of nonsphericity in the stellar collapse that triggers it, and depend strongly on the speed of collapse [i.e. on whether the collapse is nearly free-fall ("cold collapse") or is more gentle due to the resistance of thermal pressure ("hot collapse")]. See Eardley (1983), Finn (1988, 1989), and references therein.

Perfectly spherical collapse will produce no waves; highly nonspherical collapse will produce strong waves. Little is known about the degree of nonsphericity in type II supernovae (which are surely due to stellar collapse); but prejudice, until recently, suggested that the typical type II might be quite spherical and thus poorly radiating. That prejudice has been shaken by the apparent discovery (Middleditch et. al., 1989), in the remnant of the type II supernova 1987A, of a pulsar with a time interval between pulses of 0.507968 milliseconds. This interval is so extremely short that, if it is the rotational period of the remnant neutron star, then the imploding stellar core must have been driven highly nonspherical by centrifugal forces. Another possibility for large nonsphericity is the death of an accreting white dwarf in a binary system. If such white dwarfs sometimes die by collapse rather than always being disrupted by nuclear explosions, then the collapsing white dwarf will probably rotate rapidly due to the accretion, and centrifugal forces will make it highly nonspherical.

In the mid 1970s it became clear that neutral currents, in the theory of the weak interaction, should produce fairly strong coupling of neutrinos to the matter of a collapsing stellar core [KIP: CHECK – IS IT REALLY THE NEUTRAL CURRENTS?]; and, as a result, neutrinos should not be able to escape freely from the core and thus cannot carry off the heat produced by the core's compression. As a result, there was a swing of fashion away from believing that the collapse which triggers a type II supernova is cold and fast to believing it is hot and (because of the thermal pressure) slow; see, e.g., Wilson (1974) and Schramm and Arnett (1975). Some astrophysicists were aghast at the consequences of this swing: for example, in the highly nonspherical but axisymmetric collapse models of Saenz and Shapiro (1978, their tables 1–4), the maximum energy radiated as gravitational waves was reduced from $\Delta E_{GW}/M_\odot c^2 \sim 6\times10^{-3}$ for cold and fast to $\sim 1\times10^{-5}$ for hot and slow. This boded very ill for attempts to detect gravitational waves, the astrophysicists thought. However, closer scrutiny revealed relatively little change in the prospects for detection: The total energy radiated, ΔE_{GW}, is a rather poor indicator of detectability. Much more relevant is the amplitude signal-to-noise ratio $S/N \propto h_c/h_n(f_c)$ [Eq. (7.8)]. The planned full-scale interferometric detectors, when optimized for frequency f_c, have $h_n(f_c) \propto f_c$ [Fig.2.7 and Eq. (11.28a)], and this together with Eq. (7.13) gives

$$S/N \propto (\Delta E_{GW}/f_c^{\,3})^{1/2} . \tag{7.16}$$

Although the new fashion (hot and slow) corresponded to a reduction in ΔE_{GW} by a factor 600, the characteristic frequency of the waves also went down (from $\simeq$3000 Hz to $\simeq$500 Hz; see Saenz and Shapiro, 1978), and correspondingly S/N was reduced by less than a factor 2.

This illustrates the importance of thinking in terms of h_c, f_c, and $S/N \propto h_c/h_n(f_c)$, rather than in terms of energy radiated, when evaluating the detectability of gravitational waves.

A large amount of effort has gone into model calculations of gravitational collapse to a neutron star and the waves it emits; but the effort has not produced a consensus by any means! For a detailed review of the literature up to 1982 see Eardley (1983); for updates on that review see Müller (1984) and Finn (1988, 1989). In the case of rapidly rotating collapse, where the emission should be strongest but the event rate is totally unknown (most collapses *could* be slowly rotating), there is a possibility of three radically different scenarios with qualitatively different waveforms: axisymmetric collapse, triaxial collapse, and

fragmented collapse.

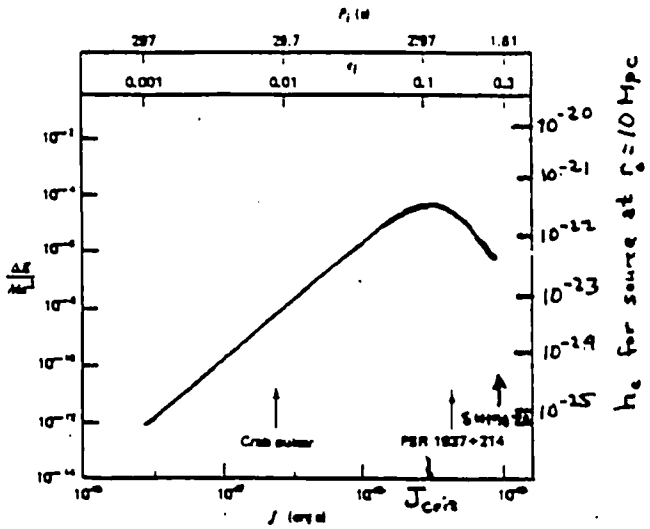

Fig. 7.3 The strengths of the gravitational waves from the axisymmetric collapse and bounce of a rotating, $0.8 M_\odot$ stellar core, as computed by Saenz and Shapiro (1981). The wave strength, plotted vertically, is characterized on the left side by the total energy emitted as gravitational waves in units of the star's rest mass–energy, and on the right side by the waves' characteristic amplitude. These wave strengths are shown as functions of the angular momentum J of the core, plotted horizontally at the bottom of the figure. The arrows indicate the estimated angular momenta of the Crab pulsar, the "millisecond pulsar" PSR 1937+214, and the pulsar remnant of supernova 1987A assuming that its rotation period is 0.507968 milliseconds as suggested by optical observations (Middleditch et. al., 1989). Plotted at the figure's top are the initial rotation period P_i and eccentricity e_i of the stellar core just before collapse begins, when the core's radius is XXXXX. For this one–parameter sequence of models, the characteristic frequency was approximately 500 Hz, independently of the angular momentum. [KIP CHECK] The models were idealized, homogeneous spheroids, with a realistic, "hot" nuclear equation of state and neutrino trapping and transport. The radiation shown is solely from the infall and first bounce. The amount of radiation from subsequent neutron–star pulsations is unknown, but may well be less than that from the infall and first bounce; see text. [Figure adapted from XXXXXX]

a. Axisymmetric collapse

If the stellar core remains axisymmetric throughout its collapse, then the details of the collapse and gravitational waves are very sensitive to the core's total angular momentum J. As was first shown by Shapiro (1977), there is a critical value of the angular momentum, J_{crit}, which gives rise to the strongest gravitational waves; see Fig. 7.3. For $J \ll J_{crit}$, centrifugal forces are weak, the star does not become

strongly flattened during its collapse, and therefore the waves are weak. For $J \gg J_{crit}$, centrifugal forces become strong so soon that they greatly slow the collapse before it reaches nuclear density, thereby (if the core remains axisymmetric) weakening the waves. For $J \sim J_{crit}$, centrifugal forces cause strong deformation just as the core is nearing nuclear densities; and the waves are strong.

When $J \lesssim J_{crit}$, the computed waveforms have time dependences and spectra that are qualitatively like those of Fig. 7.4. It is instructive (Finn, 1989), to divide these waveforms into three stages: infall, bounce, and ringdown.

The infall waveform is produced by the imploding core before it reaches nuclear density. The time dependence of the infall waveform is $h_+(t) \propto (\text{const}-t)^{-4/3}$ if the deformation is produced solely by centrifugal flattening (Evans, 1989), and $h_+(t) \propto (\text{const}-t)^{-2/3}$ if the deformation is due, instead, to nonspherical perturbations that are amplified by free-fall collapse. The waves from the infall stage were first computed, in the approximation of vanishing pressure, by Thuan and Ostriker (1974) using Newtonian theory for the star's internal gravity, and then by Epstein and Wagoner (1975) and Epstein (1976a,b) using post-Newtonian gravity. The effects of pressure were first considered by Novikov (1975).

Novikov (1975) showed that the sharp reversal of the core's implosion when it reaches nuclear density (i.e. the core's "bounce") will typically produce stronger gravitational waves than the infall. The strength of the bounce waves will depend on the sharpness of the bounce, and on the compactness of the core at bounce, and these in turn are very sensitive to the equation of state, to the trapping of neutrinos in the bouncing core, and to general relativistic effects (Shapiro, 1977; Saenz and Shapiro, 1978, 1979, 1981; Evans, 1984).

The ringdown waves in Fig. 7.4 are produced by pulsations of the newborn neutron star. If the neutron star were surrounded by vacuum, its pulsations could have a high Q (many periods of pulsation before they die away). However, the newborn neutron star is surrounded by a moderately dense, still imploding envelope; and its pulsations drive sound waves into this envelope with a resulting loss of pulsation energy. Eardley (1983) quantifies the total amount of pulsation by a parameter

$$X \equiv \left| \int dR/R \right| = \sum |\Delta \ln R| \text{ , added up over all cycles of pulsation,} \quad (7.17)$$

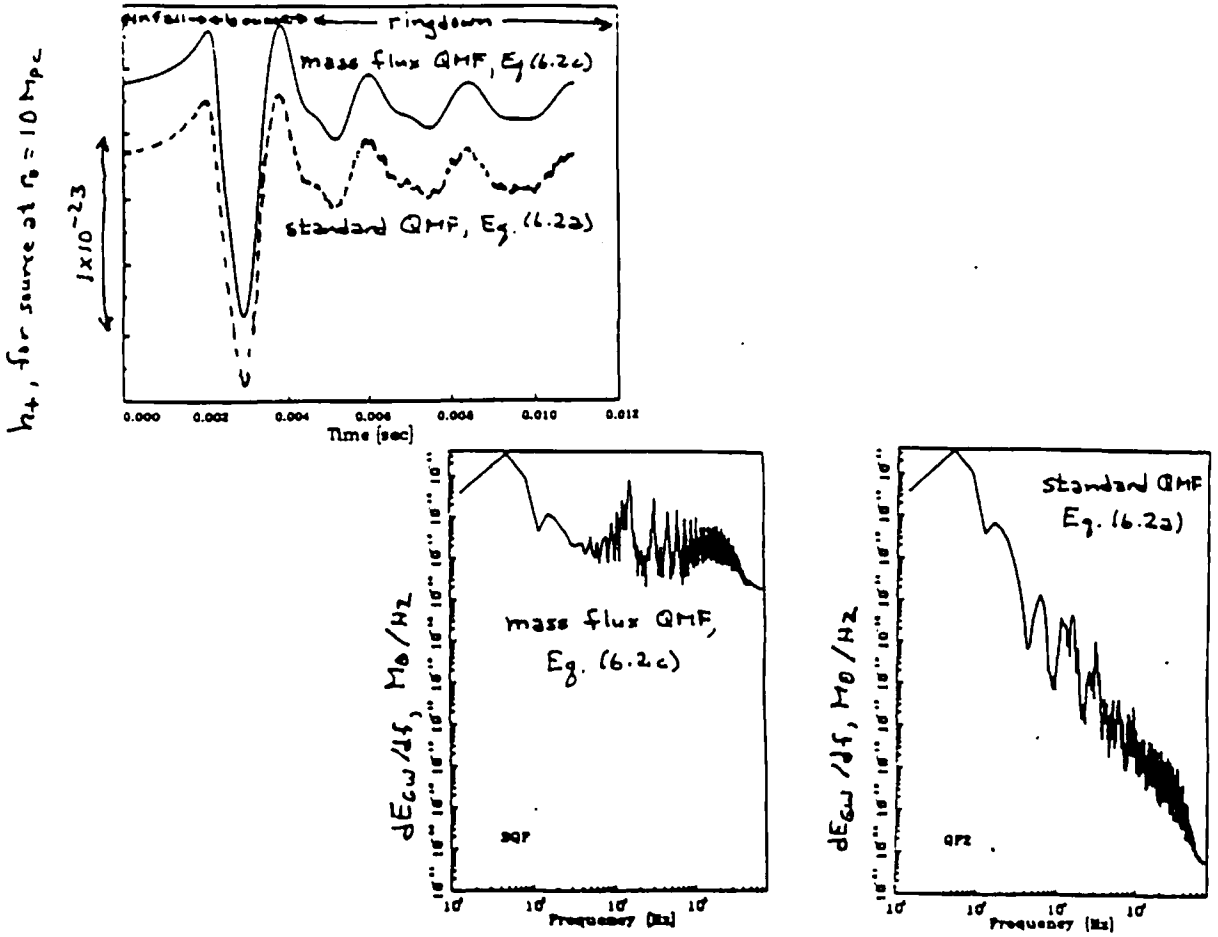

Fig. 7.4 A gravitational waveform from the axisymmetric gravitational collapse of a rotating stellar core, and the spectrum of the emitted energy, as computed by Finn and Evans (1989). The waveform (top diagram) is divided into three phases: infall, bounce, and ringdown. The waveform was computed in two different ways (solid curve and dashed curve), from the same density and velocity data produced by a two-dimensional, Newtonian simulation of the collapse. Both computations of the waveform were based on the quadrupole formalism of Sec. 6.A. The solid waveform, which is thought to be quite accurate, used the mass-flux formula (6.2c) for the second time derivative of the quadrupole moment. [KIP: SWITCH TO STRESS?] The dashed waveform (which is displaced downward from its true position so its details will not be hidden by the solid waveform) is based on the standard formula (6.2a) for the quadrupole moment. The two numerical time derivatives that are required to get the waveform h_+ [Eq. (6.XX)] from the standard formula (6.2a) produce artificial, high-frequency noise in the dashed waveform. That noise in turn produces severe errors in the standard formula's energy spectrum at frequencies above 2000 Hz (lower right-hand diagram). The astrophysical details included in this collapse simulation are not fully realistic, and thus the details of the waveform are not to be believed. This figure merely serves to illustrate the three waveform stages (infall, bounce, and ringdown), and the pitfalls of blindly applying the standard quadrupole moment formula in numerical calculations. [Figure adapted from Finn and Evans (1989)]

where R is the neutron star's radius and $\Delta \ln R$ is the amplitude of a given cycle of pulsation; and he argues, on the basis of work by Wilson (1980) and by Brown, Bethe, and Baym (1982), that damping due to sound-wave emission *may* make X be $\lesssim 1$. This is sufficiently small that: (i) although nonsphericities can be amplified by the stellar pulsations (Saenz and Shapiro, 1978, 1979, 1981; Norman and Wilson, 1979; Clark, 1979; Eardley, 1983), the amplification factor is $\lesssim 3$; (ii) the contribution of the ringdown to the characteristic amplitude h_c is likely to be less than the contribution of the initial bounce; and (iii) a waveform of the sort shown in Fig. 1.4 should be strongly modified by the sound-wave damping that was left out of its simulations. However, these conclusions, like almost all current wisdom about gravitational waves from supernovae, must be regarded as only tentative.

The characteristic amplitude and frequency of the gravitational waves from axisymmetric collapse are highly uncertain. Saenz and Shapiro (1978, 1979, 1981) have carried out the most detailed study of the effects on h_c and f_c of various input physics (the star's mass, angular momentum, equation of state, neutrino transport, etc.) Their study was thorough at the price of idealizing the collapsing stellar core to be an ellipsoidally shaped, homogeneous-density body, and thereby converting the partial differential equations that govern the collapse into ordinary differential equations. This idealization is so severe that the Saenz-Shapiro results must be regarded as only a first, crude survey. Figure 7.3 is indicative of their results: for the most realistic input physics, the characteristic frequency is $f_c \simeq 500\,\mathrm{Hz}$, and the characteristic amplitude for $J \sim J_{\mathrm{crit}}$ is $h_c \simeq (\text{several}) \times 10^{-22} (10\,\mathrm{Mpc}/r_o)$.

It is now possible to do two-dimensional (i.e. two space dimensions plus one time dimension) hydrodynamic simulations of the core collapse, and thereby gain more reliable insight into the gravitational radiation. The first such simulations, carried out by Hillebrandt and Müller (1981), and Müller (1982) using Newtonian theory and the quadrupole moment formualism, suggest that, for $J \sim J_{\mathrm{crit}}$, f_c might be 1000 Hz rather than 500, and h_c might be an order of magnitude smaller than estimated by Saenz and Shapiro. [KIP: CHECK] However, only a few models were computed by Hillebrandt and Müller, and their calculated waveforms appear to be plagued by the kind of numerical difficulties illustrated in the dashed curves of Fig. 7.4. Thus, definitive conclusions must await further, more extensive calculations. Such calculations are now underway using Newtonian theory and the quadrupole moment formalism (Finn, 1988, 1989). Techniques for similar

post-Newtonian computations are also being developed (Sec. 6.I), as are techniques for fully general relativistic, numerical-relativity calculations (Sec. 6.K).

b. Triaxial collapse

In the case of a rapidly rotating stellar core, $J \gtrsim J_{\rm crit}$, centrifugal forces might make the core unstable to an "$m=2$, bar-mode" deformation, so it rotates end-over-end like a punted American football. In other words, the collapsing star might develop a triaxial shape, with different diameters along its three axes, and with rapid rotation about one of the shorter axes. It seems fairly certain that the waves in this case will be much stronger than for axisymmetric collapse. Calculations by Ipser and Managan (1984) [KIP: WHAT METHOD?; CHECK THEIR PREDICTIONS; ALSO CITE SAENZ???] predict a highly monochromatic emission at $f \sim 1000$ Hz, lasting for ~30 cycles and producing $\Delta E_{\rm GW} \sim 3\times10^{-4} M_\odot c^2$ and $h_c \sim 5\times10^{-22}(10\,{\rm Mpc}/r_o)$. However, these calculations are only a first, crude survey of the problem. Extensive research is needed to determine whether the bar-mode instability sets in at all, and if so, just how correct these estimates are.

c. Fragmented collapse

If it is rotating very rapidly, the collapsing star may become so strongly unstable to nonaxisymmetric perturbations that on the way down it fragments into two or more discrete lumps (Ruffini and Wheeler, 1971). Even less is known about this possibility than about triaxial collapse. Radiation reaction from triaxial collapse might prevent fragmentation from occurring at all (Ipser, 1986). If the star does fragment, and if it forms just two discrete objects, then the resulting waveform should be similar to the final stages of the coalescence of a neutron-star binary (Sec. 7.D below and Fig. 1.5 above). On the basis of this similarity, Eardley (1983) argues that the resulting waves will be quite strong: $\Delta E_{\rm GW} \sim ({\rm a\ few})\times10^{-2} M_\odot c^2$ at $f_c \sim 1000$ Hz, corresponding to $h_c \sim ({\rm a\ few})\times10^{-21}(10\,{\rm Mpc}/r_o)$.

Nakamura and Fukugita (1989) and Nakamura (1989) have suggested that fragmentation occurred in the collapsing core of supernova 1987A, and have constructed a semiquantitative model of the details of the fragmentation and its consequences for gravitational-wave emission, neutrino emission, and asymmetries of the supernova remnant. Their model is able to explain several peculiar (but not 100 per cent firm) observed features of SN1987A, including: the apparent rapid

rotation of the final neutron star; the existence of two bursts of neutrinos, 9 seconds apart; and the apparent formation of a Jupiter-sized object in orbit around the neutron star. In their model the collapsing core had a mass of roughly $1.5\,M_\odot$ and an angular momentum $J \simeq 6\times10^{49}$ g cm^2 sec^{-1}, so that J was somewhat larger than $J_{\rm crit}$ [KIP: CHECK] and $J/M^2 \simeq 3$. They argue that such a rotation might be fairly common for pre-supernova stars. The core of their model star collapses nearly spherically to a radius $r \sim 100$ km, at which point its central regions have reached nuclear density and emit the first burst of neutrinos, and centrifugal forces halt its equator's collapse. In the next ~0.5 sec the polar regions collapse on inward to form a centrifugally flattened disk 20 km thick and 100 km in radius. The disk then fragments into two (or possibly three) smaller-mass neutron stars, which orbit each other, spiraling inward under the driving force of gravitational radiation reaction. During a time of ~5 to 10 sec the stars spiral together, emitting gravitational waves that sweep upward in frequency from 70 Hz toward 1 kHz; and they then coalesce with a final burst of gravitatonal waves and neutrinos. At the distance of supernova 1987A (the large Magellanic cloud, 50 kpc), the characteristic amplitude of the waves from the inspiral phase would have been $h_c \sim 4\times10^{-19}$; see Fig. 2.7.

d. Conclusions

Because the above estimates of h_c and f_c for the three scenarios (axisymmetric collapse, triaxial collapse, and fragmented collapse) are so insecure, Fig. 2.7 shows wave strengths based not on these estimates, but rather on the approximate equation (7.13). More specifically, the characteristic amplitude h_c is shown as a function of the unknown characteristic frequency f_c for the entire range of f_c that has shown up in model calculations, 200 Hz $\lesssim f_c \lesssim$ 10000 Hz. Separate curves are shown for several plausible values of the total energy radiated as gravitational waves, $\Delta E_{\rm GW}$, and the source's distance r_o. Notice from Fig. 2.7 that detectability by interferometers depends strongly on whether the waves come off at low frequencies or high: A factor 8 reduction in $\Delta E_{\rm GW}$ can be compensated by a factor 2 reduction in f_c.

Corresponding to our poor knowledge of the strengths of the waves from supernovae is a similar poor knowledge of the waveforms. It seems unlikely that theorists will be able to firm up their predictions of the waveforms before observers detect and study them. Thus, it is best to think of the computed waveforms (e.g. Saenz and Shapiro, 1978,

1981; Beltrami and Chau, 1986; Figs. 1.4 and 7.4 of this book) not as predicting what observers will see, but rather as giving us a tool for translating future observations into an understanding of what is happening in the stellar core.

We note in passing that neutron-star pulsations might be excited not only as part of the star's birth throes, but also as a consequence of a sudden strain release or phase transition in an old neutron star (Thorne 1978, Ramaty et. al. 1980, Haensel, Zdunik, and Schaeffer 1986). Since there are 10^8 to 10^9 old neutron stars in our galaxy, it is conceivable — though not highly likely — that our galaxy could produce an interesting event rate. To be detectable by full-scale interferometric detectors (Fig. 2.7), the waves would need to have $h_c \gtrsim 10^{-21}$ at $f_c \sim 3000$ Hz, corresponding to

$$\Delta E_{GW} \gtrsim 7\times10^{45}\text{ergs} \times (r_0/10\text{ kpc})^2 . \qquad (7.18)$$

7.C Collapse of a star or star cluster to form a black hole

As with collapse to form a neutron star, so also for collapse to a black hole, the strengths of the waves produced are highly sensitive to the degree of nonsphericity, and the typical degree of nonsphericity is unknown. Equally unknown in the black-hole case, by contrast with the neutron-star, is the frequency of occurrence of such collapses:

It is very likely that black holes exist in our universe with masses throughout the range $2M_\odot \lesssim M \lesssim 10^{10}M_\odot$ (Blandford, 1987). The holes of lowest mass can only form by direct collapse of a star. Those of higher mass, however, can form by many routes (direct collapse; gradual growth from a small hole by accretion; collision and coalescence of smaller holes; ...). For discussions of the routes that might occur in a dense galactic nucleus see Blandford (1979) and Rees (1983). Which routes actually occur and how often are almost totally unknown. However, roughly known upper limits on the birth rates of the smallest and the largest holes give — under the assumption that all births are by direct collapse — corresponding upper limits on the rate at which gravitational-wave bursts from such collapses hit the earth. For holes of a few solar masses the birth rate under reasonable assumptions (Sec. 3.3 of Blandford, 1987) should not exceed $\sim\frac{1}{3}$ the birth rate of neutron stars; and correspondingly, at the distance of the Virgo cluster, it should not exceed ~1/year. Bethe (1986) argues that the rate may actually be of this magnitude. At the other end of the spectrum, holes with masses $M \gtrsim 10^6 M_\odot$ probably occur only in galactic nuclei; and

over its lifetime each galactic nucleus might give birth, at maximum, to only a few such holes. Correspondingly (Thorne and Braginsky, 1976; Blandford, 1979), the maximum rate of collapse–births of supermassive holes, $M \gtrsim 10^6 M_\odot$, is a few per year throughout the observable universe — i.e. out to the Hubble distance. It is fashionable to believe that the actual rate is much less than this upper limit (e.g. Rees, 1983).

In one respect, collapse to a black hole is better understood than collapse to a neutron star: The final object is far simpler, and correspondingly the waves from its vibrations, if they are triggered by the collapse, are far better understood. Detailed calculations suggest, in fact, that black-hole vibrations are rather easy to trigger (e.g. Detweiler, 1977; Sun and Price, 1988) and that when they are triggered, the most slowly damped one or two quadrupole modes will dominate.

The waves from a given normal mode, have the form of a damped sinusoid

$$(h_+ \text{ and } h_\times) \propto \cos(2\pi f t + \text{const}) e^{-t/\tau} , \qquad (7.19)$$

with the damping caused by the flow of gravitational-wave energy down the hole and off to infinity. For a rotating black hole the frequency f and damping time τ of each normal mode, like all other properties of the hole, are determined fully by the hole's mass M and angular momentum J. It is conventional to characterize the hole by M and the dimensionless angular momentum parameter $a \equiv J^2/M$, rather than by M and J, and to characterize each mode by f and its dimensionless quality factor $Q \equiv \pi f \tau$ rather than by f and τ. Then on dimensional grounds, $f \times M$ and Q must be functions of the angular momentum parameter only. Figure 7.5 shows that functional dependence for the two most weakly damped quadrupole ($l=2$) modes, as computed by Detweiler (1980) and more accurately by Leaver (1985a,b) using the perturbation formalism of Sec. 6.J. Notice the rotationally induced splitting of each of these modes into five components with quantum numbers $m=-2,-1,0,1,2$; and notice the fact that the $m=2$ component of the lowest $l=2$ mode has a Q that becomes arbitrarily large as the hole approaches the fastest rotation rate, $a=1$, allowed by general relativity theory. This high Q makes it likely that, for very rapidly rotating holes, the $l=m=2$ mode will dominate the pulsations after the first few cycles. Echeverria (1989) has given the following approximate analytical fit to the frequency and quality factor of this mode:

$$f_{2,2} \simeq XXXXX , \qquad Q_{2,2} \simeq XXXXXXX . \qquad (7.20)$$

Fig. 7.5. The pulsation frequency f and quality factor $Q \equiv \pi f \tau$ (where τ is the amplitude damping time) for the lowest two quadrupole modes ($l=2$), as functions of the hole's angular momentum parameter a. These graphs are based on calculations by Detweiler (1980) and Leaver (1985a,b).

Return to the issue of the gravitational waves from the collapse of a star or star cluster to form a black hole. While the details of the initial burst of waves may depend on unknown details of the collapse, the late-time behavior will have a damped oscillatory form ("ringdown") dominated by one or several modes. Since the frequency and Q of each mode are unique functions of the hole's mass and angular momentum, from the final ringdown waves one can hope to get information about the mass and angular momentum (Detweiler, 1980; Leaver, 1985a,b; Stark and Piran, 1986; Piran and Stark, 1986; Echeverria, 1989).

As a specific example, Fig. 7.6 shows the waves produced by a specific model of a collapsing, rotating star as computed using numerical relativity techniques (Sec. 6.K) by Stark and Piran (1986). The solid curve is the computed waveform, and the dashed curve is a fit to it using a mixture of the two most weakly damped quadrupole modes of a nonrotating hole. The fact that the fit is so good shows: (i) that the final ringdown is, indeed, due to the black-hole vibrations; and (ii) that the hole was not rotating extremely rapidly, i.e. it had $(1-a) \gtrsim 0.3$. If the hole had had $1-a < 0.3$, the "Q" of the hole's oscillations would have been noticeably larger, and the ringdown of the waves would have been noticeably slower. (For details of the normal modes of black holes

Fig. 7.6 The gravitational waveform produced by the gravitational collapse of an axisymmetric rotating star to produce a Kerr black hole, as computed by Piran and Stark (1986) using numerical relativity techniques. The star and the black hole it forms both have $J/M^2 \equiv a = 0.63$ (where J is angular momentum and M is mass). The dashed curve is a fit, to the waveform, of a superposition of the waves from the two most slowly damped quadrupolar normal modes of a nonrotating hole with mass M: $h_+ \sim \text{Real}\{A_1 e^{-i\omega_1 t} + A_2 e^{-i\omega_2 t}\}$ and with $\omega_1 = (0.374 - 0.089i)/M$, $\omega_2 = (0.348 - 0.274i)/M$. The fitting amplitudes are $A_1 = -0.9 - 1.1i$, $A_2 = 0.9 + 1.4i$. Thus, these two modes are roughly equally excited by the collapse.

and the frequencies and damping times of the waves they should produce see Detweiler, 1980 and Leaver, 1985a,b. For "WKB" methods of computing the normal modes and their waves see Ferrari and Mashhoon, 1984, Iyer and Will, 1987, and Iyer, 1987.)

Echeverria (1989) has evaluated the accuracy ΔM and Δa with which the hole's mass M and angular momentum $J = Ma^2$ can be determined from the ringdown waves using an interferometric detector (or any other detector) whose noise is white [$S_h(f)$ = constant] in the frequency band of the hole's vibrations. Echeverria's analysis is confined to the special case where only the most slowly damped, $l = m = 2$ mode is excited. (This is likely to be the case for a hole formed by the coalescence of a black-hole or neutron-star binary system; see the next section.) In this case he finds for the one-standard-deviation accuracies

$$\frac{\Delta M}{M} \simeq 2.1 \frac{\sqrt{1-a}}{S/N}, \quad \Delta a \simeq 6.1 \frac{1-a}{S/N}, \tag{7.21}$$

where S/N is the signal-to-noise ratio at the output of an optimal filter for the ringdown waves [Eq. (7.4)], and the formulae are valid only for $S/N \gtrsim 10$. Thus, the hole's mass can be determined rather well, and its angular momentum less well unless the hole is rapidly rotating, $1-a \lesssim 0.1$. (No hole can ever rotate more rapidly than $a = 1$; see Israel, 1986).

If collapse to a black hole radiates with an efficiency $\Delta E_{GW}/Mc^2 \equiv \varepsilon$ and the hole is at a distance r_0 and has a mass M, then the characteristic frequency and amplitude of its waves will be (Stark and Piran, 1986; Piran and Stark, 1986; and Eq. (7.13) above)

$$f_c \simeq \frac{1}{5\pi M} = (1.3\times10^4\ \text{Hz})\left(\frac{M_\odot}{M}\right), \tag{7.22a}$$

$$h_c \simeq \left(\frac{15}{2\pi}\varepsilon\right)^{1/2}\frac{M}{r_0} = 7\times10^{-22}\left(\frac{\varepsilon}{0.01}\right)^{1/2}\left(\frac{M}{M_\odot}\right)\left(\frac{10\ \text{Mpc}}{r_0}\right)$$

$$= 1.0\times10^{-20}\left(\frac{\varepsilon}{0.01}\right)^{1/2}\left(\frac{10^3\ \text{Hz}}{f_c}\right)\left(\frac{10\ \text{Mpc}}{r_0}\right). \tag{7.22b}$$

If the collapse is axisymmetric, then the efficiency ε probably does not exceed 7×10^{-4} (Stark and Piran, 1986). However, in the nonaxisymmetric case (triaxial collapse or fragmented collapse, see previous section), the efficiency might be in the range 0.01 to 0.1 (see, e.g., Eardley, 1983 and Rees, 1983). The source characteristics (7.22) are shown in Fig. 2.7 for black-hole births at the Hubble distance and at the distance of Virgo, with efficiencies $\varepsilon = 10^{-2}$ and 10^{-4}.

7.D Coalescence of neutron-star and black-hole binaries

Nearly half of all stars are in close binary systems. Thus, remnants of stellar evolution may contain a significant number of binaries whose components are neutron stars or black holes, and are close enough together to be driven into coalescence by gravitational radiation reaction in a time less than the age of the universe. The binary pulsar PSR1913+16 is an example of such a system; it will coalesce 3.5×10^8 years from now (Hulse and Taylor, 1975). A second example is PSR0021-72A, a recently discovered binary pulsar in the globular cluster 47 Tuc (Ables, 1989), which will coalesce in about 10^6 years. [KIP: CHECK!! ALSO CHECK THE RECENT CALTECH BINARY PULSAR]

As the two bodies in a compact binary spiral together, they emit periodic gravitational waves with a frequency that sweeps upward

toward a maximum,

$$f_{\max} \sim (1 \text{ to } 4)\ \text{kHz} \quad \text{for neutron stars}, \tag{7.23a}$$

$$f_{\max} \sim \frac{10\ \text{kHz}}{M_1/M_\odot} \quad \text{for holes with the larger having mass } M_1 . \tag{7.23b}$$

More than 20 years ago, before pulsars had been discovered, Forward and Berman (1967) identified the coalescence of neutron-star binaries as a promising source of gravitational waves for earth-based detectors to seek, and identified this frequency sweep as a key characteristic of its waves.

During the early part of the frequency sweep, the stars or holes hardly feel each others' tidal gravitational fields at all, and they thus remain nearly spherical. We shall call this the "inspiral" stage. During the final, "coalescence stage", the stars or holes deform each other gravitationally and then merge. We shall consider these two stages in the following two subsections, coalescence first.

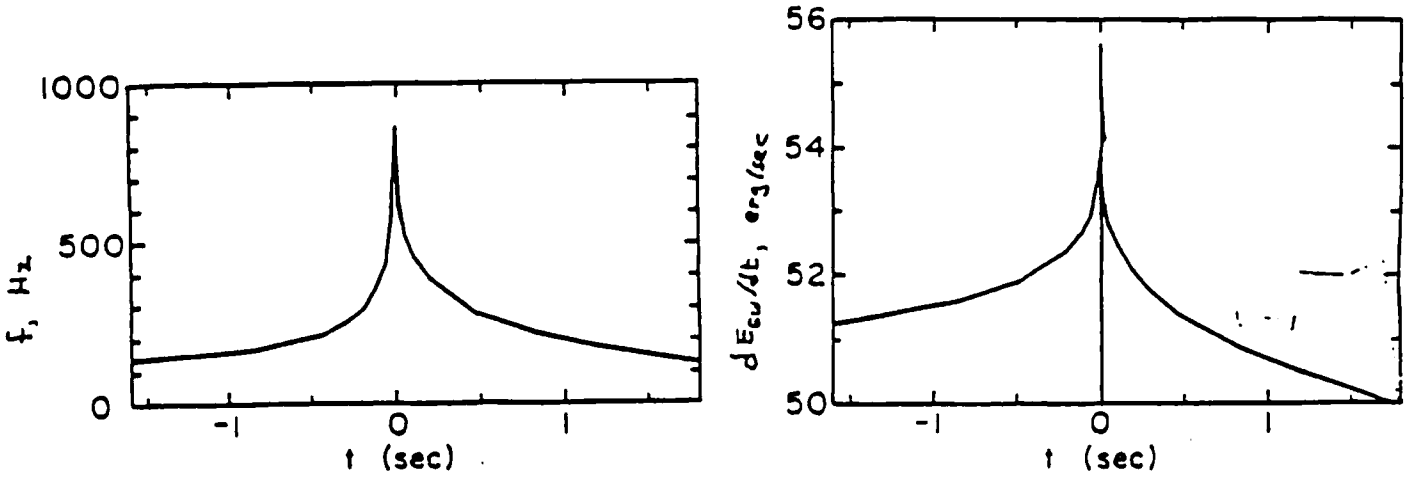

Fig. 7.7 The time evolution of the freqency f and power dE_{GW}/dt of the gravitational waves produced by the coalescence of a neutron-star binary, as computed by Clark and Eardley (1977). The stars' initial masses are $1.3M_\odot$ and $0.8M_\odot$. The reversal of the frequency sweep is caused by tidally-induced mass transfer from the less massive, secondary star to the more massive, primary star. [Figure adapted from Clark and Eardley (1977)]

a. Coalescence stage

The final, coalescence stage will be especially interesting and complex in the case of a neutron-star binary, and will be quite sensitive to the masses of the two stars. As with supernovae, we might not understand reliably what to expect until gravitational-wave observations show us.

A first, preliminary study of the coalescence stage of a neutron-star binary was carried out, using analytic estimates, [KIP: CHECK, AND CHECK DETAILS. ALSO LOOK AT BENZ ET AL (1989) FOR A RECENT SIMULATION] by Clark and Eardley (1977). They showed that, when the stars' masses are substantially different, the "secondary" star (i.e. the less massive one, which has the larger radius) is more strongly deformed, tidally, than the "primary" (more massive) star. As the stars near each other, the secondary's deformations grow larger and larger, until ultimately the primary starts pulling matter off it. This mass transfer slows, and then halts the orbital decay, and halts and reverses the upward sweep of the gravitational-wave frequency; see Fig. 7.7. Depending on the original masses and spin angular momenta of the two stars, the smaller one may be completely disrupted and form an axisymmetric disk around the larger one, or it may lose mass, retaining its identity, until it is driven below the minimum mass for a neutron star, at which point it explodes (Oppenheimer and Serber, 1938; Blinnikov et. al., 1984). The final burst of gravitational waves will be strongly influenced by which of these two fates befalls the secondary — and, correspondingly, gravitational-wave observations could reveal the fate. The waves may also be influenced by coupling of the stars' orbital motion to their quadrupolar normal modes of vibration (Kojima, 1987). The final coalescence may also be accompanied by bursts of neutrinos and gamma rays, and ejection of r-process atomic nuclei into interstellar space (Eichler et. al., 1989).

This expected evolution for neutron stars with unequal masses is quite different from expectations for the case of nearly equal masses: Major steps have been taken, in recent years, toward realistic simulations, on a supercomputer, of collisions between equal-mass neutron stars. The first step was to solve a problem that requires only two-dimensional calculations, and to do it in Newtonian theory and with the quadrupole formalism (Sec. 6.B). This initial problem was the head-on collision of two equal-mass neutron stars, and it was solved by Gilden and Shapiro (1984) and Evans (1987). The next step was to break away from axisymmetry, and use three-dimensional, Newtonian techniques

to simulate nonaxisymmetric collisions. Kochanek and Evans (1989) have accomplished this, but with initial conditions for the neutron stars that are rather far from circular orbits. Oohara and Nakamura (1989, 1990) have also succeeded; and their initial conditions are closer to those appropriate for a neutron–star binary.

In their simulations, Oohara and Nakamura used Newtonian gravity, the quadrupole formalism, and three–dimensional computations with 141 zones along each of the three axes of a Cartesian coordinate system. Figure 7.8 shows a sequence of "snapshots" of the density distribution (contours) and velocity distribution (arrows) ~~inside the binary system~~ in the binary's equatorial plane, for a simulation that did not include radiation–reaction forces (Oohara and Nakamura, 1989). A subsequent simulation, which included radiation reaction using a variant of the radiation–reaction potential (6.8), showed qualitatively similar evolution but with a factor ~2 damping of the nonaxisymmetric deformations by the time of the final snapshot in Fig. 7.8 (Oohara and Nakamura, 1990) [KIP: CHECK WITH NAKAMURA]. The gravitational waveform from this simulation, as seen by an observer on the orbit's rotational axis, is shown in Fig. 7.9. Its amplitude exhibits decay due to the gravitational radiation reaction.

The snapshots in Fig. 7.8 reveal the fate of the equal–mass binary: The two stars coalesce, with a sequence of vibrations during the coalescence, to form a triaxial neutron star, rotating end over end. Gravitational radiation reaction then gradually removes angular momentum from the star, and its long axis gradually shrinks, until (after the ends of Figs. 7.8 and 7.9) the star becomes axisymmetric and ceases radiating. The waveform (Fig. 7.9) is more or less a continuation of the sinusoidal inspiral waveform of Fig. 1.5); but once the two stars have merged significantly, its amplitude and frequency start decreasing. The net decrease in frequency, until the waves turn off, should be much less than a factor 2, by contrast with the factor ~5 decrease in the case of two neutron stars with unequal masses (Fig. 7.6). The characteristic amplitude of the entire wavetrain, from the beginning of the coalescence phase until the waves turn off, can be inferred by an extrapolation, to later times, of the Oohara–Nakamura (1990) simulations. The result is

$$h_c \simeq 1\times10^{-22}\left[\frac{M_1}{0.7M_\odot}\right]^2\left[\frac{100\ \text{Mpc}}{r_o}\right], \qquad (7.24a)$$

where $M_1 = M_2$ is the mass of one of the initial neutron stars, and r_o is

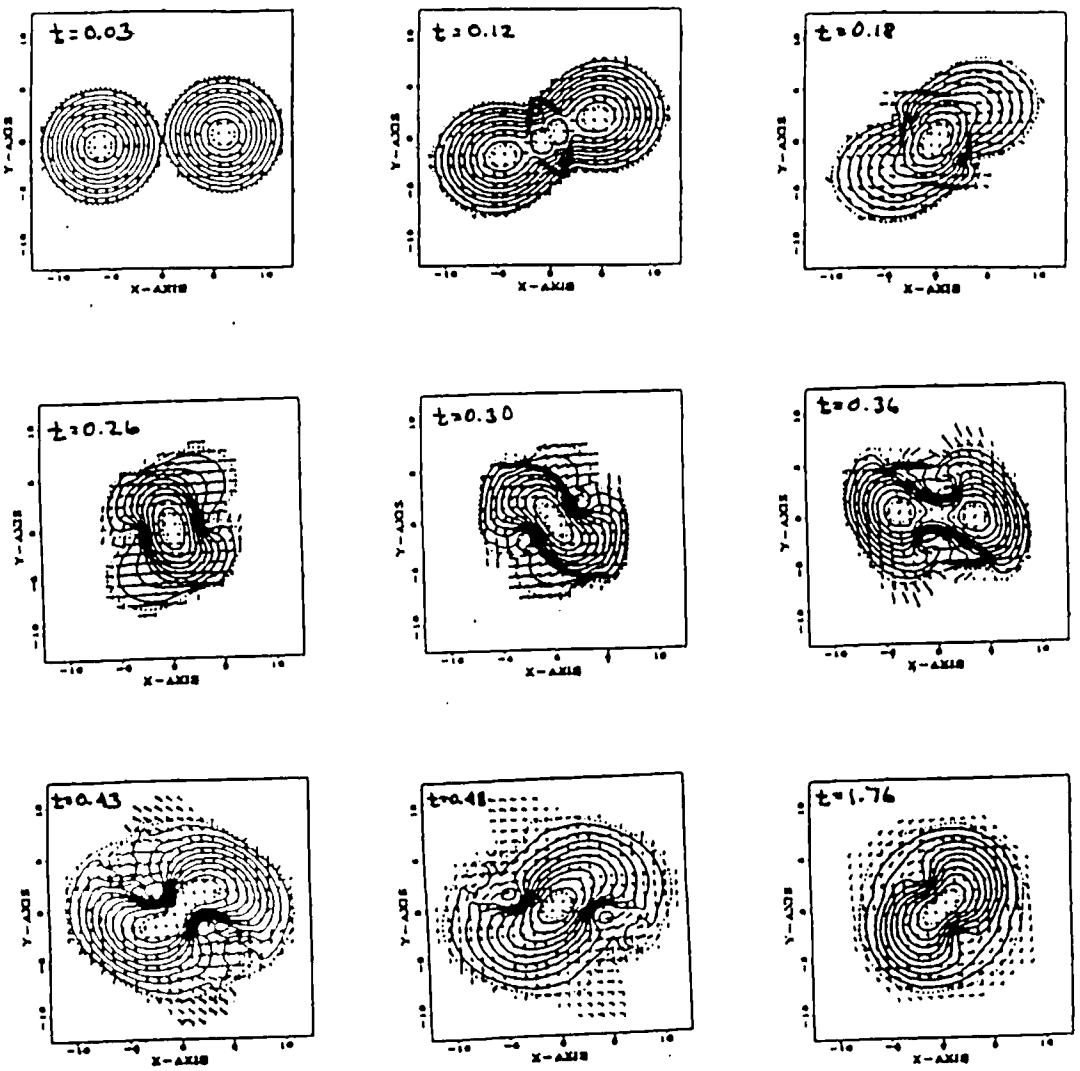

Fig. 7.8 A sequence of snapshots of the density distribution (contours) and velocity distribution (arrows) during the coalescence of a neutron–star binary with equal masses, as computed by Oohara and Nakamura (1989). The interval between contours is 0.1 of the maximum density. The equation of state was idealized as $P = K\rho^2$. The stars initially are *not* in hydrostatic equilibrium with the system's gravitational and centrifugal forces. Rather, the initial density distribution is that of two equilibrium, nonrotating stars, each with mass M_0 and radius R_0 (where R_0 is related to the constant K in the equation of state by $R_0 = \sqrt{\pi K/2}$) and with their surfaces just touching (no tidal deformation included). The initial velocity distribution is rigid rotation with angular velocity $\Omega = 0.5\sqrt{2M_0/(2R_0)^3}$, i.e. half the equilibrium angular velocity for point masses M_0 separated by $2R_0$.

Each snapshot is labeled by the time t since the initial moment of the computation, in units of $\text{msec} \times (R_1/9\,\text{km})^{3/2}(0.7M_\odot/M_1)^{1/2}$. Lengths along the x- and y-axes of each snapshot are measured in units of $R_1/6 = 1.5\,\text{km}\,(R_1/9\,\text{km})$.

the distance to the source. These simulations used an idealized equation of state designed to give rapid rotation for the final star, in accord with the observations of the apparent pulsar in SN 1987A. Correspondingly, the characteristic frequency of the final, coalescence waves was

$$f_c \simeq 4500 \text{ Hz} \left(\frac{M}{0.7M_\odot}\right)^{1/2} \left(\frac{9\text{km}}{R_1}\right)^{3/2}, \qquad (7.24b)$$

compared to a frequency of 4000 Hz which one would expect for the strongest waves from the apparent pulsar in SN 1987A. The quadratic mass dependence of h_c [Eq. (7.24a)] is an artifact of the specific equation of state used in the simulations.

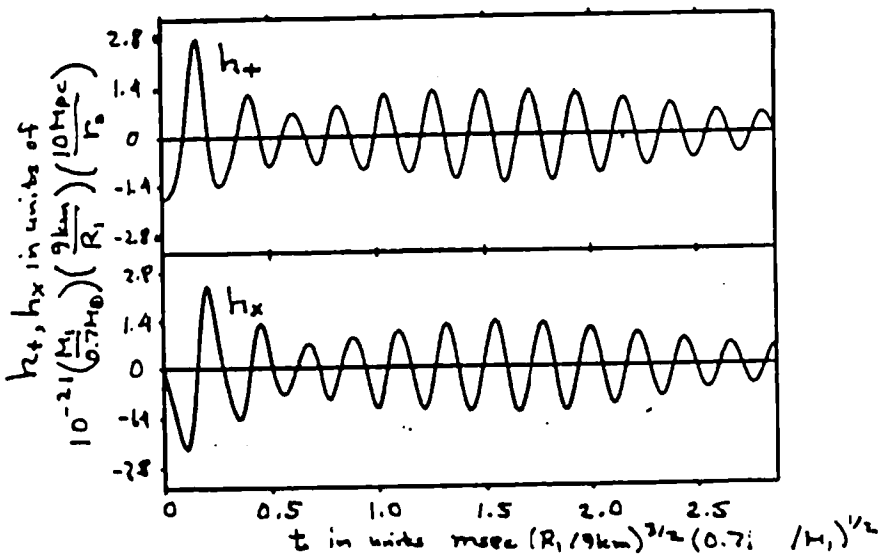

Fig. 7.9 The gravitational waveform $h_+(t)$ as measured by an observer on the rotation axis of a binary neutron star during its coalescence stage. The other waveform $h_\times(t)$ is nearly identical to this one, except for time translation by a quarter cycle. The model and simulations that produced this waveform are the same as those of Fig. 7.8, except that radiation reaction forces were included here and not there. [Figure adapted from Oohara and Nakamura (1990)].

The precise details of these simulations are not to be believed, since the equation of state and other input physics were somewhat idealized, Newtonian gravity was used rather than general relativity, and the initial configuration consisted of two undeformed stars with their surfaces touching rather than a tidally deformed configuration in quasistatic equilibrium; see Fig. 7.8. However, it seems likely that the simulations are semiquantitatively correct. Especially interesting is the fact that the characteristic amplitude (7.24a) of the final,

coalescence waveform matches smoothly, to within a factor of order 2, the characteristic amplitude of the inspiral waves which precede the coalescence [Eq. (7.28b) below].

For black-hole binaries one cannot get any information about the coalescence stage from Newtonian calculations. Full-fledged numerical relativity (Sec. 6.K) is required. Because a comparison of the theoretical and observed waveforms for black-hole coalescence is likely to give the first definitive proof that black holes exist and give the most stringent test ever of general relativity theory (Sec. 1.B), great effort is going into the computation of the waveforms. The task is very difficult, since it entails *three*-dimensional, fully relativistic simulations; and in general relativity, *two*-dimensional simulations are only now beginning to produce reliable waveforms. (The two-dimensional case of head-on collisions of equal-mass black holes was the test bed in which the foundations of numerical relativity were laid; see Smarr, 1977a, 1979, and references therein.) For early steps toward modeling the black-hole binary coalescence and determining the waveforms, see York (1984), Eardley (1986), Blackburn and Detweiler (1989), and references in Sec. 6.K.

b. Inspiral stage

Because the binary system spends far more time in the early, low-frequency part of its inspiral than in the later, high-frequency part or in the final coalescence stage, and because planned gravitational-wave detectors have less amplitude noise at low frequencies, $f \sim 100$ Hz, than at high frequencies, $f \gg 100$ Hz (cf. Fig. 2.7), it will be easier for detectors to see the Newtonian regime of the inspiral than the post-Newtonian regime or the coalescence stage — except in the case of black-hole binaries with $M_1 \sim 100$ to $1000 M_\odot$ or $M_1 \gtrsim 10^6 M_\odot$ (Fig. 2.7). In the Newtonian regime, if we orient the polarization axes $\mathbf{e}_{x'}$ and $\mathbf{e}_{y'}$ along the major and minor axes of the projection of the orbital plane on the sky, then the waveform will be

$$h_+ = 2(1+\cos^2\iota)(\mu/r)(\pi M f)^{2/3}\cos(2\pi\textstyle\int f\,dt)\,, \tag{7.25a}$$

$$h_\times = \pm 4\cos\iota(\mu/r)(\pi M f)^{2/3}\sin(2\pi\textstyle\int f\,dt)\,. \tag{7.25b}$$

Here it is assumed that the orbit is circular because radiation reaction long ago will have forced circularization (Peters and Mathews, 1963 — but see an exception later in this section); ι is the angle of inclination of the orbital plane to the tangent plane of the sky; M and μ are the

total and reduced masses

$$M = M_1 + M_2 , \quad \mu = M_1 M_2 / M ; \tag{7.25c}$$

and f, the frequency of the waves (equal to twice the orbital frequency), is given as a function of time by [MTW, Eq. (36.17)]

$$f = \frac{1}{\pi}\left[\frac{5}{256}\frac{1}{\mu M^{2/3}}\frac{1}{(t_0 - t)}\right]^{3/8} . \tag{7.25d}$$

The post-Newtonian corrections to this waveform will become more and more important as f rises toward f_{max} [Eq. (7.23)]; they have been computed by Wagoner and Will (1976); Gal'tsov, Matiukhin, and Petukhov (1980); Krolak (1988); and Blanchet and Schäfer (1989). Lincoln (1989) has taken the first step toward quantifying the higher-order corrections: he integrates the orbit using equations of motion accurate to post$^{2.5}$-Newtonian order (Damour, 1987b), and then computes the waveforms accurate to post$^{1.0}$-Newtonian order using the formalism of Wagoner and Will (1976). Blackburn and Detweiler (1989) have given a fully relativistic variational principle for the inspiral stage of black-hole binaries, from which it should be possible in the near future to compute some features of the relativistic corrections to the waveforms (7.25).

The most promising detectors for coalescing neutron-star binaries and low-mass black-hole binaries are multikilometer interferometric detectors. As we shall see in Sec. 11.D, an interferometric detector can be operated in several different optical configurations. The optimum configuration for searching for coalescing binaries is likely to be one with some variant of *light recycling* (Sec. 11.D). Thorne (1987) has calculated the spiraling binaries' signal-to-noise ratio S/N (from which follows the characteristic amplitude h_c) for the case of "broad-band recycling"; and Dhurandar, Krolak, and Lobo (1989a) have done so for "detuned recycling" (Sec. XXXX), obtaining a signal-to-noise ratio (and thence a h_c) larger by about $1/\sqrt{2}$ than for broad-band. I shall sketch the broad-band calculation; the detuned calculation is conceptually the same, but the formulas are much more complicated.

For an interferometric detector with broad-band recycling, the spectral density $S_h(f)$ of the noise is well approximated by our standard "recycling spectral density", Eq. (7.15). By Fourier transforming the waveforms (7.25), squaring, averaging over the source orientation angle ι, and inserting into Eq. (7.11), we obtain

$$\frac{dE_{GW}}{df} = \frac{\pi M \mu}{3(\pi M f)^{1/3}} . \tag{7.26}$$

By inserting this emitted spectrum (7.26) and the detector noise (7.15) into Eq. (7.12b) for the characteristic amplitude and maximizing with respect to the knee frequency f_k, we find that the experimenter will do best to choose

$$f_k = 1.44 f_{\min} . \tag{7.27}$$

For smaller choices of f_k there is not a wide enough frequency band between the seismic cutoff and the knee to take optimal advantage of the broad-band nature of the signal. For larger values of f_k the experimenter loses because the height $S_h(f)$ of the "noise floor" at $f_{\min} < f \lesssim f_k$ [Eq. (7.15)] is proportional to f_k. With this choice of knee, Eqs. (7.12a) and (7.19)–(7.27) give for the characteristic frequency $f_c = 0.909 f_k$. Below [Eq. (11.28a)] we shall characterize the sensitivities of full scale interferometric detectors, when searching for bursts, by the noise amplitude h_n *at the knee*. Correspondingly, we here shall set f_c (which after all is somewhat arbitrary) to f_k rather than $0.909 f_k$:

$$f_c = f_k = 1.44 f_{\min} . \tag{7.28a}$$

Equations (7.12a) and (7.19)–(7.27) then give for the characteristic amplitude of the waves from inspiraling binaries

$$\begin{aligned} h_c &= 0.34 \frac{\mu^{1/2} M^{1/3}}{r_0 f_c^{1/6}} \\ &= 5.8\times 10^{-22} \left[\frac{\mu}{M_\odot}\right]^{1/2} \left[\frac{M}{M_\odot}\right]^{1/3} \left[\frac{100\ \text{Mpc}}{r}\right] \left[\frac{100\ \text{Hz}}{f_c}\right]^{1/6} . \end{aligned} \tag{7.28b}$$

The characteristic amplitude (7.28b) is enhanced over the actual rms wave strength $\langle h_+^2(t_c) + h_\times^2(t_c)\rangle^{1/2}$ that the waves have at the time $t = t_c$ when they sweep through frequency f_c – enhanced by very nearly the square root of the number of periods, $n = (f^2/\dot{f})_{f=f_c} = (5/96\pi)(M/\mu) \times (\pi M f_c)^{-5/3}$, that the binary spends in the vicinity of the frequency f_c. This $\sqrt{n} \simeq 28(\mu/M_\odot)^{-1/2}(M/M_\odot)^{-1/3}(f_c/100\text{Hz})^{-5/3}$ enhancement corresponds to the enhancement in effective signal that the experimenters will achieve by optimal signal processing in their search for these frequency-sweeping bursts. [Note: In the original presentation of the above calculation (Thorne, 1987) a stupid error caused the factor 6 in (7.26) to be a 12 and correspondingly caused the numerical coefficients in (7.71b) to be too small by $1/\sqrt{2}$. I thank

Bernard Schutz for pointing out the error.]

Sheryl Smith (1987, 1988) has developed a data analysis algorithm for searching in interferometric-detector data for signals from spiraling binaries, and has used it for searches in data from the Caltech prototype detector. Her algorithm is a practical implementation of optimal signal processing, and it is sufficiently efficent to analyze the data in real time. [KIP: ADD REFS TO TINTO ET AL, ...?]

From a study of the waveform (7.25) using broad-band detectors at several widely spaced locations on the earth, it will be possible to deduce the following information: (i) the direction to the source (which comes from phase differences in the signal at different detectors in different locations); (ii) the inclination of the orbit to the line of sight (which comes from the amplitudes in the two different polarization modes); (iii) the direction the stars move in their orbit [which comes from the + or - sign in Eq. (7.25b)]; (iv) the combination $(\mu^3 M^2)^{1/5}$ of the reduced and total masses; and (v) the distance r to the source. If the mass combination $(\mu^3 M^2)^{1/5}$ is $\lesssim 1.5 M_\odot$, one can be fairly sure the binary was made of neutron stars; if it is much larger, one can be fairly sure that at least one of the bodies was a massive black hole.

Especially intriguing is the following possibility, pointed out by Schutz (1986b): In the case of neutron stars the coalescence may produce electromagnetic emission (e.g. due to the explosion of the secondary star at the end of the coalescence phase, Blinnikov et. al. 1984) that is strong enough to be detected at earth and thereby to pin down the source's location with far higher precision than can be obtained from the gravitational waves. In this case, a redshift will probably be obtainable from optical observations. That redshift together with the gravitational-wave-determined distance r will give a value for the Hubble constant. From a detailed study of the expected noise in future interferometric detectors, Schutz (1986b) concludes that the prospects are good for obtaining by this method a significantly better value of the Hubble constant than we now have. Even in the absence of electromagnetic signals from the coalescence, it may prove possible by statistical means to determine the Hubble constant using combined data for a number of coalescences; see Schutz (1986b) for details.

Clark, van den Heuvel, and Sutantyo (1979) have estimated, from neutron-star observations in our own galaxy, that to see three coalescences of neutron-star binaries per year one must look out to a distance of 100^{+100}_{-40} Mpc, where the quoted uncertainties are at the 90 per cent confidence level. Lipunov, Postnov, and Prokhorov (1988) have

obtained roughly the same estimate from statistical studies of close binary systems at earlier stages of their evolution, combined with computations of the subsequent evolution. Schutz (1988) argues that the uncertainties in this estimate are greater than Clark, van den Heuvel, and Sutantyo (1979) thought: 90 per cent confidence, Schutz concludes, corresponds to distances $10\,\mathrm{Mpc} \lesssim r \lesssim 1000\,\mathrm{Mpc}$. [KIP: ADD SUBSEQUENT ESTIMATES]

These considerations motivate the specific coalescing-binary curves shown in Fig. 2.7: There we depict the characteristic amplitude and frequency (7.28), for a range of values of the seismic cutoff $f_{\rm min}$ and corresponding values of $f_c = 1.44 f_{\rm min}$, produced by the coalescence of two 1.4 solar mass neutron stars at 100 Mpc (estimated event rate about 3 per year) and at 1/3 the Hubble distance (event rate about 10 per day).

As Fig. 2.7 shows, future earth-based interferometric detectors may be able to see black-hole coalescences throughout the universe, so long as the more massive of the two holes does not exceed $1000\,M_\odot/(1+z)$, where z is the hole's cosmological redshift. The coalescence rate for black-hole binaries of a few solar masses could be of order that for neutron-star binaries (a few per year at 100 Mpc), or might well be far lower. Particularly intriguing is a scenario, suggested as very plausible by Shapiro and Teukolsky (1985) and Quinlan and Shapiro (1987), in which a large fraction of galactic nuclei create, at some phase of their evolution, a dense cluster of neutron stars and small-mass black holes which — on a timescale of only a few years — form tight binaries that coalesce, with the coalesced holes then forming new tight binaries that coalesce, ... until the cluster goes unstable and collapses to form a single large hole. This scenario suggests that in typical years the earth might be hit by a number of wave bursts from coalescing binaries of masses $3M_\odot$ to $1000M_\odot$ at the Hubble distance, $z \sim 1$. These bursts would differ from the ones described above in that the time from binary formation to coalescence is so short as to leave many of the binaries with substantially eccentric orbits at the time their waves sweep into the detectors' frequency and sensitivity bands. Thus, the waveforms would differ from Eqs. (7.25) [see Wahlquist, 1987 and Eqs. (8.15) of this book], but in order of magnitude their characteristic amplitudes would be the same.

Also intriguing but much less likely is a scenario discussed by Bond and Carr (1984) in which a sizable fraction of the mass of the universe is in black-hole binaries with masses ~ 100 to $1000M_\odot$, for which the

coalescence rate could be several per year in the local group of galaxies (distance ~1Mpc).

One or more black hole binaries of any mass up to $\sim 10^8 M_\odot$ *might* have formed in the nuclei of a reasonable fraction of all galaxies during the past life of the universe, leading to event rates $\gtrsim 1$/year out to the Hubble distance (cf. Fig. 1 of Rees 1983) — or they might never form. There is actually observational evidence for supermassive black-hole binaries formed by the coalescence of galactic nuclei (Begelman, Blandford, and Rees 1980, Rees 1983); but the rate of such events probably does not exceed 1/100 years out to the Hubble distance (Rees 1983).

7.E The fall of stars and small holes into supermassive holes

The supermassive ($M_1 \gtrsim 10^5 M_\odot$) black holes thought to inhabit the nuclei of galaxies might typically grow by accretion on timescales as short as 10^8 years; see, e.g. Sec. 8.6 of Blandford and Thorne (1979). When such a hole grows larger than $10^9 M_\odot$, normal stars can pass near or plunge through its horizon without being torn apart tidally, and the number of stars that so scatter or plunge could well be of order one per year or more (e.g. Dymnikova, Popov, and Zentsova, 1982). For smaller supermassive holes, scattering or plunging normal stars will be tidally disrupted, reducing the amplitude and frequency of their waves; but the reduction will not be great, at least in the case of radial infall, unless the hole is below $10^6 M_\odot$ so the star is larger than the hole (Nakamura and Sasaki, 1981; Haugan, Shapiro, and Wasserman, 1982; Petrich, Shapiro, and Wasserman, 1985). For any hole, neutron stars and satellite holes can scatter or plunge through without enough disruption to strongly suppress their radiation; but the event rate (per supermassive hole) will typically be well below one per year.

Figure 7.10 illustrates the effect of finite size of the infalling star on its emitted waves, for the simple case of radial infall into a nonrotating hole. The observer is in the hole's equatorial plane, the star falls radially in along its polar axis, and the axes of the "+" polarization state are parallel to the equator and the pole. All the radiation comes out in the + state. The solid curve is the waveform $h_+(t-r)$ in the local wave zone, produced by an infalling star of arbitrarily small circumference (Petrich, Shapiro, and Wasserman, 1985; see also Davis et. al., 1971; Davis, Ruffini, and Tiomno, 1972). The dashed curve is for an infalling star which has negligible internal pressure, and is spherical with the same circumference as the hole when it passes through radius

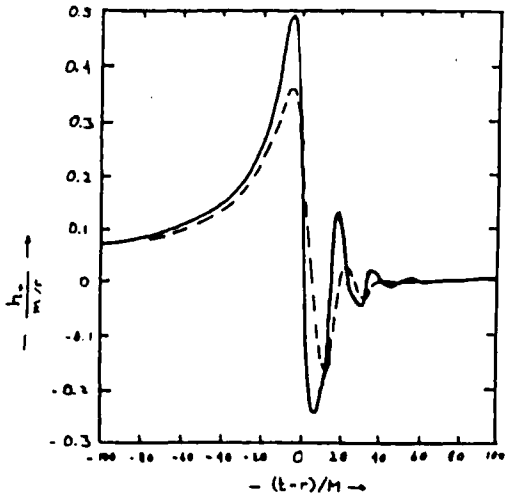

Fig. 7.10 The gravitational waveforms produced by stars falling radially into a nonrotating black hole. The observer is in the hole's equatorial plane, and the stars fall in along the polar axis. The solid curve is for a star with circumference far smaller than the hole; the dashed curve is for a star with circumference approximately equal to that of the hole, and negligible internal pressure. These waveforms are based on calculations by Petrich, Shapiro, and Wasserman (1985). Notice the similarity to the waveform produced by the collapse of a star to form a black hole (Fig. 7.6). The similarity is due in large measure to the fact that both processes produce normal-mode pulsations of the final hole. After the first burst, the radiation is due to those pulsations.

r = 12×(hole's gravitational radius, $2M$) (Petrich, Shapiro, and Wasserman, 1985). Both stars fall from rest arbitrarily far outside the hole, and both have mass m very small compared to that, M, of the hole. Notice that having a circumference the same as that of the hole reduces the characteristic amplitude and frequency in the equatorial plane to roughly 60 per cent of their compact-star values. However, the total energy radiated goes down by a bit more than a factor ten. Here, as in our discussion of waves from supernovae (Sec. 7.B), the total energy radiated is not a good indicator of detectability.

The waveforms emitted when a star or small hole is scattered by or plunges into a rotating, supermassive hole have been evaluated with high precision using perturbation formalisms; see, e.g., Detweiler and Szedenits (1979), Kojima and Nakamura (1983, 1984a), and Nakamura, Oohara, and Kojima (1987). Those waveforms typically have a much more complicated structure than the ones (Fig. 7.3) for radial infall. The characteristic frequency and amplitude for typical (non-head-on)

impact parameters are

$$f_c \cong \frac{1}{20M_1} = 10^{-4}\ \text{Hz}\left[\frac{10^8 M_\odot}{M_1}\right], \tag{7.29a}$$

$$h_c \cong \frac{M_2}{2r_o} = 2\times10^{-21}\left[\frac{M_2}{M_\odot}\right]\left[\frac{10\ \text{Mpc}}{r_o}\right], \tag{7.29b}$$

where M_1 is the mass of the large hole, M_2 is that of the infalling body, and $r_o \sim 10$ Mpc might give a reasonable event rate since there are ~100 galaxies as massive as or more massive than our own inside this distance, including M87 for which observational data suggest a central black hole of mass $M_1 \sim 4\times10^9 M_\odot$ (Sec. 3.1.4 of Blandford, 1987). These h_c and f_c are plotted in Fig. 2.7 for several interesting sets of parameters. It is conceivable that such plunge bursts will be seen by interferometric detectors in space, if and when they are flown.

7.F Cherished beliefs

From the discussion of sources in this chapter it should be clear that our electromagnetically-based knowledge of gravitational-wave sources is highly uncertain. Correspondingly, it may well be that when gravitational waves are finally seen, they will come predominantly from sources we have not thought of or have underestimated; and it seems quite possible that the waves will be stronger than the above estimates suggest.

In light of this, it is interesting to ask the following question: How strong could be the strongest bursts that strike the earth on average three times per year, without violating our "cherished beliefs" about the laws of physics and the universe? Zimmermann and Thorne (1980) have enumerated a set of cherished beliefs, including (i) that general relativity is correct, (ii) that we do not live in a special time or place in the universe, (iii) that there are no enormous primordial bursts, (iv) that no single, coherently radiating object in our galaxy has a mass exceeding $10^8 M_\odot$, and (v) that the strongest bursts were not beamed by their sources into solid angles $\ll\pi$. From these cherished beliefs, they have derived the upper limit on the 3/year burst strength which is shown in Fig. 2.7. That limit could actually be achieved at frequencies $f \gtrsim 30$ Hz by an unlikely but not implausible scenario in which a large fraction of the mass of the universe was cycled, long ago, through a pre-galactic population of massive stars ("Population III" stars), leaving much of the universe's mass in compact binary systems that

inhabit the halos of galaxies. If the mean lifetime of these binaries against spiraling together and coalescing is of order the age of the universe, then such coalescences in the halo of our own Milky Way galaxy would give bursts in the frequency domain $f \gtrsim 30$ Hz at the cherished belief level. For further discussion see Zimmermann and Thorne (1980), and Bond and Carr (1984).

While this scenario is unlikely, it is not totally implausible, and it serves to remind us that our best estimates of the waves bathing the earth could be grossly pessimistic.

7.G Bursts with memory

As Braginsky and Grishchuk (1985) have emphasized, gravitational-wave bursts can be subdivided into two classes: *normal bursts*, in which $h_+(t)$ and $h_\times(t)$ begin zero before the burst and return to zero afterward, and *bursts with memory*, in which at least one of $h_+(t)$ or $h_\times(t)$ (by convention) begins zero before the burst and then settles down into a nonzero, constant value Δh_+ or $\Delta h_\times$ (the burst's "memory") after the burst is over.

Physically, a burst with memory arises whenever the source, before the burst or afterward or both, consists of two or more free bodies that are moving with uniform velocities relative to each other. For example, the explosion of a star into several pieces will produce a burst with memory, as will a near encounter of two freely moving (not binary) stars or black holes (Zel'dovich and Polnarev, 1974), or the gravitational scattering of a star by a black hole, or an asymmetric ejection of neutrinos from a supernova (Epstein and Clark, 1979); but the birth of a black hole in nonspherical stellar collapse will produce a burst without memory. In all cases, the "memory" is the change in the total "$1/r$" coulomb-type gravitational field of the source (Braginsky and Thorne, 1987) For example, in the quadrupole approximation, when one takes account of the fact that one can add a time-independent constant to $h_{jk}^{\rm GW}$ ("gauge change" that moves stuff between the background field and the wave field) so as to make $h_{jk}^{\rm GW}$ zero initially, Eqs. (4.25), (6.1) and (6.2a) give

$$\Delta h_{jk}^{\rm GW} = \Delta h_+ e_{jk}^{+} + \Delta h_\times e_{jk}^{\times} = \Delta \sum_A \left[\frac{4 m_A v_A^j v_A^k}{r} \right]^{\rm STF} . \qquad (7.30)$$

Here the summation is over the free bodies in the system, m_A and v_A^j are the mass and velocity of body A, and Δ denotes the change from before the burst is emitted to afterward.

A specific example of a burst with memory is the gravitational radiation produced when two stars fly past each other with sufficiently high speed that they deflect each others' trajectories only slightly ("gravitational bremsstrahlung radiation"). (Such radiation is primarily of pedagogical interest, since the strength of the waves will not be terribly high.) From the quadrupole formalism one obtains, when the stars' relative speed is small compared to the speed of light,

$$h_+ = \frac{4M_1M_2}{br_o}\left[\frac{1}{2}\left(\frac{1}{D^3}+\frac{1}{D}\right)\sin^2\theta + \frac{1}{2D^3}(\sin^2\phi-\cos^2\theta\cos^2\phi) + \left(\frac{T}{D^3}+\frac{T}{D}+1\right)\cos\theta\sin\theta\cos\phi\right], \quad (7.31a)$$

$$h_\times = \frac{4M_1M_2}{br_o}\left[\frac{1}{D^3}\cos\theta\cos\phi\sin\phi - \left(\frac{T}{D^3}+\frac{T}{D}+1\right)\sin\theta\sin\phi\right] \quad (7.31b)$$

(Zel'dovich and Polnarev, 1974; Turner, 1977; Kovacs and Thorne, 1978). Here

$$T \equiv tv/b\ , \quad D \equiv \sqrt{1+T^2}\ ; \quad (7.31c)$$

b is the collisional impact parameter (distance between the stars at closest approach); v is the stars' relative speed; M_1 and M_2 are the stars' masses; r_o is the distance of the observer from the source; and (θ,ϕ) are the spherical polar angles of the direction from the source toward the observer, measured from a polar axis that is along the direction of relative motion of the stars and a $\phi = 0$ plane that is the plane of the stars' orbits. The basis vectors with respect to which the + and × polarization axes are defined are the unit vectors $\mathbf{e}_{\hat\theta}$ and $\mathbf{e}_{\hat\phi}$ along the θ and ϕ directions; i.e., the polarization tensors are $\mathbf{e}_+ = \mathbf{e}_{\hat\theta}\otimes\mathbf{e}_{\hat\theta} - \mathbf{e}_{\hat\phi}\otimes\mathbf{e}_{\hat\phi}$, and $\mathbf{e}_\times = \mathbf{e}_{\hat\theta}\otimes\mathbf{e}_{\hat\phi} + \mathbf{e}_{\hat\phi}\otimes\mathbf{e}_{\hat\theta}$.

These waveforms are depicted in Fig. 7.11. Notice how strong the memory is, for most observers' directions and polarizations. (Notice also the large changes in the waveforms' shapes as one changes the observer's direction and the polarization axes; cf. Eq. (4.23). Such large changes are not uncommon for the waves from realistic astrophysical sources. However, for many interesting sources, the waveform is nearly independent of direction and polarization. Examples include the inspiral stage of any binary system, and the waves from any axisymmetric source whose size is small compared to its wavelength so

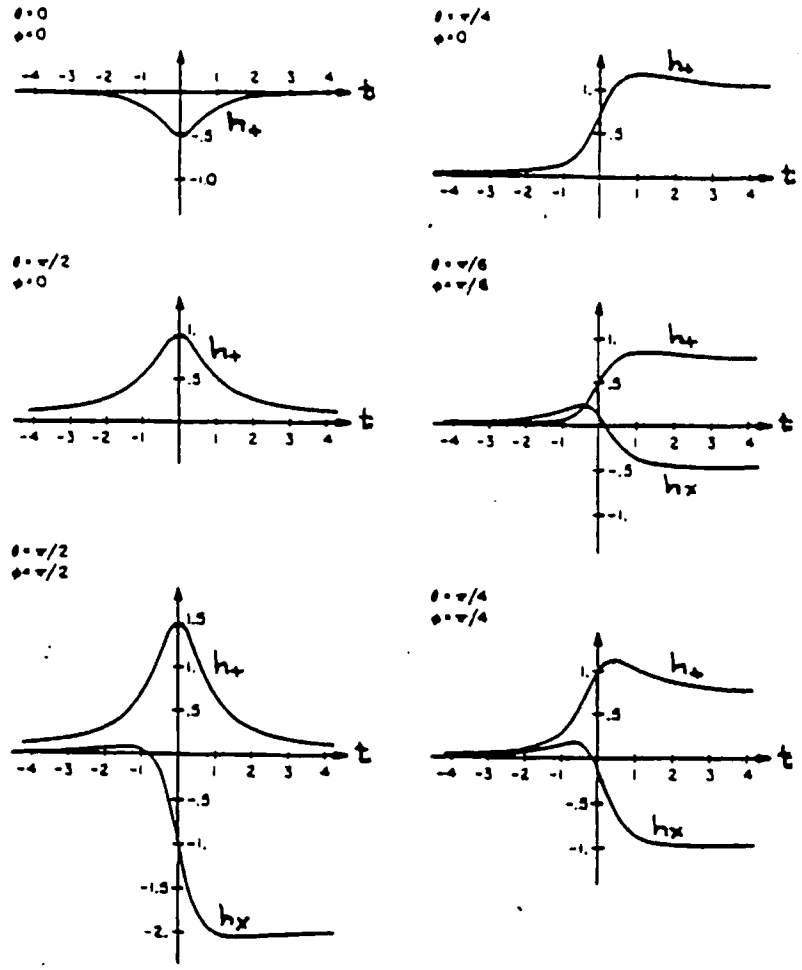

Fig. 7.11 The "gravitational bremsstrahlung" waveforms produced by two stars that fly past each other with speeds small compared to the speed of light, and with large enough impact parameter that they deflect each others' orbits only slightly. [Figure taken from Kovacs and Thorne (1978).]

only one multipolar order, usually quadrupolar, contributes.)

When the relative velocities of the two stars, as they fly past each other, are comparable with the speed of light, higher-order multipole moments contribute significantly to the radiation. As a result, the waveforms develop sharp, high-frequency features. The details have

In these waveforms h_+ and $h_\times$ are measured in units of $4M_1M_2/br_0$ and t is measured in units of b/v, where M_1 and M_2 are the masses of the stars, b is the impact parameter of the collision, r_0 is the distance to earth, and v is the stars' relative velocities. The angles θ and φ are defined in the text.

been computed by Turner and Will (1978) using the post-Newtonian formalism of Sec. 6.I (valid for relative speeds up to $v \simeq 0.5$), by Peters (1970) using the perturbation formalism of Sec. 6.J (valid for arbitrary velocities but for stars with very different masses, $M_2 \ll M_1$), by Kovacs and Thorne (1978) using the post-post-Minkowskii formalism of Sec. 6.H (valid for arbitrary velocities and masses, but for impact parameters large compared to the gravitational radii of the stars), and by D'Eath (XXXX) and XXXXX using an adaptation of the theory of colliding, planar gravitational waves, Sec. 5.H (valid for ultrarelativistic velocities $1-v \ll 1$ and for arbitrary impact parameters). Although the details can differ strongly from the low-velocity waveforms of Fig. 7.11, the memory remains a major feature of the waveforms at all velocities.

As is discussed by Braginsky and Thorne (1987), the memory part of a burst, Δh_{jk}^{GW}, can be studied by detectors (with adequate sensitivity) that operate at any frequency lower than that, f_o, of the waveform's non-memory part. Put equivalently, one can think of a burst with memory as having a signal that extends down to all frequencies below f_o (cf. the "zero-frequency limit" for gravitational waveforms, discussed by Smarr, 1977b; Bontz and Price 1979; and Wagoner, 1979). This fact shows up clearly in the form of the characteristic amplitude h_c for a burst with memory (Fig. 7.2c): If the detector's band is in the low-frequency region where the memory dominates, then h_c is independent of the detector's cutoff frequency $f_{\rm min}$.

Current prejudice suggests that the strongest of burst sources (and thus the most interesting) may produce normal bursts rather than bursts with memory; but this prejudice could perfectly well be wrong. For example, if the nucleus of our galaxy were endowed with a very dense and massive cluster of neutron stars or black holes, then memory-endowed gravitational bremsstrahlung from close encounters could be an important source of gravitational waves for space-based detectors and detectors based on pulsar timing measurements (Zel'dovich and Polnarev, 1974; Polnarev, 1988).

Grishchuk (1989) has recently pointed out that, in principle, there can also exist "bursts with memory of velocity". By this, he means bursts which have a long epoch at their beginning or end or both in which the waveform h_+ and/or $h_\times$ changes linearly with time. An example is the gravitational waveform produced by a star that oscillates up and down, vertically, though the plane of a very thin galaxy. Such a star experiences a constant downward acceleration whenever it is above the plane of the galaxy, and a constant upward acceleration

whenever it is below. This motion produces a waveform, as computed from the quadrupole formulas (6.1), (6.2a), with the qualitative form shown in Fig. 7.2e.

While bursts with memory of velocity are intriguing in principle, it is hard to conceive of any realistic astrophysical situation where such a burst would be emitted with a strong enough amplitude for detection at earth.

8 Periodic sources

This chapter describes the present (1988) knowledge and speculations about periodic sources of gravitational radiation. Section 8.A defines with care the characteristic amplitude h_c of a wave which is sinusoidal at frequency f and the corresponding sensitivity $h_{3/\mathrm{yr}}$ of a detector searching for that wave. Then the remainder of the chapter discusses specific sources of periodic waves: rotating neutron stars (Secs. 8.B, 8.C, 8.D) and binary star systems (Sec. 8.E).

8.A Characterization of the waves from periodic sources and the noise in a detector searching for them

Periodic gravitational radiation, by definition, is a superposition of precisely sinusoidal waves at a discrete set of frequencies. In this section, we shall focus on a specific frequency f and discard all others. The waves at that frequency will typically be right-hand or left-hand elliptically polarized; i.e., for some suitable choice of polarization axes $\mathbf{e}_{x'}$, $\mathbf{e}_{y'}$, they will have the form [similar to that of a decaying binary, Eq. (7.23), but with const. nt frequency]

$$h_+(t) = h_{o+}\cos(2\pi f t+\Phi)\ , \quad h_\times(t) = \pm h_{o\times}\sin(2\pi f t+\Phi)\ . \tag{8.1}$$

Here h_{o+} and $h_{o\times}$ are constant amplitudes, f is a constant frequency, and Φ is a constant phase. The corresponding energy flux at earth is [Eq. (4.33)]

$$\frac{dE_{\mathrm{GW}}}{dA\,dt} = \tfrac{1}{8}\pi f^2(h_{0+}^2+h_{0\times}^2)\ . \tag{8.2}$$

If one wishes to quantify in a precise and standard manner all the properties of these waves, including the orientations of the "preferred" x' and y' polarization axes, one might best do so using "Stokes parameters" analogous to those of electromagnetic theory (Sec. 15 of Chandrasekhar 1950). However, in this chapter we shall be concerned only with the frequencies f of the waves, and at a given emitted frequency, with a suitably defined characteristic amplitude h_c and a corresponding noise amplitude h_n in a detector searching for the waves.

As an aid in defining h_c and h_n, consider the following situation (analog of that for burst sources in Sec. 7.A): A theorist tells us the frequency f, the phase, and the amplitudes $h_{o+}(\iota,\beta,r)$ and $h_{o\times}(\iota,\beta,r)$ to be expected from a specific model for a source, with orientation angles ι,β and distance r; cf. Fig. 7.1. Suppose, further, that this type of source is distributed randomly throughout the universe and that the mean number of sources inside the distance r_o is n_o. What, then, will be (on average) the signal-to-noise ratio for the n_oth brightest source that a detector, broad-band or narrow, will see in a search (at known frequency and phase) lasting a time $\hat{\tau}$? By virtue of Eqs. (7.2) and by analogy with Eq. (7.8) for burst sources, the answer turns out to be

$$\frac{S}{N} \cong \frac{h_c}{h_n(f)} \langle [F_+(\theta,\phi,\psi)]^2 \rangle^{1/2} . \tag{8.3}$$

Here

$$h_c \equiv \sqrt{2/3} \langle [h_{o+}(\iota,\beta,r_o)]^2 + [h_{o\times}(\iota,\beta,r_o)]^2 \rangle^{1/2} \tag{8.4}$$

(with $\langle \cdots \rangle$ denoting an average over ι and β) is the characteristic amplitude of the periodic source [analog of (7.6b) for a burst source],

$$h_n(f) \equiv \sqrt{S_h(f)/\hat{\tau}} \tag{8.5}$$

is the detector's noise amplitude, and $\langle |F_+(\theta,\phi,\psi)|^2 \rangle^{1/2} \simeq 1/\sqrt{5}$ is the average of the detector's beam-pattern function over all source directions (θ,ϕ) as seen at earth, and over all polarization angles ψ; cf. Fig. 7.1. [The h_c of Eq. (8.4) is $\sqrt{4/3}$ larger than one might expect from Eq. (7.2). This factor $\sqrt{4/3}$ is an approximate correction for the fact that the angle averages in S/N should not be over squares, but rather over squares associated with the rotation of the earth during data collection, then over (squares)$^{3/2}$ covering the rest of the sky and the orientation of the source, followed by a $\frac{1}{3}$ power after averaging; cf. the discussion preceding Eq. (7.5).] By integrating the energy flux equation (8.2) over all directions around the source, noting that the angular

integral is $4\pi r^2$ times the average over ι and β, and comparing with Eq. (8.4), we see that the characteristic amplitude h_c is related to the total power being radiated by

$$h_c = \frac{1}{\pi f r}\left[\frac{4}{3}\frac{dE_{GW}}{dt}\right]^{1/2} \tag{8.6}$$

If experimenters wish to be 90% confident of having seen the n_oth brightest source after $\frac{1}{3}$ year of search, then S/N must exceed $1.655 \simeq 1.7$ (Gaussian probability distribution), and by virtue of Eq. (8.3) h_c must exceed

$$h_{3/yr} = 1.7\frac{h_n}{\langle |F_+|^2\rangle^{1/2}} = \frac{1.7\sqrt{S_h(f)\times 10^{-7}\text{Hz}}}{\langle |F_+|^2\rangle^{1/2}} \text{ if } f \text{ and phase are known}$$

$$\simeq 3.8\sqrt{S_h(f)\times 10^{-7}\text{Hz}} \text{ for interferometric or bar detectors.} \tag{8.7a}$$

Here we have used the value $1/\sqrt{5}$ for $\langle |F_+|^2\rangle^{1/2}$, which is exact for interferometric detectors, is correct to within a 15 per cent error for bar detectors, and is approximately correct for the quadrupolar beam pattern of any detector whose size is small compared to the waves' reduced wavelength. In the case that theory and electromagnetic observation have failed to tell us in advance the phase and frequency of the source, except to within Δf, the experimenters must try $\sim \hat{\gamma}\Delta f = \Delta f/10^{-7}$ Hz values of the frequency, and correspondingly the Gaussian statistics of the noise will produce

$$h_{3/yr} \simeq \frac{[2\ln(\Delta f/10^{-7}\text{ Hz})]^{1/2}}{\langle F_+^2\rangle^{1/2}}\sqrt{S_h(f)\times 10^{-7}\text{Hz}}$$

$$\text{if } f \text{ is known only to within } \Delta f. \tag{8.7b}$$

For $\Delta f \simeq f$ the factor $[2\ln(\Delta f/10^{-7}\text{Hz})]^{1/2}$ is $\simeq 7$ for earth-based detectors ($f \sim 10$ to 10^4 Hz) and $\simeq 4$ for solar-system-based detectors ($f \sim 10^{-5}$ to 10 Hz).

Figure 2.8 in Chap. 2 shows h_c, for several postulated types of source (to be discussed in the following sections), and correspondingly $h_{3/yr}$ with f and the phase known, for several types of detectors (to be discussed in Part IV below).

8.B Rotating neutron stars: formal considerations

A rotating neutron star (e.g. a pulsar) will emit periodic gravitational waves at several frequencies as a result of deviations from symmetry around its rotation axis (deviations from "axisymmetry"). The larger are those deviations and the more rapidly they rotate, the stronger will be the radiation. In this section and the next two we shall study such radiation. We shall begin our study, in this Sec. 8.B, with a formal mathematical analysis of the details of the radiation and how they depend on the star's deformations. Then in Sec. 8.C we shall estimate the strengths and frequencies of the waves from stars deformed by crystalline shear stresses or magnetic pressures; and in Sec. 8.D we shall study waves generated when a very rapidly rotating neutron star is deformed by the "CFS instability".

Typical neutron stars have masses $M \simeq 1.4 M_\odot \simeq 2\,\mathrm{km}$ and radii $R \simeq 10\,\mathrm{km}$, and correspondingly they have $M/R \simeq 0.2$. This is sufficiently large that Newtonian gravity is a somewhat poor approximation in the stars' interiors. On the other hand, most neutron stars rotate with periods $P_{\rm rot} \gtrsim 3\,\mathrm{msec}$ and produce their strongest gravitational waves at periods equal to half this rotation period, corresponding to reduced wavelengths $\lambda\!\!\!^{-} \gtrsim 70$ km and to $(R/\lambda\!\!\!^{-})^2 \lesssim 0.02$. This is sufficiently small that with good accuracy one can compute the stars' wave generation using the strong-gravity, slow-motion approximation to general relativity (Secs. 6.B and 6.G).

The slowness of a neutron star's rotation guarantees that its near zone extends to sufficiently large radii $r_{\rm max} \simeq \lambda\!\!\!^{-}$ that, in its outer reaches, gravity is weak $[M/\lambda\!\!\!^{-} \lesssim 0.03 \times (3\,\mathrm{msec}/P_{\rm rot})]$; i.e. spacetime is nearly flat. Those outer reaches are called the star's "weak-field, near zone"; and a nearly Lorentz coordinate system there, in which the star's center of mass is at rest, is called the star's *asymptotic inertial frame*. We shall denote by $\mathbf{e}_x$, $\mathbf{e}_y$, $\mathbf{e}_z$ the spatial basis vectors of this frame; see Fig. 8.1. The star's quadrupole moment I_{jk} can be regarded as residing in this asymptotic inertial frame and can be treated there as though it lived in flat spacetime. As we shall discuss below, the star will be somewhat flattened by its internal centrifugal forces, and it may differ somewhat from axisymmetry due to shear stresses produced by crystalline forces. However, the crystal lattice is likely to be weak enough that the forces it can produce are much smaller than the centrifugal forces; and, as a result, the deviations from axisymmetry are likely to be much smaller than the centrifugal flattening.

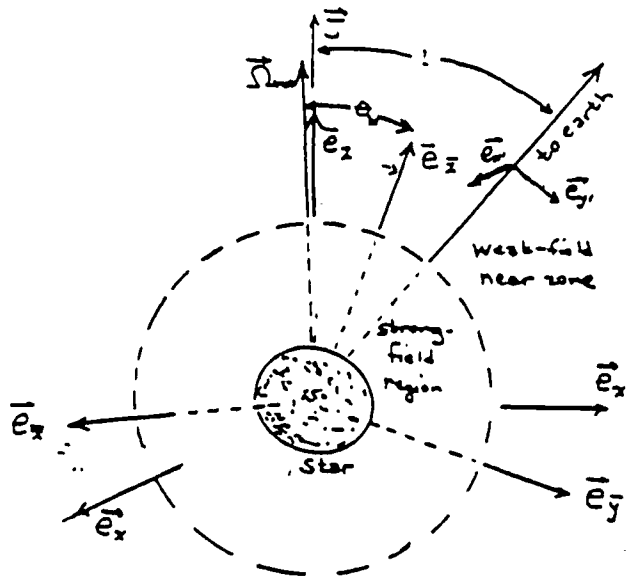

Fig. 8.1 The asymptotic inertial frame (basis vectors $\mathbf{e}_j$) and asymptotic co-rotating frame (basis vectors $\mathbf{e}_{\bar{j}}$) of a rotating neutron star. The star rotates with angular velocity $\Omega_{\rm rot}$ and is almost axisymmetric about the axis $\mathbf{e}_{\bar{z}}$.

With this justification, we shall assume that the quadrupole moment I_{jk}, which of course rotates with the star, has the following form: Denote by $\mathbf{e}_{\bar{x}}$, $\mathbf{e}_{\bar{y}}$, $\mathbf{e}_{\bar{z}}$ the unit vectors along the principal axes of I_{jk}, and let $\mathbf{e}_{\bar{z}}$ be the principal axis about which the star is almost axisymmetric. We shall call the frame of reference tied to these $\mathbf{e}_{\bar{j}}$'s the star's *asymptotic, co-rotating reference frame*. In this co-rotating frame the nonzero components of I_{jk} will be expressible in terms of the quantities

$$\varepsilon_p I \equiv I_{\bar{z}\bar{z}} , \quad \varepsilon_e I \equiv I_{\bar{x}\bar{x}} - I_{\bar{y}\bar{y}} , \quad \text{with } \varepsilon_e \ll \varepsilon_p \ll 1. \tag{8.8}$$

Here I is the star's moment of inertia (which will be defined carefully below); ε_p is the star's "poloidal gravitational oblateness"; and ε_e is its "equatorial gravitational oblateness". An explicit expression for the quadrupole moment, written in dyadic notation, is

$$\mathbf{I} = I\varepsilon_p[\mathbf{e}_{\bar{z}}\otimes\mathbf{e}_{\bar{z}} - \tfrac{1}{2}(\mathbf{e}_{\bar{x}}\otimes\mathbf{e}_{\bar{x}} + \mathbf{e}_{\bar{y}}\otimes\mathbf{e}_{\bar{y}})] + \tfrac{1}{2}I\varepsilon_e(\mathbf{e}_{\bar{x}}\otimes\mathbf{e}_{\bar{x}} - \mathbf{e}_{\bar{y}}\otimes\mathbf{e}_{\bar{y}}) . \tag{8.9}$$

The star's rotational angular velocity $\Omega_{\rm rot}$ and its angular momentum $\mathbf{J}$, like I_{jk}, can be regarded as flat-spacetime geometric objects residing in the asymptotic rest frame; cf. Thorne and Gürsel (1983). The ratio of the magnitude J of the star's angular momentum to the magnitude $\Omega_{\rm rot}$ of its angular velocity is the (scalar) moment of inertia

I

$$I \equiv J/\Omega_{\rm rot} . \tag{8.10a}$$

By angular-momentum conservation, J is a constant of the motion, and as we shall see below $\Omega_{\rm rot}$ is also a constant of the motion; therefore, I is also constant.

More generally, we can define a tensorial moment of inertia tensor as the ratio of the vectorial angular momentum J_j to the vectorial angular velocity $\Omega^k_{\rm rot}$:

$$J_j = I_{jk}\Omega^k_{\rm rot} . \tag{8.10b}$$

Because J_j and $\Omega^k_{\rm rot}$ are both vectors that reside in the star's asymptotic rest frame, I_{jk} is a tensor that resides there (Gürsel and Thorne, 1983). If gravity were nearly Newtonian inside a neutron star, then the star's quadrupole moment and moment of inertia tensor would be given by the integrals over the source's interior

$$\mathcal{I}_{jk} = \int \rho(x^j x^k - \tfrac{1}{3}r^2\delta_{jk})d^3x \ , \quad I_{jk} = \int \rho(r^2\delta_{jk} - x^j x^k)d^3x \ , \tag{8.11a}$$

and correspondingly the quadrupole moment would be the negative of the trace-free part of the moment of inertia tensor

$$\mathcal{I}_{jk} = -I_{jk} + \tfrac{1}{3}I_i{}^i\delta_{jk} . \tag{8.11b}$$

Because the star is nearly spherical, its moment of inertia tensor would be nearly diagonal, $I_{jk} = I\,\delta_{jk}$ [with I the scalar moment of inertia of Eq. (8.F)]; and the quadrupole moment would describe the moment of inertia's slight deformations from isotropy. More specifically, the poloidal and ellipsoidal oblatenesses [Eq. (8.8)] would be

$$\varepsilon_{\rm p} = \frac{2I_{zz} - I_{xx} - I_{yy}}{I_{zz} + I_{xx} + I_{yy}} \ , \quad \varepsilon_{\rm e} = \frac{I_{xx} - I_{yy}}{\frac{1}{3}(I_{zz} + I_{xx} + I_{yy})} . \tag{8.11c}$$

These relations show very precisely the manner in which the oblatenesses of a Newtonian star quantify the star's deformations from sphericity.

The relativistically strong gravity inside a neutron star invalidates the volume integrals (8.Na) for $\mathcal{I}_{jk}$ and I_{jk}, and is thought to invalidate the relation (8.11b) between $\mathcal{I}_{jk}$ and I_{jk} (Gürsel and Thorne, 1983). This invalidation may become important when gravitational-wave data are being analyzed and interpreted in terms of theoretical neutron star models. However, our present knowledge of the magnitudes of $\varepsilon_{\rm e}$ and $\varepsilon_{\rm p}$

is far cruder than the errors made by Newtonian theory; and, with this justification, in Sec. *b* we shall use Newtonian arguments to estimate the magnitudes of these ellipticities.

As the star rotates, it carries the basis vectors of its co-rotating frame around with itself. This means that, relative to the asymptotic inertial reference frame, those basis vectors change in the standard rotational manner

$$\frac{d\mathbf{e}_{\bar{j}}}{dt} = \Omega_{\rm rot}\times\mathbf{e}_{\bar{j}} \,. \tag{8.12a}$$

Just as typical Newtonian rotating bodies (such as the earth or the sun) precess, so it is reasonable to expect a neutron star to precess. However, our star's near-axisymmetry, together with symmetry considerations, guarantees that the precision will be (very nearly) like that of an axisymmetric Newtonian body: as seen in the co-rotating reference frame, the angular velocity of rotation $\Omega_{\rm rot}$ will precess at a constant rate $\Omega_{\rm prec}$ around the near-symmetry axis $\mathbf{e}_{\bar{z}}$, keeping its angle to that axis, $\theta_{\rm w}$ = ("wobble angle") fixed in time:

$$\frac{d\Omega_{\rm rot}}{dt} = \Omega_{\rm prec}\times\Omega_{\rm rot} \,, \quad \Omega_{\rm prec} = \Omega_{\rm prec}\mathbf{e}_{\bar{z}} \,,$$

$$\Omega_{\rm prec} = {\rm const} \,, \quad \Omega_{\rm rot} = {\rm const} \,, \quad \theta_{\rm w} \equiv \cos^{-1}(\Omega_{\rm rot}\cdot\mathbf{e}_{\bar{z}}) = {\rm const} \,. \tag{8.12b}$$

In Eq. (8.12b) the time derivative can be taken equal well in the inertial frame or in the body frame, since the two kinds of time derivatives differ by $\Omega_{\rm rot}\times$, which gives zero when acting on $\Omega_{\rm rot}$. We shall interpret (8.12b) and all other time derivatives as being taken in the inertial reference frame. Notice that the vectorial rate of precession, $\Omega_{\rm prec}$, has a rate of change that is precisely opposite to that of the rotational angular velocity,

$$\frac{d\Omega_{\rm prec}}{dt} = \Omega_{\rm prec}\frac{d\mathbf{e}_{\bar{z}}}{dt} = \Omega_{\rm rot}\times\Omega_{\rm prec} = -\frac{d\Omega_{\rm rot}}{dt} \,. \tag{8.12c}$$

Correspondingly, $\Omega_{\rm rot}+\Omega_{\rm prec}$ is a constant of the motion, as seen in the asymptotic inertial frame. Since (near) symmetry dictates that the conserved angular momentum $\mathbf{J}$, like $\Omega_{\rm rot}+\Omega_{\rm prec}$, must lie in the plane formed by the near-symmetry axis $\mathbf{e}_{\bar{z}}$ and the rotational angular velocity $\Omega_{\rm rot}$, and since there can only be one conserved direction in that rotating plane, $\mathbf{J}$ and $\Omega_{\rm rot}+\Omega_{\rm prec}$ must both lie along that one conserved direction. We shall take that direction to be the inertial $\mathbf{e}_z$ axis:

$$\mathbf{J} = J\mathbf{e}_z \,, \quad \Omega_{\rm rot}+\Omega_{\rm prec} = {\rm const}\,\mathbf{e}_z \,; \tag{8.12d}$$

see Fig. 8.1. Because the star's poloidal flattening is produced almost entirely by centrifugal forces (crystalline forces being much smaller), the rotation axis will be nearly aligned with the near-symmetry axis, and the precession rate will be small compared to the rotation rate:

$$\theta_w \ll 1 \ , \quad \frac{\Omega_{\rm prec}}{\Omega_{\rm rot}} \ll 1 \ . \tag{8.12e}$$

This implies, in turn, that the rotation axis is much more nearly aligned with the inertial $\mathbf{e}_z$ direction than with the body's near-symmetry axis $\mathbf{e}_{\bar{z}}$:

$$\frac{(\text{angle between } \Omega_{\rm rot} \text{ and } \mathbf{e}_z)}{(\text{angle between } \Omega_{\rm rot} \text{ and } \mathbf{e}_{\bar{z}})} = \frac{\Omega_{\rm prec}}{\Omega_{\rm rot}} \ll 1 \ . \tag{8.12f}$$

Many of the geometric relations described by Eqs. (8.12) are depicted in Fig. 8.1.

From Eqs. (8.12) it is straightforward to derive the time evolution of the star's co-rotating axes:

$$\mathbf{e}_{\bar{z}} = \mathbf{e}_z + \theta_w \cos[(\Omega_{\rm rot}+\Omega_{\rm prec})t\,]\mathbf{e}_x + \theta_w \sin[(\Omega_{\rm rot}+\Omega_{\rm prec})t\,]\mathbf{e}_y \ , \tag{8.13a}$$

$$\mathbf{e}_{\bar{x}} = -\theta_w \cos(\Omega_{\rm prec} t\,)\mathbf{e}_z + \cos(\Omega_{\rm rot} t\,)\mathbf{e}_x + \sin(\Omega_{\rm rot} t\,)\mathbf{e}_y \ , \tag{8.13b}$$

$$\mathbf{e}_{\bar{y}} = -\theta_w \sin(\Omega_{\rm prec} t\,)\mathbf{e}_z - \sin(\Omega_{\rm rot} t\,)\mathbf{e}_x + \cos(\Omega_{\rm rot} t\,)\mathbf{e}_y \ . \tag{8.13c}$$

These evolution equations are accurate only to leading order in the small wobble angle θ_w and the small ratio $\Omega_{\rm prec}/\Omega_{\rm rot}$. [KIP: CHECK]. By inserting these time evolutions into expression (8.9) for the star's quadrupole moment tensor I_{jk}, we can read off the time evolution of I_{jk} in the star's asymptotic inertial frame:

$$I_{zz} = \varepsilon_p I \ , \quad I_{xy} = \tfrac{1}{2}\varepsilon_e \sin 2\Omega_{\rm rot} t \ , \tag{8.14a}$$

$$I_{xx} = -\tfrac{1}{2}\varepsilon_p I + \tfrac{1}{2}\varepsilon_e I \cos(2\Omega_{\rm rot} t\,) \ , \quad I_{yy} = -\tfrac{1}{2}\varepsilon_p I - \tfrac{1}{2}\varepsilon_e I \cos(2\Omega_{\rm rot} t\,) \ , \tag{8.14b}$$

$$I_{xz} = 2\theta_w \varepsilon_p I \cos[(\Omega_{\rm rot}+\Omega_{\rm prec})t\,] \ , \quad I_{xy} = 2\theta_w \varepsilon_p I \sin[(\Omega_{\rm rot}+\Omega_{\rm prec})t\,] \ . \tag{8.14c}$$

Notice that the time evolving components of the quadrupole moment can be split into two sets, with different frequencies of oscillation: I_{za} with $a = x, y$ and frequency $\Omega_{\rm rot}+\Omega_{\rm prec}$; and I_{ab} with a and b equal to x, y and frequency $2\Omega_{\rm rot}$. We shall examine these two sets in turn.

The first set, I_{za} with $a = x, y$ can be regarded as a 2-dimensional vector in the plane orthogonal to the angular momentum $J\mathbf{e}_z$. This vector represents the effect of the misalignment between the near-symmetry axis and the rotation axis (as one sees from its

proportionality to the angle θ_w between those axes and to the star's poloidal oblateness θ_p). If the star is poloidally flattened but not equatorially deformed, i.e. if it is precisely axisymmetric, this I_{za} is the only time varying piece of the quadrupole moment. As time passes I_{za} rotates in the plane orthogonal to J with angular velocity $\Omega_{rot}+\Omega_{prec}$. Notice that this angular velocity is not the same as that, Ω_{rot}, of the $\mathbf{e}_x$ and $\mathbf{e}_y$ axes. It differs from Ω_{rot} because the piece I_{za} of the quadrupole moment regards all directions in the star's $\mathbf{e}_x \wedge \mathbf{e}_y$ plane as equivalent; it pays attention only to the way in which the normal $\mathbf{e}_z$ to this plane moves, and that normal is driven by the sum of the rotation and the precession; see Eq. (8.13a). By contrast, the electromagnetic pulsar beam emitted by a neutron star resides in some specific azimuthal plane in the star's asymptotic co-rotating frame, and thus like $\mathbf{e}_x$ and $\mathbf{e}_y$ it should rotate past earth with the angular velocity Ω_{rot}. It was Zimmermann and Szedenits (1979) who first recognized that I_{za} and the pulsar beam will rotate with angular velocities that differ by Ω_{prec}, and warned, therefore, that the frequency of the gravitational waves from I_{za} will be a precessional side band of the pulsar frequency. Since free (i.e. undriven) neutron-star precession has never yet been observed unequivocally, observations of gravitational waves from pulsars might bring us our first clean information about such precession. Idealized models suggest (Pines and Shaham, 1972a,b, 1974) that the relative magnitudes of the precession and rotation frequencies should be $\Omega_{prec}/\Omega_{rot} \sim 10^{-5}$ to 10^{-10}.

The second set of time varying quadrupole components, I_{ab} with a and b running over x and y, can be regarded (after subtracting off their constant time averages) as a symmetric, trace-free tensor that resides in the plane orthogonal to the star's angular momentum J. This I_{ab} represents the effect of the star's tiny equatorial oblateness ε_e [as one can see from the proportionality of I_{ab} to ε_e in Eqs. (8.Ia,b). If the star rotates about the near-symmetry axis $\mathbf{e}_z$ (so $\theta_w = 0$) and therefore does not precess, then this I_{ab} will be the only time varying piece of the quadrupole moment and will be responsible for all the gravitational waves. This I_{ab} can be thought of as an ellipse that lies in the plane orthogonal to J, and is attached to the star and thus rotates about J with the star's angular velocity Ω_{rot}. The fact that the components of I_{ab} oscillate with angular frequency $2\Omega_{rot}$ (and correspondingly the gravitational waves they emit will oscillate with that angular frequency) is a result of the 180-degree "return angle" of the I_{ab} ellipse; cf. Eq. (1.2) and associated discussion.

The gravitational-wave fields h_+ and $h_\times$ received at earth from the rotating, precessing neutron star depend on the direction to earth, as seen in the star's asymptotic inertial frame. Denote by ι the angle between the direction to earth and the star's conserved angular momentum $\mathbf{J} = J\mathbf{e}_z$. (See Fig. 8.1; and also Fig. 7.1 where, however, the $\mathbf{e}_z$ of this section is denoted $\mathbf{e}_{\bar{z}}$.) Without loss of generality we can take the earth to lie in the $\mathbf{e}_y \wedge \mathbf{e}_z$ plane, since all vertical planes in the star's asymptotic inertial frame are equivalent to this one: as time passes the star's rotation and precession make its quadrupole moment visit all such planes in the same manner. Then, choosing the wave's polarization axes to be

$$\mathbf{e}_{x'} = \mathbf{e}_x \ , \quad \mathbf{e}_{y'} = \cos\iota\, \mathbf{e}_y - \sin\iota\, \mathbf{e}_z \ , \tag{8.15}$$

we obtain for the the gravitational-wave fields [Eq. (6.1)]

$$h_+ = \frac{2}{r}\frac{d^2 I_{x'x'}}{dt^2} = -\frac{2}{r}\frac{d^2 I_{y'y'}}{dt^2} \ , \quad h_\times = \frac{2}{r}\frac{d^2 I_{x'y'}}{dt^2} \tag{8.16}$$

the following expressions:

$$h_+ = \frac{2(1+\cos^2\iota)}{r}\varepsilon_e I \Omega_{\rm rot}{}^2 \cos(2\Omega_{\rm rot} t)$$
$$+\frac{2\sin 2\iota}{r}\varepsilon_p \theta_w I \Omega_{\rm rot}{}^2 \cos[(\Omega_{\rm rot}+\Omega_{\rm prec})t] \ , \tag{8.17a}$$

$$h_\times = \frac{4\cos\iota}{r}\varepsilon I \Omega_{\rm rot}{}^2 \sin(2\Omega_{\rm rot} t)$$
$$+\frac{4\sin\iota}{r}\varepsilon_p \theta_w I \Omega_{\rm rot}{}^2 \sin[(\Omega_{\rm rot}+\Omega_{\rm prec})t] \ . \tag{8.17b}$$

Note that, in accord with the above discussion, the waves contain two frequencies: twice the star's rotation frequency (i.e. twice the pulsar frequency), emitted by the equatorial oblateness ε_e; and the precessional sideband of the rotation frequency (i.e. the pulsar frequency plus the precession frequency), emitted by precession of the poloidal oblateness $\theta_w \varepsilon_p$.

These waveforms were first derived by Zimmermann and Szedenits (1979), for the idealized case of a rigidly rotating Newtonian star. Later Gürsel and Thorne (1983) proved that a rigid, slowly rotating, fully relativistic star would precess in precisely the same manner as a nongravitating, rigid body (i.e. its precession would be governed by Euler's classic equations), and that therefore such a star's waveforms would have this same structure. More recently Alpar and Pines (1985)

have constructed a model for a Newtonian star with a spheroidally shaped fluid core and spheroidally shaped, elastic, deformable crust that are not aligned with each other but rotate in unison.† From their analysis one can infer that such a star will emit gravitational waves with this same waveform structure. The above analysis shows, more generally, that the waveforms must have this structure for any slowly rotating, weakly precessing, nearly axisymmetric star, regardless of the strength of its internal gravity or the source of its deformations. For the much more complicated waveforms emitted by a rigid body, in the case that θ_w, $\Omega_{prec}/\Omega_{rot}$, ε_p, and $\varepsilon_e/\varepsilon_p$ are not small, see Zimmermann (1980).

The characteristic amplitudes of the waves (8.17) at the two neutron star frequencies are readily worked out from Eq. (8.4):

$$h_{c1} = 8\pi^2\sqrt{2/15}\,\frac{\theta_w \varepsilon_p I (2f_1)^2}{r}$$

$$= 7.7\times10^{-20}\theta_w\varepsilon_p\left|\frac{I}{10^{45}\text{g cm}^2}\right|\left|\frac{2f_1}{1\text{ kHz}}\right|^2\left|\frac{10\text{kpc}}{r}\right| . \qquad (8.18a)$$

$$h_{c2} = 8\pi^2\sqrt{2/15}\,\frac{\varepsilon_e I f_2^2}{r}$$

$$= 7.7\times10^{-20}\varepsilon_e\left|\frac{I}{10^{45}\text{g cm}^2}\right|\left|\frac{f_2}{1\text{ kHz}}\right|^2\left|\frac{10\text{kpc}}{r}\right| . \qquad (8.18b)$$

Here h_{c1} is the characteristic amplitude at the precessional sideband of the pulsar frequency, $f_1 = (\Omega_{rot}+\Omega_{prec})/2\pi$ is the gravitational-wave frequency of that component, h_{c2} is the characteristic frequency at twice the pulsar frequency, and $f_2 = \Omega_{rot}/\pi \simeq 2f_1$ is the gravitational-wave frequency of that component. The characteristic amplitude (8.18b) is plotted in Fig. 2.8 for various values of ε_e as short-dashed lines. These same lines are valid for h_{c1} [Eq. (8.18a)] if one simply replaces the chosen, fixed value of ε_e by the same value for $4\theta_w\varepsilon_p$. The gravitational-wave powers emitted in the two components (8.11a,b) are

$$\left|\frac{dE_{GW}}{dt}\right|_1 = \frac{8}{5}(2\pi f_1)^6\theta_w^2\varepsilon_p^2 I^2 = \tfrac{3}{4}(\pi f_1 r)^2 h_{c1}^2 . \qquad (8.19a)$$

†Our notation is related to that of Alpar and Pines (1985), and the earlier Pines and Shaham (1972a,b, 1974) papers on this two-component model, by $\varepsilon_p = \varepsilon_\Omega$, $\theta_w = (b\varepsilon_o/\varepsilon_\Omega)\sin\theta_o\cos\theta_o$, $\varepsilon_e = \frac{1}{2}b\varepsilon_o\sin^2\theta_o$, where $b\varepsilon_o/\varepsilon_\Omega \ll 1$ and $b = B/A$. The coefficient 9/10 in Eq. (10) of Alpar and Pines (1985) for the total power radiated at frequency f_1 should be 8/5; see Eq. (8.19a).

$$\left|\frac{dE_{GW}}{dt}\right|_2 = \frac{32}{5}(\pi f_2)^6 \varepsilon_e^2 I^2 = \tfrac{3}{4}(\pi f_2 r)^2 h_{c2}^2 . \qquad (8.19b)$$

8.C Rotating neutron stars deformed by crystalline or magnetic stresses

Turn, now, from formal considerations to the astrophysics of realistic neutron stars. In order to estimate the characteristic amplitudes (8.18a) of the waves from such stars, we must determine plausible values of the moment of inertia I, the ellipticities ε_p and ε_e, and the wobble angle θ_w. The moment of inertia is easy: All neutron star models, independently of unknown features of the equation of state and independently of the star's mass, have $I = 10^{45}$ g cm^2, give or take a factor of ~ 3; see XXXXX. The ellipticities and wobble angles are more difficult. In subsection *a*, we shall review current theoretical understanding of the internal structures of neutron stars, and use that understanding to estimate the maximum plausible deformations that the crystalline regions of a neutron star can support. Similarly, in subsection *b*, we shall estimate the deformations that internal magnetic fields produce. Then, in subsection *c*, we shall review current, observationally based understanding of the number of fast pulsars in our galaxy and the distribution of their rotation periods, and shall combine that understanding with our theoretical estimates of the deformation to determine the prospects for future earth-based detectors to detect waves from known populations of pulsars. Finally, in subsection *d*, we shall speculate about the existence of a class of neutron stars with weak enough magnetic fields that they spin down by gravitational radiation reaction rather than electromagnetic emission, and shall estimate the strengths of the waves from such stars; and in subsection *e* we shall discuss waves from newborn neutron stars.

a. Crystalline stresses and the deformations they produce

Figure 8.2 shows several aspects of the internal structure of a neutron star, as predicted by theory, that are relevant for neutron-star deformations. For more details of this structure and its associated physics, see the reviews by Pines (1980), Shapiro and Teukolsky (1983), XXXXX, and references therein.

The star's outer crust (extending up to densities of $\sim 4\times10^{11}$ g cm^{-3}) has an isotropic pressure p provided by degenerate electrons, and its atomic nuclei are arranged in a crystal lattice that is governed by

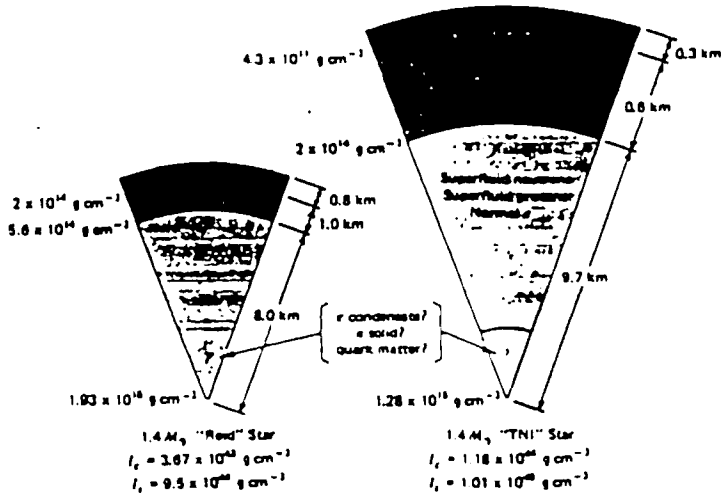

Fig. 8.2 Some features of the predicted internal structure of a neutron star. Two stellar models are shown. The one on the left, "Reid" star, has a very soft equation of state; the one on the right, "TNI" star, has a very hard equation of state. [Figure taken from Shapiro and Teukolsky (1983), but based on Pines (1980).]

Coulomb interactions. This lattice produces anisotropic, shear stresses T^S_{jk} when deformed. In the inner core (densities between $\sim 4\times10^{11}$g cm^{-3} and $\sim 2\times10^{14}$g cm^{-3}) a large fraction of the nucleons are in the form of free neutrons that have dripped off the atomic nuclei. These neutrons provide most of the isotropic pressure p — largely degeneracy pressure; and they are paired with each other in such a way as to form a superfluid. The remaining neutrons, along with protons, reside in atomic nuclei that form a Coulomb-mediated crystal lattice which supports shear stresses T^S_{jk}. The superfluid neutrons and the crystal lattice interact hardly at all; they share the same space, but they slip through each other quite happily. The principal interaction is thought to arise from the star's rotation: In the superfluid neutrons the rotation's vorticity is confined to quantized vortex lines; and these vortex lines are thought (but not known for sure) to be pinned to the crystal lattice. This pinning guarantees that the neutron superfluid and the Coulomb crystal rotate with the same angular velocity. Below this inner crust is an outer core, extending from densities $\sim 2\times10^{14}$g cm^{-3} up to some ill understood upper limit. This outer core is made of free superfluid neutrons, free superfluid protons, and normal electrons; it has an isotropic pressure p produced, largely, by strong

interactions between its nucleons; and it cannot support shear stresses. The outer core might extend all the way to the star's center, or there might be an inner core with a somewhat different structure which depends on ill understood issues of nuclear physics. One possibility (e.g. Pines, Shaham, and Ruderman, 1972; Haensel, Zdunik, and Schaeffer, 1986; XXXXX; and references therein) is that the nucleons in the inner core are arranged into a crystal structure mediated by the strong interaction, and thus can support both a shear stress T^S_{jk} and an isotropic pressure p. As is shown in Fig. 8.2, the physical sizes and masses of the various portions of the star depend quite sensitively on unknown aspects of the equation of state; they also depend sensitively on the star's mass.

The shear stress T^S_{jk} of the star's crystalline regions is the only force that can prevent the star from being axisymmetric about its rotation axis, i.e. that can produce a nonzero wobble angle θ_w and nonzero equatorial ellipticity ε_e. In producing θ_w and ε_e, this shear stress must fight against the combined forces of gravity, pressure, and rotation. Setting aside, for the moment, the possibility of a crystalline inner core, it is a difficult fight because the Coulomb interaction, which is responsible for T^S_{jk}, is far weaker than degeneracy effects and the nuclear interaction, which produce the isotropic pressure p, and also far weaker than the gravitational and centrifugal forces.

Stated more quantitatively: The gravitational forces and isotropic pressure forces are dominant and have magnitudes (on a per unit volume basis)

$$F_{\rm grav} \sim F_{\rm press} \sim \frac{M}{R^2}\rho \sim \frac{p}{R} \ , \tag{8.20a}$$

where M is the star's mass and R is its radius. The centrifugal forces

$$F_{\rm cent} \sim R\,\Omega_{\rm rot}^2 \rho \tag{8.20b}$$

are somewhat weaker, but still strong; they give rise to the star's poloidal ellipticity

$$\varepsilon_{\rm p} \sim \frac{F_{\rm cent}}{F_{\rm grav}} \sim \frac{(\Omega_{\rm rot}R)^2}{M/R} \sim \left|\frac{0.5\ {\rm msec}}{P_{\rm rot}}\right|^2 . \tag{8.20c}$$

Here $P_{\rm rot}$ is the rotation period. Weaker still are the crust's induced shear stresses. Those stresses are given by the standard stress–strain relation $T^S_{jk} = -2\mu\sigma_{jk}$, where μ is the shear modulus and σ_{jk} is the dimensionless shear strain. The shear strain is *not* the deformation

from the equilibrium shape that the star's gravitational forces, pressure forces, and centrifugal forces want to produce. Rather, σ_{jk} is the deformation of the crystal from the shape that it would have in the absence of shear forces, its "reference shape"; and that reference shape depends on the crystal's past history. An initial reference shape will be set up when the crystal first forms, in the first few seconds of the neutron star's life; and it will then change with time as a result of star quakes (i.e. crystal breakage) and plastic flow. Theoretical estimates of these changes underlie the theory of star quakes (Pines and Shaham, 1972, 1974a,b; Sec. 10.11 of Shapiro and Teukolsky, 1983). The most strongly radiating stars presumably will have reference shapes that differ from their actual shapes by as much as the crystal strength will allow; i.e., they will have shear strains σ_{jk} with magnitudes near the breaking strain $\sigma_{\rm break}$. The strongest radiators will also have strains that act coherently, over a distance of order their radius, to produce large-scale deformations; and thus their shear forces per unit volume will be

$$F_{\rm shear} \sim \frac{T^S_{jk}}{R} \sim \frac{\sigma_{\rm break}\mu}{R} . \qquad (8.20d)$$

These shear forces, acting against the balanced gravitational, pressure, and centrifugal forces, will produce deformations from the star's shear-free, nonradiating shape of magnitude

$$\varepsilon_e \sim \theta_w \varepsilon_p \sim \frac{I_c}{I}\frac{F_{\rm shear}}{F_{\rm grav}} \sim \frac{I_c}{I}\frac{\mu}{\rho}\frac{\sigma_{\rm break}}{M/R} . \qquad (8.20e)$$

Here I_c is the contribution of the crystalline material to the star's moment of inertia, and the forces and thence μ and ρ are to be evaluated in the most massive portions of the crystal – the region $\rho \sim 10^{13}$ to 2×10^{14} g cm^{-3}. Equation (8.20e) can be rewritten, in the notation of the Pines-Shaham (1972, 1974a,b) theory of starquakes and neutron-star precession, as

$$\varepsilon_e \sim \theta_w \varepsilon_p \sim \frac{B}{A}\sigma_{\rm break} ; \qquad (8.20f)$$

see also Sec. 10.11 of Shapiro and Teukolsky (1983).

How large is the breaking strain? For an idealized, perfect Coulomb lattice, theory predicts $\sigma_{\rm break}$ as large as 0.1 to 0.3. However, for laboratory crystals, impurities and defects cause $\sigma_{\rm break}$ to be far smaller: $\sigma_{\rm break} \sim 10^{-3}$ or 10^{-4}. It is thought that the crystals in neutron-star crusts will be much more perfect than laboratory

crystals, and thus may exhibit σ_{break} as large as 10^{-2} or even 10^{-1} (XXXXXX).

The shear modulus μ is better understood than σ_{break}: the theory of Coulomb lattices predicts (Baym and Pines, 1971) $\mu = 0.295 Z^2 e^2 n_N^{4/3}$, where Ze is the charge of the nuclei which form the crystal lattice, e is the electron charge, $n_N = \rho/Am_u$ is the number density of nuclei, A is the number of nucleons, including free neutrons, per nucleus, [KIP: CHECK Z and A] and m_u is one atomic mass unit. Equation-of-state calculations predict, for the more massive regions of the crystalline crust, $Z^2/A^{4/3} \simeq 1$ [KIP: CHECK], and thence $\mu/\rho \simeq 2\times10^{-4}$. For realistic neutron-star models $(I_c/I)(R/M)$ ranges from about 0.2 to 100, and it is quite sensitive to ill-understood aspects of the equation of state (XXXXX; cf. Fig. 8.2) as well as to the mass of the star: lower-mass stars have larger values. [KIP CHECK] These values of $(I_c/I)(R/M)$, μ/ρ, and σ_{break} imply that ε_e and $\theta_w\varepsilon_p$ are unlikely to exceed 10^{-4} in any neutron star; and the actual maximum might be somewhat smaller than this, say 10^{-6}. Fortunately, as Fig. 2.8 shows, these maximum ellipticities are large enough to produce gravitational waves detectable by kilometer-scale, interferometric gravitational-wave detectors.

It is important to compare these estimates, 10^{-4} to 10^{-6}, for the largest values of ε_e and $\theta_w\varepsilon_p$ with the rotationally induced poloidal ellipticity, $\varepsilon_p \simeq (0.5\ \text{msec}/P_{rot})^2$. For P_{rot} somewhat smaller than 50 msec, i.e. for gravitational-wave frequencies somewhat higher than 20 Hz, ε_p should be significantly larger than ε_e and $\theta_w\varepsilon_p$; and correspondingly, the star should be nearly axisymmetric and have a small wobble angle and the waveforms should have the form (8.17) derived above. However, for $P_{rot} \lesssim 50$ msec, i.e. for stars whose gravitational waves are at the extreme low-frequency end of the region covered by planned earth-based detectors (Fig. 2.8), the tiny deviations from sphericity might be substantially nonaxisymmetric, and the resulting waveforms might be substantially more complicated than the simple two-frequency form (8.17); cf. Zimmermann (1980) for the highly idealized (non-neutron-star-like) case of a perfectly rigidly rotating body.

b. Magnetic stresses and the deformations they produce

Soon after pulsars were discovered, Mełosh (1969), and Gunn and Ostriker (1969) pointed out that internal magnetic stresses in a pulsar might produce enough deformation to generate significant gravitational radiation. See also Ostriker and Gunn (1969) and Chau (1970);

and for highly idealized, homogeneous, fluid models of magnetically stressed stars and the waves they emit, see Tsvetkov and Tsirulev (1987, 1988), Gal'tsov, Tsvetkov and Tsirulev (1984), and references therein. Today's improved understanding of the internal structures and magnetic-field evolution of neutron stars make possible improved understanding and estimates of their magnetic-stress-induced gravitational waves:

Observations of pulsars show rather clearly that the strong surface fields they have when young, $B_{surf} \simeq 2\times10^{12}$ to 1×10^{13} Gauss, decay as the stars age, with an e-folding time of about 1×10^{7} years; see Narayan and Ostriker (1989) and references therein. This decay is believed to be due to ohmic diffusion: Inside a neutron star, at depths less than about 1 km and densities less than about 10^{12} g cm^{-3}, the electrical conductivity is small enough that the magnetic field can diffuse outward and escape from the star in 10^{7} years' time; while somewhat below this depth, the field is held in place for times longer than the age of the universe; see, e.g., Blandford, Applegate, and Hernquist (1983). These considerations dictate that we split the star's magnetic field into two parts: its temporary "crustal field", and its permanent "core field".

The crustal field in a young neutron star occupies a cross sectional area of about πR^2 at the star's surface, but only $2\pi R\,\Delta R$ as it passes through the crust and around the core; here $R \simeq 10$ km and $\Delta R \simeq 1$ km. Correspondingly, the surface field which typically is 4×10^{12} Gauss becomes $B_{crust} \simeq 2\times10^{13}$ Gauss within the crust. This field produces an anisotropic magnetic stress (pressure $p_m = B^2/8\pi \simeq 10^{25}$ dyne cm^{-2} perpendicular to the field lines and tension $-p_m$ along the field lines), which distorts the star. Gravity resists this distortion; and because of the balance between gravity and the crust's isotropic pressure $p \simeq 10^{30}$ dyne cm^{-3}, the resulting gravitational ellipticity can be written as

$$\varepsilon_e \sim \theta_w \varepsilon_p \sim \frac{p_m}{p}\frac{I_c}{I} \simeq 10^{-8}\,. \qquad (8.21)$$

[KIP: DO MORE CAREFULLY] Here $I_c \simeq 10^{-3} I$ is the moment of inertia of that portion of the crust which lies at densities below $\sim 10^{12}$ g cm^{-3}. The different field strengths and crustal thicknesses in different stars will lead to variations in the ellipticities (8.21) by perhaps one order of magnitude in either direction: from $\sim10^{-7}$ to $\sim10^{-9}$. As Fig. 2.8 shows, these ellipticities are large enough to produce waves detectable by "advanced", kilometer-scale interferometric detectors.

When the crustal field decays, it typically leaves behind a permanent field at the star's surface with strength $B_{surf} \sim 10^9$ Gauss. This is the mean field strength exhibited by old, "recycled" pulsars; see subsection *c* below. If this surface field is indicative of the permanent field in the star's core, then magnetic pressure cannot distort the core significantly. However, it is quite possible (though far from certain) that the core contains a far stronger field that got wrapped up in it during the gravitational collapse that produced the neutron star (XXXXX). Since the core is superconducting, such a field would have to be concentrated in flux tubes, with field-free matter around the tubes and field strengths $B \simeq B_{crit} \simeq 6\times10^{14}$ Gauss inside them. (At least this is so if, as we shall assume, the mean core field is $B_{core} \lesssim B_{crit}$.) The result is a mean magnetic pressure (averaged over the flux tubes and the field-free regions between them) of $p_m = B_{core}B_{crit}/8\pi$; see Easson and Pethick (1977). This magnetic pressure, acting against the gravitational forces (which are largely counterbalanced by a mean core pressure $p \sim 10^{34}$ dyne cm^{-3}), will distort the core, producing gravitational ellipticities

$$\varepsilon_e \sim \theta_w \varepsilon_p \sim \frac{p_m}{p} \sim 10^{-8} \frac{B_{core}}{10^{13}\ \text{Gauss}} . \tag{8.22}$$

Core fields as large as 10^{13} Gauss, or even 10^{15} Gauss, corresponding to ellipticities of 10^{-6} to 10^{-8} are plausible, but far from guaranteed: The core field could be as small as the remnant surface field that remains after crust fields have decayed, $\sim 10^9$ Gauss.

This core-produced ellipticity is the relevant one for old pulsars (age $\gg 10^7$ years) that have lost their crustal fields; and it might also be the relevant one for most very young pulsars (age $\lesssim 10^4$ years). The reason is that most young pulsars might be born with only small crustal fields ($B_{surf} \ll 10^{12}$ Gauss), and might acquire their large crustal fields only slowly, over a time $\sim 10^4$ years (give or take a factor 10) as a result of the thermoelectric effect; see Blandford, Applegate, and Hernquist (1983). (At least one pulsar, the Crab, has achieved a surface field of 5×10^{12} Gauss after an age of only 1000 years.)

d. Gravitational waves from known populations of pulsars

The more slowly a neutron star rotates, the weaker will be its gravitational waves; see Eqs. (8.18). Because of the limited sensitivities of planned detectors (Fig. 2.8), this means that the only stars of revelance for wave detection are those with rotation periods $P_{rot} \lesssim 0.2$

sec, i.e. gravitational-wave frequencies $f_2 \gtrsim 10$ Hz. There are two known, and fairly well studied populations of neutron stars in this fast-rotation region: "Young, fast radio pulsars" and "recycled pulsars".

Young, fast radio pulsars: Narayan and Ostriker (1989), by comparing evolutionary models with the observed distribution of pulsars, conclude that there is a fairly homogeneous population of young, fast radio pulsars. These pulsars are born with an average initial rotation period that is definitely in the region of interest to us, $\bar{P}_i < 0.2$ sec, and it is plausible that $\bar{P}_i \lesssim 10$ msec. Once the magnetic fields of these pulsars have reached their steady state strengths (after, possibly, an epoch of $\sim 10^4$ years of growth via the thermoelectric effect; see Blandford, Applegate, and Hernquist, 1983), the surface fields have an average strength of $\bar{B} = 4\times 10^{12}$ Gauss; and there is a one-standard-deviation spread about this mean that ranges from 1.7×10^{12} Gauss for the more weakly magnetized pulsars to 1.0×10^{13} Gauss for the more strongly magnetized ones. These fields, once built up, then begin to decay with an e-folding time of 10^7 years – so long that it will not be relevant for our discussion of the young, fast pulsars. Narayan and Ostriker conclude that the birth rate of these fast pulsars is about one per 200 years in our galaxy, and we shall adopt this value in the estimates that follow. However, some investigators argue for a much higher birth rate – as high as several per ten years (Blair, 1989). [KIP: CHECK]

The young pulsars gradually spin down due to emission of electromagnetic and gravitational waves. Electromagnetic emission (essentially dipole radiation from the rotation of the star's magnetic field) causes a star's rotation period to decrease at a rate $\dot{P}_{\rm rot}$ given by (XXXXX)

$$P_{\rm rot}\dot{P}_{\rm rot} \simeq 10^{-15} B_{12}^2 \ {\rm sec}\ , \qquad (8.23a)$$

where B_{12} is the surface magnetic field strength in units of 10^{12} Gauss. During the epoch when the field is constant and gravitational-radiation-reaction torques are negligible compared to electromagnetic, the resulting evolution of the rotation period is

$$P_{\rm rot}^2 = P_i^2 + (10\,{\rm msec})^2 \left| \frac{B}{4\times 10^{12}\,{\rm Gauss}} \right|^2 \frac{\tau}{100\,{\rm yr}} \ . \qquad (8.23b)$$

Here τ is the age of the pulsar. This evolution, together with the birthrate of one fast pulsar each 200 years and the average field

strength of 4×10^{12} Gauss, should produce a distribution of pulsar periods in our galaxy

$$\frac{dN}{d\ln P_{\rm rot}} \simeq \left(\frac{P_{\rm rot}}{10\ {\rm msec}}\right)^2 . \tag{8.23c}$$

Thus, assuming (as is likely) that $\bar{P}_i$ is $\lesssim 10$ msec, so Eq. (8.23c) is valid for periods as short as 10 msec, there should be ~ 4 young pulsars in our galaxy with gravitational-wave frequencies $f_2 > 100$ Hz, and ~ 400 young pulsars with gravitational-wave frequencies $f_2 > 10$ Hz.

If, as is quite plausible, most fast pulsars are born with field strengths $B \ll 10^{12}$ Gauss, and only acquire 10^{12}-Gauss fields after they age for $\sim 10^4$ years, then gravitational radiation reaction might be the dominant spindown force during the first few thousand years of their lives. By equating the energy loss rate of Eq. (8.19) to the rate of change of $\frac{1}{2}I\Omega_{\rm rot}^2$, and using $I = 1\times10^{45}$ g cm^2, we obtain for the gravitational-radiation-reaction spindown rate

$$P_{\rm rot}^3 \dot{P}_{\rm rot} \simeq 3\times10^{-11}\,\varepsilon_e^2\ {\rm sec}^3 . \tag{8.24a}$$

Here and below the equatorial ellipticity ε_e is a surrogate for $(\varepsilon_e^2+\frac{1}{4}\theta_w^2\varepsilon_p^2)^{1/2}$. This spindown rate corresponds, via Eq. (8.19), to the following value for the waves' characteristic amplitude h_c at earth:

$$\begin{aligned}[(h_{c2}^2+\tfrac{1}{4}h_{c1}^2)^{1/2}]_{\rm max} &= \frac{1}{r}\left(\frac{4I}{3}\frac{\dot{P}_{\rm rot}}{P_{\rm rot}}\right)^{1/2} \\ &\simeq 3\times10^{-25}\left(\frac{10\ {\rm kpc}}{r}\right)\left(\frac{1000\ {\rm yr}}{P_{\rm rot}/\dot{P}_{\rm rot}}\right)^{1/2} .\end{aligned} \tag{8.24b}$$

In general, this characteristic amplitude is an upper limit; if (as will usually be the case) the spindown is electromagnetic, then the waves will be weaker than (8.24b). The gravitational spindown rate (8.24a) produces the period evolution

$$P_{\rm rot}^4 = P_i^4 + (2.4\ {\rm msec})^4\left(\frac{\varepsilon_e}{10^{-6}}\right)^2\left(\frac{\tau}{10^4\ {\rm yr}}\right) . \tag{8.24c}$$

Equations (8.24a) and (8.23a) imply that, in order for gravitational spindown to dominate over electromagnetic, it is necessary that the star's surface magnetic field be

$$B < 3\times10^{10}\ {\rm Gauss}\left(\frac{\varepsilon_e}{10^{-6}}\right)^2\left(\frac{1\ {\rm msec}}{P_{\rm rot}}\right)^2 . \tag{8.24d}$$

From Eqs. (8.23b) and (8.24c) one can infer the following: If most fast pulsars are born with surface magnetic fields $B \ll 10^{12}$ Gauss and only acquire 10^{12}–Gauss fields after, on average, $\sim 10^4$ years, and if their average initial periods are $\bar{P}_i \lesssim 10$ msec, then these neutron stars will remain in the $P \lesssim 10$ msec region until their fields have grown to $B \sim 10^{12}$ Gauss; and, correspondingly, there will be ~ 100 rotating neutron stars in this region, with gravitational–wave frequencies $f_2 \gtrsim 100$ Hz. Because of their small fields, the pulsar emission from these very young neutron stars will be difficult to detect.

In summary, it is reasonable to expect in our galaxy somewhere between ~ 4 and ~ 100 young neutron stars with gravitational–wave frequencies $f_2 > 100$ Hz, and ~ 400 with 10 Hz $< f_2 <$ 100 Hz.

Known, young pulsars. No young pulsars have yet been discovered in the region $f_2 > 100$ Hz, except, possibly, an 0.5 msec object in the remnant of supernova 1987A. This is in accord with the above estimates, which predict only ~ 4 in the entire galaxy with $f_2 > 100$ Hz and strong enough magnetic fields to be bright radio emitters. Several young pulsars, however, have been discovered in the region 10 Hz $< f_2 <$ 100 Hz. Among them are three associated with supernova remnants: (i) PSR 0531+21, which has $P_{\rm rot} = 33$ msec corresponding to a gravitational–wave frequency $f_2 = 60$ Hz, and has an age $\tau \simeq 1000$ years and lies in the Crab nebula at a distance $r = 2$ kpc from earth; (ii) PSR 1951+32, which has $P_{\rm rot} = 40$ msec corresponding to $f_2 = 50$ Hz, and has an age $\tau \sim 10^5$ years and is associated with the nebula CTB 80 at a distance XXXX from earth (Kulkarni et. al., 1988); and (iii) PSR 0833–45, which has $P_{\rm rot} = 89$ msec corresponding to $f_2 = 22$ Hz, and has an age XXX and lies in the Vela nebula at a distance of only 500 pc from earth. Fig. 2.8 shows the gravitatonal–wave frequencies f_2 of these pulsars and the rate–of–spindown–inferred upper limits (8.24b) on their characteristic amplitudes h_{c2}. These observational upper limits are not quite in the plausible region of ellipticities $\varepsilon_e < 10^{-4}$. Rather, they correspond to $\varepsilon_e \simeq XXXX$ for the Crab, XXXX for Vela, and XXXXX for CTB 80. For an extensive tabulation of other known pulsars and their possible gravitational–wave properties see Barone et. al. (1988b). (Note that the characteristic amplitude h_c of this book is $\sqrt{4/3}$ times the h of Barone et. al., and the ε_e of this book is equivalent to their $\varepsilon = \theta_w \varepsilon_o$.)

Recycled pulsars. Recycled pulsars are especially common in globular star clusters. These pulsars seem to have formed in the following way (see, e.g., Kulkarni 1989 for a review): Our galaxy's first epoch of

star formation, $\sim 10^{10}$ years ago, produced a number of massive stars, which evolved quickly to form neutron stars. Those neutron stars presumably were bright pulsars until, after about 10^7 years, their magnetic fields decayed and their pulsar emission became very weak. Some of those neutron stars wound up in globular star clusters, where over the $\sim 10^{10}$ year life of the galaxy many of them captured ordinary stars to form close binary systems. As each such binary aged, a combination of the evolution of the ordinary star and gravitational radiation reaction (which drives the stars together) caused the ordinary star to start dumping its mass onto the neutron star. The neutron star was spun up by this accretion, to rotation periods in the millisecond region; and with this new, high spin rate its weak ($\sim 10^9$ Gauss) magnetic field is now able to produce observable, though weak radio waves.

Enough recycled pulsars have been discovered in globular clusters in the last several years to permit an estimate of the total number in our galaxy. The result is remarkably large: $\sim 10^4$ (Kulkarni, Narayan, and Romani, 1989). Most of these pulsars have rotation periods $P_{\rm rot} < 10$ msec and thus gravitational-wave frequencies $f_2 > 200$ Hz. Their observed spindown rates are typically so small that the constraints they place on gravitational radiation reaction imply gravitational ellipticities $\varepsilon_e \ll 10^{-6}$. For example, the best studied of the recycled pulsars, PSR1937+21, which has $P_{\rm rot} = 1.56$ msec corresponding to $f_2 = 1300$ Hz, is constrained to have $\varepsilon_e \lesssim 4\times10^{-9}$ and $h_c < 1\times10^{-27}$; see Fig. 2.8. These small values of ε_e are in good accord with the theoretical discussion in subsections *a* and *b* above: The neutron stars are very old and probably well annealed (cf. Alpar and Pines, 1985), and thus are not likely to have large crystal-induced ellipticities; and they have lost their large crustal magnetic fields and thus should have negligible crust-field-induced ellipticities. On the other hand, if only a very small fraction of these 10^4 millisecond pulsars have managed to resist annealing, or possess large magnetic fields wound up in their cores, or possess solid cores with significant deformations, then those few stars could be strong radiators of gravitational radiation.

There are also recycled pulsars outside of globular clusters (PSR1937+21 is an example); but not enough have yet been discovered, and the searches for them have not yet been extensive enough, to permit reliable estimates of their numbers.

d. Waves from as-yet-unobserved populations of neutron stars

Turn attention, now, from known populations of pulsars to possible, as-yet-undiscovered populations of rotating neutron stars. Blandford (1984) has pointed out that the most interesting such stars would be those that are spinning down by gravitational radiation reaction (since the absence of electromagnetic spindown would keep their periods as short as possible and thus enhance their detectability). The most interesting would also have strong enough waves that they have moved away from their initial periods, and thus now have $P_{\rm rot} \propto \tau^{1/4}$ [Eq. (8.24c)]. This period-age relation implies that each star in this population will have

$$(h_{c2}^2 + \tfrac{1}{4}h_{c1}^2)^{1/2} = \left[\frac{16}{3}\frac{I}{r^2\tau}\right]^{1/4}; \qquad (8.25)$$

cf. Eq. (8.24b). Of those with ages of order τ, the nearest such star to earth will be at a distance $r \simeq R_G\sqrt{\tau_B/\tau}$, where τ_B (assumed $\lesssim \tau$) is the mean time between births of these pulsars in our galaxy and $R_G \simeq 10\,\text{kpc}$ is the radius of the galaxy's disk. Correspondingly, this nearest (and brightest) pulsar will have a characteristic amplitude

$$(h_{c2}^2 + \tfrac{1}{4}h_{c1}^2)^{1/2} \simeq \left[\frac{16}{3}\frac{I}{R_G{}^2\tau_B}\right]^{1/2} \sim 2.2\times10^{-25}\left[\frac{10^4\,\text{years}}{\tau_B}\right]^{1/2}, \qquad (8.26)$$

independently of its frequency and ellipticity (Blandford, 1984). This characteristic amplitude is plotted as horizontal dashed curves in Fig. 2.8, for $h_{c1} = 0$, $h_{c2} \neq 0$, and several values of τ_B.

An example of such a family of neutron stars, based on current ideas about pulsar evolution (see above), would be very young ones ($\tau \lesssim 10^4\,\text{yr}$, $\tau_B \lesssim 200\,\text{yr}$) that have not yet acquired strong surface fields, but possess large enough crystalline deformations, say $\varepsilon_e \sim 10^{-4}$, to have achieved a $P \propto \tau^{1/4}$ spindown stage. The nearest such star, if $\tau_B \simeq 200\,\text{yr}$, would be very strong, $h_{c2} \simeq 5\times10^{-24}$, and of very high frequency, $f_{c2} \sim 1000\,\text{Hz}$. Such a neutron star would be detectable by the first interferometric detectors in the LIGO; see Fig. 2.8.

There could well be other families of neutron stars, spinning down by gravitational radiation reaction and described by Eq. (8.26), that are not even hinted at by current ideas about pulsar evolution.

e. Waves from newborn neutron stars

Also of great interest would be a newborn neutron star with strong enough deformations to spin down gravitationally; see, e.g., Piran and Nakamura (1988). The characteristic amplitude for such a star, Eq. (8.25), can be rewritten as

$$(h_{c2}^2+\tfrac{1}{4}h_{c1}^2)^{1/2} \simeq \left[\frac{16}{3}\frac{I}{r^2\tau}\right]^{1/2} \simeq 4\times10^{-23}\left[\frac{10\,\text{kpc}}{r}\right]\left[\frac{10^7\,\text{sec}}{\tau}\right]^{1/2}; \qquad (8.27a)$$

and its frequency will evolve as [cf. Eqs. (8.27a) and (8.18)]

$$f_2 \simeq 1100\,\text{Hz}\left[\frac{10^{-4}}{\varepsilon_e}\right]^{1/2}\left[\frac{10^7\,\text{sec}}{\tau}\right]^{1/4}. \qquad (8.27b)$$

Here it is assumed that ε_e does not change significantly during the early spindown, and is large enough to drive f_2 away from its initial value during the time of interest. Note that, if the waves from this newborn neutron star are studied using a detector with a "white" noise spectrum, $S_h(f)$ independent of f, then both the signal h_c [Eq. (8.27a)] and the detector noise h_n [Eq. (8.5)] will decrease as $1/(\text{time})^{1/2}$. Thus, experimenters will achieve the same signal-to-noise ratio S/N by performing a 200-day search that begins 100 days after the supernova, as by performing a two-day search that begins one day after the supernova. (On the other hand, if the spin period has not yet evolved away from its initial value, the longer, later search will be more sensitive than the shorter, earlier search.)

The wave characteristics (8.27), which represent an upper limit on the strength of periodic waves from a newborn neutron star, are shown in Fig. 2.8 for $\tau = 10^7$sec and r = 10 kpc = (distance to center of our galaxy).

An example of such a newborn neutron star is that in the remnant of supernova 1987A. One stretch of optical observations in late 1988 (Middleditch et. al., 1989) showed optical pulsations corresponding to a very rapid neutron-star rotation: $P_{\text{rot}} = 0.508$ msec, corresponding to $f_2 = 3.94$ kHz and $f_1 = 1.97$ kHz, at time τ *XXX* months after the supernova. The steadiness of the pulsation frequency implied a limit on the spindown timescale, $P_{\text{rot}}/\dot{P}_{\text{rot}} \lesssim 1600$ years. However, these optical pulsations were seen in only one, seven-day [KIP: CHECK] stretch of data. They then disappeared and had not reappered as of the time this book went to press. If we accept these observations as genuinely due to neutron-star rotation, then: (i) The neutron star was not spinning

down fast enough to have moved away from its initial spin period, so Eq. (8.27a) is not relevant for it. (ii) The rate of injection of energy into the supernova remnant's expanding gas was small enough to place a limit of $(P_{rot}/\dot{P}_{rot})_B \lesssim 10^7$ years on the electromagnetic-induced slowdown timescale. Thus, if there is any slowdown on the shorter timescale of ~ 1600 years, it must be gravitationally induced. (ii) The 1600-year limit on the spindown timescale implies an upper limit of $\varepsilon_e \lesssim 2\times10^{-7}$ on the gravitational ellipticity [Eq. (8.24a)]. (iii) The spindown timescale also implies upper limits on the waves' characteristic amplitudes, XXX months after the supernova, of $h_{c2} \lesssim 5\times10^{-26}$ at $f_2 = 3.94$ kHz, $h_{c1} \lesssim 1\times10^{-25}$ at $f_1 = 1.97$ kHz, and $h_c \lesssim 7\times10^{-25}(300\text{ Hz}/f)$ for waves at frequency f from the CFS instability (Sec. 8.D, below; Kluzniak et. al., 1989). Katz (1989) argues that the f_1 and f_2 waves may well have been of this size, with the gravitational ellipticities being induced either by crystalline stresses or by convection-induced deformations in fluid layers of the young star. Much earlier in the neutron star's life, i.e. in its first few minutes, hours, or days, there could have been much larger gravitational ellipticities and correspondingly much larger wave strengths than these. Unfortunately, the strongest waves allowed, Eq. (8.27a) with $r = 50$ kpc, were a factor ~ 20 weaker than the sensitivies of the prototype interferometric detectors that existed at the time of the supernova; see Fig. 2.8. Nevertheless, being healthily skeptical of theorists' arguments, the Caltech/MIT and Glasgow groups performed a search for such waves in the first two weeks after the supernova; see XXXXX.

D. Rotating Neutron stars deformed by the CFS instability

When a neutron star rotates more rapidly than a critical rotation period, $P_{crit} \cong 0.7$ to 1.7 msec (which depends strongly on the star's equation of state, mass, and temperature-dependent viscosity), then an instability driven by gravitational radiation reaction ["Chandrasekhar (1970)-Friedman-Schutz" (1978), or "CFS" instability] will create and maintain significantly strong pressure waves in the star's surface layers and crust. These pressure waves propagate in the opposite direction to the star's rotation, and radiate gravitational waves as they propagate. For detailed discussions see Friedman (1978, 1983), Wagoner (1984), Managan (1985), Imamura, Friedman, and Durisen (1985), Baumgart and Friedman (1986), Lindblom (1986, 1987, 1988), Friedman, Ipser and Parker (1986), Schutz (1987), Cutler and Lindblom (1987).

The physical origin of this CFS instability is easily understood: Consider a neutron star that rotates in a "positive" ("right-handed") sense with angular velocity of rotation $\Omega = d\phi/dt > 0$, as measured by observers in its asymptotic (inertial) rest frame. Here ϕ is azimuthal angle and t is proper time as measured in the asymptotic frame. Suppose that pressure (sound) waves with angular mode number $m > 0$ are propagating azimuthally inside the star, in the opposite direction to the star's rotation ("negative", "left-handed", "counterclockwise" direction), so the density perturbations as measured in the star's frame have the form

$$\delta\rho = F(r,\theta)\cos(\bar{\omega}t + m\bar{\phi}) , \tag{8.28a}$$

where

$$\bar{\phi} \equiv \phi - \Omega t \tag{8.28b}$$

is the azimuthal angle as measured in the star's frame, and $\bar{\omega} > 0$ is the hydrodynamic angular frequency. Our demands that Ω, m, $\bar{\omega}$ all be positive guarantee that the rotation is positive and the sound waves propagate negatively, as seen in the star's frame. On the other hand, as seen in the asymptotic rest frame outside the star the density perturbation has the form [inferred by inserting (8.28b) into (8.28a)]

$$\delta\rho = F(r,\theta)\cos[(\bar{\omega} - m\Omega)t + m\phi] . \tag{8.29}$$

If $\bar{\omega} - m\Omega > 0$, the sound waves propagate negatively as seen in the asymptotic rest frame; but if $\bar{\omega} - m\Omega < 0$ the rotation drags them into positive motion (Fig. 8.3). This regime of dragging, $\bar{\omega} - m\Omega < 0$, is the one of interest.

The sound waves emit gravitational radiation. Consider the energetics of that emission, from the viewpoint of the asymptotic rest frame: Since gravitational waves always carry positive energy [expression (4.33) is positive definite], the waves must reduce the star's total mass-energy [cf. Eq. (6.53)]. That reduction must come through radiation reaction acting back on the sound waves. But the energy of the sound waves, as seen in the asymptotic rest frame, is negative! This is because, as seen in the star's frame, the sound waves produce an average motion of matter in the negative direction, and thus as seen in the asymptotic rest frame they reduce the velocity of rotation of the stellar matter; and correspondingly they reduce the star's kinetic energy of rotation. [If one thinks of the sound waves quantum mechanically, i.e. as phonons, it is even more clear that their energies are negative. In

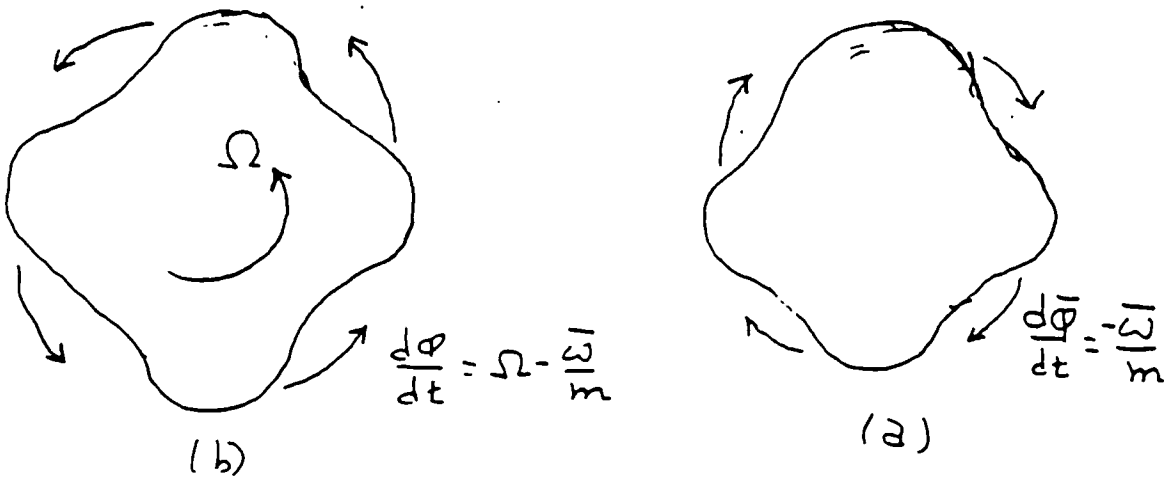

Fig. 8.3 The CFS Instability for a mode with $m = 4$: (a) As seen in the rest frame of a rotating neutron star sound waves (including currugations of the star's surface, shown exagerated here) propagate around the star periphery in a negative sense (i.e. opposite to the star's rotation), with angular velocity $d\phi/dt = -\bar{\omega}/m$. (b) As seen in the star's asymptotic (inertial) rest frame the sound waves are dragged by the star's rotation, so they move around it in a positive sense, though more slowly than the rest of the stellar matter. These waves have negative energy and thus are amplified in reaction to the emission of gravitational radiation, unless viscous damping dominates over radiation reaction.

the star's frame each phonon has components of 4-momentum $-p_{\bar{0}} = \hbar\,\bar{\omega} > 0$ and $p_{\bar{\phi}} = -m\hbar < 0$. When transformed to the laboratory frame this gives an energy

$$E = -p_0 = -\left[p_0 + \left(\frac{\partial\bar{\phi}}{\partial t}\right)_{\phi} p_{\bar{\phi}}\right] = \hbar\,(\bar{\omega} - m\Omega)\,, \tag{8.30}$$

which is negative in the regime of dragging.] As gravitational radiation carries off more and more energy, it drives the sound waves' energies more and more negative, thereby increasing the number of phonons in the star, i.e. amplifying the sound waves. Physically, radiation reaction tries to reduce the waves' forward motion and thus pushes them in the negative direction; and since this is the same direction as their motion as seen in the star's frame, the push amplifies the waves. This is the CFS instability – first discovered for $m=2$ by Chandrasekhar (1970) and later discovered in full generality by Friedman and Schutz (1978) and

Friedman (1978).

This instability is a variant of a very general phenomenon in physics: Whenever a wave is dragged "supersonically" by the medium in which it lives, it acquires negative energy and develops instabilities. Other examples are wind-driven waves on the surface of the ocean, as analyzed in the rest frame of the wind, Cerenkov radiation as analyzed in the rest frame of the charged particle that emits it, and superradiant scattering of waves off a rotating black hole.

For arbitrarily large m, one can have sound waves that circulate around the star arbitrarily close to the star's surface; and these waves will have $\bar{\omega} = mv_s/R$, where R is the star's radius and v_s is the velocity of high-frequency sound waves at the waves' location. For such waves, the condition of dragging becomes $m\Omega/\bar{\omega} = \Omega R/v_s > 0$. The larger is m, the nearer the surface the waves can circulate and the smaller will be v_s. Accordingly, for any nonzero stellar rotation rate Ω, there will be unstable modes of arbitrarily large m (Friedman, 1978 KIP: CHECK – DO I HAVE THE EXPLANATION RIGHT?); and as Ω is increased, modes of lower and lower m, reaching deeper and deeper into the star's interior, will go unstable (Friedman and Schutz, 1978). [KIP: CHECK REFS]

Viscosity inside the star can counteract the instability by damping the sound waves faster than gravitational radiation reaction makes them grow. (Lindblom and Detweiler, 1987; Detweiler and Lindblom, 1987; Lindblom and Hiscock, 1983). Viscosity is especially strong on modes of large m, since they involve especially large shears of the stellar matter. Thus, there is a competition between radiation reaction and viscosity. Viscosity always wins for arbitrarily large m, thereby stabilizing stars that rotate slowly. However, for sufficiently fast rotators and sufficiently compact stars, radiation reaction can win in some finite range of m. It is a complicated task, on which researchers are still working hard (e.g. Friedman, 1983; Managan, 1985; Imamura, Friedman and Durisen, 1985; Friedman, Ipser, and Parker, 1986; Lindblom, 1986, 1987, 1988; Cutler and Lindblom, 1987), to determine, for realistic neutron-star models, which value of m goes unstable first and at what angular velocity of stellar rotation. The answer will depend critically on the stellar temperature, since the viscosity is highly temperature dependent (Flowers and Itoh, 1979). The final story is not yet in, but preliminary results suggest that the mode with $m=3$ or 4 or 5 will go unstable first, and that the critical angular velocity at which it goes unstable will be less than that for centrifugal breakup if the star's central temperature lies between some minimum value $T_{\min}$ and some

maximum T_{max}. The minimum, which is set by shear viscosity due to XXXXXXX, is estimated to be $T_{min} \sim 10^7$ K (Cutler and Linblom, 1987; Lindblom, 1987, 1988; Friedman, 1990). The maximum, which is set by bulk viscosity due to a possible pion condensate in the stellar core (Sawyer, 1989; Friedman, 1990), is estimated to $T_{max} \sim 2\times10^9$K (XXXX; Friedman, 1990).

The great uncertainty in these minimum and maximum temperatures produces great uncertainty over whether the CFS instability is a common and important phenomenon in the real universe or never occurs. Even the frequencies of the emitted waves, in the case of instability, are highly uncertain. It is only known that they lie in the range 100 Hz to 1000 Hz (e.g. Lindblom, 1988).

If the temperature range is suitably wide, then, as Wagoner (1984) has pointed out, the CFS instability could come into play during the spinup that recycles pulsars: If the neutron star's magnetic field during the spinup is $B \gtrsim 10^7$Gauss (which is thought to be the usual case), then the spinup halts when the star's magnetosphere, at its intersection with the surrounding accretion disk, is circulating at the disk's local Keplerian velocity. If, instead, the magnetic field is $B \lesssim 10^7$Gauss, then the magnetosphere cannot hold the accretion disk back from the vicinity of the star's surface, and the star will spin up to such a high rotation rate that the CFS instability should set in. In this case, the star should live during its accretion in the unstable region, the torque due to accretion being counterbalanced by gravitational radiation reaction.

Given the extreme observational difficulty of finding by electromagnetic means evidence for rapid neutron-star rotation (see, e.g., Sec. IV of Reynolds and Stinebring, 1984 for a discussion of radio-frequency searches), it is quite possible that a number of accreting neutron stars in our galaxy are now in the CFS regime, radiating strong gravitational waves. And given the uncertainties about the effects of viscosity, and the possibility that neutron stars with fields as low as 10^7 Gauss may be exceedingly rare, it is possible there are none.

Wagoner (1984) has pointed out that, for a CFS-unstable neutron star, the energy being radiated in gravitational waves and that being radiated as accretion-induced X-rays will both be proportional to the accretion rate; and consequently the characteristic amplitude of the gravitational waves at earth will be proportional to the square root of the X-ray flux F_X arriving at earth:

$$h_c \simeq 2\times10^{-27}\left[\frac{300\ \text{Hz}}{f}\right]^{1/2}\left[\frac{F_X}{10^{-8}\ \text{erg cm}^{-2}\ \text{sec}^{-1}}\right]^{1/2} . \qquad (8.31)$$

[KIP: FIX FIGURE BECAUSE OF $f^{-1/2}$ NOT f^{-1}] The frequency f of the waves will be

$$f = \frac{m\Omega - \bar{\omega}}{2\pi} . \qquad (8.32)$$

The waves' angular frequency $\bar{\omega}$ in the star's co-rotating frame is somewhat sensitive to poorly understood aspects of the star's structure, and this uncertainty in $\bar{\omega}$ is amplified by the fact that $m\Omega$ is not far from $\bar{\omega}$. Thus, the wave frequency (8.32) is very poorly known. A rough estimate, more illuminating than (8.32), comes from noting that (i) the wave frequency f must go to zero when the star rotates with the critical angular vecocity $\Omega_{\text{crit},m}$ at which the wave pattern is at rest in the star's asymptotic inertial frame; and correspondingly, the wave frequency in the co-rotating frame is given by a power series expansion, the first two terms of which are $\bar{\omega} \simeq m\Omega_{\text{crit},m} + \text{const}\times(\Omega - \Omega_{\text{crit},m})$. Here the constant is positive because larger rotation produces larger centrifugal and Coriolis forces, which drive the frequency $\bar{\omega}$ up [KIP: CHECK WITH FRIEDMAN OR LINDBLOM; WHERE IS THIS DISCUSSED; CF. KLUZNIAK ET AL, 1989 WHO GIVE FORMULA (8.33) WITHOUT DERIVATION]. Correspondingly, Eq. (8.32) for the gravitational-wave frequency becomes

$$f \simeq \alpha\frac{m(\Omega - \Omega_{\text{crit},m})}{2\pi} , \qquad (8.33)$$

where α is a constant somewhat smaller than unity. The star typically cannot rotate much faster than $\Omega_{\text{crit},m}$ because centrifugal forces will then tear mass off the star's equator. This keeps the gravitational-wave frequency f rather low compared to $m\Omega/2\pi$. For typical models of accreting neutron stars, it is in the range KIP CHECK 100 to 1000 Hz.

The fiducial value of the X-ray flux in Eq. (8.31), $F_X \cong 10^{-8}$ erg cm^{-2} sec^{-1}, is 1/20 that of Sco X-1, the brightest quasi-steady source in the sky and itself a candidate for a CFS-unstable object. As Fig. 2.8 shows, stars with X-ray fluxes as low as 1/1000 Sco X-1 could be interestingly strong sources of gravitational waves. In such a star, the sound waves should produce oscillations of the shape of the stellar surface which should modulate the emitted X-rays at the same frequency as the gravitational radiation (Wagoner, 1984; Kluzniak, Lindblom, and Wagoner, 1979). Unfortunately, the sensitivities of past X-

ray telescopes have been too poor to detect such rapid and weak modulations. There is an interesting proposal (Wood, 1986; Wood et. al. 1986) for a new, more sensitive X-ray telescope designed to search for such modulations in Sco X-1 and other, weaker X-ray sources — especially low-mass (galactic bulge) binaries. Such a telescope, operated in coordination with gravitational-wave detectors, might one day give a wealth of new information about neutron stars.

A second possibility for waves from the CFS instability is in a newborn, very rapidly rotating neutron star, such as that which might exist in the remnant of supernova 1987A (see, e.g., Kluzniak et. al., 1989) -- KIP: GET UP TO DATE VIEWPOINT ON THIS FROM LINDBLOM.

8.E Binary stars

Ordinary binary star systems are the most reliably understood of all sources of gravitational waves. From the measured mass and orbital parameters of a binary and its estimated distance, one can compute with confidence the details of its waves. Unfortunately, ordinary binaries have orbital periods no shorter than about an hour and, correspondingly, their gravitational-wave frequencies are $f \lesssim 10^{-3}$ Hz. The shortest known binary of all is a white-dwarf/neutron-star system with orbital period 11 minutes and gravitational-wave frequency $f \simeq 3\times10^{-3}$ Hz (Stella, Priedhorsky, and White 1987). Because of seismic noise, detectors in earth laboratories cannot hope to see waves of such low frequency. However, interferometric detectors in space, tentatively planned for the turn of the century, should see them with relative ease (Secs. 2.H and 12.B).

Detailed formulas for the waves from a binary star, including the effects of the eccentricity and inclination of the orbit, have been derived from the quadrupole formalism by Peters and Mathews (1963) and Wahlquist (1987). See also Wagoner and Will (1976), and Gal'tsov, Matiukhin, and Petukhov (1980) for post-Newtonian corrections. From the quadrupole formula (6.1), Wahlquist (1987) obtains the following formulas for the waveforms at Newtonian order:

$$h_+(t-r) = H(A_0 + eA_1 + e^2A_2)\,, \quad h_\times(t-r) = H(B_0 + eB_1 + e^2B_2). \qquad (8.34a)$$

Here the polarization axes are so oriented that one of the axes of the + mode coincides with the projection on the sky of the normal to the orbital plane; H is an overall amplitude given by

$$H \equiv \frac{4\mu}{r}\frac{(2\pi f_o M)^{2/3}}{1-e^2}\,; \qquad (8.34b)$$

e is the eccentricity and f_o is the frequency (1/period) of the orbit; $M \equiv M_1+M_2$ and $\mu \equiv M_1M_2/M$ are the total and reduced masses of the stars; and r is the distance from earth to the binary system. The quantities A_i and B_i are functions of retarded time $t-r$. They are expressed most simply in terms of the angular position θ of the stars in their orbit, relative to $\theta = 0$ at periapse (when the stars are closest together). This angle θ is related to $t-r$ by

$$t-r = (t-r)_{\text{periapse}}+\frac{1}{2\pi f_o}\left[\arccos\left(\frac{e+\cos\theta}{1+e\cos\theta}\right)-\frac{e(1-e^2)^{1/2}\sin\theta}{1+e\cos\theta}\right] . \quad (8.34c)$$

Wahlquist obtains for A_i and B_i the expressions

$$A_0 = -\tfrac{1}{2}(1+\cos^2\iota)\cos2(\theta-\theta_n) , \quad B_0 = -\cos\iota\sin2(\theta-\theta_n) ,$$

$$A_1 = \tfrac{1}{4}\sin^2\iota\cos\theta-\tfrac{1}{8}(1+\cos^2\iota)[5\cos(\theta-2\theta_n)+\cos(3\theta-2\theta_n)] ,$$

$$B_1 = -\tfrac{1}{4}\cos\iota[5\sin(\theta-2\theta_n)+\sin(3\theta-2\theta_n)] ,$$

$$A_2 = \sin^2\iota-\tfrac{1}{4}(1+\cos^2\iota)\cos2\theta_n , \quad B_2 = \tfrac{1}{2}\cos\iota\sin2\theta_n . \quad (8.34d)$$

Here ι is the angle of inclination of the orbital plane to the tangent plane of the sky, and θ_n is the value of θ at the line of nodes, i.e. when the stars pass through the plane of the sky; in other words, θ_n is the angle from periapse to the line of nodes.

Figure 8.4 shows these waveforms for the special case $\iota = 0$ (orbit seen face on), and $\theta_n = 0$ (which, in this "degenerate" case, corresponds to choosing the + mode's axes to coincide with the semi-major and semi-minor axes of the orbital ellipse). Notice that for a circular orbit, $\theta = 0$, the waves are precisely sinusoidal with period half that of the orbital motion, i.e. frequency $f = f_2 = 2f_o$. This is the case embodied in Eqs. (7.25) for coalescing binaries. For eccentric orbits, the waves are a superposition of emission in all harmonics $f = f_n \equiv nf_o$ of the orbital frequency, with $n = 1, 2, 3, \ldots$. The more eccentric is the orbit, the higher are the dominant harmonics. In general, the characteristic amplitude $h_c(f_n)$ for the nth harmonic is related to the total gravitational-wave power output $(dE_{GW}/dt)_n$ in that harmonic by

$$h_c(f_n) = \frac{1}{\pi f_n r}\left[\frac{4}{3}\left(\frac{dE_{GW}}{dt}\right)_n\right]^{1/2} ; \quad (8.35)$$

see Eq. (8.5). Peters and Mathews (1963) have computed $L(f_n)$. From

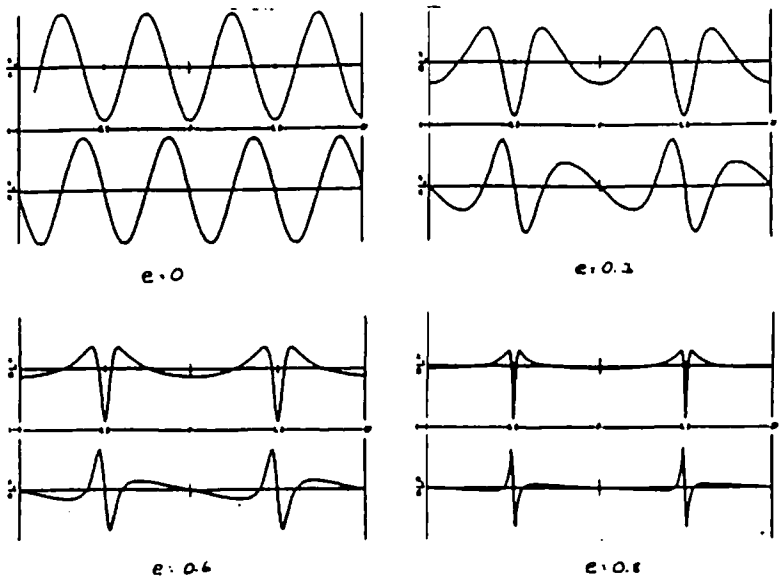

Fig. 8.4 The gravitational waveforms emitted by binary star systems of various orbital eccentricities e, as seen from directly above or below the orbital plane (inclination angle $\iota = 0$). Plotted vertically is the dimensionless wave field h_+ or $h_\times$ in units of the overall amplitude factor H [Eq. (8.34b)]. Plotted horizontally is retarded time $t-r$ in units of the orbital period $2\pi f_o$. The polarization axes of the + state are chosen to coincide with the semi-major and semi-minor axes of the orbital ellipse. [Figure adapted from Wahlquist (1987)].

their result and Eq. (8.35) one can infer that

$$h_c(f_n) = 8\left[\frac{2}{15}\right]^{1/2}\frac{\mu}{r}(\pi M f_n)^{2/3}[g(n,e)]^{1/2}$$

$$= 8.7\times10^{-21}\left[\frac{\mu}{M_\odot}\right]\left[\frac{M}{M_\odot}\right]^{2/3}\left[\frac{100\,\mathrm{pc}}{r}\right]\left[\frac{f_n}{10^{-3}\mathrm{Hz}}\right]^{2/3}[g(n,e)]^{1/2} \quad (8.36a)$$

Here

$$g(n,e) \equiv \frac{n^4}{32}[(J_{n-2}-2eJ_{n-1}+\frac{2}{n}J_n+2eJ_{n+1}-J_{n+2})^2$$

$$+ (1-e)^2(J_{n-2}-2J_n+J_{n+2})^2+\frac{4}{3n^2}(J_n)^2]\,, \quad (8.36b)$$

where $J_k \equiv J_k(ne)$ are Bessel functions with argument ne. Notice that the dependence on eccentricity e and on the harmonic n is contained entirely in the dimensionless function $g(n,e)$. This function is plotted in Fig. 8.5. Note that for eccentricity $e \lesssim 0.2$, the $n = 2$ "spectral line", at $f = 2f_{\mathrm{orb}}$ is dominant. For $e \simeq 0.5$, the lines $n = 4$ through 8 are all

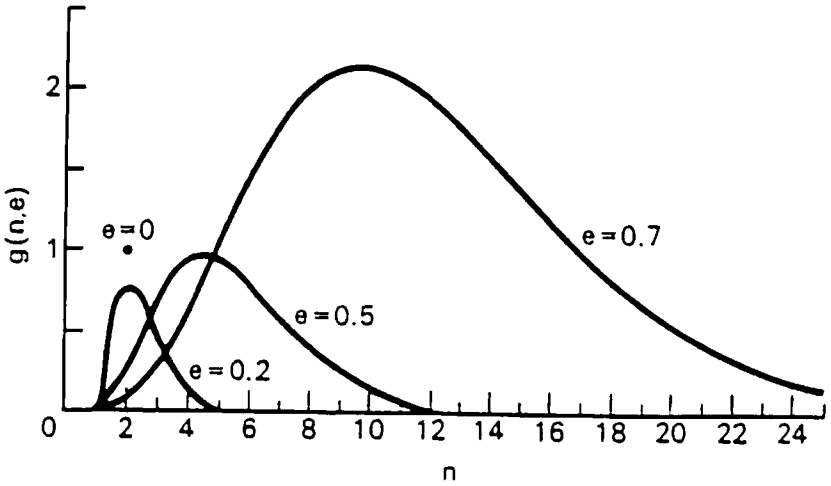

Fig. 8.5 The function $g(n,e)$ [Eq. (8.36b)] whose square root describes the dependence of a binary system's characteristic amplitude, in the "spectral line" at frequency $f_n = n \times$(orbital frequency f_o), on the order n of the line and the orbital eccentricity e. [Figure reproduced from Zel'dovich and Novikov (1967)].

strong. For $e \simeq 0.7$, the lines $n = 4$ through 20 are all strong.

The characteristic amplitude (8.36) is plotted in Fig. 2.8 for a few of the most strongly radiating, known binaries. Of the binaries shown, only the binary pulsar PSR1913+16 has a sufficiently eccentric orbit for harmonics with $n > 2$ to be important. For lists of the most strongly radiating binaries and their characteristics see Braginsky (1965), Douglass and Braginsky (1979), and Barone et. al. (1988a). For a discussion of the formation of highly eccentric binaries and their importance as gravitational-wave sources, see Fitchett (1987) - KIP MUST READ.

White-dwarf and neutron-star binaries should also be important emitters — and they should extend to higher frequencies than ordinary binaries. However, there is a paucity of observational data on them and the example of shortest known period (highest frequency) has f only 3×10^{-3} Hz (see above). From the data that do exist [summarized, e.g., by Iben and Tutukov, 1984], Lipunov and Postnov (1987), Lipunov, Postnov, and Prokhorov (1987), Evans, Iben and Smarr (1987), and Hils et. al. (1987) have estimated the charactristic amplitudes of the strongest white-dwarf and neutron-star binaries. See Fig. 2.8, where

the white-dwarf amplitudes are reduced a factor 3 from the above authors' estimates because a more recent observational search by Robinson and Shafter (1987) suggests that there are no more than 1/10 as many binary white dwarfs in our galaxy as had previously been thought. The highest frequency to be expected for any white-dwarf binary in our galaxy is 0.06 Hz since mass transfer from the less massive star to the more massive begins at or before this frequency; the highest for any neutron-star binary is 0.007 Hz since any binary of higher frequency than this would coalesce in a time less than the mean interval between coalescences, $\sim 10^4$ years.

Gravitational radiation reaction plays an important role in driving the evolution of close binary systems; see, e.g., Paczynski and Sienkiewicz (1981) and Savonije, de Kool, and van den Heuvel (1986) [KIP: CHECK] for details.

For a comparison of the strengths of binary-star gravitational waves with detector sensitivities, see Fig. 2.8

This chapter has not yet been updated for 1987 & 1988 & 1989 4/5/88

9 Stochastic Sources

This chapter describes the present (1988) knowledge and speculations about sources of stochastic gravitational radiation. Section 9.A formulates a spectral density description of stochastic gravitational waves and then uses it to define the characteristic amplitude h_c at frequency f and the corresponding sensitivity $h_{3/\mathrm{yr}}$ of a detector searching for the waves. Then the remainder of the chapter discusses specific sources of stochastic waves: huge numbers of binary stars whose waves superpose stochastically (Sec. 9.B), population III stars that might have formed and died before or during galaxy formation (Sec. 9.C), the big bang and the amplification of its waves by interaction with the subsequent expansion of the universe (Sec. 9.D), phase transitions in the early universe (Sec. 9.E), and cosmic strings (Sec. 9.F).

9.A Characterization of Stochastic Gravitational Waves and the Noise in a Detector Searching for Them

It is useful to think about stochastic gravitational waves in terms of traveling-wave normal modes of the gravitational field. As with the electromagnetic field, there are two modes (because of two polarization states) for each volume $(2\pi\hbar)^3$ in phase space; and correspondingly, one can easily show, the energy density per unit logarithmic interval of frequency divided by the critical energy density $\rho_{\mathrm{crit}} \sim 10^{-8}$ erg/cm^3 to close the universe is

$$\Omega_{\mathrm{GW}}(f) \equiv \frac{dE^{\mathrm{GW}}/d^3x\, d\ln f}{\rho_{\mathrm{crit}}} \sim \frac{\bar{n}}{10^{37}} \left| \frac{f}{1\ \mathrm{kHz}} \right|^3 . \qquad (9.1)$$

Here $\bar{n}$ is the average number of quanta in all modes with frequencies of order f. Below we shall see that $\Omega_{GW}(f)$ is likely to be $\gtrsim 10^{-14}$ at all frequencies of interest, and correspondingly the mean number of quanta in each mode is likely to be $\gtrsim 10^{20}$ — so large that a classical treatment is in order.

In any proper reference frame the gravitational-wave field of stochastic gravitational waves, evaluated at any chosen location x^i, will be a sum over contributions of all the modes of the field

$$h_{jk}^{GW}(t, x^i) = \sum_K h_K^{GW}{}_{jk}(t, x^i) \ . \tag{9.2}$$

Here the index K labels modes of the field. For stochastic gravitational waves, the wave field $h_K^{GW}{}_{jk}$ at x^i associated with mode K can be regarded as a "random process" (i.e. a stochastically fluctuating function of time t); and the total field h_{jk}^{GW} is the sum over all of the modes' random processes.

The field of a chosen mode K can be expressed as

$$h_K^{GW}{}_{jk} = h_K(t, x^i) e_{jk}^K \ , \tag{9.3}$$

where $h_K(t)$ is its scalar wave field and e_{jk}^K is its constant polarization ~~vector~~ tensor, so normalized that $e_{jk}^K e_{jk}^K = 2$ in Cartesian coordinates; cf. Eq. (7c). Then h_K is a scalar random process in time (at fixed x^i) and its statistical properties can be characterized by a spectral density $S_{hK}(f)$ KIP: FIX SUB SUB.

I shall assume that the modes are defined in such a way that there is no significant correlation between their wave fields $h_K^{GW}{}_{jk}$. As a result, when one averages the stress-energy tensor (4.28) of the waves at x^i over a sufficiently long time, all cross terms between different modes get washed out and one obtains for the time-averaged specific intensity I_f at location x^i

$$I_f(t, x^i)\Delta\Omega \equiv \frac{dE}{dA\,dt\,df\,d\Omega}\Delta\Omega = \sum_{K \text{ in } \Delta\Omega} \frac{\pi f^2}{4} S_{hK} \ . \tag{9.4}$$

Here E denotes energy, A denotes area, Ω denotes solid angle, and the sum is over all modes K with propagation directions in the infinitesimal solid angle $\Delta\Omega$. The total energy density per unit logarithmic interval (used in defining $\Omega_{GW}(f)$ above) can be expressed in terms of the specific intensity in the standard way

$$\Omega_{GW}(f)\rho_{crit} = \frac{dE}{d^3x\, d\ln f} = \int f I_f\, d\Omega = \sum_K \frac{\pi f^3}{4} S_{hK} \ , \tag{9.5}$$

where the integral is over the entire sphere and the sum is over all modes.

As for burst and periodic waves, so also for stochastic, we shall introduce a single characteristic amplitude h_c that is tied to a specific experimental situation: The experimenters use two identical gravity-wave receivers (broad-band or narrow), separated by a distance $\ll \lambda = c/2\pi f$, to search for *isotropic*, stochastic waves in the neighborhood of frequency f. The search is performed by a standard technique (Bendat 1958; Sec. 9 of Drever 1983): The outputs, $h_1(t)$ and $h_2(t)$ of detectors 1 and 2 are passed through identical filters which admit only Fourier components in a bandwidth $\Delta f \lesssim f$ centered on frequencies $\pm f$. The filtered outputs $w_1(t)$ and $w_2(t)$ are then multiplied together and integrated for a time $\hat{\tau}$ to get a single number $W = \int_{t_o}^{t_o+\hat{\tau}} w_1(t) w_2(t)$. This number will consist of a signal due to the identical stochastic backgrounds contained in $w_1(t)$ and $w_2(t)$, and a Gaussian noise due to the independent noises in the two detectors [each with the same spectral density $S_h(f)$]. It turns out (e.g. Chap. 7 of Bendat 1958) that the ratio of the signal to the root-mean-square noise is

$$\frac{S}{N} = \frac{h_c(f)}{h_n(f)} , \tag{9.6}$$

where

$$h_c(f) \equiv [\sum_K f S_{hK}(f)]^{1/2} = \left[\frac{4}{\pi f}\int I_f \, d\Omega\right]^{1/2} = \left[\frac{4}{\pi f^2}\Omega_{GW}(f)\rho_{crit}\right]^{1/2}$$

$$= 1.3\times10^{-18}\left[\frac{\rho_{crit}}{1.7\times10^{-8}\ \text{erg cm}^{-3}}\right]^{1/2}\left[\frac{1\ \text{Hz}}{f}\right][\Omega_{GW}(f)]^{1/2} \tag{9.7}$$

is the characteristic amplitude of the isotropic, stochastic waves, and

$$h_n(f) = \frac{1}{(\frac{1}{2}\hat{\tau}\Delta f)^{1/4}}\frac{[f S_h(f)]^{1/2}}{\langle F_+^2\rangle^{1/2}} \tag{9.8}$$

is the characteristic noise amplitude of the detectors. [Note: $\rho_{crit}/1.7\times10^{-8}\ \text{erg cm}^{-3} = (H_o/100\ \text{km s}^{-1}\ \text{Mpc}^{-1})^2$ where H_o is the Hubble constant.] Correspondingly, if the experimenters wish to be 90% confident of having seen the stochastic background during a search of duration $\hat{\tau} = 1/3$ year, the Gaussian probability distribution for S/N requires $S/N = 1.7$, which in turn means that h_c must exceed the noise level

$$h_{3/\mathrm{yr}}(f) = 1.7 h_n(f) = 2.0 \left| \frac{\Delta f}{10^{-7}\mathrm{Hz}} \right|^{-1/4} \frac{[f S_h(f)]^{1/2}}{\langle F_+^2 \rangle^{1/2}} \quad (9.9)$$

The characteristic amplitudes h_c of various possible stochastic sources, and the noise levels $h_{3/\mathrm{yr}}$ of various detectors are shown in Fig. 2.9 in Chap. 2.

9.B Binary Stars

So many binary stars in our galaxy and in other galaxies radiate in the frequency region $f \lesssim 0.03$ Hz that they should superpose to produce a strong stochastic background. Lipunov and Postnov (1986), Lipunov, Postnov, and Prokhorov (1987), and Hils et. al. (1987) have made careful calculations of the characteristic amplitude of this stochastic background as a function of frequency; the results of Hils et. al. are shown in Fig. 2.9 for the contribution of our own galaxy (which should be concentrated in the galactic plane). The contributions of all other galaxies (which should be isotropic) should be down from those of our own galaxy by $(h_c)_{\mathrm{other}}/(h_c)_{\mathrm{us}} \sim 0.15$.

The binary stochastic background in Fig. 2.9 is broken up into contributions from various types of binaries. Those shown as solid curves [unevolved binaries, WUMa stars (first discussed by Mironovskii 1966), and cataclysmic variables (white-dwarf/normal-star systems)] are rather firmly based on optical studies of the statistics of these types of stars, and thus are rather reliable. Those shown dashed [close white-dwarf binaries (see Evans, Iben, and Smarr 1987, and the above references), and neutron-star binaries] are based on so little observational data and so much theory that they are highly uncertain.

The binary background presents a serious potential obstacle to searches for other kinds of waves in the frequency band $0.03\mathrm{Hz} \lesssim f \lesssim 10^{-5}\mathrm{Hz}$ where space-based beam detectors will operate. A broad-band burst can be seen above this background only if it has $h_{c\,\mathrm{burst}} > h_{c\,\mathrm{background}}$ — which means, e.g., that a $1M_\odot$ star falling into a supermassive black hole in the Virgo cluster will not be discernible unless the hole's mass is $M < 3\times10^5 M_\odot$ (cf. Figs. 2.7 and 2.9). A periodic source can be seen, after an integration time $\hat{\tau}$, only if it has $h_{c\,\mathrm{periodic}} > (f\hat{\tau})^{-1/2} h_{c\,\mathrm{background}}$ — which means, e.g., that if the close white-dwarf binaries are as numerous as estimated, the binaries ι Boo and SS Cyg will be discernable only after integration times of $\hat{\tau} > 10^7$sec. For further discussion see Evans, Iben, and Smarr (1987) and Hils et. al. (1987).

9.C Population III Stars

If there was a pre-galactic population of massive stars ("Population III stars"; Carr 1986), the violent events that terminated their lives (supernovae and collapse to black holes) might have produced gravitational waves that we today would see as isotropic and stochastic. Whereas existing binary stars are a firm source of stochastic background, these Population III stars are a highly speculative one. Carr (1980) has derived an upper limit on the characteristic amplitude that could have been produced by the deaths of such stars under any reasonable scenario; it is shown in Fig. 2.9 (upper short-dashed curve) along with the maximum characteristic amplitude that could come from the remnants of these stars if they became black-hole binaries that decay by radiation reaction on a timescale $\tau_{GW} \simeq 10^{10}$ years (Bond and Carr 1984).

d) Primordial Gravitational Waves

Photons coming from the big bang last scattered off matter at a cosmological redshift $z \sim 1000$ when the universe was roughly one million years old; and neutrinos last scattered at $z \sim 10^{10}$ when it was about 0.1 second old. An order-of-magnitude calculation shows that gravitons, by contrast, last scattered at roughly the Planck time, i.e. during the first 10^{-43} seconds when spacetime was quantized and the laws of physics were exceedingly different from today (Sec. 7.2 of Zel'dovich and Novikov 1983). [KIP: GIVE THE ANALYSIS?] [An unlikely exception occurs if, at the epoch when the waves' reduced wavelength was $\lambda\!\!\!^{-} \sim$ (horizon size), much of the universe's energy density was in relativistic particles with mean free paths of order $\lambda\!\!\!^{-}$; then non-negligible absorption may occur; see Vishniac (1982).] Thus, in studying primordial gravitational waves (waves created in the big bang), one usually can ignore their subsequent interactions with matter.

Not so for their subsequent interactions with the background spacetime curvature of the universe. Grishchuk (1974, 1975a,b, 1977) has shown that, as the primordial perturbations that give rise to present-day waves "come inside the cosmological horizon" – and also before they enter the horizon – they can be parametrically amplified by their interaction with the dynamical background spacetime curvature; in other words, they can trigger further graviton creation. In this way exceedingly small initial fluctuations can be amplified into an interestingly strong stochastic background today. [KIP: GIVE THE ANALYSIS; QUOTE PARKER?]

Just how much stochastic background is produced depends crucially on ill-understood aspects of the initial singularity and on the equation-of-state-dependent and vacuum-dependent expansion rate in the very early universe. Some otherwise plausible models produce so much, $\Omega_{GW}(f) \gg 1$, as to be in violent conflict with the observed current state of the universe (e.g. page 621 of Zel'dovich and Novikov 1983). Other, equally plausible models can produce so little, $\Omega_{GW}(f) \ll 10^{-14}$, that there is no hope of detecting the waves in the foreseeable future.

In currently fashionable inflationary models of the universe vacuum fluctuations which initially are smaller than the horizon [$\lambda \ll \mathcal{R}_B$ = (background radius of curvature)] are driven outside the horizon ($\lambda \gg \mathcal{R}_B$) by the inflationary expansion. While outside the horizon, they are "frozen" with constant amplitude h. Much later, after inflation ends, noninflationary expansion brings them back inside the horizon. The number of quanta in each mode before entering and after leaving the horizon is

$$n \sim \left[\frac{1}{16\pi}\left[\frac{h}{\lambda}\right]^2\right](2\pi\lambda)^3\left[\frac{1}{\hbar/\lambda}\right] \sim \frac{\pi}{4}\frac{(h\lambda)^2}{\hbar} , \qquad (9.10)$$

where the first term is the waves' energy density, the second is the volume occupied by each mode, and the third is 1/(energy of one graviton). Before entering the horizon $n \simeq 1/2$; so the above relation says that upon leaving it,

$$n_{out} \simeq n_{enter}\frac{\lambda_{leave}}{\lambda_{enter}} = \frac{1}{2}\frac{a_{leave}}{a_{enter}} , \qquad (9.11)$$

where a is the expansion factor of the universe. Thus, the epoch of amplitude freezing is actually an epoch of parametric amplification (stimulated creation of new gravitons); and the total number of gravitons created depends on the total amount of expansion that occurs while the waves are outside the horizon. (There will be additional parametric amplification as the waves emerge from the horizon, $\lambda \sim \mathcal{R}_B$, but in inflationary models that is generally small compared to the amplification during freezing, $\lambda \gg \mathcal{R}_B$.) The total amount of inflationary expansion differs from one inflationary model to another ; and correspondingly, the models can give Ω_{GW} as large as unity or Ω_{GW} too small ($\ll 10^{-14}$) for there to be hope of detecting the waves.

For discussions of the influence of the equation of state in the early universe on the spectrum of the amplified waves, see Grishchuk

(1977) and Fig. 4 of Grishchuk and Polnarev (1980). For calculations of the waves produced by specific inflationary scenarios see Starobinsky (1979), Rubakov, Sazhin, and Veryaskin (1982), Abbott and Wise (1984), Halliwell and Hawking (1985), Mijic, Morris, and Suen (1986), and references therein. Because the range of possible strengths of primordial waves is so great, we do not bother to show it in Fig. 2.9 – aside from indicating the values of h_c corresponding to various values of $\Omega_{GW}(f)$.

9.E Phase Transitions in the Early Universe

During the early expansion of the universe, there may have been first-order phase transitions associated with QCD interactions and with electroweak interactions. In each of these phase transitions the original phase would be supercooled, by the cosmological expansion, below the equilibrium temperature of the new phase. Bubbles of the new phase would then nucleate at isolated locations and expand at near-light velocity until they have compressed the original phase enough for the two phases to coexist in equilibrium. As Witten (1984) has pointed out, and Hogan (1986) has analyzed in detail, this "cavitation" should have produced gravitational waves in two ways: (i) directly from expanding bubbles and the subsequent sound waves they generate, and (ii) subsequently from the inhomogeneities associated with the two co-existing phases (large-scale density inhomogeneities and corresponding inhomogeneities in the Hubble expansion rate). The resulting gravitational waves should possess a spectrum that peaks at wavelengths which were of order the horizon size when the cavitation occurred. Those wavelengths correspond to frequencies today $f_{max} \sim (2\times10^{-7}\ \text{Hz})(kT/1\ \text{GeV})$, where T is the temperature of the phase transition. Hogan's (1986) predicted spectra, shown in Fig. 2.9, thus peak at $f_{max} \sim 2\times10^{-8}$ Hz (QCD, $T \sim 100$ MeV) and $f_{max} \sim 2\times10^{-5}$ Hz (Electroweak, $T \sim 100$ GeV). The $f^{+1/2}$ shape of the spectra at frequencies $f > f_{max}$ is a firm prediction, but the shape f^{-1} at $f < f_{max}$ is not (it could well be f^{-p} with $p > 1$). The amplitude shown is a reasonable upper limit, unless the phase transition is unusually catastrophic with very strong supercooling.

f) Cosmic Strings

Long before the QCD and Electroweak phase transitions – i.e. nearer the initial singularity – there may have been a phase transition associated with the grand-unified interactions, and that transition may have created cosmic strings – one-dimensional "defects" in the vacuum

with mass per unit length estimated to be $\mu \sim 10^{-6}$ and with tension equal to mass per unit length (Zel'dovich 1980, Vilenkin 1981a; Sec. 2.H of this book). As the universe's horizon expands to uncover the stochastic inhomogeneities in a string's shape, those inhomogeneities should begin to vibrate with speeds up to the speed of light. By self-intersection of the string, closed loops should form; and those loops could well have acted as seeds for the condensation of galaxies and galaxy clusters (Zel'dovich 1980, Vilenkin 1981a, Turok and Brandenberger 1986, Sato 1987).

An unavoidable byproduct of this model for galaxy formation is huge amounts of stochastic gravitational waves produced by the vibrations of the closed loops (Vilenkin 1981b). Detailed calculations by Vachaspati and Vilenkin (1985) (confirming earlier, less accurate calculations by many others) predict that, if the strings are not superconducting (for the superconducting case see Ostriker *et. al.*, 1986),

$$\Omega_{GW}(f) \sim 10^{-7}\left[\frac{\mu}{10^{-6}}\right]^{\frac{1}{2}} \text{ for } 10^{5}\text{Hz} \gtrsim f \gtrsim 10^{-8}\text{Hz}\left[\frac{10^{-6}}{\mu}\right] . \qquad (9.12)$$

The upper frequency cutoff of 10^5Hz arises from the frictional damping of the motion of strings in the early universe. For the spectrum at frequencies below 10^{-8}Hz$(10^{-6}/mu)$ see Hogan and Rees, 1984. If μ is significantly less than 10^{-6} (i.e. if future gravity-wave observations constrain $\Omega_{GW}(f)$ to be $\ll 10^{-7}$), then the non-superconducting cosmic-string theory of galaxy formation will face severe difficulties. Figure 2.9 shows the predicted waves (9.12). From that figure and the corresponding discussions in Part IV it is clear that several different observational techniques have the prospect of placing cosmic string theory in jeopardy — or, hopefully, of discovering string-produced waves. [The apparent disproof of $\Omega_{GW} \sim 10^{-7}$ coming from 5°-scale anisotropy of the cosmic microwave radiation (Fig. 2.9 and Secs. 2.D, 2.H, 12.C) does not in fact constrain cosmic strings, since this observational limit is sensitive only to waves that were present and had (reduced wavelength) ~ (horizon size) at the epoch of recombination — before the strings that produce this wavelength began to vibrate and radiate.]

GRAVITATIONAL RADIATION

A New Window onto the Universe

by Kip S. Thorne

draft of 16 September 1989

California Institute of Technology

1989

This chapter has not yet been updated for 1987 & 1988 4/5/88

Part IV
Detection

A gravitational-wave detection system consisting of the XX meter diameter tracking antenna of NASA's Deep Space Network near Goldstone, California (lower left) and the Voyager X spacecraft (upper right). Monochromatic radio waves are transmitted from Goldstone to the spacecraft, then back to Goldstone. From the frequency shift of the returning radio waves a computer infers the velocity of the spacecraft relative to earth. Gravitational radiation passing through the solar system should perturb slightly the relative velocity, and those perturbations should show up in the radio tracking data. By this technique limits have been set on the strengths of low-frequency gravitational waves passing through the solar system.

10 Resonant Bar Detectors

Part IV of this book describes in detail techniques of gravitational-wave detection. Since earth-based bar detectors and beam detectors have been developed to such a high degree of sophistication and show such promise for the long-term future, they merit chapters of their own: Chapter 10 for bars, chapter 11 for beams. Other techniques of searching for gravitational waves are described in chapter 12 including, most importantly, doppler tracking of spacecraft, beam detectors in space, pulsar timing, and isotropy of the primordial micrwowave radiation.

More effort has been put into resonant bars than into any other type of gravity-wave detector. Weber's original detectors were of the resonant-bar type; all but one of the first-generation (pre-1977) earth-based detectors were of this type; and 9 of the world's 15 research groups now building and operating earth-based detectors are working with bars. Of the current bar efforts three are in the United States [the University of Maryland (Weber 1986), Stanford University (Boughn et. al. 1982, Michelson 1983), and Louisiana State University (Hamilton et. al. 1986)]; two are in Europe [the University of Rome with its detector sited at CERN (Amaldi et. al. 1984), and Moscow University (Braginsky 1983)]; .and four are in the far East [The University of Western Australia in Perth (Blair 1983), Tokyo University (Owa et. al. 1986), Guangzhou, China (Hu *et. al.*, 1986), and Beijing China (XXXX)]. The improvements in resonant-bar sensitivities since Weber's first detector have been a factor of roughly 200 in amplitude, corresponding

to 40,000 in energy; and significant further improvements are yet to come.

Resonant-bar detectors were introduced in Sec. 2.B, the history of research on them was described briefly in Sec. 3.B, and their sensitivities were compared with the best 1988 guesses of source strengths in Secs. 2.F–2.H. This chapter begins, in Sec. 10.A, by describing in some detail how a resonant bar detector works. Then Sec. 10.B discusses the parameters that determine the sensitivity of a bar detector and expresses the noise amplitude h_n and minimum detectable wave strength $h_{3/\mathrm{yr}}$ for bursts in terms of them. Section 10.C describes the physics that underlies the principal noise sources in a bar detector and how, in the face of that physics, one tries to adjust the detector's parameters to achieve optimal sensitivity to bursts. Section 10.D describes, in the light of what we have learned in Secs. 10.A–10.C, the designs and parameters of various first-generation and second-generation detectors. Up to here the chapter has dealt only with bars configured to search for gravitational-wave bursts. Bar configurations for periodic and stochastic waves are discussed in Section 10.E, along with expressions for h_n and $h_{3/\mathrm{yr}}$ in terms of those configurations. Section 10.F discusses the ultimate limits that quantum mechanics places on the sensitivities of bar detectors, if one uses the now-standard techniques for monitoring their vibrations; and it also describes the "quantum nondemolition techniques" that can circumvent those limits. The chapter concludes, in Sec. 10.G, with a brief description of some possible future directions of bar-detector research.

10.A How a Resonant Bar Detector Works

Schematically (Fig. 10.1) a resonant-bar detector consists of a large, heavy, solid bar whose mechanical oscillations are driven by gravitational waves, a transducer that converts information about the bar's oscillations into an electrical signal, an amplifier for the electrical signal, and a recording system. The transducer and amplifier together are sometimes called the sensor.

The transducer typically is mounted on one end of the bar (though other mountings are sometimes used), and it produces an output voltage or current proportional to the displacement $x(t)$ of the bar's end from equilibrium. Although $x(t)$ is a sum of contributions from all the $\sim 10^{29}$ normal modes of the bar, the transducer's output is filtered by the amplifier so that only the contribution of the bar's fundamental

Fig. 10.1 Schematic diagram of a resonant-bar detector for gravitational waves. The angles (θ,ϕ,ψ) characterizing the propagation and polarization directions of the waves relative to the detector are a specialization of the angles (θ,ϕ,ψ) shown in Fig. 7.1.

normal mode is passed on through. This is accomplished by a band-pass filter centered on the frequency f_0 of the fundamental mode, with bandwidth Δf somewhat smaller than the difference $f_1 - f_0$ between the bar's fundamental and its first harmonic. Thus, in effect, it is the fundamental mode of the bar that acts as the gravity-wave detector; and all the other normal modes are almost irrelevant.

Since the fundamental mode involves the relative in and out motion of the bar's left and right ends with just one node (at the bar's center), it corresponds to a standing sound wave with wavelength twice the length of the bar. Correspondingly, the bar's length must be

$$L \simeq \tfrac{1}{2} v_s / f_0 \ , \tag{10.1}$$

where v_s is the speed of sound in the bar. Typical solid materials have longitudinal sound speeds of order 5 km/s; astrophysics suggests (Sec. 1.C and Part III) that 1 kHz is a reasonable frequency to search for gravitational waves; and correspondingly the lengths of typical resonant bar detectors are about 2 meters and their masses are several tonnes. Notice that Eq. (10.1) gives for the ratio of the length of the bar to the reduced wavelength of the gravitational waves, $\lambda\!\!\!^{-} = c/2\pi f_0$,

$$L/\lambda\!\!\!^{-} \simeq \pi v_s / c \simeq 5\times 10^{-5} \ . \tag{10.2}$$

This justifies, with high accuracy, the use of a Newtonian-language, proper-reference-frame viewpoint in analyses of bar detectors. I shall adopt that viewpoint in this chapter.

The contribution of the fundamental mode to the displacement $x(t)$ of the bar's end can be expressed in the standard harmonic-oscillator form

$$x(t) = \text{Real}[X(t)e^{-i2\pi f_0 t}] \ , \tag{10.3}$$

where

$$X(t) = X_1 + iX_2 \tag{10.4}$$

is the mode's complex amplitude and f_0 is its eigenfrequency. It is actually the quantity $X(t)$ that the sensor monitors. To the extent that one can ignore forces from the fundamental mode's environment (e.g. very weak coupling to the other modes), only gravitational waves will produce time changes of $X(t)$. When waves hit, they drive $X(t)$ to evolve in a complicated, time-dependent way, and that evolution in principle can be deconvolved to reveal some details of the waveform $h_{jk}^{\text{GW}}(t)$.

Unfortunately, noise in the sensor is typically so severe that to control it the experimenter must use a bandwidth Δf that is far smaller than the frequency f_0 (typically $\Delta f / f_0 \sim 0.01$ in present detectors). Correspondingly, the sensor averages $X(t)$ for a time $\hat{\tau} \simeq 1/\Delta f$ that is long compared to the period $P_0 = 1/f_0$ of the gravitational waves being sought, before passing $X(t)$ on to the recording system. This means that for typical gravitational-wave bursts (e.g. from supernovae), which have durations of only a few times P_0, all that can be monitored is the total change ΔX in the complex amplitude from before the wave arrives until after it has passed. Only uncommonly long bursts, those lasting for more than $f_0/\Delta f \sim 100$ cycles, can be monitored in greater detail. In the future, however, there is hope of bringing the sensor noise under better control and thereby opening up the bandwidth to $\Delta f \simeq 0.2 f_0$ to permit detailed monitoring of much shorter bursts (Michelson and Taber 1984). (For a description of several first-generation broad-band bars see Fig. 2 of Drever 1977 and associated text, and references therein.)

9.B The Sensitivity of Bar Detectors to Short Bursts

A bar detector couples to the field [Eq. (7.1)]

$$h(t) = F_+(\theta,\phi,\psi)h_+(t;\iota,\beta) + F_\times(\theta,\phi,\psi)h_\times(t;\iota,\beta) \ , \qquad (10.5)$$

where, if the bar is axially symmetric and the direction (θ,ϕ) and polarization angle ψ are defined as in Fig. 10.1, the beam-pattern factors are

$$F_+ = \sin^2\theta\cos 2\psi \ , \quad F_\times = \sin^2\theta\sin 2\psi \ . \qquad (10.6)$$

(See chapter 37 of MTW for the key elements of a derivation.) We shall presume, throughout this section, that $h(t)$ is a burst of such short duration $\Delta t \lesssim \hat{\tau} = 1/\Delta f$ that the optimal way to search for it is to measure the mean square change $|\Delta X|^2$ it produces in the fundamental mode's complex amplitude. In this case the general formula (7.4) for the ratio S^2/N^2 of the burst's squared signal to the mean-square Gaussian noise in the detector can be reduced to the simple form (see, e.g., Giffard 1976, Pallotino and Pizella 1981, Michelson and Taber 1984)

$$\frac{S^2}{N^2} = \frac{\frac{1}{2}M_{eff}(2\pi f_0)^2|\Delta X|^2}{kT_n} \ . \qquad (10.7)$$

Here k is Boltzmann's constant, T_n is a "noise temperature" which characterizes the overall noise in the detector, and M_{eff} is an "effective mass" associated with the fundamental mode, so defined that $\frac{1}{2}M_{eff}|X|^2(2\pi f_0)^2$ is the total energy in the mode when it is vibrating with complex amplitude X. (Since X is actually the amplitude of motion of the end of the bar, for a bar that has uniform cross section and is long compared to its diameter, the effective mass is $M_{eff} = \frac{1}{2}(1+\nu^2)M$ where ν is the Poisson ratio of the bar's material and M is the bar's mass.)

Because the net wave-induced change ΔX in complex amplitude is independent of the mode's initial complex amplitude, the numerator of Eq. (10.7) is the energy that the wave would have deposited in the mode if the mode had been initially unexcited. This deposited energy can conveniently be expressed in terms of the cross section $\sigma_o(f)$ that the mode would present to the wave if the wave had hit it from an optimal direction (broadside, $\theta = \pi/2$) and with an optimal polarization (+ mode with $\psi = 0$):

$$\frac{1}{2}M_{eff}(2\pi f_0)^2|\Delta X|^2 = \int_0^\infty \frac{\pi}{2} f^2 |\hbar(f)|^2 \sigma_o(f)\,df \ . \qquad (10.8)$$

Here $\tilde{h}(f)$ is the Fourier transform of $h(t)$ [Eq. (10.5)], and for an optimal direction and polarization $(\pi/2)f^2|\tilde{h}(f)|^2$ would be the energy per unit area per unit frequency ($f \geq 0$) carried by the waves. Because $\sigma_o(f)$ is extremely sharply peaked around the resonant frequency f_0 (Sec. 37.5 of MTW), we can rewrite (10.8) and thence (10.7) in the form

$$\frac{S^2}{N^2} = \frac{\pi}{2} f_0^2 |\tilde{h}(f_0)|^2 \frac{\int \sigma_o df}{kT_n} \quad . \tag{10.9}$$

This is a special narrow-band-detector version of the general Eq. (7.4) for arbitrary detectors. Correspondingly, Eq. (7.5) for the strongest burst seen, on average, at the same rate as bursts occur inside the distance to our source, becomes

$$\frac{S^2}{N^2} \cong \frac{3}{2}\frac{\pi}{2} f_0^2 \langle |\tilde{h}_+(f_0)|^2 + |\tilde{h}_\times(f_0)|^2 \rangle \langle F_+^2 \rangle \frac{\int \sigma_o df}{kT_n} \quad , \tag{10.10}$$

where, for the F_+ and $F_\times$ of (10.6),

$$\langle F_+^2 \rangle = \langle F_\times^2 \rangle = \frac{4}{15} = 0.267 \quad . \tag{10.11}$$

Equation (10.10) motivates us to define

$$h_c \equiv \sqrt{3} f_0 \langle |\tilde{h}_+(f_0)|^2 + |\tilde{h}_\times(f_0)|^2 \rangle^{1/2} \tag{10.12}$$

as the *characteristic amplitude of the burst* [analog of (7.6b) for broad-band detectors] and

$$h_n \equiv \left[\frac{15}{\pi} \frac{kT_n}{\int \sigma_o df} \right]^{1/2} \cong 2.2 \left[\frac{G}{c^3} \frac{kT_n}{\int \sigma_o df} \right]^{1/2} \tag{10.13}$$

as the *detector's characteristic noise amplitude* [analog of (7.7) for a broad-band detector]. Correspondingly, the characteristic amplitude $h_c = h_{3/yr}$ that a source must have to be detectable with 90% confidence in a search lasting 1/3 year is

$$h_{3/yr} \cong 5h_n \cong 11 \left[\frac{G}{c^3} \frac{kT_n}{\int \sigma_o df} \right]^{1/2}$$

$$= 2.0 \times 10^{-16} \left[\frac{T_n / 1\ \mathrm{K}}{\int \sigma_o df / 10^{-21}\ \mathrm{cm^2 Hz}} \right]^{1/2} \quad . \tag{10.14}$$

For a broad-band burst that is peaked near the detector's resonant frequency f_0 (so the f_c of Eq. (7.6a) is approximately f_0) and that lasts for a time not much longer than $\Delta t = 1/f_0$, the narrow-band characteristic amplitude (10.12) will be roughly equal to the broad-band characteristic amplitude (7.6b). For such bursts, and only for such bursts, it makes sense to plot a bar detector's narrow-band $h_{3/\mathrm{yr}}$ on the same graph (Fig. 2.7) as a broad-band detector's $h_{3/\mathrm{yr}}$. Inspiraling binaries do not belong to this class of bursts, so their detection by bars must be discussed separately from Fig. 2.7.

10.C How to Optimize the Sensitivities of Bar Detectors

Equation (10.14) shows that to optimize the sensitivity of a bar detector to short, broad-band bursts, one must achieve the largest possible frequency-integrated cross section $\int \sigma_0 df$ and the smallest possible noise temperature T_n.

The integrated cross section $\int \sigma_0 df$ can be computed by analyzing the response of the bar's fundamental mode to the force field (5) produced by a sinusoidal wave with optimal direction and polarization, and by then integrating over the wave's frequency. See MTW Box 37.4 for details. For a cylindrical bar with length L somewhat greater than radius R (the usual situation), the result depends only on the bar's mass M and internal sound velocity $v_s = (E/\rho)^{1/2}$ with $E =$ (Young's modulus) and $\rho =$ (density) (Paik and Wagoner 1976):

$$\int \sigma_0 df = \frac{8}{\pi}\frac{GMv_s^2}{c^3}[1+\tfrac{1}{2}\nu(1-2\nu)(\pi R/L)^2+\cdots]$$

$$= 1.6\times10^{-21}\mathrm{cm^2Hz}\left[\frac{M}{10^3\ \mathrm{kg}}\right]\left[\frac{v_s}{5\ \mathrm{km\,s^{-1}}}\right]^2 . \qquad (10.15)$$

(Here ν is the Poisson ratio of the bar's material, and only the leading shape-dependent corrections are given.) Thus, it is desirable to build detectors that are as massive and have as high sound speed as possible.

The noise temperature T_n is determined by a combination of noise in the sensor and thermal noise in the bar.

The *thermal noise in the bar* is caused by weak coupling of the bar's fundamental mode to its environment – its $\sim 10^{29}$ other modes, the wire or cable or prongs that suspend the bar, and the residual gas in the vacuum chamber (Braginsky, Mitrofanov, and Panov 1985). If, as is normal, this environment is thermalized at some physical temperature T_b (subscript "b" for bar or for thermal bath), then these couplings

cause the mode's amplitude to execute a random walk (Brownian motion) in the domain $|X| \lesssim X_{\rm th}$ corresponding to an energy kT_b:

$$X_{\rm th} = \left[\frac{2kT_b}{M_{\rm eff}(2\pi f_0)^2}\right]^{1/2} . \qquad (10.16)$$

The fluctuation–dissipation theorem states that the timescale on which this random walk produces changes of order $X_{\rm th}$ is the same as the timescale $\tau_\cdot = Q/\pi f_0$ for large-amplitude vibrations to be damped frictionally. (Here Q is the quality factor of the mode's large-amplitude oscillations: the number of radians of oscillation required for the energy to damp by a factor e.) Consequently, the mean square Brownian change in the mode's amplitude during the sensor's averaging time $\hat{\tau} = 1/\Delta f$ is

$$|\Delta X_{\rm th}|^2 = X_{\rm th}^2 \frac{\hat{\tau}}{\tau_\cdot} = X_{\rm th}^2 \frac{\pi}{Q}\frac{f_0}{\Delta f} \qquad (10.17)$$

corresponding to

$$\tfrac{1}{2}M_{\rm eff}(2\pi f_0)^2|\Delta X_{\rm th}|^2 = \pi\frac{kT_b}{Q}\frac{f_0}{\Delta f} . \qquad (10.18)$$

The details of the *sensor noise* depend on a variety of factors, including: the detailed structure of the transducer (for a review of many transducer structures see Sec. 4.1.5 of Amaldi and Pizella 1979), the strength of coupling of the transducer to the bar (characterized by a dimensionless coupling constant β that is roughly equal to the number of cycles of oscillation required for all the fundamental mode's energy to be fed into the transducer); the impedance mismatch between the transducer and the amplifier; the noise temperature T_a of the amplifier (converted to an equivalent noise temperature $(f_0/f_a)T_a$ at the bar's frequency f_0 if the amplifier operates at a different frequency f_a than the bar); and the sensor bandwidth Δf. Although the details vary from one sensor to another (see, e.g., Weiss 1978, Pallotino and Pizella 1980, Blair 1983, Michelson and Taber 1984), the spirit of the details is captured by the following approximate expression for the mean square change $|\Delta X_{\rm sensor}|^2$ that the experimenter would infer from the sensor's output if (i) only the sensor noise were present, (ii) back-action forces of the sensor on the bar were negligible (see Sec. 10.F below), and (iii) impedances were properly matched:

$$\tfrac{1}{2}M_{\rm eff}(2\pi f_0)^2|\Delta X_{\rm sensor}|^2 \simeq \frac{kT_a(f_0/f_a)}{\beta}\frac{\Delta f}{f_0} . \qquad (10.19)$$

The sum of $\frac{1}{2}M_{eff}(2\pi f_0)^2|\Delta X_{sensor}|^2$ [Eq. (10.19)] and $\frac{1}{2}M_{eff}(2\pi f_0)^2|\Delta X_{th}|^2$ [Eq. (10.18)] is the mean square noise N^2 that appears in the denominator of Eq. (10.7); i.e., by definition, the detector's noise energy kT_n is this sum. If the experimenters choose too large a bandwidth Δf, then the sensor noise (10.19) will become inordinately large, producing a large T_n and masking the gravity-wave signal. If they choose too small a bandwidth, then the bar's thermal noise (10.18) will become inordinately large. There is an optimal bandwidth, typically $\Delta f \sim 10$ Hz in present detectors (corresponding to the averaging time $\hat{\tau} \sim 0.1$ seconds) at which roughly half the noise is from the sensor and half is from thermal motion of the bar. When the bandwidth is chosen optimally these two noise sources together produce a detector noise temperature

$$T_n \simeq \left[\frac{\pi}{\beta}\frac{T_b}{Q}\left(T_a\frac{f_0}{f_a}\right)\right]^{1/2} . \qquad (10.20)$$

In practice, the experimenters choose a bar early in their experiments, thereby fixing the integrated cross section $\int \sigma_0 df$; and they then struggle for many years to develop a sensor and its coupling to the bar, and a thermally cold environment, that will minimize the noise temperature T_n. Maximizing $\int \sigma_0 df$ is achieved by maximizing the bar's mass and its velocity of sound [and, to a small extent, optimizing its shape subject to other experimental constraints such as available cryostats.] Minimizing T_n is achieved according to Eq. (10.20) by (i) maximizing the fundamental mode's quality factor Q (i.e. minimizing its coupling to the rest of the world), (ii) cooling the bar to as low a physical temperature T_b as possible, (iii) maximizing the strength β of coupling of the transducer to the bar, (iv) using an amplifier with as low a "noise number" $kT_a/(2\pi\hbar f_a)$ as possible (the Heisenberg uncertainty principle limits the noise number to be $\gtrsim 1$; Weber 1959, Heffner 1962, Caves 1982), and (v) struggling to get good impedance matching of the transducer and amplifier (a requirement for Eq. (10.20) to be valid).

10.D Parameters of First- and Second-Generation Bar Detectors

The first-generation bar detectors (pre-1977) were all made of aluminum, weighed roughly 1.5 tonnes, and had $f_0 \simeq 1.6$ kHz and $Q \sim 10^5$; they all operated at room temperature, $T_b \cong 300$K; and most used piezo-electric transducers – i.e crystals glued to the bar which produce

small voltages when squeezed. For most the coupling of the transducer to the bar was weak, $\beta \lesssim 10^{-4}$; but those in Britain achieved strong coupling, $\beta \simeq 0.2$ and hence wide bandwidth $\Delta f / f_o \sim 1$ at the price of reducing the bar's Q from $Q \sim 10^5$ to $Q \sim 2000$. [KIP: ADD REFERENCE] The best amplifiers that could be impedance matched to the piezo-electric transducers had rather large noise numbers. For these first-generation bars the integrated cross sections were $\int \sigma_o df \simeq 2\times10^{-21}$ cm^2 Hz, and the lowest detector noise temperatures were $T_n \simeq 4$K corresponding to a minimum detectable burst amplitude with 1/3 year of observation $h_{3/yr} \cong 3\times10^{-16}$. Despite great effort in the early 70s by excellent experimenters, there was great room for improvement. (For a thorough review of the first-generation experiments see Amaldi and Pizella 1979; for other reviews see Drever, 1977, Tyson and Giffard 1978, and Weber 1986.)

In moving into the second generation, almost all the groups cooled their bars to liquid helium temperatures (T_b = 1.5 to 4 K rather than 300 K). Several of the groups (Maryland, Stanford, LSU) constructed massive bars ($M \cong$ 2 to 5 tonnes) from a new alloy of aluminum that the Tokyo group discovered has a Q 10 times higher than the old one (5×10^7 vs 5×10^6 at 10^4 K temperature; Suzuki, Tsubono, and Hirakawa, 1978). Perth and Moscow, by contrast, chose to use exotic bar materials. Perth used a 1.5 tonne Niobium bar with $Q = 2\times10^8$, while Moscow initially used a 10 kg sapphire bar with $Q = 4\times10^9$, and later when difficulty with cracking of the sapphire occurred, Moscow switched to a 10 kg silicon crystal bar with $Q = 2\times10^9$ — silicon and sapphire because of their very large Q's, an advantage bought at the price of low mass.

In the second generation each of the groups deemphasized piezo-electric transducers and developed some variant of one or another of two new transducer concepts: Moscow, LSU, Perth, and Tokyo developed *parametric transducers* in which the bar's vibrations with frequency $f_0 \sim 10^3$ Hz modulate the capacitance in a microwave cavity (or rf circuit), thereby moving microwave photons from the frequency $f_D \sim 10^9$ Hz, at which the cavity is driven, into side bands at $f = f_D \pm f_0$, at which the amplifier measures the signal. The number of photons moved is proportional to the amplitude of vibration of the bar. Stanford and Maryland developed *resonant transducers* in which a mechanical diaphragm, with a mechanical resonant frequency very nearly that of the bar's fundamental mode, is attached to the bar's end. The vibration energy is quickly transferred back and forth between the bar and the diaphragm, with the diaphragm's displacement amplitude

amplified over that of the bar by $|X_{\text{diaphragm}}|/|X_{\text{bar}}| \sim [(\text{bar mass})/(\text{diaphragm mass})]^{\frac{1}{4}}$. The vibrating diaphragm modulates the inductance of a superconducting circuit, and a SQUID (superconducting quantum interference device) amplifier is used to monitor the current in the circuit. Rome developed a similar resonant transducer with the diaphragm replaced by a toad stool which was one plate of a capacitor and with a FET transducer used to read out oscillations of the toad stool's voltage.

[KIP: UPDATE THIS PARAGRAPH] At present (late 1986) Stanford, Rome, and LSU are all on the air with systems that have resonant frequencies $f_0 = \sim 900$ Hz, cross sections $\int \sigma_0 df \cong (4 \text{ to } 8) \times 10^{-21}$ cm^2 Hz, and noise temperatures $T_n = \sim(0.01 \text{ to } 0.04)$ K. Correspondingly the weakest burst they can detect with 1/3 year of observation is $h_{3/\text{yr}} \cong 1.0 \times 10^{-17}$. Maryland and Perth are both likely to be on the air with similar characteristics before this book is published; and all five groups are hoping to push their noise levels down to $h_{3/\text{yr}} \sim 2 \times 10^{-18}$ within several years by further straightforward refinements. The Guangzhou group, having only entered the field very recently, is still at room temperature, but with a sensitivity $h_{3/\text{yr}} \simeq 1.6 \times 10^{-16}$, two times better than that of any of the first-generation room-temperature bars (Hu *et. al.* 1986). The Moscow group with its small silicon and sapphire bars operates at a much higher frequency than any of the other groups, $f_0 \cong 8$ kHz; by the time this book is published they will likely be on the air with $h_{3/\text{yr}} \sim 4 \times 10^{-17}$. The Tokyo group, on the other hand, has chosen a much lower frequency than the others, $f_0 = \sim 60$ Hz and is now operating a narrow-band search for periodic waves from the Crab pulsar (see below). These sensitivities are shown in Fig. 2.7, along with those of other kinds of detectors. For details of the present detector configurations and near-term plans, see the gravitational-wave articles in the proceedings of recent conferences (Ruffini, ed. 1986; MacCallum, ed. 1987).

e) Sensitivities of Bar Detectors to Periodic and Stochastic Waves

Although I have discussed the detectors' performances entirely in the context of searching for short bursts of gravitational waves, bar detectors can be used also to search for periodic gravitational waves and a stochastic background at frequencies within the bandwidth Δf of their sensors.

In a search for periodic gravitational waves, the experimenters will typically use a bar with eigenfrequency f_0 slightly different from the

expected frequency f of the waves. The waves then will drive the fundamental mode's complex amplitude X into oscillations with the beat frequency $f - f_0$. In searching for these oscillations the experimenters integrate for a long time; and correspondingly they can turn down the coupling strength β of the transducer to the bar, and/or narrow the bandwidth Δf, until the sensor's noise becomes negligible compared to the thermal noise of the bar (see, e.g., Michelson and Taber 1981, 1984). (The maximum resulting bandwidth with the present Stanford detector would be $\Delta f \simeq 0.5$ Hz.) When this is done, the general formulas of Sec. 8.A are valid, with $S_h(f)$ the spectral density of the bar's thermal noise, converted into an equivalent gravity-wave spectral density

$$S_h(f) = \frac{4kT_b}{\int \sigma_0 df} \frac{1}{f_0 Q} , \tag{10.21}$$

and with the beam-factor averages having the values (10.11). In particular, the detector's characteristic noise amplitude [Eq. (8.4)] is

$$h_n = \left[15 \frac{G}{c^3} \frac{kT_b}{\int \sigma_0 df} \frac{1}{Q} \frac{1}{f_0 \hat{\tau}} \right]^{1/2} , \tag{10.22}$$

and the brightest source that can be seen with 90% confidence in $\hat{\tau} = 1/3$ year of integration is

$$h_{3/\mathrm{yr}} = 1.7 h_n = 3.9\times10^{-25} \left(\frac{T_b}{1\ \mathrm{K}} \right)^{1/2} \left| \frac{10^{-21}\mathrm{cm^2\,Hz}}{\int \sigma_0 df} \right|^{1/2} \left(\frac{1000\ \mathrm{Hz}}{f_0} \right)^{1/2} \left(\frac{10^7}{Q} \right)^{1/2} \tag{10.23}$$

The Tokyo group is currently carrying out a search for gravitational waves from the Crab pulsar using the above technique (Owa et. al. 1986). Their 74 kg, cryogenically cooled antenna has $Q = 2.1\times10^7$, $T_b = 4$K, $f_0 = 60$Hz, and $\int \sigma_0 df \simeq 2.2\times10^{-27}\mathrm{cm^2}$ Hz (so low because for noncylindrical antennas with frequency f_0 lowered by special shaping, $\int \sigma_0 df \propto f_0^2$; Hirakawa *et. al.*, 1976). Correspondingly, it has $h_{3/\mathrm{yr}} \sim 3\times10^{-22}$. No other present bars are optimized for periodic waves, since there are no known sources in their frequency bands (~900 Hz and ~8 kHz). However, with the technology of present burst-optimized bars it should be possible to achieve the thermal-noise-limited sensitivity (10.23) with $T_b = 4K$, $\int \sigma_0 df \simeq 8\times10^{-21}\mathrm{cm^2}$ Hz, $f_0 \simeq 900$Hz, and $Q \simeq 5\times10^6$ corresponding to $h_{3/\mathrm{yr}} \simeq 4\times10^{-25}$ (Stanford, LSU, Rome, Maryland); and $T_b = 4K$, $\int \sigma_0 df \simeq 2\times10^{-23}\mathrm{cm^2}$ Hz, $f_0 \simeq 8$ kHz, and $Q \simeq 2\times10^9$ corresponding to $h_{3/\mathrm{yr}} \simeq 1.4\times10^{-25}$ (Moscow). See Fig. 2.8.

When searching for stochastic background it is desirable to open up the bandwidth Δf until the sensor noise becomes almost as large as the bar's thermal noise ($\Delta f \simeq 0.5$ Hz for the present Stanford bar). With $S_h(f)$ then given (approximately) by the thermal-noise spectral density [Eq. (10.21)], the noise amplitude h_n and the 90%-confidence 1/3-year sensitivity $h_{3/yr}$ for stochastic background become [Eqs. (9.8) and (9.9)]

$$h_n(f) \simeq \left[15 \frac{G}{c^3} \frac{kT_b}{\int \sigma_0 df} \frac{1}{Q} \frac{1}{\sqrt{\frac{1}{2}\hat{\tau}\Delta f}} \right]^{\frac{1}{2}} , \tag{10.24}$$

$$h_{3/yr} = 1.7 h_n \cong 8\times 10^{-22} \left(\frac{T_b}{1\ \mathrm{K}} \right)^{\frac{1}{2}} \left(\frac{10^{-21}\mathrm{cm}^2\mathrm{Hz}}{\int \sigma_0 df} \right)^{\frac{1}{2}} \left(\frac{10^7}{Q} \right)^{\frac{1}{2}} \left(\frac{1\ \mathrm{Hz}}{\Delta f} \right)^{1/4} . \tag{10.25}$$

This $h_{3/yr}$ is shown in Fig. 2.9 for the parameters of 1987 bar technology (those given in the last paragraph, plus $\Delta f \simeq 1$ Hz). For details of searches for stochastic background that were carried out using first-generation bar detectors see Hough et. al. (1975) and Hirakawa and Narihara (1975). For discussions of sensitivity that are more detailed and sophisticated than the above sketch, see Hirakawa, Owa, and Iso (1985), Weiss (1979), and references therein.

10.F Quantum Limit and Quantum Nondemolition

Quantum mechanics constrains the sensitivity that can be achieved by bar detectors using the present kinds of sensors: The fundamental mode of a bar, being highly decoupled from the rest of the world, can be regarded as a simple harmonic oscillator with mass M_{eff} and angular frequency $\omega_0 = 2\pi f_0$. As such, it is subject to the laws of quantum mechanics for oscillators: its generalized position x and momentum p must be regarded as hermitian operators that fail to commute, $[x, p] = i\hbar$; and correspondingly, the real and imaginary parts of its complex amplitude,

$$X_1 = x\cos\omega_0 t - \left(\frac{p}{M_{eff}\omega_0} \right) \sin\omega_0 t , \quad X_2 = x\sin\omega_0 t + \left(\frac{p}{M_{eff}\omega_0} \right) \cos\omega_0 t \tag{10.26}$$

are noncommuting hermitian operators with commutator

$$[X_1, X_2] = i \frac{\hbar}{M_{eff}\omega_0} . \tag{10.27}$$

From this commutation relation we infer, via the Heisenberg

uncertainty principle, an absolute limit on the variances of X_1 and X_2 in any quantum mechanical state (Thorne et al. 1978):

$$\Delta X_1 \Delta X_2 \geq \frac{\hbar}{2M_{eff}\omega_0} . \tag{10.28}$$

The principles of quantum mechanics guarantee that one can never measure X_1 and X_2 simultaneously with a precision that violates this uncertainty principle. In fact, it turns out (Caves 1982, Yamamoto and Haus 1986) that even the most ideal of measuring systems will introduce additional noise equal to (10.28), thereby producing a lower bound

$$\Delta X_1 \Delta X_2 \geq \frac{\hbar}{M_{eff}\omega_0} \tag{10.29}$$

on the products of the rms noise in the measured values of X_1 and X_2.

The sensors used in the present generation of bar detectors measure X_1 and X_2 simultaneously with equal accuracies; and correspondingly, in searches for short bursts they are subject to the "standard quantum limit" (Braginsky and Vorontsov 1974; Giffard 1976)

$$T_n = \tfrac{1}{2}M_{eff}\omega_0^2[(\Delta X_1)^2+(\Delta X_2)^2]/k \geq \hbar\omega_0/k = 4.8\times10^{-8}\mathrm{K}\left(\frac{f_0}{1000\ \mathrm{Hz}}\right) . \tag{10.30}$$

Notice that this standard quantum limit places the severe constraint

$$h_{3/\mathrm{yr}} \gtrsim 4.4\times10^{-20}\left(\frac{f_0}{1000\ \mathrm{Hz}}\right)^{1/4}\left(\frac{10^{-21}\mathrm{cm^2Hz}}{\int\sigma_0 df}\right)^{1/4} \tag{10.31}$$

on the detector's burst sensitivity (10.14). It is fairly likely, though far from certain, that the strongest kilohertz-frequency bursts striking the earth three times per year have characteristic amplitudes $h_c < 10^{-20}$ (see section 4.1); and correspondingly it may turn out to be crucial for bar detectors of the future to circumvent the standard quantum limit (10.30), (10.31).

The uncertainty principle (10.28) suggests a promising method for circumventing the standard quantum limit (Thorne *et. al.* 1978; Braginsky, Vorontsov, and Khalili 1978): One should devise a new kind of sensor that measures X_1 with high accuracy, while giving up accuracy on X_2. Such sensors, called "back-action-evading sensors" (a special case of "quantum nondemolition sensors"), are now under development in a number of laboratories (Braginsky 1983, Bocko and Johnson

1984, Oelfke 1983, Blair 1982); and they may make possible bar sensitivities in the 1990s that will beat the standard quantum limit by modest factors. For a detailed review of quantum nondemolition measurements — i.e. measurements that do not change the quantum state of the system being measured — see Caves (1983).

Although a back-action-evading sensor gives up accuracy on one of the wave's two quadrature components, that accuracy can be regained by looking at the same wave with two different detectors: On one detector, with complex amplitude $X = X_1 + iX_2$, measure X_1 with high accuracy and X_2 with poor; on the other, with complex amplitude $Y = Y_1 + iY_2$, measure Y_2 with high accuracy and Y_1 with poor. From X_1 infer the detailed evolution of one of the wave's two quadrature components; from Y_2 infer the evolution of the other. In this way, in principle, the quantum mechanical properties of the detector can be completely circumvented and the only constraints of principle on the accuracy of measurement are associated with quantization of the waves themselves. For further discussion and details see the reviews by Caves *et. al.* (1980); Caves (1983); Braginsky, Vorontsov, and Thorne (1980).

It is worth noting that a back-action-evasion measurement, ideally performed, should drive the bar's fundamental mode into a "squeezed state" (Hollenhorst 1979). Squeezed states have been studied extensively in recent years in the context of quantum optics (see, e.g. Schumaker 1986 and Walls 1983); and we shall return to them in Sec. 11.F below when discussing beam detectors.

10.G Looking Toward the Future

It may be that bar detectors in the distant future will find their greatest applications at much lower frequencies than are now common: At lower frequencies the bar can be much longer and more massive, and correspondingly more sensitive; and good bandwidth, $\Delta f \sim f_0$ will correspond to a longer averaging time and thus will be easier to achieve. For discussion see Michelson (1986).

Although individual bar detectors in the foreseeable future will be limited to moderately small bandwidths $\Delta f / f \lesssim 0.2$, and therefore will be able to acquire only very limited information about the wave form $h_{jk}^{TT}(t)$ of a gravity-wave burst, once waves are being detected in profusion it may be possible cheaply to replicate the detectors with a variety of sizes and hence a variety of fundamental-mode frequencies, thereby creating a "xylophone" of networked detectors with a large

overall bandwidth (Michelson and Taber 1984).

This chapter has not yet been updated for 1987 & 1988 4/5/88

11 Beam Detectors

Beam detectors for gravitational radiation (also called "interferometric detectors" and "laser interferometer gravitational-wave detectors") were introduced in Secs. 2.A and 2.B of this book, the history of research on them was described briefly in Sec. 3.B, and their sensitivities were compared with the best 1988 guesses of source strengths in Secs. 2.F–2.H. This chapter discusses these types of detectors in greater detail. Section 11.A describes, conceptually, the two types of beam detectors that are now in operation: "Michelson", or "delay-line" interferometric detectors and "Fabry-Perot" interferometric detectors, and discusses their common beam patterns. Section 11.B describes briefly some of the sources of noise in beam detectors explains how the overall noise is characterized by a spectral density $S_h(f)$, a noise amplitude h_n, and the sensitivities for gravitational-wave searches $h_{3/\mathrm{yr}}$. The noise in the present (1988) prototype beam detectors is discussed in Sec. 11.C. Section 11.D describes optical configurations for beam detectors that are more sophisticated than those used in the past and that hold promise of major future sensitivity improvements: "light recycling" and "light resonating". The spectra of photon shot noise in simple beam detectors, recyling beam detectors, and resonating beam detectors are also discussed in Sec. 11.D. Section 11.E describes the limits that quantum mechanics places on the sensitivities of beam detectors and possible "quantum nondemolition" procedures for circumventing those limits. Also described in Sec. 11.E is the use of "squeezed light" (more

precisely, the squeezing of the quantum electrodynamical vacuum) to improve the performance of beam detectors. Section 11.F pulls together the concepts and results of previous sections and uses them to compute the sensitivities of full-sized beam detectors that might operate in proposed Laser Interferometer Gravitational Wave Observatories. The chapter concludes, in Sec. 11.G, with a brief description of several optical configurations for beam detectors that have not yet been pursued with vigor but might prove attractive in the future.

11.A How a Beam Detector Works

The current and planned beam detectors are designed to operate at frequencies below 10 kHz because astrophysical arguments suggest that the waves will be weak above this frequency (see page 158 of Thorne, 1978); and they have their best sensitivities at frequencies below 1 kHz. Correspondingly, the waves they seek all have reduced wavelengths $\lambda\!\!\!^{-} > 5$ km and most have $\lambda\!\!\!^{-} > 50$ km. Since the planned detectors all have sizes $L \lesssim 4$ km, the condition $L \ll \lambda\!\!\!^{-}$ for use of a "proper-reference-frame analysis" is satisfied, though only marginally in extreme cases. I shall use such an analysis in the discussion below. For an outline of the alternative analysis in TT coordinates (Sec. 4.F) see e.g. Exercise 37.6 of MTW.

A beam *detector* consists of one or more *receivers* that are operated simultaneously, with cross-correlated outputs — the cross-correlation, as usual, being the key to removing spurious, non-Gaussian noise. A simple version of a *Michelson-type beam receiver* is shown in Fig. 11.1, three-dimensionally in part (a) and as seen from above in part (b). The receiver (as we saw in Secs. 2.A and 2.B) consists of three masses which hang on wires from overhead supports and swing like pendula. The masses are arranged at the ends and corner of a right-angle L. Introduce a local proper reference frame in which the receiver is at rest, with the origin of spatial coordinates riding on the corner mass and the $x-$ and $y-$axes along the receiver's two arms. Denote by $\mathbf{l} \equiv \mathbf{e}_x$ the unit vector along one arm and by $\mathbf{m} \equiv \mathbf{e}_y$ the unit vector along the other; and let both arms have the same length L when unperturbed. Let a gravitational wave with wave field $h_{jk}^{\rm TT}$ pass through the receiver, and assume that its frequencies are in the range $f \gg 1$ Hz $\sim$ (the pendular swinging frequency) so the pendular restoring force has no chance to act. Then the wave displaces a mass, whose original position was x^k, by the amount

$$\delta x^j = \frac{1}{2} h_{jk}^{\rm TT} x^k \qquad (11.1)$$

[Eq. (4.13)]. Since the corner mass has $x^k = 0$ and the end masses have $x^k = Ll^k$ and $x^k = Lm^k$, the changes in the receiver's two arm lengths L_x and L_y are

$$\delta L_x = l_j \delta x^j{}_{\text{end mass } x} = \frac{1}{2} L h_{jk}^{\text{GW}} l^j l^k \,, \tag{11.2a}$$

$$\delta L_y = m_j \delta x^j{}_{\text{end mass y}} = \frac{1}{2} L h_{jk}^{\text{GW}} m^j m^k \,. \tag{11.2b}$$

Correspondingly, the difference in arm lengths, which is monitored by laser interferometry, is perturbed by the amount

$$\Delta L \equiv \delta L_x - \delta L_y = \frac{1}{2} L h_{jk}^{\text{GW}} (l^j l^k - m^j m^k) \,. \tag{11.3}$$

Fig. 11.1 Schematic diagram of a *Michelson-type beam receiver* for gravitational waves [part (b)], and of the waves' propagation and polarization angles (θ, ϕ, ψ) relative to the receiver [part (a); cf. Fig. 7.1].

If we denote by $\mathbf{a} \equiv \mathbf{e}_{x'}$ and $\mathbf{b} \equiv \mathbf{e}_{y'}$ the unit vectors along the transverse axes used in defining the wave's + and × polarization states, then

$$h_{jk}^{\text{GW}} = h_+ (a_j a_k - b_j b_k) + h_\times (a_j b_k + b_j a_k) \,; \tag{11.4}$$

cf. Eq. (4.22). By combining Eqs. (11.3) and (11.4) we obtain for the perturbation in the arm-length difference

$$\Delta L(t) = h(t) L \,, \tag{11.5}$$

where $h(t)$ has the standard form (7.1)

$$h(t) = F_+(\theta,\phi,\psi)h_+(t;\iota,\beta) + F_\times(\theta,\phi,\psi)h_\times(t;\iota,\beta) \qquad (11.6)$$

with *beam-pattern factors* F_+ and $F_\times$ given by

$$F_+ \equiv \frac{1}{2}[(\mathbf{a}\cdot\mathbf{l})^2+(\mathbf{b}\cdot\mathbf{m})^2-(\mathbf{a}\cdot\mathbf{m})^2-(\mathbf{b}\cdot\mathbf{l})^2]$$

$$= \tfrac{1}{2}(1+\cos^2\theta)\cos2\phi\cos2\psi-\cos\theta\sin2\phi\sin2\psi \ , \qquad (11.7a)$$

$$F_\times \equiv (\mathbf{a}\cdot\mathbf{l})(\mathbf{b}\cdot\mathbf{l})-(\mathbf{a}\cdot\mathbf{m})(\mathbf{b}\cdot\mathbf{m})$$

$$= \tfrac{1}{2}(1+\cos^2\theta)\cos2\phi\sin2\psi+\cos\theta\sin2\phi\cos2\psi \ . \qquad (11.7b)$$

In these formulas (θ,ϕ) are the spherical polar angles of the source's direction as seen by the detector and ψ, the waves' *polarization angle*, is the angle between the waves' polarization axis $\mathbf{l} = \mathbf{e}_{x'}$ and the constant-ϕ plane); see Fig. 11.1(a) and also Fig. 7.1. As was discussed in Sec. 7.A and Fig. 7.1, the waveforms h_+ and $h_\times$ are to be regarded as depending on time t at the detector, and on direction (ι,β) of the detector, as seen by the source; hence the notation used in Eq. (11.6). The beam-pattern factors $F_+(\theta,\phi,\psi)$ have been derived and discussed previously by, e.g., Forward (1978), Rudenko and Sazhin, (1980), Estabrook (1985), and Schutz and Tinto (1987).

In the Michelson (delay-line) variant of a beam detector, the difference of arm lengths $\Delta L(t)$ is monitored by Michelson interferometry: A beam splitter and two mirrors are attached to the corner mass as shown in Fig. 11.1, and one mirror is attached to each end mass. A laser beam shines through a hole in the corner mass and onto the beam splitter, which directs half the beam toward each end mass. The mirrors on the end masses reflect the beams back toward the corner-mass mirrors, which in turn reflect the beams back to the end masses, which reflect the beams back through holes in the corner-mass mirrors and onto the beam splitter where they are recombined. Part of the recombined beam goes out one side of the beam splitter toward the laser [ignore for now the "recycling mirror" in Fig. 11.1(b), it is absent in the simple version of the receiver being discussed here]; the other part of the recombined beam goes out the other side toward a photodetector. Oscillations in the arm-length difference $\Delta L(t)$ produce oscillations in the relative phases of the recombining light, and thence oscillations in the fraction of the light which goes to the photodetector versus that which goes back toward the laser. The photodetector, by monitoring the oscillations in received intensity, in effect is

monitoring the oscillations $\Delta L(t)$ of arm-length difference and thence the gravity-wave oscillations $h(t)$.

In practice the laser beams are made to bounce back and forth in the arms not just twice as shown in Fig. 11.1b, but rather a large number of round-trip times B, making B distinct spots on each end mirror. In the simple case that the gravity-wave-induced arm-length difference $\Delta L = Lh$ does not change much during these many round trips (see Sec. 11.D below for the case of large change), the bouncing light beam will build up during its B trips a total phase delay

$$\Delta\Phi = \frac{2B\,\Delta L}{\lambda\!\!\!^{-}_e} = \frac{2BL}{\lambda\!\!\!^{-}_e} h \tag{11.8}$$

where $\lambda\!\!\!^{-}_e = \lambda_e/2\pi$ is the reduced wavelength of the light ($\lambda\!\!\!^{-}_e = 0.0818$ microns for the light from the argon ion lasers currently being used). This phase delay can be monitored, by the photodetector, with a precision $\Delta\Phi = 1/\sqrt{N_\gamma \eta}$, where N_γ is the total number of photons that the laser puts out during the time $\hat{\tau}$ over which the photodetector intensity is averaged, and η is the photon counting efficiency of the photodetector ($\eta \sim 0.4$ to 0.9). (In the similar discussion in Sec. 2.A we ignored the photodector efficiency.) When searching for a gravity-wave burst with characteristic frequency f, it is optimal to average the photodetector intensity for half a gravity-wave period, $\hat{\tau} \cong 1/2f$; and correspondingly the phase delay can be inferred with a photon-counting-noise ("shot-noise") precision

$$\Delta\Phi_{\rm shot} = \frac{1}{\sqrt{N_\gamma \eta}} \simeq \left[\frac{\hbar c/\lambda\!\!\!^{-}_e}{I_0 \eta (1/2f)}\right]^{1/2}, \tag{11.9}$$

where I_0 is the laser output power. By comparing Eqs. (11.8) and (11.9) we obtain a rough estimate of the amplitude of a gravity-wave burst that produces a signal of the same strength as the rms shot noise

$$h_{\rm shot} \cong \left[\frac{2\hbar c \lambda\!\!\!^{-}_e}{I_0 \eta} \frac{f}{(2BL)^2}\right]^{1/2}$$

$$\cong 7.2\times10^{-21} \frac{50}{B} \frac{1\,\text{km}}{L} \left[\frac{\lambda\!\!\!^{-}_e}{0.082\mu\text{m}}\right]^{1/2} \left[\frac{10\,\text{Watts}}{I_0 \eta}\right]^{1/2} \left[\frac{f}{1000\,\text{Hz}}\right]^{1/2} . \tag{11.10}$$

This formula and these numbers give some indication of the potential sensitivities of beam receivers.

Fabry-Perot beam receivers, have essentially the same potential sensitivities as Michelson receivers. Figure 11.2 shows a Fabry-Perot

Fig. 11.2 Schematic diagram of a *Fabry-Perot-type beam receiver* for gravitational waves.

receiver viewed from above. Here, by contrast with Fig. 11.1, the corner mass has been broken into three separate pieces, one carrying each mirror and one carrying the beam splitter. This breaking up of the corner mass, initiated in Munich, reduces spurious forces on the mirrors; since 1985 it has been standard in all beam receivers. In the Fabry–Perot system of Fig. 11.2 each arm is operated as a resonant Fabry–Perot cavity: Light from the laser is split at the beam splitter and enters the two cavities through the backs of the corner masses' partially transmitting mirrors. The two arms are arranged to have equilibrium lengths very nearly equal to a half–integral multiple of the wavelength $2\pi\lambda_e$ of the laser light. Consequently, the entering light finds itself in resonance with a mode of each cavity; and it gets resonantly trapped in the cavity, building up to high intensity before exiting back toward the beam splitter.

Slight changes in the length of each cavity drive the cavity slightly off resonance and thereby produce sharp changes in the phase of the exiting light. Consequently, when the exiting light beams from the two cavities recombine at the beam splitter, their relative phase is highly sensitive to slight modulations ΔL of the two cavities' length difference l; and correspondingly the intensity of light onto the photodetector is highly sensitive to ΔL. If the corner mirrors have a probability for reflecting photons $\mathcal{R}_C$ and a transmission probability $1-\mathcal{R}_C$ (and no

scattering), and if the end mirrors reflect much more efficiently, then this Fabry–Perot sensitivity is described by the same formulas (11.8)–(11.10) as for a Michelson receiver, with the number of round-trips B in each Michelson arm replaced by $4/(1-\mathcal{R}_C)$:

$$B \to 4/(1-\mathcal{R}_C) \ . \tag{11.11}$$

It is also possible (and, in fact, is current practice) to operate a Fabry–Perot receiver in an alternative mode where, instead of recombining and interfering the beams, the laser's frequency is locked to the eigenfrequency of one arm and the difference between the laser's frequency and that of the other arm is the gravity-wave signal; see, e.g. Hough *et. al.* (1983) or Spero (1986a) for details. This mode of operation is technically easier than beam recombination, but the ease is bought at the prices of (i) an inability to recycle unused laser light (Sec. 11.D below), and (ii) even without recycling, some debilitation in the ultimately achievable shot noise.

11.B Noise in Beam Detectors

Photon shot noise is but one of many noise sources that plague beam detectors. Almost always, thus far, the other noise sources are so strong that the effects of shot noise are lost amidst them. Typically the experimenters struggle for a long time to reduce the other noises far enough that shot noise shows up; then they improve the shot noise somewhat by increasing the laser power; then they begin a long struggle once again with the other noise sources. In this way the overall gravity-wave amplitude noise at kilohertz frequencies has been reduced during the period 1980–86 by a factor ~1000 (10^6-fold improvement in energy noise).

Among the most serious of the other noise sources are the following: Amplitude and phase fluctuations in the laser output; imperfect matching of the laser beam into the Fabry–Perot cavities or the Michelson mirror system (imperfections in beam direction, beam shape, and beam wavelength); imperfect matching of the wave fronts of the recombining beams at the beam splitter; fluctuations in the index of refraction of the gas inside the arms (even though the arms are inside vacuum pipes, residual gas can cause problems); scattering of light from one part of the optical system into another; thermal noise (thermal vibrations) in the end and corner masses and in the wires that suspend them; imperfect alignment of the mirrors; and seismic and acoustic noise from the outside world, which cause vibrations of the

wires from which the masses hang. Almost all of these effects produce a displacement noise ΔL that is independent of the arm length L; and, correspondingly, their effects on gravity-wave amplitude sensitivities scale as $h \propto 1/L$. It is this scaling that motivates the move from short prototypes to long LIGOs.

A beam receiver is intrinsically broad band: Its output, the intensity of the light into the photodetector $I_{pd}(t)$, is averaged (by filtering) over the shortest timescale, $\hat{\tau} \sim 10^{-4}$ seconds, that gravity waves are likely to contain; and then is recorded for future analysis. The future analysis can include searching in the data for signals of all frequencies $f \lesssim 1/\hat{\tau} \sim 10^4$ Hz, and for signals with complicated time dependences that embody a broad range of frequencies. Correspondingly, a beam receiver's net noise depends on the frequency f at which one studies the recorded output.

More specifically, the noise (excluding non-Gaussian, spurious events which are removed by coincident operation of two independent receivers) is characterized by the spectral density $S_{\Delta L}(f)$ of the output-inferred arm-length difference l; or, equally well, by the spectral density $S_h(f)$ of the gravity wave $h(t)$ [Eq. (11.6)]. Because the effect of the gravity wave on the arm-length difference is $\Delta L(t) = Lh(t)$, $S_h(f)$ is also called the spectral density of strain, and these two spectral densities are related by

$$S_h(f) = (1/L^2) S_{\Delta L}(f) \ . \tag{11.12}$$

It is $S_h(f)$ or its square root, or $S_{\Delta L}(f)$ or its square root, that experimenters generally quote when discussing the overall performance of their beam detectors.

In Secs. 7.A, 8.A and 9.A we derived expressions in terms of $S_h(f)$ for the minimum-amplitude signal $h_{3/yr}$ that can be detected with 90% confidence in a 1/3 year search using a detector composed of two identical cross-correlated receivers. Those expressions involve averages over the receivers' beam-pattern factors. For the L-shaped beam receivers of Figs. 11.1 and 11.2, with beam-pattern factors (11.7), the appropriate averages are

$$\langle F_+^2 \rangle = \langle F_\times^2 \rangle = 1/5 \ , \tag{11.13}$$

and correspondingly

$$h_{3/yr}(f_c) = 11\sqrt{f_c S_h(f_c)} \quad \text{for bursts [Eq. (7.9)]} \tag{11.14}$$

$$h_{3/yr}(f) = 3.8\sqrt{S_h(f) \times 10^{-7}\text{Hz}} \quad \text{for periodic waves [Eq. (8.5a)]} \ , \tag{11.15}$$

$$h_{3/\mathrm{yr}}(f) = 4.5\left|\frac{\Delta f}{10^{-7}\mathrm{Hz}}\right|^{-1/4}\sqrt{f S_h(f)}$$

for stochastic waves [Eq. (9.9)] . (11.16)

Here in the burst equation the numerical factor in Eq. (7.9) has been taken to be 5 corresponding to a characteristic frequency $f_c \sim 10$ Hz to 10^4 Hz – the largest band that earth-based receivers are likely ever to operate in; and in the periodic equation it is assumed that the frequency and phase are known in advance [Eq. (8.5a) rather than (8.5b)]. Expressions (11.14)–(11.16) are the bases of the beam-detector noise amplitudes shown in Figs. 2.7–2.9.

When the two receivers that make up a detector do not lie in the same plane (because of curvature of the earth between them) or do not have their arms parallel, their joint sensitivity is somewhat debilitated. Detailed analyses of this have been carried out by Whitcomb and Saulson (1984) and by Schutz and Tinto (1986). [KIP: ADD DETAILS?]

11.C Noise in the Present Prototypes

At present the MIT group is developing Michelson receivers using a prototype with $L = 1.5$ meters; the Munich group is developing Michelsons using $L = 30$ meters (Shoemaker et. al. 1986); the Glasgow group is developing Fabry-Perot receivers using $L = 10$ meters; and the Caltech group is developing Fabry-Perots using $L = 40$ meters. [KIP: ADD THE JAPANESE] Although the arm lengths and optics of these four prototypes are very different, their displacement sensitivities are roughly the same – and have been so throughout the past six years, during which all have improved roughly in step by about three orders of magnitude. Throughout these improvements Munich has maintained a slight (factor 2 or 3 in amplitude) lead over the other groups. (*Note added in proof*: Since this was written Glasgow has forged ahead of Munich by a factor 3 in displacement sensitivity, making them equal in h sensitivity). [KIP: FIX] Figure 11.3 shows the spectral density of strain noise for the Munich prototype as of February 1986 (Schilling 1986). The noise is due, predominantly, to seismic noise (inadequate isolation) below 250 Hz, probably seismic noise between 250 and 1000 Hz, photon shot noise between 1000 and 6000 Hz, and thermal noise in the mirrors and pockels cells above 6000 Hz. In Figs. 2.7, 2.8, and 2.9 (upper right) are shown the sensitivities $h_{3/\mathrm{yr}}$ [Eqs. (11.14)–(11.16)] for the Munich and Caltech prototypes in 1986 (Schilling 1986, Spero

1986b) and Glasgow in early 1987. As an illustration of the sensitivity progress, Fig. 2.7 also shows $h_{3/yr}$ for bursts in the Munich and Caltech prototypes a few months after each was first turned on (1980 and 1983).

Fig. 11.3 Square root of spectral density of noise $\sqrt{S_h(f)}$ plotted against frequency f for the Munich Michelson-type beam detector with 30 meter arms, as of February 1986. [KIP: REPLACE BY A MORE UP TO DATE SPECTRUM?]

11.D Simple, Recycling, and Resonating Receivers and their Shot Noise

In the present prototypes it is advantageous to store the light in the arms as long as possible, thereby building up the largest possible phase shift and gravity-wave sensitivity; cf. the B-dependence in Eqs. (11.8) and (11.10). However, in a kilometer-scale LIGO one easily can store the light longer than half a gravity-wave period, i.e. for more than $B = 75(1\text{ km}/L)(1000\text{ Hz}/f)$ round-trip traverses of an arm. Such long storage is self-defeating: the phase shift built up so laboriously during the first half period of the wave gets removed during the second half period because $h(t)$ reverses sign.

This shows up clearly in the spectral densities of shot noise $S_h(f)$ for the idealized Michelson and Fabry-Perot receivers of Figs. 11.1 and 11.2 (still without the "recycling mirrors" in place). Assuming as above that the Michelson mirrors have negligible losses during B round trips in each arm, and the Fabry-Perot end mirrors have negligible transmission compared to the corner mirrors

$$1-\mathcal{R}_E \ll 1-\mathcal{R}_C \equiv 4/B \tag{11.17}$$

[cf. Eq. (11.11)], the spectral densities of shot noise are (cf. Gürsel et. al., 1983; Meers, 1983; Vinet *et. al.*, 1988)

$$S_h(f)=\frac{2\hbar c\lambda_e}{I_o\eta}\left[\frac{1}{2BL}\right]^2\times\begin{cases}1+(2\pi BLf/c)^2 & \text{for Fabry–Perot} \quad \text{(11.5a)}\\ \left[\dfrac{2\pi BLf/c}{\sin(2\pi BLf/c)}\right]^2 & \text{for Michelson.} \quad \text{(11.5b)}\end{cases} \tag{11.18a,b}$$

These spectral densities are shown in Fig. 11.4 as a function of $2BLf/c$ = (light storage time)/(gravity-wave period), with (gravity-wave period) = $1/f$ held fixed. When (storage time)/(period)$\ll$1 the two receivers have the same shot noise, and that shot noise improves with increasing storage time as $S_h(f)\propto$(storage time)$^{-2}$. When (storage time)/(period)$\gtrsim$1 the Fabry-Perot shot noise stops improving, while the Michelson shot noise undergoes a series of oscillations with minima equal to the Fabry-Perot shot noise. Note that the minima of the Michelson oscillations occur when $2BLf/c$ = (light-storage time)/(gravity-wave period)=0.5, 1.5, 2.5, ... , while their maxima ($S_h=\infty$) occur when the light is stored for an integral number of gravity-wave periods. This is just what we would expect from the fact that $h(t)$ reverses sign every half period, thereby removing during a second half period the signal put onto the light during a first half period. In the Fabry-Perot receiver there are no oscillations of $S_h(f)$ because different photons experience different storage times — i.e. because of the probabilistic nature of the reflectivity $\mathcal{R}_C$.

Drever (1983) has devised a method for improving the sensitivity of either a Michelson or a Fabry-Perot when mirror reflectivities permit storing light for much longer than a half period. The basic idea is to extract the light after a half period, when further storage is self defeating, and then reinsert it into the cavity along with and in phase with new laser light. More specifically, for the Michelson of Fig. 11.1b, one adjusts the relative arm lengths so that very little of the recombined light emerges from the beam splitter toward the photodiode where the gravity-wave signal is read out (a mode of operation that optimizes the sensitivity, it turns out). Then most of the recombined light emerges toward the laser; and "recycling mirrors" are inserted to direct that emergent light back into the beam splitter along with fresh laser light. For the Fabry-Perot of Fig. 11.2 the same effect is achieved with a single recycling mirror.

Fig. 11.4 The improvement of photon shot noise with increasing number of bounces of light in a simple beam receiver. The receiver is of the Fabry–Perot (Fig. 11.2) or Michelson (Fig. 11.1) type with recycling mirrors absent, with $1-\mathcal{R}_E \ll 1-\mathcal{R}_C = 4/B$ in the Fabry–Perot case and with B round trips in each arm in the Michelson case. Plotted vertically is spectral density of shot noise in units proportional to f^2 but independent of the light-storage time $2BL/c$. Plotted horizontally is (light-storage time)/(gravity-wave period)$=(2BL/c)f$. The Fabry–Perot shot noise is given by the solid curve [Eq. (11.18a)]; the Michelson by the dashed curve [Eq. (11.18b)].

As an aid in quantifying the recycling-induced improvement in shot noise, consider the (realistic) situation in which the technology of mirror coatings limits the mirror reflectivities to some maximum value $\mathcal{R}_{max}$ (0.9999 at present; perhaps 0.99999 a few years from now). It obviously is optimal to place at the end of each arm a mirror with this maximum, so $\mathcal{R}_E = \mathcal{R}_{max}$. Consider, for concreteness, the Fabry–Perot receiver of Fig. 11.2. If the corner mirrors are chosen also to have the maximum reflectivity, $\mathcal{R}_C = \mathcal{R}_E$, then essentially all the unused light leaks out the end mirrors and nothing is gained by recycling. In this case of a simple, non-recycling Fabry–Perot with $\mathcal{R}_C = \mathcal{R}_E = \mathcal{R}_{max}$ the spectral density of shot noise is (cf. Gürsel et. al., 1983; Meers, 1983; Vinet *et. al.*, 1988)

$$S_h(f) = S_o[1+(f/f_o)^2] \ , \qquad (11.19a)$$

where

$$S_o = \frac{2\hbar c \lambda_e}{I_o \eta}\left(\frac{1-\mathcal{R}_E}{2L}\right)^2$$

$$= \left[\frac{3.6\times10^{-25}}{\sqrt{\text{Hz}}} \left(\frac{\lambda_e}{.0818\mu\text{m}} \right)^{1/2} \left(\frac{100\text{W}}{I_o\eta} \right)^{1/2} \left(\frac{1-\mathcal{R}_E}{10^{-4}} \right) \left(\frac{1\text{km}}{L} \right) \right]^2 \quad (11.19b)$$

$$f_o = \frac{(1-\mathcal{R}_E)c}{4\pi L} = 2.4\text{Hz} \left(\frac{1-\mathcal{R}_E}{10^{-4}} \right) \left(\frac{1\text{km}}{L} \right) . \quad (11.19c)$$

[Note that, because so much light is lost out the end mirrors, this noise is worse than the $\mathcal{R}_C \gtrsim \mathcal{R}_E$ limit of Eq. (11.18a) — worse by a factor 4 at frequencies $f \gg f_o$ and by a factor 16 at $f \ll f_o$.] This non-recycled ("simple") Fabry-Perot noise is shown as a solid curve in Fig. 11.5.

Fig. 11.5 Spectral density of shot noise for Fabry-Perot beam receivers operated in various optical configurations. The vertical and horizontal scales are both logarithmic. The solid curve is for a simple Fabry-Perot with all mirrors — corner and end — having the maximum achievable reflectivity, $\mathcal{R}_C = \mathcal{R}_E = \mathcal{R}_{max}$ [Eqs. (11.19)]. The dashed curves are for a Fabry-Perot with light recycling [Eq. (11.20c)], in which the end mirrors have the maximum achievable reflectivity $\mathcal{R}_E = \mathcal{R}_{max}$, the corner mirrors are adjusted to produce the desired knee frequency [f_{k1} and f_{k2} for the two curves shown; Eq. (11.20a)], and the recycling mirror is adjusted to minimize the noise at the knee frequency [Eq. (11.20b)]. The dotted curves are for a Fabry-Perot with light resonating [Eq. (11.22c); Fig. 11.6] in which the end mirrors have the maximum achievable reflectivity $\mathcal{R}_E = \mathcal{R}_{max}$; the corner mirrors are adjusted to produce the desired resonant frequency for gravity waves [f_{R1} and f_{R2} for the two curves shown; Eq. (11.22a)]; and the recycling mirror is adjusted to minimize the noise at the resonant frequency [Eq. (11.22b)].

An experimenter who wishes to improve on this noise level by recycling must choose a frequency $f_k \gg f_o$ near which the noise level is to

be minimized. The minimal noise level near $f = f_k$ will then be achieved by setting

$$1-\mathcal{R}_C = 8\pi L f_k / c \tag{11.20a}$$

so the effective storage time in each arm is $2BL/c = 8Lc^{-1}/(1-\mathcal{R}_c) = (\pi f_k)^{-1} = (1/\pi) \times$ (period of a gravity wave with the optimal frequency f_k). Minimal noise also requires a special choice for the reflectivity $\mathcal{R}_R$ of the recycling mirror (Fig. 11.2)

$$1-\mathcal{R}_R = \frac{4(1-\mathcal{R}_E)}{(1-\mathcal{R}_C)} \ . \tag{11.20b}$$

With these choices of reflectivity, the light-recycling Fabry-Perot receiver of Fig. 11.2 has shot noise (cf. Gürsel et. al., 1983; Meers, 1983; Vinet *et. al.*, 1988)

$$S_h(f) = \frac{f_k}{2f_o} S_o \left[1 + \left[\frac{f}{f_k} \right]^2 \right] \ . \tag{11.20c}$$

This noise is depicted in Fig. 11.5 for two choices of f_k (dashed curves). Note that this noise has a "knee" at the frequency f_k; for this reason f_k is called the *knee frequency*. Note further that recycling produces an overall improvement in $S_h(f)$, at frequencies $f \gtrsim f_k$, by a factor $f_o/2f_k$ relative to a nonrecycled Fabry-Perot with equal reflectivities for corner and end mirrors [Eqs. (11.19)] and an improvement by $2f_o/f_k$ relative to the very best nonrecycled Fabry-Perot – one with $1-\mathcal{R}_{max} = 1-\mathcal{R}_E \ll 1-\mathcal{R}_c \ll 8\pi L f_k/c$ [Eq. (11.18a)]. This improvement at $f \gtrsim f_k$ is bought at the price of worsened noise at $f \lesssim \sqrt{f_k f_o/2}$. Note further that the improvement factor, over an optimal nonrecycled Fabry-Perot at $f \gtrsim f_k$, is

$$\frac{S_h^{\text{recycled}}}{S_h^{\text{nonrecycled}}} = \frac{2f_o}{f_k} = \frac{1-\mathcal{R}_E}{1-\mathcal{R}_C} \ , \tag{11.21}$$

which is 1/(the mean number of times that the light can be recycled before it is lost by leakage through the high-reflectivity end mirrors). This is just what physical intuition should suggest.

For the recycled Michelson receiver of Fig. 11.1, recycling produces essentially the same $S_h(f)$ as for the Fabry-Perot of Fig. 11.2 at frequencies $f \lesssim f_k$. However, above the knee frequency the recycled Michelson exhibits a sequence of noise peaks and troughs analogous to those for a non-recycled Michelson [Eq. (11.18b) and Fig. 11.4].

Of all optical configurations yet invented, recycling is the best when one is searching for broad-band gravitational waves (waves with $\Delta f \gtrsim f$). However, when one is searching for narrow-band waves (waves with $\Delta f \ll f$, e.g. the periodic waves from a pulsar), recycling gives worse noise than a configuration called *light resonating* (invented by Drever 1983), which is shown in Fig. 11.6. As usual, the method is conceptually simplest in the Michelson case but is described by the simplest formulas in the Fabry-Perot case.

Fig. 11.6 Schematic diagrams of optical configurations that could be used for *resonating light* in Michelson-type [diagram (a)] and Fabry-Perot-type [diagram (b)] beam receivers (Drever, 1983).

The basic idea, as shown for a Michelson in Fig. 11.6a, is to store the light in an arm for one half cycle of the gravity-wave frequency of interest f_R (i.e. for $B = c/4f_RL$ round trips); then, instead of extracting it through the beam splitter and reinjecting it, simply move it into the other arm using a high-reflectivity, Fabry-Perot-type mirror – i.e. exchange the light between the arms. Then during the next half cycle, with arms interchanged and the sign of the gravity wave reversed, each piece of light will experience a phase shift in the same direction as during the first half cycle. At the end of the second half cycle, interchange the light in the two arms, and repeat as many times as mirror losses will permit. The arrows in Fig. 11.6a show the light, as a result of these exchanges, circulating around the interferometer in a clockwise direction, but there is an equal amount of light circulating in a

counterclockwise direction. The light circulating one way experiences a continual increase in phase shift throughout its circulation; the light circulating oppositely experiences a continual decrease in phase shift; and these oppositely circulating beams, upon reemerging through the back of the Fabry–Perot–type mirror and recombining at the beam splitter, produce a much enhanced interference signal in the photodetector.

For the Fabry–Perot receiver of Fig. 11.6b a single "resonating mirror", denoted $\mathcal{R}_R$, produces the resonant interchange of the light between the two arms: The lengths of the cavities are so adjusted as to produce in each cavity a resonance at a frequency f_e very near the laser frequency; the reflectivities $\mathcal{R}_C$ of the corner mirrors, and the path lengths between them and the resonating mirror, are then so adjusted as to produce two resonant modes of the coupled cavities at light frequencies $f_e \pm f_R/2$ – which requires

$$1-\mathcal{R}_C = 4\pi L f_R/c \ ; \qquad (11.22a)$$

the laser frequency is then adjusted so that it drives the mode at $f_e - f_R/2$; and the gravity waves with frequency f_R, by wiggling the end mirrors, then upconvert photons into the mode at $f_e + f_R/2$. In order to maximize the resulting gravity-wave–induced signal at the photodetector, the reflectivity $\mathcal{R}_R$ of the resonating mirror must be adjusted to

$$1-\mathcal{R}_R = 2\frac{1-\mathcal{R}_E}{1-\mathcal{R}_C} = 2\frac{f_o}{f_R} \ . \qquad (11.22b)$$

With these optimizations the spectral density of shot noise near f_R is (cf. Gürsel et. al., 1983; Meers, 1983; Vinet, 1986; Vinet *et. al.*, 1988)

$$S_h(f) = 4S_o\left[1+\left(\frac{f-f_R}{f_o}\right)^2\right] \quad \text{for } |f-f_R| \ll f_o \ . \qquad (11.22c)$$

As is seen in Fig. 11.5 (dotted curves), this represents an enormous improvement in noise over either a simple Fabry–Perot or a recycling Fabry–Perot. However, this improvement is bought at the price of an enormous narrow-banding of the receiver response: At frequencies $f \sim f_R/2$ and $f \sim 2f_R$ the noise is comparable to that in a simple Fabry–Perot; and at $f \ll f_R/2$ and $f \gg 2f_R$ it is far worse.

For an optimally configured, resonating Michelson the sensitivity near resonance, $|f-f_R| \ll f_o$, is similar to that of a Fabry–Perot [Eq.

(11.22c)].

Neither recycling nor resonating is potentially useful in present prototypes because present mirror reflectivities limit the prototypes to short storage times. However, in the planned full-scale LIGOs where 100-fold longer arms permit 100-fold greater storage times, recycling and resonating both give promise of substantial improvements in beam-detector sensitivities. The first attempts to implement recycling on a prototype were carried out by the Munich group in 1986, with moderate success. Resonating has not yet been attempted.

11.E Quantum Limit, Quantum Nondemolition, and Squeezed Vacuum

A beam receiver is similar to a "Heisenberg microscope", in which a photon is used to measure the position of a particle. The analog of the Heisenberg photon is the laser beam and the analogs of the Heisenberg particle are the end and corner masses. Just as the Heisenberg photon kicks the particle it is trying to measure thereby enforcing the Heisenberg uncertainty principle, $\Delta x \Delta p \geq \hbar/2$, so fluctuations in the beam's light pressure kick the end and corner masses thereby enforcing a quantum limit on the sensitivity of the beam receiver. As I shall discuss below, these quantum fluctuations have their ultimate source in the vacuum fluctuations of quantum electrodynamics (Caves 1980, 1981).

Caves (1987b) has used Feynman path-integral techniques (Caves 1986, 1987a) to derive a pseudospectral density of displacement noise that characterizes the quantum limit of any harmonic oscillator (such as a beam receiver's swinging masses) when it is studied at frequencies high above the resonant frequency f_o, using techniques that produce the minimum possible noise:

$$S_x(f) = \frac{2\hbar}{m(2\pi f)^2} , \tag{11.23}$$

where m is the oscillator's mass and x is its displacement from equilibrium. For a beam receiver, whose swinging masses have resonant frequencies $f_o \sim 1$ Hz far below the region of interest, this pseudospectral density for their displacements can be translated into a pseudospectral density for the gravity-wave field $h(t)$ that one reads off the receiver's output:

$$S_h(f) = \frac{8\hbar}{m(2\pi f)^2 L^2} . \tag{11.24}$$

Here each of the masses on which a mirror is attached is assumed to have the same mass m. This pseudospectral density can be used, in the same manner as an ordinary classical spectral density (Sec. 11.B above), to compute the standard quantum limit on the performance of a beam detector in various situations.

As for a bar detector, so also for a beam detector, there should be methods of circumventing this standard quantum limit. Unfortunately nobody has yet found a remotely practical way of doing so, except in one special case: Unruh (1982) has invented a method, which Caves' path-integral formalism says should work (Caves 1987b), for beating the standard quantum limit when performing a narrow-band measurement of periodic gravitational waves. The key idea (which was invented independently and earlier in the classical domain by Gordienko, Gusev, and Rudenko 1977) is to place a spring between each mirror and the companion mass on which it rides, thereby turning the mirror and companion into a two-mode system. By setting the ratio of the spring frequency over the gravity-wave frequency equal to the square root of the mass of the big companion over the mass of the little mirror, one can force the laser beam's fluctuating light pressure to act on the motion of the big mass and not the mirror, while the interferometer reads out the mirror's motion. The result is an improved immunity of the receiver to Heisenberg's quantum noise over a narrow frequency band. While this scheme is clever and conceptually satisfactory, whether it can be implemented in a practical manner is not yet clear.

Although, for broad-band measurements with beam receivers, there as yet is no known way of beating the standard quantum limit, Caves (1981) has invented a clever scheme for getting closer to the quantum limit when inadequate laser power causes the shot noise to exceed it. The key to Caves' idea is his discovery that the ultimate source of the photon shot noise and the fluctuating radiation-pressure noise is *not*, as people previously thought, fluctuations in the laser output. Rather, it is fluctuations in the quantum-electrodynamic vacuum state ("vacuum fluctuations") that enter the beam splitter at right angles to the incoming laser light and superpose on the laser light as it heads toward the two arms. As Caves has shown, by "squeezing the vacuum" (i.e. reducing the vacuum fluctuations in the $\cos[(ct-x)/\lambda_e]$ part of the light while increasing them in the $\sin[(ct-x)/\lambda_e]$ part; achievable in principle by sending the vacuum through a pumped, nonlinear medium), one can reduce the beam receiver's shot noise at

the expense of increasing the fluctuations in its light-pressure noise. The net result is the same as if one were using a laser of higher power: in the typical case, where the actual power is too low to permit achieving the quantum limit, one improves the sensitivity and moves toward the quantum limit.

Recently Caves (1987c) has elucidated the ultimate sensitivities achievable when one combines his squeezed-vacuum technique with light recycling and resonating. He finds that because, in a resonating system, noise associated with losses in the end mirrors is as important on resonance as vacuum fluctuations entering the beam splitter, squeezing of the vacuum is not useful. By contrast, when combined with light recycling, squeezed-vacuum techniques can reduce $S_h(f)$, over a broad band of frequencies $\Delta f \gtrsim f$, to S_0 or to the quantum limit, whichever is larger:

$$S_h(f) = \max \begin{cases} S_0 = \dfrac{2\hbar c \lambda_e}{I_0 \eta} \left| \dfrac{1 - \mathcal{K}_E}{2L} \right|^2 \\ \dfrac{8\hbar}{m(2\pi f)^2 L^2} \end{cases} \qquad (11.25)$$

Squeezed states of light have been produced by experimenters recently (Slusher et. al. 1985, Wu et. al. 1986), triggering great excitement in the field of nonlinear quantum optics. This achievement has triggered an effort by the Munich group to implement Caves' squeezed-vacuum technique – an effort that is likely to succeed within the next few years.

11.F Anticipated Sensitivities of Full-Sized LIGO Receivers

The present Munich burst sensitivity $h_{3/\mathrm{yr}} \cong 4\times10^{-17}$ at $f \sim 1000$ Hz, when scaled from the prototype arm length of 30 meters to the planned Munich LIGO arm length of 3 kilometers, would become $h_{3/\mathrm{yr}} \cong 4\times10^{-19}$. Although scaling up is not straightforward (mirror diameters must be increased a factor ten, for example), the experimenters are quite confident of doing somewhat better than this scaled-up number by the early 1990s when the first LIGOs start operating.

The upper thick, dashed curves in Figs. 2.7–2.9 show possible burst, periodic, and stochastic sensitivities (based on a 1/3-year search time and 90 per cent confidence levels), for a first generation of detectors in the full-scale LIGOs. These curves correspond, at frequencies above ~500 Hz, to receivers that are shot-noise-limited,

without recycling or resonating, with Argon-ion laser light $\lambda_e = 0.0818\mu$m, with (laser power)×(photodetector efficiency) = $I_o\eta$ = 10 Watts, and with light storage times of a half gravity-wave period or longer, so [cf. Eq. (11.18) and Fig. 11.4]

$$\sqrt{S_h(f)} = \left[\frac{2\hbar c\lambda_e}{I_o\eta}\left(\frac{\pi f}{c}\right)^2\right]^{1/2} = (2.4\times10^{-22}\ \mathrm{Hz}^{-1/2})\left(\frac{f}{1000\mathrm{Hz}}\right) \quad (11.26a)$$

and correspondingly [Eqs. (11.14)-(11.16)]

$$h_{3/\mathrm{yr}} = 11\sqrt{f_c S_h} = 8\times10^{-20}\left(\frac{f_c}{1000\mathrm{Hz}}\right)^{3/2} \quad \text{for bursts}, \quad (11.26b)$$

$$h_{3/\mathrm{yr}} = 3.8\sqrt{S_h\times10^{-7}\mathrm{Hz}} = 2.9\times10^{-25}\left(\frac{f}{1000\mathrm{Hz}}\right) \quad \text{for periodic sources},$$

$$h_{3/\mathrm{yr}} = 4.5\left(\frac{f}{10^{-7}\mathrm{Hz}}\right)^{-1/4}\sqrt{fS_h}$$

$$= 1.1\times10^{-22}\left(\frac{f}{1000\mathrm{Hz}}\right)^{5/4} \quad \text{for stochastic sources}, \quad (11.26c)$$

where the search for stochastic waves is presumed to use a bandwidth $\Delta f = f$. Below ~500Hz it is presumed that seismic noise debilitates the performance of these first-generation LIGO receivers.

During the years following the first gravity-wave searches in the LIGOs, the experimenters plan to run a sequence of detectors with ever improving sensitivities, pushing the sensitivities ever downward, and improving the seismic isolation so the detectors can operate at ever decreasing minimum frequencies. A reasonable goal by the end of the 1990s is to approach the lower-most thick-dashed curves in Figs. 2.7–2.9. These curves correspond to *advanced detectors* with the following characteristics:

L = (arm length) = 4km,

λ_e = 0.0818 μm (Argon-ion laser light),

$I_o\eta$ = (laser power)×(photodetector sensitivity) = 100 Watts,

$\mathcal{R}_E = \mathcal{R}_{\max}$ = (maximum mirror reflectivity) = 0.9999,

m = (mirror mass) = 1000 kg,

photon shot noise dominant at $100\mathrm{Hz} \lesssim f \lesssim 10^4\mathrm{Hz}$,

quantum-limit noise dominant at $10\text{Hz} \lesssim f \lesssim 100\text{Hz}$,

seismic noise dominant at $f \lesssim 10\text{Hz}$. (11.27)

It is presumed that light recycling is used for burst searches, with the knee frequency adjusted to equal the frequency of interest, so the photon shot noise [Eqs. (11.14), (11.20c), and (116b,c) with $f_k = f_c$] is

$$h_{3/\text{yr}} = 11\sqrt{f_c S_h} = 11\sqrt{S_o f_c^2/f_o} = 11\left[\frac{2\pi\hbar\lambda_e}{I_o\eta}\frac{(1-\mathcal{R}_E)}{L}f_c^2\right]^{1/2}$$

$$= 1.3\times10^{-21}\left(\frac{f_c}{1\text{kHz}}\right) \quad \text{for bursts;} \tag{11.28a}$$

and it is presumed that light resonating is used for periodic and stochastic searches, with the resonant frequency adjusted to equal the frequency of interest, so the photon shot noise [Eqs. (11.15), (11.16), (11.22c), and (116b,c) with $f_R = f$] is

$$h_{3/\text{yr}} = 3.8\sqrt{4S_o\times10^{-7}\text{Hz}} = 3.8\left[\frac{2\hbar c\lambda_e}{I_o\eta}\times10^{-7}\text{Hz}\right]^{1/2}\left(\frac{1-\mathcal{R}_E}{L}\right)$$

$$= 2.1\times10^{-28} \quad \text{for periodic waves,} \tag{11.28b}$$

$$h_{3/\text{yr}} = 4.5\left(\frac{f_o}{10^{-7}\text{Hz}}\right)^{-1/4}\sqrt{4S_o f} = 4.5\left[\frac{2\hbar c\lambda_e}{I_o\eta}f\right]^{1/2}\left[\frac{4\pi}{c}\left(\frac{1-\mathcal{R}_E}{L}\right)^3\times10^{-7}\text{Hz}\right]^{1/4}$$

$$= 5.2\times10^{-25}\left(\frac{f}{1\text{kHz}}\right)^{1/2} \quad \text{for stochastic waves.} \tag{11.28c}$$

Here it is assumed that the stochastic search is restricted to the narrow bandwidth $\Delta f = f_o$ over which the resonating receiver has good performance. The quantum-limit noise, which exceeds these shot noise levels at $f \lesssim 100\text{Hz}$, is given by [Eqs. (11.24) and (11.14)–(11.16)]

$$h_{3/\text{yr}} = 11\left[\frac{2}{\pi^2}\frac{\hbar}{mL^2}\frac{1}{f}\right]^{1/4} = 1.3\times10^{-23}\left(\frac{1000\text{Hz}}{f}\right)^{1/4} \quad \text{for bursts,} \tag{11.29a}$$

$$h_{3/\text{yr}} = 3.8\left[\frac{2}{\pi^2}\frac{\hbar}{mL^2}\frac{10^{-7}\text{Hz}}{f^2}\right]^{1/4}$$

$$= 4.4\times10^{-29}\left(\frac{1000\text{Hz}}{f}\right) \quad \text{for periodic waves,} \tag{11.29b}$$

$$h_{3/\mathrm{yr}} = 4.5\left[\frac{f_o(S_{QL}/S_o)^{1/4}}{10^{-7}\mathrm{Hz}}\right]^{-1/4}\left[\frac{4}{3}fS_{QL}\right]^{1/2}$$

$$= 4.5\left[\frac{4}{3\pi}\right]^{1/4}\left[\frac{4\hbar}{mL^2}\right]^{3/8}\left[\frac{\hbar\lambda_e}{I_o\eta c}\left[\frac{10^{-7}\mathrm{Hz}}{f}\right]^2\right]^{1/8}$$

$$= 1.5\times10^{-25}\left[\frac{1000\mathrm{Hz}}{f}\right]^{1/4} \quad \text{for stochastic waves.} \qquad (11.29c)$$

Here for stochastic waves S_{QL} is the quantum-limit spectral density [Eq. (11.24)], and the chosen bandwidth $\Delta f = f_o(S_{QL}/S_o)^{1/2}$ is that which makes shot noise [Eq. (11.22c) integrated over Δf, with $f_o<\Delta f<f_R$] equal to 1/3 the quantum noise and minimizes their sum. At frequencies $f \lesssim 10$Hz, seismic noise is presumed to strongly debilitate the receiver performances (cf. Saulson 1984).

Figs. 2.7–2.9 show, together with the above receiver sensitivities, the characteristic strengths of the gravity waves from a variety of sources that were discussed in Part III above, and the present and projected sensitivities of other kinds of detectors. As these figures suggest, the prospects for successful detection of gravity waves with the planned LIGOs are high: At the sensitivities of the "advanced detectors" one could see the coalescence of neutron-star binaries at 1/4 the Hubble distance where the event rate is estimated to be several per day, the coalescence of 10 $M_\odot$ black-hole binaries throughout the universe, supernovae in our galaxy if they put out $10^{-9}M_\odot$ of energy near 1000 Hz frequency and in the Virgo cluster if they put out $10^{-3}M_\odot$, millisecond pulsars whose frequencies are known in advance from electromagnetic measurements if they have ellipticities $10^{-8.5}$ or larger, CFS-unstable neutron stars with X-ray luminosities as small as 1/1000 that of Sco X-1, and a stochastic background at $f \sim 30$ Hz with Ω_{GW} as small as 10^{-10}. It seems likely to me that such sensitivities are more than adequate for success; waves are likely to be detected at more modest sensitivities than these — somewhere between those of the "first-generation" detectors and those of the "advanced detectors" (Figs. 2.7–2.9).

11.G Ideas for Other Types of Beam Detectors

The Michelson and Fabry-Perot configurations, on which almost all experimental work to date has focussed, are not the only possible types of beam receivers. A number of others have been conceived of, but have not been pursued vigorously. Since the LIGOs are intended to

house several different receivers simultaneously and to have lifetimes of $\gtrsim$20 years, during which a number of generations of receivers will be built and operated, some of these other configurations might one day operate in a LIGO. These other configurations include: (i) A *frequency-tagged interferometer* or *Michelson with overlapping beams* (Drever and Weiss 1983), in which the light beam in each arm is made to shift in frequency with each round-trip pass, so that the beams of successive passes can overlap each other but not interfere with each other; such an interferometer is basically a Michelson but with small, Fabry-Perot-size mirrors. (ii) *Active interferometers* (Bagaev et. al. 1981, Brillet and Tourrenc 1983), in which an active medium (atoms or molecules with transitions near the frequency of the laser light) resides in the arms (or arm – there might be only one) of the interferometer. (iii) *Spectroscopic detectors* (Nesterikhin, Rautian, and Smirnov 1978, Brillet and Tourrenc 1983, Borde et. al. 1983), in which laser spectroscopy is used to monitor the frequency shifts produced by the gravitational waves.

Although in principle these alternative types of beam detectors can achieve sensitivities comparable to those of the standard (Michelson and Fabry-Perot) types, practical issues make the active and spectroscopic detectors look substantially less promising (Brillet and Tourrenc 1983); and the frequency-tagged detector has not yet been pursued in sufficient depth to venture a tentative verdict.

This chapter has not yet been updated for 1987&1988&198 4/15/88

12 Other Types of Detectors

In Chaps. 10 and 11 we studied the two types of gravitational-wave detectors that have been most developed to the greatest degree of sophistication: bar detectors and beam detectors. This final chapter treats, in some detail, all other types of detectors that have been developed and used, or have been proposed. Section 12.A deals with earth-based detectors, designed for the high-frequency band $f \gtrsim 10\,\mathrm{Hz}$, including a variety of detectors in which electromagnetic fields play key roles, and detectors in which superfluidity or superconductivity are central. Section 12.B treats solar-system-based detectors and the low-frequency band $10\,\mathrm{Hz} \gtrsim f \gtrsim 10^{-5}\,\mathrm{Hz}$. The detectors here are doppler tracking of spacecraft, beam detectors in space, the normal modes of vibration of the earth and the sun, vibrations of blocks of the earth's crust, and an earth-orbiting skyhook. Section 12.C treats astronomical detectors and the very-low-frequency band $f \lesssim 10^{-5}\,\mathrm{Hz}$. The detectors here are the timing of pulsars; the timing of orbital motions of the moon, the planets, and binary stars; anisotropies of the primordial microwave radiation; the velocities of galaxies and clusters of galaxies, and peculiarities in primordial nucleosynthesis.

12.A Earth-Based Detectors (frequencies above 10 Hz)

In addition to bar detectors and beam detectors, a number of other types of gravity-wave detectors that could operate in an earth-bound laboratory have been conceived of. Although none of these has looked sufficiently promising to justify substantial experimental effort, some are question marks (because they have not been pursued far enough for a clear verdict) rather than discards. Because I have not looked at most of them in enough detail, I shall not venture to sort out the question marks from the total rejects. [KIP: DO SO!]

a) Electromagnetically Coupled Detectors

One type of transducer used on bar detectors (e.g. by the Moscow and Perth groups) is a reentrant microwave-cavity resonator whose capacitance is modulated by the bar's vibrations (Sec. 10 of Braginsky, Mitrofanov, and Panov 1985; Blair 1983). There is an obvious similarity of this to a Fabry-Perot beam receiver in which each arm is an optical cavity with length modulated by the motions of the swinging masses. In fact, one can imagine a continuous sequence of detector configurations that leads from one to the other, by splitting the bar into pieces and gradually moving them apart, with the microwave cavity gradually being distorted and expanded until it becomes the optical cavity of the Fabry-Perot (Caves 1978).

This argument leads to the recognition that bar detectors and beam detectors are but two examples of a large class of possible "electromagnetically coupled detectors", in which gravitational waves drive the motions of masses, and electromagnetic fields measure those motions; or, when the detector gets larger than a reduced wavelength, gravity waves drive vibrations of both the electromagnetic fields and the masses, which are coupled together. [KIP: EXPLAIN WHY OR REFER TO EARLIER FOR EXPLANATION]

Other earth-laboratory-scale electromagnetically coupled configurations, besides resonant bars and optical beams, that have been considered theoretically and show some promise but have not been pursued in a serious experimental way, include: (i) Large microwave cavities in which wall motion, driven by gravitational waves with $\lambda \gg L$, upconverts microwave quanta from one mode to another mode of slightly higher frequency (Pegoraro, Picasso, and Radicati 1978, Caves 1979).); (ii) Optical or microwave cavities with $L \lesssim \lambda$, intended for detection of high-frequency waves $f \gg 10^4$ Hz, in which the gravitational waves interact directly with the resonating electromagnetic field

to move quanta from one mode into another, or interact directly with a DC electric or magnetic field to create quanta at the gravity-wave frequency (Braginsky et. al. 1973); (iii) As a specific, much studied example of such a cavity: An optical or microwave ring resonator in which circularly polarized gravitational waves propagating orthogonal to the resonator plane resonate with the circulating electromagnetic field, producing a linearly growing phase shift in the field. This scheme, proposed by Braginsky and Menskii (1971), was incorrectly analyzed by them and by me (Box 37.6 of MTW) – a source of some embarrassment. My error was in thinking I could cover the detector with a single proper reference frame, when its diameter L is larger than the reduced wavelength λ of the gravitational waves it sees. My incorrect conclusion, and that of Braginsky and Menskii (1971) was a quadratically growing phase shift, $\Delta\Phi \propto h(ct/\lambda)(ct/\lambda_e)$. The correct conclusion (Linet and Tourrenc 1976) is a linearly growing phase shift, $\Delta\Phi \propto h(ct/\lambda_e)$, which makes this scheme no better in principle than a standard beam detector. WARNING: The literature is full of similarly incorrect analyses of the various detectors described in this section. (iv) An optical cavity filled with an isotropic medium, or an optical fiber, in which gravity-wave-produced strains induce optical effects such as birefringence (Iacopini et. al., 1979; Vinet, 1985). (vi) Detectors using the Mossbauer effect (Kauffman 1970).

For a general review of electromagnetically coupled detectors see Grishchuk (1983), and for general analyses of them see Tourrenc and Grossiord (1974), Tourrenc (1978), and Tessier du Cros (1985).

Analyses of such detectors sometimes produce wildly overoptimistic conclusions because they overlook the mundane issue of thermal noise in the mechanical parts of the detector (e.g. the walls of an electromagnetic cavity). For an example of an analysis that *does* take thermal noise into account properly see Caves (1979).

b) Superfluid Interferometers and Superconducting Circuits

Anandan (1981), Chiao (1982), and Anandan and Chiao (1982) have suggested that *if* it is possible to construct a superfluid weak link, analogous to the superconducting weak link (Josephson junction) on which SQUIDS are based, then such a link could form the basis for a superfluid ring interferometer that would be sensitive to gravitational waves. Unfortunately, such weak links do not yet exist. Schrader (1984) and independently Anandan (1985, 1986) have suggested a gravity-wave detector based on the direct interaction between the

gravitational wave and the magnetic field in superconducting solenoids, with the resulting current change monitored by a SQUID.

12.B Solar-System-Based Detectors (10 Hz to 10^{-5} Hz)

A number of solar-system-based detectors have been conceived of for operation in the low-frequency band $10\,\text{Hz} \gtrsim f \gtrsim 10^{-5}\,\text{Hz}$; and several have been constructed and have produced interesting limits on cosmic gravitational waves. In this section I shall describe these briefly.

a) Doppler Tracking of Spacecraft

At periods between a few minutes and few hours the best present gravity wave detector is the doppler tracking of spacecraft. Doppler tracking was described in elementary terms in Sec. 2.E, and its present and future sensitivities were compared with estimated source strengths in Secs. 2.F–2.H. Here I shall give a more sophisticated description of this detection technique.

In doppler tracking a highly stable clock on earth ("master oscillator") is used to control the frequency of a monochromatic radio wave, which is transmitted from earth to the spacecraft. This "uplink" radio wave is received by the spacecraft and "transponded" back to the earth; i.e. the uplink wave is used by the spacecraft to control, in a phase-coherent way, the frequency of the "downlink" radio wave that it transmits back to earth. When the downlink radio wave is received at earth, its frequency is compared with that of the master oscillator; and from that comparison a doppler shift is read out.

When gravitational radiation sweeps through the solar system — most interestingly with a reduced wavelength of order the earth-spacecraft distance so it must be analyzed by TT methods (Sec. 4.F) rather than using a proper reference frame — , it perturbs the earth, the spacecraft, and the propagating radio wave. [KIP: HERE INSERT A DERIVATION OF THE ESTABROOK-WAHLQUIST RESPONSE FORMULA BASED ON TT TECHNIQUES OF SEC. 4.F]. The net result is to produce fluctuations in the measured doppler shift with magnitude $\delta\nu/\nu \sim h_{jk}^{GW}$. Each feature in the gravitational waveform $h_{jk}^{GW}(t)$ shows up three times in the doppler shift, in a manner that can be regarded as due to interaction of the radio wave with the gravity wave at the events of emission from earth, transponding by spacecraft, and reception at earth (Estabrook and Wahlquist 1975). This triplet structure can be used to help distinguish the effects of the gravitational wave from noise in the

doppler data.

The use of doppler data for gravity-wave searches was first proposed by Braginsky and Gertsenshtein (1967), and was first pursued with pre-existing data by Anderson (1971). The response of doppler tracking to a gravity wave was worked out by Davies (1974) for special cases and by Estabrook and Wahlquist (1975) for the general case. Experimental feasibility and noise thresholds were first discussed by Wahlquist *et. al.* (1977). Experimental results have been obtained with the Viking spacecraft (Armstrong *et. al.*, 1979), the Voyager Spacecraft (Hellings *et. al.*, 1981), Pioneer 10 (Anderson *et. al.*, 1984), and Pioneer 11 (Armstrong *et. al.*; 1987). A future experiment will entail coordinated observations with the Galileo and Ulysses spacecraft (Estabrook 1987).

In all past experiments the most serious noise source was fluctuations in the interplanetary plasma (solar wind), which cause fluctuations in the dispersion of the radio waves and thence fluctuations in the doppler shift. These fluctuations have limited the sensitivity under optimal circumstances to $\sqrt{fS_h(f)} \sim 3\times10^{-14}$ in the band $10^{-4}\text{Hz} \lesssim f \lesssim 10^{-2}\text{Hz}$. Fortunately, dispersion in an ionized plasma becomes less serious when one moves to higher radio-wave frequencies – a move that is also desired to produce higher bit rates for information transfer between the spacecraft and earth. Some future spacecraft, including the Galileo mission, will use X-band radio signals (10 GHz frequency) on both the uplink and the downlink, rather than S-band (2 GHz) up and X-band down as in the past; and correspondingly their gravity-wave sensitivities should improve to $\sqrt{fS_h(f)} \sim 3\times10^{-15}$. In fact, on such spacecraft the ionized-plasma dispersion will be sufficiently low that fluctuations in dispersion due to water vapor in the earth's atmosphere may become the most serious noise source (Armstrong and Sramek 1982). Plans for monitoring the water vapor as a means of reducing this noise are being developed (Resch *et. al.*, 1984). In the more distant future, doppler tracking may be improved by using dual-frequency X-band/K-band (30 GHz) tracking to reduce and monitor the ionized plasma dispersion, by installing a highly stable clock on board the spacecraft (Smarr et. al. 1983) and/or by moving the earth-based antenna into earth orbit. These improvements might ultimately produce $\sqrt{fS_h(f)}$ as low as 10^{-17} (Estabrook 1987).

Figures 2.7–2.9 show the sensitivities $h_{3/\text{yr}}$ corresponding to these noise levels [Eqs. (34), (52a) and (67) with $\Delta f = f$].

At frequencies $f \sim 3$ Hz, far above the regime $10^{-2} - 10^{-4}$ Hz of normal doppler tracking, but below the regime of earth-based detectors, one might hope to use doppler tracking of spacecraft in earth orbit (distances $\sim c/4f \sim 25{,}000$ km). The best such spacecraft are those of the Global Positioning System (GPS). Unfortunately, even with the best projected improvements of the GPS we cannot anticipate $\sqrt{f S_h(f)}$ better than $\sim 10^{-14}$ corresponding to a burst sensitivity $h_{3/\mathrm{yr}} \sim 10^{-13}$; see Fig. 2.7 and see Hansen, Chiu, and Chao (1986) for a detailed study.

b) Beam Detectors in Space

[KIP: UPDATE THIS SECTION ON BASIS OF MATERIAL FROM BENDER] Several conceptual designs for optical beam detectors in space were suggested by Weiss et. al. (1976) and are discussed in Weiss (1979). More recently Faller and Bender (1981), Bender et. al. (1984), and Faller et. al. (1985) have been carrying out a detailed design and feasibility study for such detectors; and it is possible they will fly sometime around the turn of the century. As now conceived (Faller et. al., 1985), such a detector might consist of three "drag-free" satellites, one at the corner and two at the ends of an L. The satellites might be in the same solar orbit as the earth-moon system, but far from the earth and moon; and their arm length might be $L \sim 1$ million kilometers. Each satellite might carry its own 100-milliwatt laser, with the end lasers phase locked to the light that arrives from the corner laser. With 50 centimeter diameter telescopes on each satellite to focus the laser beams, this could result in a one-pass ($B = 1$) Michelson interferometer system with shot-noise-limited sensitivity $\sqrt{S_h(f)} = 10^{-20}\mathrm{Hz}^{-1/2}$ over the range 10^{-1} Hz $\gtrsim f \gtrsim 10^{-4}$ Hz. Above 10^{-1} Hz the sensitivity would be degraded because of too-long an arm length ($L > \lambda$). Below 10^{-4} Hz stochastic nongravitational forces might degrade the sensitivity. This projected sensitivity translates into the amplitude levels $h_{3/\mathrm{yr}}$ [Eqs. (34), (52a), and (67) with $\Delta f = f$] shown in Figs. 2.7–2.9. [KIP: DERIVE FORMULA FOR DOPPLER TRACKING?]

c) Earth's Normal Modes

Forward et. al. (1961) and Weber (1967) pioneered the use of the earth's quadrupolar normal modes as "resonant-bar" gravity-wave detectors. More recently Boughn and Kuhn (1984) have given a careful formulation of the method for inferring, from earth-normal-mode observations, limits on any stochastic gravitational waves that might be exciting the earth. Using their method on data from the IDA seismic

network, Boughn and Kuhn (1987) have derived a slightly stronger limit on stochastic background than the early Weber (1967) limit: they find $\Omega_{GW}(f) \lesssim 1$ at $f = 0.31$ mHz (Fig. 2.9). They expect, further, that a larger amount of data may permit this limit to be lowered to $\Omega_{GW} \lesssim 0.1$.

d) Sun's Normal Modes

Walgate (1983) stimulated people to think about the sun's quadrupolar normal modes as gravity-wave detectors, when he speculated (falsely; see, e.g., Kuhn and Boughn 1984, and Anderson et. al. 1984) that an observed mode was being excited by monochromatic gravitational waves from the binary star Geminga.

Boughn and Kuhn (1984) have carried out a detailed analysis of the gravity-wave implications of observed solar pulsations. From the data of Isaac (1981) on low-order p- and g-modes they find $\Omega_{GW}(f) \lesssim 100$ at $f \simeq 3\times10^{-4}$ Hz; and they argue that better observational data may produce orders of magnitude improvement, bringing $\Omega_{GW}(f)$ well below unity.

e) Vibrations of Blocks of the Earth's Crust

Braginsky et. al. (1985) have recently pointed out that blocks of the earth's crust with sizes 50 km $\lesssim L \lesssim$ 70 km could function as resonant-bar detectors for waves of frequency $f \simeq 0.03$ Hz. They propose monitoring such a block with an array of seismic stations and cross-correlating the data to pull out the seismic motions associated with the block's quadrupolar modes. Their calculations suggest a possible sensitivity $\sqrt{f S_h(f)} \sim 2\times10^{-17}$ corresponding to $h_{3/yr} \sim 2\times10^{-16}$ for bursts.

f) Skyhook

Braginsky and Thorne (1985) have suggested an earth-orbiting "skyhook" gravity-wave detector that would operate in the 0.1 to 0.01 Hz region with sensitivity $\sqrt{f S_h(f)} \sim 3\times10^{-17}$, which is much better than present or near-future doppler tracking and roughly comparable to that hoped for from blocks of the earth's crust (see Figs. 2.7–2.9). The skyhook would consist of two masses, one on each end of a long thin cable with a spring at its center. As it orbits the earth, the cable would be stretched radially by the earth's tidal gravitational field. Gravitational waves would pull the masses apart and push them together in an oscillatory fashion; their motion would be transmitted to the spring by the cable; and a sensor would monitor the spring's resulting motion.

If it ever flies, the skyhook's role will be to provide, with a simple and inexpensive device, a moderate-sensitivity coverage of the 0.1 – 0.01 Hz region during the epoch before far more sensitive beam detectors are built and installed in space.

12.C Astronomical Detectors (frequencies below 10^{-5} Hz)

At frequencies below about 10^{-5} Hz the only sources of gravitational waves are probably stochastic background from the early universe (Secs. 9.D–9.F); and the best detectors involve use of distant astronomical bodies:

a)Pulsar Timing

Remarkably good limits on very-low-frequency gravitational waves have come from the timing of pulsars (Taylor 1987). Recall from Sec. 2.E the basic idea for pulsar timing as a gravity-wave detector (an idea due to Sazhin, 1978, and Detweiler, 1979): The rotation of the pulsar's underlying neutron star is a highly stable clock, and pulsar timing compares that clock's ticking rate with the ticking of the very best atomic clocks in earth-bound laboratories. When gravity waves sweep over the pulsar, they affect the ticking rate of the pulsar's clock relative to clocks elsewhere in the universe, including earth; and those effects show up as fluctuations in the pulsar timing data. Similarly, when gravity waves sweep over the earth, they affect the ticking rates of all our clocks relative to those elsewhere in the universe; and those effects show up in pulsar timing. [KIP: DERIVE FORMULAE FOR THE SIGNAL FROM THE ANALYSIS GIVEN FOR DOPPLER TRACKING] To the extent, then, that the pulsar timing data are free of fluctuations, one can infer that gravity waves of a given strength are not sweeping over either the pulsar or the earth. (See Blandford, Narayan, and Romani, 1984 for a discussion of how to extract the gravity-wave information from the timing data and the pitfalls one encounters in doing so.) If fluctuations are seen in the timing data and are actually due to gravity waves sweeping over the pulsar, we probably will never be able to confirm that the source is gravity waves rather than fluctuations in the neutron star's rotation. However, if fluctuations are seen and are due to gravity waves sweeping over the earth, we might be able to learn their cause and study the waves' direction of propagation, polarization, and wave form by timing simultaneously several pulsars on different parts of the sky.

In response to the Sazhin–Detweiler idea, Hellings and Downs (1983) and Romani and Taylor (1983) used timing data on four especially quiet pulsars [which Downs and Reichley (1983) had tracked for over a decade with the Goldstone antenna of NASA's deep space tracking network] to place a limit $\Omega_{GW}(f) \lesssim 1\times10^{-3}(f/10^{-8}\text{Hz})^4$ (90% confidence) on any stochastic background in the frequency range $4\times10^{-9} \lesssim f \lesssim 10^{-7}$Hz; Bertotti, Carr, and Rees (1983) used data from Helfand et. al. (1980) to obtain a similar limit.

Intrinsic noise in all the pulsars used in these analyses would have made it difficult to improve on these limits at fixed frequency [though, by further observations the region covered could have been extended to lower frequencies; the lowest being of order 1/(total time since the measurements began)]. Fortunately, while these analyses were in process, they were put out of business by the discovery (Backer et. al. 1982) of a pulsar far quieter than any previously known: the millisecond pulsar PSR 1937+21. From three years of 1937+21 timing data taken with the Arecibo radio telescope, Davis et. al. (1985) and Taylor (1987) have now placed the limit

$$\Omega_{GW}(f) \leq 1\times10^{-6}\left(\frac{f}{10^{-8}\text{Hz}}\right)^4 \quad \text{for } f \gtrsim f_{\min} = 10^{-8}\text{Hz} \qquad (12.1)$$

on any isotropic stochastic background; see Fig. 2.9.

This level of sensitivity is so good that further progress at fixed frequency is limited by the long–term frequency stability of the world's best atomic clocks. Thus, unless clocks improve, we can expect the coefficient in (12.1) to improve at best as t^{-1}, while the lower frequency limit $f_{\min}$ decreases as t^{-1} producing $\Omega_{GW}(f_{\min}) \propto t^{-5}$ (with $t=0$ in 1982). Fortunately, the prospects for clock improvement are good. Ultimately, when clocks have improved by one or two orders of magnitude, noise due to interstellar scintillation may become a problem (Armstrong 1984).

Recently two other quiet, fast pulsars PSR1855+09 and PSR 1953+29 have been discovered (Segelstein et. al. 1986). Together with PSR1937+21 and others that we can hope for, they may one day form a network for gravitational–wave searches and observations. Such a network would alleviate problems with interstellar scintillations and atomic clock fluctuations.

b) The Timing of Orbital Motions

A gravitational wave with period long compared to observation times will produce a gradual secular change in the relative ticking rates of clocks in and out of the wave: $\dot{\omega}/\omega \sim (f/2\pi)h$, where f is the gravity-wave frequency, h is its amplitude, and ω is the ticking rate of the clock in the wave as monitored by any clock that is outside of the wave. For stochastic waves this gives $\dot{\omega}/\omega \sim [\Omega_{GW}(f)]^{1/2}(10^{10}\text{years})^{-1}$. Because the physical torques on pulsars are so large $[\dot{\omega}/\omega \gg (10^{10}\text{yr})^{-1}]$, pulsars cannot be useful in searches for waves with periods longer than the observation time. However (Mashhoon, Carr, and Hu 1981; Bertotti, Carr and Rees 1983), the orbit of the binary pulsar is such a good clock, with such a well-understood slow down, that it can be beat against earth-based clocks to give interesting limits on waves with frequencies $10^{-8}\text{Hz} \lesssim f \lesssim 10^{-13}$ Hz. (The low-frequency limit, 10^{-13} Hz, corresponds to waves with λ of order the distance between the earth and the pulsar.) The most recent observational data from Weisberg and Taylor (1984) give the limit

$$\int_{10^{-8}\text{Hz}}^{10^{-13}\text{Hz}} \Omega_{GW}(f) f^{-1} df \leq 0.5 H_{100}^{-2} , \qquad (12.2)$$

where H_{100} is the Hubble constant in units of 100 km/sec Mpc^{-1}.

Orbital motions are also useful as detectors of waves with frequencies f of order the orbital frequency. The orbiting bodies respond to such waves in the same manner as does a resonant-bar detector. (After all, the orbit is, in a sense, nothing but a two-dimensional oscillator.) The idea of using a lunar or planetary or binary-star orbit in this way as a gravity-wave detector has been proposed or discussed by Braginsky and Gertsenshtein (1967), Anderson (1971), Bertotti (1973), Rudenko (1975), and many others. Mashhoon, Carr, and Hu (1981) argue that Viking doppler data on the relative orbits of Mars and Earth place a limit $\Omega_{GW}(f) \lesssim 0.1$ at $f \simeq 3\times10^{-8}$ Hz (period of one year), and that laser ranging data on the moon's orbit – which now give $\Omega_{GW}(f) \lesssim 10$ – have the potential in some years to give $\Omega_{GW}(f) \lesssim 0.1$ at $f \simeq 3\times10^{-7}$ Hz (period of one month).

c)Anisotropies in the Temperature of the Cosmic Microwave Radiation

Large-scale (quadrupolar) anisotropies in the cosmic microwave radiation would be produced by gravitational waves in the vicinity of the earth today (Sachs and Wolfe 1967, Dautcourt 1969). Present observational limits on such anisotropies imply

$\Omega_{GW}(f) \lesssim 10^{-6}(f/3\times10^{-18}\ \text{Hz})^2$ for any f, even $f \lesssim 1/(\text{Hubble time})$ (Grishchuk and Zel'dovich 1978). Small-scale anisotropies (angular scales of order 5 degrees) would have been produced by gravitational waves during the epoch of plasma recombination, when the microwave radiation we now see last interacted with matter. The limit from these is remarkably good: $\Omega_{GW}(f) \lesssim 10^{-13}$ in a narrow frequency window at $f \simeq 10^{-18}$ Hz (Carr 1980, Zel'dovich and Novikov 1983, Starobinsky 1985); but this limit is much less firmly based than others. It presumes we understand thoroughly the propagation of the cosmic microwave radiation during recombination and from the epoch of recombination to the present. Note: this limit does not constrain waves from cosmic strings or any other source that emitted most of its waves later than the epoch of recombination; see Traschen, Turok, and Brandenberger (1986) for the effects of strings on the microwave anisotropy.

d) Other Astronomical Observations

In addition to the timing of pulsars and of orbital motions, and microwave anisotropies, several other astronomical observations can be used as probes of low-frequency gravitational waves: (i) The *observed velocities of galaxies and clusters of galaxies*, i.e. deviations from the Hubble flow (Rees 1971, Burke 1975, Dautcourt 1977). These give $\Omega_{GW}(f) \lesssim (f/3\times10^{-17})^2$ for 10^{-17} Hz $\lesssim f \lesssim 10^{-15}$ Hz (Carr 1980). (ii) *Peculiarities in primordial nucleosynthesis*, produced by the influence of gravitational wave energy on the expansion rate of the universe during nucleosynthesis (the "first three minutes") (Schvartzman 1969). These produce a limit $\Omega_{GW}(f) \lesssim 10^{-4}$ at $f \gtrsim 10^{-10}$ Hz, which is not fully firmly based because it presumes we thoroughly understand conditions in the first few minutes of the universe. Note that this limit is irrelevant for waves emitted since the epoch of nucleosynthesis.

For detailed reviews and references on these and other astronomical detectors of gravity waves see Dautcourt (1974), chapter 17 of Zel'dovich and Novikov (1983), and Sec. 4 of Carr (1980).

12.D Concluding Remarks

As I look back over this book, I am struck by the enormous changes in our theoretical understanding – or at least in theoretical fashion – that have occurred over the past 5, 10, and 15 years; and I am impressed even more by the progress that experimenters have made in the quest to invent, design, and build detectors of ever greater

sensitivity. That the quest ultimately will succeed seems almost assured. The only question is when, and with how much further effort. In 1981 Jerry Ostriker and I made a bet, to wit:

Whereas both Jeremiah P. Ostriker and Kip S. Thorne believe that Einstein's equations are valid

And both are convinced that these equations predict the existence of gravitational waves

And both are confident that Nature will provide what physical law predicts

And both have faith that scientists can ultimately observe whatever Nature does supply

Nevertheless, they differ on the likely strengths of natural sources and on the probability of a near-future and verifiable detection.

Therefore they agree to wager one case of good red wine (JPO to supply French wine, KST to supply California) on the detection of extraterrestrial gravitational waves before the next Millenium (January 1, 2000). KST wins the wager if at least two experimental groups observe phenomena which they agree are gravitational waves. If not, JPO wins.

Signed and officially sealed
this sixth day of May 1981

Jeremiah P. Ostriker
Kip S. Thorne

I expect to win — but I won't guarantee it.

refs.090989

Notation and Conventions

Throughout this book, unless otherwise stated, we assume that general relativity correctly describes classical gravitational waves. Our notation is that of Misner, Thorne, and Wheeler (1973) — cited as MTW throughout — including, e.g., the use of Greek indices for spacetime (running from 0 to 3) and Latin for space (running from 1 to 3), the use of commas for partial derivatives and semicolons for covariant derivatives, the use of the Einstein summation convention, and the use of geometrized units in which Newton's gravitation constant G and the speed of light c are set equal to unity. Sometimes, particularly in the introductory Part I and when discussing gravitational-wave detectors in Part III, we restore the G's and c's to the equations and use cgs units.

Mathematical symbols that appear in more than one location in the book are indexed at the end of the subject index. The pages given are those on which the symbols are defined.

GRAVITATIONAL RADIATION

A New Window onto the Universe

by Kip S. Thorne

draft of 16 September 1989

California Institute of Technology

1989

References

Abbott, L. and Wise, M. (1984). *Nuclear Physics B*, **244**, 541.

Ables, J. H., in *Proceedings of the Fifth Marcel Grossmann Meeting on General Relativity*, eds. D. G. Blair and M. J. Buckingham. World Scientific: 1989.

Abrahams, A. M. (1987). Research described by B. F. Schutz in a report on Symposium 14 in MacCallum (1987); see also Abrahams' unpublished Ph.D. dissertation, University of Illinois, 1988.

Abrahams, A. M. (1989). In Evans, Finn, and Hobill (1989), p. 110.

Abrahams, A. M. and Evans, C. R. (1988). *Physical Review D*, **37**, 318.

Adams, P. J., Hellings, R. W., and Zimmerman, R. L. (1984). *Astrophysical Journal (Letters)*, **280**, L39.

Adams, P. J., Hellings, R. W., and Zimmerman, R. L. (1985). *Astrophysical Journal*, **288**, 14.

Aglietta, M., Badino, G., Bologna, G., Castagnoli, C., Castallina, A., Fulgione, W., Galeotti, P., Saavedra, O., Trinchero, G., Vernetto, S., Amaldi, E., Cosmelli, C., Frasca, S. Pallotino, G. V., Pizzella, G., Rapagnani, P., Ricci, F., Bassan, M., Coccia, E., Modena, I., Bonifazi, P., Castellano, M. G., Dadykin, V. L., Malguin, A. S., Ryassny, V. G., Ryazhskaya, O. G., Yakushev, V. F., Zatsepin, G. T., Gretz, D., Weber, J., and Wilmot, G. (1989). *Il Nuovo Cimento*, **12**, 75.

Aguiar, O., Hamilton, W., Johnson, W., Solomonson, N., and Xu B.-X. (1989). In *Abstracts of Contributed Papers, Twelfth International Conference on General Relativity and Gravitation*. University of Colorado: Boulder, Colorado, p. 546.

Aldcroft, T., Chaing, J., Fairbank, W. M., Henderson, J., Hu En-Ke, Mann, L. D., Michelson, P. F., Price, J. C., Stevenson, T., Vaughan, B., and Zhou, Z. (1989). In *Abstracts of Contributed Papers, Twelfth International Conference on General Relativity and Gravitation*. University of Colorado: Boulder, Colorado, p. 547.

Allen, B. (1988). *Physical Review D*, **37**, 2078.

Allen, W. D. and Christodoulides, C. (1975). *Journal of Physics A*, **8**, 1726.

Alpar, M. A. and Pines, D. (1985). *Nature*, **314**, 334.

Alpar, M. A., Cheng, A. F., Ruderman, M. A., and Shaham, J. (1982). *Nature*, **300**, 728.

Amaldi, E. and Pizzella, G. (1975). *Nota Interna* 645, Istituto di Fisica G. Marconi, University of Rome.

Amaldi, E. and Pizella, G. (1979). In *Relativity, Quanta, and Cosmology in the Development of the Scientific Thought of Einstein*, Volume 1, 9.

Amaldi, E., Coccia, E., Cosmelli, C., Ogawa, Y., Pizzella, G., Rapagnani, P., Ricci, F., Bonifazi, P., Castellano, M. G., Vannaroni, G., Bronzoni, F., Carelli, P., Foglietti, V., Cavallari, G., Habel, R., Modena, I., and Pallottino, G. V. (1984). *Il Nuovo Cimento*, 7C, 338.

Amaldi, E., Bonifazi, P., Carelli, P., Castellano, M., Cavallari, G., Coccia, E., Cosmelli, C., Foglietti, V., Habel, R., Modena, I., Pallotino, G. V., Pizzella, G., Rapagnani, R., and Ricci, F. (1986). *Il Nuovi Cimento*, 9C, 829.

Amaldi, E., Aguiar, O., Bassan, M., Bonifazi, P., Carelli, P., Castellano, M. G., Cavallari, G., Coccia, E., Cosmelli, C., Fairbank, W. M., Frasca, S., Foglietti, V., Habel, R., Hamilton, W. O., Henderson, J., Johnson, W., Mann, A. G., McAshan, M. S., Michelson, P. F., Modena, L., Moskowitz, B. E., Pallottino, G. V., Pizzella, G., Price, J. C., Rapagnani, P., Ricci, F., Solomonson, N., Stevenson, T., Taber, R. C., and Xu, B.-X. (1988). Paper in press. [KIP: FIND OUT WHERE – "First Gravity wave coincidence experiment between three cryogenic resonant-mass detectors: Louisiana–Rome–Stanford".

Amaldi, E., Astone, P., Bassan, M., Bonifazi, P., Carelli, P., Castellano, M. G., Cavallari, G., Coccia, E., Cosmelli, C., Frasca, S., Modena, I., Pallottino, G. V., Pizzella, G., Rapagnani, P., Ricci, F., and Visco, M. (1989). In *Abstracts of Contributed Papers, Twelfth International Conference on General Relativity and Gravitation*. University of Colorado: Boulder, Colorado, p. 549.

Anandan, J. (1981), *Physical Review Letters*, 47, 463.

Anandan, J. (1985). *Physics Letters*, 105A, 280.

Anandan, J. (1986). In Ruffini, ed. (1986).

Anandan, J. and Chiao, R. Y. (1982). *General Relativity and Gravitation*, 14, 515.

Anderson, A. J. (1971). *Nature*, 229, 547.

Anderson, J. D., Armstrong, J. W., Estabrook, F. B., Hellings, R. W., Law, E. K., and Wahlquist, H. D. (1984). *Nature*, 308, 158.

Anderson, J. L. (1980). *Physical Review Letters*, 45, 1745.

Anderson, J. L. (1987). *Physical Review D*, 36, 2301.

Anderson, J. L., and DeCanio, T. C. (1975). *General Relativity and Gravitation*, 6, 197.

Anderson, J. L. and Hobill, D. W. (1986). In *Dynamical Spacetimes and Numerical Relativity*, ed. J. M. Centrella, p. 389. Cambridge University Press: Cambridge.

Anderson, J. L. and Hobill, D. W. (1987). *General Relativity and Gravitation*, 19, 563.

Anderson, J. L., Kates, R. E., Kegeles, L. S., and Madonna, R. G. (1982). *Physical Review D*, 25, 2038.

Aplin, P. S. (1972). *General Relativity and Gravitation*, 3, 111.

Armstrong, J. W. (1984). *Nature*, 307, 527.

Armstrong, J. W., Estabrook, F. B., and Wahlquist, H. D. (1987). *Astrophysical Journal* (in press). *Bulletin of the American Astronomical Society*, 16, 886.

Armstrong, J. W. and Sramek, R. A. (1982). *Radio Science*, 17, 1579.

Armstrong, J. W., Woo, R., and Estabrook, F. B. (1979). *Astrophysical Journal*, 230, 570.

Arnowitt, R., Deser, S., and Misner, C. W. (1962). In *Gravitation: An Introduction*

to Current Research, ed. L. Witten. Wiley: New York, p. 227
Ashtekar, A. (1981). *Journal of Mathematical Physics*, 22, 2885.
Ashtekar, A. (1983). In Deruelle and Piran, eds. (1983), p. 421.
Ashtekar, A. (1984). In *General Relativity and Gravitation*, eds. B. Bertotti *et. al.*, p. 37. Reidel: Dordrecht
Ashtekar, A. and Schmidt, B. (1990). *Asymptotic Structure of Spacetime*. Book in preparation.
Babichenko, S. I., Rudenko, V. N., and Yagola, A. G. (1984). *Soviet Astronomy—AJ*, 28, 531.
Backer, D. C., Kulkarni, S. R., Heilis, C., Davis, M. M., and Gross, W. M. (1982). *Nature*, 300, 615.
Bagaev, S. N., Chebotaev, V. P. Dychkov, A. S., and Goldort, V. G., (1981). *Appl. Phys.*, **25**, 161.
Bahcall, J. N., and Piran, T. (XXXX). RATE OF OPTICALLY SILENT SUPERNOVAE, AND NEUTRINOS SHOW NONE IN LAST 10 YEARS; SEC. 7.B.
Balbinsky, E., Detweiler, S., Lindblom, L., and Schutz, B. F. (1985). *Monthly Notices of the Royal Astronomical Society*, 213, 553.
Bardeen, J. M. and Press, W. H. (1973). *Journal of Mathematical Physics*, **14**, 7.
Bardeen, J. M. and Piran, T. (1983). *Physics Reports*, **96**, 205.
Barrow, J. D. and Silk, J. (1983). *The Left Hand of Creation*. Basic Books: New York.
Baumgart, D. and Friedman, J. L. (1988). *Proceedings of the Royal Society of London*, **A405**, 65.
Begelman, M. C., Blandford, R. D., and Rees, M. J. (1980). *Nature*, 287, 307.
Belinsky, V. A., and Francaviglia, M. (1984). *General Relativity and Gravitation*, **16**, 1189.
Belinsky, V. A., and Zakharov, E. E. (XXXX). *Soviet Physics—JETP*, **49**, 985.
Belousova, I. M., Vitushkin, L. F., Ivanov, I. P., Ivanovskaya, M. I., and Kolosnitsyn, N. I. (1983). In *General Relativity and Gravitation. Vol. 2. Relativistic Astrophysics, Experimental Gravitation, and Quantum Gravity*, ed. B. Bertotti, F. De Felice, and A. Pascolini. Consiglio Nazionale delle Ricerche, Rome, p. 1213.
Beltrami, H. and Chau, W. Y. (1986). *Astrophysics and Space Science*, **119**, 353.
Bender, P. L., Faller, J. E., Hall, J. L., Hils, D., and Vincent, M. A. (1984). Abstract for *Fifth International Laser Ranging Instrumentation Workshop*; Herstmonceaux, September 10–14, 1984.
Bender, P. L., Faller, J. E., Hils, D., Stebbins, R. T., and Vincent, M. A. (1989). *Physical Review D*, in preparation.
Bendat, J. S. (1958). *Principles and Applications of Random Noise Theory*, Wiley: New York.
Benz, W., Bowers, R. L., Cameron, A. G. W., and Press, W. H. (1989). *Astrophysical Journal*, XXXXX.
Bergmann, P. G. (1971). *Physical Review Letters*, **26**, 1398.
Bernstein, D., Hobill, D., and Smarr, L. (1989). Private communication.
Bertotti, B. (1973). *Astrophysical Letters*, **14**, 51.
Bertotti, B., Carr, B. J., and Rees, M. J. (1983). *Monthly Notices of the Royal Astronomical Society*, **203**, 945.
Bertotti, B. and Catenacci, R. (1975). *General Relativity and Gravitation*, **6**, 329.
Bertotti, B. and Iess, L. (1985). *General Relativity and Gravitation*, 17, 1043.
Bethe, H. (1986). In *Highlights in Modern Astrophysics*, ed. S. L. Shapiro and S.

A. Teukolsky. Wiley: New York, p. 45.
Bičak, J. and Schmidt, B. G. (1984). *Journal of Mathematical Physics*, 25, 600.
Bičak, J., Reilly, P., and Winicour, J. (1988). *General Relativity and Gravitation*, 20, 171.
Bičak, J. (1968). *Proceedings of the Royal Society of London A*, 302, 201.
Bičak, J. (1985). In *Galaxies, Axisymmetric Systems, and Relativity* , ed. M. H. McCallum. Cambridge University Press: Cambridge.
Bičak, J. (1988). In *Proceedings of the Second Hungarian Workshop on General Relativity*, ed. Z. Perjés. World Scientific: Singapore.
Bičak, J., Hoenselaers, C., and Schmidt, B. G. (1983), *Proceedings of the Royal Society of London A*, 390, 411.
Billing, H. and Winkler, W. (1976). *Il Nuovo Cimento*, 33, 665.
Billing, H., Kafka, P., Maischberger, K., Meyer, F., and Winkler, W. (1975). *Lettere al Nuovo Cimento*, 12, 111.
Billing, H., Maischberger, K., Ruediger, A., Schilling, R., Schnupp, L., and Winkler, W. (1978). Internal report MPI-PAE/Astro 175. Max-Planck Institut fur Quantenoptic: Munich.
Blackburn, J. K. and Detweiler, S. (1989). [KIP: FIND OUT WHERE BEING PUBLISHED -- "CLOSE BLACK HOLE BINARY SYSTEMS"]
Blair, D. G. (1980). In *Gravitational Radiation, Collapsed Objects, and Exact Solutions*, Lecture Notes in Physics vol. 124, ed. C. Edwards. Springer, Berlin, p. 299.
Blair, D. G. (1982). *Physics Letters A*, 91, 197.
Blair, D. G. (1983). In Deruelle and Piran (1983), p. 339.
Blair, D. G., Frasca, S., and Pizzella, G. (1988a). In *Proceedings of Conference on Gravitational Radiation Data Analysis* [KIP: GET REF FROM SCHUTZ]
Blair, D. G., Frasca, S., and Pizzella, G. (1988b). *Il Nuovo Cimento*, in press.
Blanchet, L. (1987a). *Proceedings of the Royal Society of London A*, 409, 383.
Blanchet, L. (1987b). Paper [KIP: on radiative tails] in preparation.
Blanchet, L. and Damour, T. (1984). *Physics Letters*, 104A, 82.
Blanchet, L. and Damour, T. (1986). *Philosophical Transactions of the Royal Society*, 320, 379.
Blanchet, L. and Damour, T. (1988a). *Physical Review D*, 37, 1410. [KIP: IN EARLY CHAPTERS WAS CITED AS 88] [CHANGE BACK TO 88]
Blanchet, L. and Damour, T. (1988b). *Annales de l/Institut Henri Poincaré — Physique Theorique*, in press. [CHANGE TO 1989] [KIP: PN WAVE GENERATION]
Blanchet, L., Damour, T., and Schäfer, G. (1989). *Monthly Notices of the Royal Astronomical Society*, in press.
Blanchet, L. and Schäfer, G. (1989). Paper in preparation.
Blandford, R. D. (1979). In Smarr, ed. (1979), p. 191.
Blandford, R. D. (1984). Private communication.
Blandford, R. D. (1987). In 300 *Years of Gravitation*, ed. S. W. Hawking and W. Israel. Cambridge University Press: Cambridge, p. 277.
Blandford, R. D., Narayan, R., and Romani, R. W. (1984). *Journal of Astrophysics and Astronomy*, 5, 369.
Blandford, R. D. and Thorne, K. S. (1979). In *General Relativity, An Einstein Centenary Survey*, ed. S. W. Hawking and W. Israel, Cambridge University Press: Cambridge.
Blinnikov, S. I., Novikov, I. D., Perevodchikova, T. V., and Polnarev, A. G. (1984). *Soviet Astronomy — Letters*, 10, 177.

Bocko, M. F. and Johnson, W. W. (1984). *Physical Review A*, 30, 2135.
Bonazzola, S., Chevreton, M., Felenbok, P., Herpe, G., and Thierry-Mieg, J. (1974). In *Colloques Internationaux CNRS No. 220, Ondes et radiations gravitationelles*, ed. Y. Choquet-Bruhat. Editions du CNRS, Paris.
Bond, J. R. and Carr, B. J. (1984). *Monthly Notices of the Royal Astronomical Society*, 207, 585.
Bondi, H. (1957). *Nature*, 179, 1072.
Bondi, H. (1960). *Nature*, 186, 535.
Bondi, H. and Pirani, F. A. E. (1988). *Nature*, KIP: GET REF.
Bondi, H., Pirani, F .A. E., and Robinson, I. (1959). *Proceedings of the Royal Society of London A*, 251, 519.
Bondi, H., van der Burg, M. G. J., and Metzner, A. W. K. (1962). *Proceedings of the Royal Society of London A*, 269, 21.
Bonnor, W. B. (1959). *Philosophical Transactions of the Royal Society of London A*, 251, 233.
Bonnor, W. B. (1983). *General Relativity and Gravitation*, 15, 535.
Bontz, R. J. and Haugan, M. P. (1981). *Astrophysics and Space Science*, 78, 204.
Bontz, R. J., and Price, R. H. (1979). *Astrophysical Journal*, 228, 560.
Bordé, C. J., Sharma, J., Tourrenc, P., and Damour, T. (1983). *Journal de Physique-LETTRES*, 44, L983.
Boughn, S. P. and Kuhn, J. R. (1984). *Astrophysical Journal*, 286, 387.
Boughn, S.P. and Kuhn, J.R. (1987). Paper in preparation.
Boughn, S. P., Fairbank, W. M., Giffard, R. P., Hollenhorst, J. N., Mapoles, E. R., McAshan, M. S., Michelson, P. F., Paik, H. J., and Taber, R. C. (1982). *Astrophysical Journal*, 261, L19.
Boulanger, J. L., Le Denmat, G., and Tourrenc, P. (1988a). *Physics Letters A*, 126, 213.
Boulanger, L. L., Duruisseau, J. P., Le Denmat, G., and Tourrenc, P. (1988b). [KIP: FIND OUT WHERE PUBLISHING, "Towards the Birth of gravitational astronomy: I. number of events expected from grav'l wave detection by interferometry"]
Boulanger, L. L., Duruisseau, J. P., Le Denmat, G., and Tourrenc, P. (1988b). [KIP: FIND OUT WHERE PUBLISHING, "Towards the Birth of gravitational astronomy: I. Directivity and number of events in coincidences expected from grav'l wave detection by interferometry"]
Braginsky, V. B. (1965). *Uspekhi Fizicheskikh Nauk*, 86, 433.
Braginsky, V. B. (1967). *Soviet Physics—JETP*, 53, 1434. [KIP CHECK: THIS IS PROBABLY THE RUSSIAN REFERENCE]
Braginsky, V. B. (1970). *Physical Experiments with Test Bodies*. Nauka, Moscow. English translation published as NASA—TT F762. National Technical Information Service, Springfield, VA.
Braginsky, V. B. (1974). In *Gravitational Radiation and Gravitational Collapse*, IAU Symposium 64, ed. C. DeWitt-Morrette. Reidel, Dordrecht, p. 28.
Braginsky, V. B. (1977). In de Sabbata and Weber, ed. (1977), p. XXXX.
Braginsky, V. B. (1983). In Deruelle and Piran (1983), p. 387.
Braginsky, V. B. and Gertsenshtein, M. E. (1967). *Soviet Physics - JETP Letters* 5, 287.
Braginsky, V. B. and Grishchuk, L. P. (1977). *Soviet Physics—JETP*, [XXXX; Russian 121, 629]
Braginsky, V. B. and Grishchuk, L. P. (1985). *Zhurnal Eksperimentalnoi i*

Teoreticheskoi Fiziki, 89, 744. English translation: *Soviet Physics - JETP*, 62, 427.
Braginsky, V. B. and Menskii, M. B. (1971). *Soviet Physics - JETP Letters* 13, 417.
Braginsky, V. B., Mitrofanov, V. P., and Panov, V. I. (1985). *Systems with Small Dissipation*. University of Chicago Press: Chicago.
Braginsky, V. B. and Nazarenko, V. S. (1971). In *Proceedings of the Conference on Experimental Tests of Gravitational Theories, November* 11-13, 1970, *California Institute of Technology*, ed. R. W. Davies. Jet Propulsion Laboratory Technical Memorandum 33-499: Pasadena, California.
Braginsky, V. B. and Thorne, K. S. (1985). *Nature*, 316, 610.
Braginsky, V. B. and Thorne, K. S. (1987). *Nature*, in press.
Braginsky, V. B. and Vorontsov, Yu. I. (1974), *Soviet Physics—Uspekhi*, 17, 644.
Braginsky, V. B., Vorontsov, Yu. I., and Khalili, F. Ya. (1978). *Soviet Physics—*JETP Letters, 27, 276.
Braginsky, V. B. Vorontsov, Yu. I., and Thorne, K. S. (1980). *Science*, 209, 547.
Braginsky, V. B., Manukin, A. B., Popov, E. I., Rudenko, V. N., and Khorev, A. A. (1972). *Soviet Physics—JETP Letters*, 16, 108.
Braginsky, V. B., Grishchuk, L. P. Doroshkevich, A. G., Zel'dovich, Ya. B., Novikov, I. D., and Sazhin, M. V. (1973). *Soviet Physics—JETP*, 38, 865.
Braginsky, V. B., Manukin, A. B., Popov, E. I., Rudenko, V. N., and Khorev, A. A. (1974). *Soviet Physics—JETP*, 39, 387.
Braginsky, V. B., Gusev, A. V., Mitrofanov, V. P., Rudenko, V. N., and Yakimov, V. N. (1985). *Uspekhi Fizicheskikh Nauk*, 147, 422. [KIP: ADD ENGLISH TRANSL]
Bramanti, D. and Maischberger, K. (1972). *Lettere al Nuovo Cimento*, 4, 1007.
Bramanti, D., Maischberger, K., and Parkinson, D. (1973). *Lettere al Nuovo Cimento*, 12, 111.
Brans, C. and Dicke, R. H. (1961). *Physical Review*, 124, 925.
Brill, D. R., and Hartle, J. B. (1964). *Phys. Rev. B* 135, 271.
Brillet, A. (1985). *Annales de Physique*, 10, 219.
Brillet, A. and Tourrenc, P. (1983). In Deruelle and Piran (1983).
Brown, G. E., Bethe, H. A., and Baym, G. (1982). *Physica Scripta*, XXXXXXX.
Buckingham, M. J., and Faulkner, E. A. (1973). *Radio Electronics Engineering*, 42, 163. [KIP: CHECK NAME OF JOURNAL]
Burlankov, D. E. (1963). *Soviet Physics—JETP*, 44, 1941. [KIP: THIS IS RUSSIAN REF; GET ENGLISH]
Burke, W. L. (1969). unpublished PhD thesis, Caltech.
Burke, W. L. (1970). *Physical Review A*, 2, 1501.
Burke, W. S. (1971). *Journal of Mathematical physics*, 12, 402.
Burke, W. L. (1975). *Astrophysical Journal*, 196, 329.
Burke, W. L. (1979). In *Isolated Gravitating Systems in General Relativity*, ed. J. Ehlers. North Holland: Amsterdam, p. 220.
Burke, W. L. and Thorne, K. S. (1970). In *Relativity*, eds. M. Carmeli, S. I. Fickler, and L. Witten. Plenum: New York, p. 209.
Campbell, W. B. and Morgan, T. (1971). *Physica*, 53, 264.
Caporali, A. (1982). *Physical Review D*, 26, 345.
Carr, B. J. (1980). *Astronomy and Astrophysics*, 89, 6.
Carr, B. J. (1986). In *Inner Space/Outer Space*, ed. E. W. Kolb, University of Chicago Press: Chicago.
Carr, B. J. and Verdaguer, E. (1983). *Physical Review D*, 28, 2995.
Carroll, K. R., Chan, H. A., Desrosier, F., Folkner, W. M., Gretz, D. J., Habib, S.,

Hamilton, J. J., Moddy, J. V., Nelson, R. A., Paik, H. J., Pang, Y., Richard, J. P., Weber, J., Wilmot, G. (1986). In Ruffini, ed. (1986), p. 533.
Carter, B. (1983). In Dereulle and Piran (1983), p. 455.
Carter, B. and Quintana, H. (1977). *Physical Review D*, **16**, 2928.
Caves, C. M. (1978). Private communication.
Caves, C. M. (1979). *Physics Letters*, **80B**, 323.
Caves, C. M. (1980a). *Physical Review Letters*, **45**, 75. [KIP: CHANGE FROM 80 TO 80a IN TEXT – IT IS QED VACUUM FLUCTUATIONS AS SOURCE OF SHOT NOISE]
Caves, C. M. (1980b). *Annals of Physics*, **125**, 35.
Caves, C. M. (1981). *Physical Review D*, **23**, 1693.
Caves, C. M. (1982). *Physical Review D*, **26**, 1817.
Caves, C. M. (1983). In *Foundations of Quantum Mechanics*, ed. S. Kamefuchi *et. al.*, p. 195. Physical Society of Japan: Tokyo.
Caves. C. M. (1986). *Physical Review D*, **33**, 1643.
Caves, C. M. (1987a). *Physical Review D*, **35**, 1815.
Caves, C. M. (1987b). In *Quantum Measurement and Chaos*, edited by E. R. Pike. Plenum: New York.
Caves, C. M. (1987c). Paper in preparation.
Caves, C. M., Thorne, K. S., Drever, R. W. P., Sandberg, V. D., and Zimmermann, M. (1980). *Reviews of Modern Physics*, **52**, 341.
Centrella, J. (1980a). *Physical Review D*, **21**, 2776.
Centrella, J. (1980b). *Astrophysical Journal*, **241**, 875.
Cespedes, J. and Verdaguer, E. (1987). *Physical Review D*, **36**, 2259.
Chanmugam, G. and Brecher, K. (1987). *Nature*, 329.
Chandrasekhar, S. (1950). *Radiative Transfer*. Oxford University Press: London.
Chandrasekhar, S. (1965). *Astrophysical Journal*, **142**, 1488.
Chandrasekhar, S. (1970). *Physical Review Letters*, **24**, 611.
Chandrasekhar, S. (1975). *Proceedings of the Royal Society of London A*, **343**, 289.
Chandrasekhar, S. (1983). *The Mathematical Theory of Black Holes*. Oxford University Press: Oxford.
Chandrasekhar, S. (1986). *Proceedings of the Royal Society of London A*, **408**, 209.
Chandrasekhar, S. and Detweiler, S. L. (1975). *Proceedings of the Royal Society of London*, **344**, 441. [KIP: CHANGE TO 75a] Chandrasekhar, S. and Detweiler, S. L. (1975b). *Proceedings of the Royal Society of London*, **345**, 145.
Chandrasekhar, S. and Detweiler, S. L. (1976). *Proceedings of the Royal Society of London, A*. **350**, 165.
Chandrasekhar, S. and Esposito, F. P. (1970). *Astrophysical Journal*, **160**, 153.
Chandrasekhar, S. and Ferrari, V. (1987). *Proceedings of the Royal Society of London, A*, **412**, 75.
Chandrasekhar, S. and Friedman, J. L. (1972). *Astrophysical Journal*, **176**, 745.
Chandrasekhar, S. and Friedman, J. L. (1973). *Astrophysical Journal*, **181**, 481.
Chandrasekhar, S. and Nutku, Y. (1969). *Astrophysical Journal*, **158**, 55.
Chandrasekhar, S. and Xanthopoulos, B. C. (1986). *Proceedings of the Royal Society of London*, **408**, 175.
Chandrasekhar, S. and Xanthopoulos, B. C. (1987). *Proceedings of the Royal Society of London*, **414**, 1.
Chau, W. Y. (1967). *Astrophysical Journal*, **147**, 664.

Chiao, R. Y. (1982). *Physical Review B*, **25**, 1655.
Chinea, F. J. (1988). *Physical Review Letters*, submitted.
(Choquet)–Bruhat, Y. (1964). *Comptes Rendues Academie Sciences Paris*, **258**, 3809.
Choquet–Bruhat, Y. (1969). *Communications in Mathematical Physics*, **12**, 16.
Christodoulou, D. and Schmidt, B. G. (1979). *Communications in Mathematical Physics*, **68**, 275.
Chrzanowski, P. L. (1975). *Physical Review D*, **11**, 2042.
Clark, J. P. A. (1979). Unpublished work described by Eardley (1983).
Clark, J. P. A. van den Heuvel, E. P. J., and Sutantyo, W. (1979). *Astronomy and Astrophysics*, **72**, 120.
Clark, J. P. A. and Eardley, D. M. (1977). *Astrophysical Journal*, **215**, 315.
Codina, J. J., Graells, J., and Martin, C. (1980). *Physical Review D*, **21**, 2731.
Cohen, J.M. and Kegeles, L.S. (1975). *Physics Letters*, **54A**, 5.
Cole, J. D. (1968). *Perturbation Methods in Applied Mathematics*. Blaisdell: Waltham, Mass.
Copeland, E., Hindmarsh, M., and Turok, N. (1987). *Physical Review Letters*, **58**, 1910.
Corkill, R. W. and Stewart, J. M. (1983). *Proceedings of the Royal Society of London A*, **386**, 373.
Courant, R. and Hilbert, D. (1953). *Methods of Mathematical Physics*, Vol. 1, pp. 510ff. Interscience: New York.
Crowley, R. J. and Thorne, K. S. (1977). *Astrophysical Journal*, **215**, 624.
Cruise, A. M. (1983). *Monthly Notices of the Royal Astronomical Society*, **204**, 485.
Cunningham, C. T., Price, R. H., and Moncrief, V. (1978). *Astrophysical Journal*, 224, 643.
Cunningham, C. T., Price, R. H., and Moncrief, V. (1979). *Astrophysical Journal*, **230**, 870.
Curtis, G. E. (1978). *General Relativity and Gravitation*, **9**, 987 and 999.
Cutler, C. and Lindblom, L. (1987). *Astrophysical Journal*, 314, 234.
Cyranski, J. F. and Lubkin, E. (1974). *Annals of Physics*, **87**, 205.
Damour, T. (1983). In Deruelle and Piran (1983). p. 59. [KIP: CHANGE THROUGHOUT TO 1983A]
Damour, T. (1983b). *Physical Review Letters*, **51**, 1019.
Damour, T. (1986a). In *Proceedings of the Fourth Marcel Grossmann Meeting on the Recent Developments of General Relativity*, ed. R. Ruffini. North Holland: Amsterdam. [KIP: CITED ORIGINALLY AS DAMOUR 1986]
Damour, T. (1986b). In *Gravitational Collapse and Relativity*, eds. H. Sato and T. Nakamura, p. 63. World Scientific: Singapore.
Damour, T. (1987a). In *Gravitation in Astrophysics*, B. Carter and J. B. Hartle, eds. Plenum: New York. [KIP: PREVIOUSLY CITED AS DAMOUR 1987]
Damour, T. (1987b). In 300 *Years of Gravitation*, eds. S. W. Hawking and W. Israel. Cambridge University Press: Cambridge, p. 128.
Damour, T. and Deruelle, N. (1981). *Physics Letters*, **87A**, 81.
Damour, T. and Deruelle, N. (1986). *Annales Institut Henri Poincaré (Physique Théorique)*, **44**, 263.
Dautcourt, G. (1969). *Monthly Notices of the Royal Astronomical Society*, **144**, 255.
Dautcourt, G. (1974). In *Confrontation of Cosmological Theories with*

Observational Data, Proceedings of IAU Symposium 63, ed. M. S. Longair. Reidel: Dordrecht, p. 299.
Dautcourt, G. (1977). *Astronomische Nachrichten* 298, 81.
Davies, R. W. (1974). In *Colloque Internationaux CNRS No. 220, "Ondes et Radiations Gravitationelles."* Institut Henri Poincaré: Paris, p. 33.
Davis, W. S. and Richard, J.-P. (1980). *Physical Review D*, 22, 2297.
Davis, M. R., Ruffini, R., and Tiomno, J. (1972). *Physical Review D*, 5, 2932.
Davis, M. R., Ruffini, R., Press, W. H., and Price, R. H. (1971). *Physical Review Letters*, 27, 1466.
Davis, M. M., Taylor, J.H., Weisberg, J.M., and Backer, D.C. (1985). *Nature*, 315, 547.
deDonder, T. (1921). *La gravifique einsteinienne*. Paris.
D'Eath, P. D. (1978). *Physical Review D*, 18, 990.
Dehnian, H., Romero, F., and Schaefer, G. (1984). *Classical and Quantum Gravity*, 1, 305.
De Logi, W. K. and Kovacs, S. J. (1977). *Physical Review D*, 16, 2331.
Deruelle, N. and Piran, T. (1983). *Gravitational Radiation*. North Holland: Amsterdam.
de Sabbata, V. and Weber, J. eds. (1977). *Topics in Theoretical and Experimental Gravitation Physics*. Plenum: London.
Deser, S. (1970). *General Relativity and Gravitation*, 1, 9.
DeSitter, W. (1916). *Monthly Notices of the Royal Astronomical Society*, 76, 699; and 77, 155.
Detweiler, S. L. (1975). *Astrophysical Journal*, 197, 203.
Detweiler, S. L. (1977). *Proceedings of the Royal Society of London A*, 352, 381.
Detweiler, S. L. (1978). *Astrophysical Journal*, 225, 687.
Detweiler, S. L. (1979). *Astrophysical Journal*, 234, 1100.
Detweiler, S. L. (1980). *Astrophysical Journal*, 239, 292.
Detweiler, S. L. (1987). *Physical Review D*, 35, 1095.
Detweiler, S. L. and Ipser, J. R. (1973). *Astrophysical Journal*, 185, 685.
Detweiler, S. L. and Lindblom, L. (1985). *Astrophysical Journal*, 292, 12.
Detweiler, S. L. and Szedenits, E. (1979). *Astrophysical Journal*, 231, 211.
Dewey, D. (1987). *Physical Review D*, 36, 1577.
DeWitt, B. S. (1967a). *Phys. Rev.* 160, 1113.
DeWitt, B. S. (1967b). *Phys. Rev.* 162, 1239.
DeWitt, B. S. (1971). *Lectures on Relativity*—Stanford, Fall 1971. Unpublished manuscript.
DeWitt, B. S. and Brehme, R. W. (1960). *Annals of Physics*, 9, 220.
DeWitt, B. S. and DeWitt, C. M. (1964). *Physics*, 1, 1.
Dhurandhar, S. V., Krolak, A., and Lobo, J. A. (1989a). *Monthly Notices of the Royal Astronomical Society*, submitted. [KIP: CHECK THIS AND FOLLOWING REF]
Dhurandhar, S. V., Krolak, A., and Lobo, J. A. (1989b). *Monthly Notices of the Royal Astronomical Society*, submitted.
Dhurandhar, S. V., and Tinto, M. (1988). *Monthly Notices of the Royal Astronomical Society*, in press.
Dicke, R. H. (1962). *Physical Review*, 125, 2163.
Dicke, R. H., Peebles, P. J. E., Roll, P. G., and Wilkinson, D. T. (1965). *Astrophysical Journal*, 142, 414.
Douglass, D. H., Cromar, M. W., Gram, R. Q., Johnson, W. W., Lam, C., and

Macaluso, D. (1982). In *Proceedings of the Second Marcel Grossmann Meeting on General Relativity*, ed. R. Ruffini. North-Holland, Amsterdam, p. 1149.
Douglass, D. H., Gram, R. Q., Tyson, J. A. and Lee, R. W. (1975). *Physical Review Letters*, **35**, 480.
Douglass, D. H. and Braginsky, V. B. (1979) in *General Relativity, an Einstein Centenary Survey*, ed. S. W. Hawking and W. Israel. Cambridge University Press: Cambridge.
Downs, G. S. and Reichley, P. E. (1983). *Astrophysical Journal Supplement Series*, **53**, 169.
Drever, R. W. P. (1977). *Quarterly Journal of the Royal Astronomical Society*, **18**, 9.
Drever, R. W. P. (1983). In Deruelle and Piran (1983). p. 321.
Drever, R. W. P. and Weiss, R. (1983). unpublished work reported briefly in Appendix B.2(c) of Drever et. al. (1985).
Drever, R. W. P., Hough, J., Bland, R., and Lessnoff, G. W. (1973). *Nature*, **246**, 340.
Drever, R. W. P., Hough, J., Bland, R., and Lessnoff, G. W. (1974). In *Colloques Internationaux du CNRS: Ondes et Radiations Gravitationelles*, ed Y. Choquet-Bruhat. CNRS Report 220, Paris, p. 113.
Drever, R. W. P., Hough, J., Edelstein, W., Pugh, J. R., and Martin, W. (1977). In *Cravitazione Sperimentale*, ed. B. Bertotti. Accademia Nazionale dei Lincei: Rome, p. 365.
Drever, R. W. P., Ford, G. M., Hough, J., Kerr, I., Munley, A. J., Pugh, J. R., Robertson, N. A., and Ward, H. (1980). *Proceedings of the Ninth International Conference on General Relativity and Gravitation*, ed. E. Schmutzer, p. 265. VEB Deutscher Verlag der Wissenschaften: Berlin.
Drever, R. W. P., Weiss, R., Linsay, P. S., Saulson, P. R., Spero, R., and Schutz, F. (1985). A Detailed Engineering Design Study and Development and Testing of Components for a Laser Interferometer Gravitational Wave Observatory. Caltech: Pasadena, California, and MIT: Cambridge, Massachusetts. (unpublished)
Drever, R. W. P., Spero, R., Chen, Y-T., Čadež, A., Abramovici, A., Gürsel, Y., Zucker, M. E., Smith, S., Bostick, A., and Ward, H. (1988). In *Proceedings of the International Symposium on Experimental Gravitational Physics*, Guangzhou China, August 1987, ed. Hu Enke. World Scientific: Singapore, in press.
Droste, J. (1916). *Versl. K. Akad. Wet. Amsterdam*, **25**, 460.
Dymnikova, I.G., Popov, A.K., and Zentsova, A.S. (1982). *Astrophysics and Space Science*, **85**, 231.
Dyson, F.J. (1969), *Astrophysical Journal*, **156**, 529.
Eardley, D. M. (1983). In Deruelle and Piran (1983), p. 257.
Eardley, D. M. (1986). In *Dynamical Spacetimes and Numerical Relativity*, ed. J. M. Centrella. Cambridge University Press: Cambridge.
Eardley, D. M., Lee, D. L., and Lightman, A. P. (1973). *Physical Review D*, **8**, 3308.
Eardley, D. M., Lee, D. L., Lightman, A. P. Wagoner, R. V., and Will, C. M. (1973). *Physical Review Letters*, **30**, 884.
Echeverria, F. (1989). *Physical Review D*, submitted.
Eddington, A. S. (1922). *Proceedings of the Royal Society A*, **102**, 268.
Eddington, A. S. (1924). *The Mathematical Theory of Relativity*, second edition, Cambridge University Press: Cambridge; see especially supplementary notes

7 and 8.
Edelstein, L. A. and Vishveshwara, C. V. (1970). *Physical Review D*, 1, 3514.
Ehlers, J., ed. (1979). *Isolated Gravitating Gravitating Systems in General Relativity*. North Holland: Amsterdam, p. 220.
Ehlers, J. and Kundt, W. (1962). In *Gravitation: An Introduction to Current Research*, ed. L. Witten. Wiley: New York.
Ehlers, J., Prasanna, A. R., and Breuer, R. A. (1986). *Classical and Quantum Gravity*, 4, 253.
Ehlers, J. and Walker, M. (1984). In *General Relativity and Gravitation*, ed. B. Bertotti et. al., p. 125. Reidel: Dordrecht.
Ehlers, J., Rosenblum, A., Goldberg, J. N., and Havas, P. (1976). *Astrophysical Journal Letters*, 208, L77.
Eichler, D., Livio, M., Piran, T., and Schramm, D. N. (1989). KIP: GET REF -- APJ LETT? -- "COALESCING NEUTRON STARS, NAKED NEUTRINO BURSTS, GAMMA RAYS, GRAV RADN, MS PULSARS, AND R-PROCESS NUCLEOSYNTHESIS"
Einstein, A. (1915). *Preuss. Akad. Wiss. Berlin, Sitzungsberichte der physikalisch-mathematischen Klasse*, p. 844.
Einstein, A. (1916). *Preuss. Akad. Wiss. Berlin, Sitzungsberichte der physikalisch-mathematischen Klasse*, p. 688.
Einstein, A. (1918). *Preuss. Akad. Wiss. Berlin, Sitzungsberichte der Physikalisch-mathematischen Klasse*, p. 154.
Einstein, A. (1936). Letter to Max Born published in *The Born-Einstein Letters*, translated by I. Born, p. 125. Macmillan & Co.: London, 1971.
Einstein, A. and Grossmann, M. (1913). *Zeit. Math. Physik.*, 62, 225.
Einstein, A., Infeld, L. and Hoffmann, B. (1938). *Annals of Mathematics*, 39, 65.
Einstein, A. and Rosen, N. 1937. *Journal of the Franklin Institute*, 223, 43.
Epstein, R. (1976a). Unpublished PhD thesis, Stanford University. KIP: CITED IN SEC. 7.B
Epstein, R. (1976b). KIP: GW'S IN PN APPROX FROM DUST IMPLOSION; PROBABLY REFERENCED BY FINN IN CARDIFF VOLUME. CITED IN SEC. 7.B
Epstein, R. and Clark, J. P. A. (1979). In Smarr, ed. (1979), p. 477.
Epstein, R. and Wagoner, R. V. (1975). *Astrophysical Journal*, 197, 717.
Eriguchi, Y., Futamase, T., and Hachisu, I. (1989). *Astronomy and Astrophysics*, submitted.
Ernst, F. J., Garcia, D. A., and Hauser, I. (1986). *Journal of Mathematical Physics*, 29, 681.
Esposito, F. P. (1971a) *Astrophysical Journal*, 165, 165.
Esposito, F. P. (1971b) *Astrophysical Journal*, 168, 495.
Estabrook, F. B. (1985). *General Relativity and Gravitation*, 17, 719.
Estabrook, F. B. (1987). *Acta Astronautica*, in press.
Estabrook, F. B. and Wahlquist, H. D. (1975). *General Relativity and Gravitation*, 6, 439.
Estabrook, F. B., Wahlquist, H., Christensen, S., DeWitt, B., Smarr, L., and Tsiang, E. (1973). *Physical Review D*, 7, 2814.
Evans, C. R. (1984). Ph.D. thesis, University of Texas at Austin, unpublished.
Evans, C. R. (1986). In *Dynamical Spacetimes and Numerical Relativity*, ed. J. M. Centrella. Cambridge University Press: Cambridge, p. 3.
Evans, C. R. (1987). In *Proceedings of the 13th Texas Symposium on Relativistic Astrophysics*, ed. M. Ulmer. New York Academy of Sciences: New York, 152.
Evans, C. R. (1989). KIP: GET REF FROM CHUCK: "Rotationally-induced

deformation during stellar collapse: perturbations of the Goldreich–Weber model".
Evans, C. R., Finn, L. S., and Hobill, D. W., eds. (1989). *Frontiers in Numerical Relativity. Cambridge University Press: Cambridge.*
Evans, C.R., Iben, I., and Smarr, L. (1987). *Astrophysical Journal*, submitted.
Fairbank, W. M., Boughn, S. P., Paik, H.–J., McAshan, M. S., Opfer, J. E., Taber, R. C., Hamilton, W. O., Pipes, B., Bernat, T., and Reynolds, J. M. (1974). In *Experimental Gravitation*, ed. B. Bertotti. Academic Press, New York, pp. 294 and 515.
Fairbank, W. M., Bassan, M., Mapoles, E. R., McAshan, M. S., Michelson, P. F., and Moskowitz, B. E. (1986). In Ruffini, ed., (1986), p. 543.
Faller, J. E. and Bender, P. L. (1981). Abstract for the *International Conference on Precision Measurements and Fundamental Constants*, June 8–12, 1981.
Faller, J. E., Bender, P. L., Hall, J. L., Hils, D., and Vincent, M. A. (1985). In *Proceedings of the Colloquium "Kilometric Optical Arrays in Space"*, Cargese (Corsica) 23–25 October 1984. ESA SP–226.
Ferrari, V. and Mashhoon, B. (1984). *Physical Review D*, 30, 295.
Ferrari, V., Ibanez, J., and Bruni, M. (1987). *Physics Letters A*, 122, 459.
Feynman, R. P. 1963a. *Acta Physica Polonica* 24, 697: also published in *Proceedings of the* 1962 *Warsaw Conference on the Theory of Gravitation.* PWN–Editions Scientifiques de Pologne: Warsaw (1964). [KIP: CITED IN SOME PLACES AS FEYNMAN 1963]
Feynman, R. P. 1963b. *Feynman, R. P.* (1963). *Lectures on Gravitation.* Unpublished lecture notes prepared by F. B. Morinigo and W. G. Wagner, and occasionally duplicated for private distribution by the California Institute of Technology, Pasadena.
Finn, L. S. (1985). *Classical and Quantum Gravity*, 2, 381.
Finn, L. S. (1986). *Monthly Notices of the Royal Astronomical Society*, 222, 393.
Finn, L. S. (1988). In *Proceedings of the NATO Advanced Research Workshop on Gravitational Radiation Data Analysis*, ed. B. Schutz, XXXXXX.
Finn, L. S. (1989). In Evans, Finn, and Hobill, eds. (1989), p. 126.
Finn, L. S. and Evans, C. R. (1989). *Astrophysical Journal*, submitted.
Flowers, E. and Itoh, N. (1979). *Astrophysical Journal*, 230, 847.
Fock, V. A. (1939). *Journal of Physics (Moscow)*, 1, 81.
Fock, V. A. (1955). [KIP: GET REF -- RUSSIAN VERSION OF 59]
Fock, V. A. (1959). *Theory of Space, Time, and Gravitation.* Pergamon: London. Section 87. [KIP: MOVE THE SECTION 87 CITATION INTO TEXT, NOT SEC. 6.E]
Ford, L. H. (1982). *Annals of Physics*, 144, 238.
Forster, J. and Newman, E. T. (1967). *Journal of Mathematical Physics*, 8, 189.
Forward, R. L. (1964). Personal Journal No. C1338, p. 66, entry for 13 September 1984 (unpublished).
Forward, R. L. (1978). *Physical Review D*, 17, 379.
Forward, R. L. and Berman, D. (1967). *Physical Review Letters*, 18, 1071.
Forward, R. L. and Moss, G. E. (1972). *Bulletin of the American Physical Society*, 17, 1183(A).
Forward, R. L., Zipoy, D., Weber, J., Smith, S., and Benioff, H. (1961). *Nature*, 189, 473.
Friedman, J. L. (1978). *Communications in Mathematical Physics*, 62, 247.
Friedman, J. L. (1983). *Physical Review Letters*, 51, 11.
Friedman, J. L., Ipser, J. R., and Parker, L. (1986). *Astrophysical Journal*, 304,

115.
Friedman, J. L. and Schutz, B. F. (1975a). *Astrophysical Journal (Letters)*, 199, L157.
Friedman, J. L. and Schutz, B. F. (1975b). *Astrophysical Journal*, 200, 204.
Friedman, J. L. and Schutz, B. F. (1978). *Astrophysical Journal*, 222, 281.
Friedrich, H. (1986). *Communications in Mathematical Physics*, 103, 35.
Futamase, T. (1983). *Physical Review D*, 28, 2373.
Futamase, T. (1985). *Physical Review D*, 32, 2566.
Futamase, T. (1987). *Physical Review D*, 36, 330.
Futamase, T. and Schutz, B. F. (1983). *Physical Review D*, 28, 2363.
Futamase, T. and Schutz, B. F. (1985). *Physical Review D*, 32, 2557.
Futterman, XXX, Handler, XXX, and Matzner, XXX (1988). *Scattering from Black Holes*. [KIP CHECK TITLE] Cambridge University Press: Cambridge.
Gal'tsov, D. V., Matiukhin, A. A., and Petukhov, V. I. (1980). *Physics Letters*, 77A, 387.
Gal'tsov, D. V., and Tsvetkov, V. P. (1984). *Physics Letters A*, 103, 193.
Gal'tsov, D. V., Tsvetkov, V. P., and Tsirulev, A. N. (1984). *Soviet Physics — JETP*, 59, 472.
Garfinkle, D. and Wald, R. M. (1985). *General Relativity and Gravitation*, 17, 461.
Garriga, J. and Verdaguer, E. (1987). *Physical Review D*, 36, 2250.
Garwin, R. L. and Levine, J. L. (1973). *Physical Review Letters*, 31, 176.
Gayer, S. and Kennel, C. F. (1979). *Physical Review D*, 19, 1070.
Gel'fand, I. M., Minlos, R. A., and Shapiro, Z. Ya. (1963). *Representations of the Rotation and Lorentz Groups*. Pergamon: Oxford.
Gerlach, U. H. (1980). *Physical Review D*, 22, 1300.
Geroch, R., Held, A., and Penrose, R. (1973). *Journal of Mathematical Physics* 14, 874.
Gertsenshtein, M. E. (1962). *Soviet Physics* — JETP, 14, 84.
Gertsenshtein, M. E. and Pustovoit, V. I. (1962). *Soviet Physics — JETP*, 16, 433.
Giazotto, A., Campani, E., Passuello, D., and Stefanini, A. (1986). In Ruffini, ed. (1986), p. 1329.
Giazzoto, A., Del Fabbro, R., Di Virgilio, A., Kautzky, H., Montelatici, V., Passuello, D., Arnaldo, S. (INFN sezione di Pisa e Universita' di Pisa); Barone, F., Bruzzese, R., Cutolo, A., Longo, M., Milano, L., Pinto, I., Solimeno, S. (Universita' di Napoli e di Salerno); Bordoni, F., Fuligni, F., Iafolla, V. (CNR, Franscati); Brillet, A., Man, C. N., Shoemaker, D., Tourrenc, P., and Vinet, J-Y. (CNRS-Univ. P. et M. Curie, Orsay-Paris) (1987). *Proposta di Antenna interferometrica a grande base per la ricerca di Onde Gravitazionali*. Universita degli Studi di Pisa and Istituto Nazionale di Fisica Nucleare Sezione di Pisa; Pisa, Italy.
Gibbons, G. W. and Hawking, S. W. (1971). *Physical Review D*, 4, 2191.
Gilden, D. L. and Shapiro, S. L. (1984). *Astrophysical Journal*, 287, 728.
Giffard, R. P. (1976). *Physical Review D*, 14, 2478.
Gliner, E. (XXXX). KIP: CITED IN SEC. 3.B, PARAGRAPH BEGINNING "IN THE SOVIET UNION"
Goebel, C. J. (1972). *Astrophysical Journal (Letters)*, 172, L95.
Goldberg, J. N. (1958). *Physical Review*, 111, 315.
Gomez, R. and Winicour, J. (1989). In Evans, Finn, and Hobill (1989), p. 385.
Gomez, R., Isaacson, R.A., Welling, J.S., and Winicour, J. (1986). In *Dynamical Spacetimes and Numerical Relativity*, ed. J. M. Centrella. Cambridge University Press: Cambridge, p. 236.

Gordienko, N. V., Gusev, A. V., and Rudenko, V. N. (1977). Vestnik Moskovskovo Universiteta, 18, 48.
Grigor'ev, V. I. (1982). *Moscow University Physics Bulletin*, 37, 39.
Grindlay, J. E. and Bailyn, C. D. (1989). *Nature*, 336, 48.
Grishchuk, L.P. (1974). *Soviet Physics* — JETP, 40, 409.
Grishchuk, L. P. (1975a). *Lettere al Nuovo Cimento*, 12, 60.
Grishchuk, L. P. (1975b). *Soviet Physics* — JETP, 40, 409.
Grishchuk, L. P. (1977). *Annals of the New York Academy of Sciences*, 302, 439. [CHANGE TO 1977A]
Grishchuk, L. P. (1977). *Soviet Physics—Uspekhi*, [XXXX Russian 121, 169] [KIP: FIX – THIS IS A NEW 1977; THERE IS ALSO AN OLD ONE. MAKE THIS ONE 1977B]
Grishchuk, L. P. (1983). In *Proceedings of the Ninth International Conference on General Relativity and Gravitation*, ed. E. Schmutzer, Cambridge University Press: Cambridge, p. 255.
Grishchuk, L. P. (1988a). Private communication.
Grishchuk, L. P. (1988b). *Proceedings of Eleventh International Conference on General Relativity and Gravitation*, ed. M. A. H. MacCallum. Cambridge University Press: Cambridge, p. 86. [KIP: FIX – THIS IS A NEW 1988; THERE IS ALSO AN OLD ONE; OLD IS NOW A, NEW IS NOW B -- EXCEPT THAT I HAVE ELIMINATED OLD ONE FROM SEC 3.B AND IT MAY NOW BE TOTALLY GONE!]
Grishchuk, L. P. (1989). [KIP: GET REF FROM HIS VITAE, ON BURSTS WITH MEMORY OF VELOCITY; CITED IN LAST FEW PARAGRAPHS OF CHAP. 7]
Grishchuk, L. P. and Kopeikin, S. M. (1986). In: *Relativity in Celestial Mechanics and Astrometry*, eds. J. Kovalevsky and V. A. Brumberg. North–Holland: Amsterdam, p. 19.
Grishchuk, L. P. and Petrov, A. N. (1987). *Zhurnal Eksperimentalnoi i Teoreticheskoi Fiziki*, 92, 9.
Grishchuk, L. P., Petrov, A. N., and Popova, A. D. (1984). *Communications in Mathematical Physics*, 94, 379.
Grishchuk, L. P. and Polnarev, A. G. (1980). In *General Relativity and Gravitation*, vol. 2, ed. A Held. Plenum: New York, p. 393.
Grishchuk, L. P. and Zel'dovich, Ya. B. (1978). *Soviet Astronomy—AJ*, 22, 125.
Gupta, S. N. (1957). *Reviews of Modern Physics*, 29, 334.
Gürsel, Y., Linsay, P., Saulson, P., Spero, R., Weiss, R., and Whitcomb, S. (1983). Unpublished Caltech/MIT manuscript.
Gürsel, Y., and Tinto, M. (1989). *Physical Review D*, submitted.
Gusev, A. V. and Rudenko, V. N. (1976). *Radiotekhnika i Electronika*, 3, 1865.
Haensel, P., Zdunik, J. L., and Schaeffer, R. (1986). *Astronomy and Astrophysics*, 160, 251.
Halliwell, J. J. and Hawking, S. W. (1985). *Physical Review D*, 31, 1777.
Halpern, L. E. (1963). *Bull. Acad. Roy. Belg. Cl. Sci.*, 53, 226. [KIP: WHAT IS FULL TITLE OF JOURNAL?]
Halpern, L. E. and Desbrandes, R. (1969). *Annales Institut Henri Poincaré*, 9, 309.
Hamilton, W. O. (1977). In de Sabbata and Weber, eds. (1977).
Hamilton, W. O., Darling, D., Kadlec, J, and DeWitt, D. (1983). In *Proceedings of the Third Marcel Grossmann Meeting on General Relativity*, ed. H. Ning. North Holland: Amsterdam, p. 1175.
Hamilton, W. O., Xu, B.–X., Solomonson, N., Mann, A. G., and Sibley, A., (1986). "Performance of the LSU Tuned Bar Gravitational Wave Detector."

unpublished technical memorandum. Louisiana State University: Baton Rouge, LA.
Hansen, P. M., Chiu, Y. T., and Chao, C.-C. (1986). Aerospace Report No. ATR-86(8421)-2. The Aerospace Corporation: El Segundo, CA.
Havas, P. (1957). *Physical Review*, 108, 398.
Havas, P. (1979). In *Isolated Gravitating Systems in General Relativity*, ed. J. Ehlers. North Holland: Amsterdam, p. 74.
Havas, P. and Goldberg, J. N. (1962). *Physical Review*, 128, 398.
Hawking, S. W. (1985). *Physics Letters*, 150B, 339.
Hawking, S. W. and Israel, W., eds. (1987). 300 *Years of Gravitation*. Cambridge University Press: Cambridge
Haugan, M. P., Shapiro, S. L. and Wasserman, I. (1982). *Astrophysical Journal*, 257, 283.
Heffner, H. (1962). *Proceedings of the IRE*, 50, 1604.
Helfand, D. H., Taylor, J. H., Backus, R. R., and Cordes, J. M. (1980). *Astrophysical Journal*, 237, 206.
Hellings, R. W. and Downs, G. S. (1983). *Astrophysical Journal (Letters)*. 265, L39.
Hellings, R. W., Callahan, P. S., Anderson, J. D., and Moffett, A. T. (1981). *Physical Review D*, 23, 844.
Hertz, H. (1892). *Untersuchungen* über die Ausbreitung der elektrischen Kraft. Johann Ambrosius Barth, Leipzig.
Hillebrandt, W. and Müller, E. (1981). *Astronomy and Astrophysics*, 103, 147.
Hils, D. L., Bender, P., Faller, J. E., and Webbink, R. F. (1987). Paper in preparation.
Hirakawa, H. and Narihara, K. (1975). *Physical Review Letters*, 35, 330.
Hirakawa, H., Narihara, K., and Fujimoto, M.-K. (1976). *Journal of the Physical Society of Japan*, 41, 1093.
Hirakawa, H., Owa, S., and Iso, K. (1985). *Journal of the Physical Society of Japan*, 54, 1270.
Hobill, D. W. (1984). *Journal of Mathematical Physics*, 25, 3527.
Hobson, E. W. (1931). *The Theory of Spherical and Ellipsoidal Harmonics*. Cambridge University Press: Cambridge, p. 119. Republished in 1955 by Chelsea Publishing Co.: New York.
Hogan, C. J. (1986). *Monthly Notices of the Royal Astronomical Society*, 218, 629.
Hogan, C. J. and Rees, M. J. (1984). *Nature*, 311, 109.
Hollenhorst, J. N. (1979). *Physical Review D*, 19, 1669.
Hough, J., Meers, B. J., Newton, G. P., Robertson, N. A., Ward, H., Schutz, B. F., and Drever, R. W. P. (1986). *A British Long Baseline Gravitational Wave Observatory*, unpublished report submitted by Glasgow University to the SERC.
Hough, J., Pugh, J. R., Bland, R., and Drever, R. W. P. (1975). *Nature*, 254, 498.
Hough, J., Drever, R. W. P., Munley, A. J., Lee, S.-A., Spero, R., Whitcomb, S. E., Pugh, J., Newton, G., Meers, B., Brooks, E., and Gürsel, Y. (1983). In *Quantum Optics, Experimental Gravity, and Measurement Theory*, eds. P. Meystre and M. O. Scully, p. 515. Plenum: New York.
Hu, B. L. (1978). *Physical Review D*, 18, 969.
Hu En Ke, Guan Tongren, Yu Bo, Tang Menxi, Chen Shusen, Zheng Qingzhang, Michelson, P. F., Moskowitz, B. E., McAshan, M. S., Fairbank, W. M., and Bassan, M. (1986). *Chinese Physics Letters*, No. 11-12, 1.
Hu, N. (1947). *Proceedings of the Royal Irish Academy*, 51A, 87.
Hu R., Jiang N., Liu Y., Qin R.-X., Tan D., Tian J., Wang G., Zhang P. Zhao Z., and

Zheng L. (1982). In *Proceedings of the Second Marcel Grossmann Meeting on General Relativity*, ed. R. Ruffini. North-Holland, Amsterdam, p. 1133.
Hulse, R. A. and Taylor, J. H. (1975). *Astrophysical Journal (Letters)*, **195**, L51.
Iacopini, E., Picasso, E., Pegoraro, F., and Radicati, L. A. (1979). *Physics Letters*, **73A**, 140.
Iben, I. (1988). *Astrophysical Journal*, **324**, 355.
Iben, I. and Tutukov, A. V. (1984). *Astrophysical Journal Supplements*, **54**, 335.
Imamura, J. N., Friedman, J. L., and Durisen, R. H. (1985). *Astrophysical Journal*, **294**, 474.
Infeld, L. and Plebansky, J. (1960). *Motion and Relativity*. Pergamon: London.
Infeld, L. and Scheidegger, A. E. (1951). *Canadian Journal of Mathematics*, 3, 195.
Ipser, J. R. (1971), *Astrophysical Journal*, **166**, 175.
Ipser, J. R. (1986). Private communication.
Ipser, J. R. and Managan, R. A. (1984). *Astrophysical Journal*, **282**, 287.
Ipser, J. R. and Thorne, K. S. (1973) *Astrophysical Journal*, **181**, 181.
Isaac, G. R. (1981). *Solar Physics*, **74**, 43.
Isaacson, R. A. (1968a) *Physical Review* **166**, 1263.
Isaacson, R. A. (1968b) *Physical Review* **166**, 1272.
Isaacson, R. A., Welling, J. S., and Winicour, J. (1983). *Journal of Mathematical Physics*, **24**, 1824.
Isaacson, R. A. Welling, J. S., and Winicour, J. (1984). *Physical Review Letters*, **53**, 1870.
Isaacson, R. A., Welling, J. S., and Winicour, J. (1985). *Journal of Mathematical Physics*, **26**, 2859.
Israel, W. (1986). [KIP: PRL ON PROOF OF THIRD LAW]
Iyer, S. (1987). *Physical Review D*, **35**, 3632.
Iyer, S. and Will, C. M. (1987). *Physical Review D*, **35**, 3621.
Jackson, J. D. (XXXX), *Classical Electrodynamics*. Wiley: New York.
Janis, A. I. (1985). *General Relativity and Gravitation*, **17**, 599.
Jordan, P. (1959). *Z. Phys.*, **157**, 112.
Kahn, K. and Penrose, R. (1971). *Nature*, **229**, 185.
Kafka, P. (1977). In de Sabbata and Weber (1977), p. 161.
Kafka, P. and Schnupp, L. (1978). *Astronomy and Astrophysics*, 70, 97.
Kaufmann, W. J. (1970). *Nature*, **227**, 157.
Kawashima, N. (1989). In *Abstracts of Contributed Papers, Twelfth International Conference on General Relativity and Gravitation*. University of Colorado: Boulder, Colorado, p. 574.
Kegeles, L. S. and Cohen, J. M. (1979). *Physical Review D*, **19**, 1641.
Kellerman, K. I. and Sheets, B. (1983). *Serendipitous Discoveries in Radio Astronomy*. National Radio Astronomy Observatory: Green Bank, West Virginia.
Kelvin, Lord (Sir William Thomson) and Tate, P. G. (1879). *Treatise on Natural Philosophy*, Appendix B of Chap. 1 of Vol. 1. Cambridge University Press: Cambridge.
Kerlick, G. D. (1975). *General Relativity and Gravitation*, 12, 467 and 521.
Kinnersley, W. and Walker, M. (1970). *Physical Review D*, 2, 1359.
Kluzniak, W., Lindblom, L., and Wagoner, R. V. (1989). Paper in preparation.
Kochanek, C. S. and Evans, C. R. (1989). In Evans, Finn, and Hobill (1989), p. 297.

Kojima, Y. (1987). *Progress of Theoretical Physics*, 77, 297.
Kojima, Y. and Nakamura, T. (1983). *Physics Letters A*, 99, 37.
Kojima, Y. and Nakamura, T. (1984a). *Progress of Theoretical Physics*, 71, 79.
Kojima, Y. and Nakamura, T. (1984b). *Progress of Theoretical Physics*, 72, 494.
Kovacs, S. J. and Thorne, K. S. (1977). *Astrophysical Journal*, 217, 252.
Kovacs, S. J. and Thorne, K. S. (1978). *Astrophysical Journal*, 224, 62.
Kraichnan, R. H. (1955). *Physical Review*, 98, 1118.
Kramer, D., XXXXXXX (1980). *Exact Solutions of Einstein's Field Equations*. XXXXXXX.
Krauss, L. M. (1986). *General Relativity and Gravitation*, 18, 723.
Krolak, A. (1988). [KIP: GET REF. – PN CORRS TO SPIRALING BINARY WAVEFORMS]
Kuhn, J. R. and Boughn, S. P. (1984). *Nature*, 308, 164.
Lanczos, C. (1923). *Physikalische Zeitschrift*, 23, 537.
Landau, L. D. and Lifshitz, E. M. (1941). *Teoriya Polya*. Nauka: Moscow. [English translation of a later edition, *The Classical Theory of Fields*. Addison–Wesley: Cambridge, Mass. (1951).]
Landau, L. D. and Lifshitz, E. M. (1962). *The Classical Theory of Fields*, revised second edition. Addison–Wesley: Cambridge, Mass.
Leaver, E. W. (1985a). "Solutions to a Generalized Spheroidal Wave Equation in Molecular Physics and General Relativity, and an Analysis of the Quasi–Normal Modes of Kerr Black Holes", unpublished PhD thesis, University of Utah: Salt Lake City.
Leaver, E. W. (1985b). *Proceedings of the Royal Society of London A*, 402, 285.
Leaver, E. W. (1986). *Physical Review D*, 34, 384.
Leen, T. K., Parker, L., and Pimentel, L. O. (1983). *General Relativity and Gravitation*, 15, 761.
Levine, J. L. and Garwin, R. L. (1973). *Physical Review Letters*, 31, 173.
Levine, J. L. and Garwin, R. L. (1974). *Physical Review Letters*, 33, 794.
Levi–Civita, T. (1918). *Atti Accademia Nazionale dei Lincei., RendXXXX.*, 27, 343.
Levi–Civita, T. (1937). *American Journal of Mathematics*, 59, 9 and 225.
Leusch, G., Maischberger, K., Rüdiger, A., Schilling, R., Schnupp, L., ans Winkler, W. (1987). *Vorschlag zum Bau eines groß*en Laser–Interferometers zur Messung von Gravitationswellen, Report MPQ 129. Max–Planck–Institut für Quantenoptik: Garching bei Munchen, Germany.
Lichnerowicz, A. (1955). *Théo*ries relatavistes de la gravitation et de l'électromagnétisme. Masson, Paris.
Lifshitz, E. M. (1946). *Zhurnal Eksperimentalnoi i Teoreticheskoi Fiziki*, 16, 587.
Lindblom, L. (1986). *Astrophysical Journal*, 303, 146.
Lindblom, L. (1987). *Astrophysical Journal*, 317, 325.
Lindblom, L. (1988). In *Proceedings of International Symposium on Experimental Gravitational Physics*, Guangzhou, China, August 1987, ed Hu En Ke. World Scientific, Singapore, in press.
Lindblom, L. and Detweiler, S. L. (1977), *Astrophysical Journa.*, 211, 1965.
Lindblom, L. and Detweiler, S. L. (1983), *Astrophysical Journal*, 53, 73. [KIP: SOMETHING IS WRONG WITH VOLUME NUMBER]
Lindblom, L. and Hiscock, W. A. (1983). *Astrophysical Journal*, 267, 384.
Linet, B. (1982). *General Relativity and Gravitation*, 14, 479.
Linet, B. (1984). *General Relativity and Gravitation*, 16, 89.
Linet, B. and Tourrenc, P. (1976). *Canadian Journal of Physics*, 54, 1129.
Lincoln, C. W. (1989). Paper in preparation.

Linsay, P., Saulson, P., and Weiss, R. (1983). *A Study of a Long Baseline Gravitational Wave Antenna System*, report prepared for The National Science Foundation. MIT: Cambridge, Massachusetts (unpublished).

Lipunov, V. M. and Postnov, K. A. (1987). *Soviet Astronomy—AJ*, 31, 228.

Lipunov, V. M., Postnov, K. A., and Prokhorov, M. E. (1987). *Astronomy and Astrophysics*, 176, L1.

Lipunov, V. M., Postnov, K. A., and Prokhorov, M. E. (1988). In *The Physics of Neutron Stars: Their Formation, Structure, and Evolution*, Proceedings of a conference of the Astronomical Council of the Academy of Sciences of the USSR. Ioffe Physico–Technical Institute: Leningrad.

Livas, J., Benford, R., Dewey, D., Jeffries, A., Linsay, P., Saulson, P., Shoemaker, D., and Weiss, R. (1986). In Ruffini, ed. (1986), p. 591.

Livas, J., Saulson, P., Spero, R., and Thorne, K. S. (1987). *Final Report of the LIGO Site Selection Working Group*, unpublished report, Caltech and MIT: Pasadena, CA and Cambridge MA.

Logunov, A. A., and Vlasov, A. A. (1984). *Theoretical and Mathematical Physics (USSR)*, 60, 635.

Logunov, A. A., Loskutov, Yu. M., and Mestvirishvili, M. A. (1988). *Soviet Physics—Uspekhi*, 155, 369. [KIP: THIS IS RUSSIAN REF, CHANGE TO ENGLISH; ALSO CHECK TO BE SURE THIS PAPER REALLY SHOULD BE CITED IN SEC. 6.E.]

Lorentz, H. A. (1900). *Proc. K. Ak. Amsterdam* 8, 603. [KIP: CHECK AND FIX REF; SAME JOURNAL AS BELOW?]

Lorentz, H. A. and Droste, J. (1917). *Versl. K. Akad. Wet. Amsterdam*, 26, 392 and 649. Reprinted in *Collected Papers of H. A. Lorentz*, 5, p. 330. Nijhoff: The Hague (1937).

Lucacs, B., Perjes, Z., Porter, J., and Sebestyen, A. (1984). *General Relativity and Gravitation*, 16, 691.

Lyamov, V. E. and Rudenko, V. N. (1975). *Soviet Physics - JETP*, 40, 787.

MacCallum, M. H., ed. (1987). *Proceedings of the Tenth International Conference on General Relativity and Gravitation*. Cambridge University Press: Cambridge.

MacCallum, M. A. H. and Taub, A. H. (1973). *Communications in Mathematical Physics* 30, 153.

Macedo, P. G. and Nelson, A. H. (1983). *Physical Review D*, 28, 2382.

Maeda, K., Sasaki, M. Nakamura, T. and Miyama, S. (1980). *Progress of Theoretical Physics*, 63, 719.

Maeder, D. G. (1974). *Journal of Physics A*, 5, L113.

Maischberger, K. (1974). In Colloques Internationaux CNRS No. 220, *Ondes et radiations gravitationelles*, ed. Y. Choquet–Bruhat. Editions du CNRS: Paris.

Maischberger, K., Rudiger, A., Schilling, R., Schnupp, L., Shoemaker, D., and Winkler, W. (1985). *Vorschlag zum Bau eines grossen Laser-Interferometers zur Messung von Gravitationswellen*. Max–Planck Institut fur Quantenoptic: Munich. (unpublished).

Managan, R. A. (1985). *Astrophysical Journal*, 294, 463.

Mashhoon, B., Carr, B. J., and Hu, B. L. (1981). *Astrophysical Journal*, 246, 569.

Matzner, R. A., DeWitt–Morette, C., Nelson, B., and Zhang, T.–R. (1985). *Physical Review D*, 31, 1869.

Matzner, R. A. and Ryan, M. (1978). *Astrophysical Journal Supplement Series*, 36, 451.

Matzner, R. A. and Tipler, F. J. (1984). *Physical Review D*, 29, 1575.

Meers, B. (1983). Unpublished PhD thesis, University of Glasgow.
Melosh, H. J. (1969). *Nature*, **224**, 781.
Michelson, P. F. (1983). In Deruelle and Piran (1983), p. 465.
Michelson, P.F. (1986). *Physical Review D*, **34**, 2966.
Michelson, P.F. and Taber, R.C. (1981). *Journal of Applied Physics* , **52**, 4313.
Michelson, P. F. and Taber, R. C. (1984). *Physical Review D*, **29**, 2149.
Michelson, P. F., Price, J. C., and Taber, R. C. (1987). *Science*, **237**, 150.
Middleditch, J., Pennypacker, C., Morris, D. E., Muller, R. A., Perlmutter, S., Sasseen, T., Kristian, J. A., Kunkel, W. E., Hamuy, M. A., Imamura, J. N., Steiman-Cameron, T. Y., Shelton, I. K., Tuohy, I. R., and Rawlings, S. (1989). *I.A.U. Circular* No. 4735. [KIP: GET NATURE REFERENCE AND REPLACE IAU BY IT]
Mijić, M., Morris, M., and Suen, W.-M. (1986). *Physical Review D*, **34**, 2934.
Miller, B. D. (1974). *Astrophysical Journal*, **187**, 609.
Mironovskii, V. N. (1966). *Soviet Astronomy — AJ*, **9**, 752.
Misner, C. W., Thorne, K. S., and Wheeler, J. A. (1973). *Gravitation*. W. H. Freeman & Co.: San Francisco. *Cited in text as* MTW
Moncrief, V. (1974). *Annals of Physics*, **88**, 323.
Moss, G. E., Miller, L. R., and Forward, R. L. (1971). *Applied Optics*, **10**, 2495.
Müller, E. (1982). *Astronomy and Astrophysics*, **114**, 53.
Müller, E. (1984). In *Problems of Collapse and Numerical Relativity*, ed. D. Bancel and M. Signore, Reidel: Dordrecht, p. 271
Nagashima, Y., Owa, S., Tsubono, K., and Hirakawa, H. (1988). *Reviews of Scientific Instruments*, **59**, 112.
Nakamura, T. (1983). In Deruelle and Piran (1983).
Nakamura, T. (1987). In *Gravitational Collapse and Relativity*, eds. H. Sato and T. Nakamura, p. 295. World Scientific: Singapore.
Nakamura, T. (1989). *Progress of Theoretical Physics*, **81**, 1006.
Nakamura, T. (1990). In *Procedings of Twelfth International Conference on General Relativity and Gravitation*, XXXXXX, ed. Cambridge University Press: Cambridge, in preparation.
Nakamura, T. and Fukugita, M. (1989). *Astrophysical Journal*, **337**, 466.
Nakamuara, T. and Oohara, K. (1989). In Evans, Finn, and Hobill (1989).
Nakamura, T., Oohara, K., and Kojima, Y. (1987). *Progress of Theoretical Physics Supplement No.* 90.
Nakamura, T. and Sasaki, M. (1981). *Physics Letters*, **106B**, 69.
Nesterikhin, Y. E., Rautian, S. G., and Smirnov, G. I. (1978). *Soviet Physics — JETP*, **48**, 1.
Newman, E. T. and Penrose, R. (1962). *Journal of Mathematical Physics*, **3**, 566, and **4**, 998.
Newman, E. T. and Penrose, R. (1965). *Physical Review Letters*, **15**, 231.
Newman, E. T. and Tod, K. P. (1980). In *General Relativity and Gravitation Volume* 2, ed. A. Held. Plenum: New York, p. 1.
Ni, W.-T. and Zimmermann, M. E. (1978). *Physical Review D*, **17**, 1473.
Nordtvedt, K. (1968). *Physical Review*, **169**, 1017.
Norman, M. and Wilson, J. R. (1979). Unpublished research reported by Wilson (1979).
Novikov, I. D. (1975). *Soviet Astronomy—AJ*, **19**, 398.
Nutku, Y. and Halil, M. (1977). *Physical Review Letters*, **39**, 1379.
Oelfke, W. C. (1983). In *Quantum Optics, Experimental Gravitation and Measurement Theory*, eds. P. Meystre and M. O. Scully. Plenum: New York, p. 387.

Ogievetsky, V. I., and Polubarinov, I. V. (1965). *Annals of Physics*, 35, 167.
Oohara, K. I. and Nakamura, T. (1984). *Progress of Theoretical Physics*, 71, 91.
Oohara, K. I. and Nakamura, T. (1989). *Progress of Theoretical Physics*, 82, in press.
Oohara, K. I. and Nakamura, T. (1990). *Progress of Theoretical Physics*, paper in preparation.
Oppenheimer, J. R. and Serber, R. (1938). *Physical Review*, 54, 540.
Ostriker, J. P., Thompson, C., and Witten, E. (1986). *Physics Letters*, B180, 231.
Owa, S., Fujimoto, M.–K., Hirakawa, H., Morimoto, K., Suzuki, T., and Tsubono, K. (1986). In *Proceedings of Fourth Marcel Grossmann Meeting on Recent Developments of General Relativity*, ed. R. Ruffini. North Holland: Amsterdam.
Paczynski, B. and Sienkiewicz, R. (1981). *Astrophysical Journal (Letters)*, 248, L27.
Paik, H.–J. (1976). *Journal of Applied Physics*, 47, 1168.
Paik, H.–J. (1980). *Il Nuovo Cimento B*, 55, 15.
Paik, H.–J. and Wagoner, R. V. (1976). *Physical Review D*, 13, 2694.
Pandharipande, V. R., Pines, D., and Smith, R. A. (1976). *Astrophysical Journal*, 208, 550.
Pallotino, G. V. and Pizella, G. (1981). *Nuovo Cimento*, 4C, 237.
Papadopoulos, D. and Esposito, F. P. (1985). *Astrophysical Journal*, 282, 330.
Papapetrou, A. (1948). *Procedings of the Royal Irish Academy*, Series A, 52, 11.
Papapetrou, A. (1962). *Comptes Rendues Acad. Sci. Paris*, 255, 1578.
Papapetrou, A. (1971). *Annales Institut Henri Poincaré*, 14, 79.
Papapetrou, A. (1977). In de Sabbata and Weber (1977), p. 83.
Payne, P. N. (1983). *Gravitational Radiation in High Speed Black-Hole Collisions*. Unpublished PhD dissertation. Cambridge University: Cambridge.
Pegoraro, F., Picasso, E., and Radicati, J. (1978). *Journal of Physics A*, 11, 1949.
Pei–Yuan, XXXXXXXXX.
Penrose, R. (1963a). *Physical Review Letters* 10, 66.
Penrose, R. (1963b). *Relativity, Groups, and Topology*, ed. C. DeWitt and B. DeWitt. Gordon and Breach: New York, p. 565.
Penrose, R. and Rindler, W. (1986). *Spinors and Space-time*, vol. 2. Cambridge University Press: Cambridge.
Penzias, A. A. and Wilson, R. W. (1965). *Astrophysical Journal*, 142, 419.
Peres, A. (1960). *Nuovo Cimento*, 15, 351.
Peters, P. C. (1964). *Physical Review* 136, B1224.
Peters, P. C. and Mathews, J. (1963). *Physical Review*, 131, 435.
Petrich, L. L., Shapiro, S. L., and Wasserman, I. (1985). *Astrophysical Journal Supplement Series*, 58, 297.
Petrov, A. Z. (1954). *Scientific Notices, Kazan State University* (USSR), 114, 55.
Pines, D. (1980). *Science*, 207, 597.
Piran, T. (1979). In Smarr, ed. (1979), p. 409.
Piran, T. (1983). In Deruelle and Piran, ed. (1983), p. 203.
Piran, T. (1985). *Physical Review D*, 32, 3101.
Piran, T. (1987). In MacCallum, ed. (1987), p. 177.
Piran, T. and Safier, P. (1985). *Nature*, 318, 271.
Piran, T., Safier, P., and Katz, J. (1986). *Physical Review D*, 34, 331.
Piran, T., Safier, P., and Stark, R. (1985). *Physical Review D*, 32, 3101.
Piran, T. and Stark, R. F. (1986). In *Dynamical Spacetimes and Numerical*

Relativity, ed. J. M. Centrella. Cambridge University Press: Cambridge, p. 40.
Pirani, F. A. E. (1956). *Acta Physica Polonica*, **15**, 389.
Pirani, F. A. E. (1957). *Physical Review* **105**, 1089.
Pirani, F. A. E. (1962a). In *Recent Developments in General Relativity*. Pergamon Press, Oxford, and PWN—Polish Scientific Publishers, Warsaw, p. 89.
Pirani, F. A. E. (1962b). In *Gravitation: An Introduction to Current Research*, ed. L. Witten. Wiley, New York, p. 199.
Pirani, F. A. E. (1964). In *Lectures on General Relativity*, A. Trautman, F. A. E. Pirani, and H. Bondi. Prentice-Hall: Englewood Cliffs, NJ.
Pizzella, G. (1984). *Lettere al Nuovo Cimento*, **40**, 240.
Poincaré, H. (1905). *Comptes Rendues Academie Sciences Paris*, **140**, 1504. Reprinted in *Ouvres de Henri Poincaré*, IX, p. 489. Gauthier-Villars: Paris (1954). [KIP: CHECK]
Poincaré, H. (1908). *Revue générale des sciences pure et appliquées*, **19**, 386. Reprinted in *Ouvres de Henri Poincaré*, IX, p. 551. Gauthier-Villars: Paris (1954).
Polnarev, A. G. (1985). *Soviet Astronomy—AJ*, **29**, 607.
Polnarev, A. G. (1988). KIP: GET REF: "Bremsstrahlung grav'l radn and its astrophysical manifestation"
Power, E. A. and Wheeler, J. A. (1957). *Reviews of Modern Physics*, **29**, 480.
Press, W. H. (1971). *Astrophysical Journal (Letters)*, **170**, L105.
Press, W. H. (1977). *Physical Review D*, **15**, 965.
Press, W. H. (1979). *General Relativity and Gravitation*, **11**, 105.
Price, R. H. (1972a). *Physical Review D* **5**, 2419.
Price, R. H. (1972b). *Physical Review D* **5**, 2439.
Price, R. H. and Thorne, K. S. (1969). *Astrophysical Journal*, **155**, 163.
Priedhorsky, W., Stella, L., and White, N.E. (1986). *International Astronomical Union Circular* No. 4247, Aug. 28, 1986.
Quinlan, G. and Shapiro, S. L. (1987). *Astrophysical Journal*, in press.
Rapagnani, P. (1982). *Il Nuovo Cimento C*, **5**, 385.
Rawley, L. A., Taylor, J. H., Davis, M. M., and Allan, D. W. (1987). *Science*, **238**, 761.
Ramaty, R., Bonazzola, S., Cline, T. L., Kazanas, D., and Meszaros, P. (1980). *Nature*, **287**, 122.
Rees, M. J. (1971). *Monthly Notices of the Royal Astronomical Society*, **154**, 187.
Rees, M. J. (1983). In Deruelle and Piran (1983), p. 297.
Regge, T. (1961). *Il Nuovo Cimento*, **19**, 558.
Regge, T. and Wheeler, J. A. (1957). *Physical Review*, **108**, 1063.
Resch, G. M., Hogg, D. E., and Napier, P. G. (1984). *Radio Science*, **19**, 411.
Reynolds, S. P. and Stinebring, D. R. (1984). *Millisecond Pulsars*, National Radio Astronomy Observatory: Green Bank, West Virginia
Richard, J.-P. (1979). In *Gravitational Radiation, Collapsed Objects, and Exact Solutions*, ed. C. Edwards. Springer: Berlin, p. 370. [KIP: CHECK -- THERE MAY BE A BETTER 1979 REF ON RICHARD'S 2-MODE OR 3-MODE TRANSDUCER; CITED IN SEC. 3.B, PARAGRAPH BEGINNING "THIS SECOND".
Richard, J.-P. (1982). In *Proceedings of the Second Marcel Grossmann Meeting on General Relativity*, ed. R. Ruffini. North-Holland, Amsterdam, p. 1239.
Richard, J.-P. (1984). *Physical Review Letters*, **52**, 165. [KIP: DELETE AND REPLACE BY 82, 86?]
Richard, J.-P. (1986). *Reviews of Scientific Instruments*, **47**, 423.

Richard, J.-P., Pang Yi, and Hamilton, J. J. (1989). In *Abstracts of Contributed Papers, Twelfth International Conference on General Relativity and Gravitation*. University of Colorado: Boulder, Colorado, p. 558.
Robertson, D. S. and Carter, W. E. (1984). *Nature*, **310**, 572.
Robinson, E. L. and Shafter, W. (1987). *Astrophysical Journal*, **322**, 296.
Robinson, I., and Trautman, A. (1962). *Proceedings of the Royal Society of London*, **265A**, 463.
Romani, R. W. and Taylor, J. H. (1983). *Astrophysical Journal (Letters)*, **265**, L35.
Rosen, N. (1937). *Physikalische Zeitschrift Sowjetunion*, **12**, 366.
Rosen, N. (1940). *Physical Review*, **57**, 147.
Rosen, N. (1963). *Annals of Physics*, **22**, 1.
Rubakov, V., Sazhin, M. C., and Veryaskin, A. (1982). *Physics Letters*, **115B**, 189.
Rudenko, V. N. (1975). *Soviet Astronomy — AJ*, **19**, 270.
Rudenko, V. N. and Grishchuk, L. P. (1988). Private communication.
Rudenko, V.N. and Sazhin, M.V. (1980). *Kvantovaya Elektronika*, **7**, 2344.
Ruderman, M. (1969). *Nature*, **223**, 597.
Ruffini, R., ed. (1986). *Proceedings of the Fourth Marcel Grossmann Meeting on Recent Developments of General Relativity*. North Holland: Amsterdam.
Ruffini, R. and Wheeler, J. A. (1971). In *Proceedings of the Conference on Space Physics*. European Space Research Organization: Paris, p. 45.
Sachs, R. K. (1961). *Proceedings of the Royal Society of London A*, **264**, 309; especially Appendix B.
Sachs, R. K. (1962). *Proceedings of the Royal Society of London A*, **270**, 103.
Sachs, R. K. (1963). In *Relativity, Groups, and Topology*, ed. C. DeWitt and B. DeWitt. Gordon and Breach. New York, p. 521.
Sachs, R. K. and Bergmann, P. G. (1958). *Physical Review*, **112**, 674.
Sachs, R. K. and Wolfe, A. M. (1967). *Astrophysical Journal*, **147**, 73.
Saenz, R.A. and Shapiro, S.L. (1978). *Astrophysical Journal*, **221**, 286.
Saenz, R.A. and Shapiro, S.L. (1979). *Astrophysical Journal*, **229**, 1107.
Saenz, R.A. and Shapiro, S.L. (1981). *Astrophysical Journal*, **244**, 1033.
Sasaki, M. (1984). In *Problems of Collapse and Numerical Relativity*, ed. D. Bancel and M. Signore. Reidel: Dordrecht, p. 203.
Sasaki, M. and Nakamura, T. (1982). *Progress of Theoretical Physics*, **67**, 1788.
Sato, H. (1987). *Progress of Theoretical Physics*, **75**, 1342.
Saulson, P. (1984). *Physical Review D*, **30**, 732.
Sazhin, M. V. (1978). *Soviet Astronomy — AJ*, **22**, 36.
Schäfer (1983). *Lettere al Nuovo Cimento*, **36**, 105.
Schäfer (1985). *Annals of Physics*, **161**, 81.
Schäfer (1989). In *Proceedings of the Fifth Marcel Grossmann Meeting on General Relativity*, eds. D. G. Blair and M. J. Buckingham. World Scientific: Singapore.
Scheidegger, A. E. (1955). *Physical Review*, **99**, 1883.
Schmidt, B. G. (1981). *Communications in Mathematical Physics*, **78**, 447.
Schmidt, B. G. (1979). In *Isolated Gravitating Systems*, ed. J. Ehlers, p. 11. North Holland: Amsterdam.
Schmidt, B. G. (1986). "Gravitational Radiation Near Spatial and Null Infinity," preprint XXXXXX.
Schmidt, B. G. (1987). "Existence of Solutions of the Robinson-Trautman Equation and Spatial Infinity", preprint XXXXXXX.
Schilling, R. (1986). Private communication.

Schrader, R. (1984). *Physics Letters B*, 143B, 421.
Schramm, D. N. and Arnett, W. D. (1975). *Astrophysical Journal*, 198, 629.
Schumaker, B. L. (1986). *Physics Reports*, 135, 318.
Schumaker, B. L. and Thorne, K. S. (1983). *Monthly Notices of the Royal Astronomical Society*, 203, 457.
Schutz, B. F. (1972). *Astrophysical Journal Supplement Series*, 24, 343.
Schutz, B. F. (1980). *Physical Review D*, 22, 249.
Schutz, B. F. (1986a). In *Relativity, Supersymmetry, and Cosmology*, eds. O. Bressan, M. Castagnino, and V. Hamity, p. 3. World Scientific: Singapore.
Schutz, B. F. (1986b). *Nature*, 323, 310.
Schutz, B. F. (1986c). In *Dynamical Spacetimes and Numerical Relativity*, ed. J. Centrella. Cambridge University Press: Cambridge. p. 446.
Schutz, B. F. (1987). In *Gravitation in Astrophysics*, ed. B. Carter and J. Hartle. Plenum: New York. [KIP: MUST BE CHANGED TO 1987A]
Schutz, B. F. (1987b). In MacCallum (1987), p. 369.
Schutz, B. F. (1988). In Proceedings of the NATO Advanced Research Workshop on *Gravitational Radiation Data Analysis*, ed. B. Schutz, in press.
Schutz, B. F. and Futamase, T. (1983). *Physical Review D*, 28, 2373.
Schutz, B. F. and Tinto, M. (1987). *Monthly Notices of the Royal Astronomical Society*, 224, 131.
Schvartzman, V. F. (1969). *Soviet Physics* — JETP Letters, 9, 184.
Segelstein, D. J., Rawley, L. A., Stinebring, D. R., Fruchter, A. S., and Taylor, J. H. (1986). *Nature*, 322, 714.
Seidel, E. and Moore, T. (1987). *Physical Review D*, 35, 2287.
Seidel, E. and Moore, T. (1989). In Evans, Finn, and Hobill (1989), p. 146.
Shapiro, S. L. (1977). *Astrophysical Journal*, 214, 566.
Shapiro, S. L. and Teukolsky, S. A. (1985). *Astrophysical Journal (Letters)*, 292, L41.
Shapiro, S. L. and Teukolsky, S. A. (1986a). *Astrophysical Journal*, 307, 575.
Shapiro, S. L. and Teukolsky, S. A. (1986b). In *Dynamical Spacetimes and Numerical Relativity*, ed. J. M. Centrella. Cambridge University Press: Cambridge.
Shoemaker, D., Winkler, W., Maischberger, K., Rudiger, A., Schilling, R., and Schnupp, L. (1986). In Ruffini, ed. (1986).
Shoemaker, D., Schilling, R., Schnupp, L., Winkler, W., Maischberger, K., and Ruediger, A. (1988). *Physical Review D*, in press.
Silk, J. (1980). *The Big Bang*. Freeman, San Francisco. KIP: REPLACE THIS BY BARROW AND SILK (1983) THROUGHOUT THE BOOK; AND DELETE THIS REFERENCE
Slusher, R. E., Hollberg, L. W., Yurke, B., Mertz, J. C., and Valley, J. F. (1985). *Physical Review Letters*, 55, 2409.
Smarr, L. (1977a). *Annals of the New York Academy of Sciences*, 302, 569.
Smarr, L. (1977b). *Physical Review D*, 15, 2069.
Smarr, L., ed. (1979). *Sources of Gravitational Radiation*. Cambridge University Press: Cambridge.
Smarr, L. and York, J. W. (1978). *Physical Review D*, 17, 2529.
Smarr, L., Vessot, R. F. C., Lundquist, C. A., Decher, R., and Piran, T. (1983). *General Relativity and Gravitation*, 15, 129.
Smith, S. (1987). *Physical Review D*, 36, 2901.
Smith, S. (1988). Unpublished PhD thesis. California Institute of Technology: Pasadena.

Smith, S. F. and Havas, P. (1965). *Physical Review*, 138, 495.
Spero, R. (1986a). In Ruffini, ed. (1986).
Spero, R. (1986b). Private communication.
Stark, R. F. and Piran, T. (1985). *Physical Review Letters*, 55, 891 and 56, 97.
Stark, R. F. and Piran, T. (1986). In Ruffini (1986).
Starobinsky, A. A. (1973). *Soviet Physics — JETP*, 65, 20.
Starobinsky, A. A. (1979). *Soviet Physics* — JETP Letters, 30, 682.
Starobinsky, A. A. (1983). *Soviet Astronomy—AJ*, 9, 302.
Starobinsky, A. A. (1985). *Soviet Astronomy Letters*, 11, 133.
Stewart, J. M. and Friedrich, H. (1983). *Proceedings of the Royal Society of London A*, 384, 427.
Strayer, D. M., Papini, G., Ramadan, B., and Tward, E. (1982). In *Proceedings of the Second Marcel Grossmann Meeting on General Relativity*, ed. R. Ruffini. North–Holland: Amsterdam, p. 1227.
Sun, Y. and Price, R. H. (1988). *Physical Review D*, in press.
Suzuki, T., Tsubono, K., and Hirakawa, H. (1978). *Physics Letters A*, 67, 10.
Sullivan, W. T. (1982). *Classics in Radio Astronomy*. Reidel: Dordrecht.
Sullivan, W. T. (1984). *The Early Years of Radio Astronomy*, Cambridge University Press: Cambridge.
Szekeres, P. (1971). *Annals of Physics* 64, 599.
Tammann, G. A. (1981). In *Supernovae: A Survey of Current Research*, eds. M. J. Rees and R. J. Stoneham, p. 371. Reidel: Dordrecht.
Taylor, E. F. and Wheeler, J. A. (1966). *Spacetime Physics*. W. H. Freeman: San Francisco.
Taylor, J. H. (1987). In *Proceedings of Eleventh International Conference on General Relativity and Gravitation*. Cambridge University Press: Cambridge; in press.
Teissier du Cros, F. (1985). *Annales de Physique*, 10, 263.
Teukolsky, S. A. (1972), *Physical Review Letters*, 29, 1114.
Teukolsky, S. A. (1973). *Astrophysical Journal*, 185, 635.
Teukolsky, S. A. and Press, W. H. (1974). *Astrophysical Journal*, 193, 443.
Thirring, W. (1961). *Annals of Physics*, 16, 96.
Thorne, K. S. (1965a). *Physical Review*, B138, 251.
Thorne, K. S. (1965b). Unpublished Ph.D. thesis, Princeton University.
Thorne, K. S. (1969a). *Astrophysical Journal*, 158, 1.
Thorne, K. S. (1969b). *Astrophysical Journal*, 158, 997.
Thorne, K. S. (1972). In *Magic Without Magic: John Archibald Wheeler*. W. H. Freeman: San Francisco; Appendix A, p.243.
Thorne, K. S. (1977). In de Sabbata and Weber (1977). p. 1.
Thorne, K. S. (1978). In *Theoretical Principles in Astrophysics and Relativity*, ed. N. R. Lebovitz, W. H. Reid, and P. O. Vandervoort. University of Chicago Press: Chicago., p. 149.
Thorne, K. S. (1980a). Reviews of Modern Physics, 52, 285.
Thorne, K. S. (1980b). Reviews of Modern Physics, 52, 299.
Thorne, K. S. (1983). Chapter 1 of Deruelle and Piran (1983).
Thorne, K. S. (1985). In *Nonlinear Phenomena in Physics*, ed. F. Claro. Springer–Verlag: Berlin, p. 280.
Thorne, K. S. (1987). In Hawking and Israel (1987), p. 330.
Thorne, K. S. (1988). In *Near Zero: The Frontiers of Physics*, eds. J. D. Fairbank, B. S. Deaver, Jr., C. W. F. Everitt, and P. F. Michelson. Freeman: New York, p.

573.
Thorne, K. S. and Braginsky, V. B. (1976). *Astrophysical Journal (Letters)*, 204, L1.
Thorne, K. S. and Campolattaro, A. (1967). *Astrophysical Journal*, 149, 591; and 152, 673.
Thorne, K. S., Caves, C. M., Sandberg, V. D., Zimmermann, M., and Drever, R. W. P. (1979), in Smarr (1979), p. 49.
Thorne, K. S., Drever, R. W. P., Caves, C. M., Zimmermann, M., and Sandberg, V. D. (1978). *Physical Review Letters*, 40, 667.
Thorne, K. S. and Gürsel, Y. (1983). *Monthly Notices of the Royal Astronomical Society*, 205, 809.
Thorne, K. S. and Hartle, J. B. (1985). *Physical Review D*, 31, 1815.
Thorne, K. S. and Kovacs, S. J. (1975). *Astrophysical Journal*, 200, 245.
Thorne, K. S., Price, R. H., and Macdonald, D. M., eds. (1986). *Black Holes: The Membrane Paradigm*. Yale University Press: New Haven, Connecticut.
Thorne, K. S. and Will, C. M. (1971). *Astrophysical Journal*, 163, 595.
Thuan, T. X. and Ostriker, J. P. (1974). *Astrophysical Journal (Letters)*, 191, L105.
Tinto, M. (1987a). *Monthly Notices of the Royal Astronomical Society*, 226, 829.
Tinto, M. (1987b). *Monthly Notices of the Royal Astronomical Society*, 229, 315.
Tipler, F. J. (1980). *Physical Review D*, 22, 2929.
Tomimatsu, A. (1987). *Journal of Mathematical Physics*, 28, 2720.
Tourrenc, P. (1978). *General Relativity and Gravitation*, 9, 123 and 141.
Tourrenc, P. and Crossiord, J.-L. (1974). *Nuovo Cimento*, 19B, 105.
Traschen, J., Turok, N., and Brandenberger, R. (1986). *Physical Review D*, 34, 919.
Trautman, A. (1958a). *Bulletin de l'Académie* Polonaise des Sciences, Série des Sciences Mathématiques, Astronomiques, et Physiques, 6, 403, 407, and 627.
Trautman, A. (1958b). *Lectures in General Relativity*, mimeographed notes. Kings College, London.
Trautman, A., Pirani, F. A. E., and Bondi, H. (1964). *Lectures on General Relativity*. Prentice-Hall: Englewood Cliffs, NJ.
Tsubono, K. (1989). Private communication.
Tsvetkov, V. P. (1984). *Soviet Astronomy—AJ*, 28, 394.
Tsvetkov, V. P. (1984). *Physics Letters A*, 105, 34. [KIP: THIS IS A NEW 1984; NOTE THERE IS AN OLD ONE]
Tsvetkov, V. P. and Tsirulev, A. N. (1983). *Soviet Astronomy—AJ*, 27, 67.
Tsvetkov, V. P. and Tsirulev, A. N. (1987). *Soviet Astronomy—AJ*, 31, 584.
Turner, M. and Wagoner, R. V. (1979). In Smarr (1979), p. 383.
Turner, M. and Will, C. M. (1978). *Astrophysical Journal*, 220, 1107.
Turok, N. and Brandenberger, R.H. (1986). *Physical Review D*, 33, 2175.
Tyson, J. A. (1973). *Physical Review Letters*, 31, 326.
Tyson, J. A. and Giffard, R. P. (1978). *Annual Reviews of Astronomy and Astrophysics*, 16, 521.
Unruh, W. G. (1979). *Physical Review D*, 19, 2888.
Unruh, W. G. (1982). Unpublished work reported at NATO Advanced Study Institute on Gravitational Radiation, Les Houches, France, June 1982.
Vachaspati, T. and Vilenkin, A. (1985). *Physical Review D*, 31, 3052.
van den Heuvel, E. P. J. (1984). In Reynolds and Stinebring, ed. (1984).
Veitch, P. J., Blair, D. G., Linthorne, N. P., Mann, L. D., and Ramm, D. K. (1987).

Reviews of Scientific Instruments, 58, 1910.
Vilenkin, A. (1981a). *Physical Review D*, 24, 2082.
Vilenkin, A. (1981b). *Physics Letters*, 107B, 47.
Vilenkin, A. (1987). In 300 *Years of Gravitation*, ed. S. W. Hawking and W. Israel. Cambridge University Press: Cambridge, p. 499.
Vinet, J. Y. (1985). *Annales de Physique*, 10, 253.
Vinet, J. Y. (1986). *Journal de Physique*, 47, 639.
Vinet, J. Y., Meers, B., Man, C. N., and Brillet, A. (1988). *Physical Review D*, in press.
Vishniac, E. T. (1982). *Astrophysical Journal*, 257, 456.
Vishveshwara, C. V. (1970a). *Nature*, 227, 936.
Vishveshwara, C. V. (1970b). *Physical Review D*, 1, 2870.
Vlasov, A. A., Logunov, A. A., and Mestvirishvili, M. A. (1984). *Theoretical and Mathematical Physics (USSR)*, 61, 323.
Vogt, R. E., Drever, R. W. P., Thorne, K. S., and Weiss, R. (1987). *Caltech/MIT Project for a Laser Interferometr Gravitational Wave Observatory*, Proposal submitted to National Science Foundation December 1987. Caltech and MIT: Pasadena, CA and Cambridge, MA (unpublished).
Vogt, R. E., Drever, R. W. P., Raab, F. XXX., Thorne, K. S., and Weiss, R. (1989). [CONSTRUCTION PROPOSAL: PRECISE TITLE ETC. NEEDED]
Wagoner, R. V. (1977). In *Gravitazione Sperimentale*, ed. B. Bertotti. Accademia Nazionale dei Lincei: Rome.
Wagoner, R. V. (1979). *Physical Review D*, 19, 2897.
Wagoner, R. V. (1984). *Astrophysical Journal*, 278, 345.
Wagoner, R. V. and Will, C. M. (1976). *Astrophysical Journal*, 210, 764.
Wahlquist, H. D. (1987). *General Relativity and Gravitation*, 19, 1101.
Wahlquist, H. D., Anderson, J. D., Estabrook, F. B., and Thorne, K. S. (1977). In *Gravitazione Sperimentale*, ed. B. Bertotti, p. 335. Accademia Nazionale dei Lincei: Rome.
Wainstein, L. A. and Zubakov, V. D. (1962). *Extraction of Signals from Noise*, Prentice–Hall: London.
Wald, R. M. (1973). *Journal of Mathematical Physics*, 14, 1453.
Walgate, R. (1983). *Nature*, 305, 665.
Walker, M. (1983). In *Relativistic Astrophysics and Cosmology*, eds. X. Fustero and E. Verdaguer. World Scientific: Singapore.
Walker, M. (1984). In *General Relativity and Gravitation*, eds. B. Bertotti et. al., p. 107. Reidel: Dordrecht.
Walker, M. (1986). *Physical Review D*, 33, 612.
Walker, M. and Will, C. M. (1979). *Physical Review D*, 19, 3483 and 3495.
Walker, M. and Will, C. M. (1980). *Astrophysical Journal (Letters)*, 242, L129.
Walls, D.F. (1983). *Nature*, 306, 141.
Ward, H., Hough, J., Kerr, G. A., Mackenzie, N. L., Mangan, J. B., Meers, B. J., Newton, G. P., Robertson, D. I., and Robertson, N. A. (1988). In *Proceedings of International Symposium on Experimental Gravitational Physics*, Guangzhou, China, August 1987, ed Hu En Ke. World Scientific, Singapore, in press.
Weber, J. (1959). *Reviews of Modern Physics*, 31, 681 (see especially section V).
Weber, J. (1960). *Physical Review*, 117, 306.
Weber, J. (1967). *Physical Review Letters*, 18, 498.
Weber, J. (1969). *Physical Review Letters*, 22, 1302.
Weber, J. (1977). In de Sabbata and Weber (1977).

Weber, J. (1979). In *General Relativity and Gravitation*, ed. A. Held. Plenum, New York.
Weber, J. (1983). XXXXXX: KIP – TRY TO FIND – MISSING REFERENCE ON HIS SECOND-GENERATION BAR WORK; SEE SEC. 3.B, PARAGRAPH BEGINNING "FORTURNATELY"
Weber, J. (1984). *Foundations of Physics*, **14**, 1185.
Weber, J. (1986). In *Proceedings of the Sir Arthur Eddington Centenary Symposium. Volume* 3 - *Gravitational Radiation and Relativity*, eds. J. Weber and T. M. Karade. World Scientific: Singapore, p. 1.
Weber, J. and Wheeler, J. A. (1957). *Reviews of Modern Physics*, **29**, 509.
Weinberg, S. (1965). *Physical Review*, B **138**, 988.
Weinberg, S. (1965). *Physical Review*, B **140**, 516. [KIP: NOTE THIS IS A NEW 1965; CALL IT 1965B. THERE WAS AN OLD ONE ABOVE; CHANGE IT TO 1965A]
Weisberg, J. M. and Taylor, J. H., and Fowler, L. A. (1981). *Scientific American*, **245**, No. 4 (October), 66.
Weisberg, J. M. and Taylor, J. H. (1981). *General Relativity and Gravitation*, **13**, 1.
Weisberg, J. M. and Taylor, J. H. (1984). *Physical Review Letters*, **52**, 1348.
Weiss, R. (1972). *Quarterly Progress Report of the Research Laboratory of Electronics of the Massachusetts Institute of Technology*, **105**, 54.
Weiss, R. (1978). In *Sources of Gravitational Radiation*, ed. L. Smarr. Cambridge University Press: Cambridge, p. 7. [KIP: CHANGE THROUGHOUT TO WEISS 1979, AND DELETE THIS REF]
Weiss, R. (1979). In Smarr (1979), p. 7.
Weiss, R., Bender, P. L., Misner, C. W., and Pound, R. V. (1976). *Report of the Sub-Panel on Relativity and Gravitation, Management and Operations Working Croup for Shuttle Astronomy*. NASA: Washington, D. C.
Westpfahl, K. (1985). *Fortschritte der Physik*, **33**, 417.
Weyl, H. (1922). *Space-Time-Matter*. Metheun: London.
Wheeler, J. A. (1955). *Physical Review*, **97**, 511.
Wheeler, J. A. (1962). *Geometrodynamics*. Academic Press: New York.
Wheeler, J. A. (1964). In *Relativity, Croups, and Topology*, ed. C. DeWitt and B. DeWitt. Gordon and Breach: New York.
Whitcomb, S. E., Anderson, D. A., Drever, R. W. P., Gürsel, Y., Hereld, M., and Spero, R. (1983). In *Proceedings of the Third Marcel Grossmann Conference on General Relativity*, e. H. Ning. North-Holland: Amsterdam, p. 1399.
Whitcomb, S. E. and Saulson, P. (1984). Unpublished research at Caltech and MIT; a few of the results are given in figure E.3 of Drever, Weiss, et al. (1985).
Whiting, B. (1989). *Journal of Mathematical Physics*, **30**, 1301.
Wiener, N. (1949). *The Extrapolation, Interpolation and Smoothing of Stationary Time Series with Engineering Applications*. Wiley: New York.
Will, C. M. (1974). *Astrophysical Journal*, **190**, 403.
Will, C. M. (1981). *Theory and Experiment in Gravitational Physics*. Cambridge University Press, Cambridge.
Will, C. M. (1986). *Canadian Journal of Physics*, **64**, 140. [KIP: CHANGE TO 1986A]
Will, C. M. (1986b). *Was Einstein Right?* Basic Books, New York.
Wilson, J. R. (1974). *Physical Review Letters*, **32**, 849.
Wilson, J. R. (1979). In Smarr, ed. (1979), p. 423.
Wilson, J. R. (1980). *Annals of the New York Academy of Sciences*, **336**, 358.
Winkler, W. (1977). In *Gravitazione Sperimentale*, ed. B. Bertotti. Academia

Nazionale dei Lincei: Rome.
Winkler, W., Maischberger, K., Rüdiger, A., Schilling, R., Schnupp, L., and Shoemaker, D. (1986). In Ruffini, ed. (1986).
Winicour, J. (1987a). *Journal of Mathematical Physics*, 28, 668.
Winicour, J. (1987b). *General Relativity and Gravitation*, 19, 281.
Winicour, J. (1988). [KIP: GET REF – "Radiative Space–Times: Physical Properties and Parameters"]
Witten, E. (1984). *Physical Review D*, 30, 272.
Wood, L., Zimmermann, G., Nukolls, J., and Chapline, G. (1971). *Bulletin of the American Physical Society*, 16, 609.
Wood, K. S., Michelson, P. F., Boynton, P., Yearian, M. R., Gursky, H., Friedman, H., and Dieter, J. (1986). *A Proposal to NASA for an X-Ray Large Array (XLA) for the NASA Space Station*. Stanford: Palo Alto, California.
Woosley, S. E. and Weaver, T. A. (1986). *Annual Reviews of Astronomy and Astrophysics*, 24, 205.
Wu, L.–A., Kimble, H. J., Hall, J. L., and Wu, H. (1986). *Physical Review Letters*, 57, 2520.
Yamamoto, Y. and Haus, H.A. (1986). *Reviews of Modern Physics*, 58, 1001.
York, J. W. (1979). In Smarr (1979), p. 83.
York, J. W. (1983). In Deruelle and Piran (1983), p. 175.
York, J. W. (1984). *Physica*, 124A, 629.
Yurtsever, U. (1986). *Abstracts of Contributed Papers. 11th International Conference on General Relativity and Gravitation*, Stockholm, Sweden, July 6–12, 1986. University of Stockholm: Stockholm, p. 287.
Yurtsever, U. (1987a). *Physical Review D*, in press [KIP: GRP–161].
Yurtsever, U. (1987b). *Physical Review D*, in press [KIP: GRP–162].
Yurtsever, U. (1988). *Physical Review D*, submitted [KIP: JULY 88 PAPER].
Zel'dovich, Ya. B. (1980). *Monthly Notices of the Royal Astronomical Society*, 192, 663.
Zel'dovich, Ya. B. and Novikov, I. D. (1967). *Relativistic Astrophysics Vol. 1. Stars and Relativity*. University of Chicago Press: Chicago.
Zel'dovich, Ya. B. and Novikov, I. D. (1983). *Relativistic Astrophysics Vol. 2. The Structure and Evolution of the Universe*. University of Chicaago Press: Chicago.
Zhang, X.–H. (1986). *Physical Review D*, 34, 991.
Zel'dovich, Ya. B. and Grishchuk, L. P. (1986). *Soviet Physics—Uspekhi*, 139, 695 [KIP: THIS IS THE RUSSIAN REF; WHAT IS THE ENGLISH?]
Zel'dovich, Ya. B. and Grishchuk, L. P. (1987). *Soviet Physics—Uspekhi*, 149, 780. [KIP: IS THIS THE RUSSIAN CITATION OR THE ENGLISH?]
Zel'dovich, Ya. B. and Grishchuk, L. P. (1988). *Soviet Physics—Uspekhi*, 155, 517. [KIP: THIS IS THE RUSSIAN CITATION]
Zel'dovich, Ya. B. and Polnarev, A. G. (1974). *Soviet Astronomy—AJ*, 18, 17. [KIP: CHECK: IS THIS THE ENGLISH?]
Zerilli, F. J. (1970). *Physical Review D*, 2, 2141.
Zimmermann, M. (1978). *Nature*, 271, 524.
Zimmermann, M. (1980). *Physical Review D*, 21, 891.
Zimmermann, M. and Szedenits, E. (1979). *Physical Review D*, 20, 351
Zimmermann, M. and Thorne, K. S. (1980). In *Essays in General Relativity*, ed. F. J. Tipler. Academic Press: New York, p. 139.
Zipoy, D. (1966). *Physical Review*, 142, 826.